UNIVERSITAT DE BARCELONA

New Analytical Methodologies based on Chromatography-Atmospheric Pressure Ionization-Mass Spectrometry for the Determination of Halogenated Organic Contaminants

Juan Francisco Ayala Cabrera

Juan Francisco Ayala Cabrera

PhD Thesis

2020

UNIVERSITAT DE BARCELONA

New Analytical Methodologies based on Chromatography-Atmospheric Pressure Ionization-Mass Spectrometry for the Determination of Halogenated Organic Contaminants

Juan Francisco Ayala Cabrera

UNIVERSITAT DE BARCELONA

New Analytical Methodologies based on Chromatography-Atmospheric Pressure Ionization-Mass Spectrometry for the Determination of Halogenated Organic Contaminants

Juan Francisco Ayala Cabrera

UNIVERSITAT DE
BARCELONA

FACULTY OF CHEMISTRY
DEPARTMENT OF CHEMICAL ENGINEERING AND ANALYTICAL CHEMISTRY
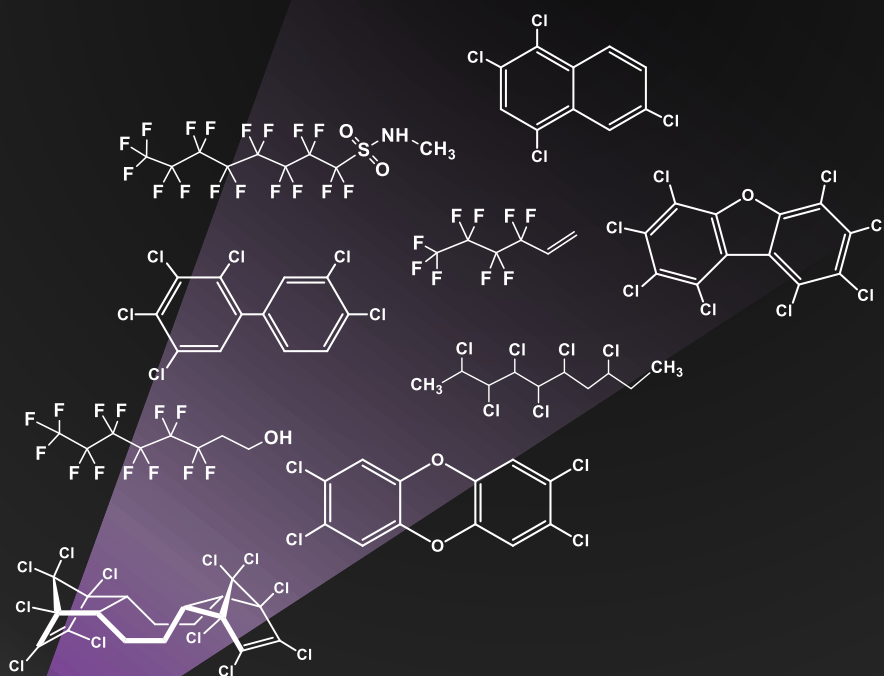
PhD Program:
Analytical Chemistry and the Environment

New Analytical Methodologies based on Chromatography-Atmospheric Pressure Ionization-Mass Spectrometry for the Determination of Halogenated Organic Contaminants

Thesis presented by
Juan Francisco Ayala Cabrera
to obtain the doctor's degree by the University of Barcelona

Under the supervision of
Dra. Encarnación Moyano Morcillo
Dr. Francisco Javier Santos Vicente
from the Department of Chemical Engineering and Analytical Chemistry

La **Dra. Encarnación Moyano Morcillo**, Catedrática de Universidad, y el **Dr. Francisco Javier Santos Vicente**, Profesor Titular de Universidad del Departamento de Ingeniería Química y Química Analítica de la Universidad de Barcelona,

HACEN CONSTAR

Que la presente memoria de tesis doctoral titulada "*New analytical methodologies based on chromatography-atmospheric pressure ionization-mass spectrometry for the determination of halogenated organic contaminants*" ha sido realizada por el Sr. **Juan Francisco Ayala Cabrera** bajo su supervisión en el Departamento de Ingeniería Química y Química Analítica de la Universidad de Barcelona, y que los resultados presentados son frutos de la investigación realizada por el mencionado doctorando.

Y para que así conste, expedimos y firmamos el presente certificado.

Barcelona, junio de 2020

Dra. Encarnación Moyano Morcillo
Catedrática de Universidad del Departamento de Ingeniería Química y Química Analítica

Dr. Francisco Javier Santos Vicente
Profesor Titular de Universidad del Departamento de Ingeniería Química y Química Analítica

When you get into a tight place and everything goes against you until it seems that you cannot hold on for a minute longer, never give up then, for that is just the place and time when the tide will turn.

Harriet Beecher Stowe

AGRADECIMIENTOS

No suelo decir lo que siento y, quizás por ello, estas han sido las páginas más difíciles y a la vez más fáciles de escribir. En primer lugar, me gustaría agradecer todo el tiempo dedicado a mis directores. A la Dra. Encarnación Moyano, por todas sus ideas, su afán de que mejorara continuamente y su predisposición e interés constante en esta tesis. No solo me gustaría agradecérselo desde un punto de vista académico, sino también personal. Han sido muchos años compartiendo tiempo, reuniones, llamadas o cafés lo que me ha permitido valorarte no solo como una gran investigadora, sino también como una persona que tiene un corazón enorme. Igualmente, me gustaría agradecer al Dr. Javier Santos, por todo el tiempo que le he robado, su ayuda constante, su sinceridad y su colaboración en todo momento para que esta tesis saliera adelante. También su continua preocupación por mi día a día, sus consejos y su precaución sobre mi futuro, pero, sobre todo, por obligarme a ser en cada momento la mejor versión de mí mismo. Quizás por ser tan parecidos en muchas cosas tendemos a tener debates muy profundos sobre muchos temas durante cafés, reuniones o descansos, pero todo eso me ha ayudado a mejorar tanto personal como científicamente y eso es algo que nunca te podré terminar de agradecer.

También me gustaría agradecer al Dr. Óscar Núñez todo su apoyo, sus consejos y su esfuerzo desinteresado por aportar todo lo posible para que pudiera mejorar como investigador. Además de gran cocinero eres una gran persona y echaré de menos todos esos ratitos que compartíamos en el laboratorio. Por otro lado, me gustaría agradecer enormemente el apoyo a mis amigos del CECEM (Élida, Javi, Adrià, Sergio, Claudia, Albert, Nerea, etc.). A Raquel, per tots els moments compartits, las muntanyes russes i pel teu recolzament davant qualsevol situació. També voldria agrair especialment a Guillem y Noemí per tots els moments tant dintre com fora del lab, per les mirades còmplices i per ser un pilar molt important per a mi durant tots aquests anys. Recordaré totes les cerveses *"tontes"* i cadascuna de les aventures que hem viscuts junts. Anentzako, inoiz ezingo dizut eskertu neregatik egin dezun dana. Eskerrik asko nere albuan eoteagatik, beti irribarre bat edukitzeagatik eta neregan sinisteagatik nik enunian iten. Hau re bai zuregatik da. Esperoet noizbait zuk emandako danan zati bat bueltatzeko kapaza izatia behintzat.

Todo esto también ha sido posible gracias al maravilloso grupo del departamento que hacía que todo fuera más divertido y ameno. Me gustaría agradecer a Roger, Sara, Laura y Montse todos los momentos de carcajadas, locura y apoyo a lo largo de esta etapa. De manera especial, a Alejandro y a Clara, por todos esos cafés, escapadas a la playa y a la montaña, los *random fucks* y por los consejos y apoyo a lo largo de todos estos años.

A todos gracias, porque habéis sido los mejores compañeros de viaje que podría haber tenido.

I would also like to thank Prof. Oliver Schmitz for the opportunity to work in your laboratory during my Ph. D, all your advice and your friendliness. To all the people from the Applied Analytical Chemistry group in Essen (Sven, Martin, Maria, Florian, Dominik, Kristina, Timo, Claudia, and Gina). Especially, I would like to thank Lidia, Christian, Julia, and Martin for their friendship, their support and all the time we spent, and we will spend together. *Vielen Dank!*

Por otro lado, me gustaría dar las gracias a todas esas caras invisibles que tanto me han ayudado a lo largo de esta tesis. A mis amigos de Barcelona, por habernos conocido, por compartir la vida, por los vermuts, por las charlas, por animarme y por creer en mí en todo momento. Me gustaría dar las gracias especialmente a Alex, Belén, Bea, Simone, Borja y Triana. No ha sido fácil, con confinamiento incluido, pero lo hemos conseguido. Alguien me dijo una vez que las ciudades son bonitas por la gente con las que la compartes y, sin duda, ustedes habéis hecho que Barcelona se convierta en la ciudad más bonita del mundo. A mis amigos de Tenerife, los de siempre, porque habéis seguido estando igual de cerca, por no olvidarse del *catalán*, por las llamadas, las conversaciones, las visitas, los abrazos y por animarme y creer en mí cual padres orgullosos de su hijo. Este triunfo también es de ustedes.

Sobre todo, me gustaría agradecer a mi familia. A mis padres y a mi hermano por apoyarme en esta experiencia, aunque eso significara no poder darme un abrazo cada día. Gracias por vuestra paciencia, valores, cariño y por hacerme sentir la persona más afortunada del mundo. Todos los malos momentos han sido mucho más fáciles gracias a ustedes, sois mi ejemplo en la vida y no hay papel que pueda aguantar todo lo que les aprecio. A mis padres postizos (Sissi y Edu), por hacerme sentir como en casa, por traer un trocito de Canarias a Barcelona, por todo el apoyo y por haberme cuidado tanto y tan bien. Finalmente, a mis abuelas y a la memoria de mis abuelos, por demostrarme que hay que perseguir tus sueños, que en esta vida todo se puede siempre que creas en ello, que le pongas empeño y que tengas al lado una buena guitarra.

A todos ellos y a todas las personas que directa o indirectamente han formado parte de esta tesis,

Gracias.

INDEX

RESUMEN

La incesante emisión de contaminantes supone una amenaza tanto para el medio ambiente como para los seres vivos. Entre estos contaminantes, los compuestos orgánicos persistentes halogenados y los nuevos contaminantes emergentes han despertado una gran preocupación debido a su toxicidad, persistencia, capacidad de bioacumulación y biomagnificación y por su elevada movilidad en el medio ambiente. Además, sus efectos toxicológicos se manifiestan incluso a niveles de trazas, siendo necesario el uso de metodologías analíticas muy sensibles y selectivas para afrontar su detección en muestras ambientales. En este sentido, el uso de fuentes de ionización a presión atmosférica (API) como la ionización química (APCI) y la fotoionización a presión atmosférica (APPI) para sistemas de cromatografía de líquidos (LC-MS) y de gases acoplados a la espectrometría de masas (GC-MS) puede ofrecer ventajas importantes para superar limitaciones observadas en la determinación de estos contaminantes.

En esta Tesis se ha evaluado la aplicabilidad de las fuentes API, especialmente APPI, para desarrollar metodologías LC-API-MS y GC-API-MS que permitan monitorizar contaminantes halogenados en muestras medioambientales. Se han estudiado ampliamente los mecanismos de ionización para maximizar la eficiencia de la ionización de sustancias neutras per- y polifluoroalquiladas (nPFAS). Para ello se ha optimizado la composición de la fase móvil, la adición de sustancias o dopantes que modifican la ionización y los parámetros operacionales más relevantes. Estos estudios han llevado al desarrollo de métodos selectivos y sensibles (fg inyectados en columna) tanto de cromatografía de líquidos acoplados a la espectrometría de masas en tándem (LC-MS/MS) como de cromatografía de gases acoplados a la espectrometría de masas de alta resolución (GC-HRMS). Además, se ha establecido un método eficiente de extracción en fase sólida y uno rápido de microextracción en fase sólida para el análisis de los nPFAS en muestras de agua evitando las pérdidas por volatilización. También se han propuesto rutas de fragmentación para los iones generados en las fuentes API, utilizando la información obtenida en la fragmentación en la fuente y en los estudios de espectrometría de masas en tándem y de alta resolución. Estas rutas de fragmentación pretenden proporcionar una información muy útil para desarrollar estrategias de análisis dirigidas y no dirigidas que hagan posible la identificación tanto de familias conocidas como desconocidas de nPFAS en muestras ambientales.

En esta Tesis se propone por primera vez el uso del novedoso sistema GC-APPI-HRMS (Orbitrap) para hacer frente a las limitaciones observadas en la determinación analítica de contaminantes clorados como el declorano plus (DP) y análogos, los naftalenos policlorados (PCNs), las dibenzo-ρ-dioxinas y dibenzofuranos policlorados (PCDD/Fs), los bifenilos policlorados similares a las dioxinas (dl-PCBs) y las parafinas cloradas de cadena corta (SCCPs). Se ha aprovechado la ionización suave de la fuente GC-APPI para favorecer la formación de iones moleculares o *quasi*-moleculares, así como otros iones característicos como el ion fenoxido, permitiendo desarrollar metodologías sensibles y selectivas. Se ha

estudiado en profundidad la ionización asistida por dopantes para detectar los parámetros críticos que permiten maximizar la eficiencia de ionización. Además, también se ha evaluado la estrategia de ionización *anion-attachment* para minimizar la fragmentación en la fuente y mejorar tanto la selectividad como la sensibilidad en la determinación de SCCPs. También se ha evaluado el uso de estrategias de separación multidimensional utilizando novedosas fases estacionarias y/o movilidad iónica para mejorar la separación de aquellos compuestos que normalmente presentan coeluciones en las separaciones monodimensionales (PCNs y SCCPs). Los métodos de GC-APPI-HRMS propuestos en esta Tesis han demostrado gozar de una gran capacidad de detección (hasta pocos fg inyectados en columna), una alta selectividad debido tanto a la alta resolución como a la baja fragmentación obtenida en la fuente GC-APPI y un buen rendimiento para determinar estos compuestos a niveles bajos de concentración en muestras complejas de interés ambiental.

.

ABSTRACT

The environment sustainability is being threatened by the continuous release of pollutants that can negatively affect not only environmental compartments but also wildlife and human beings. Among these pollutants, halogenated persistent organic pollutants and new emerging contaminants have cause great concern due to their toxicity, persistence, bioaccumulation and biomagnification capacity and/or their high mobility in the environment. Moreover, their hazardous effects are manifested even at trace levels, thus requiring very selective and sensitive analytical methodologies to face their detection in environmental samples. In this sense, atmospheric pressure ionization (API) sources such as atmospheric pressure chemical ionization (APCI) and atmospheric pressure photoionization (APPI) for both liquid-mass spectrometry (LC-MS) and gas chromatography-mass spectrometry (GC-MS) could offer great advantages to overcome the limitations observed in the determination of these group of substances.

In the present Thesis, the feasibility of these ionization sources, especially APPI, has been evaluated to develop sensitive and selective LC-API-MS and GC-API-MS methodologies to monitor relevant halogenated contaminants in environmental samples. API sources have been thoroughly tested to achieve an efficient ionization of neutral per- and polyfluoroalkyl substances (nPFAS). The ionization behavior of these compounds was assessed through optimization of the mobile phase composition, the addition of additives or dopants as well as critical ion source working parameters. These studies have led to highly selective and sensitive liquid chromatography-tandem mass spectrometry (LC-MS/MS) and gas chromatography-high-resolution mass spectrometry (GC-HRMS) methodologies (up to fg injected on column). Furthermore, an efficient solid-phase extraction and a fast and *in-situ* preconcentration headspace solid-phase microextraction procedures have been developed to analyze nPFAS in river water samples avoiding analyte losses observed during evaporation steps. Additionally, the fragmentation pathways of ions generated for these compounds in API sources has been tentatively proposed using the combined information of in-source fragmentation, tandem mass spectrometry and high-resolution mass spectrometry. These fragmentation pathways aim to provide useful information for the development of target, suspect and non-targeted analysis strategies for the identification of known and new families of nPFAS in complex environmental samples.

Furthermore, in this Thesis, the novel GC-APPI-HRMS (Orbitrap) system is proposed to face the main limitations that have been observed in the currently used analytical determinations of relevant chlorinated contaminants such as dechlorane plus (DP) and analogs, polychlorinated naphthalenes (PCNs), polychlorinated dibenzo-ρ-dioxins and dibenzofurans (PCDD/Fs), dioxin-like polychlorinated biphenyls (dl-PCBs), and short-chain chlorinated paraffins (SCCPs). The soft ionization of GC-APPI has been used to promote molecular or quasi-molecular ions as well as characteristic cluster ions such as [M–Cl+O]⁻, allowing the development of sensitive and selective methods. The use of dopant vapors has been

thoroughly investigated to detect the critical parameters that allow maximizing the ionization efficiency of the analytes. Additionally, anion-attachment ionization strategies have been also studied to reduce the in-source fragmentation and to improve sensitivity and selectivity for SCCPs. Furthermore, multidimensional separation strategies (using novel stationary phases and/or ion mobility separation) have also been evaluated to improve the separation of those compounds that often coelute (PCNs or SCCPs).The GC-APPI-HRMS methods developed in this Thesis have shown a great detection capability (up to low fg injected on column) and a high selectivity due to both the exact mass measurements (Orbitrap) and the soft ionization provided by the GC-APPI source. Moreover, they have demonstrated a good performance to determine these compounds in marine sediments, fly ashes, gull eggs, or fishes among other complex environmental samples.

ABBREVIATIONS AND ACRONYMS

A

ADONA	Ammonium 4,8-dioxa-3H-perfluorononanoate
AKMD	Adjusted kendrick mass defect
AMAP	Arctic Monitoring and Assessment Programme
APCI	Atmospheric pressure chemical ionization
µAPCI	Microchip-based atmospheric pressure chemical ionization
APGC	Atmospheric pressure gas chromatography
API	Atmospheric pressure ionization
APPI	Atmospheric pressure photoionization
µAPPI	Microchip-based atmospheric pressure photoionization

B

BAT	Best available techniques
BEP	Best environmental practices

C

cAPPI	Capillary atmospheric pressure photoionization
CCS	Collision cross-section
CEN	European Committee for Standardization
CEPA	Canada Environmental Protection Act
CI	Positive ion chemical ionization
CID	Collision-induced dissociation
Cl-PFESAs	Chlorinated polyfluoroalkyl ether sulfonic acids
Cl_{10}-DP	Cl_{10}-Dechlorinated Dechlorane Plus
Cl_{11}-DP	Cl_{11}-Dechlorinated Dechlorane Plus
CPs	Chlorinated paraffins
CPI	Capillary pressure photoionization

D

Dec-602	Dechlorane 602
Dec-603	Dechlorane 603
Dec-604	Dechlorane 604
dl-PCBs	Dioxin-like polychlorinated biphenyls
DP	Dechlorane Plus
DTIMS	Drift tube ion mobility spectrometry

E

ECHA	European Chemical Agency
EEA	European Environment Agency
EFSA	European Food Safety Authority
EI	Electron ionization
ELV	Emission limit value
ESI	Electrospray ionization

F

FAPA	Flowing atmospheric pressure afterglow
FBSAs	*N*-alkyl fluorobutane sulfonamides
FBSEs	*N*-alkyl fluorobutane sulfonamido-ethanols
FIA	Flow injection analysis
FOSAs	*N*-alkyl fluorooctane sulfonamides
FOSEs	*N*-alkyl fluorooctane sulfonamido-ethanols
FTCAs	Fluorotelomer carboxylic acids
FTOs	Fluorotelomer olefins
FTOHs	Fluorotelomer alcohols
FWHM	Full width at half maximum

G

GC	Gas chromatography
GC-APCI	Atmospheric pressure chemical ionization for GC-MS
GC-APLI	Atmospheric pressure laser ionization for GC-MS
GC-APPI	Atmospheric pressure photoionization for GC-MS
GC-ESI	Multichannel electrospray ionization for GC-MS
GCxGC	Comprehensive two-dimensional gas chromatography
GC-LTP	Low temperature plasma for GC-MS

H

HBCD	Hexabromocyclododecane
HCB	Hexachlorobenzene
HPLC	High performance liquid chromatography
HRMS	High-resolution mass spectrometry
HS-SPME	Headspace solid-phase microextraction

I

IARC	International Agency of Research on Cancer
IE	Ionization energy
IL	Ionic liquid
iLOD	Instrumental limit of detection
IM	Ion mobility
IT	Ion-trap

J

JISC	Japanese Industrial Standards Committee

K

KMD	Kendrick mass defect

L

LC	Liquid chromatography
LCCPs	Long-chain chlorinated paraffins
LLE	Liquid-liquid extraction
LRMS	Low-resolution mass spectrometry

M

MAE	Microwave-assisted extraction
MCCPs	Medium-chain chlorinated paraffins
mLOD	Method limit of detection
mLOQ	Method limit of quantification
MRM	Multiple reaction monitoring
MS	Mass spectrometry
MS^n	Multiple-stage mass spectrometry
MS/MS	Tandem mass spectrometry

N

NATO	North Atlantic Treaty Organization
nPFAS	Neutral per- and polyfluoroalkyl substances
NICI	Negative ion chemical ionization
NTP	National Toxicology Program

O

OECD	Organization for Economic Co-operation and Development

P

PA	Proton affinity
PBDEs	Polybrominated diphenyl ethers
PCBs	Polychlorinated biphenyls
PCDDs	Polychlorinated dibenzo-ρ-dioxins
PCDFs	Polychlorinated dibenzofurans
PCNs	Polychlorinated naphthalenes
PFAS	Per- and polyfluoroalkyl substances
PFCAs	Perfluoroalkyl carboxylic acids
PFECAs	Polyfluoroalkyl ether carboxylic acids
PFESAs	Polyfluoroalkyl ether sulfonic acids
PFOA	Perfluorooctanoic acid
PFOS	Perfluorooctane sulfonic acid
PFSAs	Perfluoro-alkane sulfonic acids
PLE	Pressurized liquid extraction
POP	Persistent organic pollutant
PS-APPI	Paper spray-atmospheric pressure photoionization
pSFC	Packed column supercritical fluid chromatography
PTV	Programmed temperature vaporization

Q

Q	Quadrupole
QqQ	Triple quadrupole
QuEchERS	Quick, easy, cheap, effective, rugged, and safe

R

RDB	Ring double bond equivalent
REACH	Registration, Evaluation, Authorization, and Restriction of Chemicals
RP	Relative potency

S

SCCPs	Short-chain chlorinated paraffins
SE	Solvent extraction
SIM	Selected ion monitoring
S/N	Signal-to-noise
SPE	Solid-phase extraction
SPME	Solid-phase microextraction

T

TEF	Toxic equivalency factor
TEQ	Toxic equivalent
TOF	Time-of-flight
TWI	Tolerable weekly intake

U

UAE	Ultrasound-assisted extraction
UHPLC	Ultra-high performance liquid chromatography
UNEP	United Nations Environment Programme
U.S. EPA	U.S. Environmental Protection Agency

W

WHO	World Health Organization

OBJECTIVES AND STRUCTURE

OBJECTIVES AND STRUCTURE

The objective of this Thesis is to establish new analytical methodologies, mainly based on chromatography-atmospheric pressure ionization-mass spectrometry, for the determination of halogenated organic contaminants in environmental samples. These methodologies may face the main limitations of the current methods to improve the chromatographic separation, detection capability and/or selectivity in front of potential interferences.

This main goal can be divided into the following sub-objectives that are reflected in the experimental work included in this Thesis:

- Evaluation of the ionization mechanisms of several families of halogenated organic contaminants in atmospheric pressure ionization sources (mainly APCI and APPI) and identification of the most critical parameters to promote the generation of molecular or quasi-molecular ions. To achieve this goal, the effect of mobile phase composition (for LC-MS determinations) and the addition of different additives (acid and basic species, dopants, or other substances affecting the ionization mechanism) that can improve the ionization efficiency of the target compounds will be studied. Moreover, these studies should help to better understand the behaviour of the novel GC-APPI source.

- Study of in-source and tandem mass spectrometry fragmentation of the compounds included in this Thesis to identify fragmentation pathways and common fragmentation patterns. This valuable information should allow to establish reliable targeted and non-targeted strategies for the detection of halogenated organic contaminants in samples of environmental interest.

- Development of LC-API-MS/MS and GC-API-HRMS methods to improve the detection capability and the selectivity on the determination of the halogenated organic contaminants. These methods may involve highly efficient chromatographic systems, ionization strategies that reduce in-source fragmentation and mass analyzers that provide highly selective structural information (tandem mass spectrometry and high-resolution mass spectrometry). These methodologies will be combined with suitable sample treatment procedures and applied to the analysis of these halogenated organic contaminants in different environmental samples.

- Study of the capabilities of multidimensional separation techniques using novel stationary phases to improve the chromatographic separation of closely eluting compounds. This goal will be addressed by the use of comprehensive two-dimensional gas chromatography and ion mobility to better separate PCNs and SCCPs congeners, respectively.

To achieve these objectives, the current Thesis has been structured into three chapters:

- Chapter 1 includes a general introduction to the halogenated organic contaminants, involving both persistent organic pollutants and emerging contaminants. In this introduction, the families of compounds evaluated in this Thesis are presented and the state-of-the-art of their toxicity and legislation has been included to better understand the hazardous effects and restrictions of these contaminants. This chapter also includes an extensive review of the current analytical methodologies commonly used to determine these halogenated organic contaminants. These methodologies are discussed considering the sample treatment, chromatographic separation, mass spectrometry analysis (including both ionization sources and mass analyzers), and the quantification approaches generally applied. This revision highlights the main limitations of the current analytical methodologies as well as the most promising trends to improve the determination of these compounds in environmental samples. Finally, a section dealing with the last trends in the use of atmospheric pressure ionization (API) sources for both liquid chromatography-tandem mass spectrometry (LC-MS/MS) and gas chromatography-mass spectrometry (GC-MS) has been included to highlight the great potential of these ionization techniques to efficiently ionize halogenated organic contaminants.

- Chapter 2 is focused on the determination of fluorinated organic compounds. API sources are evaluated to ionize neutral per- and polyfluoroalkyl substances (nPFAS) and to establish their fragmentation pathways. These studies allow to identify fragmentation patterns and the most characteristic and abundant ions to be monitored to develop sensitive and selective methodologies by LC-MS/MS and gas chromatography-high-resolution mass spectrometry (GC-HRMS) for the determination of these contaminants in river water samples, as well as for the establishment of identification and characterization strategies to help in the detection of target and related compounds in complex matrices. This chapter consists of 3 sections, an introduction related to the main properties and applications, the classification, and the analytical determination of PFAS, as well as the main limitations of analytical determination of neutral PFAS and their environmental occurrence; the experimental work and results section that includes the research articles focused in the development of the determination methodologies for the analysis of these compounds; and the discussion of the results obtained in the research papers, focusing in the most relevant aspects for the determination of fluorinated compounds using the methodologies developed. The research articles included in this chapter are: "*Negative-ion atmospheric pressure ionisation of semi-volatile fluorinated compounds for ultra-high-performance liquid chromatography tandem mass spectrometry analysis*" (Analytical and Bioanalytical Chemistry, (2018) 410: 4913-4924), "*Gas chromatography and liquid chromatography coupled to mass spectrometry for the determination of fluorotelomer olefins, fluorotelomer alcohols, perfluoroalkyl*

sulfonamides and sulfonamido-ethanols in water" (Journal of Chromatography A, (2020) 1609: 460463), *"Fragmentation studies of neutral per- and polyfluoroalkyl substances by atmospheric pressure ionization-multiple stage mass spectrometry"* (Analytical and Bioanalytical Chemistry, (2019) 411: 7357-7373) and *"A novel methodology for the determination of neutral perfluoroalkyl and polyfluoroalkyl substances in water by gas chromatography-atmospheric pressure photoionisation-high resolution mass spectrometry"* (Analytica Chimica Acta, (2020) 1100: 97-106).

- Chapter 3 is focused on the determination of several families of chlorinated organic contaminants using GC-HRMS with API sources. To this end, the feasibility of GC-HRMS mainly using atmospheric pressure photoionization, as well as the use of novel multidimensional separation techniques are evaluated to overcome the main limitations of the currently applied analytical determinations for chlorinated organic contaminants. This chapter includes a general introduction that highlights the main properties, applications, environmental occurrence, and determination issues of the chlorinated organic contaminants, an experimental work and results section that includes 5 research articles (2 of them related to the analysis of polychlorinated naphthalenes are the result of a research stay of 3.5 months at the Analytical Applied Chemistry group of the University of Duisburg-Essen) that focus in the development of GC-HRMS methods or multidimensional methods, and a further joint discussion of the results to extract the main conclusions of these publications. The experimental work and results are included in the following research articles: *"Analysis of dechlorane plus and analogues in gull eggs by GC-HRMS using a novel atmospheric pressure photoionization source"* (sent to Analytical and Bioanalytical Chemistry), *"Ionic liquid stationary phase for improving comprehensive multidimensional gas chromatographic separation of polychlorinated naphthalenes"* (sent to Journal of Chromatography A), *"Atmospheric pressure ionization for gas chromatography-high resolution mass spectrometry determination of polychlorinated naphthalenes in marine sediments"* (sent to Chemosphere), *"Feasibility of gas chromatography-atmospheric pressure photoionization-high-resolution mass spectrometry for the analysis of polychlorinated dibenzo-ρ-dioxins, dibenzofurans, and dioxin-like polychlorinated biphenyls in environmental and feed samples* (Analytical and Bioanalytical Chemistry, (2020), 412: 3703-3716), and *"Chloride-attachment atmospheric pressure photoionisation for the determination of short-chain chlorinated paraffins by gas chromatography-high-resolution mass spectrometry"* (sent to Analytica Chimica Acta).

Finally, the main conclusions extracted from this Thesis are summarized in the corresponding section and the bibliography section includes the references considered to support the dissertation of the different chapters.

CHAPTER 1.
INTRODUCTION

CHAPTER 1.INTRODUCTION

Human beings have always been trying to simplify our existence to achieve the best life quality. Thus, there was a significant change in our lifestyle at the end of the 18th century due to the industrial revolution. This affected social, economic, and technological processes and completely transformed our reality. This transition involved moving from hand production methods to the use of machines, new chemical manufacturing, and iron production processes, as well as the increasing use of water and steam power, the development of machine tools, and the rise of the industrial mechanization systems. However, the industrial revolution also led to an unprecedented rise in the pollution levels, and, after that, this threat has exponentially increased, becoming a well-known worldwide concern. Pollutants have shown to produce harmful effects in the environment, causing irreparable damage to the earth through multiples compartments, such as soil, air, or water, among others. As human beings increase their control over nature, new needs arise in society, trying to adapt ourselves to the continuously changing environment. Thus, both technological development and demographic growth have led to the disruption of the environment. Nowadays, environmental pollution is one of the main problems that the world is facing, which requires taking strong actions to find sustainable technological and economic growth that helps to preserve the environment.

According to the release into the environment, the most critical pollutants have been classified by the European Environment Agency (EEA) into the following categories: pesticides, halogenated organic contaminants, greenhouse gases (CH_4, CO_2, N_2O, perfluorocarbons, etc.), heavy metals (Hg, As, Cd, Pb, Zn, Cr, etc.), inorganic substances (chloride, cyanide, bromide, fluoride, particulate matter, etc.), other gases (chlorofluorocarbons, nitrogen oxides, sulfur oxides, etc.) and other organic substances (polyaromatic hydrocarbons, benzene, toluene, xylenes, etc.). All of them have been shown to cause adverse effects on both the environment and human beings as they are involved in the greenhouse effect or are linked with several diseases. In the last century, most of the efforts of the scientific community have been focused on monitoring halogenated organic contaminants and pesticides (especially organohalogen pesticides) since they are extremely hazardous compounds even at ultra-trace levels. Additionally, their adverse effects frequently manifest after the exposure, being difficult to find a relationship between the contamination source and the disease until the consequences are irreparable. This Thesis is focused on the study of one of these pollutant groups, the halogenated organic contaminants.

1.1.Halogenated Organic Contaminants

Among all the halogenated organic contaminants released to the environment, persistent organic pollutants (POPs) have aroused great interest. These compounds have a high resistance to degradation, remaining intact for exceptionally long periods, and they are prone to be long-distance transported throughout the environment as a result of natural processes involving soil, water, and air. These releases into the environment over the years, mainly due

to anthropogenic activities, have caused that POPs are worldwide distributed, affecting both environmental media and living organisms through many foodstuffs and resulting in the exposure of many species, including humans, for periods that span generations. Moreover, POPs can easily incorporate to fatty tissues, where concentrations can magnify up to 70,000 times the background levels, through a process called bioaccumulation. This bioaccumulation capacity increases through the food chain since mammals and humans can absorb high concentrations (biomagnification). Due to these processes, POPs can be found even in humans and animals living in remote regions that are far away from any major POP source. Additionally, POPs show high toxicity that can cause important diseases such as cancer, allergies, damages to the nervous system, reproductive disorders, disruption of the immune system as well as, in some cases, they are considered as endocrine disrupters [1].

For these reasons, POPs have become a global problem and, consequently, the scientific community and different administrative organizations, like the United Nations, through the United Nations Environment Programme (UNEP), have introduced restrictive actions to regulate their control. In this sense, the most ambitious project has been the Stockholm Convention, which was adopted and ratified by over 150 countries on the 22nd of May of 2001 and entered into force on the 17th of May of 2004. The main objective of the Stockholm Convention is to protect human health and the environment in front of POPs, by eliminating or at least reducing the emissions of these pollutants. Currently, over 30 POPs are listed by the Stockholm Convention, while few others are proposed for listing as potential POPs (Fig. 1.1). In the beginning, twelve groups of chemicals, known as the *dirty dozen*, were listed as POPs in 2001. These POPs included organochlorine pesticides, as aldrin, chlordane, dichloro-diphenyl-trichloroethane (DDT), dieldrin, endrin, heptachlor, hexachlorobenzene (HCB), mirex and toxaphene, industrial chemicals, such as HCB and polychlorinated biphenyls (PCBs), and industrial by-products, such as the already mentioned HCB and PCBs as well as polychlorinated dibenzo-ρ-dioxins (PCDDs) and dibenzofurans (PCDFs). These pollutants were classified under different annexes, according to the decisions achieved by the Conference of the Parties of the Stockholm Convention about their production and use (Table 1.1). Hence, most of the organohalogen pesticides are listed in Annex A for their elimination with specific exemptions for their use. In contrast, DDT was included in Annex B to the Stockholm Convention with restrictions on its production and/or use for disease vector control purposes following the recommendations and guidelines of the World Health Organization (WHO). Regarding industrial chemicals, such as PCBs and HCB, they were not only included under Annex A but also in Annex C as well as PCDD/Fs, since they are also unintentional industrial by-products. The Stockholm Convention also focuses its efforts on identifying, characterizing, quantifying, and prioritizing potential sources of releases of unintentional POPs. To reduce these anthropogenic releases, parties of the Stockholm Convention must implement best available techniques (BAT) and best environmental practices (BEP) for the POPs listed in Annex C. Among the BAT and BEP strategies to reduce releases of unintentional POPs we can find the following actions: (i) closing down ineffective obsolete

facilities and replacing them by cleaner technologies, (ii) modifying existing facilities to increase efficiency, (iii) taking measures to reduce the total amount of waste and improving design and management of landfills, and (iv) separating household waste and composting rather than back-yard burning.

POPs added in 2001 (Dirty dozen)

Aldrin	*Chlordane*	*Dieldrin*	*Endrin*

| *Heptachlor* | *Hexachlorobenzene (HCB)* | *Mirex* | *Toxaphene* |

| *Polychlorinated biphenyls (PCBs)* | *Dichlorodiphenyltrichloroethane (DDT)* | *Polychlorinated dibenzo-ρ-dioxins (PCDDs)* | *Polychlorinated dibenzofurans (PCDFs)* |

POPs added in 2009

| *α-Hexachlorocyclohexane (α-HCH)* | *β-Hexachlorocyclohexane (β-HCH)* | *Chlordecone* | *Hexabromobiphenyl (HBB)* |

| *Polybrominated diphenyl ethers (PBDEs)* | *Lindane (γ-HCH)* | *Pentachlorobenzene* | *Perfluorooctane sulfonic acid (PFOS) and its salts* |
| | | | *Perfluorooctane sulfonyl fluoride (PFOSF)* |

POPs added in 2011

Endosulfan and its related isomers

POPs added in 2013

Hexabromocyclododecane (HBCD)

Fig. 1.1. Persistent organic pollutants listed or proposed to be included in the Stockholm Convention.

5

POPs added in 2015

Pentachlorophenol, its
salts and esters

Hexachlorobutadiene

Polychlorinated naphthalenes
(PCNs)

POPs added in 2017

POPs added in 2019

Decabromodiphenyl ether
(Deca-BDE)

Short-chain chlorinated paraffins
(SCCPs)

Dicofol

Perfluorooctanoic acid (PFOA),
its salts and PFOA-related
compounds

Candidate POPs (Under review)

Dechlorane Plus (DPs)

Methoxychlor

Perfluorohexane sulfonic acid
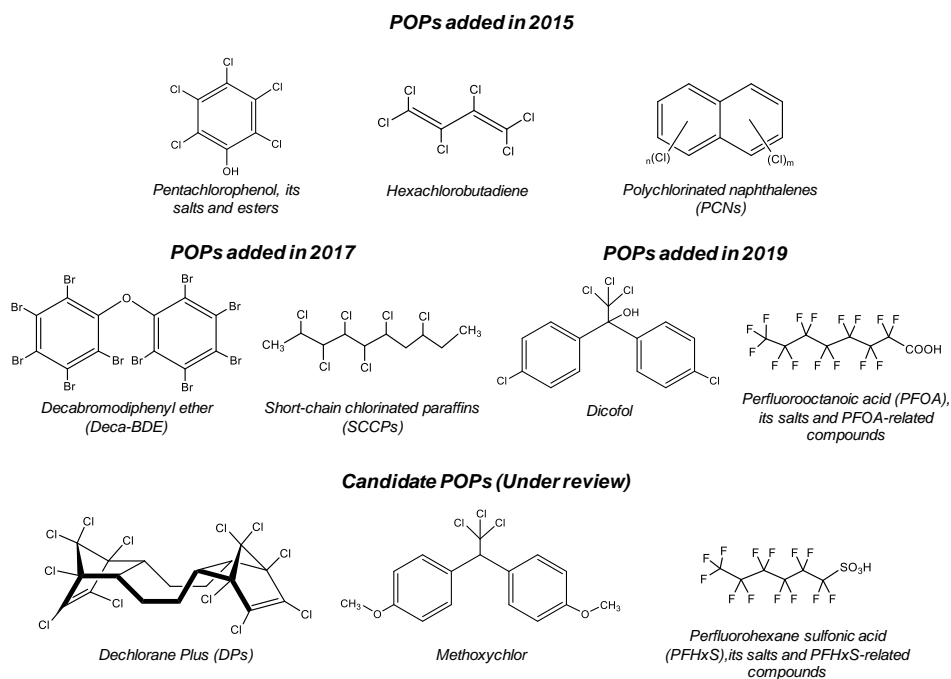(PFHxS),its salts and PFHxS-related
compounds

Fig. 1.1. (cont.) Persistent organic pollutants listed or proposed to be included in the Stockholm Convention.

The Stockholm Convention list has been increasing during the years due to the decisions accomplished by the Conference of the Parties of the Stockholm Convention. During the fourth meeting celebrated in May of 2009, new pesticides like α-hexachlorocyclohexane (α-HCH), β-hexachlorocyclohexane (β-HCH), lindane (γ-HCH), and chlordecone, as well as industrial chemicals, such as hexabromobiphenyl (HBB), tetra- (Tetra-BDEs), penta- (Penta-BDEs) as the main components of the commercial pentabromodiphenyl ether mixture, as well as hexa- (Hexa-BDEs) and heptabromodiphenyl ethers (Hepta-BDEs), from the commercial octabromodiphenyl ether mixture, were added to Annex A for their elimination. Additionally, perfluorooctane sulfonic acid (PFOS) and its salts, and perfluorooctane sulfonyl fluoride (PFOSF), were listed in Annex B, allowing their production and use as photomasks in the semiconductor and liquid crystal display industries, metal plating, electric and electronic parts for color printers and color copy machines, chemically driven oil production and insecticides for control red imported fire ants and termites. As happened for PCBs, HCB, and PCDD/Fs, pentachlorobenzene was also added to Annex A and C for controlling their unintentional production. The fifth (May 2011) and sixth meetings (May 2013) of the Conference of the Parties included endosulfan and hexabromocyclododecane (HBCD) in Annex A, respectively; while pentachlorophenol, its salts, and esters, hexachlorobutadiene were listed in this annex during the seventh meeting (May 2015) at the same time as polychlorinated naphthalenes (PCNs), which were added to Annex A and C. Hexachlorobutadiene was later included in Annex C after considering its risk profile and risk management evaluation.

Table 1.1. Classification of POPs included in the Stockholm Convention list.

Annex	Group of pollutants
A *(Elimination)*	Aldrin, chlordane, chlordecone, dicofol, dieldrin, endosulfan, endrin, heptachlor, hexabromobiphenyl, HBB, HBCD, HCB, hexachlorobutadiene, α-HCH, β-HCH, γ-HCH, mirex, pentachlorobenzene, pentachlorophenol, and its salts and esters, Tetra-BDEs, Penta-BDEs, Hexa-BDEs, Hepta-BDEs and Deca-BDE, PCBs, PCNs, PFOA, its salts and PFOA-related compounds, SCCPs, and toxaphene
B *(Restriction)*	DDT, PFOS, its salts and PFOSF
C *(Unintentional Production)*	HCB, hexachlorobutadiene, pentachlorobenzene, PCBs, PCDD/Fs, and PCNs
D *(Under review)*	Dechlorane Plus, methoxychlor, PFHxD, its salts, and PFHxS-related compounds

After that, two more meetings of the Conference of the Parties were celebrated in May 2017 and 2019 proposing the inclusion in Annex A (elimination) of decabromodiphenyl ether (Deca-BDE, commercial mixture, c-decaBDE), short-chain chlorinated paraffins (SCCPs), dicofol, perfluorooctanoic acid (PFOA), its salts and PFOA-related compounds [2]. Moreover, other chemicals such as Dechlorane Plus (DP) [3], methoxychlor [4], perfluorohexane sulfonic acid (PFHxS), its salts, and PFHxS-related compounds [5] have already been proposed as candidates for listing under the Stockholm Convention.

Although the profile risks elaborated for these compounds and their inclusion in the Stockholm Convention list have reduced their use and production, the European Environment Agency has reported a continuous significant release of POPs into the environment (ca. 3800 tonnes/year in Europe). These releases significantly vary between years and the environmental compartments (Fig. 1.2).
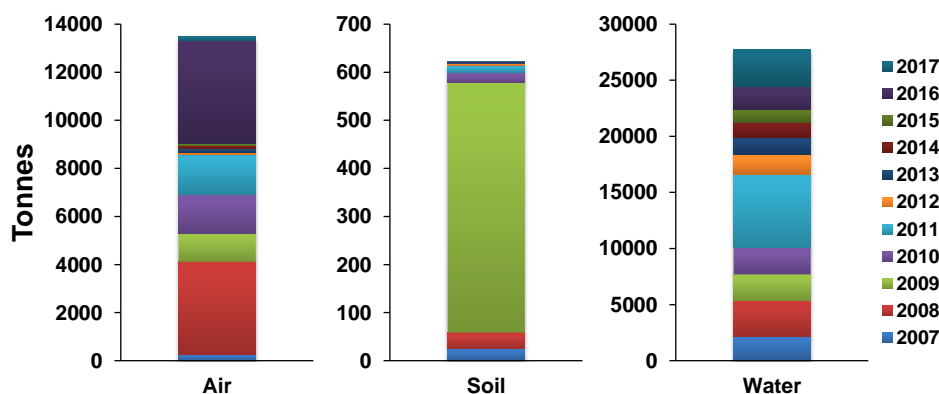
Fig. 1.2. Accumulated release of POPs into the environment from 2007 to 2017.

Thus, the discharges to the aquatic environments correspond to 66.3% of the total POP release to the environment, whereas the release of these pollutants to air and soil accounts for 32.2% and 1.5%, respectively. Considering the main activities that contribute to the release of these pollutants, the production, and processing of metals, as well as waste and wastewater management, are the main sources of POPs emissions in Europe according to EEA (Fig. 1.3). Moreover, both the energy sector and the chemical industry contribute significantly to generate 20% and 13% of these pollutants release, respectively. Other sectors, such as mineral industry and paper and wood production and processing show a lower contribution emitting less than 5% of these contaminants.
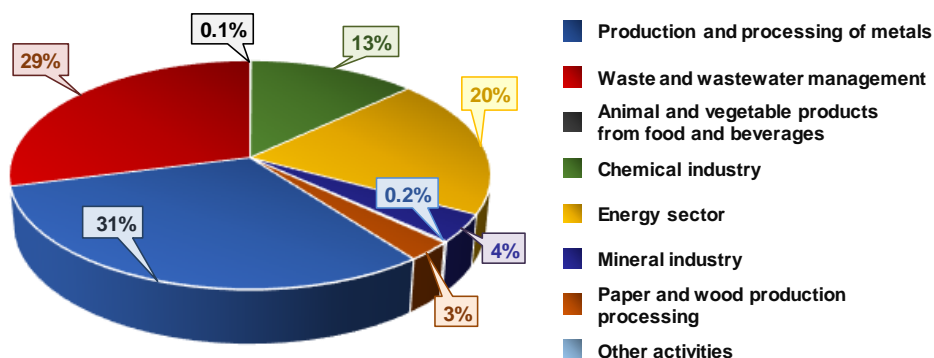
Fig. 1.3.   Release of POPs to the environment according to the emission source.

The emission of these pollutants and their physicochemical properties, especially their persistence and mobility in the environment, have led to basal and ubiquitous levels of these pollutants in the environment. Hence, they are subjected to a large-scale global monitoring plan (GMP) that provides a harmonized organizational framework to collect comparable data on the presence of POPs from different regions. This GMP helps with the identification of potential changes in POP concentration over time as well as their regional and global environmental transport. At the same time, it allows to periodically verify the effectiveness of measures adopted by the Convention to eliminate or significantly reduce POP releases into the environment. Until now, two data collection campaigns have been carried out, generating global and regional monitoring reports endorsed by the Conference of Parties (COPs). The first GMP data collection (2008) on POPs levels in the environment was focused on the initial 12 POPs (*dirty dozen*) while the second campaign (2014) included information about 23 POPs listed in the Stockholm Convention which can be visualized using the GMP data warehouse [6]. The third GMP data collection campaign has been ongoing until the end of March 2020 and it will provide information about POP levels and trends from ambient air, human tissues (breast milk and blood), and water matrices.

Besides POPs, other halogenated pollutants, generally called emerging halogenated contaminants, have also caused great concern. This group of chemicals involves per- and polyfluorinated alkyl substances (PFAS), brominated/iodinated disinfection by-products

(DBPs) for drinking water and swimming pools (halonitromethanes, iodo-acids, haloamides, halofuranones or halobenzoquinones, etc.) and halogenated flame retardants like tetrabromobisphenol-A (TBBPA) or halogenated organophosphates, among others [7–9]. Among these emerging halogenated contaminants, PFAS have focused great attention due to the large number of compounds documented within this group (more than 6,300 PFAS) that show a wide range of physicochemical properties, characteristics, and effects. Perfluoroalkyl carboxylic acids (PFCAs) and perfluoro-alkane sulfonic acids (PFSAs) have been the compounds most widely studied, paying special attention to PFOA and PFOS [9]. The levels of these persistent pollutants have started to decline may be partly due to their inclusion in the Stockholm Convention list and partly due to the shift in the production to alternative fluorinated compounds [10]. In this sense, increased use of neutral PFAS have been observed since they are generally not environmentally persistent and less toxic compounds. In contrast, they are quite volatile and, therefore, suitable for long-range atmospheric transport. The main families of neutral PFAS are summarized in Fig. 1.4.
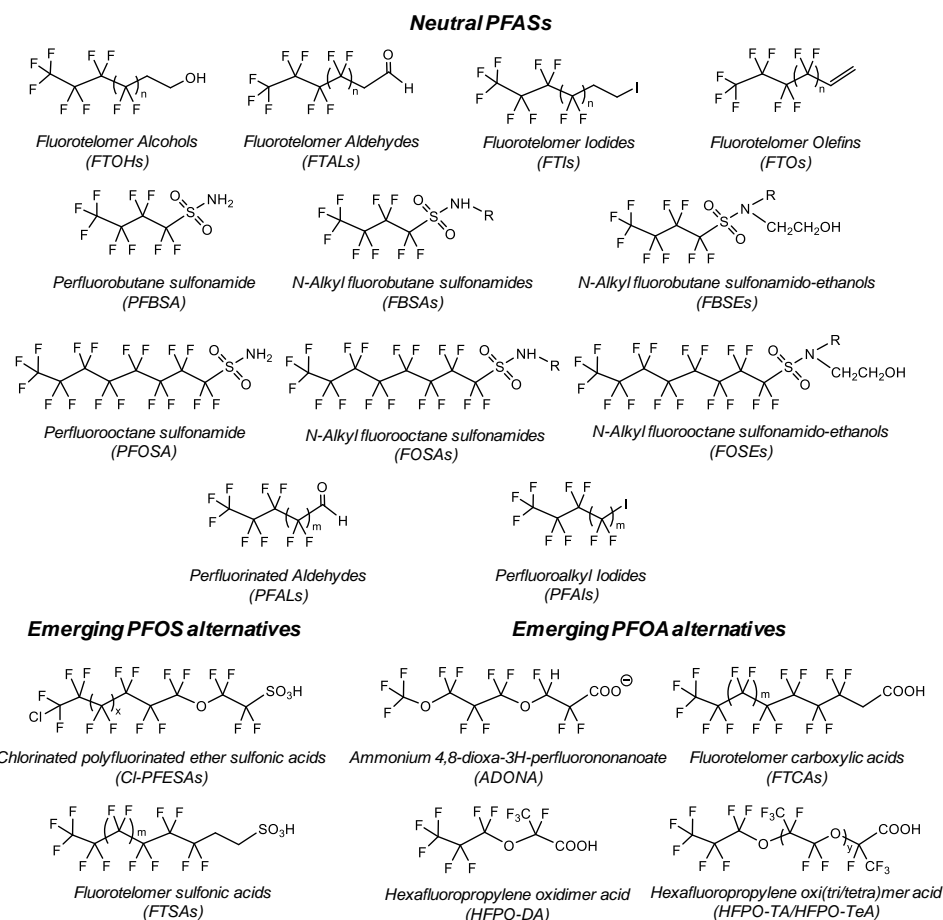

Fig. 1.4. Neutral PFAS and emerging alternatives to PFOS and PFOA.

9

Neutral PFAS have been suggested to be precursors of persistent ionic PFAS, becoming a global problem as they contribute to increasing the basal levels of these POPs in the environment. Additionally, as neutral PFAS are eventually biotransformed in the environment or atmospherically degraded to partly form final breakdown products like PFSAs and PFCAs, Jahnke *et al.* [11] proposed the environmental fates of PFAS as shown in Fig. 1.5.

Fig. 1.5. Environmental fates of ionic PFAS from neutral PFAS [11]. (*FBSAs: N-alkyl fluorobutane sulfonamides, FBSEs: N-alkyl fluorobutane sulfonamido-ethanols, FOSAs: N-alkyl fluorooctane sulfonamides, FOSEs: N-alkyl fluorooctane sulfonamido-ethanols, FTALs: fluorotelomer aldehydes, FTCAs: fluorotelomer carboxylic acids, FTOs: fluorotelomer olefins, FTOHs: fluorotelomer alcohols, FTSAs: fluorotelomer sulfonic acids, FTUCAs: fluorotelomer unsaturated carboxylates, PFALs: perfluorinated aldehydes, PFBSA: perfluorobutane sulfonamide, PFCAs, perfluoroalkyl carboxylic acids, PFOSA: perfluorooctane sulfonamide, PFOSi: perfluorooctane sulfinate, PFSAs: perfluoro-alkane sulfonic acids*).

Other emerging PFAS have recently been identified, increasing the concern about these chemicals as they have been suggested as substitutes to PFOS and PFOA (Fig. 1.4). The use of polyfluoroalkyl ether sulfonic acids (PFESAs) has been introduced in the electroplating industry instead of PFOS [12], whereas polyfluoroalkyl ether carboxylic acids (PFECAs) have replaced PFOA in high-performance materials such as processing aids [13]. Regarding PFOS alternatives, chlorinated polyfluoroalkyl ether sulfonic acids (Cl-PFESAs) were firstly identified by Wang *et al*. [14] through the discovery of 6:2 Cl-PFESA, also known as F-53B, in wastewater. Since then, the occurrence of F-53B has not only been reported in environmental matrices like sewage sludge [15] but also in living organisms [16,17] and human beings [18,19]. Fluorotelomer sulfonic acid (FTSAs), mainly 6:2 FTSA, have also been proposed as PFOS alternatives [20,21] in the surface treatment of metal and plastic components in the emulsion polymerization of fluoropolymers [22,23]. Concerning PFOA alternatives, they mainly include hexafluoropropylene oxide dimer acid (HFPO-DA), HFPO trimer acid (HPFO-TA), HFPO tetramer acid (HFPO-TeA) and ammonium 4,8-dioxa-3H-perfluorononanoate (ADONA). The presence of these compounds has been reported in surface waters [13] and plasma samples in the case of ADONA [24]. Among them, HFPO-DA has been identified in

surface waters [25] and its ammonium salt, commercially known as GenX, is widely used as an alternative to the legacy PFAS [26]. Additionally, another kind of novel fluorinated substitutes to PFOA are the fluorotelomer carboxylic acids (FTCAs), being 6:2 FTCA the chemical most widely used in China [27,28].

The increasing threat of halogenated organic contaminants (POPs and new emerging contaminants) to the environment makes necessary to go deeper into their accurate and sensitive analysis to monitor their distribution and fates in the environment even at low concentration levels. Therefore, this Thesis is mainly focused on some families of these pollutants that have aroused great interest in the scientific community, but also show some significant drawbacks in their analytical determination. The families of halogenated compounds studied in this Thesis are presented in Table 1.2.

Table 1.2. Families of halogenated organic contaminants included in this Thesis

Family of compound	Subgroup
POPs	
Chlorinated paraffins (CPs)	Short-chain chlorinated paraffins (SCCPs)
Polychlorinated biphenyls (PCBs)	Dioxin-like polychlorinated biphenyls (dl-PCBs)
Polychlorinated dibenzo-p-dioxins (PCDDs)	
Polychlorinated dibenzofurans (PCDFs)	
Polychlorinated naphthalenes (PCNs)	
Candidate POPs	
Dechlorane Plus (DP) and analogs	*Anti*-Dechlorane Plus (Anti-DP)
	Syn-Dechlorane Plus (Syn-DP)
	Dechlorane 602 (Dec-602)
	Dechlorane 603 (Dec-603)
	Dechlorane 604 (Dec-604)
	Cl_{10}-Dechlorinated Dechlorane Plus (Cl_{10}-DP)
	Cl_{11}-Dechlorinated Dechlorane Plus (Cl_{11}-DP)
Emerging halogenated organic contaminants	
Neutral per- and polyfluoroalkyl substances (nPFAS)	Fluorotelomer alcohols (FTOHs)
	Fluorotelomer olefins (FTOs)
	N-Alkyl fluorooctane sulfonamides (FOSAs)
	N-Alkyl fluorooctane sulfonamido-ethanols (FOSEs)

1.1.1. Toxicology

Due to the physicochemical characteristics and properties of these families of contaminants, most of them are considered POPs. These compounds often show high resistance to biodegradation and a high tendency to be accumulated and biomagnified through the food chain. Besides that, toxicologic studies reported that their presence in the living organisms is particularly harmful due to the high toxicity observed for some of these compounds. Among them, the toxicity of POPs such as 2,3,7,8-PCDD/Fs and dioxin-like PCBs is well-known, and it has been extensively reported [29]. In addition to these compounds, the scientific community has denoted as dioxin-like compounds those POPs like some PCNs that show similar toxicology properties and similar biochemical and toxic responses in testing animals. The planar structure of these POPs may help them to permeate through the cell membrane and achieve the cytoplasm, where they have a similar behavior than some hormones (endocrine disruptors). The high toxic effects are mainly due to the interaction with the aryl hydrocarbon receptor [30–33]. Briefly, this cytosolic protein receptor generates a complex with the dioxin-like compound that then dimerizes and, therefore, migrates to the cell nucleus. There, it can be associated with a transfer ribonucleic acid, causing changes in the deoxyribonucleic acid. Consequently, these changes affect the production of enzymes, like cytochrome P450, that induce cytochrome-dependent enzymatic activities that may produce the genotoxic estradiol hormone, among others. Moreover, these pollutants can also modify the action of the aryl hydrocarbon receptor over the intracellular signal transduction and transmission, causing skin and liver alterations. For instance, one of the best-known skin alterations induced by dioxin-like compounds is the dermatological response of chloracne. These alterations and the endocrinological effects could be related to their carcinogenic effects.

Some of these POPs, such as 2,3,7,8- tetraclorodibenzo-*p*-dioxin (2,3,7,8-TCDD), 2,3,4,7,8-pentaclorodibenzo-*p*-dioxin (2,3,4,7,8-PeCDF), and dl-PCBs, have been included in the list of carcinogenic to humans by the International Agency of Research on Cancer (IARC) while more evidence is still required for other PCDD/Fs as well as PCNs. The toxicity of dioxin-like compounds differs between families and depends on the number of chlorine atoms. Only 17 compounds (2,3,7,8-chloro-substituted dibenzo-*p*-dioxins and dibenzofurans) of the 210 PCDD/Fs, as well as non-ortho and mono-ortho PCBs, have shown this high toxicity. The toxicological studies concluded that the 2,3,7,8-TCDD shows the highest toxicity among them, although nowadays 1,2,3,7,8-PeCDD has denoted the same toxicity. Taking into account the interest of the toxicity supported by each congener in environmental samples, the Ontario Ministry of the Environment (Canada) proposed for the first time the use of the toxic equivalency factor (TEF) for 2,3,7,8-PCDD/Fs in 1984 [34]. This term considers the following testing facts: (i) all 2,3,7,8-PCDD/Fs have the same action mechanism with the aryl hydrocarbon receptor, although the potential toxicity may differ between *congeners,* and (ii) the mixture of these compounds produces an additive effect on the total toxic response. Thereby, the toxicological potential of each congener is measured as the toxic equivalency

factor, which is a relative value to the most toxic 2,3,7,8-TCDD (TEF = 1). Thus, the toxic equivalent (TEQ) of a real sample can be determined as the sum of the concentration of each congener multiplied by the TEF value.

$$TEQ = \sum (TEF_i \cdot [\text{dioxin-like compound}]_i)$$

Table 1.3 summarizes the TEF values assigned to each dioxin-like compound over the years and organizations, such as international TEFs (I-TEF) established by the North Atlantic Treaty Organization (NATO) or the present World Health Organization TEFs (WHO-TEF), which already includes dioxin-like PCBs.

Table 1.3. Toxic equivalency factors proposed by the NATO and WHO organizations.

Group	Congener	I-TEF (*1988*)	WHO-TEF (*1998*)	WHO-TEF (*2005*)
PCDDs	2,3,7,8-TCDD	1	1	1
	1,2,3,7,8-PeCDD	0.5	1	1
	1,2,3,4,7,8-HxCDD	0.1	0.1	0.1
	1,2,3,6,7,8-HxCDD	0.1	0.1	0.1
	1,2,3,7,8,9-HxCDD	0.1	0.1	0.1
	1,2,3,4,6,7,8-HpCDD	0.01	0.01	0.001
	OCDD	0.001	0.0001	0.0003
PCDFs	2,3,7,8-TCDF	0.1	0.1	0.1
	1,2,3,7,8-PeCDF	0.05	0.05	0.03
	2,3,4,7,8-PeCDF	0.5	0.5	0.3
	1,2,3,4,7,8-HxCDF	0.1	0.1	0.1
	1,2,3,6,7,8-HxCDF	0.1	0.1	0.1
	1,2,3,7,8,9-HxCDF	0.1	0.1	0.1
	2,3,4,6,7,8-HxCDF	0.1	0.1	0.1
	1,2,3,4,6,7,8-HpCDF	0.01	0.01	0.01
	1,2,3,4,7,8,9-HpCDF	0.01	0.01	0.01
	OCDF	0.001	0.0001	0.0003
dl-PCBs	3,3',4,4'-TCB (CB-77)[a]	-	0.0001	0.0001
	3,4',4,5-TCB (CB-81)[a]	-	0.0001	0.0003
	2,3,3',4,4'-PeCB (CB-105)[b]	-	0.0001	0.00003
	2,3,4,4',5-PeCB (CB-114)[b]	-	0.0005	0.00003
	2,3',4,4',5-PeCB (CB-118)[b]	-	0.0001	0.00003
	2',3,4,4',5-PeCB (CB-123)[b]	-	0.0001	0.00003
	3,3',4,4',5-PeCB (CB-126)[a]	-	0.1	0.01
	2,3,3',4,4',5-HxCB (CB-156)[b]	-	0.0005	0.00003
	2,3,3',4,4',5'-HxCB (CB-157)[b]	-	0.0005	0.00003
	2,3',4,4',5,5'-HxCB (CB-167)[b]	-	0.00001	0.00003
	3,3',4,4',5,5'-HxCB (CB-169)[a]	-	0.01	0.03
	2,3,3',4,4',5,5'-HpCB (CB-189)[b]	-	0.0001	0.00003

[a] Non-ortho PCB; [b] Mono-ortho PCB.

In 1988, the NATO reported the I-TEF values for PCDD/Fs based on the evaluation of the *in vitro* and *in vivo* toxicity data as well as the current TEF practices of several countries [35]. These values are still applied to determine the TEQ in emissions from landfills, waste incinerator plants, etc. After that, an expert committee organized by the WHO revised the I-TEF values using experimental data on the relative effect potencies (RPs) of PCDD/Fs and also dl-PCBs for mammalian, avian, and fish species [36]. In 2005, WHO-TEF values for humans and mammalians were re-evaluated [37] and, today, they are commonly used to determine the WHO-TEQ in biological and food samples, although they have also been applied to abiotic environmental matrices. In this last revision, Van den Berg *et al.* [37] indicated that different families of pollutants like PCNs might be considered for possible inclusion in the TEF scheme since they also induce dioxin-like effects. Other arguments supporting this claim are that several PCNs have similar aryl hydrocarbon receptor activities to PCDD/Fs but less potent [38–40]. Moreover, they show a chemical structural relationship to PCDD/Fs while showing persistence and a tendency to bioaccumulate through the food chain, fulfilling all the criteria for their inclusion in the TEF concept. Although some RP values have been determined for some PCN congeners, there are no unification criteria to establish common TEF values for PCNs. Recently, Suzuki *et al.* [41] have reported RP values for PCNs showing dioxin-like toxicity using the same analytical approach. Authors concluded that some PCNs, especially some PeCN and HxCN congeners, have an aryl hydrocarbon receptor-mediated activity comparable with that of PCDD/Fs. This could be the first step to include dioxin-like PCNs into the TEF concept.

Another family of halogenated pollutants that has been thoroughly evaluated is the short-chain chlorinated paraffins (SCCPs) not only by the research community but also by different institutions. For instance, IARC classified them as possibly carcinogenic to humans (group 2B) in 1990 based on different studies reporting morphological changes in liver, kidney and thyroid hormone systems that were later correlated with the growth of tumors (carcinomas and adenomas) [42,43]. The liver damage is associated with peroxisome proliferation, while the thyroids effects are correlated to altered thyroid hormone status and glucoronyl transferase induction [44]. One of the most recent assessments of the EU concluded that the potential toxicological effects of SCCPs in mammals on the organs and hormonal systems reported are those causing hepatic enzyme induction and thyroid hyperactivity, which can cause cancer diseases in these organs in the long term [45]. SCCPs are also listed as endocrine disruptors of category 1 human health by the EU [46]. In addition to EU considerations, the National Toxicology Program (NTP) of the U.S. Department of Health and Human Services also classified in 2014 (13th report on carcinogens) SCCPs as reasonably anticipated to be human carcinogens [47].

Concerning the toxicity of neutral PFAS (FTOs, FTOHs, FOSAs, and FOSEs), the available data is limited. For instance, some studies conducted in rats found that 6:2 FTOH (*where 6 and 2 are the number of CF$_2$- and CH$_2$- units in the fluoroalkyl chain*) was slightly toxic by oral (LD$_{50}$ = 1750 mg kg^{-1}) and dermal (LD$_{50}$ > 5000 mg kg^{-1}) exposure. However, an increment in

mortality was observed when administering oral doses of 125 mg kg^{-1} per day [48,49]. Different studies also denoted the proliferation of thyroid follicular cell adenomas as well as an increase in stillbirths and neonatal mortality in rats exposed to *N*-EtFOSE [50]. Although neutral PFAS do not show strong toxicity, their degradation to legacy PFAS like PFOS or PFOA has focused most of the toxicological studies [51]. For instance, PFOA is classified as possibly carcinogenic to humans (group 2B) by the IARC as well as carcinogenic (group 2) and affecting reproducibility (group 1B) by the EU Regulation No. 944/2013 [52]. Moreover, both PFOS and PFOA have been classified as suggestive carcinogens by the U. S. Environmental Protection Agency (U.S. EPA). The risk profile reported by the UNEP (Stockholm Convention) concluded that PFOA also produces adverse health effects such as high cholesterol levels, altered reproductive and developmental effects, endocrine disruption, or immunotoxicity, among others [53]. In the case of PFOS, it has shown toxicity towards mammals in sub-chronic repeated dose studies at low concentrations as well as altered reproductive effects, increasing the mortality of rat pups [54].

Regarding Dechlorane Plus (DP) and analogs, toxicological information is still quite limited and most of the studies are focused on the effects of the exposure to these compounds. Oxidative stress after exposure to DP has been reported in different organisms, such as marine bivalves [55], fishes [56–58], earthworms [59], birds [60] and mice [61]. For instance, studies about short-time exposure of zebrafish to DP suggest that this compound can induce oxidative stress and neurobehavioral changes that may be linked to axonal and muscular lesions [56,58]. Similar effects were observed for earthworm with longer time exposures [59]. According to available assessments, studies with mammals indicated DP is not carcinogenic, mutagenic, or toxic to reproduction [62,63]. However, other effects have been reported in mammals. Generally, oral exposure to DP isomers can lead to oxidative stress and hepatic damages as well as alternations on the metabolism or in the transduction signal in mice [61]. Also, DP isomers show to be preferentially accumulated in the liver with *syn*-DP as the dominating isomer [64]. Additionally, some indication of endocrine disruption potential of DP has also been observed. For instance, Kang *et al.* observed transcriptional responses of both thyroid and sex hormone-related genes in the adult zebrafish brain [57]. A relation between thyroid hormone and DP levels was also reported in human mother-infant pairs near an e-waste recycling area in China [65]. Moreover, some studies show that DP can cross the blood-brain barrier in fish [66] and frogs [67], and it is maternally transferred to offspring in several species such as fishes [66], frogs [68], birds [69], female sharks [70] an even in humans [65,71]. This DP transference *in utero* generates a risk for embryonic development and may constitute the largest source of flame-retardant input to offspring during the first years of life.

1.1.2. Legislation

The toxicity potential of halogenated organic contaminants, as well as the physicochemical properties of halogenated POPs, has brought authorities to take measures to protect human health and the environment through international agreements leading to international and national regulations. The Aarhus Protocol (1998) was one of the first international agreements about POPs to promote the monitoring, reduction, and/or elimination of 16 selected substances including eleven pesticides, two industrial contaminants and three unintentional industrial by-products (including PCDD/Fs and PCBs) [72]. This protocol included different actions to eliminate any discharges, emissions, and residues of POPs, as well as measures to reduce the emission of unintentional by-products, suggesting for the first-time emission limit values (ELV) for the incineration of municipal (0.1 ng TEQ Nm^{-3}), hazardous (0.2 ng TEQ Nm^{-3}) and medical waste (0.5 ng TEQ Nm^{-3}). Some years later, the Stockholm Convention on POPs adopted these measures, under the auspices of the UNEP. Building on the Aarhus Protocol, the Stockholm Convention raised the profile of POPs to the global level. In 2009, the Aarhus Protocol was amended to cover other seven new substances (PFOS, PCNs, and SCCPs, among them) and revised the ELVs for waste incineration. The Parties of the Stockholm Convention also adopted decisions to update guidance on the BAT to control emissions of POPs (Annex V) and turn part of them into a guidance document (Annex VII) [73]. Besides, Parties introduced flexibilities regarding the time frames for the application of the ELVs and BAT to facilitate the ratification of the Protocol by countries with economies in transition in Eastern Europe, Caucasus, and Central Asia. The amended annexes entered into force for most of the Parties in 2010, whereas the remained annexes still require ratification of at least two-thirds of the Parties.

According to the considerations denoted by the Aarhus Protocol, the Stockholm Convention, as well as other programs all over the world, international institutions have established different legislations to regulate the presence of these compounds in the environment as well as in other relevant fields such as food and commercial products. Thus, in May of 2004, the EU 850/2004 regulation entered into force with the main objective of establishing a common legal framework for both the Stockholm Convention and Aarhus Protocol [74]. The regulation reported the mandatory elaboration of national plans, including different actions like the creation of emission inventories of unintentional industrial by-products to the atmosphere, water, and soils. After that, this regulation has been updated to include all substances considered as POPs by the Stockholm Convention and exceptional uses for some of them (e.g., PFOS, PCBs, or SCCPs) [75]. Moreover, this regulation also established maximum concentration limits of POPs in generated waste residues ranging from 5 mg kg^{-1} for PCDD/Fs up to 10,000 mg kg^{-1} for SCCPs. Some specific directives have been reported for the elimination of some POPs like PCBs [76]. Additionally, all POPs have been categorized as substances of very high concern (DP is under evaluation) in the Registration, Evaluation, Authorization, and Restriction of Chemicals (REACH) regulation of the European Chemical

Agency (ECHA). All these actions have led to the EU Regulation 166/2006, where different thresholds were set for releases of pollutants such as SCCPs (1 kg year^{-1}) to water and land, as well as for PCDD/Fs (0.0001 kg TEQ year^{-1}) and PCBs (0.1 kg year^{-1}) to air, water and land. In the case of those pollutants that are not individually regulated, it was also considered releases of halogenated pollutants to water and soil (1,000 kg year^{-1}, expressed as Cl^{-}) [77]. The Spanish national pollutant and transfer register (E-PRTR), according to *Real Decreto* 508/2007 [78], is based on this EU regulation.

After that, different directives have been entered into force to regulate both emissions to the environment and quality control of the natural resources. Regarding industrial emissions, the Directive 2010/75/EU of the European Parliament involves all the European legislation about the emissions of big combustion industrial facilities [79]. This regulation force operators to invest the best available technologies and obey the ELVs to obtain production rights. These average ELVs for PCDD/Fs were fixed at 0.1 ng TEQ Nm^{-3} over a sampling period of 6 to 8 hours.

Concerning water sources, the Directive 2013/39/EU of the European Parliament on environmental quality standards (EQS) in the field of water policy reported annual average (AA) and maximum allowable concentrations (MAC) for a list of priority substances and other specific pollutants [80]. The values concerning the target and related compounds evaluated in this Thesis are summarized in Table 1.4. For instance, SCCPs and PFOS are regulated in inland surface waters (rivers, lakes, and related artificial or heavily modified water bodies) as well as in other surface waters (transitional and coastal waters, among others). Additionally, some of these compounds are also regulated in biota samples with very restrictive EQS values (expressed as µg kg^{-1} wet weight, ww), especially for dioxin-like compounds (including PCDD/Fs and dl-PCBs). These EU considerations have also been transferred to the Spanish national *Real Decreto 817/2015* [81].

Table 1.4. Environmental quality standards for selected priority substances in water and biota.

Name of substance	Inland surface waters (µg L^{-1})		Other surface waters (µg L^{-1})		Biota (µg kg^{-1} ww)
	AA-EQS	MAC-EQS	AA-EQS	MAC-EQS	EQS
SCCPs	0.4	0.4	1.4	1.4	-
PFOS	6.5 10^{-4}	1.3 · 10^{-4}	36	7.2	9.1
Dioxin-like compounds	-	-	n.a.[a]	n.a.[a]	0.0065[b]

[a] Not applicable; [b] Sum of PCDD/Fs and dl-PCBs (µg TEQ kg^{-1}).

About drinking water, the Directive 98/83/EC [82] and its latest amendments, including Directive 2015/1787/EU [83], established the quality criteria for water intended for human consumption. Most of the compounds studied in this Thesis are not considered to be present in drinking water. Nevertheless, in the last years, the European citizens' *Right2Water* initiative

has triggered a proposal to modernize the 20-years old directive on drinking water (98/83/EC). Thus, the General Secretariat of the Council published on the 24th of February of 2020 a proposal for a new drinking water directive [84] that update the requirements to guarantee the safety of drinking water. Among the compounds included in this new directive, PFAS has been considered for the first time, establishing maximum levels of 0.1 µg L^{-1} for the sum of 20 legacy PFAS (including PFOA and PFOS and others) and 0.5 µg L^{-1} for the total PFAS concentration (including neutral PFAS). The U.S. EPA has also considered monitoring these pollutants in drinking water through the third Unregulated Contaminant Monitoring Rule 3 published in 2012 [85]. The data obtained serves as a primary source of occurrence and exposure with the intent of being used on the development of regulatory decisions. Meanwhile, a health advisory concentration level of 70 ng L^{-1} has already been proposed for the sum of PFOA and PFOS [86]. In the case of Spanish legislation, the latest update (1st of August of 2018) of *Real Decreto* 140/2003 does not include any information about PFAS yet [87].

In the case of soil samples, information is lacking on the regulation of the contaminants evaluated in this Thesis. The *Real Decreto* 9/2005 (updated in November 2017) includes a list of pollutants and maximum reference levels, based on the use of the soils, which are required to protect human health [88]. For instance, reference levels for PCBs in soils have been established for industrial (0.8 mg kg^{-1} dry weight, dw), urban (0.08 mg kg^{-1} dw) and other soil uses (0.01 mg kg^{-1} dw), being considered a contaminated soil if the concentration found exceeds more than 100 times these reference levels.

The European Food Safety Authority (EFSA) has also thoroughly studied the effect of halogenated organic contaminants in foodstuffs, establishing tolerable weekly intake (TWI) for some of these compounds. For instance, the TWI that EFSA fixed for PCDD/Fs and dl-PCBs was 2 pg TEQ kg^{-1} body weight (bw) $week^{-1}$ [89]. The detection of these compounds in food samples has created great concern in the food field during the last decades, which has led to their inclusion in the EU 1881/2006 regulation (last update: 28th of November of 2019) [90]. This regulation has set maximum concentration levels in fish and meat products (2.00-20 pg TEQ g^{-1} ww), oils and fats (1.25-6.0 pg TEQ g^{-1} fat), eggs and dairy products (5.0-5.5 pg TEQ g^{-1} fat) as well as in baby and toddler foods (0.2 pg TEQ g^{-1} ww). Nowadays, EFSA has set working groups to determine the risk profile of different families of halogenated pollutants such as PFAS, SCCPs, as well as other brominated flame retardants. Regarding PFAS, EFSA has already established a TWI of 8 ng kg^{-1} bw $week^{-1}$ for the total PFAS content (including FTOHs, FOSAs, and FOSEs) according to new data on the risk assessment to human health in food [91]. Concerning CPs, the EFSA Panel selected a benchmark dose lower bound with a 10% increased incidence ($BMDL_{10}$) of 2.3 mg kg^{-1} bw day^{-1} for an increased incidence of nephritis in male rats due to their exposure to SCCPs, and of 36 mg kg^{-1} bw day^{-1} for the increased relative kidney weights in male and female rats from exposure to medium-chain chlorinated paraffins (MCCPs) [92]. Further interpretation of mammal and human risk exposure may require more data to perform a robust and thorough exposure assessment and risk characterization. Due to the growing importance of these halogenated

pollutants, the European Union Reference Laboratory (EURL) network has extended the scope from PCBs and PCDD/Fs to halogenated POPs (including PFAS, SCCPs, and PCNs) to provide reliable analytical methodologies and ensure both feed and food safety [93].

Finally, regulations about DP are still scarce since these compounds have recently been proposed as a candidate to be included on the POP list of the Stockholm Convention. For instance, U.S. EPA has taken some preventive actions like listed them in the Toxic Substances Control Act inventory and subjecting them to the Chemical Data Reporting Rule, which requires manufacturers and importers to report their production, import, and use volumes. Moreover, the Government of Canada, under the Canada Environmental Protection Act (CEPA), included DP in the Domestic Substances List that regulates its use in plastic materials and where its content cannot exceed 35% (*w/w*). Recently, DP has also been included in the List of Toxic Substances and further actions are expected after a risk evaluation [63].

1.2. Analytical Determination of Halogenated Organic Contaminants

The determination of halogenated organic contaminants in environmental samples is the first step to monitor and know their distribution and fates in the environment. These contaminants are generally found at ultra-trace level concentrations, which is enough to produce harmful effects in both the environment and living organisms. Therefore, sensitive and selective methods are needed to achieve accurate and precise detection/identification and quantitation of these analytes in environmental matrices. In this way, thousands of publications based on the analytical determination of these compounds have appeared during the last decades proposing reliable methodologies to monitor their occurrence and ensure the quality of the reported results.

This section will provide a broad overview of the main advances in the analytical methodologies for halogenated organic contaminants, in terms of sample treatment, chromatographic separation and mass spectrometry determination (*Section 1.2.1*) as well as the latest trends on the use of atmospheric pressure ionization (API) techniques for both liquid chromatography (LC-MS) and gas chromatography coupled to mass spectrometry (GC-MS) determinations (*Section 1.2.2*).

1.2.1. Trends in Analytical methodologies

As mentioned above (*Section 1.1.2*), the evaluation of the risk profile of these pollutants has enabled many governments to legislate them setting restrictions or even banning their production and use. Hence, reliable information about the environmental occurrence of these compounds is required to help on the investigation of their distribution, environmental fates, spatial and temporal trends as well as potential sources of release. Moreover, these chemicals are hazardous even at extremely low concentration levels, so powerful analytical methodologies are required to ensure their reliable monitoring in the environment at very low concentration levels. These methodologies need to meet some requirements, such as the high capacity for the detection/identification of pollutants at ultra-trace levels and high selectivity to avoid potential interferences. Authorities, like the U.S. EPA, the European Committee for Standardization (CEN), or the Japanese Industrial Standards Committee (JISC), have proposed comprehensive analytical protocols for monitoring these compounds. However, the requirements to be met by the analytical protocols for the reliable determination of these compounds in environmental samples leads to the development of many analytical methodologies, which is continuously increasing. This section provides an overview of the most relevant advances in analytical methodologies of halogenated organic contaminants. In addition to the main group of compounds of interest studied in this Thesis (Table 1.2.), other relevant pollutants such HBCD and polybrominated diphenyl ethers (PBDEs) have also been included to provide a more representative overview of methodology trends for halogenated contaminants. Therefore, advances in sample treatment protocols, chromatographic separations, and mass spectrometry (MS) determinations/identifications are discussed based on the most relevant papers published in the last decades for these families of compounds.

Sample treatment

Sample treatment is a critical step in determining halogenated organic contaminants that involves isolation of these compounds from potential matrix interferences or structurally similar compounds, as well as preconcentration of extracts to allow the detection of these pollutants at low concentration levels in environmental samples. Generally, sample treatment procedures for the analysis of these substances in environmental samples are extensive, laborious, and they are usually subjected to strict quality control protocols. For these reasons, surrogates standards (internal standards and isotopically labeled compounds) are frequently added before the extraction for establishing the recovery rate and allowing the reliable quantification of the target compounds.

Regarding the extraction, clean-up, and fractionation procedures, many protocols have been proposed to analyze halogenated pollutants in different environmental matrices. The most representative sample treatment protocols used in this field for the analysis of liquid, solid, and gas matrices are summarized in Fig. 1.6. Concerning liquid samples (e.g., surface water, river water, wastewater, etc.), liquid-liquid extraction (LLE) or solid-phase extraction (SPE) are

usually selected for the extraction of these compounds. Dichloromethane has often been proposed for the LLE of DPs, PBDEs and dioxin-like PCBs from environmental water samples [94,95], while methyl tert-butyl ether, hexane or ethyl acetate have also been used to extract FTOHs [96], PBDEs [97], and PCNs [98], respectively. Regarding SPE, Oasis HLB [99], and Oasis WAX [100] cartridges are often used to extract neutral PFAS that are later eluted with methanol. However, for the extraction of flame retardants such as HBCD and PBDEs, as well as other compounds with dioxin-like toxicity such as PCBs and PCNs, the use of C_{18} cartridges with hexane-based mixtures as elution solvent is generally recommended [101,102].
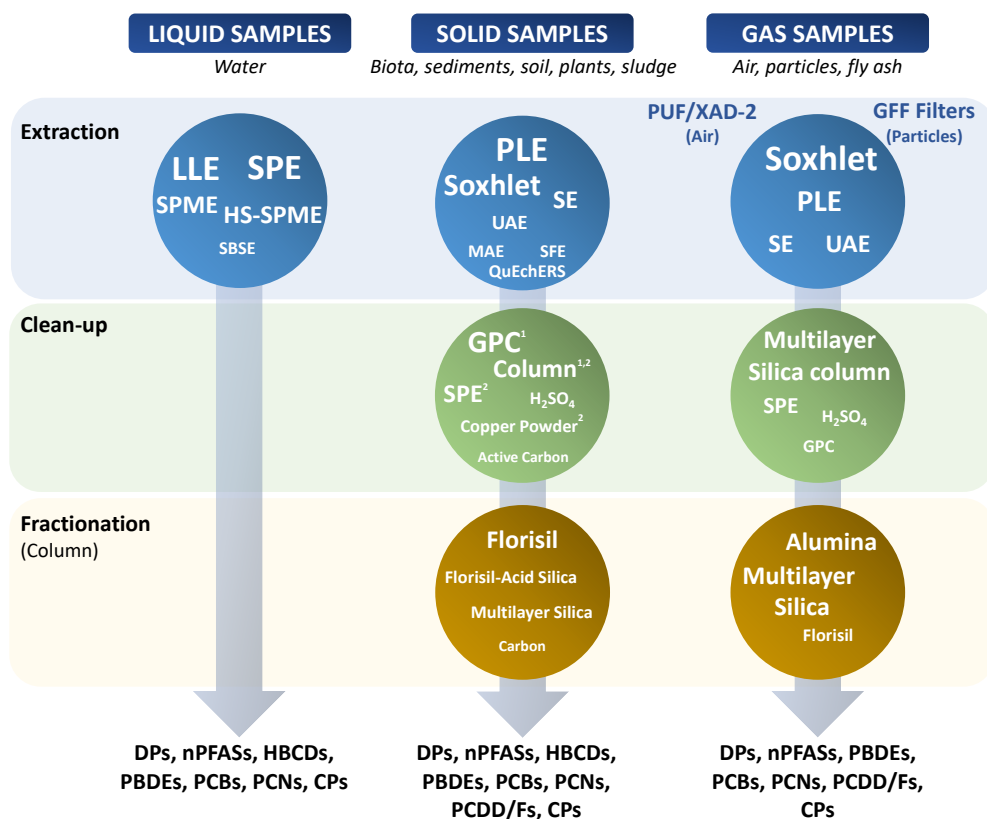
Fig 1.6. Main sample treatments proposed for the determination of halogenated organic contaminants in environmental samples (*[1]Biota samples; [2]Sediment, soil, plant, and sludge samples*).

Recovery rates that have been reported using these procedures are higher than 70% for most of the compounds [94,95,98,101,103], although for most volatile compounds, such as neutral PFAS, these values seem to be lower. Taniyasu *et al.* [100] indicated that the low recoveries (35-55%) achieved with these compounds sometimes are associated to other factors that are not related to the cartridge nature, such as the adsorption of the analytes on the polypropylene container as well as the losses of more volatile FTOHs during the evaporation of the solvent extracts. In the last decade, the use of rapid, inexpensive, and solvent-free alternative

extraction techniques has been increased to improve recoveries and to avoid excessive sample manipulation. For instance, headspace solid-phase microextraction (HS-SPME) has been used for the analysis of neutral PFAS (FTOHs and FOSAS). Direct immersion SPME has also been proposed for the determination of SCCPs, PBDEs, and PCBs in water, while stir bar sorptive extraction (SBSE) has been used for the analysis of SCCPs [104–107]. All these extraction techniques allow *in-situ* preconcentration of analytes and avoid evaporation steps that could yield losses of the most volatile compounds.

On the other hand, pressurized liquid extraction (PLE) [108–113] and Soxhlet extraction [94,114–116] with dichloromethane or dichloromethane/hexane mixtures as solvents are the most widely used methods for extracting halogenated organic contaminants from solid matrices. For instance, DP and their analogs have been extracted from sediments using both Soxhlet extraction [114] and PLE [108]. Soxhlet extraction has also been proposed for the extraction of PCBs, PCNs, and SCCPs from sediments [117] and PBDEs from sewage sludge [95], while PLE has also been proposed to extract PBDEs, HBCDs and PCDD/Fs from sewage sludges and sediments. In some cases, the use of adsorbents such as alumina [118] or mixtures of silica, alumina, and Florisil [109] allows a more selective PLE extraction, which can simplify further clean-up steps. Besides, other extraction techniques avoiding the use of specific and sophisticated instrumentation have also been successfully applied to extract these compounds from solid matrices. For instance, solvent extraction (SE) has been used to extract neutral PFAS from sediments and biota samples [119,120] and PBDEs, PCDD/Fs, and PCBs from fatty fish tissues [121]. Ultrasound-assisted extraction (UAE) has also been proposed to extract DPs, HBCDs, PBDEs, and PCBs from marine sediments [101,122]. Additionally, microwave-assisted extraction (MAE) has been used to extract PBDEs and PCBs from sediments [123], while the QuEchERS (Quick, Easy, Cheap, Effective, Rugged, and Safe) technique has also been satisfactorily applied to extract HBCD from fish [124]. The analysis of samples with high lipid content requires the use of multilayer sorbents, generally, silica or acidic silica columns, to remove lipids (through hydrolysis) and hydrocarbons [112,125], as well as to fractionate the extracts for the isolation of the different families of contaminants. For instance, a multi-layer silica gel column has been used to remove hydrocarbons and to isolate HBCDs from related halogenated compounds when analyzing sediments [112]. Direct sample treatment with concentrated H_2SO_4 has also been considered for the same purpose in the determination of PBDEs, DP and analogs in biota and sludge samples [108,115,126]. For biota samples, gel permeation chromatography (GPC) is often recommended, as permeation gels such as porous styrene-divinylbenzene resin (Bio-beads S-X3) allow for more efficient removal of lipids through size exclusion chromatography [111,113,115,116,121,122,127]. Moreover, GPC could be automated, offering an important advantage for laboratory throughput. On the other hand, SPE adsorbents such as silica, wax, Florisil, or alumina cartridges have also been recommended to remove matrix components that interfere in the analysis of sediments and sludges [110,114,120,126]. Additionally, the presence of high sulfur content from sediments samples requires the use of activated copper powder, which also avoids chromatographic

baseline distortions [122]. The fractionation of extracts to separate different groups of compounds is usually followed by sample clean-up. Florisil and sometimes combined with acidic silica are the adsorbents most commonly used. For the fractionation, solvent mixtures with high hexane content are used to elute DP and analogs, HBCDs, PBDEs, and PCBs from these sorbents. In contrast, solvent mixtures with a higher content of dichloromethane or toluene are recommended to favor the elution of CPs, PCDD/Fs, and PCNs. Additionally, carbon cartridges are usually backflushed with toluene to isolate planar compounds (PCNs, PCDD/Fs, and dioxin-like PCBs) from other related non-planar contaminants (DP, *ortho* PCBs, PBDEs or CPs, among others) [69,115,117,125].

For the analysis of gaseous samples (e.g., air), both the gas- and the particulate-phase are often collected using polyurethane foams/styrene-divinylbenzene copolymer resin (PUF/XAD-2) and glass-fiber filters (GFF), respectively. These materials are generally extracted by Soxhlet or PLE and clean-up by multilayer silica [128–130]. Regarding PCNs, dioxin like-PCBs, and PCDD/Fs, which are often determined in fly ashes, the fractionation is usually carried out on multilayer silica columns followed by alumina or Florisil ones [131,132]. It is important to highlight that with this protocol more volatile compounds such as mono- and diCNs led to low recoveries due to losses during the solvent evaporation process with a nitrogen stream. In this sense, Li *et al.* have proposed to limit evaporation steps to the use of rotary evaporation for improving the recoveries of mono- and diCN congeners [130].

Chromatographic Separation

Mass spectrometry-based analytical strategies frequently require previous efficient chromatographic separations to simplify and ensure the correct detection and quantitation of analytes present in complex samples. Among the separation techniques, the most frequently used for the analysis of these pollutants are gas chromatography (GC) and liquid chromatography (LC) [133]. However, during the last decade, some authors have also proposed the use of packed column supercritical fluid chromatography (pSFC) for the analysis of PCDD/Fs, PCBs, DPs, and HBCDs [134–136]. This section reports an overview of the separation techniques frequently employed for the determination of halogenated organic contaminants in environmental samples and Table 1.5 summarizes the most relevant references in this field.

Gas Chromatography

Gas chromatography with capillary columns is the method of choice for the separation of most of these analytes due to their relatively high volatility properties. As most of them are non-polar compounds, 5% phenyl-(95% dimethylpolysiloxane) (e.g., DB-5MS, DB-5HT, etc.) is the "gold standard" stationary phases that generally provides good chromatographic resolution for these families of compounds. However, other columns have also been proposed for the determination of specific families of halogenated contaminants. Regarding neutral PFAS, poly(ethylene glycol)-based stationary phases are commonly chosen to achieve the separation

of semi-volatile neutral PFAS (FTOHs, PFOSA, FBSAs, FOSAs FBSEs, and FOSEs) [99,137]. Concerning HBCDs, 100% dimethylpolysiloxane as well as 5% phenyl-(95% dimethylpolysiloxane) stationary phases, are typically selected for their gas chromatography separation. Nevertheless, GC-based methods are generally focused on the determination of the total concentration of the 16 potential HBCDs (six enantiomers and diastereomeric pairs). This is because the GC separation of HBCD isomers is not well resolved and the interconversion between isomers generally occurs in the GC injector system or the ionization source because of the high temperatures applied [138]. Regarding the capillary column length, the separation of dioxin-like compounds (PCDD/Fs, dioxin like-PCBs, and PCNs) usually requires 60 m-capillary columns to achieve a satisfactory chromatographic separation of most representative isobaric compounds [130,134,139].

In contrast, the analysis of HBCDs, PBDEs, DP and analogs, is normally performed on 15 m-capillary columns. These short columns provide enough chromatographic resolution and significantly reduce analysis time [140–143]. Additionally, Stapleton *et al.* [144] reported that the use of longer columns could favor the degradation of highly brominated PBDEs (e.g., PBDE-209) during the GC analysis. In this sense, the 15 m-Rtx®-1614 column, which consists of a 5% phenyl-(95% dimethylpolysiloxane) stationary phase deactivated with an optimized procedure, is commonly recommended to improve the response of these thermally labile PBDEs [143]. Moreover, Rjabova *et al.* [145] also indicated some chromatographic improvement for Dec-604 using the same capillary column. Concerning CPs, even though the total separation of isobaric congener groups is not possible (more than 10,000 compounds) in these short capillary columns, they are employed to increase signal-to-noise (S/N) ratios and to reduce analysis time [146,147].

Helium is the most common carrier gas by far to achieve the separation of these substances using flow rates around 1.0 mL min^{-1}. However, it is important to highlight that when gas chromatography is coupled to mass spectrometry by using API, especially atmospheric pressure chemical ionization (APCI), relatively high flow rates (from 1.4 up to 4 mL min^{-1}) are required, probably to prevent potential post-column peak broadening in the API source. This effect could also be avoided by using nitrogen as a make-up gas at the ion source to improve the ion transmission to the mass spectrometer inlet [99,141,143,148–151]. Regarding the injection, split/splitless injector port in the splitless mode is generally preferred as most of the halogenated contaminants are found at very low levels in environmental samples. In some cases, extra pressure is applied during the splitless injection (pulsed splitless) to improve the analyte transfer to the column, especially for those compounds with high molecular weight and low vapor pressure like DP and analogs, HBCDs, MCCPs, and long-chain chlorinated paraffins (LCCPs) [140,141,146,147].

Table 1.5. Chromatographic techniques for the separation of halogenated organic contaminants.

Separation	Analyte	Stationary Phase	Mobile Phase		Injection	Ref.
HPLC	DP and analogs	Rtx Pinnacle DB Biphenyl (10 cm × 2.1 mm; 3 µm)	CH_3OH/CH_3CN-H_2O (3:1 v/v) (0.3 mL min⁻¹)	1 µL	n.r.[a]	[152]
	PCBs	XSELECT HSS T3 (10 cm × 2.1 mm; 2.5 µm)	CH_3OH/H_2O (0.1 mL min⁻¹)	5 µL	Full Loop	[94]
	PCNs	Hypersil Green PAH (10 cm × 2.1 mm; 3 µm)	(5% CH_3OH) CH_3CN/H_2O (0.08 mL min⁻¹)	5 µL	Full Loop	[98]
UHPLC	FTOHs	Acquity BEH C18 (10 cm × 2.1 mm; 1.7 µm)	CH_3OH/H_2O (0.1% HCOOH) (0.3 mL min⁻¹)	5 µL	n.r.[a]	[120]
	FOSAs, FOSEs and PFOSA	HSS T3 (10 cm × 2.1 mm; 1.8 µm)	CH_3OH/H_2O (5 mM NH₄Ac[b]) (0.3 mL min⁻¹)	10 µL	Full Loop	[153]
	HBCDs	Acquity Phenyl-Hexyl (10 cm × 2.1 mm; 1.7 µm)	$CH_3CN/CH_3OH/H_2O$ (0.3 mL min⁻¹)	1 µL	n.r.[a]	[154]
	HBCDs	Acquity BEH C18 (5 cm × 2.1 mm; 1.7 µm)	CH_3CN-CH_3OH (1:1 v/v)/H_2O (0.2 mL min⁻¹)	1 µL	n.r.[a]	[112]
	PBDEs	BEH C18 (15 cm × 2.1 mm; 1.7 µm)	CH_3OH/H_2O (0.25 mL min⁻¹)	5 µL	Partial Loop	[118]
	SCCPs, MCCPs and LCCPs	C18 Eclipse Plus (5 cm × 2.1 mm; 1.8 µm)	CH_3OH/H_2O (0.5 mM NH₄Cl) (0.2 mL min⁻¹)	5 µL	n.r.[a]	[155]
pSFC	PCDD/Fs	Torus 1-AA (10 cm × 3.0 mm; 1.7 µm)	CO_2/CH_3OH (1 mL min⁻¹)	n.r.[a]	n.r.[a]	[134]
GC	DP and analogs	DB-5MS (30 m × 0.25 mm; 0.25 µm)	He (1.0 mL min⁻¹)	1 µL	Splitless	[145]
	DP	DB-5HT (15 m × 0.25 mm; 0.1 µm)	He (1.0 mL min⁻¹)	1 µL	Pulsed Splitless	[140]
	FTOs, FTOHs, FOSAs; FOSEs, PFOSA, N-MeFBSA, N-MeFBSE	CP-Wax 57 CB (25 m × 0.25 mm; 0.2 µm)	He (1.0 mL min⁻¹)	1 µL	Splitless	[137]
	FTOHs, FOSAs and FOSEs	TG-WaxMS (30 m × 0.25 mm; 0.25 µm)	He (1.4 mL min⁻¹)	2 µL	Pulsed Splitless	[99]
	HBCDs	DB-1HT (15 m × 0.25 mm; 0.1 µm)	He (4.0 mL min⁻¹)	1 µL	Pulsed Splitless	[141]
	PBDEs	Rtx-1614 (15 m × 0.25 mm; 0.1 µm)	He or N_2 (3.0 mL min⁻¹)	1 µL	Splitless/Split	[143]
	PBDEs	DB-5HT (15 m × 0.25 mm; 0.1 µm)	He (1.0 mL min⁻¹)	10 µL	PTV[c]	[142]
	PCDD/Fs and dl-PCBs	HP-5MS (30 m × 0.25 mm; 0.25 µm)	He (1.2 mL min⁻¹)	1 µL	Splitless, PTV	[139]
		DB-5MS (60 m × 0.25 mm; 0.25 µm)	He (1.0 mL min⁻¹)	1 µL	Splitless	
	PCDD/Fs	DB-5 (60 m × 0.25 mm; 0.25 µm)	He (1.0 mL min⁻¹)	1 µL	Splitless	[134]
	PCNs	Rtx-5MS (60 m × 0.25 mm; 0.25 µm)	He (1.0 mL min⁻¹)	1 µL	Splitless	[130]
	SCCPs	DB-5 (15 m × 0.25 mm; 0.25 µm)	He (0.9 mL min⁻¹)	2 µL	Pulsed Splitless	[146]
	SCCPs and MCCPs	TG-5SilMS (15 m × 0.25 mm; 0.25 µm)	He (1.4 mL min⁻¹)	n.r.[a]	Pulsed Splitless	[147]
		HP5-MS UI (15 m × 0.25 mm; 0.25 µm)	He (1.0 mL min⁻¹)	5 µL	PTV[c]	
GCxGC	PCNs	Rt-β DEXcst (30 m × 0.25 mm; 0.25 µm) DB-WAX (2 m × 0.1 mm; 0.1 µm)	He (2.49 mL min⁻¹)	1 µL	Splitless, PTV	[156]
	PBDEs, PCBs and PCDD/Fs	InertCap-5MS/Sil (60 m × 0.25 mm; 0.1 µm) SGE BPX-50 (1.5 m × 0.1 mm; 0.1 µm)	He (488.8 kPa at 70 °C)	1 µL	Splitless	[157]
	SCCPs and MCCPs	DB-5MS (30 m × 0.25 mm; 0.25 µm) BPX-50 (1 m × 0.1 mm; 0.1 µm)	He (1.0 mL min⁻¹)	1 µL	Splitless	[111]

[a] not reported; [b] ammonium acetate; [c] solvent vent mode.

Programmed temperature vaporization (PTV) injection has also been performed showing important advantages in front of non-programmable injection modes (split and splitless). PTV injection avoids syringe discrimination and holding back of non-volatile compounds in the liner, and it allows large volume injections by removing solvent vapors before the transference of the analytes to the column head [142,147].

Comprehensive Two-dimensional Gas Chromatography

Comprehensive two-dimensional gas chromatography (GCxGC) is the most common multidimensional chromatographic separation technique used for the determination of halogenated pollutants. This technique significantly increases the peak capacity (selectivity) and the sensitivity over single-dimensional GC by connecting two columns through a modulator, which traps the compounds eluted in the first column and then efficiently transfers them onto a second column with an orthogonal selectivity [133]. GCxGC allows the separation of compounds that are closely eluted in one-dimension GC (structurally related compounds, isomers, etc.) in complex matrices. Generally, the GCxGC separation of these compounds is based on a first column with a stationary phase of low polarity and a second shorter column with a more polar stationary phase. As an example, Hanari *et al.* [156] proposed a GCxGC separation for closely eluting PCNs (from tetraCNs to octaCN) based on a 14% cyanopropylphenyl-(86% dimethylpolysiloxane) stationary phase as the first dimension column with a poly(ethylene glycol)-based stationary phase as the second dimension column using a modulation time of 8 s. Indeed, they achieved the separation of all PCN congeners, although a slow-temperature program was required, leading to a total run time of 204 minutes. Other compounds with dioxin-like toxicity such as dioxin like-PCBs and PCDD/Fs as well as PBDEs present in complex samples have also been separated using GCxGC [157,158]. Besides, the separation of overly complex mixtures such as SCCPs and MCCPs has also been evaluated by GCxGC. Xia *et al.* [111] proposed a method for simultaneously profiling and quantify SCCPs and MCCPs obtaining good orthogonality on the separation and allowing the determination of 48 CP congener groups in one injection analysis with high selectivity. This method allowed not only the separation of SCCPs and MCCPs but also their separation from other related compounds such as PCBs, PBDEs, and other organohalogen compounds, minimizing potential interferences. Therefore, the high separation capacity of GCxGC combined with the high identification capacity of high-resolution mass spectrometers provides a powerful tool for the characterization of complex environmental samples. It also allows the selective quantification of target compounds and non-targeted approaches to detect other contaminants, although it also involves a long analysis time and complex data treatment [111,157,158].

Liquid Chromatography and Supercritical Fluid Chromatography

In the last decades, liquid chromatography has increased its use for the analysis of a wider range of halogenated contaminants, including polar, ionic, non-volatile, and thermally labile compounds, which were more difficult to analyze by GC [133]. Reversed phases, mainly C_{18}, are the stationary phases most widely used in the chromatographic separations of many of these compounds. Other columns, like the biphenyl-embedded stationary phase, have also been proposed to improve the separation of DP isomers since it also allows π-π and steric interactions in addition to hydrophobic ones. The influence of π-π interactions may allow a better selectivity between those species with and without π electrons, while steric interactions may yield shape recognition of the different chemical structures [152]. Moreover, following the general trends in liquid chromatography during this last decade, the use of ultra-high performance liquid chromatography (UHPLC) columns (sub-2 μm particle size) has also been generalized for the LC-MS analysis of these substances taking advantage of the improved chromatographic efficiency and the higher chromatographic resolution offered by these UHPLC columns. For instance, UHPLC separations have been widely applied for the determination of HBCDs. Zhao *et al.* proposed a UHPLC method that used a reversed-phase stationary phase (C_{18}) and a ternary mobile phase (methanol/acetonitrile/water) to separate the HBCD diastereomers, α-HBCD, β-HBCD, and γ-HBCD, allowing their selective individual determination [112]. Nevertheless, new HBCD diastereomers (mainly δ-HBCD and ε-HBCD) have been recently detected in industrial mixtures and it has been observed that the selectivity of the phenyl-hexyl stationary phase combined with a ternary mobile phase is required for their chromatographic separation [154]. Moreover, the separation of HBCD enantiomers has also been achieved using a chiral permethylated cyclodextrin column [159]. For PBDEs, PCBs and PCNs, the LC separation is usually achieved using columns that favor hydrophobic (C_{18}) as well as π-π interactions (Hypersil Green PAH) combined with binary hydro-organic mobile phases (methanol/water or acetonitrile/water) [94,98,118]. The separation of CPs has also been tested by liquid chromatography but showing a lower chromatographic resolution than that obtained on GC columns [155].

Concerning mobile phase composition, hydro-organic solvent gradients without the addition of acid or base species are generally employed since they allow enough retention and satisfactory peak shape for these non-polar compounds. An aspect to highlight is that the composition of the mobile phase can also affect the ionization efficiency of analytes when working with API sources. This fact makes necessary a careful optimization of the mobile phase composition to fulfill the minimum requirements in terms of sensitivity for the determination of these compounds. As an example, Zhou *et al.* achieved for all the API sources better responses of the DP and analogs using a methanol/water mobile phase than those achieved with an acetonitrile/water mixture [152]. Moreover, when neutral PFAS are determined simultaneously with legacy PFAS, ammonium acetate (NH4Ac) is usually added to

the mobile phase to ensure the retention of these polar and ionic compounds [153], although it also involves a loss of sensitivity for neutral PFAS, especially for FTOHs and FOSEs.

Other separation technique like packed column supercritical fluid chromatography (pSFC), has also been reported with the main advantages of facilitating the simultaneous analysis of different families of compounds or the determination of thermally labile compounds. For instance, the separation of PCDD/Fs in a Torus 1-AA column (anthracene-based column) employing supercritical CO_2 and methanol as cosolvent provided a similar elution profile than that achieved using a DB-5 column, although lower resolution was obtained [134]. Nonetheless, few co-elutions with non-2,3,7,8 substituted congeners were observed, which makes this technique promising for the analysis of halogenated pollutants, although further investigation would be required to propose pSFC as a potential alternative to GC separations.

Mass Spectrometry

Mass spectrometry is a powerful technique, especially when coupled with chromatography, allowing to overcome the lack of confirmation of classical selective detection systems (e.g., electron capture detector, fluorescent detection, or even electrochemical detection) for the determination of halogenated organic contaminants. Some of the important advantages offered by mass spectrometry techniques in front of classical detectors are the unequivocal identification/confirmation, the structural and isotope information needed for analyte characterization, selectivity to prevent interference problems and differentiate isobaric coeluting compounds as well as reduce the background noise improving sensitivity. Additionally, recent advances in mass spectrometry have increased the number of commercially available instruments that provide high sensitivity and selectivity while being easy to handle with reduced cost and maintenance. Thus, mass spectrometry has become a universal and specific technique for targeted and non-targeted analysis of these contaminants in environmental applications.

Ionization Techniques

In addition to the sample introduction, ionization is one of the first steps in the mass spectrometric analysis. Table 1.6 summarizes the main ionization techniques employed in the analysis of halogenated organic contaminants by chromatography-mass spectrometry. Regarding high-vacuum ionization techniques (applied in GC-MS determinations), electron ionization (EI) has been widely used for compounds such as PCDD/Fs, dioxin-like PCBs, and PCNs. These compounds generally yield the molecular ion $[M]^{+\bullet}$ in EI. However, low ionization energies have often been used to reduce the fragmentation of PCDD/Fs and PCBs. This also happens for PBDEs, although highly brominated congeners still show the ion $[M–Br_2]^{+\bullet}$ as the base peak of the mass spectrum even at low ionization energies [142,160,161]. On the other hand, the ionization of CPs, DPs, HBCDs, and neutral PFAS under EI conditions has shown a high fragmentation that hinders the detection capability and the selectivity of the method. This fact is especially critical for the determination of CPs, where the highly fragmented mass

spectra make difficult the quantitation of the congener groups (more than 10,000 compounds). Thus, the EI-based methods are generally focused on the determination of total CPs concentration. In contrast to EI, chemical ionization techniques are typically proposed to reduce fragmentation of these compounds improving both selectivity and sensitivity. Among them, few of the target compounds usually are determined using positive ion chemical ionization (CI)-based methods. For instance, FTOHs, FOSAs and FOSEs were ionized leading to the protonated molecule [M+H]$^+$ as the base peak of the mass spectra improving both selectivity and sensitivity over that obtained with EI [137,162]. Regarding negative-ion chemical ionization (NICI), different ionization trends can be observed. CPs were primarily ionized generating the [M–Cl]$^-$ and [M–HCl]$^{-\bullet}$ ions that facilitate the individual quantitation of each congener group [163]. Despite the advantages of NICI, Zencak *et al.* [164] reported that EI combined with tandem mass spectrometry (MS/MS) was still more selective than NICI-MS to overcome potential interferences such as PCBs or PBDEs, which enable the use of simple clean-up procedures. A similar ionization pattern was observed by NICI for PCDD/Fs, PCBs, PCNs, and even DP and chlorinated analogs, where the molecular ion [M]$^{-\bullet}$ is typically monitored although losses of Cl or HCl are also observed. This kind of fragmentation may hinder the selectivity on the determination of these compounds in front of other structurally similar compounds. Additionally, low chlorinated congener groups of PCDD/Fs, dl-PCBs, and PCNs show a relatively low response in NICI. At the same time, significant differences in the intensity have also been observed for compounds from the same homologue group of congeners [165] that makes necessary the use of isotope dilution for avoiding quantitation problems. Sometimes, NICI also provides highly fragmented mass spectra. For example, FOSAs and FOSEs show a high fragmentation with low characteristic ions while mass spectra FTOHs are characterized by fragment ions originated by losses of HF units from the molecular ion. Therefore, NICI is usually employed for confirmation purposes in the analysis of neutral PFAS [137,162]. This selectivity disadvantage is also manifested for brominated organic contaminants. For instance, an intense but low selective [Br]$^-$ ion is normally selected to determine Dec-604 [108] and tri- to heptaBDEs whereas highly brominated PBDEs show a lower fragmentation being possible to select more characteristic ions at high *m/z* values in the mass spectra [126].

Concerning API sources, the number of publications that propose these techniques for the ionization of halogenated pollutants has exponentially increased in the last years. These ionization sources are mainly used for LC-MS systems, but in this last decade, the number of applications using the API sources for GC-MS has greatly increased. API techniques provide a soft ionization promoting the formation of molecular ion or quasi-molecular ions (protonated or deprotonated molecule) and, therefore, reducing the in-source fragmentation. Among the API sources, atmospheric pressure chemical ionization (APCI) and atmospheric pressure photoionization (APPI) are the techniques most widely used for the determination of these compounds using both LC-MS and GC-MS. These sources ionize both moderate-polar and non-polar compounds, while electrospray (ESI) is mainly applied for the ionization of ionic,

polar, and less volatile halogenated compounds. Regardless of the coupling used (LC-MS, GC-MS, etc.), the ions observed for each family of compounds are generally similar in each API source. The nature of these ions will only depend on the liquid-phase (ESI) or gas-phase composition (APCI and APPI), leading to small variations in the mass spectra.

Halogenated aromatic contaminants (PBDEs, PCBs, PCDD/Fs, and PCNs) have been widely analyzed by APCI and APPI, for LC-MS and pSFC-MS couplings, yielding the molecular ion $[M]^{+\bullet}$ and the phenoxide ion $[M–X+O]^-$ (X: Cl, Br) in positive and negative ion mode, respectively, regardless of the mobile phase composition in APCI or the dopant used in APPI. However, the gas-phase composition can have a significant effect on the ionization efficiency. For instance, Perazzolli *et al.* [166] reported the post-column addition of benzene in LC-APCI to dramatically increase the ionization efficiency of TCDD/Fs in positive ion mode. Besides, Debrauwer *et al.* [167] used the post-column addition of toluene as dopant in LC-APPI (positive ion mode) to favor the formation of the molecular ion for PBDEs. In contrast, Riddell *et al.* [135] proposed the use of fluorobenzene, instead of the more toxic toluene, to promote charge-exchange reactions in the ionization of PCDD/Fs in pSFC-APPI positive ion mode.

Concerning LC-APCI and LC-APPI negative ion mode, the formation of $[M–X+O]^-$ ion occurs by the gas-phase reaction of analyte neutral molecules with superoxide ions, which are generated in these ionization sources even when oxygen is present at trace concentration levels [168]. In dopant-assisted negative APPI ionization, toluene has been often used for PCBs [94], PCDD/Fs [168] and PCNs [98] yielding the $[M–Cl+O]^-$ ion, while for PBDEs [97,116] the best results have been reported using toluene and acetone, which favor the formation of $[M–Br+O]^-$ ion for highly brominated PBDEs. In contrast, di- and triBDEs showed a very low response working in negative ion APPI mode [167,169]. In the case of BDE-209 the ion $[C_6Br_5O]^-$ was the base peak of the mass spectrum instead of the phenoxide ion observed for other highly brominated BDEs [116,118,170]. Furthermore, when using $[M–X+O]^-$ ions as precursor ions in tandem mass spectrometry experiments, it yielded product ions due to losses of chlorine or bromine atoms, providing high selectivity for the corresponding LC-MS/MS methods [94,98,168]. Additionally, the product ion mass spectra of $[M–Br+O]^-$ precursor ion also yielded a non-specific intense $[Br]^-$ ion as it was reported by Bacaloni *et al.* for BDE-153 [97].

On the other hand, the atmospheric pressure ionization of non-aromatic halogenated contaminants has also been evaluated in negative ion mode for LC-MS determinations. Concerning ESI, HBCDs yielded the deprotonated molecule [112,171], while neutral PFAS and DP have shown a high tendency to form adduct ions. For neutral PFAS, ammonium acetate is employed in the mobile phase to favor the chromatographic retention of ionic PFAS. Under these conditions, FOSAs generated the deprotonated molecule, while FTOHs and FOSEs yielded $[M+CH_3COO]^-$ adduct ions, which only led to an unselective acetate ion in the tandem mass spectrum [153,172]. To overcome this lack of selectivity, the ammonium acetate must be removed to favor the formation of the deprotonated molecule for FTOHs [96].

Table 1.6. Mass spectrometry systems used for the determination of halogenated organic contaminants.

Analyte	Inlet System	Ionization Technique	Ion Source Conditions	Precursor Ion	Mass Analyzer	iLOD (pg μL⁻¹)	Ref.
CPs	GC	EI	70 eV	$[C_7H_7]^+/[C_5H_7Cl]^{+\bullet}$	QqQ	90-230	[107,125,163,164]
			70 eV	$[M]^\bullet$ (²H-*dechlorinated analogs*)	QTOF	1.5ᵃ	[173]
		NICI	Methane/NH3ᵇ	$[M-Cl]^-/[M-HCl]^{-\bullet}$	QqQ	n.r.ᶜ	[163,164]
			n.r.ᶜ	$[M-Cl]^-/[M-2Cl]^{-\bullet}$	QTOF	24-170	[174]
			Methaneᵇ	$[M-Cl]^-/[M-HCl]^{-\bullet}$	Q-Orbitrap	0.03-2.02ᵈ	[147]
			Methaneᵇ	$[M-Cl]^-$	Q	100-700	[125]
	GCxGC	NICI	Methaneᵇ	$[M-Cl]^-/[M-HCl]^{-\bullet}$	TOF	n.r.ᶜ	[111]
	LC	ESI (−)	NH4Clᵉ	$[M+Cl]^-$	QTOF	10-20	[155]
	FIAᶠ	ESI (−)	CH2Cl2ᵍ	$[M+Cl]^-$	QTOF	50-400	[175]
		APCI (−)	CH2Cl2ᵍ	$[M+Cl]^-$	QTOF	30-1200 / 0.2-100ᵈ	[176–178]
			CHBr3ᵍ	$[M+Br]^-$	QTOF	0.1-160ᵈ	[179]
DPs	GC	EI	35 eV	$[C_5Cl_6]^{+\bullet}/[C_7H_2Cl_5]^+/[C_5H_xCl_y]^{+\bullet \#}$	QqQ	n.r.ᶜ	[122]
			35 eV	$[C_5Cl_6]^{+\bullet}/[C_7H_2Cl_5]^+/[C_5H_xCl_y]^{+\bullet \#}$	Sectors	0.003-0.064	[140,145]
		NICI	Methaneᵇ	$[M]^{\bullet-}/[Br]^-$	Q	0.005-0.096ᵃ	[108]
			Methaneᵇ	$[M]^{\bullet-}/[Br]^-$	QqQ	0.017-0.075ᵃ	[108]
		GC-APCI (+)	–	$[C_7H_2Cl_5]^+/[M+H-Cl]^{+\bullet}$	QTOF	n.r.ᶜ	[113]
	LC	ESI (−)	NH4Clᵍ	$[M+Cl]^-$	QqQ	n.r.ᶜ	[152]
		APCI (−)	−/NH4Clᵍ	$[M+H]^-/[M-X+O]^{-\ast\ast}$	QqQ	n.r.ᶜ	[152]
		APPI (−)	Acetoneᵍ	$[M+H]^-/[M-Br+O]^-/[M-xH+yCl-zO]^{-\perp}$	QqQ	25-50ᵃ	[152]
HBCDs	GC	EI	70 eV	$[M-Br-4HBr]^+$	QqQ	n.r.ᶜ	[180]
		GC-APCI (+)	–	$[M-Br]^+$	QqQ	0.1	[141]
	LC	ESI (−)	–	$[M-H]^-$	QqQ	0.09-0.19	[112,180,181]
			–	$[M-H]^-$	Orbitrap	0.39-0.90ᵃ	[182]
		APCI (−)	–	$[M-H]^-$	QqQ	0.3-0.4ᵃ	[183]
		APPI (−)	Toluene + 1,4-DBBᵍ,ʰ	$[M+Br]^-$	QqQ	4.3-23	[184]
	pSFC	APPI (−)	Fluorobenzeneᵍ	$[M-H]^-$	Q	n.r.ᶜ	[135]
	–	FAPA (−)	Helium	$[M-H]^-$	QITʲ	10,000	[185]

ᵃ pg injected on column; ᵇ reagent gas; ᶜ not reported; ᵈ individual CP homologues; ᵉ mobile phase component; ᶠ Flow injection analysis; ᵍ post-column addition; ʰ 1,4-dibromobutane; ⁱ modifier in the source; ʲ quadrupole-ion trap; # x=1-2, y=4-5; * X=Cl, Br; ⊥ x=2-3, y=4-5, z=4-5; ** R=−CH₃, −C₂H₅; ‡ x=1-4.

Table 1.6 (cont.). Mass spectrometry systems used for the determination of halogenated organic contaminants.

Analyte	Inlet System	Ionization Technique	Ion Source Conditions	Precursor Ion	Mass Analyzer	iLOD (pg µL⁻¹)	Ref.
nPFAS	GC	EI	70 eV	[M+H–xHF]⁺‡/[NSO₂HR]⁺**	Q	0.2-6	[105]
		CI	Methaneᵇ	[M+H]⁺/[M–F]⁺	Q	0.06-4	[137,162]
		NICI	Methaneᵇ	[M–xHF]⁻•‡/[NSO₂HR]⁻*/[C₂H₅ONSO₂R]⁺**	Q	n.r.ᶜ	[137,162]
		GC-APCI (+)	H₂Oⁱ	[M+H]⁺	QqQ	0.001-0.005ᵃ	[99]
	LC	ESI (–)	NH₄Acᵉ	[M+CH₃COO]⁻	QqQ	n.r.ᶜ	[153]
			–	[M–H]⁻	QqQ	n.r.ᶜ	[96]
		APPI (–)	Tolueneᵍ	[M–H]⁻/[M+O₂]⁻•	QqQ	0.08-1	[119]
PBDEs	GC	EI	70 eV	[M]⁺•	Q	0.2-200ᵃ	[129]
			65 eV	[M]⁻•/[M–Br₂]⁺•	QqQ	0.04-24ᵃ	[160]
			45 eV/–	[M]⁻•/[M–Br₂]⁺•	Sectors	0.010-11	[127,161,186]
		NICI	Methane/NH₃ᵇ	[Br]⁻	Q	n.r.ᶜ	[126,187]
		GC-APCI (+)	–	[M+H]⁺/[M]⁺•	QTOF	0.013-2.5	[186]
			–	[M+H]⁺/[M]⁺•	QqQ	0.001-0.01	[188]
			H₂O/HCOOH (1%)ⁱ	[M+H]⁺	QqQ	0.001-0.025	[188]
		GC-APPI (+)	–	[M]⁺•	TOF	n.r.ᶜ	[143]
	LC	APCI (–)	–	[M–Br+O]⁻	QqQ	0.10-0.72ᵃ	[118]
		APPI (+)	Tolueneᵍ	[M]⁺•	QqQ	n.r.ᶜ	[167]
		APPI (–)	Toluene/Acetoneᵍ	[M–Br+O]⁻/[M–2Br+O]⁻•	QqQ	0.11-6.3ᵃ	[97,118]
			Tolueneᵍ	[M–Br+O]⁻	Q-Orbitrap	0.2-2.2ᵃ	[116]
	–	APCI (–)	–	[M–Br+O]⁻	DTIMS-QTOF	n.r.ᶜ	[189]
		APPI (–)	Toluene/Acetoneᵉ	[M–Br+O]⁻	DTIMS-QTOF	n.r.ᶜ	[189]
PCDD/Fs	GC	EI	70 eV	[M]⁺•	QqQ	0.07-0.75ᵃ	[139]
			70 eV	[M]⁺•	IT	0.04-0.86ᵃ	[121]
			32 eV	[M]⁺•	Sectors	0.007-0.026ᵃ	[139]
			70 eV	[M]⁺•	Orbitrap	0.009-0.045ᵃ	[190]
		GC-APCI (+)	–	[M]⁺•	QqQ	0.001-0.002ᵃ	[148,191,192]
	LC	APCI (+)	Benzeneᵍ	[M]⁺•	IT	n.r.ᶜ	[166]
	pSFC	APPI (+)	Fluorobenzeneᵍ	[M]⁺•	QqQ	n.r.ᶜ	[135]
	FIAᶜ	APPI (–)	Tolueneᵉ	[M–Cl+O]⁻	QqQ	0.17-4.61ᵃ	[168]

ᵃ pg injected on column; ᵇ reagent gas; ᶜ not reported; ᵈ individual CP homologues; ᵉ mobile phase component; ᶠ Flow injection analysis; ᵍ post-column addition; ʰ 1,4-dibromobutane; ⁱ modifier in the source; ＃ x=1-2, y=4-5; ** X=Cl, Br; ⁺ x=2-3, y=4-5, z=4-5; ** R=–CH₃, –C₂H₅; ‡ x=1-4.

Table 1.6 (cont.). Mass spectrometry systems used for the determination of halogenated organic contaminants.

Analyte	Inlet System	Ionization Technique	Ion Source Conditions	Precursor Ion	Mass Analyzer	iLOD (pg μL^{-1})	Ref.
PCBs	GC	EI	70 eV	$[M]^{+\bullet}$	QqQ	0.05-0.63	[139]
			32 eV	$[M]^{+\bullet}$	Sectors	0.004-0.007	[139]
		NICl	Methane[b]	$[M]^{-\bullet}$	Q	n.r.[c]	[109]
		GC-APCI (+)	–	$[M]^{+\bullet}$	QqQ	0.0025	[149,150,193]
			–	$[M]^{+\bullet}$	QTOF	0.02-0.5	[194]
		GC-µAPCI (−)	–	$[M-Cl+O]^-$	IT	1-1000	[195]
		GC-µAPPI (−)	Toluene[i]	$[M-Cl+O]^-$	IT	1-2000	[195]
	LC	APPI (−)	Toluene[g]	$[M-Cl+O]^-$	QqQ	0.29-8.3[a]	[94]
		APCI (−)	–	$[M-Cl+O]^-$	DTIMS-QTOF	n.r.[c]	[189]
	–	APPI (−)	Toluene/Acetone[e]	$[M-Cl+O]^-$	DTIMS-QTOF	n.r.[c]	[189]
PCNs	GC	EI	70 eV	$[M]^{+\bullet}$	Sectors	0.06-0.13[a]	[196]
		EI	70 eV	$[M]^{+\bullet}$	QqQ	n.r.[c]	[130]
		NICl	NH$_3$[b]	$[M]^{-\bullet}$/$[M-HCl]^{-\bullet}$	Q	n.r.[c]	[197]
	GCxGC	EI	70 eV	$[M]^{+\bullet}$	TOF	0.09-0.06	[158]
	LC	APPI (−)	Toluene[g]	$[M-Cl+O]^-$	QqQ	0.8-16[a]	[98]

[a] pg injected on column; [b] reagent gas; [c] not reported; [d] individual CP homologues; [e] mobile phase component; [f] Flow injection analysis; [g] post-column addition; [h] 1,4-dibromobutane; [i] modifier in the source; # x=1-2, y=4-5; ** X=Cl, Br; + x=2-3, y=4-5, z=4-5; ** R=−CH$_3$, −C$_2$H$_5$; ‡ x=1-4.

Moreover, Peng *et al.* [120] proposed dansyl derivatization of FTOHs to improve their ionization, preventing adduct formation. Regarding DP and analogs, Zhou *et al.* [152] reported that ESI only allows the ionization of Dec-603, *syn-* and *anti-*DP in the negative ion mode through the generation of [M+Cl]$^-$ ions when NH$_4$Cl is added to the mobile phase. In contrast, negative ion APCI and APPI (dopant: acetone) showed similar results mainly consisting in displacement products ions such as [M−Br+O]$^-$ and [M−xH+yCl–zO]$^-$ (where x=2-3, y=4-5, z=4-5) or association product ions [M+H]$^-$, although negative ion APPI provided the best sensitivity. The use of LC-APPI or LC-APCI in negative ion mode also improved the ionization efficiency of neutral PFAS and HBCDs. For instance, Chu *et al.* [119] reported that FTOHs and FOSAs led to deprotonated molecule ions under gas-phase API conditions. Besides, these authors indicated that when analyzing biota samples, negative ion APPI (gas-phase ionization) showed the additional advantage of a significantly lower matrix effect over FTOHs response compared to ESI (liquid-phase ionization). In the case of HBCDs, Feng *et al.* [183] indicated that APCI achieved 2-3 times higher sensitivity than ESI for the formation of the deprotonated molecule, thus becoming an interesting alternative to overcome potential matrix effect. In the last few years, the use of API sources has also been deeply evaluated to achieve the ionization of CPs by promoting stable adduct ions through an anion-attachment ionization mechanism. Thus, Bogdal *et al.* [176] proposed the post-column addition of dichloromethane to an acetonitrile mobile phase, which allowed the generation of an APCI plasma of Cl$^-$ ions to promote the formation of [M+Cl]$^-$ adduct ions. The chlorine-enhanced ionization conditions suppressed the formation of multiple fragment ions, which improved the sensitivity and the selectivity for the determination of CPs by negative ion APCI. However, under these ionization conditions, Yuan *et al.* [179] observed that [M+Cl]$^-$ ions of C$_{10}$Cl$_5$ to C$_{10}$Cl$_8$ congeners overlapped with [M+Cl–HCl]$^-$ ions coming from the ionization of C$_{10}$Cl$_6$ to C$_{10}$Cl$_9$ congener groups. In contrast, the post-column addition of bromoform produced an APCI plasma of [Br]$^-$ ions that favored the formation of nearly exclusive [M+Br]$^-$ ions for C$_{10}$Cl$_5$ to C$_{10}$Cl$_9$ congeners that increased the selectivity and avoided complex data deconvolution processes. Recently, this anion-attachment ionization strategy is being applied in ESI. For instance, Li *et al.* [175] have evaluated the use of negative ion ESI for the analysis of CPs by using a post-column addition of dichloromethane to promote the formation of [M+Cl]$^-$ ions. Zheng *et al.* [155] also proposed the use of NH$_4$Cl in the methanol mobile phase to form chloride adduct ions thus increasing 3-fold the response of [M+Cl]$^-$ ions compared to the use of CH$_2$Cl$_2$. The authors suggested that the concentration of Cl$^-$ ion would be enhanced by the decomposition of NH$_4$Cl into ammonia and HCl (at 300 ^{o}C), whereas the volatilization of dichloromethane would reduce the presence of Cl$^-$ ions in the ESI source.

The use of API techniques has significantly increased in the last decades not only for LC-MS determinations but also for GC-MS analysis due to the specific development of atmospheric pressure chemical ionization (GC-APCI) and atmospheric pressure photoionization (GC-APPI) sources for the GC-MS coupling [198,199]. Among them, positive ion GC-APCI have been extensively used owing to its great sensitivity for the determination of halogenated

contaminants. The use of the GC-APCI source significantly prevented the fragmentation observed in EI as it could be observed in Fig. 1.7 for PCB-157. PCDD/Fs as well as dl-PCBs show very intense molecular ion with negligible APCI in-source fragmentation, thus allowing the detection of the target compounds at the low fg level (ca. 2-25 fg injected on column) [148–150,191]. Moreover, Sales *et al.*[141] reported that HBCDs efficiently formed the [M–Br]$^+$ ion in GC-APCI, that allowed the selective and sensitive screening of these compounds up to 100 fg µL^{-1}, while Portolés *et al.* [99] indicated that FTOHs, FOSEs, and FOSAs were efficiently ionized by yielding the protonated molecule as the base peak in GC-APCI-MS. The addition of an uncapped vial with water into the ion source has been proposed to promote proton-transfer reactions, which allowed the detection of neutral PFAS at the low fg level (1-5 fg injected on column). This strategy has also been evaluated to ionize PBDEs, which formed both the molecular ion and the protonated molecule. However, it was observed that the absence of water or other substances such as formic acid for preventing proton-transfer reactions provided the highest sensitivity for PBDEs by monitoring product ions coming from the [M]$^{+\bullet}$ ion [188].
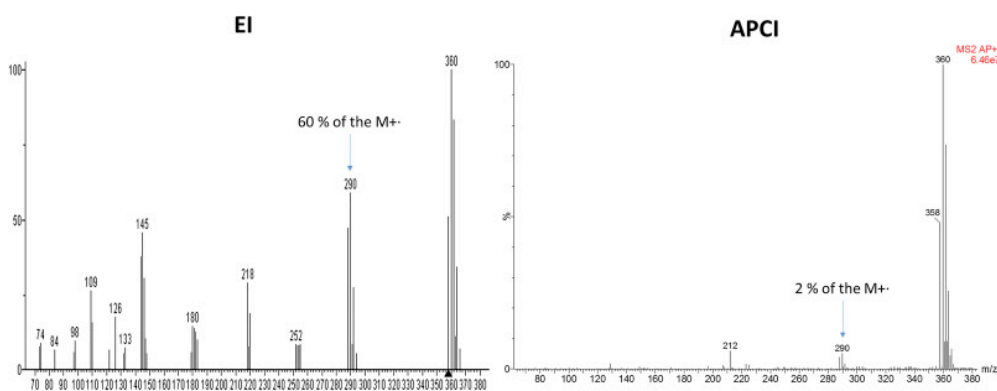

Fig. 1.7. Comparison of the ionization for the 2,3,3',4,4',5-hexachlorobiphenyl dioxin like-PCB in EI (*left*) and APCI (*right*) sources [149].

The GC-APPI source has been commercialized in the last years and it has demonstrated a great potential to efficiently ionize halogenated pollutants. For instance, Di Lorenzo *et al.* [143] demonstrated that under dopant-assisted photoionization PBDEs only yielded the molecular ion in contrast to the ion mixture [M]$^{+\bullet}$/[M+H]$^+$ observed in the GC-APCI source. Besides, some photooxidation products such as [M–Br+O]$^+$ or [M–Br+O$_2$]$^+$ were also observed working in positive ion GC-APPI mode which allowed the differentiation between coeluting BDE isomers like BDE-49 and BDE-71. Regarding negative ion mode, Luosujärvi *et al.* [195] evaluated the ionization of PCBs using both GC-APCI and GC-APPI and observed the generation of the corresponding phenoxide ions as happen in LC-APCI and LC-APPI sources.

Mass Analyzers

Halogenated organic contaminants have been analyzed using both low-resolution (LRMS) and high-resolution mass spectrometry (HRMS) (Table 1.6). Low-resolution mass analyzers, especially quadrupoles (Q), have been used for both GC-MS and LC-MS determinations. Earlier GC-MS applications were quadrupole-based using EI due to the rich information that it could provide and the capability for mass library searching. For instance, the analysis of neutral PFAS in animal plasma and tissues [200] as well as PBDEs in long-finned pilot whale [201] have been proposed by GC-EI-MS working in selected ion monitoring (SIM) mode. In contrast to ion traps (IT), where sensitive full-scan acquisition mode could be performed, quadrupole systems often operate in SIM mode to enhance the selectivity and sensitivity, especially for quantitative purposes when the analytes are present at very low concentration levels. The use of single quadrupoles is more limited when using soft ionization techniques (CI, NICI, and API sources) [99,125] because of the lower fragmentation observed in the mass spectra does not allow to obtain chemical structural information necessary for confirmation purposes by searching in the mass library. However, the lower fragmentation and the promotion of molecular and quasi-molecular ions provide better sensitivity than EI-SIM mode methods using single quadrupoles. For instance, neutral PFAS showed low fragmentation by GC-CI-MS (Q) with intense quasi-molecular ions. However, the few fragment ions observed had very low abundances thus requiring the re-analysis of positive samples by an orthogonal technique such as GC-NICI-MS to confirm the presence of the target compounds [137]. Besides, Iozza *et al.* [125] determined SCCPs by GC-NICI-MS (based on the monitoring of [M–Cl]$^-$ ions) although an extensive clean-up was required to avoid interferences from other related halogenated compounds that can coelute with them at the same retention time. Thereby, tandem mass spectrometry with triple quadrupole (QqQ) instruments has been often chosen to improve the selectivity and detection capability of the methods, as well as to offer significant structural information for confirmation purposes. To overcome the lack of fragment ions in soft ionization sources, MS/MS is carried out to generate product ions that allow the improvement of selectivity, sensitivity, and characterization capabilities of the methods. For instance, although the analysis of PCDD/Fs and PCBs has been usually carried out by HRMS (sectors), new advances on fast and sensitive QqQ instruments have allowed the determination of these compounds by using EI and positive-ion APCI without sacrificing the selectivity required and avoiding some coeluting isobaric interferences such as other dioxin-like compounds [139,148,149,191,192]. However, García-Bermejo *et al.* [139] pointed out that variations in the measurement of the ion transition ratios (for MS/MS systems) could be higher than the ion ratio estimated for GC-HRMS systems (in SIM mode), which could limit method precision. Moreover, LC-MS and GC-MS applications using soft API sources have been performed exclusively in MS/MS when working with low-resolution mass spectrometers. For example, Sales *et al.* [141] proposed a GC-APCI-MS/MS method to determine HBCDs by monitoring product ions from the [M–Br]$^{+\bullet}$ precursor ion in multiple reaction monitoring (MRM) mode. Besides, Moukas *et al.* proposed the LC-APPI-MS/MS (QqQ) methods to determine PCBs [94]

and PCNs [98] by monitoring selective transitions such as $[M–Cl+O]^- \rightarrow [M–2Cl+O]^-$ and $[M–Cl+O]^- \rightarrow [M–3Cl+O]^-$. LC-MS/MS methods have also been proposed for other contaminants such as DP [152], PBDEs [118], and HBCDs [181,183]. Although MRM mode generally improves both selectivity and sensitivity for the analysis of these halogenated compounds, $[Cl]^-$ and $[Br]^-$ ions are usually selected as product ions for their monitoring. However, these transitions are not selective enough and can compromise the selectivity of these methods against other coeluting chlorinated or brominated isobaric interferences. In the case of the MS/MS determination of neutral PFAS, especially FTOHs and FOSEs, the product ions monitored in negative ion APPI [119] or positive ion GC-APCI [99] (combined losses of HF, fluoroalkyl chain or functional group moieties) are more selective than the non-characteristic acetate product ion observed in negative ion ESI since only $[M+CH_3COO]^-$ ions are generally formed for these families of compounds.

Additionally, with the advances in modern triple quadrupoles, MS/MS has also been used to reduce background noise even for analytes showing high fragmentation. For instance, Barón *et al.* [108] observed that the QqQ instrument increased the S/N ratio of DPs compared to a single quadrupole system when analyzing biota samples by GC-NICI-MS(/MS). Furthermore, the GC-EI-MS/MS analysis of CPs, which are based on the monitoring of common fragment ions at low *m/z* values, allows that isobaric interferences could be filtered, thus increasing method sensitivity by acquiring data in MRM mode [125]. On the other hand, although ion-trap analyzers offered better sensitivity than quadrupoles working in full-scan mode, it surprises the reduced number of applications for the determination of these substances. This fact can be due to the slow scanning rate of these mass analyzers in tandem mass spectrometry in front of modern QqQ and quadrupole-time-of-flight (QTOF) instruments, which could hinder the correct monitoring of narrow chromatographic peaks. However, Smoluch *et a*l. [185] and Roszko *et al*. [121] have proposed the used of an ion-trap mass analyzer for the screening of HBCDs using an ambient ionization mass spectrometry technique such as flowing atmospheric pressure afterglow (FAPA)-MS/MS and the determination of PCDD/Fs by GC-MS/MS, respectively.

One interesting aspect of tandem mass spectrometry is the capability to study the fragmentation pathway of families of compounds to identify common fragmentation patterns, product ions, or even losses among closed related compounds. For instance, Riu *et al.* [169] tentatively proposed fragmentation pathways for PBDEs, identifying general fragmentation trends (losses of Br, Br$_2$, or COBr moieties) and common product ions using LC-APPI-MS/MS (ion trap). The fragmentation studies may assist in the identification of new and unknown related compounds, as well as in the development of non-targeted strategies, such as fragmentation flagging approaches or mass defect plots.

Despite the advantages of tandem mass spectrometry, the difficulties of LRMS to differentiate isobaric ions may hinder the quantitation of some complex mixtures. For instance, the LRMS analysis of CPs is mainly based on the determination of the total CP content due to the

limitations in separating the individual response of each CP homologue group without the contribution of CP groups with different chlorination degree and/or carbon chain-length or other halogenated contaminants like pesticides or PCBs [125]. Most of the problems and limitations observed in the LRMS determination of these pollutants can be overcome by using HRMS coupled to both GC and LC, with the additional advantage of reducing the number of false positives and negatives. Traditionally, the environmental occurrence of PBDEs [186] and compounds with dioxin-like toxicity (PCDD/Fs, dioxin like-PCBs and some PCNs) [139,196] has been addressed through the GC-EI-HRMS analysis with double-focusing magnetic sectors to overcome isobaric interferences from coeluting congeners and/or matrix components. Regarding DPs, EI leads to low-specific fragment ions, such as $[C_5Cl_6]^+$ or $[C_5HCl_5]^+$, and the use of HRMS affords the selective determination [145]. The use of double-focusing magnetic sectors mass analyzers not only could improve selectivity by removing potential interferences, but also could increase the sensitivity on the analysis of complex matrices by reducing the background noise. Nonetheless, these HRMS instruments have to work in SIM mode due to the low sensitivity that they show when they operate in full-scan acquisition mode. In this sense, the new generation of HRMS analyzers like time-of-flight (TOF) and Orbitrap offers important advantages, such as high scanning speed and sensitivity over traditional double-focusing magnetic sectors mass analyzers. Thus, Hayward *et al.* [190] proposed a GC-EI-Orbitrap method to determine PCDD/Fs in cow and human milk, since Orbitrap could keep a high selectivity operating at a resolution of 120,000 (FWHM, full width at half maximum, at *m/z* 200) with high sensitivity in full-scan acquisition mode. These advantages allowed achieving instrumental limits of detection (iLODs) comparable to those obtained using double-focusing magnetic sectors. The easy operation of modern HRMS instruments, but keeping and enhancing the HRMS capabilities, have exponentially increased the number of publications using TOF and Orbitrap analyzers in the field of the analysis of halogenated pollutants in the last decades. For instance, Zacs *et al.* [116,182] proposed the use of highly sensitive and selective UHPLC-ESI-Orbitrap and UHPLC-APPI-Orbitrap methods for the determination of HBCDs and PBDEs, respectively. These authors highlighted that a compromise between selectivity and sensitivity might be considered due to the reduced scanning speed of Orbitrap (comparing to TOF instruments). These mass analyzers have been particularly relevant for the determination of CPs. Typically, GC-NICI-HRMS (TOF and Orbitrap) methods have been usually carried out for both the determination of the total CP content and the characterization of individual CP homologue groups [147,174]. For instance, the GC-NICI-Orbitrap determination achieved the lowest iLODs for SCCPs (0.03-2.02 pg μL^{-1}) and MCCPs (0.11-0.41 pg μL^{-1}). Moreover, working at a resolution of 60,000 FWHM authors found that relative deviation between the experimental and theoretical ion ratios was lower than 10% when the response of the homologue CP groups was lower than 1% of the total 'hump' area, demonstrating the high selectivity of the method [147]. However, a mass resolution of 94,000 FWHM is required to solve some overlapping signals due to the high number of CP isomers. The rich CP isotope clusters and the multiple fragmentations of CP congeners lead to overly complex mass spectral data, which may result in mass interferences between and within CP

homologue groups [177]. In the last few years, flow injection analysis (FIA)-HRMS (TOF) methods have also been developed for the determination of CPs, showing important advantages. As mentioned above, the use of anion-attachment APCI and ESI through the formation of [M+Cl]⁻ ions led to less complex mass spectra than those obtained by NICI [178], and the combination with a mathematical deconvolution approach and the TOF mass analyzer has made possible the selective and sensitive determination of CPs. The deconvolution approach allowed the identification of ion signals within a pull of overlapping masses since [M+Cl]⁻ ions of C_nCl_m homologue groups were not resolved from other ions, especially [M+Cl–HCl]⁻ ions coming from C_nCl_{m+1} homologue groups (Fig. 1.8), thus avoiding an overestimation on the concentration of 1.4-39% [179].
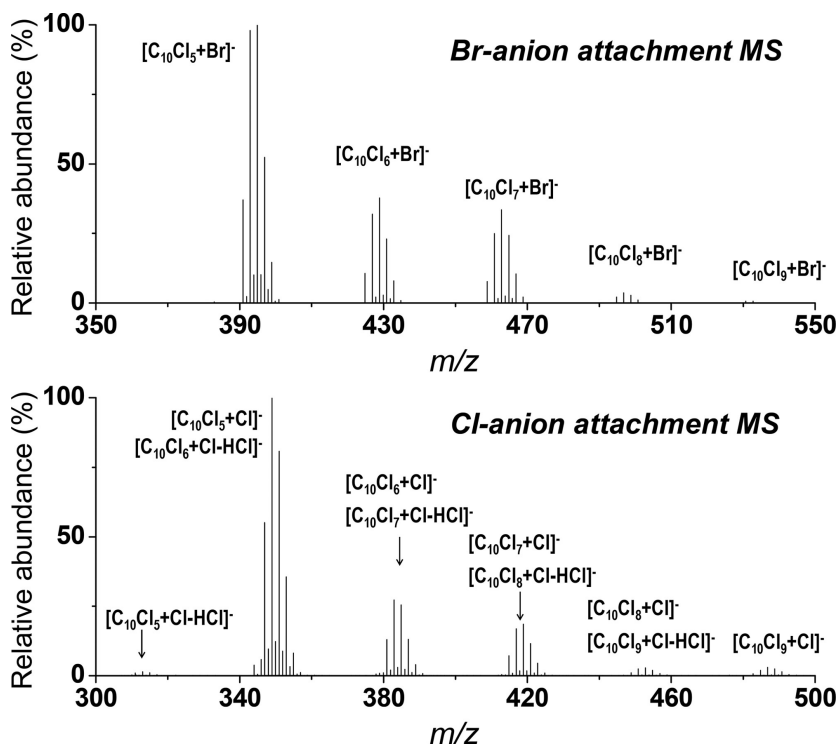
Fig. 1.8. Bromine- and chlorine-enhanced APCI mass spectra of five CP congeners in a congener standard mixture *(MIX-2)* [179] (*https://pubs.acs.org/doi/10.1021/acs.estlett.8b00216, further permissions related to the material excerpted should be directed to the ACS*).

Meanwhile, a minimum mass resolution of 10,000 FWHM was required to overcome other potential interferences before the deconvolution step [177]. This procedure was even simplified by Yuan *et al.* [179] by using a bromide-attachment APCI-TOF method where the measured isotopic distributions of the [M+Br]⁻ ions perfectly matched with the theoretical values because there was no fragmentation (Fig. 1.8). Thus, these results would suggest that using this methodology there would be no need to use the deconvolution approach, which simplifies the

data treatment analysis and even it would open the door for the application of this methodology using LRMS.

The high sensitive full-scan acquisition provided by HRMS mass analyzers like TOF or Orbitrap allow not only targeted analysis but also non-targeted approaches such as screening analysis of a large number of suspect compounds and the identification of new related pollutants, among others. For instance, Ieda *et al.* [202] proposed a workflow for targeted and non-targeted screening of contaminants in environmental samples based on GCxGC-EI-HRMS (TOF) analysis. Regarding the non-targeted approach, the authors propose the use of specialized software (NMF with DBcreator) to achieve the deconvolution of the mixture of components and improve the mass spectral library searching. Mass defect plots are another useful tool based on full-scan HRMS data that can simplify and make faster the identification of halogenated pollutants in complex mixtures. In this strategy, the whole set of acquired *m/z* values are transformed into the H/Cl mass scale by multiplying each ion mass by the exchange factor 1.0011 (34/33.96102). A mass defect graph is then built by plotting the ion nominal mass in front of the H/Cl mass defect. This graph shows series of ions aligned in different classes ("bands") indicating that all ions within the same series have the same repeating unit. In this example, hydrocarbon ions, silicon-containing ions, and halogen-containing ions were separated in different "bands" [203].

As mentioned before, the use of an API source for GC-MS has become very popular in the last few years and this methodology is often used in combination with HRMS. The use of GC-APCI-HRMS (TOF) has shown significant advantages over GC-EI-HRMS (magnetic sectors). For instance, Portolés *et al.* [204] proposed a multiclass screening of organic pollutants, including PBDEs, PCBs, and PCNs in water by GC-APCI-HRMS (QTOF) facilitating a rapid, wide-scope, more sensitive and effective screening based on molecular ion and/or protonated molecule searching. Additionally, the possibility of performing both full-scan and product ion scan in hybrid instruments such as Q-TOF or quadrupole-Orbitrap (Q-Orbitrap) provides useful chemical structural information to support the tentative analyte identification. In this way, Liu *et al.* [113] reported the use of a Q-TOF mass analyzer using the GC-APCI source in the positive ion mode and combining HRMS and MS/HRMS experiments to identify two novel dechlorane analogs, structurally related to Dec-603.

GC-HRMS and LC-HRMS methods can provide accurate determinations of halogenated contaminants, but in some cases, the separation of isomeric compounds that have an identical or close elemental composition is complicated. The use of GCxGC could overcome this problem, but long analysis times and complex data processing may limit its use. A promising alternative technique is the ion mobility (IM) combined with high-resolution mass spectrometry because it could provide a selective and fast determination of close related halogenated organic contaminants by separating isobaric/isomeric compounds in very complex samples and improving environmental laboratory throughput. In IM separation, ions traveling through a drift cell filled with a buffer gas (e.g., N_2) and under the influenced of a weak electric field are

separated according to their shape and volume (collision cross-section, CCS) in addition to their *m/z* value. Despite having an identical elemental composition, compounds with a compact structure (lower CCS) will travel faster through the IM cell than compounds with more extended shapes (higher CCS). Zheng *et al.* [189] evaluated the capabilities of IM-QTOF (using APCI and APPI) and demonstrated that both isobaric PCBs and PBDEs can be almost baseline separated. For instance, IM is a powerful technique to separate *ortho* and *non-ortho* PCB congeners (Fig. 1.9a). *Non-ortho* PCBs mainly exist in a planar structure leading to a larger size and, therefore, a higher CCS value than that observed for *ortho* PCBs, which are more likely to adapt to more compact three-dimensional structures and consequently show lower CCS values. The authors also reported that the CCS values measured for PCBs and hydroxyl-PCBs (OH-PCBs) in the drift tube IM (DTIMS) are larger than those obtained for PBDEs and hydroxyl-PBDEs with the same *m/z* values (Fig. 1.9b). This fact indicates that PCBs have a larger structure than PBDEs, which may be explained because the electron density conjugation between the phenyl rings and the oxygen allows PBDEs to form a more stable planar structure.
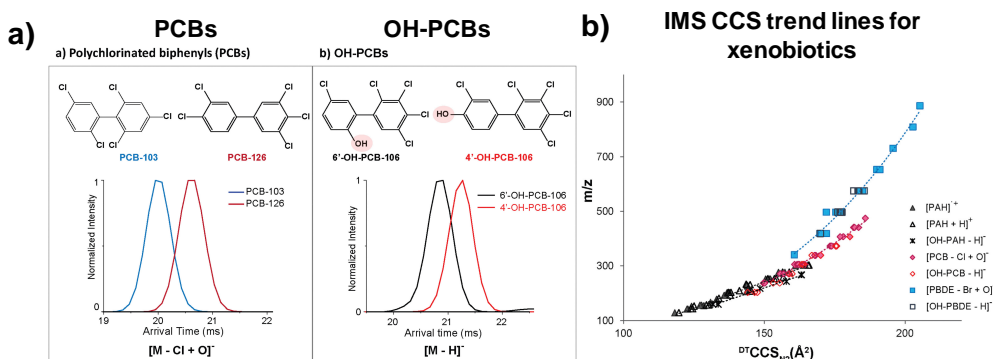

Fig. 1.9. a) IM separations of isobaric PCBs and OH-PCBs and b) CCS values versus *m/z* trend lines for polycyclic aromatic hydrocarbons (PAHs), PCBs, PBDEs and their metabolites *(adapted from Zheng et al.* [189]*)*.

Quantification methods

The quantification method applied for the determination of halogenated pollutants in environmental samples depends on the family of compounds, the main goal of the quantitative method (determination of the content of total or specific congeners) and the analytical methodology applied, especially the separation and the ionization techniques used in GC-MS and LC-MS. One of the main advantages of working with mass spectrometry is the possibility of quantifying by using isotope-labelled compounds regardless of the mass analyzer employed. These isotopically labelled analogs are generally used to guarantee accurate and precise quantitative data since they behave similarly to native analytes during sample processing (surrogates), chromatographic separations (internal standards), and mass spectrometry analysis (internal standards and isotope dilution). Traditionally, the determination of 2,3,7,8-PCDD/Fs and dl-PCBs has been performed by isotope dilution, providing accurate

results despite the high cost of labelled standards for all the compounds [121,139]. Nowadays, isotopically labelled compounds are also commercially available for broader families of compounds such as DP [186], HBCDs [181], and neutral PFAS [105]. In the case of PBDEs, the applicability of the isotope dilution method depends on the ionization source selected. For instance, monitoring of non-specific [Br]− ions in NICI make the isotope dilution method unsuitable for quantitative purposes. In contrast, when ionization techniques such as EI and API are used, more specific ions are monitored that often keep up the ^{13}C atoms in their chemical structure [118]. Regarding PCNs, there are 75 potential toxic congeners and it is unfeasible to have labelled compounds for all of them, therefore, the quantitation is generally performed by using only one ^{13}C-labelled compound for each homologue group [196,205]. Although the use of isotopically labelled compounds provides significant advantages, they are expensive and for some compounds like SCCPs, they are not available for each specific congener. Consequently, other compounds with similar properties are often used as internal standards for quantitation purposes and/or calculate recovery rates [133]. For instance, in the determination of CPs, ^{13}C-trans chlordane [111,125,164], pentachlorobenzene [107], or Dec-603 [163] have often been proposed as internal standards for quantification purposes to avoid expensive isotope-labelled CPs, while ε-hexachlorocyclohexane has been frequently used as recovery standard [111,125]. On the other hand, for PCNs analysis, PCBs [130,197] and ^{13}C$_6$-hexachlorobenzene [117] have been proposed injection internal standards for quantification purposes whereas tetrabromobenzene and PCB-209 have been applied as surrogates to estimate recovery rates [197]. When surrogates and/or internal standards are not used, which often occurs when working with API sources in LC-MS/MS determinations, the matrix effect takes significant relevance because it may lead to underestimated or overestimated results. In these cases, the matrix effect could be corrected by using a matrix-matched calibration approach. Moreover, the use of APCI or APPI sources (gas-phase ionization) instead of ESI (liquid-phase ionization) could also help to overcome matrix effects (compared to ESI) as it was reported by Chu *et al.* for neutral PFAS [119].

Especially attention must be paid in the determination of CPs. Mixtures with different chlorine content and the lack of isotope-labelled compounds lead to different quantitative approaches according to the ionization technique used. For instance, the EI response factors of different SCCP mixtures are not dependent on the chlorine content, although the low selectivity only allows the determination of the total SCCP content [125]. In contrast, NICI responses of these compounds are strongly affected by their chlorination degree, which requires the use of a different approach like Reth's method to overcome quantification errors [206]. A similar quantitative method has been carried out when using APCI-HRMS but with a previous deconvolution approach [178]. Nevertheless, this methodology has important advantages over NICI-based methods such as lower quantitation errors and the ability to detect a larger number of homologue groups (from Cl$_3$ to Cl$_{12}$-homologue groups) than those observed in NICI based-methods (from Cl$_5$ to Cl$_{10}$-homologue groups), becoming a reliable alternative to reduce quantification errors in the analysis of SCCPs.

1.2.2. Atmospheric Pressure Ionization Trends

As it was concluded in the previous Section 1.2.1., one of the most significant trends in the analytical determination of halogenated contaminants is the suitable applicability of API techniques. These API sources are softer ionization techniques than the traditional high-vacuum EI and chemical ionization (CI and NICI), providing low in-source fragmentation and, therefore, a high abundance of analyte ions. Additionally, API techniques may enable not only the ionization of polar compounds but also non-polar or semi-polar compounds such as most of the halogenated pollutants evaluated in this Thesis, highlighted in bold in Fig. 1.10.
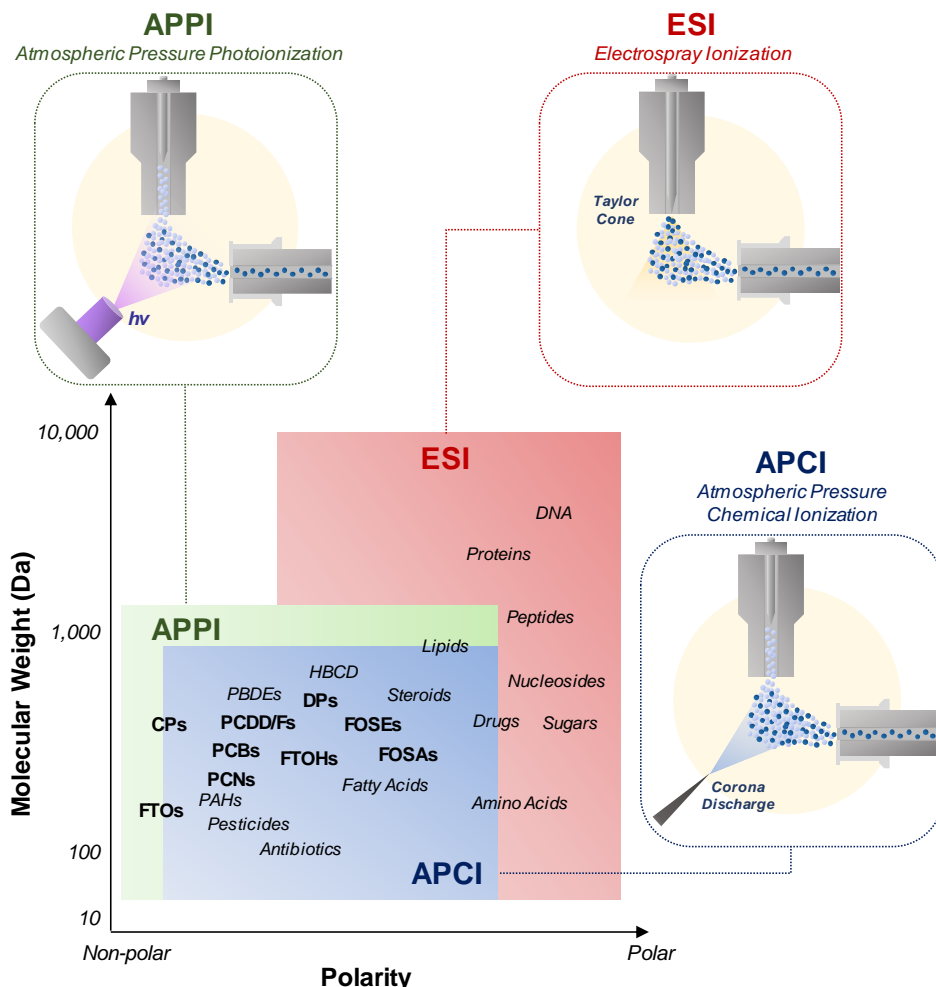

Fig. 1.10. Feasibility of atmospheric pressure ionization techniques for polar and non-polar compounds.

The main characteristics of the API techniques are summarized in Table 1.7. Among the API sources, electrospray ionization (ESI) has been the most widely used for the LC-MS coupling. However, ESI allows the ionization of polar compounds in the liquid-phase mainly through the control of pH, thus the presence of acid or basic functional groups in the analyte structure is

essential. Thereby, ESI may provide an inefficient ionization for most of the analytes evaluated in this Thesis. Indeed, only ESI based methods for the determination of FTOHs, FOSAs, and FOSEs as well as few methods for SCCPs have already been reported. Additionally, ion suppression nor ion enhancement are usually observed using electrospray due to the presence of another ionizable compound, as it could be a competition during the ion evaporation process. These effects can lead to an artificial and irreproducible reduction or amplification of the analyte signal causing problems in the quantitative analysis.

Table 1.7. Characteristics of atmospheric pressure ionization techniques.

	ESI	APCI	APPI
Ionization	Liquid-phase	Gas-phase	Gas-phase
Influenced by	pH	PA[a] and IE[b]	IE[b] and PA[a]
Compounds	Polar	Polar and non-polar	Polar and non-polar
Ion suppression	High	Low	Low
Structural information	Low	Low	Low
Thermal degradation	Low	Medium	Medium
Adduct formation	High	Medium	Medium
Mass spectra complexity	Low	Medium	High

[a] Proton affinity, [b] Ionization energy.

On the other hand, APCI and APPI present important advantages over ESI since they allow the ionization of both polar and non-polar compounds, and thus may be suitable to ionize halogenated organic contaminants. Besides that, they show a low ion suppression and less tendency to form adduct ions which lead to the establishment of methodologies less affected by the matrix. Nevertheless, some disadvantages must be also pointed out such as the possibility to produce thermal degradation due to the high temperatures applied (ca. 200-500 °C) and the acquisition of more complex mass spectra that might difficult mass spectral interpretation. Moreover, API sources provide less structural information than EI, although they often generate the molecular or quasi-molecular ion, which can be later fragmented by tandem mass spectrometry experiments to obtain this information. APCI and APPI sources have shown a great efficiency to ionize the target compounds and, consequently, the LC-API-MS methods based on these sources provide high sensitivity to detect these compounds at ultra-trace levels in environmental samples. However, the reported LC-MS determinations usually do not show as satisfactory chromatographic resolution as GC-MS (high-vacuum ionization) determinations, which still makes GC-MS the method of choice.

In the last decade, the use of atmospheric pressure ionization sources for GC-MS determinations has exponentially increased combining the high chromatographic resolution of GC and the high sensitivity and selectivity of API sources (Fig. 1.11). The main advantages of GC-atmospheric pressure ionization are:

- The use of API sources allows GC separation to be combined with advanced mass spectrometers originally developed for LC separations,
- The molecular or quasi-molecular ion is largely preserved,
- Due to the low in-source fragmentation, a compromise between sensitivity and selectivity is not necessary on the selection of precursor ions for MS/MS experiments,
- Accurate mass measurements and elemental composition are enabled when coupling to HRMS,
- Throughput improvement and reduced cost is possible as the same mass analyzer could alternatively be coupled to LC or GC instruments,
- Different ionization techniques may open new fields of applications for the detection of organic compounds.
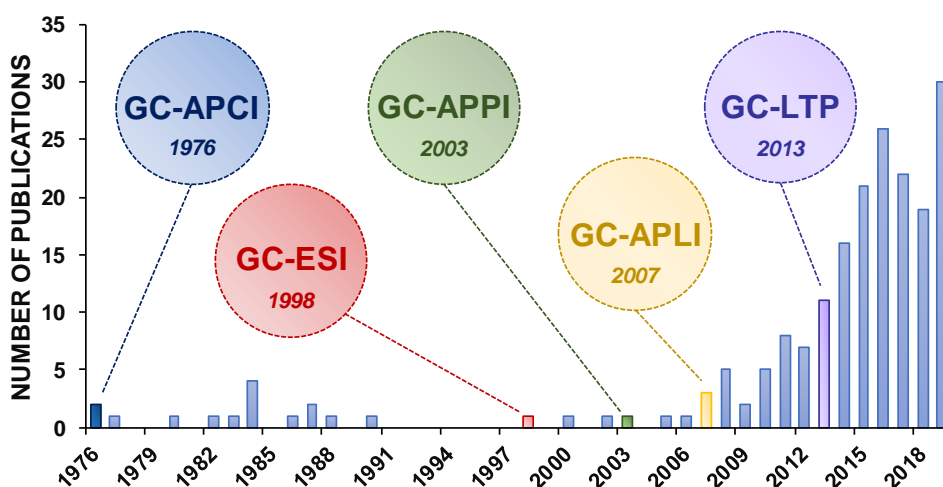

Fig. 1.11. Chronological distribution of the number of publications based on GC-API-MS methods.

The first GC-API coupling based on atmospheric pressure chemical ionization (GC-APCI) was pioneered by Horning *et al.* in the 70s [207,208]. This setup consisted of a GC system with a packed column coupled to an API-MS system designed for operation in the negative ion *via* electron capture. After that, Mitchum *et al.* [209,210] changed Horning's setup by coupling the API source to both glass capillary and fused capillary GC columns. This system was successfully applied during the 80s for the analysis of environmental samples to determine tetrachlorinated dibenzo-ρ-dioxins [209–212], 2,3,7,8-tetrachlorinated dibenzofuran [213], nitro-polycyclic aromatic hydrocarbons (nitro-PAHs) [214–217], and amino-PAHs [218]. In 1998, Lee *et al.* [219] reported the multichannel electrospray ionization for the GC-MS coupling (GC-ESI) for the ionization of volatile organic compounds. The eluate of the GC column flowed through the center channel of the source, while the other six surrounding channels were used to electrospray a methanol solution containing 1% of acetic acid to allow the protonation of analytes by ion-molecule reactions. Thus, the authors avoided the interference from gas

bubbles that could occur if the eluent from the GC column is directed into the liquid in the electrospray needle, leading to instability of both electrospray and analytes signal. Two years later, Wu *et al.* [220] also proposed the use of secondary electrospray ionization (SESI) for coupling LC and GC to ion mobility-mass spectrometry (LC-IM-MS and GC-IM-MS) as a powerful technique to determine illicit drugs. Although these sources show a great potential to ionize polar compounds, they are not suitable to ionize semi-polar and non-polar compounds such as most of the halogenated contaminants.

Despite the power demonstrated by the GC-API techniques for the determination of organic compounds, the number of publications reporting their use did not increase exponentially until the beginning of the 21st century (Fig. 1.11). Hence, in 2003, Revelsky *et al.* [198] reported the first study using an atmospheric pressure photoionization source for GC-MS (GC-APPI). Using this source, the ionization of several compounds, including alcohols, alkanes, amines, and esters, was achieved without in-source fragmentation. At the same time, in 2005 McEwen and McKay [199] introduced a new APCI interface for GC-MS and LC-MS couplings, whereas in 2007 and 2008 Schiewek *et al.* [221–223] proposed an atmospheric pressure laser ionization source for GC-MS (GC-APLI). After that, Nørgaard *et al.* [224] also reported a new interface based on low temperature plasma for GC-MS (GC-LTP). The LTP allowed the ionization of low to moderate polar compounds through the formation of analyte molecular ions, protonated molecules, and adduct ions like $[M+NO]^+$, achieving proper detection limits (0.5 ng injected on column) for volatile organic compounds. However, the GC-LTP source has not been used too much in the last years. Regarding GC-APCI and GC-APLI techniques, they had been interfaced with commercial instruments although they had never become popular until McEwen [199] and Schiewek [222] developed ion sources for multipurpose analysis, including both LC-MS and GC-MS determinations in the same instrument. Nowadays, among the almost 200 publications describing the application of GC-API techniques, most of them (ca. 75%) are based on the use of the GC-APCI source, while GC-APPI and GC-APLI cover only 10% and 9% of the publications, respectively. Among them, GC-APLI has been mainly applied to the determination of PAHs [225–230] while GC-APCI and GC-APPI have covered a wider range of applications.

Atmospheric Pressure Chemical Ionization for GC-MS Determinations

In 2009, Waters commercialized and launched the GC-APCI source under the nickname of Atmospheric Pressure Gas Chromatography (APGC) for their use with both QqQ and TOF mass spectrometers. Later, the GC-APCI source was also developed for their used in TOF mass analyzer instruments from Bruker and Agilent Technologies. Briefly, the APCI mechanism is initiated by a corona discharge that generates primary ions, which ionize analyte molecules through gas-phase ion-molecule reactions (Fig. 1.12). The corona discharge needle releases electrons that react with the nitrogen plasma (when N_2 make-up gas used in this source), leading to $N_2^{+\bullet}$ and $N_4^{+\bullet}$. Then, if the ionization potential of the analyte is lower than $N_2^{+\bullet}$ or $N_4^{+\bullet}$, charge-exchange reactions may occur (Fig. 1.12a). On the other hand, when water

is present in the source, these nitrogen ion species can react with water leading to the formation of water clusters that would participate in proton-transfer reactions with analyte molecules (Fig. 1.12b). This proton-transfer-reaction could even be produced with water vapor traces presented in the ion chamber [208,231]. So, both the source and the environment must be under strict control to prevent ionization and corona/plasma fluctuations due to changes in the ionization source environmental gas composition. However, modifiers such as water or methanol could be used to enhance proton-transfer reactions and to promote the protonated molecules of analytes in GC-APCI [231].
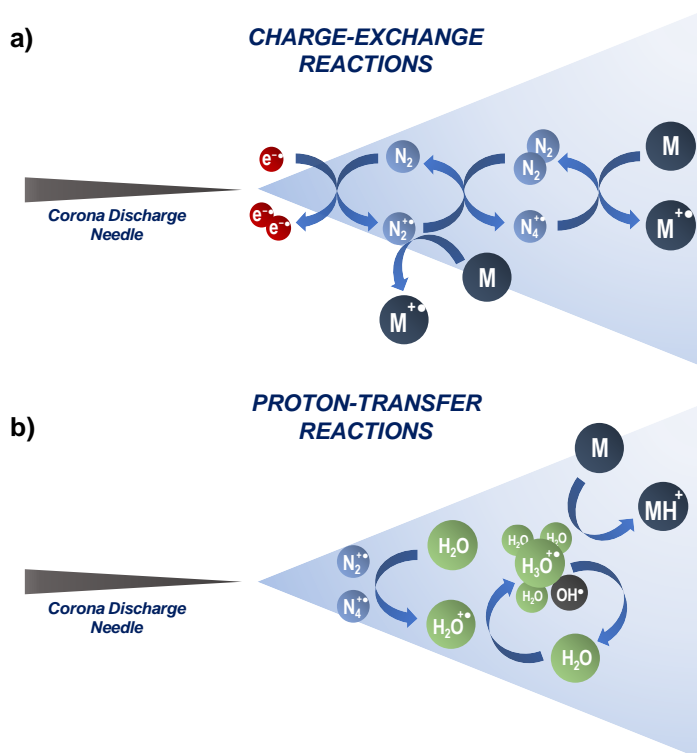

Fig. 1.12. APCI ionization mechanisms by (a) charge-exchange or (b) proton-transfer reactions (*where M: analyte*).

Portolés *et al.* [232] observed that the introduction of water vapor in the APCI source by means of an uncapped vial located within a designed holder decreases the fragmentation of several families of pesticides and made the [M+H]$^+$ ion the base peak of their mass spectra. Moreover, Wachsmuth *et al.* [233] proposed the use of a syringe pump to increase the water vapor concentration in the APCI source. The continuous infusion of water provided a very sensitive and selective method to determine methyl chloroformate derivatives.

The feasibility of this APCI source to ionize halogenated contaminants have been widely demonstrated. Highly sensitive and selective GC-APCI-MS methods have been reported for the determination of DP and analogs [113], PCBs [149–151,193] and PCDD/Fs [148,191–

193,234], all of them under charge-exchange conditions to promote the molecular ion, while the methods reported for neutral PFAS [99] demonstrated that the ionization was significantly improved under proton-transfer conditions to generate the protonated molecule. Moreover, other related halogenated pollutants such as PBDEs [143,180,186,188] and HBCD [141] have also been efficiently ionized by positive ion GC-APCI through $[M]^{+\bullet}/[M+H]^+$ overlapped clusters and $[M–Br]^+$ ions, respectively.

Atmospheric Pressure Chemical Photoionization for GC-MS Determinations

After the pioneering GC-APPI source was developed by Revelsky *et al.* [198] in 2003, different prototypes of this ion source were also developed, demonstrating the high capabilities of this ionization technique. The ion source setups of these prototypes mainly depended on the lamp position because it affects both the signal stability and the ionization efficiency. The UV lamp provides a selective ionization by releasing photons with an energy higher than the ionization potential of most analytes but lower than those of the carrier gas and the make-up gas, which significantly increases the sensitivity by reducing the background noise [235]. In this way, a krypton discharge lamp (10.0 and 10.6 eV) is commonly selected for the APPI source since it produces a more universal ionization than vacuum UV lamps (9.8 eV) [236]. Hence, the lamp in the APPI source can be positioned in 45º tangent [237] or orthogonal geometry [238]. When the lamp is fixed at 45º tangent ion source setup, the best signal stability was achieved when the eluate from the GC was directed toward the tip of the MS capillary at an angle of 45º. Later, Kersten *et al.* [239] and Kauppila *et al.* [238] reported a gas-tight vortex geometry for the APPI source. In this design, the GC-capillary outlet and the make-up gas entrance were set below the lamp and the ionization volume had a conical shape with the outlet to the MS located at the apex of the cone, which favored the main flow to generate a vortex. This vortex flow path allows a balance between the chromatographic efficiency and the residence time of compounds to achieve high ionization efficiency and prevent chromatographic band broadening. In contrast to the GC-APCI source, the GC-APPI ionization region is hermetically isolated from the surrounding environment and it allows both dopant-free and dopant-assisted ionization with high stability, low background noise, and low adduct ions formation [240]. This GC-APPI source setup idea was developed in collaboration with MasCom Technologies that, in 2013, launched the first commercially available GC-APPI source as an interface for Orbitrap mass analyzers (Fig. 1.13).

Many gas-phase reactions could be involved during the photoionization process. Since APPI is coupled to GC instruments, the inert mobile phase (He) does not participate in the ionization mechanism.
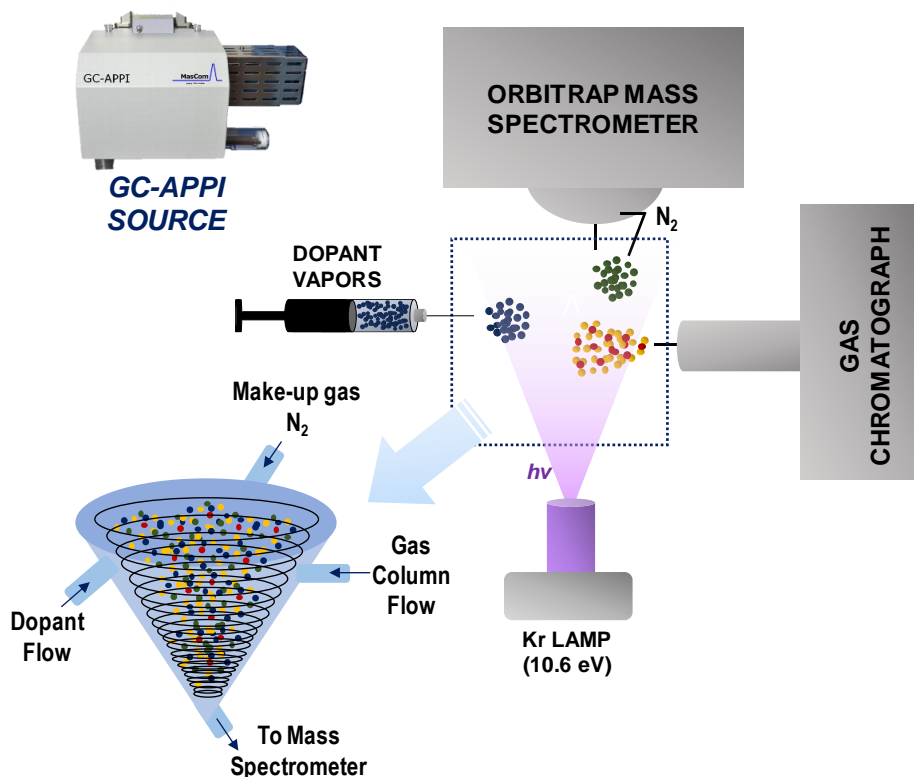
Fig. 1.13. GC-APPI source developed by MasCom Technologies based on a vortex design.

Fig. 1.14. shows the main ionization mechanisms than can usually take place in positive ion mode. If the analyte has an ionization energy (IE) lower than 10.6 eV, direct photoionization can occur due to the direct interaction with photons emitted by the krypton discharge lamp to generate the [M]$^{+•}$ ion (Fig. 1.14a). After that, a self-protonation of the analyte by reaction with the analyte radical cation could be produced to form the [M+H]$^+$ ion if the proton affinity (PA) of the molecule (M) is higher than PA of the [M-H]$^•$ radical [241]. The addition of a suitable substance (dopant, D) in relatively larger amounts than the analyte could significantly increase the ionization efficiency. For a substance to act as dopant, two different criteria must be attained:

- The substance must be photoionizable by the krypton discharge lamp (IE < 10.6 eV),
- The photoionizable specie may be able to interact with analyte molecules through proton-transfer or charge-exchange reactions, among others.

Typically, organic solvents such as toluene, acetone, chlorobenzene, tetrahydrofuran, and anisole have been considered as dopants, although other compounds such as fluorobenzene have also been evaluated.
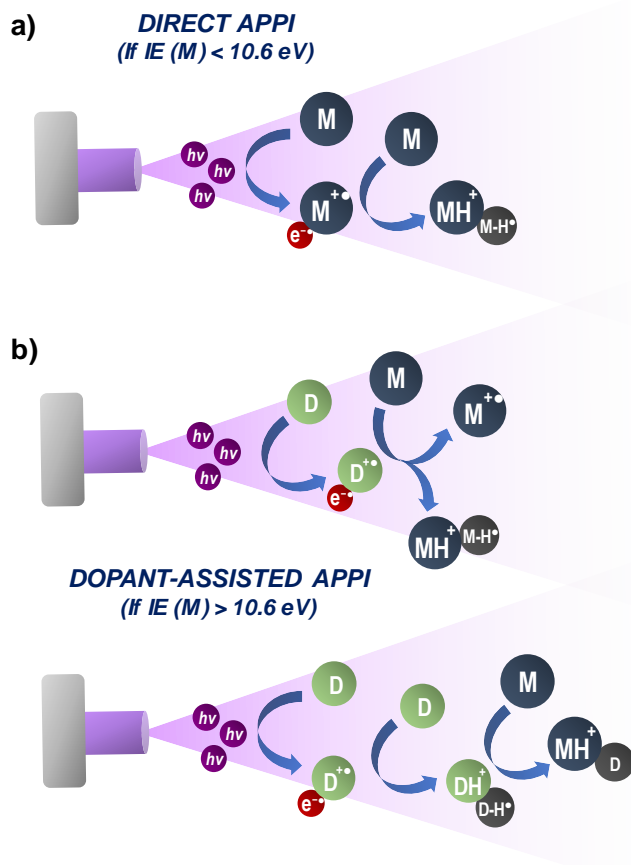
Fig. 1.14. Positive ion APPI ionization mechanisms by (a) direct or (b) dopant-assisted photoionization reactions (*where D: dopant and M: analyte*).

The dopant-assisted photoionization takes more relevance when direct photoionization processes are hindered (IE (M) > 10.6 eV) (Fig. 1.14b). However, it might be pointed out that the addition of dopants could also suppress the ionization of analytes with IEs above the IE of the dopant [238]. After the generation of the dopant radical ion during the photoionization process, it could directly interact with the neutral analyte molecule to promote charge-exchange (if IE (M) < IE (D)) or proton-transfer reactions (if PA (M) > PA ([D-H]·)). Sometimes, a self-protonation dopant reaction can occur (if PA (D) > PA ([D-H]·)) leading to the dopant protonated molecule ion [D+H]+ that may later interact with the neutral molecule by proton-transfer reactions (if PA (M) > PA (D)) [241].

Regarding the ionization mechanisms in negative ion APPI mode, the main gas-phase reactions that often take place are shown in Fig. 1.15. These gas-phase reactions must be necessarily mediated by a dopant agent, which releases electrons after the dopant photoionization process. Then, the electrons released can interact with both neutral analytes, if they have functional groups with enough electron affinity [242], or with the oxygen present in

the ion chamber to generate the superoxide ion $[O_2]^{-\bullet}$ by electron capture reactions. This superoxide ion could also interact later by charge-exchange reactions with neutral molecules (Fig. 1.15a). Additionally, the formation of the deprotonated molecule may also be enabled for analytes with low proton affinity. Indeed, proton-transfer reactions may take place due to the strong gas-phase basicity (high proton affinity) of the superoxide ion that may react with analytes to yield the deprotonated molecules [242]. Finally, clustering reactions can also take place in negative ion APPI mode. Thus, the formation of phenoxide ions $[M-X+O]^{-}$ (where X: H, Cl or Br), that can be generated even at trace concentration of oxygen in a nitrogen atmosphere, have also been reported for halogenated compounds not only for the GC-APPI source but also for negative ion GC-APCI [195] (Fig. 1.15b).
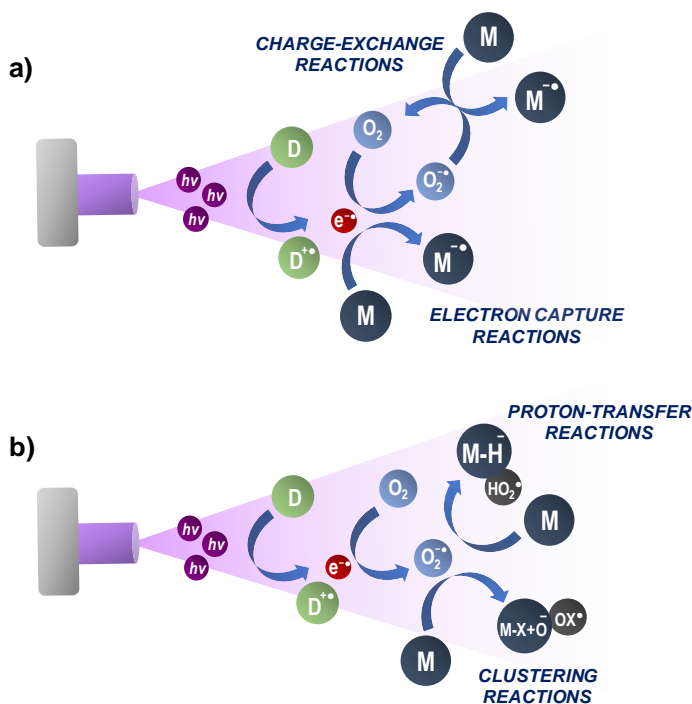

Fig. 1.15. Negative ion dopant-assisted APPI ionization mechanisms by (a) charge-exchange and electron capture reactions or (b) proton transfer or clustering reactions *(where D: dopant, M: analyte and X: H, Cl or Br)*.

Since the GC-APPI source has been recently commercialized, the number of applications is still reduced in front of the GC-APCI source, which has been launched by three different mass spectrometry companies. Most of the applications used home-made or prototype ionization sources, although they have shown a high potential for the determination of different families of compounds. The more relevant applications reported using the GC-APPI technique for the analysis of organic compounds are summarized in Table 1.8.

Table 1.8. Applications of the GC-APPI source to the analysis of organic compounds.

Type	Mode	Dopant	Mass Analyzer	Compounds	Sample	Ref.
		Ion Source				
APPI	+	Acetone	Q	Derivatized amino acids	Standards	[198]
APPI	+	–	Q	Aromatic hydrocarbons, PAHs y phthalates	Crude oil	[243]
APPI	+	Toluene	LIT-Orbitrap[a]	Volatile compounds	Perfume	[244]
APPI	+	Chlorobenzene	QqQ	Derivatized neurosteroids	Urine	[237]
APPI	+	Acetone, anisole, chlorobenzene and toluene	Orbitrap	Aromatic compounds	Standards	[238]
APPI	+	Acetone, anisole, chlorobenzene and toluene	Orbitrap	EPA contaminants	Standards	[241]
APPI	+	Toluene	Orbitrap	Volatile compounds	Crude oil	[245]
APPI	+	–	QTOF	PBDEs	Soil, sediments and dust	[143]
cAPPI	+/–	–	QIT	Volatile compounds	Standards	[246]
CPI	+	Toluene	IT	PAHs, amphetamines and steroids	Urine	[247]
µAPPI	+	Toluene	QqQ	PAHs, amphetamines and steroids	Standards	[248]
µAPPI	–	Toluene	IT	Marker PCBs	Soil	[195]
µAPPI	+	Toluene	QqQ	Selective androgen receptor modulators	Urine	[249]
µAPPI	+	Toluene	QqQ	Anabolic Steroids	Urine	[250]
µAPPI	+	Chlorobenzene	QqQ	Anabolic Steroids	Urine	[251]

[a] Linear Ion Trap-Orbitrap.

Most of the applications have been carried out in positive ion GC-APPI mode. Firstly, Revelsky *et al.* [198] evaluated the capabilities of the new ion source through the analysis of derivatized amino acids obtaining both the molecular ion and the protonated molecule for most of the compounds and achieving iLODs from 0.1 µg L^{-1} to 1 µg L^{-1} that were at least 10 times lower than those obtained using EI. Additionally, they also determined aromatic hydrocarbons, PAHs, and phthalates in crude oil obtaining the molecular ion and/or the protonated molecule for all the compounds [243]. The analysis of crude oil samples has also been investigated using the GC-APPI source. For instance, Kondyli *et al.* [245] proposed the complementary use of GC-APPI to EI in GC-MS for the characterization of the light fraction of crude oil due to the capability to ionize semi-polar and non-polar compounds. Lee *et al.* [244] reported the analysis of volatile compounds in perfume samples showing the improvement over the ionization efficiency and the reduction of oxidative ionization of analytes using dopants, while Suominen *et al.* [237] analyzed derivatized neurosteroids in urine obtaining low method limits of detection (mLODs) from 0.01 µg L^{-1} to 10 µg L^{-1} when using chlorobenzene as dopant. Kauppila *et al.* [238,241] helped to understand the dopant-assisted ionization mechanisms in GC-APPI using traditional dopant-solvents (acetone, anisole, chlorobenzene, and toluene) for aromatic compounds and other environmental contaminants, explaining differences in the ionization efficiency and the nature of the generated ions. In the case of EPA contaminants, authors reported that the use of dopants reduced the number of compounds ionized (e.g. 54/77 using toluene) but, in many cases, the response of the ionized analytes increased comparing with direct photoionization. In general, direct photoionization led to the generation of molecular ions whereas dopant-assisted photoionization also promoted charge-exchange and transfer-reactions. The best ionization efficiency was achieved for PAHs and aromatic compounds with O- and N-functional groups, while aliphatic ethers and nitro-compounds showed the worst results. Moreover, acetone showed a different behavior than toluene, chlorobenzene, and anisole since it allowed the formation of the protonated molecule for many analytes [241].

New APPI source geometries have also been developed to improve the ionization (nature and abundance of ions) and the transmission of ions to the inlet of the mass spectrometer, enhancing the sensitivity from 10 to 100-fold. Hence, capillary photoionization (CPI) [247] and capillary atmospheric pressure photoionization (cAPPI) [246] have emerged as alternatives to the GC-APPI. In both ionization sources, the photoionization process occurs in a confined capillary volume, although they differ from each other by the vacuum UV lamp (CPI: Kr UV lamp, cAPPI: DC-spark discharge VUV lamp) used and whether they use a vacuum UV glass window (usually MgF$_2$ and LiF glass windows). Both ion sources were designed for their coupling to chromatographic systems, improving the ion transmission to the MS inlet and reducing unfavorable ion-molecule reactions. CPI allows the detection of both volatile and non-volatile compounds without taking care of compound polarity since it provides additional sample heating [247] while cAPPI is only suitable for the analysis of volatile compounds [246].

Miniaturized ion source has also been tested with a focus on generation and transmission to the mass spectrometer inlet of APPI ions. The interest around miniaturized systems is growing because it implies higher sensitivity, shorter analysis time, reduced sample and solvent consumption, and lower manufacturing cost. Thus, miniaturized heated nebulizers have been performed for microchip-based APPI (μAPPI) [252] and APCI (μAPCI) [253] for both LC-MS and GC-MS coupling. The analytical determination by GC-μAPPI-MS was evaluated by Haapala *et al.* [248] analyzing PAHs, amphetamines, and steroids. The authors achieved very high detection capability (down to 0.8 fmol for benzo[a]pyrene), good repeatability, and linearity. Luosujärvi *et al.* [249] determined derivatized selective androgen receptor achieving iLODs from 0.2 μg L^{-1} to 20 μg L^{-1} and thus demonstrating the high detection capability of this ion source. Hintikka et *al.* also tested the μAPPI for the detection of anabolic steroids in urine for anti-doping control. They indicated that the use of toluene as dopant led to the generation of the protonated molecule for most of the compounds (mLODs: 0.2-1 μg L^{-1}) [250], while the use of chlorobenzene mainly favored the molecular ion formation (mLODs: 0.05-0.1 μg L^{-1}) [251].

The GC-APPI source has demonstrated a great potential to favor the ionization of organic compounds, being of great interest the evaluation of their capabilities to ionize halogenated contaminants. In fact, Luosujärvi *et al.* [195] evaluated the GC-μAPPI-MS for the determination of marker PCBs in soil samples whereas Di Lorenzo *et al.* [143] tested the GC-APPI-HRMS for the analysis of PBDEs in soil, sediment and dust samples. In both cases, the analysis of these compounds was compared with the GC-μAPCI and GC-APCI sources, respectively. Luosujärvi *et al.* [195] concluded that μAPCI was slightly more sensitive (2-3 times) while μAPPI was found to be a more repeatable ionization method for PCBs within a wider linear range than μAPCI. On the other hand, Di Lorenzo *et al.* [143] demonstrated that the ionization of PBDEs by GC-APPI only generated the molecular ion in contrast to the overlapped isotope clusters of [M]$^{+\bullet}$ and [M+H]$^+$ ions observed in the GC-APCI source and thus leading to higher iLODs. Besides, some photooxidation products were also observed in the positive ion GC-APPI mode, which may help with the differentiation of critical PBDE isomers. These recent findings highlight the important advantages that GC-APPI could have over the already reported methodologies for the detection and quantification of halogenated organic contaminants in environmental samples.

CHAPTER 2.

DETERMINATION OF FLUORINATED ORGANIC COMPOUNDS

CHAPTER 2.DETERMINATION OF FLUORINATED ORGANIC COMPOUNDS

In this chapter, the performance of atmospheric pressure ionization sources is studied for the development of reliable LC-MS/MS and GC-HRMS methods to the accurate determination of neutral PFAS, including fluorotelomer alcohols and olefins, perfluoroalkyl sulfonamides and sulfonamido-ethanols, in water samples. To achieve this goal, ionization behavior of target compounds is thoroughly explored using API sources, such as ESI, APCI, and APPI sources for LC-MS/MS determinations, while the use of novel GC-APPI source is examined for GC-HRMS analysis opening the door to couple GC to a Quadrupole-Orbitrap mass spectrometer. The methodologies proposed are studied from the point of view of evaluating the ionization behavior of these families of compounds by selecting the most appropriate mobile phase composition (for LC-MS determinations) and ionization source conditions to achieve maximum sensitivity and selectivity in the determination of the target compounds. Additionally, the fragmentation pathways of ions generated for neutral PFAS in the API sources were also investigated to provide useful tools and rules for the identification of these analytes and related compounds in environmental, food, or biological samples of great interest.

This chapter includes a brief introduction about PFAS, including their main physicochemical properties, their production and uses, their classification, and both the analytical determination issues and the environmental occurrence of those neutral PFAS included in this Thesis. Furthermore, this chapter also contains an experimental and results section with four research publications. Two of them propose methodologies based on APPI (*Article I*) and APCI (*Article II*) ionization for the UHPLC-MS/MS determination of PFAS in river waters. A third publication is devoted to the study of tandem mass spectrometry fragmentation of the ions generated for neutral PFAS in API sources to propose for the first time tentative fragmentation pathways of these compounds (*Article III*). Finally, the last article studies the implementation of a novel GC-APPI source for the development of a GC-HRMS (Quadrupole-Orbitrap) methodology for the determination of PFAS in water samples (*Article IV*). This chapter ends with a cross-sectional discussion of the results obtained in these research publications.

2.1. Introduction

As defined by Buck *et al.* [254], "*PFASs are aliphatic substances containing one or more C atoms on which all the H substituents (present in the nonfluorinated analogues from which they are notionally derived) have been replaced by F atoms, in such a manner that they contain the perfluoroalkyl moiety $C_nF_{2n+1}–$*". Since 1950, PFAS as well as surfactants and polymers made from them, have been used in many applications. PFAS have unique biological and physicochemical properties mainly due to the high-energy carbon-fluoride bond and the high electronegativity of fluorine atoms that confer strength and stability to these bonds [255]. These characteristics contribute to the high chemical and thermal stability of the PFAS perfluoroalkyl moiety that, in combination with the lipophilic and hydrophobic characteristics, make them suitable for a wide range of applications. Thus, PFAS have been extensively used in industrial and household applications, including aqueous fire-fighting foams, surfactants, lubricants, pesticides, water, and stein-resistance coatings (in textile products or packaging materials) as well as the production of fluoropolymers, among others [256].

Historically, two main manufacturing processes have been carried out to synthesize compounds containing perfluoroalkyl chains:

- *Electrochemical fluorination:* this process was licensed by 3M company and it consists of submerging an organic raw material (e.g., octane sulfonyl fluoride) in anhydrous hydrogen fluoride solution and subjecting it to an electric current to favor the exchange of H atoms by F atoms. This is not a selective process and leads to isomeric and short-perfluoroalkyl chain by-products [257].

- *Telomerization:* this process was firstly developed by Haszeldine in 1949 [258] and further adapted by DuPont company in 1969 [259]. It consists of the addition of tetrafluoroethylene to a perfluoroalkyl iodide (PFAI), generally perfluoroethyl iodide, to generate a mixture of linear perfluoroalkyl iodides and the later substitution of the iodide by an appropriated functional group, depending on the application. Nowadays, this is the process most widely used for PFAS production.

Because of the widespread use of PFAS and their emission, a broad range of them has been detected in the environment, wildlife, and human beings. This global spread was firstly demonstrated by Giesy and Kannan in 2001 [260], which reported the occurrence of PFOS in wildlife. At the same time, Hansen *et al.* [261] discovered the presence of PFOS, PFOA and other PFAS in human blood, suggesting that PFAS were responsible for a significant fraction of the organic fluorine detected in human serum in earlier pioneering studies in humans not occupationally exposed to PFAS. Thus, 3M company, after negotiations with the U.S. EPA, announced that it would voluntarily phased-out its C_8-based production at the end of 2002 [262]. Additionally, in 2006, eight leading companies reached an agreement to submit baseline data on emissions from their facilities and the content of PFOA and related chemicals in their

products. The PFOA Stewardship Program involved ambitious goals, including a 95% reduction in the emissions and product content by 2010 and the removal of these chemicals from industrial processing by 2015 [263]. A similar agreement was also ratified in Canada where Environment Canada, Health Canada, and some of these companies signed in 2010 the "*Environmental Performance Agreement Respecting Perfluorocarboxylic Acids (PFCAs) and their Precursors in Perfluorinated Products Sold in Canada*" [264]. The Organization for Economic Co-operation and Development (OECD) also created a global per- and polyfluorinated chemicals group to "*consider the development, facilitation and promotion in an open, transparent and inclusive manner of national and international stewardship programmes and regulatory approaches to reduce emissions and the content of relevant perfluorinated chemicals of concern in product and to work toward global elimination, where appropriate and technically feasible*" [265]. All these actions and the inclusion of the persistent PFOS and PFOA in the Stockholm Convention list [266,267] led to the restriction on the production of PFAS under regional, national or international regulatory frameworks. These global actions to phase-out legacy PFAS have resulted in compensatory usage of alternative fluorinated compounds that would be inevitably released into the environment [268]. Thus, relevant international scientists and regulators have been discussing future directions on the regulation and management of PFAS. They recommend global cooperation on more streamlined research, including prioritizing certain substances, adopting a group-based approach instead of studying individual substances, and updating regulations for highly-persistent PFAS [269].

As it was mentioned in the introduction of this Thesis (*Section 1.1*), more than 6,300 PFAS have been detected in the last decades, drawing great attention since they have a wide variety of molecular structures. Until now, both Buck *et al.* [254] and the OECD [270] have proposed classifications for PFAS and they are today among the most accepted ones. Taking into account the advantages of both classifications, Fig. 2.1 shows the new classification proposed to consider all families of compounds discovered until now. Generally, PFAS are classified into fluorinated polymers and non-polymer per- and polyfluoroalkyl substances. Regarding fluorinated polymers, they can be divided into fluoropolymers, perfluoropolyethers (PFPEs), and side-chain fluorinated polymers. Fluoropolymers, which are normally used as plastics, are only based on fluorocarbon-only polymer backbone (e.g., polytetrafluoroethylene). On the other hand, PFPEs are polymers in whose fluoroalkyl backbone units are separated by oxygen atoms and have been functionalized with a hydrophilic group. These functionalized PFPEs are marketed for surface protection treatments on natural stone, metal, glass, plastic, or paperboard treatment for food-contact applications, among others. In contrast to these polymers, side-chain fluorinated polymers are constituted partly by a non-fluorinated polymer backbone and partly by a fluoroalkyl chain. These polymers are mainly employed as surfactants and products for surface protection. Concerning non-polymer PFAS, they could be classified into perfluoroalkyl and polyfluoroalkyl substances. Among the first one, most of perfluoroalkyl acids (PFAAs) have been commercialized as surfactants or used as "processing aid" in the manufacture of fluoropolymers, especially PFCAs and PFSAs. These families of

compounds include known persistent PFAS such as PFOA and PFOS. Other perfluoroalkyl families such as perfluoroalkane sulfonyl fluorides (PASFs), perfluoroalkanoyl fluorides (PFAs), or perfluoroalkyl iodides (PFAIs) are the major raw material for the manufacturing of surfactants and products for surface protection, while perfluoroalkyl aldehydes (PFALs) are intermediate environmental transformation products.

On the other hand, non-polymer polyfluoroalkyl substances mainly involve three different groups of PFAS: (i) perfluoroalkane sulfonamido substances (PASF-based derivatives), (ii) fluorotelomer-based substances (FT-based derivatives), and (iii) polyfluoroalkyl ether-based substances (PFPE-based derivatives). Perfluoroalkane sulfonamido substances are mainly manufactured from PASFs (Fig. 2.2a). Although PASFs could generate PFSAs by direct hydrolysis, they are mainly transformed into *N*-alkyl perfluoroalkane sulfonamides (FASAs) by reacting them with an amine compound. These FASAs are sometimes commercialized, like *N*-EtFOSA (also known as the pesticide sulfluramid), but they can also be reacted with ethylene carbonate to give *N*-alkyl perfluoroalkane sulfonamido-ethanols (FASEs) [271,272]. As FASEs have an alcohol group, they can be transformed in *N*-alkyl perfluoroalkane sulfonamido-ethyl acrylates (FASACs) and methacrylates (FASMACs), as well as into phosphates and other derived products. FASACs and FASMACs are generally used as co-monomers to synthesize commercially available acrylic polymers for surface protection applications [271]. All these PFAS are also the main building blocks of fluorochemical products for surface treatment and protection of paper packaging [254]. In the same way as the PASFs for perfluoroalkane sulfonamido substances, PFAIs and fluorotelomer iodides (FTIs) are raw materials to produce FT-based derivatives (Fig. 2.2. b). For instance, FTOs, which are widely used to manufacture PFCAs or silanes, are produced by dehydrohalogenation of FTIs, but they might also be generated as an impurity during the synthesis of FTOHs. Meanwhile, FTOHs are the major raw material in the production of fluorotelomer acrylates (FTACs) and methacrylates (FTMACs), that are further copolymerized to manufacture side-chain fluorinated polymers [255]. Fluorotelomer mono- (monoPAPs) and diphosphates (diPAPs), which can also be formed from FTOHs, are commercial fluorinated surfactants that are used as grease-proofing agents for food-contact paper. Although most of PASF- and FT-based derivatives have shown low toxicity, their degradation has been reported as a potential source of PFSA and PFCA release into the environment, respectively. The occurrence of these compounds in the environment, especially FASAs, FOSEs, FTOHs, FTOs, monoPAPs, and diPAPs, has been extensively reported in the last decades [254]. Finally, and as mentioned in Section 1.1, another subgroup consists of PFPE-based derivatives, such as polyfluoroalkyl ether carboxylic (PFECAs) and sulfonic acids (PFESAs), has been recently used for replacing the persistent PFOA and PFOS in the manufacture of fluoropolymers.
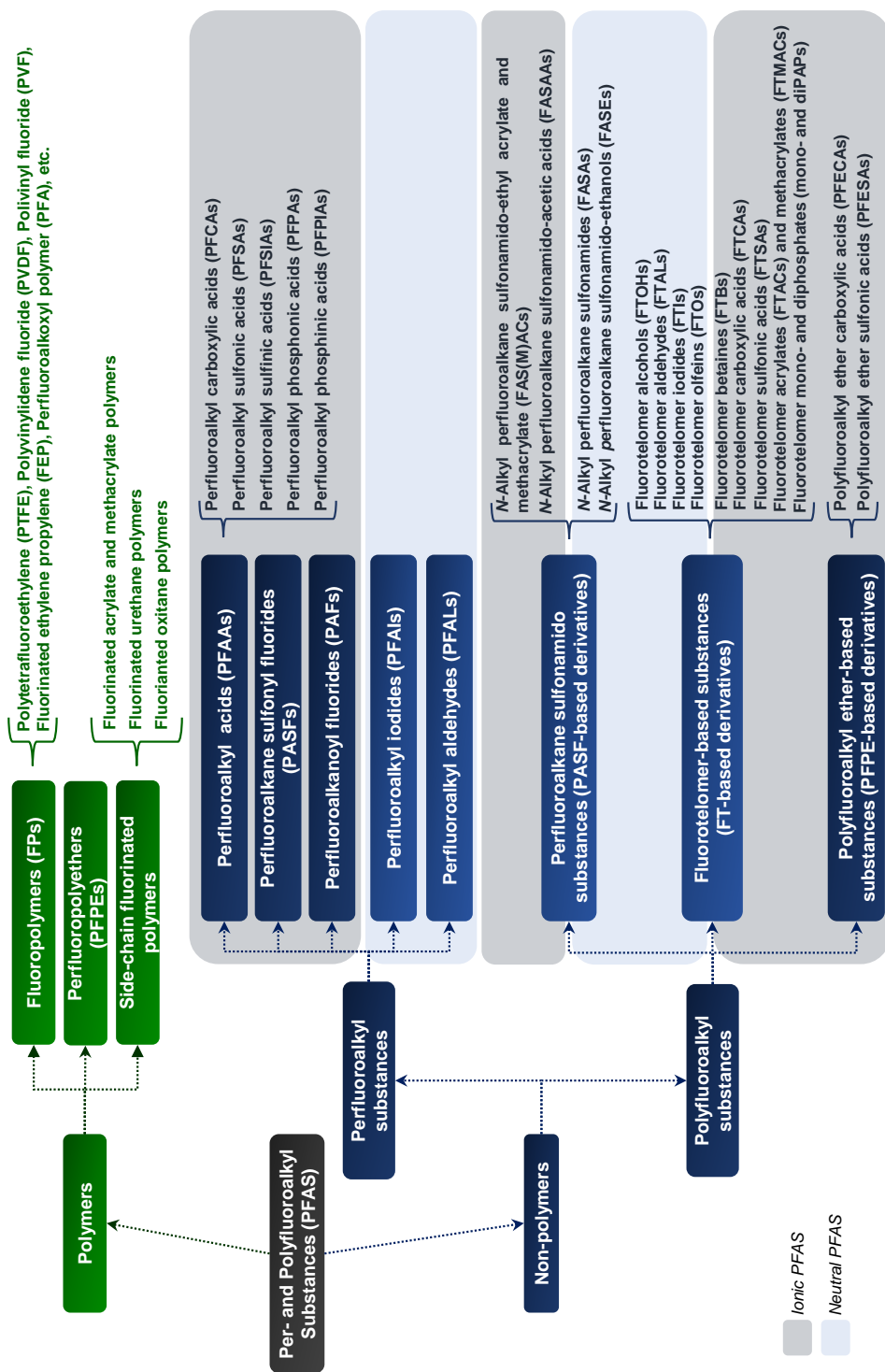
Fig. 2.1. Classification of main PFAS families based-on their chemical structure.
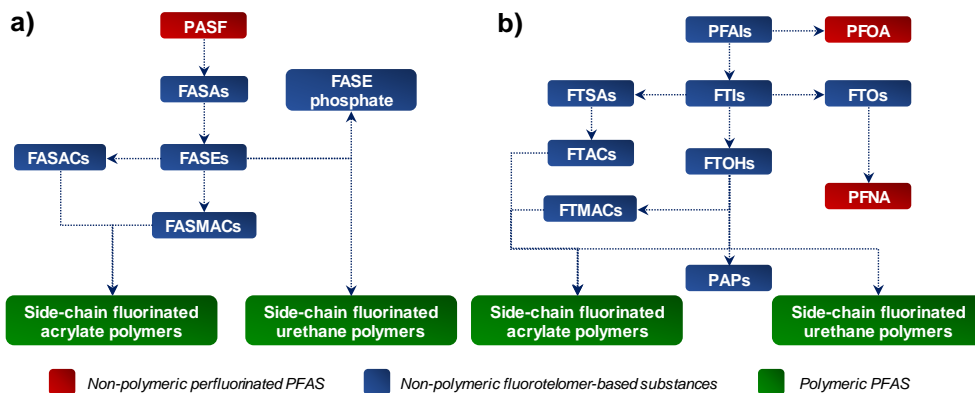
Fig. 2.2. Synthesis of a) perfluoroalkane sulfonamido substances *(from PASF with 8 C atoms)* and b) PFCAs and fluorotelomer-based substances *(from PFAI with 8 C atoms)*.

Regarding the toxicity of PFPE-based derivatives, it remains unclear, although it is suggested that some of these compounds, like F-53B (Cl-PFESA), have acute toxicity similar to PFOS [14], while ADONA may be less toxic than PFOA or PFOS [273–275]. Although information related to their toxicology, occurrence, and environmental fate is incomplete, less bioaccumulation may be expected for PFPE-based derivatives compared to legacy PFAS due to the presence of alkyl ether linkages (C-O-C) in the fluoroalkyl chain, as indicated by the REACH criterion for highly bioaccumulative substances [276]. However, a recent study has shown the high occurrence of 6:2 Cl-PFESA in human samples [19]. Thus, this compound could have a higher bioaccumulation potential than PFOS [277,278], becoming a new potential environmental threat.

In the early stages of PFAS research, analytical methods were mainly developed for the analysis of legacy PFAS, including PFOS and PFOA, in various matrices such as air, water, solid matrices, human samples and wildlife [11]. According to the shift toward manufacturing alternatives, recent research has focused on the identification of new PFAS and the development of analytical methods that can detect, characterize, and determine these new chemicals [279]. However, cost-effective analytical methods that can cover a wide range of PFAS families have been difficult to develop [280]. In this way, establishing fragmentation pathways could help in the detection and characterization of new related PFAS.

In general, the analytical determination of PFAS has been usually carried out by liquid chromatography coupled to mass spectrometry using electrospray ionization and operating in negative ion mode [11,268]. In fact, U.S. EPA reported a methodology for the determination of PFAS in drinking water by LC-MS/MS using the ESI source and a solid-phase extraction method for sample treatment [281]. This methodology is suitable for PFAS, such as legacy PFAS and novel alternatives (PFECAs, PFESAs, etc.) since they are ionic compounds. Nevertheless, as explained above (*Section 1.2.1*), neutral PFAS usually show ionization difficulties by ESI in negative ion mode, especially FTOHs and FOSEs, due to ion suppression

induced by buffers used in the mobile phase [8,282]. Some neutral PFAS like FTOs cannot even be ionized by ESI, requiring other ionization techniques to allow their detection. Thus, the use of gas chromatography coupled to mass spectrometry has been widely recommended for the determination of these families of neutral PFAS (FTOs, FTOHs, FOSAs, and FOSEs) [11]. Nonetheless, high-vacuum ionization techniques (EI and CI) have shown a low ionization efficiency, which may lead to difficulties in detecting these compounds [283]. At the same time, the high volatile FTOs are generally poorly retained in gas chromatography, compromising their determination [137,284,285]. Moreover, the joint determination of these compounds is challenging due to their physicochemical properties and structural differences, requiring from different methodologies to achieve their detection. Thus, the evaluation of other chromatographic and ionization techniques could provide reliable alternatives for a sensitive and selective determination of these compounds at those low concentration levels (pg L^{-1}) frequently found in environmental samples.

The occurrence of the neutral PFAS evaluated (FTOs, FTOHs, FOSAs, and FOSEs) depends on the matrices analyzed. Regarding the consumer products containing PFAS, they cover a wide range of goods intended for both human consumption and use, such as food contact materials, cleaning agents, lubricants, waxes, outdoor textiles, or carpets, among others. The highest concentration levels of neutral PFAS have been reported in liquid products including lubricants, cleaning agents, and impregnation sprays. For instance, Kotthoff *et al.* [286] determined levels of FTOHs ranging from 19 to 146.2 mg kg^{-1} in impregnation sprays while Favreau *et al.* [287] reported levels of FTOHs from 2 to 1,840 mg kg^{-1} in waterproofing and protector materials as well as high concentrations of FTOHs (2-180 mg kg^{-1}), FOSAs (0.1-11.7 mg kg^{-1}) and FOSEs (0.2-494 mg kg^{-1}) in aqueous film-forming foams. Gremmel *et al.* [172] also reported the presence of FTOHs and FOSEs in outdoor jackets at concentrations up to 516 µg m^{-2} and 5.02 µg m^{-2}, respectively. Neutral PFAS, especially FTOHs, have also been detected in non-stick cookware and microwave popcorn packaging materials as well as in different kinds of food contact materials. Thus, Liu *et al.* [288] identified FTOHs at concentrations up to 12.7 mg kg^{-1} in treated food contact paper, while Yuan *et al.* [289] reported concentrations of these compounds ranging from 0.08 to 93.50 mg kg^{-1} in popcorn bags.

Despite of the high amounts of these compounds in consumer products, they are identified at very low concentration levels in the environment. The different families of neutral PFAS are widely distributed according to their physical properties (Fig. 2.3). As FTOs, FTOHs, FOSAs, and FOSEs are semi-volatile compounds, their presence has been widely reported in air samples. Thus, Xie *et al.* [290] determined concentration levels ranging from 2.3 to 75 pg m^{-3} for FTOHs, from 1.0 to 21 pg m^{-3} for FOSAs, and from 0.3 to 8.6 pg m^{-3} for FOSEs in air samples from the North Sea. These concentration levels were lower than those obtained in Asian countries such as Japan, India, China, or Taiwan. Li *et al.* [285] reported similar median concentration levels in Asian countries for FOSEs (2.27-16.4 pg m^{-3}) and FOSAs (0.96-7.40 pg m^{-3}) and higher median concentration levels for FTOHs (3.31-709 pg m^{-3}), especially for

the 8:2 FTOH. Additionally, 8:2 FTO was also identified at median concentrations ranging from 46.2 to 401 pg m^{-3}. These concentrations exponentially increase when analyzing indoor air samples as it has been reported for FTOs, FTOHs, FOSAs and FOSEs (114-6,626 pg m^{-3}) in Tromsø (Norway) [137], and in Singapore for FTOHs, FOSAs, and FOSEs (77-10,458 pg m^{-3}) [291].
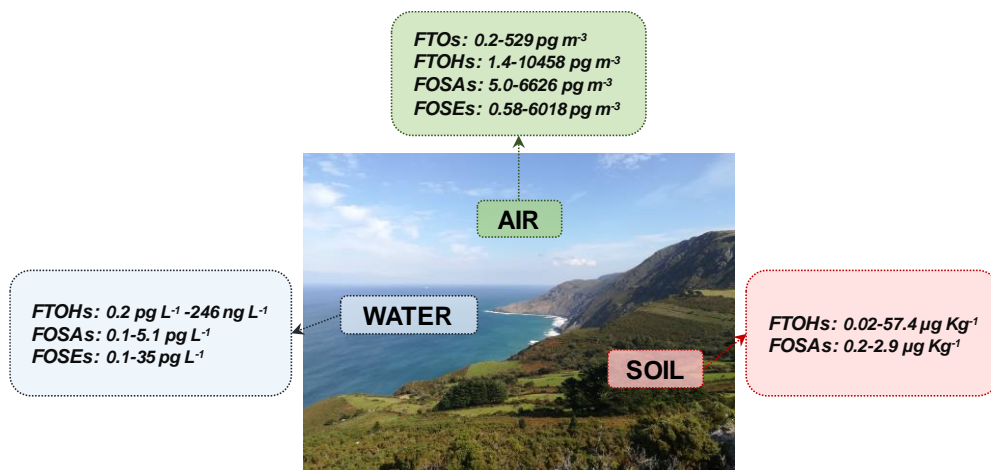

Fig. 2.3. Environmental occurrence of FTOs, FTOHs, FOSAs and FOSEs.
[99,105,295,296,120,137,285,290–294].

Regarding soil and sediment samples, the presence of some of these families of compounds has also been found, especially for FTOHs and *N*-EtFOSA. For instance, Zhang *et al.* [294] reported the presence of 6:2 FTOH and 8:2 FTOH in biosolids-amended soils and plants (1.74-57.4 µg kg^{-1} dry weight, dw), whereas Zabaleta *et al.* [296] and García-Valcárcel *et al.* [293] detected *N*-EtFOSA in cultivated carrots (2.9 µg kg^{-1}) and sludge amended soil (0.2 µg kg^{-1}), respectively. Concentration levels of main FTOHs (4:2 FTOH, 6:2 FTOH, 8:2 FTOH, and 10:2 FTOH) have also been reported in sediment samples from Liaodong Bay (0.02-0.26 µg kg^{-1} dw) [120].

Nonetheless, the lowest levels of these families of neutral PFAS are found in water samples. For instance, Portolés *et al.* [99] detected the presence of FTOHs (45-97.5 pg L^{-1}), FOSAs (1.0-3.5 pg L^{-1}) and FOSEs (1.5-20.5 pg L^{-1}) in river water and wastewater samples from Barcelona (Spain) while relatively higher concentrations of 8:2 FTOH were found in surface water from a river located at 40 km from a fluoropolymer manufacturing plant in France (102-246 ng L^{-1}) [105]. Chen *et al.* [295] investigated the occurrence of FTOHs in wastewater from China (0.15-12.4 ng L^{-1}), being 8:2 FTOH the predominant neutral PFAS. Mahmoud *et al.* [292] also detected FTOHs in surface water (1.09-9.17 ng L^{-1}), waste water treatment plant effluents (5.08-17.4 ng L^{-1}), as well as in rainwater (0.3-3.18 ng L^{-1}) from Japan, demonstrating their capability to be incorporated into water environmental compartment from the air.

Considering the importance of water resources for humans and wildlife, the releases of these compounds to the rivers, but also taking into account the difficulties and the drawbacks of the available analytical methodologies, the capabilities of API sources to develop selective and sensitive LC-MS and GC-MS methods for the determination of neutral PFAS in environmental water samples have been evaluated in this chapter of the Thesis. Additionally, the fragmentation of these classes of compounds under tandem mass spectrometry has also been thoroughly studied to establish the fragmentation pathways and identify common product ions and neutral losses to help on the identification of the increasing number of new families of PFAS detected in the environment.

2.2. Experimental work and results

This section includes four publications related to the determination of neutral PFAS. The *Article I,* entitled "*Negative-ion atmospheric pressure ionisation of semi-volatile fluorinated compounds for ultra-high performance liquid chromatography tandem mass spectrometry analysis*" lies on the evaluation of the ionization of neutral PFAS (FTOHs, FOSAs, and FOSEs) using different API techniques (ESI, APCI, and APPI) to achieve their sensitive and selective determination in surface river water samples. Additionally, the *Article II* entitled "*Gas chromatography and liquid chromatography coupled to mass spectrometry for the determination of fluorotelomer olefins, fluorotelomer alcohols, perfluoroalkyl sulfonamides and sulfonamido-ethanols in water*" comprises a comparative study of both chromatographic systems (GC *vs.* UHPLC) and ionization techniques (high-vacuum ionization techniques *vs.* API sources) for the determination of FTOs, FTOHs, FOSAs and FOSEs in river water samples. This was the first time that FTOs were ionized using API techniques.

On the other hand, this section also includes the article entitled "*Fragmentation studies of neutral per- and polyfluoroalkyl substances by atmospheric pressure ionization-multiple stage mass spectrometry*" (*Article III*) that describes the fragmentation pathways of the ions generated by these compounds in API sources to establish fragmentation pathways and to identify common fragment/product ions that could help in the identification of currently known PFAS and new related PFAS in real samples. Finally, *Article IV* entitled "*A novel methodology for the determination of neutral perfluoroalkyl and polyfluoroalkyl substances in water by gas chromatography-atmospheric pressure photoionization-high resolution mass spectrometry*" reports for the first time the application of the APPI source for the GC-HRMS determination of neutral PFAS in water samples. This article combines the advantages of APPI over the ionization efficiency of neutral PFAS, the separation capacity of gas chromatography, and the sensitivity and selectivity of a high-resolution mass spectrometer such as Orbitrap to determine these compounds at ultra-trace levels. Moreover, GC-APPI-HRMS (Orbitrap) was combined with a powerful headspace solid-phase microextraction to ensure a selective extraction, avoiding evaporation steps that could cause losses of the most volatile analytes.

2.2.1. Article I

Negative-ion atmospheric pressure ionisation of semi-volatile fluorinated compounds for ultra-high-performance liquid chromatography tandem mass spectrometry analysis

Juan F. Ayala-Cabrera, F. Javier Santos, Encarnación Moyano

Analytical and Bioanalytical Chemistry, (**2018**) 410: 4913-4924

RESEARCH PAPER

CrossMark

Negative-ion atmospheric pressure ionisation of semi-volatile fluorinated compounds for ultra-high-performance liquid chromatography tandem mass spectrometry analysis

Juan F. Ayala-Cabrera[1] · F. Javier Santos[1,2] · Encarnación Moyano[1,2]

Abstract

In this work, the feasibility of negative-ion atmospheric pressure chemical ionisation (APCI) and atmospheric pressure photoionisation (APPI) for ultra-high-performance liquid chromatography tandem mass spectrometry (UHPLC-MS/MS) determination of fluorotelomer alcohols (FTOHs), fluorinated octanesulfonamides (FOSAs) and fluorinated octanesulfonamido-ethanols (FOSEs) was evaluated. The study of the effect of mobile phase composition on the atmospheric pressure ionisation of these compounds indicated that methanol/water mixtures provided the best responses in APCI, while acetonitrile/water with a post-column addition of toluene as dopant was the most appropriated mixture in APPI. Under the optimal working conditions, most of the target compounds produced the ion $[M–H]^-$ as base peak, although in-source collision-induced dissociation fragment ions in APCI and APPI and superoxide adduct ions $[M+O_2]^{-\bullet}$ in APPI were also present. These ions proved to be more useful as precursor ions for MS/MS determination than the adduct ions generated in electrospray. Although the UHPLC-APCI-MS/MS method allowed the determination of these semi-volatile compounds at low concentration levels, the analysis by UHPLC-APPI-MS/MS provided the lowest limits of detection and it was applied to the analysis of water samples in combination with solid-phase extraction. Quality parameters demonstrated the good performance of the proposed method, providing low method limits of detection (0.3–6 ng L^{-1}), good precision (RSD % < 5%) and an accurate quantification (relative error % < 14%). Among the river water samples analysed by the developed method, 4:2 FTOH and *N*-EtFOSA were determined at 30 and 780 ng L^{-1}, respectively.

Introduction

Per- and polyfluorinated alkyl substances (PFASs) comprise a large group of chemicals that have been produced for more than 50 years. They consist on a hydrophilic group attached to an alkyl chain of variable length where the hydrogen atoms

✉ Encarnación Moyano
  encarna.moyano@ub.edu

1   Department of Chemical Engineering and Analytical Chemistry, University of Barcelona, Av. Diagonal 645, 08028 Barcelona, Spain

2   Water Research Institute (IdRA), University of Barcelona, Montalegre 6, 08001 Barcelona, Spain

are either completely (perfluorinated) or partially (polyfluorinated) replaced by fluorine atoms. Carbon-fluorine is one of the strongest covalent bonds, providing stability to PFASs, making them resistant to biodegradation and increasing their presence in the environment [1–3]. These characteristics make them suitable for their use in a wide range of industrial and commercial applications [4, 5].

Nevertheless, there is a concern regarding the potential toxicity of some PFASs, such as perfluorooctanoic acid (PFOA) and perfluorooctanesulfonic acid (PFOS), since they cause estrogenic effects in living organisms. This fact and their persistent and bioaccumulative properties [1] have led the Stockholm Convention to include PFOS in the annex B of the list of persistent organic pollutants, while PFOA is still under revision [6, 7]. As a consequence, classical PFASs are being substituted in industrial and commercial applications by semi-volatile fluorinated compounds, such as fluorinated

⦚ Springer

alkyl sulfonamides (FASAs), fluorinated alkyl sulfonamido-ethanols (FASEs) and fluorotelomer alcohols (FTOHs), among others. However, the chemical and biological degradation of these other PFASs into the persistent PFOA and PFOS [4], in addition to their growing use and potential risk to human health, have led to an interest in their environmental occurrence.

Gas chromatography coupled to mass spectrometry (GC-MS) [8–10] and liquid chromatography tandem mass spectrometry (LC-MS/MS) [11–13] are the techniques most commonly used for the determination of these semi-volatile PFASs. Their GC separation is usually achieved using polar stationary phases, and electron ionisation and chemical ionisation techniques have been widely employed for their MS detection [14, 15]. Nevertheless, GC-MS methods provide relatively high limits of detection due to poor ionisation efficiency [16–18]. Thus, reversed-phase LC coupled to MS/MS is presented as an alternative to GC-MS, being the electrospray ionisation (ESI) technique most frequently used for the determination of these compounds. Under negative-ion ESI conditions, FASAs are easily ionised, yielding abundant [M–H]⁻ ions, while FTOHs and FASEs only generate carboxylate adduct ions [M+RCOO]⁻ [12]. Unfortunately, the fragmentation by collision-induced dissociation (CID), in the collision cell, of these adduct ions leads to non-characteristic product ions as [RCOO]⁻, which limits the confirmation capabilities of ESI. The use of other atmospheric pressure ionisation (API) sources such as atmospheric pressure chemical ionisation (APCI) or atmospheric pressure

photoionisation (APPI) could be an excellent alternative to overcome the limitations of the existing LC-ESI-MS/MS methods. However, to our knowledge, there is only one article that uses APPI for the analysis of some of these compounds, but it is mainly focused on the reduction of matrix effect observed in ESI [17]. Therefore, there is a need for more information on the ionisation of FTOHs, FASAs and FASEs by APCI and APPI. Recently, the use of GC-APCI(+)-MS/MS has also been reported [19], showing the feasibility of APCI for the ionisation of these compounds.

The aim of the present work was to assess the applicability of APCI and APPI for the efficient ionisation of FTOHs, fluorinated octanesulfonamides (FOSAs) and fluorinated octanesulfonamido-ethanols (FOSEs), since some of them show ionisation problems when using electron and chemical ionisation and even ESI. These studies were the base for the development of a new selective and sensitive UHPLC-MS/MS method for the determination of the semi-volatile fluorinated compounds in river water samples.

Materials and methods

Reagents and standards

FTOHs, FOSAs and FOSEs have been selected as target compounds for this study (Fig. 1). Fluorotelomer alcohols, $1H,1H,2H,2H$-perfluorohexan-1-ol (4:2 FTOH), $1H,1H,2H,2H$-perfluorooctan-1-ol (6:2 FTOH) and $1H,1H,2H,2H$-perfluoro-7-trifluoromethyl-octan-1-ol (7-Me-

Fig. 1 Chemical structure of studied semi-volatile fluorinated compounds

n	R	Compound
3	–F	4:2 FTOH
5	–F	6:2 FTOH
5	–CF₃	7-Me-6:2 FTOH
7	–F	8:2 FTOH
9	–F	10:2 FTOH

FTOHs

R	Compound
–CH₃	N-MeFOSA
–C₂H₅	N-EtFOSA

FOSAs

R	Compound
–CH₃	N-MeFOSE
–C₂H₅	N-EtFOSE

FOSEs
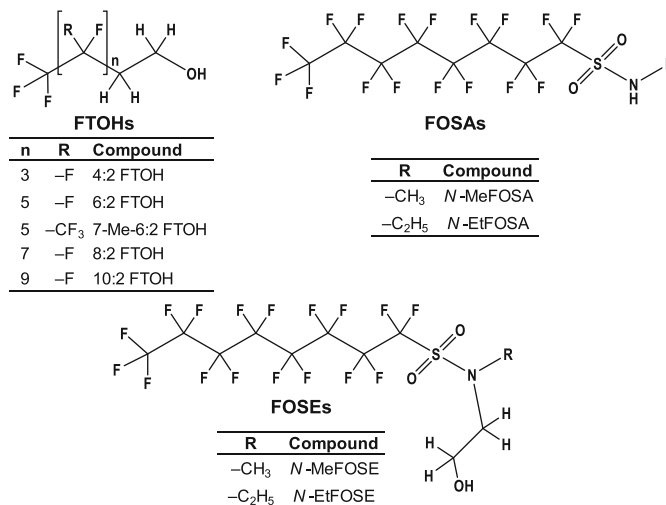
6:2 FTOH), were supplied by Fluorochem, Ltd. (Derbyshire, UK), while 1H,1H,2H,2H-perfluorodecan-1-ol (8:2 FTOH) and 1H,1H,2H,2H-perfluorododecan-1-ol (10:2 FTOH) were purchased from Alfa Aesar GmbH & Co KG (Karlsruhe, Germany) at a purity higher than 96%. Individual stock standard solutions (1000 mg L^{-1}) of each compound were prepared in acetonitrile from their respective pure standard. 2-(N-Methylperfluoro-1-octanesulfonamido)-ethanol (N-MeFOSE), 2-(N-ethylperfluoro-1-octanesulfonamido)-ethanol (N-EtFOSE) and N-methylperfluoro-1-octanesulfonamide (N-MeFOSA) were supplied by Wellington Laboratories, Inc. (Guelph, Ontario, Canada) as individual standard solutions (50 mg L^{-1} in methanol, ≥ 98%), while N-ethylperfluoro-1-octanesulfonamide (N-EtFOSA) (99%) was obtained from Dr. Ehrenstorfer GmbH (Augsburg, Germany). Standard mixtures of all compounds were obtained by dilution of the stock standard solutions in acetonitrile/water (1:1, v/v) and stored at 4 °C until their analysis.

Acetonitrile, methanol and water (LC-MS Chromasolv® grade) were purchased from Sigma-Aldrich (St. Louis, MO, USA) for preparing mobile phases. Dopants such as toluene and chlorobenzene (Chromasolv® Plus for HPLC) were obtained from Sigma-Aldrich, anisole and acetone (pesticide residue analysis grade) were supplied by Fluka® Analytical (St. Louis, MO, USA) and tetrahydrofuran (Photrex™ Reagent) was purchased from J.T. Baker (Deventer, Holland). All solvents were of purity higher than 99.8%.

Formic acid (≥ 98%) and acetic acid (≥ 99.7%) were purchased from Sigma-Aldrich while ammonium hydroxide (33%) was obtained from J.T. Baker. They have been used as mobile phase additives. Moreover, ultra-pure water was obtained from a Milli-Q system coupled to an Elix 3 (Millipore, Bedford, MA, USA).

Argon (≥ 99.999%) was supplied by Air Liquide (Madrid, Spain) and was employed as collision gas in tandem mass spectrometry experiments, while nitrogen (> 99.995%) was purchased from Linde (Barcelona, Spain) and was used as auxiliary and nebuliser gas in the API sources.

Samples

Surface water samples were collected from river sampling sites near to industrialised and rural areas in Catalonia (Spain). They were used to demonstrate the applicability of the developed method for the analysis of semi-volatile fluorinated compounds. Two samples were sampled in the Llobregat River (Barcelona, Spain), which runs through very densely populated and industrialised areas, receiving large urban and industrial wastewater discharges from more than three million habitants. They were collected at the lower section of the Llobregat River, before and after the industrialised region of Sant Boi-Cornellà. Another two samples were collected at the Ebro River, before and after the industrial area

near Tortosa (Tarragon, Spain). Moreover, a blank surface water sample was also collected from the Fluvià River that runs through rural areas. Amber glass bottles (1000 mL) were filled with the surface water sample without leaving a head-space and stored in the dark at 4 °C until analysis.

Sample treatment

Analytes were extracted from river water samples by solid-phase extraction (SPE) using a Visiprep System (Supelco, Bellefonte, PA, USA). The SPE procedure was carried out as follows: 500 mL of surface water sample was loaded onto an Oasis HLB® cartridge (500 mg, 6 mL) (Waters, Milford, MA, USA) previously conditioned (20 mL of methanol and 20 mL of Milli-Q water) and dried under a gentle nitrogen stream during 15 min. Water samples were percolated through the SPE sorbent at a flow rate of 10 mL min^{-1}, then the SPE cartridge was washed with 10 mL of methanol/Milli-Q water (5:95, v/v) and, finally, the target compounds were eluted with 4 mL of methanol. An aliquot of 1 mL of the eluent was diluted 1:3 (v/v) with Milli-Q water, and 10 μL of the final extract was injected into the UHPLC-MS/MS system. To optimise and validate the analytical method, a blank river water sample collected from the Fluvià River spiked with target compounds was used.

Instrumentation

The chromatographic separation of the target compounds was carried out on an Accucore C$_{18}$ column (100 × 2.1 mm, 2.6 μm superficially porous particles) (Thermo Fisher Scientific, San Jose, CA, USA) using an Accela UHPLC system equipped with an autosampler (Accela Open AS) and a quaternary pump (Accela 1250 Pump) (Thermo Fisher Scientific). The UHPLC system was coupled to a triple quadrupole TSQ Quantum Ultra AM mass spectrometer (Thermo Fisher Scientific) equipped with heated-ESI, APCI and APPI sources.

For the analysis of semi-volatile PFASs by UHPLC-APCI-MS/MS method, the methanol/water gradient elution program for a total runtime of 19 min was as follows: initial conditions, a 50% methanol isocratic step for 3 min, from 50 to 90% methanol in 6 min and a final isocratic step at 90% methanol for 5 min before returning to the initial conditions (5 min of re-equilibration time). For the UHPLC-APPI-MS/MS method, an acetonitrile/water mobile phase was employed and the gradient elution program for a total runtime of 14 min was as follows: initial conditions, an isocratic step at 50% acetonitrile for 1 min, from 50 to 70% acetonitrile in 1.5 min, an isocratic step at 70% acetonitrile for 1 min, from 70 to 100% acetonitrile in 4.5 min and a final isocratic step at 100% acetonitrile for 1 min before returning to the initial conditions (5 min of re-equilibration time). In addition, toluene was post-column

added (5%, *v/v*) as a dopant. The injection volume was 10 μL, and the flow rate was 300 μL min⁻¹ for both chromatographic methods.

The ionisation source parameters for APCI and APPI were as follows: vaporiser and capillary temperatures were 250 and 275 °C, respectively; nebuliser gas and auxiliary gas pressures were 50 and 25 arbitrary units (a.u.), respectively; the discharge current in APCI was held at 10 μA; and the krypton lamp emitted photons with an energy level of 10.6 eV in APPI. Finally, the tube lens offset voltage was optimised for each compound and the values ranged from − 80 to − 100 V.

For both UHPLC-MS/MS methods (APCI and APPI), data acquisition was performed in multiple reaction monitoring (MRM) mode (see Electronic Supplementary Material (ESM) Table S1) with a dwell time in the range of 50–150 ms, depending on the compound, which was enough to acquire at least 12 data point across each peak width. Argon collision gas pressure was set at 1.0 bar. Quadrupoles run always at a scan width of 0.1 *m/z* with a peak width of 0.7 *m/z*, except for 6:2 FTOH which was 0.1 *m/z* to avoid interferences on its signal. Xcalibur™ v 2.1 software was used to control the instrument setup and for the data acquisition.

Results and discussion

Atmospheric pressure ionisation behaviour of FTOHs, FOSAs and FOSEs

Limited information on the applicability of APCI and APPI for the ionisation of FTOHs, FOSAs and FOSEs is available. Thus, we studied the effect of mobile phase components (solvent and additives) on both the nature and the intensity of the ions generated in the API sources. For this purpose, target compounds were injected in both positive- and negative-ion modes using different organic modifiers and mobile phase additives. After the initial experiments, the positive-ion mode was discarded since none of the compounds could be ionised using any of the API sources tested at any working conditions. Therefore, further studies were focused on the negative-ion atmospheric pressure ionisation of these semi-volatile PFASs.

Electrospray

ESI was tested to be compared with APCI and APPI. The ESI mass spectra were obtained by infusing standard solutions of target compounds into both acetonitrile/water (80:20, *v/v*) and methanol/water (80:20, *v/v*) mobile phases with and without the addition of organic acids or ammonia at 0.1% (*v/v*). As an example, Fig. 2 shows the ESI mass spectra of 8:2 FTOH, *N*-MeFOSE and *N*-EtFOSA. It was observed that FOSAs ionised via proton abstraction [M–H]⁻, while FTOHs and FOSEs showed a high tendency to form adduct ions, [M+

RCOO]⁻ (R: –H, –CH₃) and [M+Cl]⁻, when organic acids and/or anions as chloride are present in the LC-MS system. Nevertheless, these adduct ions only yielded non-characteristic product ions, such as [RCOO]⁻ and [Cl]⁻, which are not suitable for the UHPLC-MS/MS determination in MRM mode (see ESM Fig. S1a). In order to favour the generation of deprotonated molecules and prevent the formation of adduct ions, a labour-intense cleaning of the LC-MS system was required. For instance, adduct ions are still observed in the ESI mass spectrum of 10:2 FTOH after 72 h of cleaning the UHPLC-MS system (ESM Fig. S1b). These results agreed with those previously published [20] that also indicated the high tendency of FTOHs to form adduct ions and the difficulty to prevent them. Thus, ESI was discarded for the UHPLC-MS/MS determination of these families of compounds and other API sources were explored as alternative.

APCI and APPI

Regarding APCI and APPI, the ionisation behaviour depended on the mobile phase composition, which was reflected in the nature and the abundance of the ions generated. To compare both sources, mass spectra were acquired using the mobile phase composition that produces the maximal ion response. In general, semi-volatile fluorinated compounds were ionised by APCI using hydro-organic mobile phases without additives, while for APPI, a post-column addition of a dopant was required. Regarding FOSAs and FOSEs, the ions generated in both API sources were almost the same, even using different mobile phase compositions. The [M–H]⁻ was always the base peak in the FOSA mass spectra, although some in-source CID fragment ions were also observed due to the loss of N(F)R and NHR (R: –CH₃, –CH₂CH₃), as can be seen in Fig. 2 for *N*-EtFOSA. However, the [M–H]⁻ of FOSEs was not detected in any of API sources, which might be due to a strong in-source CID fragmentation. In this case, the ions at *m/z* 494 for *N*-MeFOSE and at *m/z* 508 for *N*-EtFOSE were the base peaks in the APCI mass spectra of these compounds (Fig. 2) and they were assigned to the loss of CH₂CH₂OF. For the APPI source, different abundances of the in-source CID fragment ions were observed, being [M–CH₂CH₂OH–RN]⁻ (R: –CH₃, –CH₂CH₃) the most intense one. Moreover, FOSEs showed an additional abundant and characteristic ion in APPI, which might be assigned to the superoxide adduct ion [M+O₂]⁻• as it is shown in Fig. 2 for *N*-MeFOSE.

Concerning FTOHs, the mobile phase composition significantly affects the nature of the ions generated in APCI. For instance, when using a methanol/water mobile phase, the [M–H]⁻ was the base peak (Fig. 2, APCI mass spectrum of 8:2 FTOH), while the ionisation under an acetonitrile/water mobile phase only led to the generation of in-source CID fragment radical ions (see ESM Fig. S2). This could be a
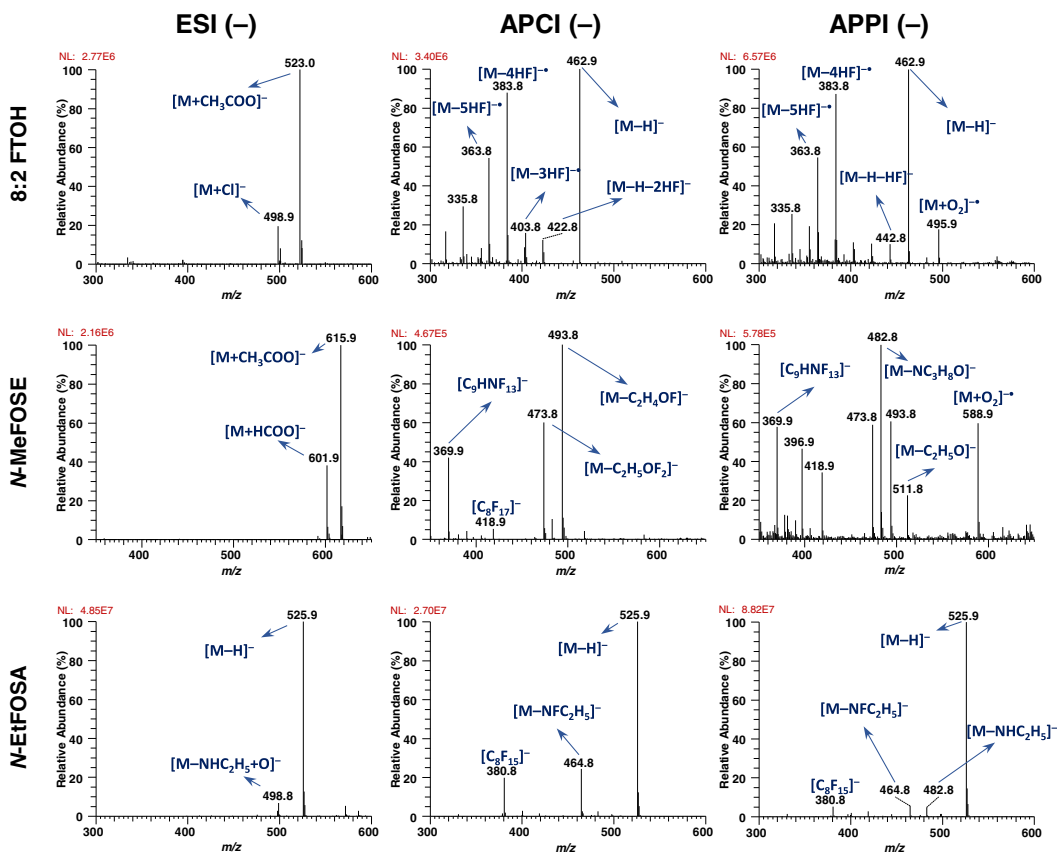
Fig. 2 Negative-ion ESI, APCI and APPI mass spectra of 8:2 FTOH, *N*-MeFOSE and *N*-EtFOSA under the optimal conditions. (ESI (−): acetonitrile/0.1% (*v/v*) acetic acid (80:20, *v/v*); APCI (−): methanol/ water (1:1, *v/v*); APPI (−): acetonitrile/water (1:1, *v/v*) with a toluene (5%, *v/v*) post-column addition)

consequence of the different proton affinity behaviour of methanol/water and acetonitrile/water clusters compared to the organic solvent molecules alone [21]. Regarding APPI, the mass spectra obtained using acetonitrile/water and methanol/water mobile phases (toluene as dopant) were similar to those obtained by APCI using methanol/water, except for the presence of the superoxide adduct ion $[M+O_2]^{-\bullet}$, which was only observed in the APPI mass spectrum, as can be seen in Fig. 2 for 8:2 FTOH.

FTOHs showed strong in-source CID fragmentation in APCI and APPI. As an example, Fig. 3a shows the APCI mass spectrum obtained for 10:2 FTOH using methanol/water. Tandem mass spectrometry was used to characterise these in-source CID fragment ions, and the obtained data showed that two different ionisation-fragmentation mechanisms could be taking place simultaneously. For instance, ions observed at odd *m/z* values for 10:2 FTOH could be produced by the

losses of *n* HF units and CO from the $[M–H]^-$ (e.g., ions at *m/z* 523 $[M–H–2HF]^-$, *m/z* 503 $[M–H–3HF]^-$ and *m/z* 455 $[M–H–4HF–CO]^-$) (Fig. 3b). Meanwhile, ions at even *m/z* values might be originated from the in-source CID fragmentation of an unstable molecular ion $[M]^{-\bullet}$. In fact, the fragmentation by CID in the collision cell of the radical ion at the highest even *m/z* value (*m/z* 524) generated the same product ions at even *m/z* values than those observed via in-source CID fragmentation. These ions correspond to successive losses of *n* HF units (*m/z* 504 $[M–3HF]^{-\bullet}$, *m/z* 484 $[M–4HF]^{-\bullet}$ and *m/z* 464 $[M–5HF]^{-\bullet}$) and CO group (*m/z* 436 $[M–5HF–CO]^{-\bullet}$) (Fig. 3c).

The effect of mobile phase composition on the APCI and APPI ion intensity was also evaluated to achieve the best ionisation efficiency. The intensity of the ions observed for FOSAs and FOSEs was independent of the mobile phase composition in both API sources, while FTOH responses were
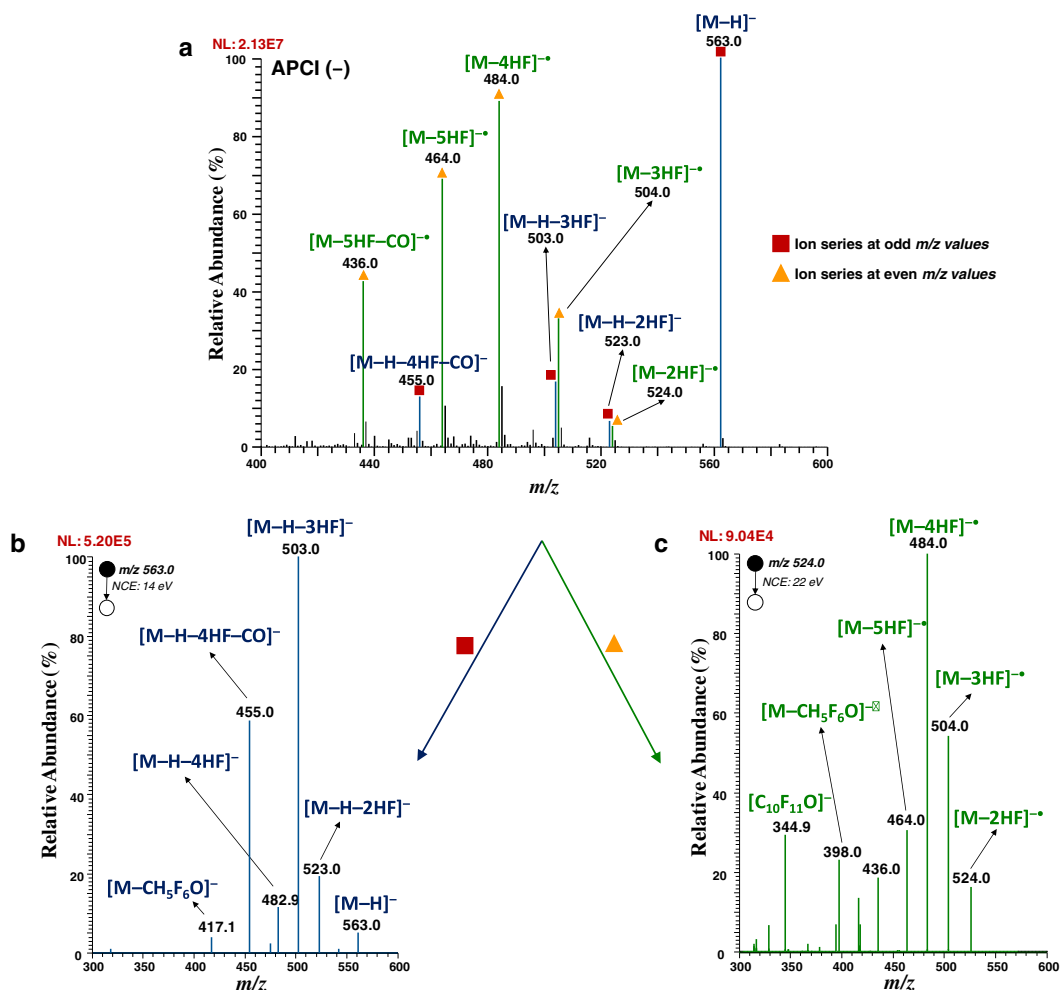
Fig. 3 (**a**) Negative-ion APCI mass spectrum of 10:2 FTOH and product ion mass spectrum of (**b**) [M–H]$^-$ (m/z 563) and (**c**) [M–2HF]$^{-\bullet}$ (m/z 524). (Ions generated by different in-source CID fragmentation mechanisms are shown in blue empty squares and green-coloured empty triangle)

strongly affected. Regarding APCI, methanol/water was selected as the best mobile phase since acetonitrile/water did not allow the formation of the deprotonated molecule for FTOHs. Additionally, when using a methanol/water mobile phase in APCI, the signal improved by increasing the water content above 50% (see ESM Fig. S3a).

In APPI, acetonitrile/water provided higher signal intensities than those obtained with methanol/water for all FTOHs using the tested dopants (see ESM Fig. S4). The high capacity of methanol to compete with FTOHs in the proton abstraction process could lead to the suppression of the [M–H]$^-$. In contrast, the absence of this competitive process using acetonitrile (aprotic character) might favour the deprotonation of FTOHs.

Furthermore, the percentage of the organic modifier in the mobile phase also affected the ionisation efficiency of FTOHs and the maximum responses were observed at acetonitrile content above 50% (v/v) (see ESM Fig. S3b).

Finally, several solvents (toluene, acetone, anisole, chlorobenzene and tetrahydrofuran) were tested as dopant. The ions generated in APPI for each fluorinated compound, regardless of the dopant, were quite similar. Figure 4 shows the normalised signal intensity achieved for the most abundant ions, [M–H]$^-$ for FTOHs and FOSAs and [M–CH$_2$CH$_2$OH–RN]$^-$ (R: –CH$_3$, –CH$_2$CH$_3$) for FOSEs, using the tested dopants. Toluene provided the highest signal intensity for most of the analytes, although anisole also produced satisfactory results for FOSAs

Fig. 4 Effect of different dopants (post-column addition of 5%, v/v) on the response of fluorinated compounds in negative-ion APPI using a mixture of acetonitrile/ water (80:20, v/v)
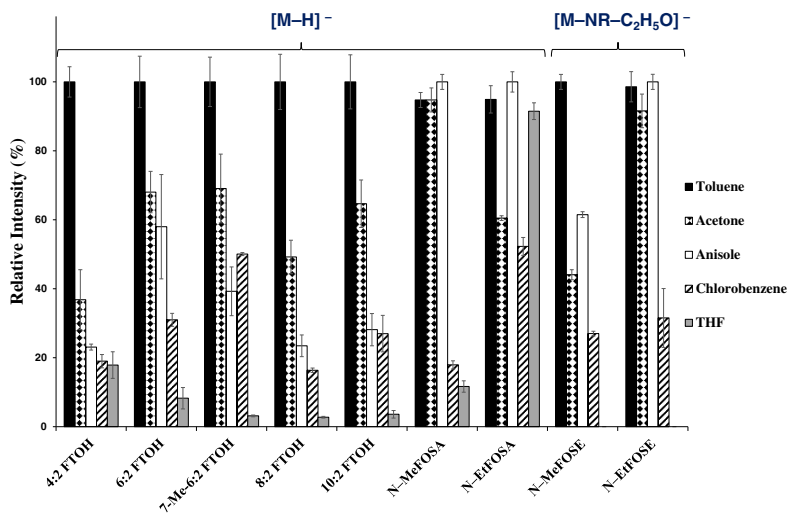
and N-EtFOSE. The toluene percentage added into the total mobile phase flow rate was also optimised within the range of 1–10% (v/v), obtaining the highest responses at 5% (v/v), and no significant improvement was achieved at higher toluene percentages.

Among the MS operating parameters, the tube lens offset voltage was the most critical one. It is a compound-dependent parameter, which focuses the ion beam, controls the ion kinetic energy and affects the in-source CID fragmentation. After optimisation, the optimal working range was narrower (from − 90 to − 110 V) for FTOHs than for FOSAs and FOSEs. For instance, Fig. S5 (see ESM) shows the effect of the tube lens offset voltage in the signal intensity of [M–H]⁻ for 10:2 FTOH compared to that observed for N-EtFOSA. Besides, the tube lens offset voltage can change with running time as the lens become dirty; therefore, a careful control of this parameter and a frequent maintenance of the lens are recommended to achieve the maximum response for FTOHs.

UHPLC-MS/MS

Those ions generated in the API sources were fragmented by CID in the collision cell, and the two most selective and sensitive product ions (quantitation and confirmation) were selected for the UHPLC-MS/MS determination in MRM mode.

Table 1 shows the precursor and product ion assignment as well as the optimal collision energies established for each transition. The fragmentation by CID in the collision cell of [M–H]⁻ for FTOHs followed the same pattern, providing two intense product ions, [M–H–4HF–CO]⁻ and [M–H–3HF]⁻. In the case of FOSAs, the fragmentation by CID in the collision cell yielded two main common product ions produced from

the cleavage of the sulfonamide group (SO₂NR, R: –CH₃, –CH₂CH₃) and n CF₂ units to generate the ions at m/z 169 (5 CF₂ units, quantitation) and m/z 219 (4 CF₂ units, confirmation). Concerning FOSEs, the precursor ions selected in both API sources were different. For APPI, the fragmentation of the most abundant ion, [M–CH₂CH₂OH–RN]⁻ (R: –CH₃, –CH₂CH₃), resulted in a high background noise, which increased limits of detection. On that way, the less abundant [M+O₂]⁻• (65% relative abundance) was selected since it yielded two intense product ions with less background noise. These two product ions were generated by the loss of ethanol (–CH₂CH₂OH) and the alkyl chains (–CH₃ or –CH₂CH₃) in the sulfonamido-ethanol group. On the other hand, the most intense in-source CID fragment ion [M–CH₂CH₂OF]⁻ was selected as precursor ion in APCI, which yielded product ions originated by losses of n HF units (n = 3, 4, 6) and SO₂, except for N-EtFOSE that only lost 1 HF unit.

Regarding the UHPLC method and taking into account the ionisation behaviour of these compounds in APCI and APPI, two chromatographic separations were optimised depending on the best mobile phase composition needed to maximise the responses. In APCI, although the best ionisation efficiency was achieved at methanol percentage lower than 50% (v/v), a higher methanol content was required to elute all the analytes from the reversed-phase column. As a compromise, it was proposed as a 50% methanol isocratic step of 3 min in order to elute the analytes within the lowest methanol content. On that way, it was possible to achieve a chromatographic separation in less than 12 min. Concerning the APPI source, the high eluotropic strength of acetonitrile and the wide acetonitrile percentage range (50–100%, v/v) in which the analyte signals were higher, allow to achieve the chromatographic

Table 1 MRM transitions, normalised collision energies (NCEs) and ion assignments used in APCI and APPI

Analyte	API source	Precursor ion		MRM transition					
				Quantification product ion			Confirmation product ion		
		m/z	Assignment	m/z	Assignment	NCE (V)	m/z	Assignment	NCE (V)
4:2 FTOH	APCI/APPI	263	$[M–H]^-$	203	$[M–H–3HF]^-$	10	155	$[M–H–4HF–CO]^-$	24
6:2 FTOH	APCI/APPI	363	$[M–H]^-$	255	$[M–H–4HF–CO]^-$	22	303	$[M–H–3HF]^-$	10
7-Me-6:2 FTOH	APCI/APPI	413	$[M–H]^-$	305	$[M–H–4HF–CO]^-$	24	353	$[M–H–3HF]^-$	10
8:2 FTOH	APCI/APPI	463	$[M–H]^-$	355	$[M–H–4HF–CO]^-$	30	403	$[M–H–3HF]^-$	8
10:2 FTOH	APCI/APPI	563	$[M–H]^-$	503	$[M–H–3HF]^-$	12	455	$[M–H–4HF–CO]^-$	26
N-MeFOSA	APCI/APPI	512	$[M–H]^-$	169	$[M–H–CH_3NSO_2–C_5F_{10}]^-$	30	219	$[M–H–CH_3NSO_2–C_4F_8]^-$	25
N-EtFOSA	APCI/APPI	526	$[M–H]^-$	169	$[M–H–C_2H_5NSO_2–C_5F_{10}]^-$	32	219	$[M–H–CH_3NSO_2–C_4F_8]^-$	28
N-MeFOSE	APCI	494	$[M–CH_2CH_2OF]^-$	370	$[M–CH_2CH_2OF–3HF–SO_2]^-$	20	350	$[M–CH_2CH_2OF–4HF–SO_2]^-$	20
	APPI	589	$[M+O_2]^{-\bullet}$	512	$[M+O_2–CH_2CH_2OH]^-$	15	542	$[M+O_2–CH_3]^-$	15
N-EtFOSE	APCI	508	$[M–CH_2CH_2OF]^-$	488	$[M–CH_2CH_2OF–HF]^-$	24	324	$[M–CH_2CH_2OF–6HF–SO_2]^-$	22
	APPI	603	$[M+O_2]^{-\bullet}$	526	$[M+O_2–CH_2CH_2OH]^-$	15	542	$[M+O_2–CH_2CH_3]^-$	15

separation in less than 8 min (Fig. 5). Despite all the compounds were not separated at baseline, the selected MRM transitions were selective enough and neither ion suppression nor ion enhancement was observed for any of the partially coeluting compounds. Instrumental limits of detection (ILODs) were established for both UHPLC-API-MS/MS systems (Table 2) using the optimal conditions (section "Instrumentation"). ILODs were determined as three times the signal-to-noise ratio (S/N) on the selected quantification product ion. As it can be observed, ILODs using APPI were 8–150 times lower than those obtained by APCI. Therefore, the UHPLC-APPI-MS/MS method was selected for the determination of polyfluoroalkyl substances at very low concentration levels in water samples. Moreover, instrumental run-to-run precision was estimated at low (2–30 µg L^{-1}) and medium (20–300 µg L^{-1}) concentration levels, obtaining relative standard deviation values (RSD, %) lower than 5% ($n = 3$).

Analysis of river water samples by UHPLC-APPI-MS/MS

Semi-volatile fluorinated compounds are currently detected at low concentration levels in river water, making

necessary a preconcentration step to determine them. In this work, a solid-phase extraction method, previously reported for the GC-MS analysis of these compounds [19], was modified to be compatible with the UHPLC-APPI-MS/MS method. For the analysis of river water samples, methanol and acetonitrile were tested to elute the analytes from Oasis HLB$^{®}$ cartridges. The best results were achieved with methanol (4 mL) because it provided cleaner extracts than those obtained with acetonitrile. The SPE extraction efficiency (EE, %) was evaluated using a blank river water (Fluvià River) spiked with target compounds at two concentration levels (50 and 400 ng L^{-1}). The EE (%) values achieved for all the compounds ranged from 96 to 102%, with RSD (%) lower than 5%. Matrix effect (ME, %) for each compound was estimated as the relative difference between the peak area of a spiked extract of a blank river water and that obtained from standard mixtures at the same concentration level. The ME (%) values ranged from 15 to 60%, which indicate an important matrix effect. To minimise this effect, an aliquot of 1 mL of the extract was diluted 1:3 (*v/v*) with Milli-Q water and the ME (%) decreased down to 20% improving the S/N ratio four to five times. Under these conditions, the total recovery, including
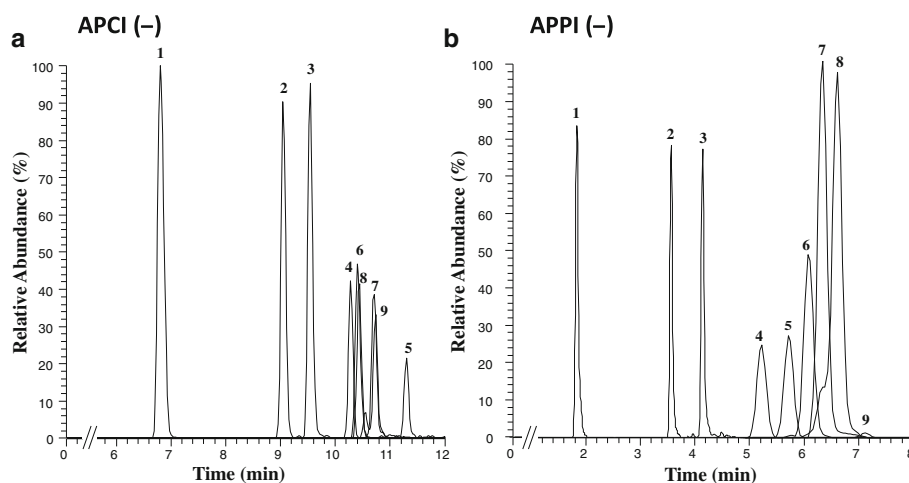
Fig. 5 UHPLC-MS/MS chromatograms (conditions in the "Materials and Methods" section) of a standard mixture of target compounds at a concentration of 500 μg L^{-1} using (**a**) negative-ion APCI and (**b**) negative-ion APPI sources. Compounds are as follows: (1) 4:2 FTOH, (2) 6:2 FTOH, (3) 7-Me-6:2 FTOH, (4) 8:2 FTOH, (5) N-MeFOSE, (6) N-MeFOSA, (7) N-EtFOSE, (8) N-EtFOSA and (9) 10:2 FTOH

extraction efficiency and matrix effect, ranged from 78 to 100% for all the compounds (Table 3).

Quality parameters of the developed SPE UHPLC-APPI-MS/MS method were estimated using a spiked blank river water (Table 3). Method limits of detection (MLODs) based on the S/N ratio of 3 ranged from 0.3 to 6 ng L^{-1}, while method limits of quantification (MLOQs), defined as a S/N ratio of 10, were comprised between 1 and 20 ng L^{-1}. To our knowledge, there are no data published on LC-MS/MS using APCI or APPI to determine these semi-volatile fluorinated compounds in water samples. For this reason, the results obtained were compared with those previously determined by GC-MS and LC-ESI-MS/MS in water samples. The MLODs obtained in the present work were ten times lower than those

previously reported for FTOHs using LC-ESI-MS/MS (60–90 ng L^{-1}) [16], while for FOSAs and FOSEs, the MLODs were quite similar (FOSAs, 0.29 to 0.62 ng L^{-1}; FOSEs, 2.2 ng L^{-1}) [22–24]. Regarding GC-MS, the MLOQs reported refer only to some of the FTOHs and FOSAs included in the present work and they are 5–20 times higher (20 to 100 ng L^{-1}) using headspace solid-phase microextraction for the water analysis [25].

In order to correct the slight matrix effect observed, a matrix-matched calibration was performed for quantitative analysis, providing a good linearity in the working range ($R^2 > 0.994$) (see ESM Table S2). Moreover, the precision of the method was also determined, using a blank river water sample spiked at two concentration levels (low, 5–

Table 2 Instrumental limits of detection in APCI and APPI and run-to-run precision in APPI

Analyte	APCI	APPI	APPI	
	ILOD (μg L^{-1})[a]	ILOD (μg L^{-1})[a]	Run-to-run precision (RSD, %)	
			Low level[b]	Medium level[c]
4:2 FTOH	50	1	5	3
6:2 FTOH	15	0.4	2	3
7-Me-6:2 FTOH	14	0.3	5	4
8:2 FTOH	50	0.5	4	4
10:2 FTOH	75	0.5	5	3
N-MeFOSA	0.7	0.08	4	5
N-EtFOSA	0.8	0.1	4	5
N-MeFOSE	12	0.1	2	1
N-EtFOSE	0.9	0.09	2	4

[a] Injection volume of 10 μL

[b] Low level of 2–30 μg L^{-1} (depending on the compound)

[c] Medium level of 20–300 μg L^{-1} (depending on the compound)

Table 3   Quality parameters of the SPE UHPLC-APPI-MS/MS method

Analyte	4:2 FTOH	6:2 FTOH	7-Me-6:2 FTOH	8:2 FTOH	N-MeFOSE	N-MeFOSA	N-EtFOSE	N-EtFOSA	10:2 FTOH
$t_R \pm$ SD (min)[a]	1.82 ± 0.01	3.62 ± 0.01	4.17 ± 0.01	5.31 ± 0.01	5.81 ± 0.01	6.17 ± 0.01	6.46 ± 0.02	6.77 ± 0.02	7.18 ± 0.01
MLOQ (ng L^{-1})	20	7	6	8	8	1	1	2	2
MLOD (ng L^{-1})	6	2	2	2	2	0.3	0.4	0.6	0.5
Ion ratio (Q/q) (RSD, %)	1.3 (12)	1.0 (12)	1.3 (17)	1.1 (6)	1.5 (11)	1.1 (11)	7.9 (2)	1.2 (10)	17.1 (1)
Recovery ± SD (%)[a]	100 ± 3	85 ± 4	100 ± 2	79 ± 5	80 ± 3	91 ± 6	78 ± 1	100 ± 6	95 ± 5
Spiked concentration (ng L^{-1})									
Low level	100	40	30	50	5	5	5	5	50
Medium level	1000	400	300	500	200	200	200	200	500
Found concentration ± SD[a] (ng L^{-1})									
Low level	114 ± 5	43.6 ± 0.7	32 ± 1	55 ± 1	4.6 ± 0.1	4.69 ± 0.07	5.32 ± 0.05	5.4 ± 0.2	52 ± 2
Medium level	1065 ± 24	396 ± 10	308 ± 12	524 ± 26	205 ± 6	188 ± 7	197 ± 4	209 ± 9	515 ± 19
Precision (RSD, %)[a]									
Low level	4	2	4	2	3	1	1	4	4
Medium level	2	3	4	5	3	4	2	4	4
Trueness (Rel. error, %)[a]									
Low level	14	9	5	10	−8	−6	6	8	4
Medium level	6	−1	3	5	3	−6	−2	4	3

[a] $n = 3$

100 ng L^{-1}, and medium, 200–1000 ng L^{-1}). The RSD (%) values based on the concentration were lower than 5% ($n = 3$), while the trueness (the same spiked levels) was lower than 14% (relative error, $n = 3$). These results indicate the good performance of the SPE UHPLC-APPI-MS/MS method developed.

The method was applied to the determination of FTOHs, FOSAs and FOSEs in water samples collected from river basins (two samples from the Llobregat River, two from the Ebro River and one from the Fluvià River) located on the north-east area of Spain (Catalonia). The samples were analysed by triplicate, and procedural blanks were also analysed to ensure the absence of possible carryover between samples, assessing the quality of the results. Among the river waters analysed, the presence of 4:2 FTOH (30 ± 1 ng L^{-1}) was detected in a sample from the Llobregat River collected upstream of a wastewater treatment plant located in the metropolitan area of Barcelona. Meanwhile, in a sample from the Ebro River collected downstream of an industrial area near Tortosa (Tarragona, Spain), *N*-EtFOSA was detected (780 ± 12 ng L^{-1}).

Conclusions

The study of the atmospheric pressure ionisation of FTOHs, FOSAs and FOSEs highlighted the differences on the nature and the abundance of the generated ions in the API sources tested. The ionisation was only possible in negative-ion mode, and the use of APCI and APPI sources provided advantages over ESI since they prevented the formation of adduct ions and yielded characteristic product ions for the UHPLC-MS/MS determination in MRM mode. To maximise APCI responses, a methanol/water (methanol below 50%, *v/v*) mobile phase is recommended, while acetonitrile/water (acetonitrile above 50%, *v/v*) and a post-column addition of toluene (5%, *v/v*) are suggested in APPI. Under these conditions, FTOHs and FOSAs were mainly ionised via proton abstraction, although FTOHs also showed the formation of abundant radical ions. In contrast, the high in-source CID fragmentation observed for FOSEs led to the selection of [M–CH$_2$CH$_2$OF]$^-$ in APCI and [M+O$_2$]$^{-\bullet}$ in APPI as precursor ions.

Taking into account these results, a chromatographic separation for each API source was proposed. Although both methods allowed the determination of the target compounds at low concentration levels, UHPLC-APPI-MS/MS provided lower ILODs (8 and 150 times) than those achieved by UHPLC-APCI-MS/MS and it was proposed as a good alternative to GC-MS and LC-ESI-MS/MS for the determination of semi-volatile PFASs in water samples.

Compliance with ethical standards

Conflict of interest The authors declare that they have no conflict of interest.

References

1. Fromme H, Tittlemier SA, Völkel W, Wilhelm M, Twardella D. Perfluorinated compounds—exposure assessment for the general population in western countries. Int J Hyg Environ Health. 2009;212:239–70.
2. Hekster FM, Laane RWPM, de Voogt P. Environmental and toxicity effects of perfluoroalkylated substances. Rev Environ Contam Toxicol. 2003;179:99–121.
3. Lehmer H-S. Synthesis of environmentally relevant fluorinated surfactants—a review. Chemosphere. 2005;58:1471–96.
4. Buck RC, Franklin J, Berger U, Conder JM, Cousins IT, de Voogt P, et al. Perfluoroalkyl and polyfluoroalkyl substances in the environment: terminology, classification, and origins. Integr Environ Assess Manag. 2011;7:513–41.
5. Kissa E. Fluorinated surfactants and repellents. 2nd ed. New York: Marcel Dekker; 2001.
6. Council Decision (EU) 2015/633 of 20 April 2015 on the submission, on behalf of the European Union, of a proposal for the listing of additional chemicals in Annex A to the Stockholm Convention on Persistent Organic Pollutants. Official Journal of the European Union. 2015;L 104:14–15.
7. Decision SC-4/17 of 4–8 May 2009 of Listing of perfluorooctane sulfonic acid, its salts and perfluorooctane sulfonyl fluoride. United Nation Environment Programme. Stockholm Convention on Persistent Organic Pollutants. UNEP/POPS/COP.4/38:66-9.
8. Jahnke A, Ahrens L, Ebinghaus R, Berger U, Barber JL, Temme C. An improved method for the analysis of volatile polyfluorinated alkyl substances in environmental air samples. Anal Bioanal Chem. 2007;387:965–75.
9. Wu Y, Chang VW-C. Development of analysis of volatile polyfluorinated alkyl substances in indoor air using thermal desorption-gas chromatography–mass spectrometry. J Chromatogr A. 2012;1238:114–20.
10. Kim S-K, Shoeib M, Kim K-S, Park J-E. Indoor and outdoor poly- and perfluoroalkyl substances (PFASs) in Korea determined by passive air sampler. Environ Pollut. 2012;162:144–50.
11. Kuklenyik Z, Needham LL, Calafat AM. Measurement of 18 perfluorinated organic acids and amides in human serum using on-line solid-phase extraction. Anal Chem. 2005;77:6085–91.
12. Gremmel C, Frömel T, Knepper TP. Systematic determination of perfluoroalkyl and polyfluoroalkyl substances (PFASs) in outdoor jackets. Chemosphere. 2016;160:173–80.
13. Lacina O, Hradkova P, Pulkrabova J, Hajslova J. Simple, high throughput ultra-high performance liquid chromatography/tandem mass spectrometry trace analysis of perfluorinated alkylated substances in food of animal origin: milk and fish. J Chromatogr A. 2011;1218:4312–21.
14. Martin JW, Muir DCG, Moody CA, Ellis DA, Kwan WC, Solomon KR, et al. Collection of airborne fluorinated organics and analysis

by gas chromatography/chemical ionization mass spectrometry. Anal Chem. 2002;74:584–90.

15. Szostek B, Prickett KB. Determination of 8:2 fluorotelomer alcohol in animal plasma and tissues by gas chromatography–mass spectrometry. J Chromatogr B. 2004;813:313–21.

16. Szostek B, Prickett KB, Buck RC. Determination of fluorotelomer alcohols by liquid chromatography/tandem mass spectrometry in water. Rapid Commun Mass Spectrom. 2006;20:2837–44.

17. Chu S, Letcher RJ. Analysis of fluorotelomer alcohols and perfluorinated sulfonamiddes in biotic samples by lquid chromatography-atmospheric pressure photoionization mass spectrometry. J Chromatogr A. 2008;1215:92–9.

18. Krusic PJ, Marchione AA, Davidson F, Kaiser MA, Kao C-PC, Richardson RE, et al. Vapor pressure and intramolecular hydrogen bonding in fluorotelomer alcohols. J Phys Chem A. 2005;109:6232–41.

19. Portolés T, Rosales LE, Sancho JV, Santos FJ, Moyano E. Gas chromatography–tandem mass spectrometry with atmospheric pressure chemical ionization for fluorotelomer alcohols and perfluorinated sulfonamides determination. J Chromatogr A. 2015;1413:107–16.

20. Berger U, Langlois I, Oehme M, Kallenborn R. Comparison of three types of mass spectrometer for high-performance liquid chromatography/mass spectrometry analysis of perfluoroalkylated

substances and fluorotelomer alcohols. Eur J Mass Spectrom. 2004;10:579–88.

21. Chai Y, Hu N, Pan Y. Kinetic and thermodynamic control of protonation in atmospheric pressure chemical ionization. J Am Soc Mass Spectrom. 2013;24:1097–101.

22. Arvaniti OS, Asimakopoulos AG, Dasenaki ME, Ventouri EI, Stasinakis AS, Thomaidis NS. Simultaneous determination of eighteen perfluorinated compounds in dissolved and particulate phases of wastewater, and in sewage sludge by liquid chromatography-tandem mass spectrometry. Anal Methods. 2014;6:1341–9.

23. González-Barreiro C, Martínez-Carballo E, Sitka A, Scharf S, Gans O. Method optimization for determination of selected perfluorinated alkylated substances in water samples. Anal Bioanal Chem. 2006;386:2123–32.

24. Boulanger B, Vargo J, Schnoor JL, Hornbuckle KC. Detection of perfluorooctane surfactants in great lakes water. Environ Sci Technol. 2004;38:4064–70.

25. Bach C, Boiteux V, Hemard J, Colin A, Rosin C, Munoz JF, et al. Simultaneous determination of perfluoroalkyl iodides, perfluoroalkane sulfonamides, fluorotelomer alcohols, fluorotelomer iodides and fluorotelomer acrylates and methacrylates in water and sediments using solid-phase microextraction-gas chromatography/mass spectrometry. J Chromatogr A. 2016;1448:98–106.

Analytical and Bioanalytical Chemistry

Electronic Supplementary Material

Negative-ion atmospheric pressure ionisation of semi-volatile fluorinated compounds for ultra-high-performance liquid chromatography tandem mass spectrometry analysis

Juan F. Ayala-Cabrera, F. Javier Santos, Encarnación Moyano

Table of Contents

Supporting Tables

Table S1 Acquisition parameters of the UHPLC-APPI-MS/MS determination

Analyte	$t_R \pm SD$	Tube Lens	Segment	Dwell Time	Quantification Transition		Confirmation Transition		Ion Ratio
	(min)	Offset (V)	(min)	(ms)	$m/z \rightarrow m/z$	NCE (V)	$m/z \rightarrow m/z$	NCE (V)	Q/q (RSD, %)
4:2 FTOH	1.82 ± 0.01	80	0.00–2.50	150	$263 \rightarrow 203$	10	$263 \rightarrow 155$	24	1.3 (12%)
6:2 FTOH	3.62 ± 0.01	80	2.50–3.85	150	$363 \rightarrow 255$	22	$363 \rightarrow 303$	10	1.0 (12%)
7-Me-6:2 FTOH	4.17 ± 0.01	85	3.85–4.85	150	$413 \rightarrow 219$	24	$413 \rightarrow 159$	10	1.3 (17%)
8:2 FTOH	5.31 ± 0.01	95	4.85–15.00	50	$463 \rightarrow 355$	30	$463 \rightarrow 403$	8	1.1 (6%)
N-MeFOSE	5.81 ± 0.01	100	4.85–15.00	50	$589 \rightarrow 512$	15	$589 \rightarrow 350$	15	1.5 (11%)
N-MeFOSA	6.17 ± 0.01	95	4.85–15.00	50	$512 \rightarrow 169$	30	$512 \rightarrow 219$	25	1.1 (11%)
N-EtFOSE	6.46 ± 0.02	80	4.85–15.00	50	$603 \rightarrow 526$	15	$603 \rightarrow 542$	15	7.9 (2%)
N-EtFOSA	6.77 ± 0.02	95	4.85–15.00	50	$526 \rightarrow 169$	32	$526 \rightarrow 219$	28	1.2 (10%)
10:2 FTOH	7.18 ± 0.01	100	4.85–15.00	50	$563 \rightarrow 503$	12	$563 \rightarrow 455$	26	17.1 (1%)

Table S2   SPE UHPLC‑APPI‑MS/MS matrix matched calibration data

Analyte	Calibration Range (ng L^{-1})	Slope	±	$t_{n-2} \cdot SD^a$	R^2
4:2 FTOH	20–2000	90	±	11	0.995
6:2 FTOH	7–700	151	±	16	0.997
7‑Me‑6:2 FTOH	6–600	140	±	13	0.995
8:2 FTOH	8–800	112	±	15	0.994
10:2 FTOH	8–800	73	±	8	0.994
N-MeFOSA	1–1,000	5,910	±	762	0.996
N-EtFOSA	1–1,000	5,346	±	303	0.998
N-MeFOSE	1–1,000	9,320	±	105	0.996
N-EtFOSE	1–1,000	9,228	±	427	0.999

[a] t_{n-2} for 5 degrees of freedom and $\alpha = 0.05$.

Supporting Figures
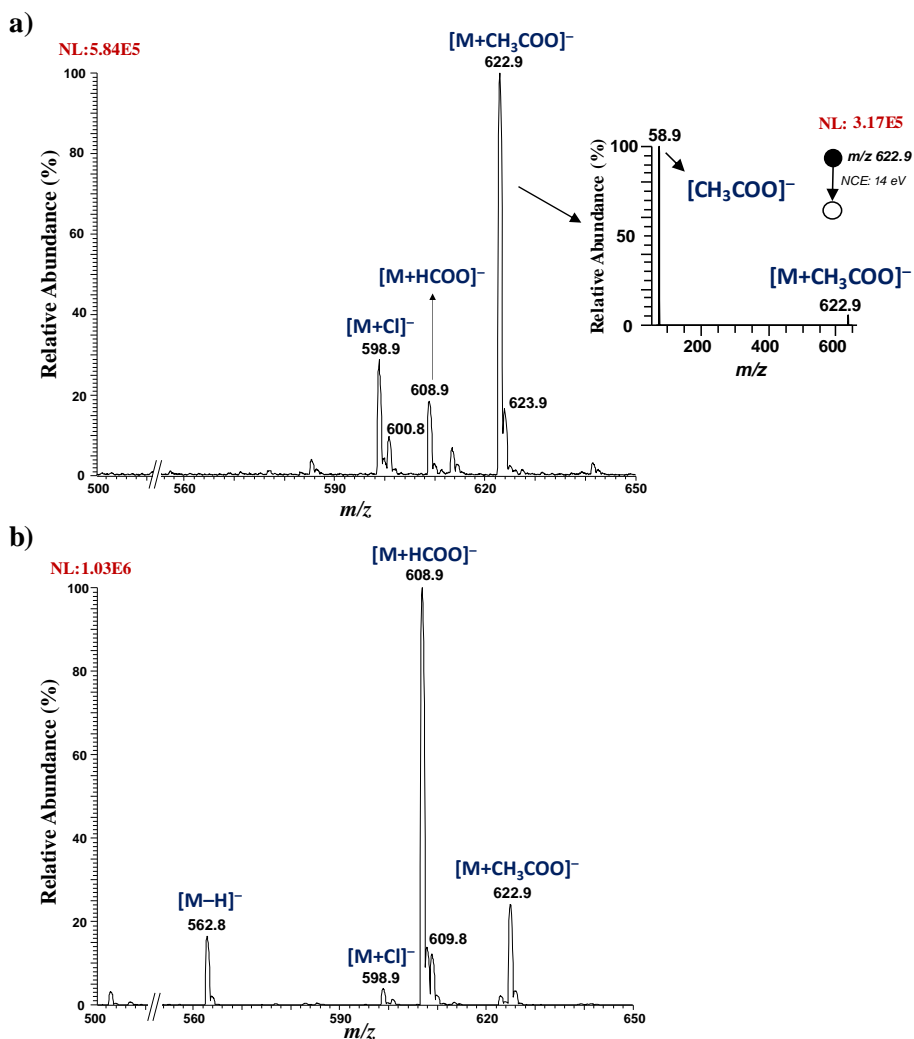
Fig. S1 a) Negative-ion ESI mass spectrum of 10:2 FTOH using a methanol/water (80:20 *v/v*) as mobile phase and tandem mass spectrum of [CH₃COO]⁻ adduct ion. b) Negative-ion ESI mass spectrum of 10:2 FTOH using a methanol/water (80:20 *v/v*) as mobile phase after 72 h cleaning the LC-MS system
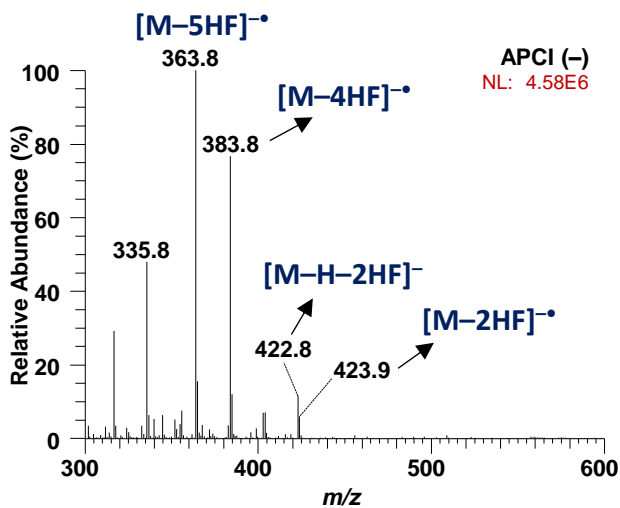
Fig. S2   Negative‑ion APCI mass spectrum of 8:2 FTOH using an acetonitrile/water (1:1 *v/v*) mobile phase
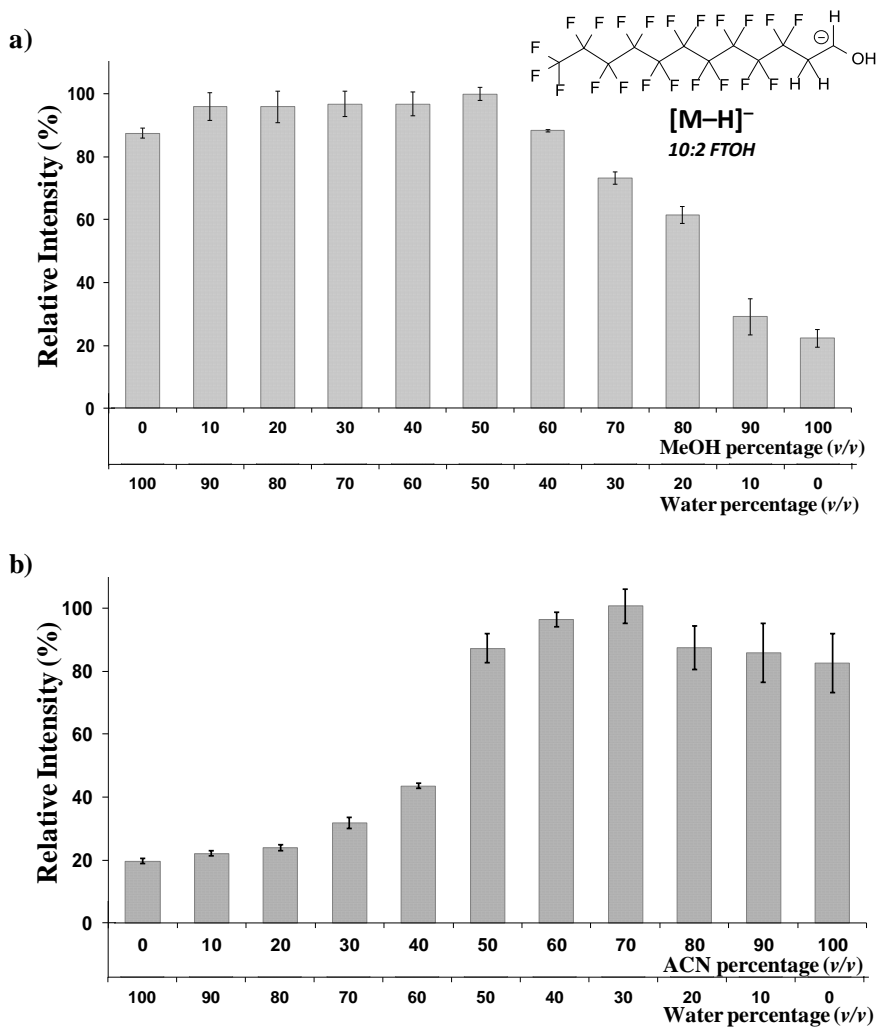
Fig. S3   Effect of water content on the ionization efficiency of 10:2 FTOH in a) APCI and b) APPI. (MeOH: methanol; ACN: acetonitrile)

Fig. S4   Effect of mobile phase composition on negative-ion APPI signal intensity of 10:2 FTOH using methanol/water (80:20, *v/v*) and acetonitrile/water (80:20, *v/v*) as mobile phase (dopant post-column addition, 5%, *v/v*).

Fig. S5   Effect of tube lens offset voltage on the intensity of [M–H]⁻ ion for 10:2 FTOH and *N*-EtFOSA

2.2.2. Article II

Gas chromatography and liquid chromatography coupled to mass spectrometry for the determination of fluorotelomer olefins, fluorotelomer alcohols, perfluoroalkyl sulfonamides and sulfonamido-ethanols in water

J. F. Ayala-Cabrera, E. Moyano, F. J. Santos

Gas chromatography and liquid chromatography coupled to mass spectrometry for the determination of fluorotelomer olefins, fluorotelomer alcohols, perfluoroalkyl sulfonamides and sulfonamido-ethanols in water

J.F. Ayala-Cabrera [a], E. Moyano [a,b], F.J. Santos [a,b,*]

[a] *Department of Chemical Engineering and Analytical Chemistry, University of Barcelona. Av. Diagonal 645, E–08028 Barcelona, Spain*
[b] *Water Research Institute (IdRA), University of Barcelona, Montalegre 6, E–08001 Barcelona, Spain*

ABSTRACT

In this work, the suitability of gas chromatography-mass spectrometry (GC–MS) and liquid chromatography-tandem mass spectrometry (LC–MS/MS) for the multi-class determination of different families of neutral per- and polyfluoroalkyl substances (PFASs), such as fluorotelomer olefins (FTOs), alcohols (FTOHs) and fluorooctanesulfonamides (FOSAs) and sulfonamido-ethanols (FOSEs), was investigated and compared. Regarding GC–MS, the use of a semi-polar GC column (DB-624, 6%-cyanopropilphenyl 94%-dimethyl polysiloxane) allowed the adequate separation of all the compounds while chemical ionisation (CI) of positive ions as ionisation technique provided the best responses. Concerning UHPLC–MS/MS, atmospheric pressure chemical ionisation (APCI) and photoionisation (APPI) sources allowed the ionisation of all studied neutral PFASs, including FTOs for the first time. High vaporizer temperatures (450 °C) and acetonitrile/water mobile phase mixtures were required to favour the ionisation of FTOs, with adequate ionisation for FTOHs, FOSAs and FOSEs. The chromatographic separation, performed on a totally porous column (Luna C18), allowed the successful separation of the four families of neutral PFASs. After comparing the performance of the studied methods, the highest detectability was achieved using UHPLC–APCI–MS/MS and it was chosen in combination with a solid-phase extraction (SPE) procedure for the analysis of neutral PFASs in water samples. The whole method provided low limits of detection (0.003–6 µg L^{-1}), good precision (RSD < 9%) and trueness (relative error < 10%). The methodology was applied to the analysis of river water samples and the presence of some neutral PFASs were detected (8:2 FTO) and quantified (4:2 FTOH and *N*-EtFOSA) at low concentration levels (ng L^{-1}).

© 2019 Elsevier B.V. All rights reserved.

1. Introduction

Per- and polyfluoalkyl substances (PFASs) are widely used in industrial and consumer products as surfactants in coating and firefighting foams and in polymer applications, such as textile, soil repellents, food-contact paper, on account of their water and stain-resistant properties [1–4]. The concern about PFASs, especially for ionic compounds (e.g., perfluoroalkylsulfonates and perdluoroalkyl-carboxylates), has increased in recent years because they are potentially toxic, persistent, ubiquitous in the environment, and can be transported long-distances in the atmosphere [5–7]. In addition, the ability of PFASs to bioaccumulate through the food chain [8–10] makes them frequently detected at significant concentration levels in humans and wildlife [11,12]. These properties have led to include some ionic PFASs, such as perfluorooctanesulfonic acid (PFOS) and its related compounds, in the list of Stockholm Convention as persistent organic pollutants [13]. In addition, the European Union have regulated their use and production due to their potential harmful effects on the human health [14]. Consequently, several families of neutral PFASs, such as fluorotelomer alcohols (FTOHs), fluorotelomer olefins (FTOs) as well as *N*-alkylated fluorooctane-sulfonamides (FOSAs) and sulfonamido-ethanols (FOSEs) have been used for replacing the toxic PFASs. Nevertheless, they are easily degraded in the environment and/or are metabolised in living organisms, leading to the formation of more toxic compounds, such as PFOS and other derivatives [2,15]. Therefore, the accurate monitoring of neutral PFASs in the environment is of great interest to assess the real exposure of humans and wildlife.

---

* Corresponding author at: Department of Chemical Engineering and Analytical Chemistry, University of Barcelona, Av. Diagonal 645, E–08028 Barcelona, Spain.
E-mail address: javier.santos@ub.edu (F.J. Santos).

Gas chromatography (GC) and liquid chromatography (LC) coupled to mass spectrometry (MS) are the methods of choice for the determination of neutral PFASs. The current GC–MS methods involve the use of electron ionisation (EI) [16–18] and chemical ionisation (CI) [19–21] for quantitative purposes, and negative ion chemical ionisation (NICI) for confirmation of target compounds [16,17,21]. In addition, GC columns with stationary phases of different polarity have been used depending on the families of neutral PFASs. For instance, Piekarz et al. [20] proposed the use of a polar column, poly(ethylene glycol)-based stationary phase, for the separation of FTOHs, FOSAs and FOSEs, while a non-polar column (DB-5ms, 5%-diphenyl 95%-dimethyl polysiloxane) was used for achieving an adequate retention of FTOs. Li et al. [22] were able to determine 8:2 FTO – where 8 and 2 are the number of fluorinated and non-fluorinated carbons, respectively– and also FTOHs, FOSAs and FOSEs using a polar GC column, poly(ethylene glycol)-based stationary phase, but the most volatile FTOs could not be analysed because they showed a poor retention. To solve this problem Barber et al. [23] investigated the coupling of two GC columns of different polarity, a semi-polar poly(trifluoropropyldimethylsiloxane)–based column with a polar poly(ethylene glycol) column, to the analysis of FTOs, FTOHs, FOSAs and FOSEs. Nevertheless, peak tailing and a poor peak shape were observed under these conditions. Besides, some problems regarding the ionisation efficiency have also been observed for the GC–MS determination of these compounds [24]. Thus, further investigation is required in order to propose a reliable GC–MS multi-class method for the determination of neutral PFASs.

Liquid chromatography (LC) coupled to tandem mass spectrometry (MS/MS) has also been applied for the determination of different class of neutral PFASs, mainly using electrospray (ESI) as ionisation source [25–27]. However, FTOHs and FOSEs generate non-characteristic adduct ions with some mobile phase components, such as acetate, formate or chloride, making difficult their identification and confirmation [27,28]. To overcome this problem, Berger et al. [29] demonstrated that removal of ammonium acetate from the LC–MS system allows the formation of deprotonated molecules of FTOHs in negative-ion ESI, but this methodology was only addressed to the analysis of this family of PFASs. Atmospheric pressure chemical ionisation (APCI) [30] and atmospheric pressure photoionisation (APPI) [28,31] have also been proposed as alternative ionisation techniques to ESI for the analysis of FTOHs, FOSAs and FOSEs. Nevertheless, to the best of our knowledge, there is no information regarding the ionisation of FTOs using these sources or even their chromatographic separation by LC. Consequently, developing a multi-class methods capable of analyzing these families of PFASs remains a challenge.

In this work, the performance of GC–MS and LC–MS/MS for the simultaneous determination of FTOs, FTOHs, FOSAs and FOSEs were evaluated to propose a sensitive and selective multi-class method for the analysis of river water. Thus, classical ionisation techniques (EI, CI and NICI) in GC–MS and atmospheric pressure ionisation sources (ESI, APCI and APPI) in LC–MS as well as their chromatographic separation were investigated and compared.

2. Materials and methods

2.1. Reagents and standards

The neutral PFASs studied in this work are summarised in Table S1. Individual pure standards of fluorotelomer alcohols, 3,3,4,4,5,5,6,6,6-nonafluoro-1-hexanol (4:2 FTOH), 3,3,4,4,5,5,6,6,7,7,8,8,8-tridecafluoro-1-octanol (6:2 FTOH), and 3,3,4,4,5,5,6,6,7,8,8,8-dodecafluoro-7-(trifluoromethyl)-1-octanol (7-Me-6:2 FTOH), were purchased from Fluorochem Ltd. (Derbyshire, UK), while

3,3,4,4,5,5,6,6,7,7,8,8,9,9,10,10,10-heptadecafluoro-1-decanol (8:2 FTOH) and 3,3,4,4,5,5,6,6,7,7,8,8,9,9,10, 10,11,11,12,12,12-henicosafluoro-1-dodecanol (10:2 FTOH) were supplied by Alfa Aesar GmbH & Co KG (Karlsruhe, Germany) at a purity higher than 96%. The fluorotelomer olefins, 3,3,4,4,5,5,6,6,6-nonafluoro-1-hexene (4:2 FTO), 3,3,4,4,5,5,6,6,7,7,8,8,8-tridecafluoro-1-octene (6:2 FTO) and 3,3,4,4,5,5,6,6,7,7,8,8,9,9,10,10,10-heptadecafluoro-1-decene (8:2 FTO) were also obtained from Fluorochem Ltd. Individual stock standard solutions at 1000 mg L^{-1} were prepared in methanol and acetonitrile from their respective pure standards. Individual standard solutions at 50 mg L^{-1} in methanol of perfluoroalkyl sulfonamides and sulfonamido-ethanols, 1,1,2,2,3,3,4,4,5,5,6,6,7,7,8,8,8-heptadecafluoro- N-(2-hydroxy ethyl)- N-methyl-1-octanesulfonamide (N-MeFOSE), 1,1,2,2,3,3,4,4,5,5,6,6,7,7,8,8,8-heptadecafluoro- N-(2-hydroxyethyl)- N-ethyl-1-octanesulfonamide (N-EtFOSE) and N-methyl-1,1,2,2,3,3,4,4,5,5,6,6,7,7,8,8,8-heptadecafluoro-1-octanesulfonamide (N-MeFOSA), were supplied by Wellington Laboratories Inc. (Guelph, Ontario, Canada), while N-ethyl-1,1,2,2,3,3,4,4,5,5,6,6,7,7,8,8,8-heptadecafluoro-1-octanesulfonamide (N-EtFOSA) was purchased from Dr. Ehrenstorfer GmbH (Ausburg, Germany). Standard mixtures of all compounds at 1 mg L^{-1} were prepared by appropriate dilution of the stock standard solutions in methanol, for GC–MS experiments, and acetonitrile/water (1:1 v/v), for LC–MS analysis. A set of six calibration solutions containing FTOHs, FOSAs and FOSEs at concentrations ranging from 10 to 800 ng L^{-1} and FTOs at concentrations from 0.25 to 200 μg L^{-1} were prepared by dilution of the corresponding standard mixtures. All these solutions were stored at 4 °C until analysis.

Water and acetonitrile (LC–MS Chromasolv™, purity ≥ 99%), tert-butyl methyl ether (Chromasolv™, purity ≥ 99.8%), ethyl acetate (Chromasolv™), and dichloromethane for pesticide residual analysis, were purchased from Sigma-Aldrich (St Louis, MO, USA), while methanol (LiChrosolv™, purity ≥ 99.9%) was supplied by Merck (Darmstadt, Germany). Furthermore, acetone for pesticide residue analysis, anisole (anhydrous, purity at 99.7%), toluene and chlorobenzene (Chromasolv™ Plus for HPLC analysis, purity ≥ 99.8%) from Sigma-Aldrich, and tetrahydrofuran (Photrex™ reagent, purity at 99%) from J. T. Baker (Deventer, Holland), were used as APPI dopants. Besides, ultra-pure water was obtained from a Milli-Q system coupled to an Elix 3 (Millipore, Bedfore, MA, USA). All glassware was treated with chromosulphuric acid and rinsed consecutively with Milli-Q water and acetone before use.

Helium (purity ≥ 99.9993%), employed as GC carrier gas, and nitrogen as auxiliary and nebulizer gas for ESI, APCI and APPI sources, were supplied by Linde (Barcelona, Spain), while methane (purity ≥ 99.95%), used as chemical ionisation reagent gas in GC–MS analysis, and argon (purity ≥ 99.999%), employed as collision gas in MS/MS experiments, were purchased from Air Liquide (Madrid, Spain).

2.2. Sampling and sample treatment

Five river water samples were collected from areas highly influenced by human and industrial activities to assess the applicability of the proposed methodology and to know the real occurrence of the target compounds in surface waters. From the five surface waters, two samples were collected in the last part of the Llobregat River (Barcelona, Spain), which runs through very densely populated and industrialised areas, receiving extensive urban and industrial wastewater discharges from more than 3 million inhabitants. Another two samples were taken from the Ebro River (Tarragona, Spain) before and after the industrial region of Tortosa. Finally, one water sample was collected from Fluvià River, which crosses towns and industrialised areas with a low-medium contamination impact. Glass bottles (1000 mL) fitted with black Viton septa were

filled with water without headspace and stored in the dark at 4 °C before being analysed. Field blanks consisting of 1000 mL of natural mineral water were prepared at the same sampling points and they were analysed along with the water samples.

The target compounds were extracted from the river water samples employing a solid-phase extraction (SPE) method previously described elsewhere [28]. Briefly, a volume of 500 mL of water sample was loaded into an Oasis HLB® cartridge (500 mg, 6 mL) (Waters, Milford, MA, USA) at a flow rate of 10 mL min^{-1} using a Visiprep System (Supelco, Bellefonte, PA, USA). Before use, SPE cartridge was conditioned with 20 mL of methanol and 20 mL of Milli-Q water, and then it was dried under a nitrogen stream during 15 min. Once the sample was extracted, the cartridge was washed with 10 mL of methanol/Milli-Q water mixture (5:95, v/v), dried with a gentle nitrogen current during 30 min and analytes were then eluted with 4 mL of methanol. For LC–MS analysis, an aliquot of 1 mL of the extract was diluted 1:3 (v/v) with Milli-Q water and then 10 μL of the final extract were injected.

2.3. GC–MS analysis

The GC–MS determination of neutral PFASs was carried out on a Trace GC 2000 Series coupled to a DSQ II mass spectrometer equipped with an AS 2000 autosampler (Thermo Fisher Scientific, San Jose, CA, USA). The chromatographic separation of target compounds was performed on a DB-624 (6%-cyanopropylphenyl 94%-dimethyl polysiloxane) fused-silica capillary column (Agilent Technologies, Santa Clara, CA, USA) of 60 m of length, 0.25 mm I.D., and 1.40 μm film thickness, using helium as carrier gas at constant flow rate of 1.0 mL min^{-1}. The injector was operated at 250 °C in split mode (split ratio: 1:15), injecting a volume of 1 μL for standards and sample extracts. The oven temperature was programmed from 50 °C (held for 2 min) to 120 °C at 10 °C min^{-1}, and then to 250 °C (held for 6 min) at 25 °C min^{-1}. The MS was operated in electron ionisation (EI), chemical ionisation (CI) and negative ion chemical ionization (NICI) modes using an ion source temperature of 200 °C, 180 °C and 180 °C, respectively. In addition, electron energy was set to 70 eV for EI and NICI, and 120 eV for CI, while the emission current was fixed to 50 μA for EI and CI, and 100 μA for NICI, us-

ing in all cases a transfer line temperature of 250 °C. Methane was used as reagent gas at an optimum flow rate of 1.5 mL min^{-1} for CI and 2.0 mL min^{-1} for NICI. The optimisation of the MS operating parameters was carried out in full-scan mode over 40–650 *m/z* range using a scan time of 0.50 s. After MS optimisation, acquisition was performed in selected ion monitoring (SIM) mode using a dwell time of 100 ms and a delay time of 20 ms. Table 1 shows the ions selected for the identification and confirmation of the target compounds. Xcalibur™ υ 1.4 software was used to control the instrument setup, data acquisition and processing.

2.4. LC–MS analysis

The analyses were performed on an UHPLC system equipped with an autosampler (Accela Open AS) and a quaternary pump (Accela 1250 Pump) (Thermo Fisher Scientific). The chromatographic separation of target compounds was investigated using two fused-core columns: Accucore C18 (100 × 2.1 mm I.D., 2.6 μm) and Accucore PFP (pentafluorophenyl bonded phase, 150 × 2.1 mm I.D., 2.6 μm) (Thermo Fisher Scientific), and two totally porous particle columns: Luna C18 (100 × 2.1 mm I.D., 1.6 μm) and Luna Polar C18 (100 × 2.1 mm I.D., 1.6 μm) (Phenomenex, Torrance, CA, USA). After optimisation of the separation, Luna C18 column was chosen for the determination of the target compounds. The UHPLC system was coupled to a triple quadrupole TSQ Quantum Ultra AM mass spectrometer (Thermo Fisher Scientific) equipped with heated-electrospray (H-ESI), atmospheric pressure chemical ionisation (APCI) and atmospheric pressure photoionisation (APPI) sources, operating in both ion modes (positive and negative). For the separation of target compounds, the acetonitrile/water gradient elution program was as follows: from 55% to 75% acetonitrile (ACN) in 3 min; from 75% to 100% ACN in 7 min followed by an isocratic step at 100% ACN for 1 min before returning to the initial conditions. For APPI conditions, toluene was used as dopant (5%, v/v). All LC–MS analyses were performed by injecting 10 μL of sample extracts and standards. The vaporizer and the capillary temperatures were fixed at 450 °C and 275 °C, respectively. Moreover, the nebuliser and auxiliary gas pressure were set at 50 and 25 arbitrary units (a.u.). The current discharge was fixed at 12 μA for

Table 1
Ions selected for GC–MS determination of the target compounds using EI, CI and NICI techniques.

Compound	EI		CI		NICI	
	m/z	Assignation	*m/z*	Assignation	*m/z*	Assignation
4:2 FTO	77	$[C_3H_3F_2]^+$	227	$[M-F]^+$	226	$[M-HF]^{-\bullet}$
	227	$[M-F]^+$	228	$[M_{13}-F]^+$	186	$[M-2HF-F_2]^{-\bullet}$
6:2 FTO	77	$[C_3H_3F_2]^+$	327	$[M-F]^+$	286	$[M-3HF]^{-\bullet}$
	327	$[M-F]^+$	328	$[M_{13}-F]^+$	306	$[M-2HF]^{-\bullet}$
8:2 FTO	77	$[C_3H_3F_2]^+$	427	$[M-F]^+$	386	$[M-3HF]^{-\bullet}$
	427	$[M-F]^+$	428	$[M_{13}-F]^+$	406	$[M-2HF]^{-\bullet}$
4:2 FTOH	95	$[C_3H_2F_3]^+$	265	$[M+H]^+$	222	$[M-H_4F_2]^{-\bullet}$
	244	$[M-HF]^{+\bullet}$	227	$[M-H_2O-F]^+$	184	$[M-4HF]^{-\bullet}$
6:2 FTOH	95	$[C_3H_2F_3]^+$	365	$[M+H]^+$	304	$[M-3HF]^{-\bullet}$
	344	$[M-HF]^{+\bullet}$	327	$[M-H_2O-F]^+$	284	$[M-4HF]^{-\bullet}$
7-Me-6:2 FTOH	95	$[C_3H_2F_3]^+$	415	$[M+H]^+$	306	$[M-CF_2-HF-F_2]^{-\bullet}$
	394	$[M-HF]^{+\bullet}$	377	$[M-H_2O-F]^+$	316	$[M-3HF-F_2]^{-\bullet}$
8:2 FTOH	95	$[C_3H_2F_3]^+$	465	$[M+H]^+$	386	$[M-3HF-H_2O]^{-\bullet}$
	444	$[M-HF]^{+\bullet}$	427	$[M-H_2O-F]^+$	384	$[M-4HF]^{-\bullet}$
10:2 FTOH	95	$[C_3H_2F_3]^+$	565	$[M+H]^+$	484	$[M-4HF]^{-\bullet}$
	505	$[M-H_2F_3]^+$	527	$[M-H_2O-F]^+$	486	$[M-3HF-H_2O]^{-\bullet}$
N-MeFOSA	94	$[CH_3NSO_2H]^+$	528	$[M+H]^+$	94	$[CH_3NSO_2H]^-$
	448	$[M-SO_2H]^+$	529	$[M_{13}+H]^+$	493	$[M-HF]^{-\bullet}$
N-EtFOSA	108	$[C_2H_5NSO_2H]^+$	514	$[M+H]^+$	108	$[C_2H_5NSO_2H]^-$
	448	$[M-CH_3SO_2H]^+$	515	$[M_{13}+H]^+$	483	$[M-C_2H_5NH]^-$
N-MeFOSE	526	$[M-CH_2OH]^+$	558	$[M+H]^+$	138	$[C_3H_8NSO_3]^-$
	462	$[C_{10}H_5NF_{17}]^+$	540	$[M+H-H_2O]^+$	512	$[M-C_2H_4OH]^-$
N-EtFOSE	540	$[M-CH_2OH]^+$	572	$[M+H]^+$	152	$[C_4H_{10}NSO_3]^-$
	448	$[C_9H_3NF_{17}]^+$	554	$[M+H-H_2O]^+$	526	$[M-C_2H_4OH]^-$

Table 2

Multiple reaction monitoring (MRM) transitions selected for UHPLC–API–MS/MS determination of FTOs, FTOHs, FOSAs and FOSEs.

Compound	Precursor ion		Product ion		NCE (%)[a]
	m/z	Assignment	*m/z*	Assignment	
4:2 FTO	186	$[M-3HF]^{-\bullet}$	117	$[M-3HF-CF_3]^-$	20
			136	$[M-3HF-CF_2]^-$	20
6:2 FTO	286	$[M-3HF]^{-\bullet}$	167	$[M-3HF-C_2F_5]^-$	16
			217	$[M-3HF-CF_3]^-$	22
8:2 FTO	386	$[M-3HF]^{-\bullet}$	267	$[M-3HF-C_2F_5]^-$	24
			317	$[M-3HF-CF_3]^-$	22
4:2 FTOH	184	$[M-4HF]^{-\bullet}$	136	$[M-4HF-CHOF]^{-\bullet}$	16
			164	$[M-4HF-HF]^{-\bullet}$	12
6:2 FTOH	284	$[M-4HF]^{-\bullet}$	236	$[M-4HF-CHOF]^{-\bullet}$	18
			264	$[M-4HF-HF]^{-\bullet}$	14
7-Me-6:2 FTOH	306	$[M-CHF_5]^{-\bullet}$	236	$[M-CHF_5-CH_3]^{-\bullet}$	28
			286	$[M-CHF_5-HF]^{-\bullet}$	20
8:2 FTOH	384	$[M-4HF]^{-\bullet}$	295	$[M-4HF-CHF_4]^-$	25
			298	$[M-4HF-CHOF_3]^-$	22
10:2 FTOH	484	$[M-4HF]^{-\bullet}$	295	$[M-4HF-C_3HF_8]^-$	26
			464	$[M-4HF-HF]^{-\bullet}$	14
N–MeFOSA	512	$[M-H]^-$	169	$[M-H-CH_3NSO_2-C_5F_{10}]^-$	30
			219	$[M-H-CH_3NSO_2-C_4F_8]^-$	25
N–EtFOSA	526	$[M-H]^-$	169	$[M-H-CH_2CH_3NSO_2-C_5F_{10}]^-$	32
			219	$[M-H-CH_2CH_3NSO_2-C_4F_8]^-$	28
N–MeFOSE	494	$[M-CH_2CH_2OF]^-$	350	$[M-CH_2CH_2OF-4HF-SO_2]^-$	20
			370	$[M-CH_2CH_2OF-3HF-SO_2]^-$	20
N–EtFOSE	508	$[M-CH_2CH_2OF]^-$	488	$[M-CH_2CH_2OF-HF]^-$	24
			324	$[M-CH_2CH_2OF-6HF-SO_2]^-$	22

[a] NCE: normalised collision energy.

APCI, while in APPI the krypton lamp emitted photons with an energy of 10.6 eV. The tube lens potential values were optimised for each compound ranging from –70 to –100 V.

For UHPLC–APCI–MS/MS and UHPLC–APPI–MS/MS methods, data acquisition was performed in negative-ion mode using multiple reaction monitoring (MRM), dwell times ranging from 50 to 150 ms and argon as collision gas at a pressure of 1.0 bar. The scan width and the peak width were set at 0.3 *m/z* and 0.7 *m/z*, respectively. Table 2 shows the MRM transitions selected for the determination of the target compounds. Xcalibur™ *v* 2.1 software was used to control the instrument setup and data acquisition.

2.5. Quality control

Criteria for ensuring the quality of the data included specific tests for checking the chromatographic separation, the sensitivity of the GC–MS and UHPLC–MS systems using standards and quality control water samples, the validity of the calibration, and the possible carryover between samples. Procedural blanks covering both the instrumental and the sample treatment procedure were routinely analysed to evaluate the contribution of potential interfering compounds on the neutral PFAS responses. In addition, each water sample was accompanied by a field blank to ensure the accurate tracing of any contamination. Quality parameters of the method, such as limits of detection (LODs) and quantification (LOQs), and precision were routinely checked to ensure the quality of the results. In addition, recoveries of the analytes were periodically tested by analysing a blank river water spiked at low concentration levels.

3. Results and discussion

3.1. Gas chromatography-mass spectrometry determination

As first step, the chromatographic retention and separation of these compounds, especially short alkyl chain FTOs, was evaluated testing three different capillary columns. The non-polar poly(diphenyldimethyl siloxane) containing 5% diphenylsiloxane monomer (DB-5MS, 30 m × 0.25 mm I.D; 0.25 μm) and the

polar poly(ethylene glycol)-based (TG-WAX, 30 m × 0.25 mm I.D; 0.25 μm) columns did not allow a correct retention and separation of the target compounds. In light of these results, a semi-polar poly(cyanopropylphenyldimethyl siloxane)-based column (DB-624, 60 m × 0.25 mm I.D., 1.4 μm film thickness) was evaluated and it provided the best chromatographic separation for all the compounds. Considering the low retention times observed for FTOs, different solvents such as methanol, acetonitrile, methyl tert-butyl ether, dichloromethane, acetone and ethyl acetate were tested in order to elute the most volatile FTOs far enough from the solvent peak tailing. Since methanol showed the lowest retention on GC column, it was selected as solvent for GC–MS determination. Fig. 1 shows the chromatographic separation of the target compounds obtained under optimal conditions. As can be seen, all the neutral PFASs can be analysed in a single run, although the most volatile olefin (4:2 FTO) slightly overlapped with the tail of the solvent peak.

The ionisation efficiency of EI, CI and NICI techniques were tested to select the best conditions for the sensitive determination. Concerning EI, a high fragmentation was observed for FTOs, FTOHs and FOSAs, generating abundant ions at low *m/z* values, while FOSEs yielded less fragmentation. For instance, Fig. 2 shows the EI mass spectra obtained for 8:2 FTO and *N*-EtFOSE, where $[C_3H_3F_2]^+$ (*m/z* 77) and $[M-CH_2OH]^+$ (*m/z* 540) were the base peaks, respectively. As expected, CI provided less fragmentation than EI (Fig. 2 and Fig. S1), being the protonated molecule the base peak of the mass spectra for most of the analytes (Fig. S1), while FTOs led to $[M-F]^+$ ions (Fig. 2). In the case of NICI, all the compounds showed a high fragmentation and their mass spectra included radical ions originated from successive losses of HF units (20 Da) from the molecular ion for FTOs and FTOHs, and fragment ions at low *m/z* values for FOSAs and FOSEs. This can be observed in Fig. 2 for 8:2 FTO and *N*-EtFOSE and in Fig. S1 for *N*-EtFOSA. Comparing the capabilities and performances of the three MS ionisation techniques for detecting all target compounds in a single run, CI seems to be the most adequate ionisation technique since it provides less fragmented mass spectra and, therefore, a more selective determination for most of the compounds.
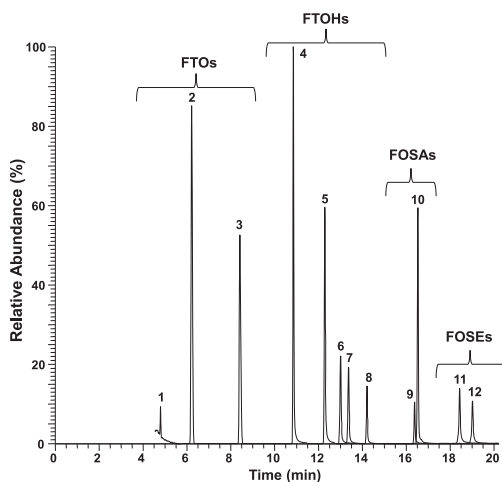
Fig. 1. GC–MS SIM chromatogram of a standard mixture of the target compounds at a concentration of 100 µg L^{-1} using a DB-624 column (60 m length, 0.25 mm I.D., 1.4 µm film thickness). Peaks: (1) 4:2 FTOH, (2) 6:2 FTO, (3) 8:2 FTO, (4) 4:2 FTOH, (5) 6:2 FTOH, (6) 7-Me-6:2 FTOH, (7) 8:2 FTOH, (8) 10:2 FTOH, (9) *N*-MeFOSA, (10) *N*-EtFOSA, (11) *N*-MeFOSE, (12) *N*-EtFOSE.

3.2. Ultra-high performance liquid chromatography-tandem mass spectrometry determination

In a previous work, we examined the applicability of several atmospheric pressure ionisation (API) sources for the sensitive determination of FTOHs, FOSAs and FOSEs by LC–MS/MS [28], demonstrating the efficient ionisation of these families of compounds by negative-ion APCI and APPI. To develop a multi-class method for neutral PFASs, including FTOs, a thorough optimisation of the chromatographic separation and mass spectrometry determination was required. Since there is no information about the behaviour of the FTOs using API sources, preliminary experiments were conducted to investigate their ionization efficiency by APCI and APPI techniques. For this purpose, both positive and negative-ion modes were tested using water/organic solvent (acetonitrile and methanol) mobile phase mixtures (1:1, v/v) and only the negative-ion mode allowed the ionisation of FTOs using APCI. In addition, the use of a dopant (toluene, acetone or anisole, among others) was required to allow their ionisation in negative-ion APPI. To achieve the highest responses for FTOs, a vaporizer temperature of 450 °C was required, although it also caused in-source fragmentation by collision-induced dissociation (CID) for the other families of neutral PFASs. Under these conditions, mass spectra were quite similar using both APCI and APPI ionisation techniques for all the compounds. Thus, FTOs showed [M−3HF]$^{-\bullet}$ as the base peak of the

mass spectra due to the losses of three HF units from the molecular ion, as it can be seen in Fig. 3a for 8:2 FTO. In addition, it could be observed some fragment ions corresponding to the loss of HF units and fluorine atoms or CF$_2$ units. Regarding FTOHs, two different ionisation mechanisms *via* radical and deprotonation can take place simultaneously [28]. However, the high vaporizer temperature required to maximise FTOs ionisation led to the formation of radical ions for FTOHs, since the proton transfer mechanism was not favoured in APPI and even hindered in APCI. For instance, Fig. 3b shows the negative-ion APPI mass spectrum of 10:2 FTOH, where the presence of abundant odd-electron ions was observed. In the case of FOSAs, the deprotonated molecule was the base peak of the mass spectra (Fig. 3c for *N*-MeFOSA), while for FOSEs the main ions observed were in-source CID fragments corresponding to [M−C$_2$H$_5$ORN]$^-$ (R: −CH$_3$, −−CH$_2$CH$_3$) ions (Fig. 3d). Therefore, 450 °C was chosen as optimal vaporizer temperature for the multi-class LC–MS determination, although at this temperature the ionisation efficiency of FTOHs, FOSAs and FOSEs was slightly reduced.

Considering that the mobile phase composition significantly affects the ionisation efficiency of these compounds [28], several mixtures of methanol/water and acetonitrile/water were tested as mobile phases. The best performance in terms of ionization efficiency for both APCI and APPI were observed using acetonitrile/water mixtures with an acetonitrile content higher than 50% (v/v). As an example, Fig. S2 shows the effect of the mobile phase composition on the 8:2 FTO response using methanol and acetonitrile as organic modifier. Concerning APPI, different dopants were evaluated and toluene provided the highest responses for FTOs (Fig. S3a), as well as for FTOHs, FOSAs and FOSEs, working at a flow rate of 15 µL min^{-1}, which corresponded to a 5% (v/v) of the total flow rate (Fig. S3b). The most abundant ions generated by APCI and APPI were selected as precursor ions for tandem mass spectrometry experiments. However, the selected precursor ions for FOSEs ([M−C$_2$H$_5$ORN]$^-$, with R: −CH$_3$, −CH$_2$CH$_3$) yielded product ions with low signal-to-noise ratios. To improve the detectability of these compounds by MS/MS, the [M−C$_2$H$_4$OF]$^-$ in-source CID fragment ions were selected as precursor ions since they yielded more intense product ions. Table 2 summarises the two most intense MRM transitions chosen for the UHPLC–MS/MS determination of neutral PFASs.

Once established the API conditions, several UHPLC columns, fused-core and totally porous particle technology (see Section 2.4), were tested to achieve the retention and separation of the analytes. The four UHPLC columns are packed with particles of different sizes (2.6 and 1.6 µm) and technologies (fused-core and totally porous), but also different bonded stationary phases (C18 and PFP), which are adequate for the simultaneous retention of semi-polar (FTOHs, FOSAs and FOSEs) and non-polar PFASs (FTOs). Fused-core columns such as Accucore C18 and Accucore PFP provided poorest resolution, column efficiency, peak asymmetry and run-to-run precision than those obtained using the totally porous columns (Table 3). Considering Luna C18 column was able to resolve the

Table 3
Comparison of UHPLC columns for the separation of the target compounds.

Column	Number of peaks resolved			H (µm)[a]	A$_s$[b]	Peak area precision (RSD, %)[c]
	$R_s < 1$	$1 < R_s < 1.5$	$R_s > 1.5$			
Accucore C18	5	3	4	3–54	1.0–1.5	0.7–8.9
Accucore PFP	8	1	3	15–77	0.9–2.7	3.8–37.2
Luna C18	2	2	8	1–15	0.8–1.2	1.8–5.0
Luna Polar C18	2	6	4	1–12	0.8–1.2	2.5–4.7

[a] H: Height equivalent to a theoretical plate (HETP).
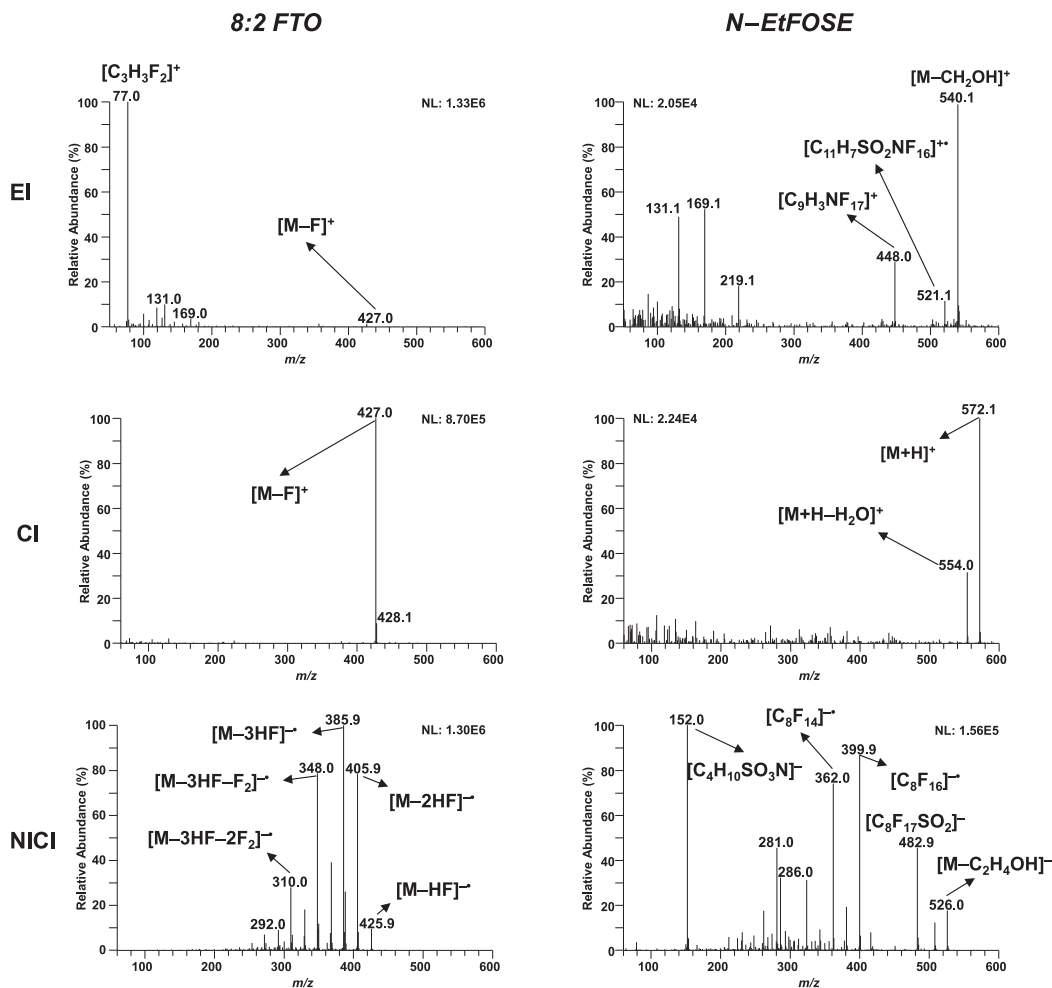[b] A$_s$: Peak asymmetry.
[c] $n = 3$.

Fig. 2. Mass spectra of 8:2 FTO and *N*-EtFOSE under EI, CI and NICI ionisation conditions.

separation of a greater number all compounds in less than 9 min ($R_s > 1.5$) that with the Luna Polar C18 column, it was selected for the chromatographic separation of neutral PFASs by LC–MS (Fig. 4). Besides, ion suppression and ion enhancement were considered negligible for partially co-eluting compounds ($R_s < 1.5$) because the differences observed between responses obtained for the compound analysed individually and in a mixture were lower than 7%.

3.3. Comparison of GC–MS and UHPLC–MS/MS methods

Once established the UHPLC–MS/MS and GC–MS methods, quality parameters, such as instrumental limit of detection (ILOD), defined as three times the signal-to-noise ratio, and run-to-run precision, were compared to select the most appropriated method for the determination of the target compounds. As it can be observed in Table 4, negative-ion APPI provided the highest ILODs with val-

ues for FTOHs and FTOs ranging from 0.9 to 4000 µg L^{-1}. This could be attributed to the lower ionization efficiency of these compounds at the established APPI conditions. In contrast, negative-ion APCI provided better detectability of target compounds, achieving ILODs from 0.2 to 1 µg L^{-1} except for 6:2 FTOH and 4:2 FTO, which were 23 and 100 µg L^{-1}, respectively. For the classical GC–MS ionisation techniques, NICI was discarded because it provided a poor run-to-run precision (RSD 10–55%), while EI and CI provided ILODs between 0.06 and 6 µg L^{-1}, except for 4:2 FTO which were 17 and 429 µg L^{-1}, respectively. Comparing CI and negative-ion APCI, ILODs were very similar, although 4:2 FTO was slightly suppressed by the solvent peak in GC–MS. Taking into account that negative-ion APCI provided better intra-day precision (RSD 1.2–5.0%, $n = 3$) than those obtained with CI, and the good retention of FTOs observed in the UHPLC column, the UHPLC–APCI–MS/MS method is proposed for the analysis of the target compounds.
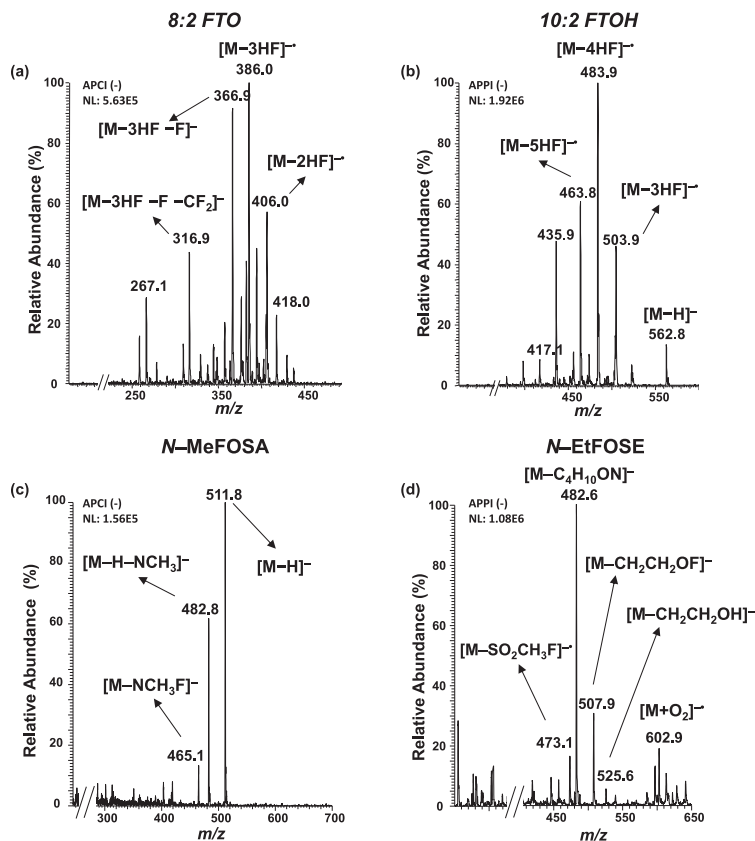
Fig. 3. Mass spectra of (a) 8:2 FTO and (c) *N*-MeFOSA, obtained under negative-ion APCI conditions, and (b) 10:2 FTOH and (d) *N*-EtFOSE obtained under negative-ion APPI conditions.
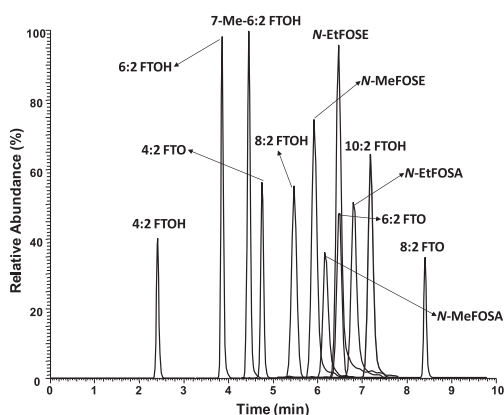
Fig. 4. UHPLC–APCI–MS/MS chromatogram of a standard mixture of target compounds obtained using a Luna C18 column (100 × 2.1 mm I.D., 1.6 μm).

Table 4

Instrumental limits of detection for both GC–MS and UHPLC–MS/MS methods.

Compound	Instrumental LOD (μg L^{-1})			
	GC–MS[a]		UHPLC–MS/MS[b]	
	EI	CI	APCI (−)	APPI (−)
4:2 FTO	17	429	100	4000
6:2 FTO	2	0.3	23	1800
8:2 FTO	1	0.2	0.9	500
4:2 FTOH	2	0.2	0.8	225
6:2 FTOH	2	0.2	0.2	7
7-Me-6:2 FTOH	0.2	0.06	0.1	0.9
8:2 FTOH	5	0.5	0.9	23
10:2 FTOH	6	1	0.3	2
N-MeFOSA	1	4	0.7	0.08
N-EtFOSA	2	1	1	0.1
N-MeFOSE	1	4	0.3	0.2
N-EtFOSE	1	1	0.3	0.3

[a] Injection volume: 1 μL.
[b] Injection volume: 10 μL.

Table 5
Quality parameters of the SPE UHPLC–APCI–MS/MS method.

Compound	MLOD (ng L^{-1})	MLOQ (ng L^{-1})	Matrix effect (± SD) (%)[a]		Recovery (± SD) (%)[a]		Intra-day precision (RSD, %)[a]		Inter-day precision (RSD, %)[a]		Trueness (RE, %)[a]	
			Low[b]	Medium[c]	Low[b]	Medium[c]	Low[b]	Medium[c]	Low[b]	Medium[c]	Low[b]	Medium[c]
4:2 FTO	6000	13000	5 ± 3	1 ± 2	94 ± 1	100 ± 3	3	3	3	3	−6	7
6:2 FTO	2000	7000	7 ± 6	2 ± 1	96 ± 9	98 ± 1	7	2	7	2	−7	−3
8:2 FTO	70	200	8 ± 3	8 ± 6	95 ± 4	93 ± 6	7	6	9	7	−10	−3
4:2 FTOH	12	40	5 ± 5	2 ± 2	95 ± 3	98 ± 2	4	3	5	3	−3	−5
6:2 FTOH	6	13	7 ± 9	2 ± 1	95 ± 4	97 ± 2	5	4	7	3	1	−7
7-Me-6:2 FTOH	3	10	4 ± 7	2 ± 3	95 ± 9	99 ± 1	6	2	7	2	2	−7
8:2 FTOH	19	77	4 ± 5	4 ± 4	97 ± 4	100 ± 3	6	2	6	2	−9	−6
10:2 FTOH	7	23	2 ± 5	4 ± 3	100 ± 6	98 ± 3	2	3	4	3	7	−8
N-MeFOSA	11	37	1 ± 5	3 ± 4	94 ± 4	97 ± 1	3	2	4	2	−1	−8
N-EtFOSA	17	56	10 ± 3	2 ± 3	95 ± 4	96 ± 2	3	1	4	3	3	−1
N-MeFOSE	8	26	15 ± 4	7 ± 2	90 ± 3	96 ± 1	6	2	6	3	−9	−2
N-EtFOSE	7	23	8 ± 8	1 ± 1	94 ± 9	98 ± 1	1	1	5	2	−1	−4

[a] $n = 5$.
[b] Low level: 50–150 ng L^{-1} for FTOHs, FOSAs and FOSEs, and 500–20,000 ng L^{-1} for FTOs.
[c] Medium level: 200–600 ng L^{-1} for FTOHs, FOSAs and FOSEs, and 2000–80,000 ng L^{-1} for FTOs.

3.4. Analysis of water samples

The developed UHPLC–APCI–MS/MS method combined with a SPE procedure previously developed [28] was applied to the analysis of river water samples. To examine the validity of the whole method, quality parameters were investigated. Method limits of detection (MLOD) and quantification (MLOQ), defined as the concentration that produces respectively a signal-to-noise ratio of three and ten, were determined using a blank river water spiked with target compounds at very low concentration levels. MLODs and MLOQs for FTOHs, FOSAs and FOSEs ranged from 3 to 19 ng L^{-1} and between 10 and 77 ng L^{-1}, while for FTOs the values were between 70 and 6000 ng L^{-1}, and from 200 to 13000 ng L^{-1}, respectively (Table 5). These results confirm the good detectability of the SPE UHPLC–APCI–MS/MS method.

Other quality parameters, such as matrix effect, recovery, precision and trueness, were estimated ($n = 5$) at low (50–150 ng L^{-1} for FTOHs, FOSAs and FOSEs, and 500–20,000 ng L^{-1} for FTOs) and medium concentration levels (200–600 ng L^{-1} for FTOHs, FOSAs and FOSEs, and 2000–80,000 ng L^{-1} for FTOs). Matrix effect (ME, %) was calculated as the relative difference on the peak area between spiked blank extract and standard solution at the same concentration level. The ME (%) values were lower than 15% for all the compounds (Table 5). Therefore, a matrix-matched calibration was carried out to correct this slight deviation. Moreover, recoveries of the target compounds, involving matrix effect and extraction efficiency, ranged from 90 to 100% (Table 5). The intraday and inter-day precision were studied by analysing spiked water samples on one day and two non-consecutive days, respectively. Relative standard deviations (RSD %) for the intra-day and inter-day precision were respectively lower than 7% and 9%. Finally, the trueness was also determined achieving relative errors up to 10% for all the compounds. These results showed the good performance of the developed method and it was then applied to the simultaneous determination of FTOs, FTOHs, FOSAs and FOSEs in river water samples. The presence of 4:2 FTOH and N-EtFOSA were detected at 45 ± 1 ng L^{-1} in the Llobregat River and 690 ± 20 ng L^{-1} in the Ebro River, respectively. These values were in agreement with those previously reported [28], confirming that the concentrations of these compounds remain almost constant over time (more than one year). Besides, 8:2 FTO could be also detected at concentration lower than the limit of quantification (< 200 ng L^{-1}) in the Ebro River water. The presence of the other compounds was not detected in any of the analysed samples. These findings suggest a constant release of 4:2 FTOH and N-EtFOSA to the Llobregat and Ebro River basin and further studies should be done to identify potential source of this pollution.

4. Conclusions

This work demonstrates, for the first time, the good efficiency of the atmospheric pressure ionisation sources (APCI and APPI) for the simultaneous determination of FTOs with other families of neutral PFASs (FTOHs, FOSAs and FOSEs) using a UHPLC–MS/MS method. Although gas chromatography-mass spectrometry methods offer good performance for the analysis of these compounds, the UHPLC–MS/MS provided interesting advantages over them, such as adequate retention of FTOs, high efficiency on the ionisation of the studied neutral PFASs and low detection limits for a suitable analysis of water samples. The required high vaporizer temperature necessary to maximise the ionisation of FTOs by negative-ion APCI and APPI also allowed an acceptable response for the rest of compounds. Moreover, the use of a totally porous (1.6 µm) Luna C18 UHPLC column combined with an acetonitrile/water mobile phase provided the best performance for both the chromatographic separation and the ionisation of neutral PFASs. The combination of a SPE Oasis HLB® sample treatment with the UHPLC–APCI–MS/MS method provided low limits of detection, good precision and trueness. Therefore, this method was proposed for the simultaneous determination of FTOs, FTOHs, FOSAs and FOSEs in river water samples. The concentration levels found in the river water samples suggested a constant release of some neutral PFASs, might be coming from industrial activities.

Declaration of Competing Interest

The authors declare that they have no conflict of interest.

Acknowledgements

Supplementary materials

Supplementary material associated with this article can be found, in the online version, at doi:10.1016/j.chroma.2019.460463.

References

[1] E. Kissa, Fluorinated Surfactants and Repellents, 2nd ed., Marcel Dekker, New York, 2001.

[2] R.C. Buck, J. Franklin, U. Berger, J.M. Conder, I.T. Cousins, P. De Voogt, A.A. Jensen, K. Kannan, S. a. Mabury, S.P.J. van Leeuwen, Perfluoroalkyl and polyfluoroalkyl substances in the environment: terminology, classification, and origins, Integr. Environ. Assess. Manag 7 (2011) 513–541 http://dx.doi.org/10.1002/ieam.258.

[3] J. Campo, A. Masiá, Y. Picó, M. Farré, D. Barceló, Distribution and fate of perfluoroalkyl substances in Mediterranean Spanish sewage treatment plants, Sci. Total Environ. 472 (2014) 912–922 http://dx.doi.org/10.1016/j.scitotenv.2013.11.056.

[4] G. Munoz, J.-L. Giraudel, F. Botta, F. Lestremau, M.-H. Dévier, H. Budzinski, P. Labadie, Spatial distribution and partitioning behavior of selected poly- and perfluoroalkyl substances in freshwater ecosystems: a French nationwide survey, Sci. Total Environ. 517 (2015) 48–56 http://dx.doi.org/10.1016/j.scitotenv.2015.02.043.

[5] F.M. Hekster, R.W.P.M. Laane, P. de Voogt, Environmental and toxicity effects of perfluoroalkylated substances, in: G.W. Ware (Ed.), Rev. Environ. Contam. Toxicol., 179, Springer, New York, 2003, pp. 99–121.

[6] H.J. Lehmler, Synthesis of environmentally relevant fluorinated surfactants - a review, Chemosphere 58 (2005) 1471–1496 http://dx.doi.org/10.1016/j.chemosphere.2004.11.078.

[7] H. Fromme, S.A. Tittlemier, W. Völkel, M. Wilhelm, D. Twardella, Perfluorinated compounds - exposure assessment for the general population in western countries, Int. J. Hyg. Environ. Health 212 (2009) 239–270 http://dx.doi.org/10.1016/j.ijheh.2008.04.007.

[8] Y. Picó, M. Farré, M. Llorca, D. Barceló, Perfluorinated compounds in food: a global perspective, Crit. Rev. Food Sci. Nutr. 51 (2011) 605–625 http://dx.doi.org/10.1080/10408391003721727.

[9] A. Galatius, R. Bossi, C. Sonne, F.F. Rigét, C.C. Kinze, C. Lockyer, J. Teilmann, R. Dietz, PFAS profiles in three North Sea top predators: metabolic differences among species? Environ. Sci. Pollut. Res. 20 (2013) 8013–8020 http://dx.doi.org/10.1007/s11356-013-1633-x.

[10] S. Fang, X. Chen, S. Zhao, Y. Zhang, W. Jiang, L. Yang, L. Zhu, Trophic magnification and isomer fractionation of perfluoroalkyl substances in the food web of Taihu Lake, China, Environ. Sci. Technol. 48 (2014) 2173–2182 http://dx.doi.org/10.1021/es405018b.

[11] A.M. Calafat, X. Ye, M.J. Silva, Z. Kuklenyik, L.L. Needham, M. Kolossa, J. Tuomisto, A. Astrup Jensen, Human exposure assessment to environmental chemicals using biomonitoring, Int. J. Androl. 29 (2006) 166–171 http://dx.doi.org/10.1111/j.1365-2605.2005.00570.x.

[12] M. Llorca, M. Farré, Y. Picó, M.L. Teijón, J.G. Álvarez, D. Barceló, Infant exposure of perfluorinated compounds: levels in breast milk and commercial baby food, Environ. Int. 36 (2010) 584–592 http://dx.doi.org/10.1016/j.envint.2010.04.016.

[13] Decision SC-4/17 of 4–8 May 2009 of Listing listing of perfluorooctanesulfonic acid, its salts and perfluorooctano sulfonyl fluoride. United Nation Environment Programme. Stockholm Convention on Persistent Organic Pollutants. UNEP/POPS/COP-4/38:66–9. Available at: http://www.pops.int/TheConvention/Overview/TextoftheConvention/tabid/2232/Default.aspx (accessed 20.03.19).

[14] Council Decision (EU), 2015/633 of 20 April 2015 on the submission, on behalf of the European Union, of a proposal for the listing of additional chemicals in Annex A to the Stockholm Convention on Persistent Organic Pollutants, Off. J. Eur. Union. L 104 (2015) 14–15.

[15] A. Jahnke, L. Ahrens, R. Ebinghaus, C. Temme, Urban versus remote air concentrations of fluorotelomer alcohols and other polyfluorinated alkyl substances in Germany, Environ. Sci. Technol. 41 (2007) 745–752 http://dx.doi.org/10.1021/es0619861.

[16] B. Szostek, K.B. Prickett, Determination of 8:2 fluorotelomer alcohol in animal plasma and tissues by gas chromatography-mass spectrometry, J. Chromatogr. B Anal. Technol. Biomed. Life Sci. 813 (2004) 313–321 http://dx.doi.org/10.1016/j.jchromb.2004.10.031.

[17] M. Shoeib, T. Harner, M. Ikonomou, K. Kannan, Indoor and outdoor air concentrations and phase partitioning of perfluoroalkyl sulfonamides and polybrominated diphenyl ethers, Environ. Sci. Technol 38 (2004) 1313–1320 http://dx.doi.org/10.1021/es0305555.

[18] C. Bach, V. Boiteux, J. Hemard, A. Colin, C. Rosin, J.F. Munoz, X. Dauchy, Simultaneous determination of perfluoroalkyl iodides, perfluoroalkane sulfonamides, fluorotelomer alcohols, fluorotelomer iodides and fluorotelomer acrylates and methacrylates in water and sediments using solid-phase microextraction-gas chromatography/mas, J. Chromatogr. A. 1448 (2016) 98–106 http://dx.doi.org/10.1016/j.chroma.2016.04.025.

[19] J.W. Martin, D.C.G. Muir, C.A. Moody, D.A. Ellis, W.C. Kwan, K.R. Solomon, S.A. Mabury, Collection of airborne fluorinated organics and analysis by gas chromatography / chemical ionization mass spectrometry, Anal. Chem. 74 (2002) 584–590 http://dx.doi.org/10.1021/ac015630d.

[20] A.M. Piekarz, T. Primbs, J.A. Field, D.F. Barofsky, S. Simonich, Semivolatile fluorinated organic compounds in Asian and western U.S. air masses, Environ. Sci. Technol. 41 (2007) 8248–8255 http://dx.doi.org/10.1021/es0713678.

[21] Y. Wu, V.W.C. Chang, Development of analysis of volatile polyfluorinated alkyl substances in indoor air using thermal desorption-gas chromatography-mass spectrometry, J. Chromatogr. A. 1238 (2012) 114–120 http://dx.doi.org/10.1016/j.chroma.2012.03.053.

[22] J. Li, S. Del Vento, J. Schuster, G. Zhang, P. Chakraborty, Y. Kobara, K.C. Jones, Perfluorinated compounds in the asian atmosphere, Environ. Sci. Technol. 45 (2011) 7241–7248 http://dx.doi.org/10.1021/es201739t.

[23] J.L. Barber, U. Berger, C. Chaemfa, S. Huber, A. Jahnke, C. Temme, K.C. Jones, Analysis of per- and polyfluorinated alkyl substances in air samples from Northwest Europe, J. Environ. Monit. 9 (2007) 530–541 http://dx.doi.org/10.1039/b701417a.

[24] W.M. Henderson, E.J. Weber, S.E. Duirk, J.W. Washington, M.A. Smith, Quantification of fluorotelomer-based chemicals in mammalian matrices by monitoring perfluoroalkyl chain fragments with GC/MS, J. Chromatogr. B Anal. Technol. Biomed. Life Sci. 846 (2007) 155–161 http://dx.doi.org/10.1016/j.jchromb.2006.08.042.

[25] A. Jahnke, U. Berger, Trace analysis of per- and polyfluorinated alkyl substances in various matrices-how do current methods perform? J. Chromatogr. A. 1216 (2009) 410–421 http://dx.doi.org/10.1016/j.chroma.2008.08.098.

[26] O. Lacina, P. Hradkova, J. Pulkrabova, J. Hajslova, Simple, high throughput ultra-high performance liquid chromatography/tandem mass spectrometry trace analysis of perfluorinated alkylated substances in food of animal origin: milk and fish, J. Chromatogr. A. 1218 (2011) 4312–4321 http://dx.doi.org/10.1016/j.chroma.2011.04.061.

[27] C. Gremmel, T. Frömel, T.P. Knepper, Systematic determination of perfluoroalkyl and polyfluoroalkyl substances (PFASs) in outdoor jackets, Chemosphere 160 (2016) 173–180 http://dx.doi.org/10.1016/j.chemosphere.2016.06.043.

[28] J.F. Ayala-Cabrera, F. Javier Santos, E. Moyano, Negative-ion atmospheric pressure ionisation of semi-volatile fluorinated compounds for ultra-high-performance liquid chromatography tandem mass spectrometry analysis, Anal. Bioanal. Chem. 410 (2018) 4913–4924 http://dx.doi.org/10.1007/s00216-018-1138-z.

[29] U. Berger, I. Langlois, M. Oehme, R. Kallenborn, Comparison of three types of mass spectrometer for high-performance liquid chromatography/mass spectrometry analysis of perfluoroalkylated substances and fluorotelomer alcohols, Eur. J. Mass Spectrom 10 (2004) 579–588 http://dx.doi.org/10.1255/ejms.679.

[30] T. Portolés, L.E. Rosales, J.V. Sancho, F.J. Santos, E. Moyano, Gas chromatography-tandem mass spectrometry with atmospheric pressure chemical ionization for fluorotelomer alcohols and perfluorinated sulfonamides determination, J. Chromatogr. A. 1413 (2015) 107–116 http://dx.doi.org/10.1016/j.chroma.2015.08.016.

[31] S. Chu, R.J. Letcher, Analysis of fluorotelomer alcohols and perfluorinated sulfonamides in biotic samples by liquid chromatography-atmospheric pressure photoionization mass spectrometry, J. Chromatogr. A. 1215 (2008) 92–99 http://dx.doi.org/10.1016/j.chroma.2008.10.103.

Supporting Data for

Gas chromatography and liquid chromatography coupled to mass spectrometry for the determination of fluorotelomer olefins, fluorotelomer alcohols, perfluoroalkyl sulfonamides and sulfonamido-ethanols in water

J. F. Ayala-Cabrera[1], E. Moyano[1,2], F. J. Santos[1,2]*

[1] Department of Chemical Engineering and Analytical Chemistry, University of Barcelona. Av. Diagonal 645, E–08028 Barcelona, Spain

[2] Water Research Institute (IdRA), University of Barcelona, Montalegre 6, E–08001 Barcelona, Spain

*Corresponding author: F. J. Santos

Table of Contents

Supporting Tables

Table S1. Chemical structures of the target compounds.

Family of Compounds	Structure	Substituent		
Fluorotelomer Olefins (FTOs)		R:	$-C_4F_9$	4:2 FTO
			$-C_6F_{13}$	6:2 FTO
			$-C_8F_{17}$	8:2 FTO
Fluorotelomer Alcohols (FTOHs)		R:	$-C_4F_9$	4:2 FTOH
			$-C_6F_{13}$	6:2 FTOH
			$-C_4F_8(CF_3)CF_3$	7-Me-6:2 FTOH
			$-C_8F_{17}$	8:2 FTOH
			$-C_{10}F_{21}$	10:2 FTOH
Fluororooctane Sulfonamides (FOSAs)		R:	$-CH_3$	*N*-MeFOSA
			$-C_2H_5$	*N*-EtFOSA
Fluorooctane Sulfonamido-Ethanols (FOSEs)		R:	$-CH_3$	*N*-MeFOSE
			$-C_2H_5$	*N*-EtFOSE

Supporting Figures
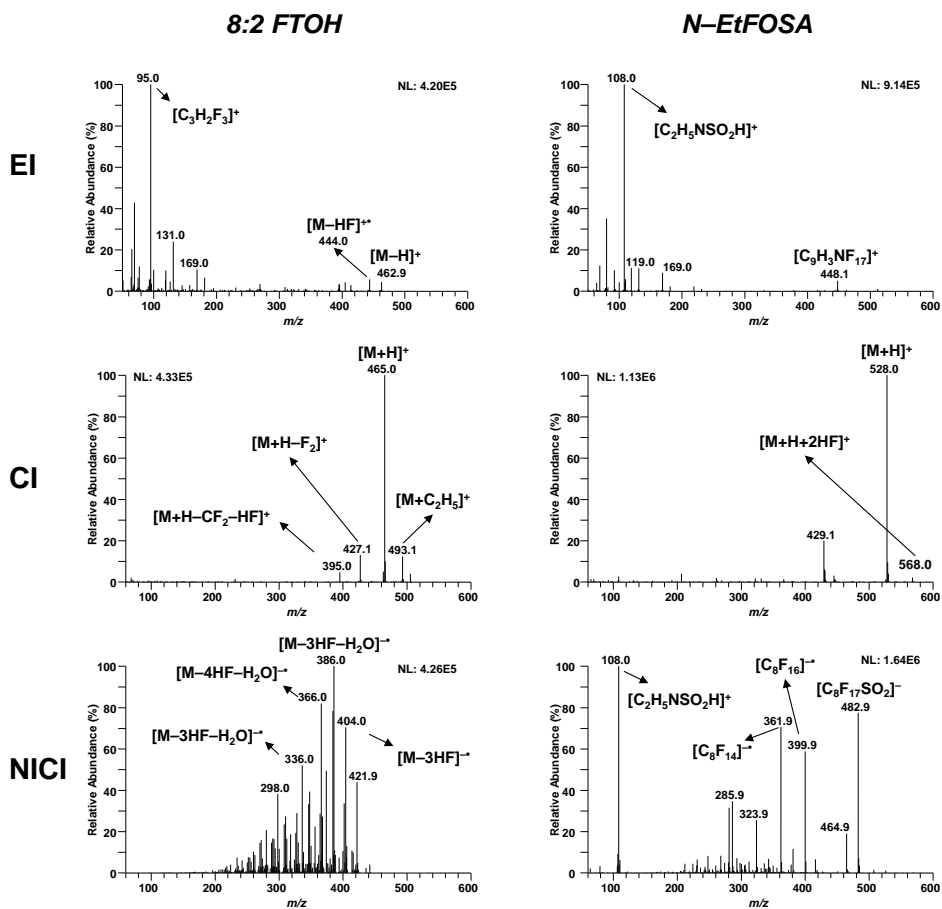
Figure S1. EI, CI and NICI mass spectra of 8:2 FTOH and *N*-EtFOSA.
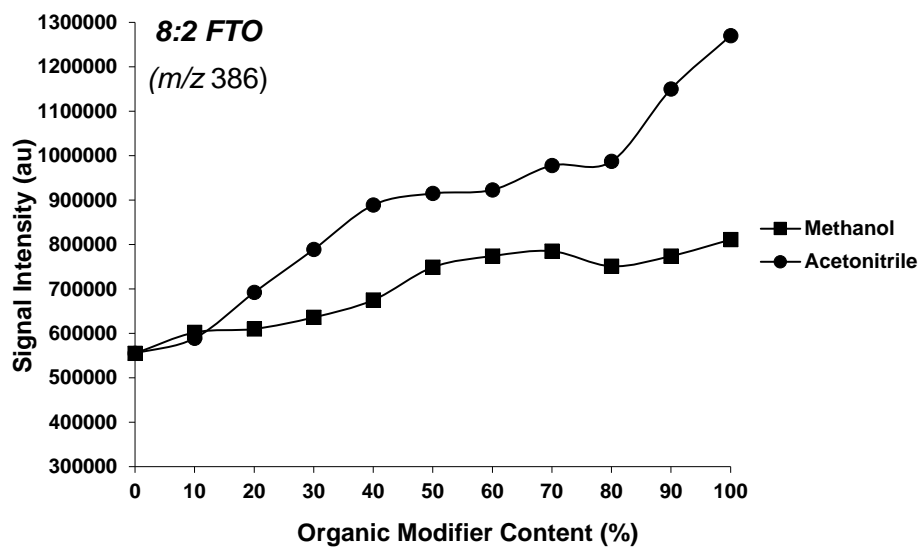
Figure S2. Effect of the organic modifier on the *m/z* 386 signal intensity of 8:2 FTO using negative-ion APCI.
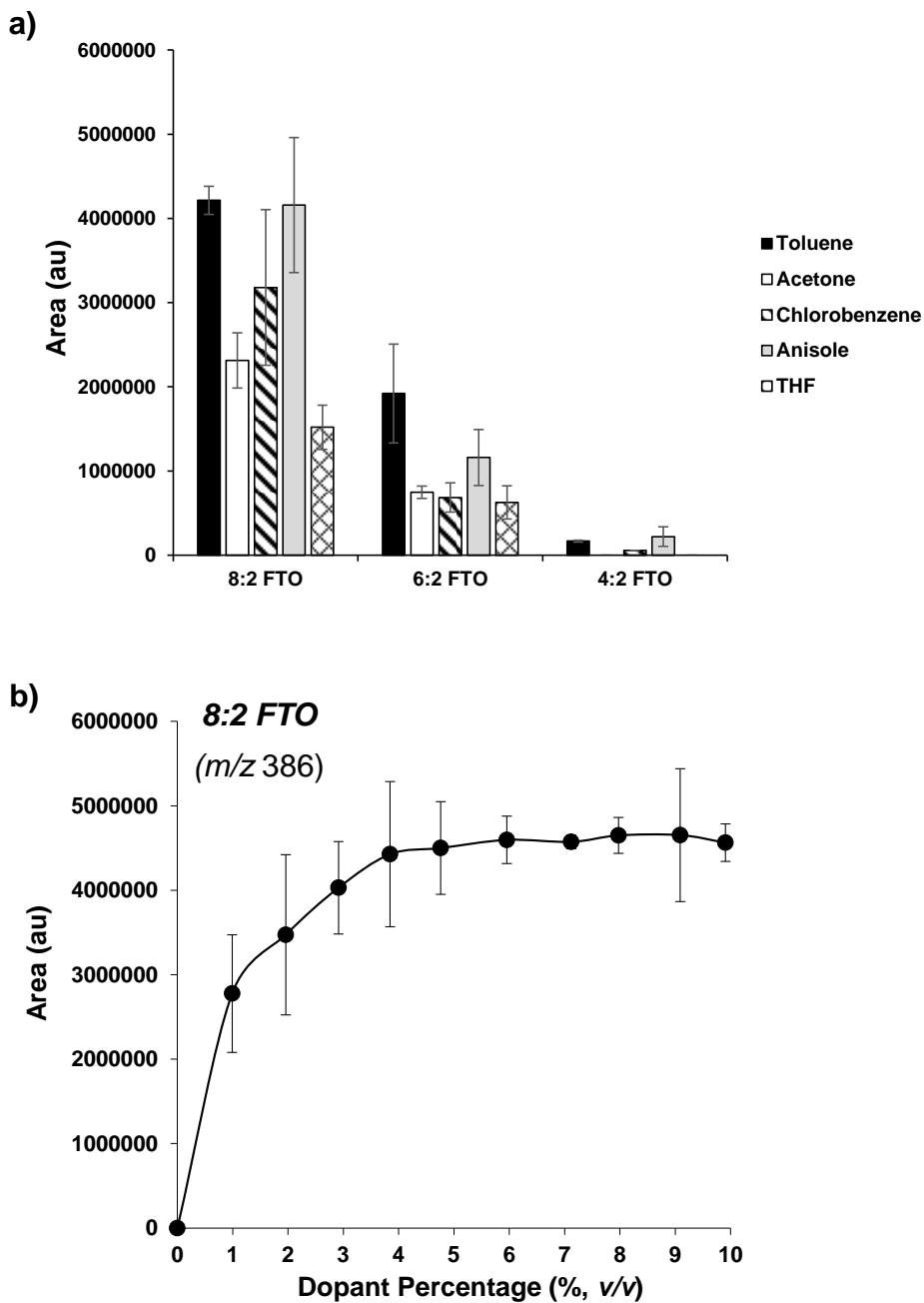
Figure S3. Effect of the (a) dopant and (b) dopant percentage on the peak areas of FTOs and 8:2 FTO using negative-ion APPI.

2.2.3. Article III

Fragmentation studies of neutral per- and polyfluoroalkyl substances by atmospheric pressure ionization-multiple stage mass spectrometry

Juan F. Ayala-Cabrera, F. Javier Santos, Encarnación Moyano

PAPER IN FORERRONT

Fragmentation studies of neutral per- and polyfluoroalkyl substances by atmospheric pressure ionization-multiple-stage mass spectrometry

Juan F. Ayala-Cabrera [1] · F. Javier Santos [1,2] · Encarnación Moyano [1,2]

Abstract

The establishment of fragmentation pathways has a great interest in the identification of new or unknown related compounds present in complex samples. On that way, tentative fragmentation pathways for the ions generated by atmospheric pressure ionization of neutral per- and polyfluorinated alkyl substances (PFASs) have been proposed in this work. Electrospray (ESI), atmospheric pressure chemical ionization (APCI) and photoionization (APPI) were evaluated using mobile phases and source conditions that enhance the ionization efficiency of ions generated. A hybrid mass spectrometer consisting of a linear ion trap and an Orbitrap was used to combine the information of both multiple-stage mass spectrometry (MS^n) and mass accuracy measurements to characterize and establish the genealogical relationship between the product ions observed. The ionization mechanisms to generate ions such as $[M–H]^-$, $[M]^{-\bullet}$, and $[M+O_2]^{-\bullet}$ or the in-source collision-induced dissociation (CID) fragment ions in each API source are discussed in this study. In general, fluorotelomer olefins (FTOs) ionized in negative-ion APCI and APPI generated the molecular ion, while fluorotelomer alcohols (FTOHs) also provided the deprotonated molecule. Besides, fluorooctane sulfonamides (FOSAs) and sulfonamido-ethanols (FOSEs) led to the deprotonated molecule and in-source CID fragment ions, respectively. The fragmentation pathways from these precursor ions mainly involved initial α,β-eliminations of HF units and successive losses of CF_2 units coming from the perfluorinated alkyl chain. Moreover, FTOHs and FOSEs showed a high tendency to generate adduct ions under negative-ion ESI and APPI conditions. The fragmentation study of these adduct ions has demonstrated a strong interaction with the attached moiety.

Keywords Fluorotelomer olefins · Fluorotelomer alcohols · Fluorooctane sulfonamides and sulfonamido-ethanols · Atmospheric pressure ionization · Multiple-stage mass spectrometry · Fragmentation pathway

Introduction

Mass spectrometry is an important tool for structural elucidation but also for the selective and sensitive detection of analytes in complex samples of multitude application fields.

✉ Encarnación Moyano
  encarna.moyano@ub.edu

1   Department of Chemical Engineering and Analytical Chemistry, University of Barcelona, Av. Diagonal 645, 08028 Barcelona, Spain

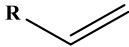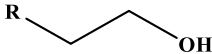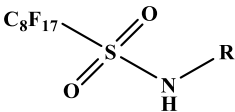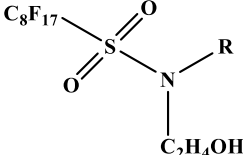2   Research Institute in Water (IdRA), University of Barcelona, Montalegre 6, 08001 Barcelona, Spain

Thus, the establishment of fragmentation pathways is of great relevance. Besides the characterization of target compounds, the fragmentation studies also allow the identification of characteristic product ions and common fragmentation patterns, which could be useful for the identification of new and unknown related compounds. Generally, triple–quadrupole instruments and ion trap instruments have been traditionally used to get structural information via tandem mass spectrometry experiments, mainly for the identification of the ions used for quantitative and confirmatory purposes [1–4]. Nevertheless, these analyzers operate at low resolution and the correct assignment of some product ions might be compromised. Hybrid high-resolution instruments help to solve this problem [5, 6], since they generally isolate precursor ions at low resolution, but the acquisition of product ions is performed at high resolution after their fragmentation via

⌀ Springer

collision-induced dissociation (CID) in a collision cell [7–11]. Particularly, the hybridization of a linear ion trap with an Orbitrap mass analyzer (LIT-Orbitrap) has provided a powerful tool for the study of fragmentation pathways since this instrument allows the accurate molecular formula assignment of both precursor and product ions (mass accuracy lower than 5 ppm) and the establishment of the genealogical relationship of ions generated via multiple-stage mass spectrometry [12–15].

In the present study, the fragmentation behavior of four different families of neutral per- and polyfluoroalkyl substances (PFASs), consisting on fluorotelomer olefins (FTOs), fluorotelomer alcohols (FTOHs), fluorooctane sulfonamides (FOSAs), and sulfonamido-ethanols (FOSEs), has been studied. These compounds are widely used in commercial products, such as packaging materials or fire foams fighters, as a consequence of their water- and stain-resistant properties [16, 17], although their degradation leads to persistent PFASs, which have been regulated due to their toxicity effects over the environment and living organisms [17–20]. Gas chromatography-mass spectrometry (GC-MS) [21–23] and liquid chromatography-tandem mass spectrometry (LC-MS/MS) [24–26] are the techniques normally employed for the determination of these neutral PFASs. However, in the development of GC-MS methods, only some studies pay attention to discuss the fragmentation observed, as reported for FOSAs under electron ionization conditions [27, 28]. On the other hand, it has been reported that, under atmospheric pressure ionization (API) conditions, these compounds generate ions that are highly fragmented through CID, thus providing complex tandem mass spectra [26, 29], especially in both atmospheric pressure chemical ionization (APCI) and photoionization (APPI) sources [30, 31]. However, most of the published studies just focused on the assignment of those product ions selected for quantitative analysis and confirmatory purposes. To our knowledge, there are no previous publications where the CID fragmentation of the ions generated under API conditions of neutral PFASs have been thoroughly studied.

The aim of this work was to study the ions generated for neutral PFASs under atmospheric pressure using electrospray (ESI), atmospheric pressure chemical ionization (APCI) and photoionization (APPI) sources and the complex tandem mass spectral data that frequently are obtained from them using multiple-stage mass spectrometry (MS^n) and high-resolution mass spectrometry (HRMS). These studies have also searched for the establishment of fragmentation pathways for these families of compounds since they may be also of interest to develop mass spectrometry strategies for the screening of similar/related fluorinated compounds in environmental, food, and consumer product analyses.

Material and methods

Reagents and standards

Neutral per- and polyfluoroalkyl substances included in this work are summarized in Table 1. FTOHs—1H,1H,2H,2H-perfluorohexan-1-ol (4:2 FTOH), 1H,1H,2H,2H-perfluorooctan-1-ol (6:2 FTOH), and 1H,1H,2H,2H-perfluoro-7-trifluoromethyl-octan-1-ol (7-Me-6:2 FTOH)—were obtained from Fluorochem Ltd. (Derbyshire, UK), while 1H,1H,2H,2H-perfluorodecan-1-ol (8:2 FTOH) and 1H,1H,2H,2H-perfluorododecan-1-ol (10:2 FTOH) were purchased from Alfa Aesar GmbH & Co KG (Karlsruhe, Germany), all of them at a purity higher than 96%. The FTOs—1H,1H,2H-perfluoro-1-hexane (4:2 FTO), 1H,1H,2H-perfluoro-1-octane (6:2 FTO), and 1H,1H,2H-perfluoro-1-decene (8:2 FTO)—were also supplied by Fluorochem Ltd. Moreover, *N*-ethylperfluoro-1-octanesulfonamide (*N*-EtFOSA) was obtained from Dr. Ehrenstorfer GmbH (Ausburg, Germany), all of them at a purity higher than 99%. Individual stock standard solutions (1000 mg L^{-1}) of each compound were prepared in acetonitrile from their respective pure standards. Besides, individual standard solutions (50 mg L^{-1} in methanol) of 2-(*N*-methylperfluoro-1-octanesulfonamido)-ethanol (*N*-MeFOSE), 2-(*N*-ethylperfluoro-1-octanesulfonamido)-ethanol (*N*-EtFOSE), and *N*-methylperfluoro-1-octanesulfonamide (*N*-MeFOSA) were purchased from Wellington Laboratories Inc. (Guelph, Ontario, Canada). Working solutions were obtained by dilution of stock standard solutions prepared in acetonitrile/water (1:1, *v/v*) or methanol/water (1:1, *v/v*) and stored at 4 °C.

Acetonitrile, methanol, and water LC-MS Chromasolv®, used as mobile phase solvents, and toluene Chromasolv® Plus for HPLC, used as dopant solvent in the APPI source, were purchased from Sigma-Aldrich (St Louis, MO, USA). Acetic acid (≥ 99.7%) was also supplied by Sigma-Aldrich, while ammonium hydroxide (33%) was obtained from J. T. Baker (Deventer, Holland). Both of them have been used as additives in mobile phases.

Nitrogen (> 99.995%) was purchased from Linde (Barcelona, Spain) and it was used as auxiliary and nebulizer gas in the atmospheric pressure ionization sources, while helium (99.999%), obtained from Air Liquide (Madrid, Spain), was employed as buffer gas in the linear ion trap (LIT).

Instrumentation and MS conditions

A hybrid mass spectrometer (linear ion trap-Orbitrap), LTQ Orbitrap Velos (Thermo Fisher Scientific, San Jose, CA, USA), was used for the fragmentation studies of neutral per- and polyfluoroalkyl substances. Three atmospheric pressure ionization sources (ESI, APCI, and APPI) could be swapped

Table 1　Selected neutral per- and polyfluoroalkyl substances

Analyte	Abbreviation	Chemical Structure
1H,1H,2H–Perfluoro–1–hexane	4:2 FTO	
1H,1H,2H–Perfluoro–1–octane	6:2 FTO	
1H,1H,2H–Perfluoro–1–decene	8:2 FTO	
1H,1H,2H,2H–Perfluorohexan–1–ol	4:2 FTOH	
1H,1H,2H,2H–Perfluorooctan–1–ol	6:2 FTOH	
1H,1H,2H,2H–Perfluoro–7–trifluoromethyl–octan–1–ol	7-Me-6:2 FTOH	
1H,1H,2H,2H–Perfluorodecan–1–ol	8:2 FTOH	
1H,1H,2H,2H–Perfluorododecan–1–ol	10:2 FTOH	
N–methylperfluoro–1–octane sulfonamide	*N*-MeFOSA	
N–ethylperfluoro–1–octane sulfonamide	*N*-EtFOSA	
2–(N–methylperfluoro–1–octane sulfonamido)–ethanol	*N*-MeFOSE	
2–(N–ethylperfluoro–1–octane sulfonamido)–ethanol	*N*-EtFOSE	

in the LTQ-Orbitrap instrument and coupled to an UHPLC pump system (Accela, Thermo Fisher Scientific). The ionization source working conditions and the mobile phase composition depended on the API source used. Thus, individual standard solutions, prepared in the most adequate solvent mixture, were infused at 15 μL min^{-1} using a syringe pump. The standard solution was infused and introduced in the stream of the mobile phase (200 μL min^{-1}) by means of a Valco zero dead volume T-piece to deliver a final concentration of 5 mg L^{-1} into the ionization source. Regarding ESI, both acidic (0.1% acetic acid) and basic (0.1% ammonia) acetonitrile/water (1:1, *v/v*) mobile phases were evaluated.

The ESI optimal working conditions were as follows: spray voltage, 2.5–3.0 kV; sheath gas pressure, 50 a.u. (arbitrary units); auxiliary gas pressure, 15 a.u.; and vaporizer and capillary temperatures, 40 and 275 °C, respectively. Concerning APCI and APPI, the mobile phase composition was selected considering those hydro-organic mixtures that achieved the best ionization efficiency of analytes [26, 29]. In APCI, water/methanol (1:1, *v/v*) mobile phase was the best option for FTOHs, FOSAs, and FOSEs, while water/acetonitrile (1:1, *v/v*) was the most appropriated for FTOs' ionization. Regarding APPI, the optimal mobile phase was water/acetonitrile (1:1, *v/v*), and the dopant used for all the compounds was toluene, which was introduced into the mobile phase stream by post-column addition at 15 µL min^{-1} using a T-piece (Valco). A discharge current of 10 µA was set in APCI and the krypton lamp, used in APPI, emitted photons of 10.6 eV. Sheath and auxiliary gas pressures and the capillary temperature were fixed as in ESI experiments, while the vaporizer temperature was set at 250 °C for FTOHs, FOSAs, and FOSEs and at 450 °C for FTOs in both APCI and APPI sources, respectively. Regarding the ion trap parameters, the isolation width was 1.0 *m/z*, while the activation time and activation *Q* were fixed at 30 ms and 0.25, respectively. Multiple-stage mass spectrometry (MS^n) data was acquired in full scan negative-ion mode (50–650 *m/z*) at a resolution of 30,000 full width at half maximum (FWHM). The S-lens RF was fixed at 50%, while the maximum injection time and the AGC target were adjusted at 200 ms and 10^6, respectively. Xcalibur™ v. 2.2 software was used for instrument control, MS^n data acquisition, and data processing.

Results and discussion

In the present work, ions generated by atmospheric pressure ionization (ESI, APCI, and APPI) were fragmented by collision-induced dissociation (CID) in a linear ion trap-Orbitrap (LIT-Orbitrap) mass spectrometer. Multiple-stage mass spectrometry (MS^n) was used to establish the genealogical relationships of product ions, and accurate mass measurements on the Orbitrap allowed the correct assignment of elemental compositions of ions.

The full scan mass spectra of target compounds were obtained under working conditions that maximized the formation of molecular ions or deprotonated molecule ions and minimized the in-source CID fragmentation. The nth generation ions were obtained by MS^n experiments and the product ions generated in each step were immediately stabilized after their formation, which generally reduced subsequent fragmentations by multiple collisions. Nevertheless, in some cases, fast kinetics dissociation processes could also yield product ions via multiple collisions hindering the interpretation of the genealogical relationships of ions observed. Therefore,

exhaustive mass spectra analysis has been performed to establish the fragmentation pathways of neutral PFASs.

Fluorotelomer olefins

The absence of neither acidic hydrogen nor basic functional group did not allow the ionization of FTOs by ESI. Otherwise, the ionization of these compounds was possible in negative-ion mode APCI and APPI via electron-capture or ion-molecule reactions (charge exchange) in the gas phase. The use of high vaporizer temperatures (450 °C) and acetonitrile/water mobile phases improved the ionization efficiency of these analytes [26]. Figure 1 shows the MS^n spectra of the most characteristic ions obtained by negative-ion APCI for 8:2 FTO as model compound. As it can be observed in the MS spectrum, the [M]$^{-•}$ (*m/z* 445.9962, −1.5 ppm) is present at very low relative abundance (< 5%), and two groups of in-source CID fragment ions (odd- and even-electron ion series) dominate the mass spectrum (relative abundances > 40%). These ion series could come from the in-source CID fragmentation of less stable molecular ion. Moreover, ions within these series shifted 20.0062 Da (mass error 0.01 mDa), which may indicate the loss of HF units. These ions were further fragmented up to MS^3 to establish the genealogical relationship among the fragment/product ions observed. Figure 2 shows the tentative fragmentation pathway proposed for the molecular ion of 8:2 FTO, which also serves as a general fragmentation pathway for this family of compounds. The fragmentation of the radical molecular ion starts by losing several HF units, which might occur consecutively by α,β-elimination between adjacent carbons on the fluoroalkyl chain, yielding product ions with a higher number of double bonds. Conjugation would favor the subsequent losses of HF units until exhausting the hydrogen atoms, as can be seen in the MS^n of the consecutive ions (Fig. 1). For instance, the MS^2 spectrum of [M–2HF]$^{-•}$ (*m/z* 405.9836, −2.0 ppm) shows as base peak the ion at *m/z* 385.9772 assigned to [M–3HF]$^{-•}$ (−2.6 ppm), while the MS^2 from [M–HF$_2$]$^-$ and the MS^3 from [M–HF$_2$–HF]$^-$ show the ions obtained by these consecutive losses of HF units, although some of them could have occurred via hydrogen rearrangement. After exhausting all hydrogens, two types of fragmentation alternated: the elimination of F atoms and the loss of CF$_2$, which may be produced through the cleavage of a terminal C–C bond and the subsequent reattachment of one F atom, thus losing the last –CF$_2$ moiety (49.9968 Da). For instance, the MS^2 spectrum corresponding to the in-source CID fragment ion [M–3HF]$^{-•}$ showed a product ion at *m/z* 366.9782, which could be assigned to [M–3HF–F]$^-$ (−4.3 ppm) in agreement with the fragmentation pathway
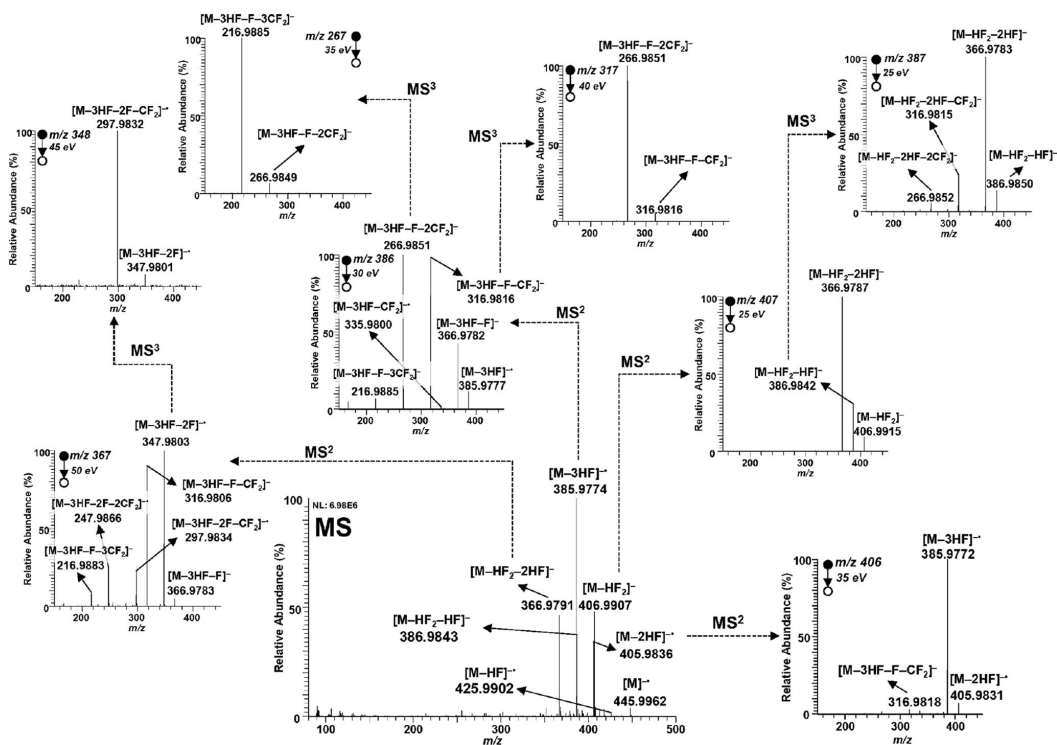
Fig. 1 Full scan mass spectra of 8:2 FTO and MS^n spectra of the most important product ions under negative-ion APCI conditions

suggested. Additionally, the other even-electron ions present in this MS^2 mass spectrum, which shifted 49.9966 Da, could be explained through the fragmentation of the perfluoroalkyl chain by successive losses of CF$_2$ units (−0.2 mDa). Thus, ions at m/z 316.9816 (−4.3 ppm) and m/z 266.9851 (−4.0 ppm) were assigned to [M–3HF–F–CF$_2$]$^-$ and [M–3HF–F–2CF$_2$]$^-$, respectively. The genealogical relationship between these ions was confirmed by their MS^3 spectra, where only the ions at m/z 266.9851 [M–3HF–F–2CF$_2$]$^-$ and m/z 216.9885 [M–3HF–F–3CF$_2$]$^-$ were respectively observed. On the other hand, the loss of one F atom from [M–3HF–F]$^-$ (m/z 347.9803, −3.1 ppm) yielded an odd-electron product ion series which could be also explained by consecutive losses of CF$_2$ units. The genealogical relationship of the different odd-electron ions can also be followed through the MS^3 spectrum of [M–3HF–2F]$^{-\bullet}$ (m/z 347.9803), which only yielded the formation of one ion at m/z 297.9832, that may correspond to [M–3HF–2F–CF$_2$]$^{-\bullet}$ (−1.4 ppm).

This tentative fragmentation pathway has also been observed for the different FTOs included in this study, so it could

be proposed as a general fragmentation pathway for the whole FTO family.

Fluorotelomer alcohols

FTOHs were ionized by negative-ion APCI or APPI (toluene) using hydro-organic mobile phases (methanol or acetonitrile/water mixtures, respectively) to improve their ionization efficiency [26, 29, 32]. Under these conditions, two main ionization mechanisms could explain the ions observed in the full scan mass spectra of FTOHs: (i) proton abstraction via ion-molecule reactions in the gas phase to produce the deprotonated molecule [M–H]$^-$ and (ii) electron capture/charge exchange via the interaction with gas phase ionic species to form the molecular ion [M]$^{-\bullet}$ [29]. Further, these ions also fragmented via in-source CID, even under optimal conditions. As an example, Table 2 summarizes the main product ions observed in MS^n ($n = 1$–3) for 8:2 FTOH using negative-ion APCI and APPI. The MS^2 and MS^3 spectra were characterized by an important number of product ions that may have been originated by multiple collisions, probably due to fast kinetic fragmentations. In fact, changes on the activation time
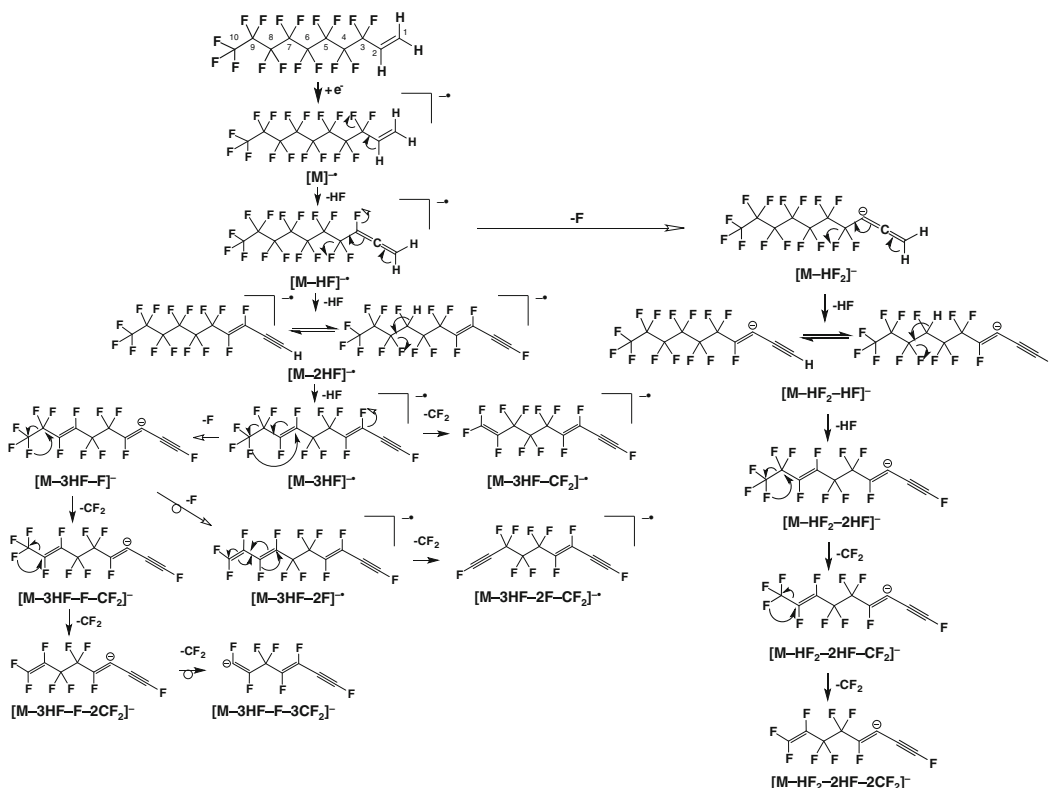
Fig. 2 Tentative fragmentation pathway of 8:2 FTO from the molecular ion using negative-ion APCI and APPI

and activation Q did not produce any improvement on the stabilization of the corresponding precursor ions in the linear ion trap. These data were studied in order to propose fragmentation pathways for both the deprotonated molecule ion and the molecular ion. Figure 3 shows the tentative fragmentation pathways proposed for 8:2 FTOH, as model compound for the FTOH family. As it has been observed for FTOs ("Fluorotelomer olefins" section), FTOHs also showed successive losses of HF units via α,β-elimination with charge retention, generating conjugated double bonds (RDB equivalent was increasing in each HF loss) until exhausting the hydrogens in the molecule. After that, the fragmentation of the resulting product ions continued through the loss of CO or CF_2O within the even-electron ion series (Fig. 3a), or the loss of CO in the case of the odd-electron ion series (Fig. 3b). These mechanisms are still challenging but they should involve the rearrangement of a fluorine atom. After that, the fragmentation for the even-electron ion series ended with the cleavage of CF_2 units, as it happened for FTOs. However, the fragmentation of the molecular radical ion also included steps where a F atom was lost followed by possible losses of CO,

CF_2, or CF_2O. For instance, it could be observed in Table 2 that the fragmentation of $[M–5HF–F]^-$ (m/z 344.9766, − 3.8 ppm) led to $[M–5HF–F–CO]^-$ (m/z 316.9819, − 3.4 ppm), $[M–5HF–F–CF_2O]^-$ (m/z 278.9850, − 4.2 ppm), and $[M–5HF–F–CF_2]^-$ (m/z 294.9799, − 4.0 ppm). After this step, the new product ion could be further fragmented either by losing CF_2 and CO units or by losing a CF_2O moiety.

On the other hand, FTOHs also show a high tendency to generate adduct ions. Table 3 shows the fragmentation of the adduct ions frequently generated in API sources. When using mobile phases with acetic acid/sodium acetate buffers [24, 25], FTOHs generated the acetate adduct ion $[M+CH_3COO]^-$, which directly fragmented into the acetate ion in the MS/MS experiments, thus preventing the generation of analyte-specific product ions. When ammonia (0.1%, v/v) was added to the mobile phase, FTOHs formed the ion $[M–H+CO_2]^-$ as the base peak of the mass spectra. These adduct ions were relatively stable and they were only fragmented using normalized collision energies (NCE) above 30%, which indicates the intense strength of the interaction between the alcohol moiety and the CO_2. These results are in agreement

Table 2 Full scan, MS², and MS³ main product ions obtained for 8:2 FTOH under negative-ion APCI and APPI conditions

API source	Full scan m/z (rel. ab., %)	Full scan Ion assignment	Full scan Error (ppm)	MS² m/z	MS² Ion assignment	MS² Error (ppm)	MS³ m/z	MS³ Ion assignment	MS³ Error (ppm)
APCI	462.9984 (100%)	[M–H]⁻	–2.7	462.9979 (3%)	[M–H]⁻	–3.7	442.9914 (30%)	[M–H–HF]⁻	–4.5
				442.9918 (100%)	[M–H–HF]⁻	–3.6	422.9853 (100%)	[M–H–2HF]⁻	–4.4
				422.9856 (25%)	[M–H–2HF]⁻	–3.7	402.9790 (36%)	[M–H–3HF]⁻	–4.8
				402.9792 (5%)	[M–H–3HF]⁻	–4.3	382.9732 (13%)	[M–H–4HF]⁻	–3.9
							354.9783 (5%)	[M–H–4HF–CO]⁻	–4.2
							422.9854 (3%)	[M–H–2HF]⁻	–4.2
							402.9803 (8%)	[M–H–3HF]⁻	–1.6
							382.9729 (100%)	[M–H–4HF]⁻	–4.7
							354.9786 (4%)	[M–H–4HF–CO]⁻	–3.4
							402.9792 (4%)	[M–H–3HF]⁻	–4.3
							382.9734 (100%)	[M–H–4HF]⁻	–3.4
							354.9785 (61%)	[M–H–4HF–CO]⁻	–3.6
							316.9817 (29%)	[M–H–4HF–CF₂O]⁻	–4.0
							266.9849 (2%)	[M–H–4HF–CF₂O–CF₂]⁻	–4.6
	423.9933 (6%)	[M–2HF]•⁻	–3.9	423.9931 (18%)	[M–2HF]•⁻	–4.4	403.9805 (5%)	[M–3HF]•⁻	–3.1
				403.9883 (100%)	[M–3HF]•⁻	–4.0	383.9808 (100%)	[M–4HF]•⁻	–4.5
				383.9812 (5%)	[M–4HF]•⁻	–3.4	383.9809 (4%)	[M–4HF]•⁻	–4.5
				363.9746 (7%)	[M–5HF]•⁻	–4.6	363.9747 (100%)	[M–5HF]•⁻	–4.5
				335.9800 (4%)	[M–5HF–CO]•⁻	–3.9	344.9763 (6%)	[M–5HF–F]⁻	–4.5
							335.9798 (4%)	[M–5HF–CO]•⁻	–4.6
							316.9816 (4%)	[M–5HF–CO–F]⁻	–4.4
							294.9797 (7%)	[M–5HF–F–CF₂]⁻	–4.7
							244.9831 (5%)	[M–5HF–F–2CF₂]⁻	–4.8
							363.9746 (7%)	[M–5HF]•⁻	–4.7
							344.9765 (27%)	[M–5HF–F]⁻	–4.1
							335.9798 (13%)	[M–5HF–CO]•⁻	–4.7
							316.9815 (31%)	[M–5HF–CO–F]⁻	–4.7
							294.9797 (100%)	[M–5HF–F–CF₂]⁻	–4.7
							266.9851 (3%)	[M–5HF–CO–F–CF₂]⁻	–4.0
							244.9832 (18%)	[M–5HF–F–2CF₂]⁻	–4.4
							335.9799 (22%)	[M–5HF–CO]•⁻	–4.4
							316.9818 (100%)	[M–5HF–CO–F]⁻	–3.7
							285.9733 (11%)	[M–5HF–CO–CF₂]•⁻	–4.8
							266.9851 (56%)	[M–5HF–CO–F–CF₂]⁻	–4.0
	422.9859 (8%)[a]	[M–H–2HF]•⁻	–3.1	402.9793 (2%)	[M–H–3HF]⁻	–4.0	382.9729 (22%)	[M–H–4HF]⁻	–4.6
	403.9871 (14%)[a]	[M–3HF]•⁻	–4.1	382.9732 (100%)	[M–H–4HF]⁻	–3.9	354.9781 (8%)	[M–H–4HF–CO]⁻	–4.8
	402.9797 (9%)	[M–H–3HF]⁻	–3.2	354.9784 (56%)	[M–H–4HF–CO]⁻	–3.8	316.9815 (100%)	[M–H–4HF–CF₂O]⁻	–4.6
				316.9816 (29%)	[M–H–4HF–CF₂O]⁻	–4.3	266.9850 (5%)	[M–H–4HF–CF₂O–CF₂]⁻	–4.5
				266.9848 (1%)	[M–H–4HF–CF₂O–CF₂]⁻	–4.9	354.9781 (28%)	[M–H–4HF–CO]⁻	–4.8
							304.9816 (100%)	[M–H–4HF–CO–CF₂]⁻	–4.5
							316.9815 (32%)	[M–H–4HF–CF₂O]⁻	–4.7
							266.9849 (100%)	[M–H–4HF–CF₂O–CF₂]⁻	–4.8
	383.9813 (80%)[a]	[M–4HF]•⁻	–3.2	363.9748 (6%)	[M–5HF]•⁻	–4.1	344.9764 (30%)	[M–5HF–F]⁻	–4.3
	363.9751 (26%)	[M–5HF]•⁻	–3.3	344.9766 (29%)	[M–5HF–F]⁻	–3.8	316.9819 (5%)	[M–5HF–F–CO]⁻	–3.4
				335.9801 (12%)	[M–5HF–CO]•⁻	–3.8	294.9799 (3%)	[M–5HF–F–CF₂]⁻	–4.0
				316.9815 (30%)	[M–5HF–CO–F]⁻	–4.7	278.9850 (100%)	[M–5HF–F–CF₂O]⁻	–4.2
				294.9798 (100%)	[M–5HF–F–CF₂]⁻	–4.4	294.9799 (22%)	[M–5HF–F–CF₂]⁻	–4.0
				266.9851 (5%)	[M–5HF–CO–F–CF₂]⁻	–4.0	266.9849 (14%)	[M–5HF–CO–F–CF₂]⁻	–4.8

Table 2 (continued)

API source	Full scan			MS²			MS³		
	m/z (rel. ab., %)	Ion assignment	Error (ppm)	m/z	Ion assignment	Error (ppm)	m/z	Ion assignment	Error (ppm)
APPI toluene (5%)	335.9803 (8%)[a]	[M-5HF-CO]⁻•	-3.2	244.9833 (16%)	[M-5HF-F-2CF$_2$]⁻	-4.0	244.9834 (3%)	[M-5HF-F-2CF$_2$]⁻	-3.6
	495.9962 (36%)	[M+O$_2$]⁻•	-2.2				228.9883 (100%)	[M-5HF-F-CF$_2$-CF$_2$O]⁻	-4.7
	462.9987 (100%)[a]	[M-H]⁻	-2.0						
	442.9926 (4%)[a]	[M-H-HF]⁻	-1.7						
	422.9865 (10%)[a]	[M-H-2HF]⁻	-1.5						
	403.9870 (7%)[a]	[M-3HF]⁻•	-4.3						
	402.9805 (28%)[a]	[M-H-3HF]⁻	-1.0						
	383.9823 (75%)[a]	[M-4HF]⁻•	-0.7						
	363.9761 (14%)[a]	[M-5HF]⁻•	-0.5						

[a] As previously mentioned

with Zhou et al., which reported the formation of CO_2 adduct ions with monohydric alcohols in negative-ion ESI [33]. For short-fluoroalkyl chain FTOHs such as 4:2 FTOH and 6:2 FTOH, the MS/MS fragmentation of the adduct ion led to both the loss of the CO_2, which yields the deprotonated molecule [M–H]⁻, and the simultaneous loss of the CO_2 and CH_3OF to form the ion [M+CO_2–CO_2CH_3OF]⁻. The fragmentation mechanism is still unclear, although it may include the elimination of a fluorine atom and the α,β-cleavage to form a double bond (RDB equivalent, 1.5). After that, the fragmentation follows the main fragmentation pathways previously described. Concerning long-fluoroalkyl chain FTOHs such as 7-Me-6:2 FTOH, 8:2 FTOH, and 10:2 FTOH, the fragmentation of CO_2 adduct ions also occurred by the loss of the CO_2, yielding the deprotonated molecule, but also the combined loss of CO and CH_2O due to the α,β-cleavage. Then, the fragmentation continued as explained above for short-fluoroalkyl chain FTOHs.

Finally, the formation of characteristic superoxide adduct ions was also observed for all FTOHs in negative-ion APPI [29, 32]. As what happened with the CO_2 adduct ions, the fragmentation of these superoxide adduct ions required high NCE (25 to 40%), which indicates their high stability. Moreover, the MS² spectra of [M+O_2]⁻• shows successive losses of HF units with oxygen atoms remaining in the new product ions and, therefore, showing the strong interaction between the FTOH molecule and the superoxide ion.

Perfluorooctane sulfonamido-ethanols

The mass spectrometry studies of FOSEs were performed in negative-ion APCI and APPI using hydro-organic mobile phases, methanol/water and acetonitrile/water, respectively, and toluene as dopant in APPI. Under these conditions, neither the molecular ion [M]⁻• nor the deprotonated molecule [M–H]⁻ were observed, because of the intense in-source CID fragmentation of these ions, which led to the ion [M–C_2H_4OF]⁻ through the loss of the alcohol alkyl chain [29]. Table 4 shows the precursor ions observed for *N*-EtFOSE, as an example for this family of compounds, using the different API sources. As it can be observed, FOSEs also showed a high tendency to form adduct ions under ESI conditions, promoting the formation of the ions [M+CH_3COO]⁻ and [M–H+CO_2]⁻ under acidic and basic conditions, respectively. Nevertheless, the low stability of some of these adduct ions led to their fragmentation when isolating them in the linear ion trap or to the formation of the carboxylate as the only product ion in MS/MS. Concerning APCI and APPI, the ion [M–C_2H_4OF]⁻ was the base peak for both *N*-MeFOSE (see Electronic supplementary material, ESM Table S1) and *N*-EtFOSE, m/z 493.9700 (−2.6 ppm) and m/z 507.9860

Fig. 3 Proposed fragmentation pathway for 8:2 FTOH from the **a** deprotonated molecule and **b** molecular ion using negative-ion APCI and APPI
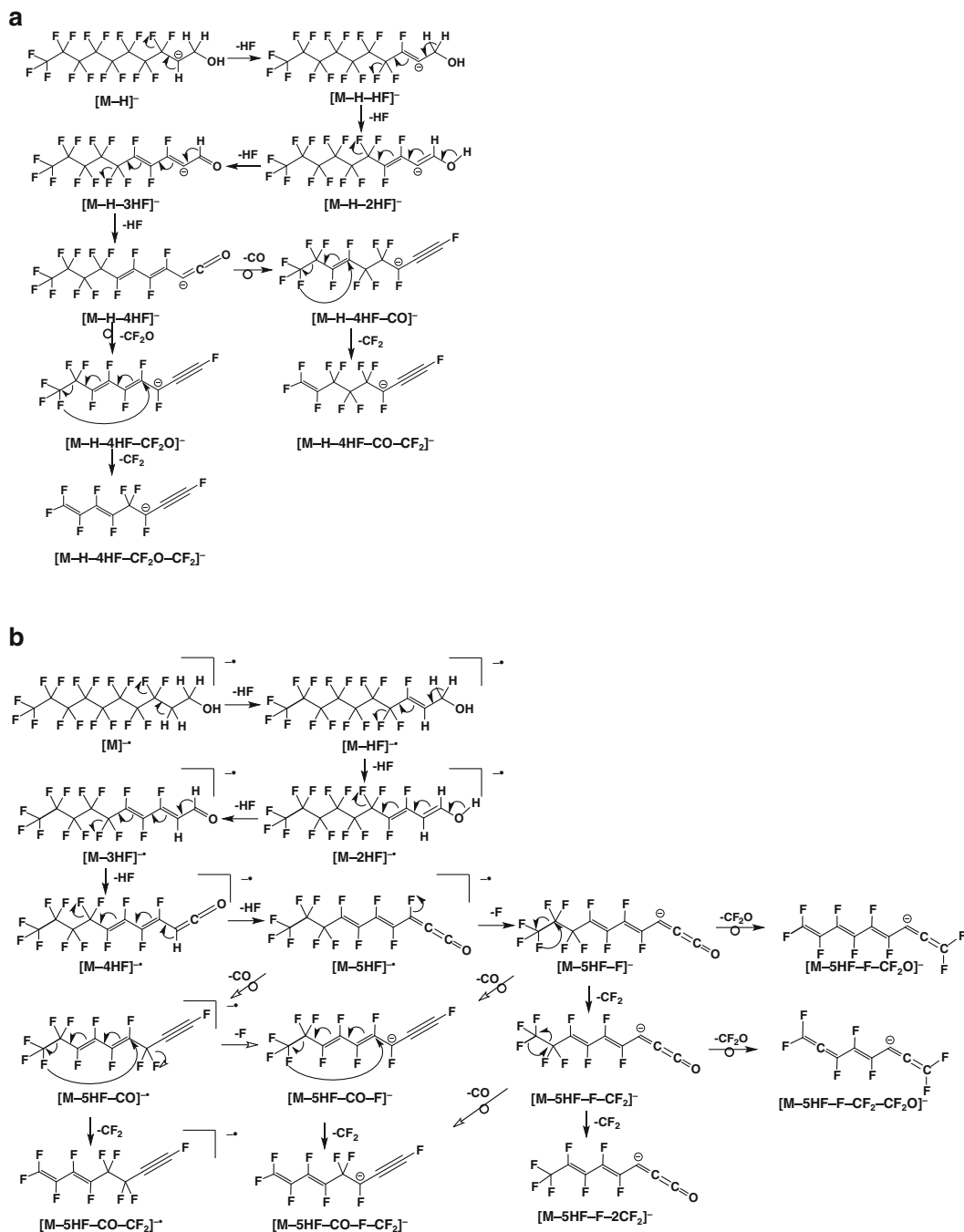
Table 3 MS² and MS³ main product ions obtained for 4:2 FTOH and 7-Me-6:2 FTOH adduct ions generated under negative-ion ESI and APPI conditions

Compound	API source	Full scan			MS²			MS³		
		m/z (rel. ab., %)	Ion assignment	Error (ppm)	m/z (rel. ab., %)	Ion assignment	Error (ppm)	m/z (rel. ab., %)	Ion assignment	Error (ppm)
4:2 FTOH	ESI HAc (0.1%)	323.0329 (100%)	$[M+CH_3COO]^-$	−1.9	323.0324 (12%)	$[M+CH_3COO]^-$	−3.5			
					59.0138 (100%)	$[CH_3COO]^-$	−0.8			
	ESI NH₃ (0.1%)	307.0012 (100%)	$[M-H+CO_2]^-$	−3.3	307.0008 (100%)	$[M-H+CO_2]^-$	−4.6	212.9947 (22%)	$[M-H-CH_3OF]^-$	−4.6
					263.0111 (2%)	$[M-H]^-$	−5.2	192.9886 (100%)	$[C_5F_7]^-$	−4.2
					243.0049 (4%)	$[M-H-HF]^-$	−5.0			
					222.9988 (11%)	$[M-H-2HF]^-$	−5.2			
					212.9945 (17%)	$[M-H-CH_3OF]^-$	−5.2			
					202.9927 (16%)	$[M-H-3HF]^-$	−5.2			
					192.9884 (15%)	$[C_5F_7]^-$				
	APPI toluene (5%)	296.0089 (11%)	$[M+O_2]^{•-}$	−3.7	296.0087 (41%)	$[M+O_2]^{•-}$	−4.5	276.0029 (3%)	$[M+O_2-HF]^{•-}$	−3.3
					276.0025 (100%)	$[M+O_2-HF]^{•-}$	−4.7	255.9967 (100%)	$[M+O_2-2HF]^{•-}$	−3.1
					255.9963 (36%)	$[M+O_2-2HF]^{•-}$	−4.7			
7-Me-6:2 FTOH	ESI HAc (0.1%)	473.0232 (100%)	$[M+CH_3COO]^-$	−1.6	473.0229 (10%)	$[M+CH_3COO]^-$	−2.2			
					59.0138 (100%)	$[CH_3COO]^-$	−0.9			
	ESI NH₃ (0.1%)	456.9910 (100%)	$[M-H+CO_2]^-$	−3.5	456.9909 (4%)	$[M-H+CO_2]^-$	−3.8	382.9905 (14%)	$[M-H-CH_2O]^-$	−4.6
					413.0015 (2%)	$[M-H]^-$	−3.1	362.9844 (100%)	$[M-H-CH_2O-HF]^-$	−4.4
					393.9948 (100%)	$[M-H-HF]^-$	−4.5	362.9846 (10%)	$[M-H-CH_2O-HF]^-$	−3.9
					382.9906 (27%)	$[M-H-CH_2O]^-$	−4.4	342.9785 (100%)	$[M-H-CH_2O-2HF]^-$	−3.8
					362.9844 (14%)	$[M-H-CH_2O-HF]^-$	−4.6			
					342.9780 (2%)	$[M-H-CH_2O-2HF]^-$	−5.1			
	APPI toluene (5%)	445.9993 (4%)	$[M+O_2]^{•-}$	−2.7	445.9990 (30%)	$[M+O_2]^{•-}$	−3.3	425.9923 (100%)	$[M+O_2-HF]^{•-}$	−4.5
					425.9928 (100%)	$[M+O_2-HF]^{•-}$	−3.3	405.9861 (45%)	$[M+O_2-2HF]^{•-}$	−4.7
					405.9866 (68%)	$[M+O_2-2HF]^{•-}$	−3.4			
					385.9805 (39%)	$[M+O_2-3HF]^{•-}$	−3.4			

Table 4 Full scan mass spectra ions obtained for FOSAs and FOSEs under negative-ion ESI, APCI, and APPI conditions

Compound	ESI			APCI			APPI (toluene, 5% v/v)		
	m/z (rel. ab., %)	Ion assignment	Error (ppm)	m/z (rel. ab., %)	Ion assignment	Error (ppm)	m/z (rel. ab., %)	Ion assignment	Error (ppm)
N-MeFOSA	511.9610 (100%)	$[M-H]^-$	−1.3	511.9600 (100%)	$[M-H]^-$	−3.7	511.9613 (100%)	$[M-H]^-$	−1.0
				482.9334 (10%)	$[M-NHCH_3]^-$	−3.8	482.9348 (39%)	$[M-NHCH_3]^-$	−1.1
				464.9429 (70%)	$[M-NFCH_3]^-$	−3.9	464.9445 (60%)	$[M-NFCH_3]^-$	−0.5
				380.9749 (22%)	$[C_8F_{15}]^-$	−4.5	434.9680 (31%)	$[M-NHCH_3SO]^-$	−0.7
							380.9764 (22%)	$[C_8F_{15}]^-$	−0.4
N-EtFOSA	525.9756 (100%)	$[M-H]^-$	−3.6	525.9768 (100%)	$[M-H]^-$	−1.3	525.9769 (100%)	$[M-H]^-$	−1.1
	498.9290 (4%)	$[M+ O-NHC_2H_5]^-$	−2.4	482.9343 (6%)	$[M-NHC_2H_5]^-$	−2.0	482.9345 (13%)	$[M-NHC_2H_5]^-$	−1.6
				464.9439 (47%)	$[M-NFC_2H_5]^-$	−1.7	464.9440 (5%)¹	$[M-NFC_2H_5]^-$	−1.5
				380.9755 (6%)	$[C_8F_{15}]^-$	−2.8			
N-MeFOSE	616.0075 (100%)ᵃ	$[M+CH_3COO]^-$	−2.8	493.9700 (100%)	$[M-C_2H_4OF]^-$	−2.6	588.9848 (12%)	$[M+O_2]^{\bullet -}$	−1.6
	591.9636 (6%)ᵃ	$[M+Cl]^-$	−2.0	482.9338 (10%)	$[M-C_2H_5O-NCH_3]^-$	−3.2	511.9611 (3%)	$[M-C_2H_5O]^-$	−1.4
	599.9775 (100%)ᵇ	$[M-H \cdot CO_2]^-$	−0.6	473.9635 (31%)	$[M-C_2H_4OF-HF]^-$	−3.4	493.9708 (100%)	$[M-C_2H_4OF]^-$	−1.1
	555.9873 (3%)ᵇ	$[M-H]^-$	−1.3	369.9892 (6%)	$[M-C_2H_4OF-3HF-SO_2]^-$	−3.2	482.9352 (57%)	$[M-C_2H_5O-NCH_3]^-$	−0.3
	511.9609 (7%)ᵇ	$[M-C_2H_5O]^-$	−1.9				473.9649 (37%)	$[M-C_2H_4OF-HF]^-$	−0.3
	418.9725 (57%)ᵇ	$[C_8F_{17}]^-$	−2.3				434.9680 (31%)	$[M-N(C_2H_5O)CH_3SO]^-$	−0.8
							369.9906 (19%)	$[M-C_2H_4OF-3HF-SO_2]^-$	−0.2
N-EtFOSE	630.0232 (100%)ᵃ	$[M+CH_3COO]^-$	−2.5	507.9860 (100%)	$[M-C_2H_4OF]^-$	−1.8	603.0007 (15%)	$[M+O_2]^{\bullet -}$	−1.2
	605.9795 (7%)ᵃ	$[M+Cl]^-$	−1.5	487.9798 (21%)	$[M-C_2H_4OF-HF]^-$	−1.8	525.9770 (4%)	$[M-C_2H_5O]^-$	−1.0
	613.9915 (100%)ᵇ	$[M-H \cdot CO_2]^-$	−3.3	482.9341 (8%)	$[M-C_2H_5O-NC_2H_5]^-$	−2.5	507.9867 (100%)	$[M-C_2H_4OF]^-$	−0.4
	605.9789 (11%)ᵇ	$[M+Cl]^-$	−2.5				487.9805 (20%)	$[M-C_2H_4OF-HF]^-$	−0.3
	570.0018 (2%)ᵇ	$[M-H]^-$	−3.3				482.9349 (64%)	$[M-C_2H_5O-NC_2H_5]^-$	−0.9
	525.9756 (3%)ᵇ	$[M-C_2H_5O]^-$	−3.6				434.9679 (38%)	$[M-N(C_2H_5O)C_2H_5SO]^-$	−1.1
	418.9716 (49%)ᵇ	$[C_8F_{17}]^-$	−4.4						

ᵃ ESI full scan mass spectra acquired under acidic conditions (acetic acid, 0.1% v/v)

ᵇ ESI full scan mass spectra acquired under basic conditions (NH₃, 0.1% v/v)

Ⓐ Springer

(−1.8 ppm), among the in-source CID fragment ions observed. Figure 4 shows the fragmentation pathways proposed for this family of compounds from the ion $[M-C_2H_4OF]^-$. This ion might be generated by the loss of the alcohol alkyl chain, which would involve the rearrangement of a hydrogen atom to favor the cleavage of a fluorine atom. The MS^n fragmentation of this ion could begin with the formation of a cyclic structure to yield the ion $[M-C_2H_4OF-HF]^-$. This hypothesis is in agreement with previous studies that indicate the possibility of fluorooctane sulfonamides to from cyclic structure ions [27, 28]. Additionally, this tentative ion assignment allows the justification of following fragmentations due to consecutive losses of HF units, as can be seen in the corresponding MS^2 and MS^3 spectra of $[M-C_2H_4OF]^-$. These HF losses occurred until two hydrogen atoms remained in the product ion $[M-C_2H_4OF-2HF]^-$ (m/z 453.9588, −3.7 ppm) for N-MeFOSE and $[M-C_2H_4OF-4HF]^-$ (m/z 427.9620, −2.8 ppm) for N-EtFOSE. After that, the cleavage of the sulfone group

occurred to yield $[M-C_2H_4OF-2HF-SO_2]^-$ (m/z 389.9953, −4.1 ppm) for N-MeFOSE and $[M-C_2H_4OF-4HF-SO_2]^-$ (m/z 363.9986, −4.3 ppm) for N-EtFOSE. Later, the fragmentation followed through two additional consecutive losses of HF until exhaust of the hydrogen atoms and the fragmentation of the fluoroalkyl chain by the loss of n CF_2 units. Regarding N-MeFOSE, an additional product ion was observed from the fragmentation of the ion $[M-C_2H_4OF-2HF]^-$, which was tentatively assigned to $[M-C_2H_4OF-2HF-NCH]^-$ (m/z 426.9464, −3.6 ppm), although this fragmentation mechanism is still unclear.

Other fragmentation pathways have been also proposed for less intense precursor ions observed by APCI and APPI (see ESM, Fig. S1a and S1b), which mainly involved losses of the functional group and simultaneous α,β-cleavages in the fluoroalkylchain. Finally, it is also interesting to highlight that the adduct ion $[M+O_2]^{-\bullet}$ was observed working in negative-ion APPI conditions. The MS^2 spectrum of this ion led to two main product ions as a result of the cleavage of the O_2 moiety,
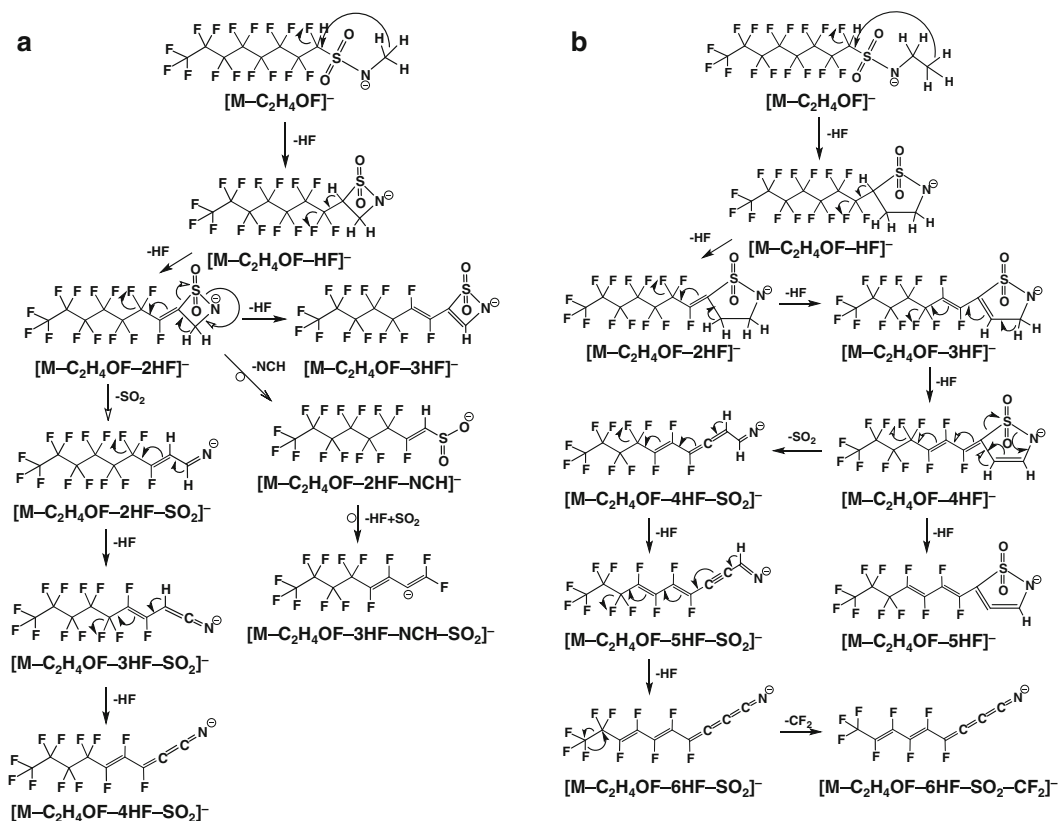

Fig. 4 Main fragmentation pathway of **a** N-MeFOSE and **b** N-EtFOSE from the $[M-C_2H_4OF]^-$ ion using negative-ion APCI and APPI

Table 5　MS² and MS³ main product ions obtained from precursor ions for N-EtFOSA and N-EtFOSE under negative-ion API conditions

Compound	Full scan Ion assignment	MS² m/z (rel. ab., %)	MS² Ion assignment	MS² Error (ppm)	MS³ m/z (rel. ab., %)	MS³ Ion assignment	MS³ Error (ppm)
N-EtFOSA	$[M-H]^-$	525.9767 (10%)	$[M-H]^-$	−1.6	418.9719 (10%)	$[C_8F_7]^-$	−0.5
		477.9386 (14%)	$[M-H-C_2H_4F]^-$	−2.6	268.9818 (34%)	$[C_5F_{11}]^-$	−4.4
		418.9721 (100%)	$[C_8F_7]^-$	−3.2	218.9852 (100%)	$[C_4F_9]^-$	−4.5
		401.9957 (23%)	$[M-H-3HF-SO_2]^-$	−3.0	168.9886 (28%)	$[C_3F_7]^-$	−4.6
		361.9832 (91%)	$[M-H-5HF-SO_2]^-$	−3.4	401.9955 (12%)	$[M-H-3HF-SO_2]^-$	−3.5
		268.9818 (42%)	$[C_5F_{11}]^-$	−4.3	381.9893 (18%)	$[M-H-4HF-SO_2]^-$	−3.7
		218.9853 (94%)	$[C_4F_9]^-$	−4.1	361.9831 (100%)	$[M-H-5HF-SO_2]^-$	−3.8
		168.9886 (39%)	$[C_3F_7]^-$	−4.4	361.9832 (10%)	$[M-H-5HF-SO_2]^-$	−3.5
					311.9864 (100%)	$[M-H-5HF-SO_2-CF_4]^-$	−4.2
	$[M+O-NHC_2H_5]^-$	498.9286 (20%)	$[M+O-NHC_2H_5]^-$	−3.3	329.9401 (35%)	$[M+O-NHC_2H_5-C_4F_7]^{-\bullet}$	−4.0
		418.9719 (100%)ᵃ	$[C_8F_7]^-$	−3.6	179.9501 (100%)	$[M+O-NHC_2H_5-C_6F_{13}]^{-\bullet}$	−4.7
		329.9400 (42%)	$[M+O-NHC_2H_5-C_4F_7]^{-\bullet}$	−4.1			
		279.9432 (65%)	$[M+O-NHC_2H_5-C_4F_9]^{-\bullet}$	−4.7			
	$[M-NHC_2H_5]^-$	482.9341 (3%)	$[M-NHC_2H_5]^-$	−2.4			
		418.9722 (100%)ᵃ	$[C_8F_7]^-$	−3.0			
	$[M-NFC_2H_5]^-$	464.9426 (6%)	$[M-NFC_2H_5]^-$	−4.5	444.9372 (15%)	$[M-NFC_2H_5-HF]^-$	−2.9
		444.9362 (3%)	$[M-NFC_2H_5-HF]^-$	−4.6	380.9753 (100%)	$[M-NFC_2H_5-HF-SO_2]^-$	−3.4
		400.9810 (5%)	$[M-NFC_2H_5-SO_2]^-$	−4.6	400.9819 (25%)	$[M-NFC_2H_5-SO_2]^-$	−2.2
		380.9747 (100%)	$[C_8F_{15}]^-$	−4.2	380.9749 (100%)	$[C_8F_{15}]^-$	−4.5
					380.9755 (28%)	$[C_8F_{15}]^-$	−2.9
					330.9786 (7%)	$[C_7F_{13}]^-$	−3.3
					311.9802 (29%)	$[C_7F_{12}]^{-\bullet}$	−3.2
					230.9851 (61%)	$[C_5F_9]^-$	−4.8
					168.9886 (100%)	$[C_3F_7]^-$	−4.1
					118.9921 (81%)	$[C_2F_5]^-$	−4.2
N-EtFOSE	$[M+CH_3COO]^-$	630.0226 (9%)	$[M+CH_3COO]^-$	−3.5	487.9797 (8%)	$[M-C_2H_4OF-HF]^-$	−2.0
		59.0136 (100%)	$[CH_3COO]^-$	−2.6	467.9733 (27%)	$[M-C_2H_4OF-2HF]^-$	−2.5
					447.9670 (3%)	$[M-C_2H_4OF-3HF]^-$	−2.7
					427.9608 (4%)	$[M-C_2H_4OF-4HF]^-$	−2.8
					363.9989 (73%)	$[M-C_2H_4OF-4HF-SO_2]^-$	−3.3
					343.9927 (61%)	$[M-C_2H_4OF-5HF-SO_2]^-$	−3.5
					323.9865 (100%)	$[M-C_2H_4OF-6HF-SO_2]^-$	−3.6
					467.9728 (7%)	$[M-C_2H_4OF-2HF]^-$	−3.6
					447.9664 (13%)	$[M-C_2H_4OF-3HF]^-$	−4.1
					427.9604 (100%)	$[M-C_2H_4OF-4HF]^-$	−3.8
					407.9541 (3%)	$[M-C_2H_4OF-5HF]^-$	−4.2
					363.9985 (26%)	$[M-C_2H_4OF-4HF-SO_2]^-$	−4.4
					343.9924 (86%)	$[M-C_2H_4OF-5HF-SO_2]^-$	−4.4
					323.9861 (43%)	$[M-C_2H_4OF-6HF-SO_2]^-$	−4.7
					427.9605 (11%)	$[M-C_2H_4OF-4HF]^-$	−3.6
					407.9544 (2%)	$[M-C_2H_4OF-5HF]^-$	−3.4
					363.9986 (100%)	$[M-C_2H_4OF-4HF-SO_2]^-$	−4.3
					343.9925 (46%)	$[M-C_2H_4OF-5HF-SO_2]^-$	−4.1
					323.9862 (31%)	$[M-C_2H_4OF-6HF-SO_2]^-$	−4.5
					363.9986 (9%)	$[M-C_2H_4OF-4HF-SO_2]^-$	−4.0
					343.9924 (100%)	$[M-C_2H_4OF-5HF-SO_2]^-$	−4.2
					323.9862 (81%)	$[M-C_2H_4OF-6HF-SO_2]^-$	−4.5
					343.9924 (3%)	$[M-C_2H_4OF-5HF-SO_2]^-$	−4.3
					323.9862 (100%)	$[M-C_2H_4OF-6HF-SO_2]^-$	−4.4
	$[M-C_2H_4OF]^-$	507.9859 (3%)	$[M-C_2H_4OF]^-$	−2.0			
		487.9794 (100%)	$[M-C_2H_4OF-HF]^-$	−2.7			
		467.9732 (41%)	$[M-C_2H_4OF-2HF]^-$	−2.7			
		447.9670 (6%)	$[M-C_2H_4OF-3HF]^-$	−2.8			
		427.9608 (32%)	$[M-C_2H_4OF-4HF]^-$	−2.8			
		407.9547 (2%)	$[M-C_2H_4OF-5HF]^-$	−2.7			
		363.9989 (25%)	$[M-C_2H_4OF-4HF-SO_2]^-$	−3.5			
		343.9927 (54%)	$[M-C_2H_4OF-5HF-SO_2]^-$	−3.5			
		323.9865 (60%)	$[M-C_2H_4OF-6HF-SO_2]^-$	−3.7			

Table 5 (continued)

Compound	Full scan	MS²			MS³		
	Ion assignment	m/z (rel. ab., %)	Ion assignment	Error (ppm)	m/z (rel. ab., %)	Ion assignment	Error (ppm)
	[M+O₂]⁻	602.9996 (11%) 541.9710 (9%) 525.9759 (100%)	[M+O₂]⁻ [M+O₂–C₂H₅O₂]⁻ [M+O₂–C₂H₅O₃]⁻	−2.9 −2.7 −3.1	323.9862 (17%) 273.9895 (100%)	[M–C₂H₄OF–6HF–SO₂]⁻ [M–C₂H₄OF–6HF–SO₂–CF₂]⁻	−4.4 −4.8
	[M–NHC₂H₅SO]⁻	434.9672 (9%) 368.9754 (100%) 218.9852 (11%) 168.9886 (12%)	[M–NHC₂H₅SO]⁻ [C₇F₁₅]⁻ [C₄F₉]⁻ [C₃F₇]⁻	−2.6 −3.4 −4.2 −4.3	368.9751 (7%) 218.9851 (74%) 169.9886 (100%)	[C₇F₁₅]⁻ [C₄F₉]⁻ [C₃F₇]⁻	−3.9 −4.9 −4.7

[a] As previously mentioned

as well as the alkyl chain and the ethanol group, [M+O₂–C₂H₄OH–O₂]⁻ and [M+O₂–R–O₂]⁻ (R: –CH₃, –C₂H₅) (see ESM, Fig. S2).

Perfluorooctane sulfonamides

Regarding FOSAs, the acidity of sulfonamide group may favor their ionization via proton abstraction, leading to the formation of the deprotonated molecule [M–H]⁻ as base peak under API conditions (Table 4). As an example, the MS^n (n = 1–3) data obtained for *N*-EtFOSA from the fragmentation of the main precursor ions, including the deprotonated molecule, are summarized in Table 5. Considering all these information, Fig. 5 shows the fragmentation pathway proposed for *N*-EtFOSA as an example for this family of compounds. The ion [M–H]⁻ for both FOSAs mainly generated the product ion at m/z 418.9734, [M–H–SO₂NR]⁻ (R: –CH₃, –C₂H₅), as a result of the cleavage of the sulfonamide group, being the most favored fragmentation mechanism. Later, the MS³ of this product ion yielded three product ions, m/z 268.9830, m/z 218.9862, and m/z 168.9894, because of the fragmentation of the perfluoalkyl chain by losing n CF₂ units. Besides, the ion [M–H]⁻ also fragmented to led to the product ion at m/z 477.9400, which can be assigned to [M–H–RF]⁻ (R: –CH₃, –C₂H₅) due to the combined loss of the alkyl chain and a fluorine atom.

Concerning *N*-EtFOSA, the deprotonated molecule [M–H]⁻ fragmentation also yielded the product ion [M–H–3HF–SO₂]⁻ (m/z 401.9957, −3.0 ppm), which may involve intermediate steps through low-stable ions, as shown in Fig. 5 (dash square). As commented above for FOSEs, we hypothesize that these intermediate steps might also involve cyclic species to rationalize the formation of the ion [M–H–3HF–SO₂]⁻. The fragmentation of this product ion would continue through the loss of successive HF units until exhausting the hydrogens in the molecule. After that, the perfluoroalkyl chain would be fragmented through the elimination of n CF₂ units. It must be mentioned that the ions corresponding to this additional fragmentation pathway were not observed for *N*-MeFOSA, may be due to the lower stability of the four-member ring ion.

The fragmentation of other less intense ions observed in the API sources has also been studied and the MS^n spectral data are detailed in Table 5. Tentative fragmentation pathways for these precursor ions are summarized in Fig. S1 (ESM). Regarding ESI, *N*-EtFOSA full scan mass spectrum presented an additional low intense ion at m/z 498.9290 (see ESM, Fig. S1c), which might be assigned to [M+O–NHC₂H₅]⁻ (−2.4 ppm), probably due to an oxidation process in the ESI source. This ion coincides with the deprotonated molecule of the perfluorooctane sulfonate (PFOS), which could produce
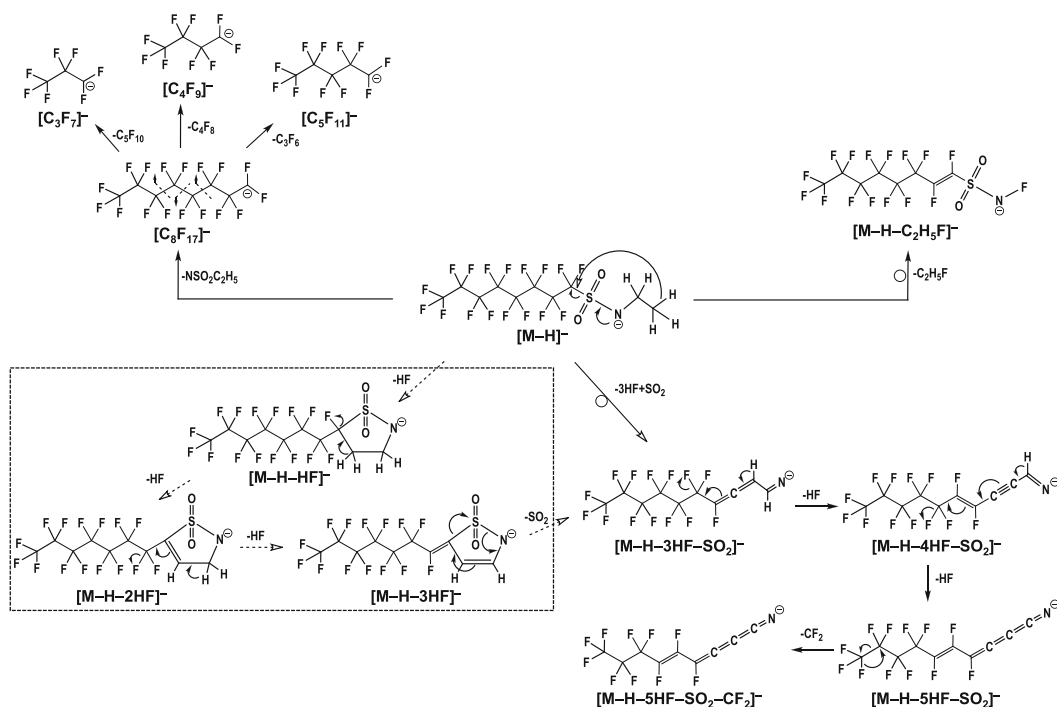
122

Fig. 5 Main fragmentation pathway of *N*-EtFOSA from the deprotonated molecule using negative-ion API sources

false positives in the analysis of samples. In relation to APCI and APPI, two common in-source CID fragment ions (m/z 464.9447 and m/z 482.9353) were observed, which can be explained because of the nitrogen α-cleavage to yield the ions $[M–NFR]^-$ and $[M–NHR]^-$ (R: $–CH_3$, $–C_2H_5$), respectively. The proposed fragmentation pathway of the ion $[M–NFR]^-$ (ESM, Fig. S1d) may start with consecutive losses of HF and SO_2 to yield the perfluoroalkyl ion $[C_8F_{15}]^-$, which was further fragmented by losing the characteristic n CF_2 units. Concerning the ion $[M–NHR]^-$, it may be generated by the cleavage of the N–S bond. The MS^2 spectra of these ions showed the generation of stable perfluoroalkyl chain ions $[C_8F_{17}]^-$ (m/z 418.9722, $-$ 3.0 ppm) and $[C_8F_{15}]^-$ (m/z 380.9747, -4.2 ppm), respectively, because of the loss of the sulfonamide group (ESM, Fig. S1a). Additionally, in APPI, the *N*-MeFOSA also generated the ion $[M–NHCH_3SO]^-$ (m/z 434.9680, -0.7 ppm) (see ESM, Table S1) that fragmented following the same fragmentation pathway than the ion $[M–N(C_2H_5O)RSO]^-$ (R: $–CH_3$, $–C_2H_5$) observed for FOSEs (ESM, Fig. S1b). This ion could be formed due to the attachment of oxygen to the perfluoroalkyl chain moiety, probably due to the presence of oxygen in the ion

trap because of the dissociation of the superoxide ion. After that, different C–C bond cleavages could take place, leading to product ions at m/z 218.9854 and m/z 168.9886, which have been assigned to $[C_4F_9]^-$ ($-$ 3.8 ppm) and $[C_3F_7]^-$ (-4.6 ppm), respectively.

Conclusions

In this work, tentative fragmentation pathways have been established for ions observed for neutral PFASs using API sources. The ions generated have been assigned and the genealogical relationships between them have been established through the combined used of multiple-stage mass spectrometry and high-resolution mass spectrometry. Fragmentation pathways proposed for precursor ions of FTOs (molecular ion) and FTOHs (molecular ion and deprotonated molecule) included initial α,β-eliminations of HF units through the formation of conjugated double bonds, until exhausting hydrogens in the ions generated. Afterwards, these compounds mainly fragmented by losing F atoms and CO (in the case of FTOHs), but also CF_2 units, which came from the perfluoroalkyl chain. Additionally, it has been shown the tendency of FTOHs to form adduct ions such as $[M–H+CO_2]^-$ (under negative-ion ESI) and $[M+O_2]^{-\bullet}$ (under

negative-ion APPI) and the required high NCE (%) has suggested the strength of the adduct moiety interaction. Concerning FOSAs and FOSEs, common fragmentation pathways were proposed. FOSAs showed the deprotonated molecule as the base peak ion in all the API mass spectra, and its fragmentation pattern mainly led to the loss of the sulfonamide group and, after that, to the loss of n CF_2 units from the perfluoroalkyl chain. Moreover, under ESI conditions, an oxidation reaction generated the ion $[M+O–NHC_2H_5]^-$ for N-EtFOSA, which has the same exact mass than the persistent PFOS ion, being susceptible of causing identification errors. In the case of FOSEs, the tentative fragmentation pathway for the main ion $[M–C_2H_4OF]^-$ observed under negative-ion APCI and APPI proposes the initial formation of a four- (for N-MeFOSE) or five-membered ring (for N-EtFOSE) intermediate, which would favor the elimination of HF units until two hydrogen atoms remain in the cyclic structure. After that, the loss of the SO_2 moiety would also be favored and the rings opened to further fragment through the loss of HF units and successive losses of CF_2 moieties.

The fragmentation patterns proposed in this work for the different neutral PFAs show general fragmentation trends and common product ions, which could be really useful for the identification and characterization of new and unknown neutral PFASs in real samples as well as on the differentiation of potential isobaric neutral PFASs.

Compliance with ethical standards

Conflict of interest The authors declare that they have no conflict of interest.

References

1. Toribio F, Moyano E, Puignou L, Galceran MT. Multistep mass spectrometry of heterocyclic amines in a quadrupole ion trap mass analyser. J Mass Spectrom. 2002;37:812–28.
2. Alechaga É, Moyano E, Galceran MT. Atmospheric pressure ionization-tandem mass spectrometry of the phenicol drug family. J Mass Spectrom. 2013;48:1241–51.
3. De La Iglesia P, Fonollosa E, Diogène J. Assessment of acylation routes and structural characterisation by liquid chromatography/tandemmass spectrometry of semi-synthetic acyl ester analogues of lipophilic marine toxins. Rapid Commun Mass Spectrom. 2014;28:2605–16.
4. Huang M, Cheng Z, Wang L, Feng Y, Huang J, Du Z, et al. A targeted strategy to identify untargeted metabolites from in vitro to in vivo: rapid and sensitive metabolites profiling of licorice in rats using ultra-high performance liquid chromatography coupled with triple quadrupole-linear ion trap mass spectrometry. J Chromatogr B. 2018;1092:40–50.
5. Núñez O, Moyano E, Galceran MT. High mass accuracy in-source collision-induced dissociation tandem mass spectrometry and multi-step mass spectrometry as complementary tools for fragmentation studies of quaternary ammonium herbicides. J Mass Spectrom. 2014;39:873–83.
6. Yu D, Liang X. Fragmentation pathways and differentiation of positional isomers of sorafenib and structural analogues by ESI-IT-MSn and ESI-Q-TOF-MS/MS coupled with DFT calculations. J Mass Spectrom. 2018;53:579–89.
7. Sekuła K, Zuba D, Lorek K. Analysis of fragmentation pathways of new-type synthetic cannabinoids using electrospray ionization. J Am Soc Mass Spectrom. 2018;29:1941–50.
8. Huysman S, Van Meulebroek L, Janssens O, Vanryckeghem F, Van Langenhove H, Demeestere K, et al. Targeted quantification and untargeted screening of alkylphenols, bisphenol A and phthalates in aquatic matrices using ultra-high-performance liquid chromatography coupled to hybrid Q-Orbitrap mass spectrometry. Anal Chim Acta. 2018;1049:141–51.
9. Qi H, Chen F, Liu T, Zhang F, Zhang F, Zhai J, et al. Development of an analytical method for twelve Dioscorea saponins using liquid chromatography coupled to Q-exactive high resolution mass spectrometry. Talanta. 2018;191:11–20.
10. Chen L, Chen X, Wang S, Bian Y, Zhao J, Li S. Analysis of triterpenoids in Ganoderma resinaceum using liquid chromatography coupled with electrospray ionization quadrupole–time-of-flight mass spectrometry. Int J Mass Spectrom. 2019;436:42–51.
11. Asare SO, Huang F, Lynn BC. Characterization and sequencing of lithium cationized β-O-4 lignin oligomers using higher-energy collisional dissociation mass spectrometry. Anal Chim Acta. 2019;1047:104–14.
12. Li Y, Liu Y, Liu R, Liu S, Zhang X, Wang Z, et al. HPLC-LTQ-orbitrap MS^n profiling method to comprehensively characterize multiple chemical constituents in xiao-er-qing-jie granules. Anal Methods. 2015;7:7511–26.
13. Shan J, Zhao X, Shen C, Ji J, Xu J, Wang S, et al. Liquid chromatography coupled with linear ion trap hybrid OrbitrapMass spectrometry for determination of alkaloids in Sinomenium acutum. Molecules. 2018. https://doi.org/10.3390/molecules23071634.
14. Prothmann J, Spégel P, Sandahl M, Turner C. Identification of lignin oligomers in Kraft lignin using ultra-high-performance liquid chromatography/high-resolution multiple-stage tandem mass spectrometry (UHPLC/HRMSn). Anal Bioanal Chem. 2018;410:7803–14.
15. Lv X, Sun JZ, Xu SZ, Cai Q, Liu YQ. Rapid characterization and identification of chemical constituents in Gentiana radix before and after wine-processed by UHPLC-LTQ-orbitrap MSn. Molecules. 2018. https://doi.org/10.3390/molecules23123222.
16. Kissa E. Fluorinated surfactants and repellents. second ed. New York: Marcel Dekker; 2001.
17. Buck RC, Franklin J, Berger U, Conder JM, Cousins IT, De Voogt P, et al. Perfluoroalkyl and polyfluoroalkyl substances in the environment: terminology, classification, and origins. Integr Environ Assess Manag. 2011;7:513–41.
18. Council Decision (EU) 2015/633 of 20 April 2015 on the submission, on behalf of the European Union. of a proposal for the listing of additional chemicals in Annex A to the Stockholm Convention on persistent organic pollutants. Off J Eur Union. 2015;L 104:14–5.
19. Jahnke A, Ahrens L, Ebinghaus R, Temme C. Urban versus remote air concentrations of fluorotelomer alcohols and other polyfluorinated alkyl substances in Germany. Environ Sci Technol. 2007;41:745–52.
20. Decision SC-4/17 of 4–8 May 2009 of Listing of perfluorooctane sulfonic acid, its salts and perfluorooctano sulfonyl fluoride. United

Nation Environment Programme. Stockholm Convention on persistent organic pollutants. UNEP/POPS/COP-4/38:66–9.

21. Martin JW, Muir DCG, Moody CA, Ellis DA, Kwan WC, Solomon KR, et al. Collection of airborne fluorinated organics and analysis by gas chromatography / chemical ionization mass spectrometry. Anal Chem. 2002;74:584–90.

22. Wu Y, Chang VWC. Development of analysis of volatile polyfluorinated alkyl substances in indoor air using thermal desorption-gas chromatography-mass spectrometry. J Chromatogr A. 2012;1238:114–20.

23. Bach C, Boiteux V, Hemard J, Colin A, Rosin C, Munoz JF, et al. Simultaneous determination of perfluoroalkyl iodides, perfluoroalkane sulfonamides, fluorotelomer alcohols, fluorotelomer iodides and fluorotelomer acrylates and methacrylates in water and sediments using solid-phase microextraction-gas chromatography/mas. J Chromatogr A. 2016;1448:98–106.

24. Lacina O, Hradkova P, Pulkrabova J, Hajslova J. Simple, high throughput ultra-high performance liquid chromatography/tandem mass spectrometry trace analysis of perfluorinated alkylated substances in food of animal origin: milk and fish. J Chromatogr A. 2011;1218:4312–21.

25. Gremmel C, Frömel T, Knepper TP. Systematic determination of perfluoroalkyl and polyfluoroalkyl substances (PFASs) in outdoor jackets. Chemosphere. 2016;160:173–80.

26. Ayala-Cabrera JF, Moyano E, Santos FJ. Gas chromatography and liquid chromatography coupled to mass spectrometry for the determination of fluorotelomer olefins, fluorotelomer alcohols, perfluoroalkyl sulfonamides and sulfonamidoethanols in water. J Chromatogr A. 2019. https://doi.org/10.1016/j.chroma.2019.460463.

27. Kuehl DW, Rozynov B. Chromatographic and mass spectral studies of perfluorooctanesulfonate and three perfluorooctanesulfonamides. Rapid Commun Mass Spectrom. 2003;17:2364–9.

28. Arsenault G, Chittim B, McAlees A, McCrindle R, Potter D, Tashiro C, et al. Mass spectral studies of native and mass-labeled perfluorooctanesulfonamide. Rapid Commun Mass Spectrom. 2007;21:929–36.

29. Ayala-Cabrera JF, Santos FJ, Moyano E. Negative-ion atmospheric pressure ionisation of semi-volatile fluorinated compounds for ultra-high-performance liquid chromatography tandem mass spectrometry analysis. Anal Bioanal Chem. 2018;410:4913–24.

30. Rafaelli A, Saba A. Atmospheric pressure photoionization mass spectrometry. Mass Spectrom Rev. 2003;22:318–31.

31. Wang C. The ionization technology of LC-MS, advantages of APPI on detection of PPCPs and hormones. Austin Chromatogr. 2015;2: 1032–4.

32. Chu S, Letcher RJ. Analysis of fluorotelomer alcohols and perfluorinated sulfonamides in biotic samples by liquid chromatography-atmospheric pressure photoionization mass spectrometry. J Chromatogr A. 2018;1215:92–9.

33. Zhou X, Zhang Y, Zhao S, Hsu CS, Shi Q. Observation of CO2 and solvent adduct ions during negative mode electrospray ionization Fourier transform ion cyclotron resonance mass spectrometric analysis of monohydric alcohols. Rapid Commun Mass Spectrom. 2013;27:2581–7.

Juan F. Ayala-Cabrera is a PhD student at the University of Barcelona. His work focuses on the development of GC-MS and LC-MS methods, using atmospheric pressure ionization techniques, for the determination of organic pollutants in environmental and food samples.

F. Javier Santos is an associate professor at the University of Barcelona. His research is mainly focused on the development of GC-MS methods for the determination of legacy and emerging organic pollutants as well as food authentication using advanced mass spectrometry strategies.

Encarnación Moyano is a full professor at the University of Barcelona. Her research focuses on the evaluation of mass spectrometry strategies and novel ionization techniques such as GC-APPI or ambient MS to deal with analytical problems in both environmental analysis and food safety.

Analytical and Bioanalytical Chemistry

Electronic Supplementary Material

Fragmentation studies of neutral per- and polyfluoroalkyl substances by atmospheric pressure ionization - multiple-stage mass spectrometry

Juan F. Ayala-Cabrera, F. Javier Santos, Encarnación Moyano
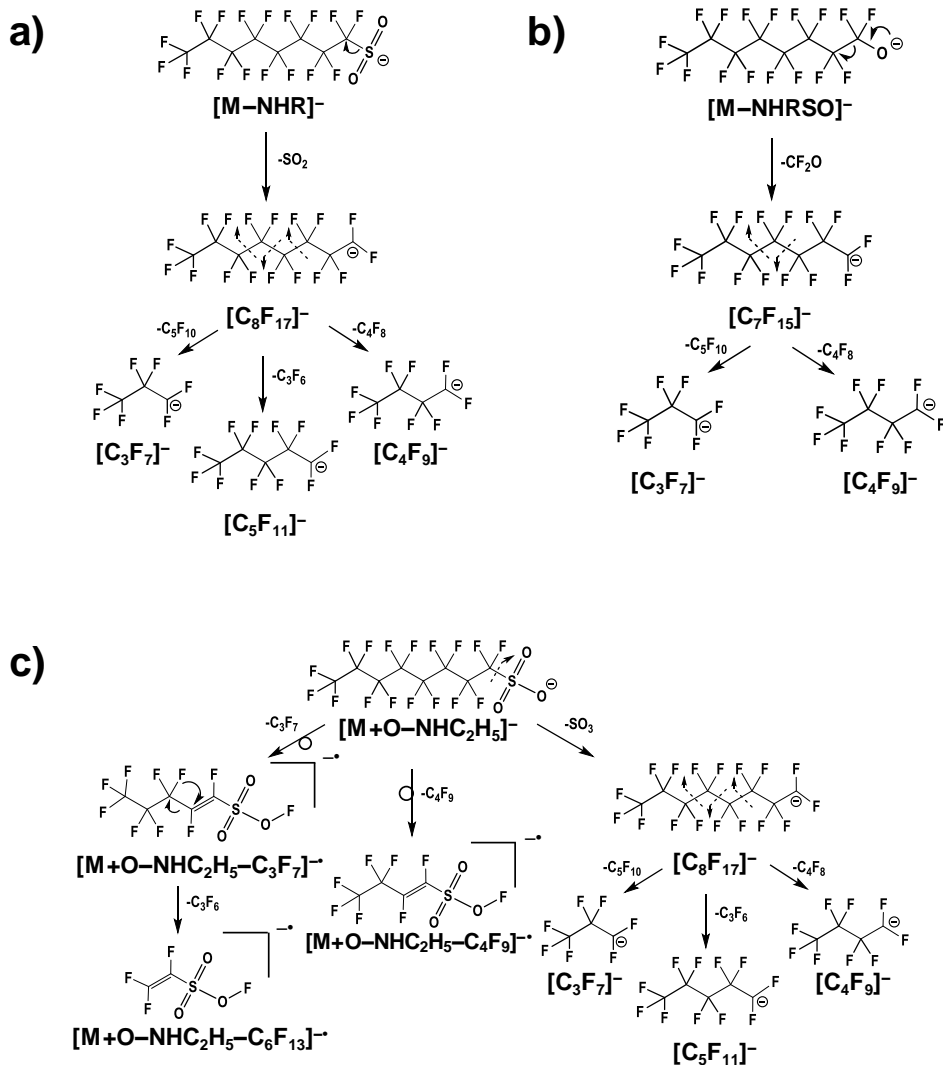
Table of Contents

Supporting Tables

Table S1 MS ² and MS ³ main product ions obtained from precursor ions for *N*-MeFOSA and *N*-MeFOSE under negative-ion API conditions

Compound	Full Scan Ion Assignment	MS² m/z (Rel. Ab. %)	MS² Ion Assignment	MS² Error (ppm)	MS³ m/z (Rel. Ab. %)	MS³ Ion Assignment	MS³ Error (ppm)
N-MeFOSA	[M-H]⁻	511.9606 (4%)	[M-H]⁻	-2.4			
		477.9389 (16%)	[M-H-CH₃F]⁻	-2.2			
		418.9726 (100%)	[C₈F₁₇]⁻	-1.9	418.9726 (8%)	[C₈F₁₇]⁻	-3.1
					268.9817 (41%)	[C₅F₁₁]⁻	-4.8
					218.9851 (100%)	[C₄F₉]⁻	-4.8
					138.9887 (27%)	[C₃F₇]⁻	-4.0
		268.9822 (24%)	[C₅F₁₁]⁻	-2.8			
		218.9853 (76%)	[C₄F₉]⁻	-3.7			
		138.9889 (34%)	[C₃F₇]⁻	-2.8			
	[M-NHCH₃]⁻	482.9331 (5%)	[M-NHCH₃]⁻	-4.6			
		418.9720 (100%)ᵃ	[C₈F₁₇]⁻	-3.4			
	[M-NFCH₃]⁻	464.9434 (17%)	[M-NFCH₃]⁻	-2.8			
		444.9373 (2%)	[M-NFCH₃-HF]⁻	-2.8			
		400.9815 (4%)	[M-NFCH₃-SO₂]⁻	-3.4			
		380.9754 (100%)	[C₈F₁₅]⁻	-3.2	380.9751 (22%)	[C₈F₁₅]⁻	-4.0
					330.9782 (2%)	[C₇F₁₃]⁻	-4.8
					311.9799 (15%)	[C₇F₁₂]⁻•	-4.7
					230.9852 (60%)	[C₅F₉]⁻	-4.8
					168.9886 (100%)	[C₃F₇]⁻	-4.5
					118.9920 (95%)	[C₂F₅]⁻	-4.4
	[M-NHCH₃SO]⁻	434.9670 (14%)	[M-NHCH₃SO]⁻	-3.1			
		368.9752 (100%)	[C₇F₁₅]⁻	-3.7	368.9751 (6%)	[C₇F₁₅]⁻	-4.0
					218.9854 (74%)	[C₄F₉]⁻	-3.8
					168.9886 (100%)	[C₃F₇]⁻	-4.6
		218.9852 (11%)	[C₄F₉]⁻	-4.6			
		168.9886 (12%)	[C₃F₇]⁻	-4.8			
N-MeFOSE	[M+CH₃COO]⁻	616.00717 (10%)	[M+CH₃COO]⁻	-3.3			
		59.0136 (100%)	[CH₃COO]⁻	-4.3			
	[M-H]⁻	555.9863 (2%)	[M-H]⁻	-3.2	535.9798 (18%)	[M-H-HF]⁻	-3.8
		535.9801 (100%)	[M-H-HF]⁻	-3.3	515.9733 (100%)	[M-H-2HF]⁻	-4.6
					495.9672 (30%)	[M-H-3HF]⁻	-4.5
					475.9610 (27%)	[M-H-4HF]⁻	-4.6

m/z (%)	Assignment	ppm	m/z (%)	Assignment	ppm
515.9739 (9%)	[M−H−2HF]−	-3.3	515.9732 (15%)	[M−H−2HF]−	-4.7
			495.9673 (69%)	[M−H−3HF]−	-4.2
			475.9610 (100%)	[M−H−4HF]−	-4.6
495.9676 (3%)	[M−H−3HF]−	-3.7			
475.9613 (3%)	[M−H−4HF]−	-3.8			
[C8F17]−a					
[M−C2H4OF]−					
493.9695 (11%)	[M− C2H4OF]−	-3.6			
473.9636 (60%)	[M− C2H4OF−HF]−	-3.1	473.9634 (20%)	[M− C2H4OF−HF]−	-3.4
			453.9572 (100%)	[M− C2H4OF−2HF]−	-3.7
			426.9467 (2%)	[M−C2H4OF−2HF−NCH]−	-2.9
			369.9892 (3%)	[M−C2H4OF−3HF−SO2]−	-3.9
			349.9830 (13%)	[M−C2H4OF−4HF−SO2]−	-4.3
			342.9783 (9%)	[M−C2H4OF−3HF−NCH−SO2]−	-4.3
453.9574 (100%)	[M− C2H4OF−2HF]−	-3.0	453.9572 (11%)	[M−C2H4OF−2HF]−	-3.5
			433.9512 (3%)	[M−C2H4OF−3HF]−	-3.2
			426.9464 (13%)	[M−C2H4OF−2HF−NCH]−	-3.6
			389.9953 (1%)	[M−C2H4OF−2HF−SO2]−	-4.1
			369.9894 (2%)	[M−C2H4OF−3HF−SO2]−	-4.2
			349.9830 (55%)	[M−C2H4OF−4HF−SO2]−	-4.2
			342.9784 (100%)	[M−C2H4OF−3HF−NCH−SO2]−	-4.0
426.9466 (3%)	[M−C2H4OF−2HF−NCH]−	-3.2	426.9462 (9%)	[M−C2H4OF−2HF−NCH]−	-4.5
			342.9783 (100%)	[M−C2H4OF−3HF−NCH−SO2]−	-4.4
389.9954 (1%)	[M−C2H4OF−2HF−SO2]−	-3.9			
369.9894 (9%)	[M−C2H4OF−3HF−SO2]−	-3.4	369.9891 (10%)	[M−C2H4OF−3HF−SO2]−	-4.8
			349.9830 (100%)	[M−C2H4OF−4HF−SO2]−	-4.2
349.9831 (42%)	[M−C2H4OF−4HF−SO2]−	-3.8			
342.9786 (35%)	[M−C2H4OF−3HF−NCH−SO2]−	-3.6			
[M−C2H5O−NCH3]−					
482.9335 (9%)	[M−C2H5O−NC2H5]−	-3.7			
418.9718 (100%)a	[C8F17]−	-3.8			
[M+O2]−•					
588.9843 (19%)	[M+O2]−•	-2.4			
541.9710 (10%)	[M+O2−CH3O2]−	-2.6			
511.9603 (100%)	[M+O2−C2H5O3]−•	-3.1			
[M−NHCH3SO]−					
434.9676 (8%)	[M−NHCH3SO]−	-1.6			
368.9761 (100%)	[C7F15]−	-1.4	368.9761 (7%)	[C7F15]−	-2.7
			218.9853 (71%)	[C4F9]−	-4.0
			168.9886 (100%)	[C3F7]−	-4.6
218.9856 (15%)	[C4F9]−	-2.6			
168.9890 (15%)	[C3F7]−	-2.2			

a As previously mentioned.

128

Supporting Figures

d)

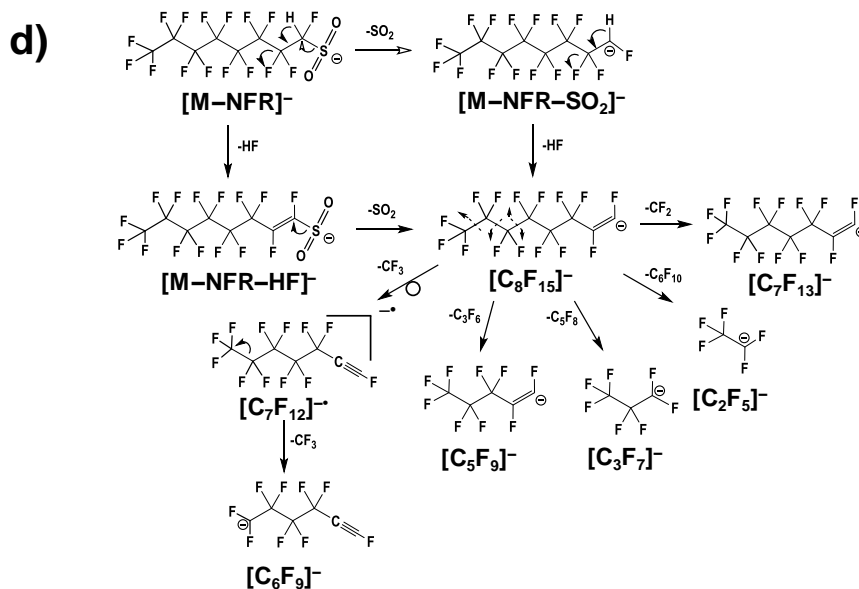**Figure S1** Secondary fragmentation pathways of FOSA and FOSEs: a) [M–NHR]⁻ (*analogue to [M–C₂H₅O–NR]⁻ being R: –CH₃, –C₂H₅*) fragmentation pathway under negative-ion APCI and APPI conditions; b) [M–NHRSO]⁻ fragmentation pathway under negative-ion APPI conditions (*for N-MeFOSA and also for FOSEs*); c) [M+O–NHC₂H₅]⁻ fragmentation pathway for *N-EtFOSA* under negative-ion ESI conditions and d) [M–NFR]⁻ fragmentation pathway for FOSAs under negative-ion APCI and APPI conditions
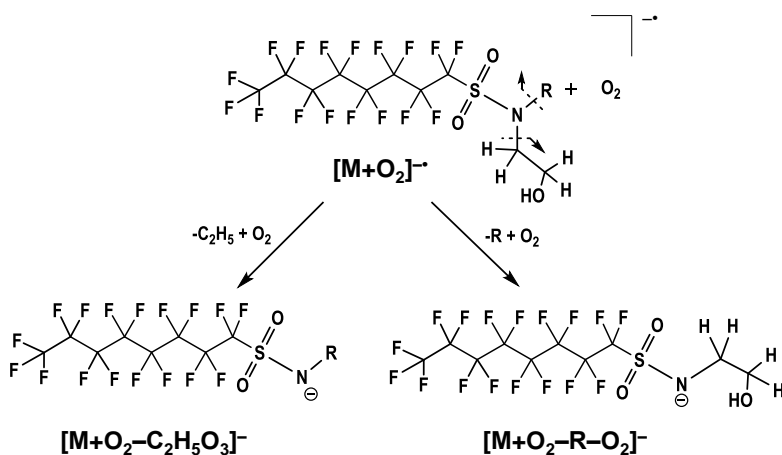
Figure S2 Secondary FOSEs fragmentation pathway of [M+O₂]⁻˙ under negative-ion APPI conditions

2.2.4. Article IV

A novel methodology for the determination of neutral perfluoroalkyl and polyfluoroalkyl substances in water by gas chromatography-atmospheric pressure photoionisation-high resolution mass spectrometry

J. F. Ayala-Cabrera, A. Contreras-Llin, E. Moyano, F. J. Santos

Analytica Chimica Acta, (**2020**) 1100: 97-106

A novel methodology for the determination of neutral perfluoroalkyl and polyfluoroalkyl substances in water by gas chromatography-atmospheric pressure photoionisation-high resolution mass spectrometry

J.F. Ayala-Cabrera [a], A. Contreras-Llin [a], E. Moyano [a, b], F.J. Santos [a, b, *]

[a] *Department of Chemical Engineering and Analytical Chemistry, University of Barcelona, Av. Diagonal 645, E–08028, Barcelona, Spain*
[b] *Water Research Institute (IdRA), University of Barcelona, Montalegre 6, E–08001, Barcelona, Spain*

HIGHLIGHTS

- GC-APPI-HRMS was applied for the first time to determine neutral PFASs in water.
- GC-APPI($-$) with acetone as dopant allowed an efficient ionisation of neutral PFASs.
- GC-APPI-HRMS method significantly improved in the detectability of the analytes.
- HS-SPME allowed a fast and effective extraction of neutral PFASs from water.
- The new method allowed a sensitive determination of neutral PFASs in river water.

GRAPHICAL ABSTRACT
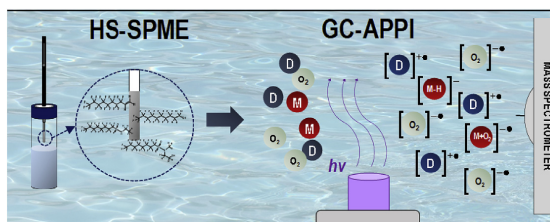
ABSTRACT

Here, we developed and validated a new gas chromatography-atmospheric pressure photoionisation-high-resolution mass spectrometry (GC–APPI–HRMS) method combined with headspace solid-phase microextraction (HS–SPME) for the determination of neutral perfluoroalkyl and polyfluoroalkyl substances (PFASs) in water samples. The method includes fluorotelomer olefins (FTOs), fluorotelomer alcohols (FTOHs), fluoroctanesulfonamides (FOSAs) and sulfonamido-ethanols (FOSEs). The feasibility of the GC-APPI interface for the ionisation of the target compounds was evaluated, achieving the best results using negative-ion dopant-assisted ionisation with acetone and a source and capillary temperatures of 225 °C and 175 °C, respectively. Under optimal conditions, FTOs and FTOHs mass spectra showed intense in-source CID fragment ions from the fluoroalkyl chain but also the superoxide $[M+O_2]^{-\bullet}$ adduct ion. For FOSAs, $[M-H]^-$ was the main ion generated, while FOSEs mass spectra showed fragment ions corresponding to the different cleavages of the functional group. The high ionisation efficiency achieved with the GC-APPI interface provided limits of the detection lower than those obtained using traditional GC-MS ionisation techniques, with a high sensitivity, selectivity and precision. For water analysis, a fast and simple HS-SPME procedure was developed, avoiding evaporation steps, which could lead to the loss of the most volatile compounds. The developed HS-SPME GC-APPI-HRMS method showed a good

* Corresponding author. Department of Chemical Engineering and Analytical Chemistry, University of Barcelona, Av Diagonal 645, E–08028, Barcelona, Spain.
E-mail address: javier.santos@ub.edu (F.J. Santos).

analytical performance for the analysis of river water samples, providing very low limits of detection (0.02–15 ng L^{-1}), good repeatability (RSD < 11%) and trueness (relative error < 12%).

1. Introduction

Perfluoroalkyl and polyfluoroalkyl substances (PFASs) consist on a functional group attached to a fully or partially fluorinated alkyl chain. Since 1950, PFASs have been produced in high volumes due to their high chemical and thermal stability, their ability to repel both water and oil, and their stain resistance. These unique properties have made them useful in numerous industrial and domestic applications, including polymer manufacture, food-contact paper coatings, fire-fighting foams, textile, and carpet and leather treatments [1–5]. Among them, fluorotelomer olefins (FTOs), fluorotelomer alcohols (FTOHs), fluorooctane sulfonamides (FOSAs), and sulfonamido-ethanols (FOSEs), have been used as precursors and/or intermediates in the telomerisation process to manufacture other PFASs and fluorotelomer-based polymers [2]. However, these neutral PFASs are easily biodegraded and/or oxidised in the environment leading to persistent and more toxic PFASs, such as perfluorooctane sulfonate (PFOS) and perfluorooctanoic acid (PFOA), that can be easily bioaccumulated and biomagnified by living organisms [5–7] and are subjected to international regulations (i.e., PFOS) or under evaluation process (i.e., PFOA) [8,9]. Until now, most of the targeted and non-targeted strategies have been focused on the analysis of other ionic and non-ionic precursors and toxics PFASs [10–12]. However, the determination of FTOs, FTOHs, FOSAs and FOSEs has still a long way to go to facilitate accurate measurements of their environmental levels and estimate their real relevance in the environment. In fact, there are still a limited number of studies conducted to determine the presence of these compounds in environmental samples, especially in water, and therefore, there is a great need for reliable data about their occurrence and distribution in the aquatic media.

Neutral PFASs have been currently determined by gas chromatography coupled to mass spectrometry (GC-MS) using electron ionisation (EI) and chemical ionisation (CI) of positive ions [13–18], while negative ion chemical ionisation (NICI) has been applied for confirmation purposes [14,18]. Although these ionisation techniques have proven useful in detecting neutral PFASs, relatively high instrumental limits of detection are usually achieved, ranging from 0.06 to 429 μg L^{-1} [19,20]. In the last years, GC-MS applications are moving from conventional ionisation techniques (e.g., EI and CI) to the atmospheric pressure chemical ionisation (APCI) and photoionisation (APPI) technologies [21,22]. Thus, the GC-APCI and GC-APPI interfaces are being introduced progressively in the analytical laboratories, opening new fields of applications due to their capabilities to ionise a great range of compounds. In addition, these sources are soft ionisation techniques that decrease the fragmentation of the molecular ion and improve the sensitivity of the instrumental methods [23]. GC-APCI has been the most used interface because it was firstly commercialised, but methods based on GC-APPI have also been developed, although to a lesser extent. Thus, GC-APPI interface has been applied to the analysis of steroids [24], polycyclic aromatic hydrocarbons (PAHs) [24,25], polychlorinated biphenyls (PCBs) [26], polibrominated diphenyls ethers (PBDEs)[27], some environmental priority pollutants [28], and light crude oil fraction [29], among others. However, the GC-APPI interface has not yet been evaluated for the determination of the neutral PFASs, although the effectiveness of the APPI source has

been demonstrated in the analysis of these compounds by liquid chromatography-tandem mass spectrometry (LC–MS/MS) [20]. Recently, an efficient GC-APPI interface based on a vortex design for GC-Orbitrap mass analyser has been commercialised [30], and it could be an excellent alternative to traditional GC-MS ionisation methods for the analysis of neutral PFASs.

Currently, the extraction methods most commonly used for the determination of neutral PFASs in water samples are based on liquid-liquid extraction or solid-phase extraction [31–33]. These extraction techniques require the use of large sample volumes and several preconcentration steps to achieve limits of detection low enough for water analysis. Nevertheless, the use of these methods resulted in losses of the analytes during the evaporation step, especially for FTOs (from 75 to 85%) and FTOHs (from 23 to 72%), and a significant matrix effect (15–60%) that caused an important decrease in the LC-MS/MS responses [34]. In this way, headspace solid-phase microextraction (HS-SPME) could be an excellent alternative for the determination of neutral PFASs. SPME is a rapid, inexpensive and solvent-free extraction technique that allows an *in-situ* preconcentration of the analytes. This technique offers a reliable and easy method for the determination of volatile organic compounds [35–37], avoiding the evaporation steps currently required in solid-phase extraction, which could cause losses of volatile analytes.

The aim of the present work is to evaluate the potential of the atmospheric pressure photoionisation source in GC-HRMS using an Orbitrap mass analyser for a selective and sensitive determination of neutral PFASs in water samples. For this purpose, several parameters that affect the ionisation behaviour of the target compounds, such as source and capillary temperatures, and the use of dopants, were optimised. In addition, the feasibility of headspace solid-phase microextraction (HS-SPME) for a rapid and reliable extraction of the target compounds from water samples was also examined. The developed HS-SPME GC-APPI-HRMS method was validated and its applicability to the analysis of river water samples was investigated to propose a new analytical method for the accurate determination of neutral PFAS at low concentration levels.

2. Materials and methods

2.1. Reagents and standards

Twelve neutral semi-volatile PFASs were selected from the families of FTOs, FTOHs, FOSAs and FOSEs as target compounds (Table 1). Individual standards of FTOs (4:2 FTO, 6:2 FTO and 8:2 FTO) and FTOHs (4:2 FTOH, 6:2 FTOH, 7-Me-6:2 FTOH) were obtained from Fluorochem Ltd. (Derbyshire, UK), while 8:2 FTOH and 10:2 FTOH were supplied by Alfa Aesar GmbH & Co KG (Karlsruhe, Germany) at a purity higher than 96%. Individual stock standard solutions of FTOs and FTOHs (1000 μg mL^{-1}) were prepared in methanol (LiChrosolv® grade, Merck, Darmstadt, Germany) from the respective pure standards. Standard solutions (50 μg mL^{-1}) of *N*-MeFOSA, *N*-MeFOSE and *N*-EtFOSE in methanol were purchased from Wellington Laboratories Inc. (Guelph, Ontario, Canada), while a stock standard solution (1000 μg mL^{-1}) of *N*-EtFOSA was prepared in methanol from a solid standard (purity > 99%) supplied by Dr. Ehrenstorfer GmbH (Ausburg, Germany). Individual standards of

Table 1
Chemical names, acronyms, linear structures and molecular formula of the target compounds.

Compound	Acronym	Linear structure	Molecular Formula	Vapour Pressure[a] (mm Hg, 25 °C)
1H, 1H, 2H–perfluoro-1-hexene	4:2 FTO	$CF_3(CF_2)_3CH=CH_2$	$C_6H_3F_9$	332
1H, 1H, 2H–perfluoro-1-octene	6:2 FTO	$CF_3(CF_2)_5CH=CH_2$	$C_8H_3F_{13}$	43.9
1H, 1H, 2H–perfluoro-1-decene	8:2 FTO	$CF_3(CF_2)_7CH=CH_2$	$C_{10}H_3F_{17}$	6.36
1H, 1H, 2H, 2H–perfluorohexan–1–ol	4:2 FTOH	$CF_3(CF_2)_3CH_2CH_2OH$	$C_6H_5F_9O$	12.9
1H, 1H, 2H, 2H–perfluorooctan–1–ol	6:2 FTOH	$CF_3(CF_2)_5CH_2CH_2OH$	$C_8H_5F_{13}O$	0.382
1H, 1H, 2H, 2H–perfluoro–7–methyloctan–1–ol	7–Me–6:2 FTOH	$(CF_3)_2CF(CF_2)_4CH_2CH_2OH$	$C_9H_5F_{15}O$	0.807
1H, 1H, 2H, 2H–perfluoro–1–decanol	8:2 FTOH	$CF_3(CF_2)_7CH_2CH_2OH$	$C_{10}H_5F_{17}O$	0.17
1H, 1H, 2H, 2H–perfluoro–1–dodecanol	10:2 FTOH	$CF_3(CF_2)_9CH_2CH_2OH$	$C_{12}H_5F_{21}O$	0.0208
2–(N–methylperfluoro–1–octanesulfonamido)–ethanol	N–MeFOSE	$CF_3(CF_2)_7SO_2N(CH_3)\,(CH_2CH_2OH)$	$C_{11}H_8F_{17}NO_3S$	0.000116
2–(N–ethylperfluoro–1–octanesulfonamido)–ethanol	N–EtFOSE	$CF_3(CF_2)_7SO_2N(CH_2CH_3)\,(CH_2CH_2OH)$	$C_{12}H_{10}F_{17}NO_3S$	0.0000339
N–methylperfluoro–1–octanesulfonamide	N–MeFOSA	$CF_3(CF_2)_7SO_2NH(CH_3)$	$C_9H_4F_{17}NO_2S$	0.078
N–ethylperfluoro–1–octanesulfonamide	N–EtFOSA	$CF_3(CF_2)_7SO_2NH(CH_2CH_3)$	$C_{10}H_6F_{17}NO_2S$	0.0269

[a] Predicted values by the ACD/Labs Percepta Platform.

1H, 1H-pentadecafluoro-1-octanol (7:1 FA), 1H, 1H-perfluoro-1-nonanol (8:1 FA), 1H, 1H-perfluoro-1-decanol (9:1 FA) and 1H, 1H-perfluoro-1-dodecanol (11:1 FA), supplied by Fluorochem Ltd., were used as internal standards for FTOs and FTOHs, while N-ethyl-$^2H_5$-perfluoro-1-octanesulfonamide (d$_5$-N-EtFOSA) and 2-(N-Ethyl-$^2H_5$-perfluoro-1-octane-sulfonamido)-ethan-$^2H_4$-ol) (d$_9$-N-EtFOSE) from Wellington Laboratories Inc. were employed for FOSAs and FOSEs, respectively. All the internal standards were at a purity higher than 95%. For optimising the GC-APPI-HRMS method, a standard mixture of all the target compounds were prepared in methanol at 1 μg mL^{-1}. For validation purposes, a set of seven calibration solutions ranging from 0.1 ng mL^{-1} to 100 ng mL^{-1} (FTOs between 1 ng mL^{-1} and 500 ng mL^{-1}) were prepared by successive dilution of stock standard solutions. All these standard solutions contained appropriate amounts of the internal standards to give concentrations of 10 ng mL^{-1} for 7:1 FA and d$_5$-N-EtFOSA, 5 ng mL^{-1} for 8:1 FA and 9:1 FA, and 2 ng mL^{-1} for 11:1 FA and d$_5$-N-EtFOSE. All these solutions were stored at 4 °C until their analysis (1 μL) by GC-APCI-HRMS.

Anisole anhydrous (purity 99.7%), toluene and chlorobenzene for HPLC (Chromasolv™ Plus, purity ≥ 99%) were supplied by Sigma-Aldrich (Merck, Darmstadt, Germany). Tetrahydrofuran (Photrex™ reagent, purity of 99%) was purchased from J. T. Baker (Deventer, The Netherland) and acetone (LiChrosolv®, purity ≥ 99.8%) was obtained from Merck. Vapours of all these solvents were used as dopants for the optimisation of APPI source conditions. Moreover, a Milli-Q system coupled to an Elix 3 (Millipore, Bedfore, MA, USA) was used to obtain ultra-pure water. All glassware was cleaned with chromo-sulphuric acid and rinsed with Milli-Q water and acetone before use. Helium Alphagaz™ 1 (purity ≥ 99.9993%), supplied by Air Liquide (Madrid, Spain), was employed as GC carrier gas while nitrogen (purity > 99.9995%), purchased from Linde (Barcelona, Spain), was used as make-up gas for the GC-APPI interface.

2.2. Water samples

River water samples were collected from the lower section of Llobregat River (Barcelona, Spain). This river runs through a densely populated and industrialised area before flowing into the Mediterranean Sea, receiving extensive urban and industrial wastewater discharges coming from different factories and populations inhabiting its surroundings. The water samples were taken upstream and downstream of an industrial area located at the towns of Sant Boi de Llobregat and Cornellà, dedicated to textile, clothing and footwear manufacturing. In addition, tap water samples were also taken from the supply of the city of Barcelona to assess the possible contribution of the pipeline network. All these samples

were collected using 1000 mL glass bottles filled without leaving headspace, to prevent possible losses, and stored in the refrigerator at 4 °C before being analysed. Field blanks consisting of 100 ml of natural mineral water (Font Vella, San Hilari Sacalm, Spain) were prepared at the same sampling points and analysed along with the river and tap water samples.

2.3. Sample treatment

Target compounds were extracted from water samples by headspace solid-phase microextraction (HS-SPME) using a manual fibre holder supplied by Supelco (Bellefonte, PA, USA). Five SPME fibres, purchased from Supelco, were tested: 100-μm poly-dimethylsiloxane (PDMS), 85-μm polydimethylsiloxane/carboxen (PDMS/CAR), 65-μm polydimethylsiloxane/divinylbenzene (PDMS/DVB), 85-μm polyacrylate (PA) and 50/30-μm divinylbenzene/car-boxen/polydimethylsiloxane (DVB/CAR/PDMS). These fibres cover different polarities, which could interact with different parts of the molecules, to improve the extraction of the different families of compounds from non-polar FTOs to relatively polar FOSAs. Before use, each fibre was conditioned in the GC injection port under helium flow according to the manufacturer's recommendation. After conditioning, fibre blanks were periodically analysed to ensure there were no contaminants or carryover present.

After optimisation, the HS-SPME procedure was carried out as follows: 10 mL of water were placed in a 20 mL screw-cap glass vial fitted with rubber septa containing a 10 mm × 5 mm stir bar and an appropriate amount of the internal standards was added through the sample vial septum. The internal standard concentrations in the final vial were 20 ng L^{-1} for 7:1 FA, 10 ng L^{-1} for 8:1 FA and 9:1 FA, 30 ng L^{-1} for d$_5$-N-EtFOSA, and 4 ng L^{-1} for 11:1 FA and d$_9$-N-EtFOSE. Polytetrafluoroethylene (PTFE) coating of stir bar was removed before use. Before HS-SPME analysis, the sample vial was conditioned for 15 min in a thermostatic water bath at the extraction temperature. Then, water samples and calibration solutions were extracted from the headspace with a DVB/CAR/PDMS fibre at 60 °C for 30 min using a constant agitation rate of 750 rpm. Finally, thermal desorption of the target compounds was carried out by exposing the fibre into a GC injection port at 250 °C for 3 min in splitless injection mode. After desorption, the fibre was kept in the GC injector for an additional time of 20 min in split mode (purge on) for cleaning the fibre and preventing possible carryover between samples. For quantification of neutral PFASs, seven calibration water standard solutions were prepared by adding adequate amounts of standard mixtures into a 20 mL screw-cap glass vial containing 10 ml of Milli-Q water to give concentrations ranging from 0.2 to 2000 ng L^{-1}. In addition, appropriate amounts of internal standard were added to each calibration solution to obtain

similar concentrations than those used for water samples. Further details about the optimisation of the HS-SPME procedure are given in section 3.3.

2.4. Instrumentation

Neutral PFASs were determined on a Trace 1300 gas chromatograph coupled to a Q-Exactive Orbitrap mass spectrometer (Thermo Fisher Scientific, San Jose, CA, USA), using an atmospheric pressure photoionisation source for GC-MS analysis (GC-APPI) (MasCom Technologies GmbH, Bremen, Germany). For the chromatographic separation, a DB-624 (6% cyanopropylphenyl 94% dimethyl polysiloxane) GC fused-capillary column of 60 m of length, 0.25 mm I.D. and 1.40 μm of film thickness (Agilent Technologies, Santa Clara, CA, USA) was employed. The injector was operated at 250 °C in the splitless injection mode (3 min) using a glass inlet liner (I.D., 0.75 mm, Agilent Technologies) for the HS-SPME experiments. Helium was used as carrier gas at a constant flow rate of 1.3 mL min^{-1} held by electronic flow control. The oven temperature program was as follow: from 50 °C (held for 3 min) to 120 °C at 10 °C min^{-1} and then to 250 °C at 25 °C min^{-1} (held for 10 min). The transfer line, source and capillary temperatures were set at 250 °C, 225 °C and 175 °C, respectively. The GC-APPI source was equipped with a 10.6 eV krypton lamp (Syagen, Santa Ana, CA, USA) and it worked in the negative-ion mode using nitrogen as make-up gas (gas pressure of 5 a.u.) and acetone vapours (70 μL min^{-1}) as dopant. Data acquisition was performed in full-scan mode from m/z 100 to m/z 800 at a resolution of 35,000 (FWHM, at 200 m/z), using a maximum injection time of 200 ms for good peak reconstruction with at least 12 data points per peak and an automatic gain control (AGC) of $3 \cdot 10^6$ to achieve the highest sensitivity. With identification and quantification purposes, extracted ion chromatograms (EICs) were obtained using ±5 ppm precision extraction windows. Xcalibur v 3.1 software was used to control the instrument setup and process the data acquisition. ACD/Labs Percepta software (Advanced Chemistry Development Inc., Toronto, Canada) was used to estimate the vapour pressure values of the target compounds.

2.5. Quality control and method validation

Quality control standard solutions and procedural blanks were introduced among the analysis of standards and samples for ensuring the quality of the results and for checking the GC separation, the sensitivity of the GC-APPI-HRMS system and the validity of the calibration. The accurate mass calibration in the Orbitrap was performed every 72 h using an electrospray source with a calibration solution containing caffeine, MRFA peptide, Ultramark 1621 and butylamine in acetonitrile/methanol/water (2:1:1, $v/v/v$) with 1% (v/v) formic acid. Procedural blanks covering both the instrumental and HS-SPME procedure were periodically analysed to evaluate the potential contribution of interfering compounds on the neutral PFASs measurements and the possible carryover between samples. Instrumental (ILODs) and method limits of detection (MLODs) were estimated as the smallest analyte concentration that provides a well-defined chromatographic peak with a good peak shape and a mass error on the HRMS mass spectrum lower than 5 ppm for the characteristic ions. These criteria were used because almost no baseline noise was recorded in the extracted ion chromatograms due to the narrow mass error threshold (<5 ppm) and the high resolution used (FWHM 35,000 at m/z 200) on the Orbitrap mass analyser. Instrumental (ILOQs) and method limits of quantification (MLOQs) were experimentally established by analysing standards and spiked blank water samples at low concentration levels according with the respective limits of detection and linearity. Intra-

day precision (n = 3) was routinely tested by analysing blank river water samples spiked with the target compounds at low ng L^{-1} levels.

3. Results and discussion

3.1. Determination of neutral PFASs by GC-APPI-HRMS

Since FTOHs, FTOs, FOSAs and FOSEs cannot be directly photoionised using APPI, the ionisation was assisted by a dopant which was introduced into the source as a gas-phase. In addition, positive-ion APPI mode did not allow the ionisation of the target compounds, may be due to their high electronegativity. Therefore, the ionisation behaviour of these compounds in negative-ion mode was investigated using different solvents, such as toluene, acetone, chlorobenzene, tetrahydrofuran and anisole, as potential APPI dopants. All these experiments were carried out using a source and capillary temperatures of 250 °C and 200 °C, respectively. Generally, the mass spectra obtained using these solvents showed ions that did not depend of the dopant used, although differences in their ion intensities were observed (see Table S1). As an example, Fig. 1 shows the GC-APPI-HRMS mass spectra obtained for 8:2 FTOH, 8:2 FTO, N-MeFOSA and N-EtFOSE using acetone as dopant. The mass spectra for most of FTOHs using acetone as dopant showed the presence of the superoxide [M+O$_2$]$^{-•}$ ion as base peak and some in-source CID fragments corresponding to different cleavages of the fluorinated alkyl chain (Fig. 1a). For FTOs, mass spectra were characterised by the odd-electron fragment ions generated from the unstable [M+O$_2$]$^{-•}$ adduct (i.e., [M+O$_2$−HF$_2$O]$^-$, [M+O$_2$−HF$_2$]$^-$ or [C$_9$OF$_{15}$]$^-$) and some ions coming from the fragmentation of the fluorinated alkyl chain, being the [M−CH$_3$F$_2$]$^-$ the base peak in all the spectra (i.e., [C$_9$F$_{15}$]$^-$ for 8:2 FTO, Fig. 1b). The presence in the mass spectra of superoxide-related fragment ions could be attributed to the entry of dopant mixed with air into the APPI source, which promoted the formation of a non-stable superoxide adduct ion that yielded characteristic fragment ions. These superoxide adduct-related ions are not observed in LC-APPI-MS [29,32] because the dopant is introduced in the APPI source in liquid-phase. Concerning FOSEs, they were ionised by the formation of a superoxide adduct ion but also generating fragment ions corresponding to the loss of the ethanol chain [M−C$_2$H$_4$OH]$^-$ (base peak of the spectra) or even the functional group [M−NRC$_2$H$_4$OH]$^-$ (R: CH$_3$, C$_2$H$_5$) (Fig. 1c for N-EtFOSE). Otherwise, FOSAs showed the deprotonated molecule as the base peak of the mass spectrum, although some low abundant in-source CID fragment ions generated by the loss of the sulfonamide group from the deprotonated molecule were also observed (Fig. 1d). The presence of these characteristic fragment ions in the mass spectra provided valuable structural information for confirming the identification of the analytes and detecting related unknown compounds. To select the most suitable dopant for the efficient ionisation of the target compounds the responses of the most abundant ions were compared. Among the dopants studied, acetone provided the best result for most of the compounds, especially for FTOHs (Fig. 2). This fact could be related with the high vapour pressure of acetone that may allow a higher generation of O$_2^{-•}$ in the gas-phase and, consequently, a more efficient ionisation of superoxide adduct ions. In the case of 4:2 FTO, tetrahydrofuran showed the highest response, although acetone also provided an adequate ionisation efficiency (Fig. 2). Therefore, acetone was selected as APPI dopant for the subsequent experiments. To maximise the response of the target compounds, the acetone vapours flow-rate was then optimised from 30 to 70 μL min^{-1}, obtaining the best results at 70 μL min^{-1} (Fig. S1), which is close to the recommended maximum value for avoiding turbulent flow. Moreover,
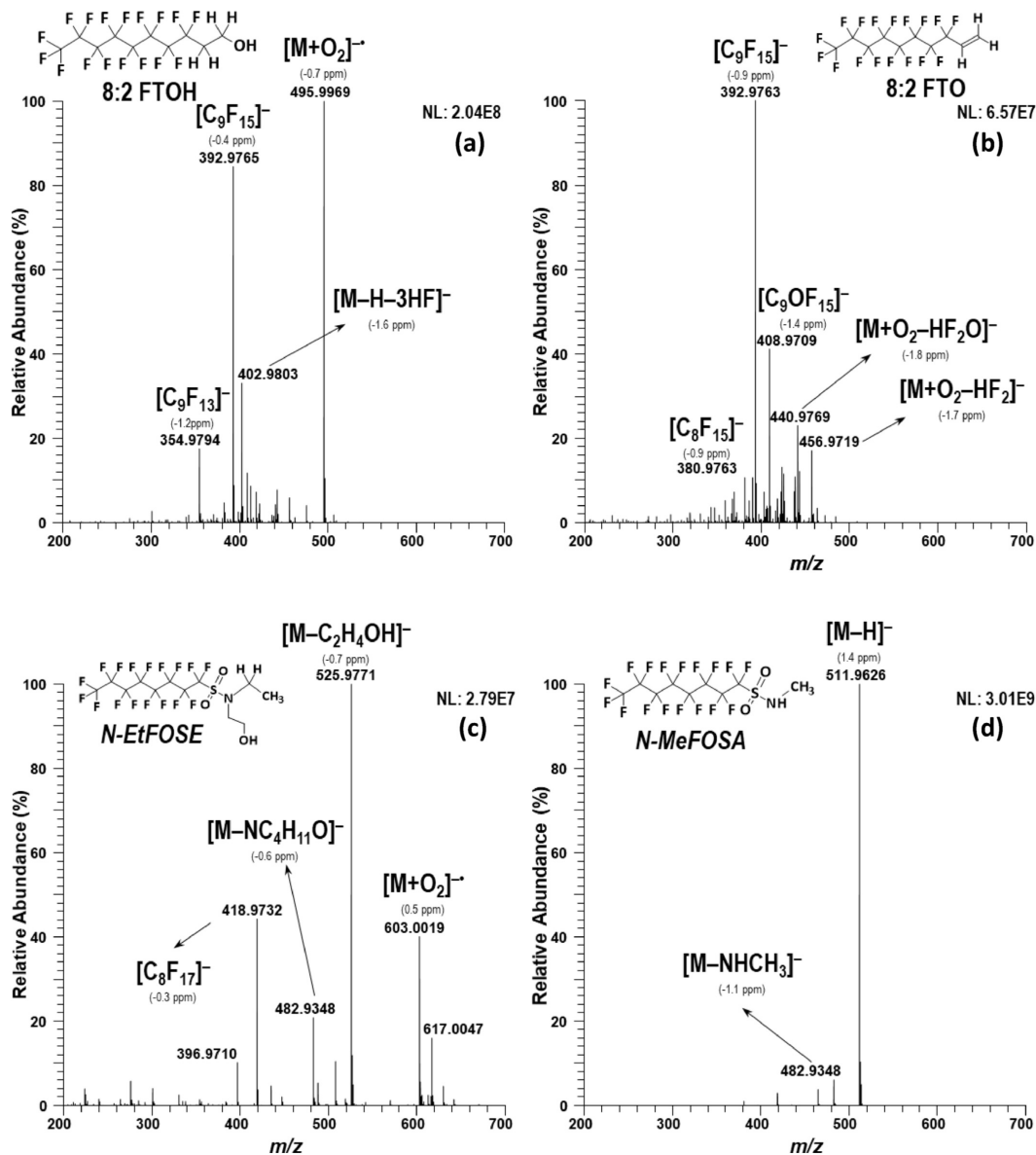
Fig. 1. Negative-ion APPI mass spectra of (a) 8:2 FTOH, (b) 8:2 FTO, (c) *N*-EtFOSE and (d) *N*-MeFOSA using acetone as APPI-dopant.

APPI source (from 200 °C to 250 °C) and capillary temperatures (from 175 °C to 225 °C) were also evaluated to maximise the ionisation efficiency by reducing the in-source CID fragmentation. Since no significant differences in the response were observed at the temperatures tested, a source temperature of 225 °C and a capillary temperature of 175 °C were chosen. Table 2 summarises

the two most intense ions selected from each high-resolution full-scan mass spectrum for the GC-APPI-HRMS determination of neutral PFASs. Concerning *N*-EtFOSA, the $[M-NFC_2H_5]^-$ fragment ion (m/z 464.9447) was chosen as qualifier ion because the second most intense ion, $[M-NHC_2H_5]^-$ (m/z 482.9353, $[C_8F_{17}O_2S]^-$), was interfered by the same fragment ion from d_5-*N*-EtFOSA internal
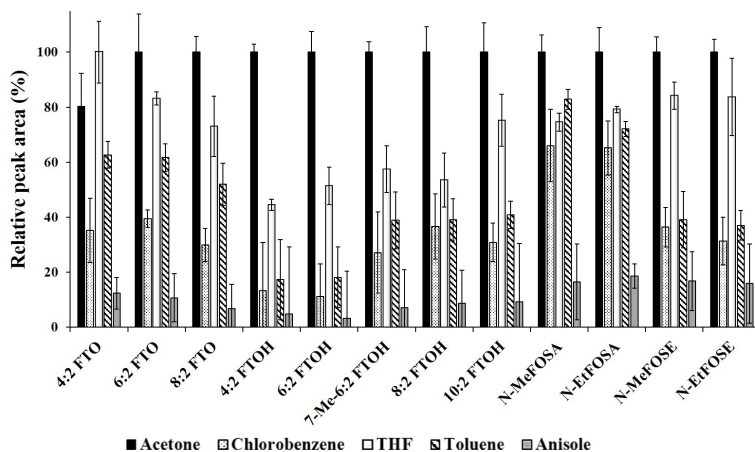
Fig. 2. Effect of APPI-dopants on the response of neutral PFASs using negative-ion GC-APPI-HRMS. (THF: tetrahydrofuran).

Table 2
Selected ions from GC-APPI-HRMS high-resolution full-scan for the quantification of target compounds.

Compound	Quantification Ion		Confirmation Ion	
	m/z	Assignation	m/z	Assignation
4:2 FTO	192.9894	$[C_5F_7]^-$	208.9843	$[C_5OF_7]^-$
6:2 FTO	292.9830	$[C_7F_{11}]^-$	308.9779	$[C_7OF_{11}]^-$
8:2 FTO	392.9766	$[C_9F_{15}]^-$	408.9715	$[C_9OF_{15}]^-$
4:2 FTOH	192.9894	$[C_5F_7]^-$	296.0101	$[M+O_2]^{-\bullet}$
6:2 FTOH	396.0037	$[M+O_2]^{-\bullet}$	292.9830	$[C_7F_{11}]^-$
7-Me-6:2 FTOH	305.9908	$[C_8HF_{11}]^{-\bullet}$	446.0005	$[M+O_2]^{-\bullet}$
8:2 FTOH	495.9973	$[M+O_2]^{-\bullet}$	392.9766	$[C_9F_{15}]^-$
10:2 FTOH	595.9909	$[M+O_2]^{-\bullet}$	492.9702	$[C_{11}F_{19}]^-$
N-MeFOSA	511.9612	$[M-H]^-$	482.9353	$[M-NHCH_3]^-$
N-EtFOSA	525.9775	$[M-H]^-$	464.9447	$[M-NFC_2H_5]^-$
N-MeFOSE	511.9619	$[M-C_2H_5O]^-$	588.9857	$[M+O_2]^{-\bullet}$
N-EtFOSE	525.9775	$[M-C_2H_5O]^-$	603.0014	$[M+O_2]^{-\bullet}$
Internal Standards				
7:1 FA	398.9872	$[M-H]^-$	431.9848	$[M+O_2]^{-\bullet}$
8:1 FA	448.9840	$[M-H]^-$	481.9817	$[M+O_2]^{-\bullet}$
9:1 FA	498.9808	$[M-H]^-$	531.9784	$[M+O_2]^{-\bullet}$
11:1 FA	598.9748	$[M-H]^-$	631.9720	$[M+O_2]^{-\bullet}$
d_5-*N*-EtFOSA	531.0089	$[M-H]^-$	465.9510	$[M-NFC_2H^2H_4]^-$
d_9-*N*-EtFOSE	531.0089	$[M-C_2H^2H_4O]^-$	612.0579	$[M+O_2]^{-\bullet}$

standard.

The performance of the developed GC-APPI-HRMS method was evaluated by determining the linearity, instrumental limits of detection and quantification, sensitivity, precision and trueness (Table S2). Linearity was tested by injecting seven calibration solutions at concentrations ranging from 0.1 ng mL^{-1} to 100 ng mL^{-1} (FTOs in the range 1—500 ng mL^{-1}). Internal standard calibration curves were established by least-squares regression analysis obtaining correlation coefficients (r) for all the compounds higher than 0.999. The sensitivity of instrumental method was determined from the slope of the calibration curves and were from 10 to 500 times higher than those obtained in a previous work with LC-APCI-MS/MS [34], demonstrating the good performance of the method. Instrumental limits of detection (ILODs) ranged from 0.03 to 0.3 ng mL^{-1} for most of the target compounds, although for 4:2 FTO and 6:2 FTO the ILOD values were 1 and 8 ng mL^{-1}, respectively (Table S2). To improve the ILODs of FTOs an increase of the source temperature is required, since the ionisation efficiency of these compounds in APCI and APPI sources is favoured at high temperatures (around 400 °C) [20], but the GC-APPI source does not allow to operate at temperatures higher than 250 °C. In general, GC-APPI-HRMS provided ILODs lower than those obtained with both LC-APCI-MS/MS and GC-MS using chemical ionisation (CI) [34,38,39]. In addition, the ILOD values were around 50 times better than those obtained with LC-APPI-MS/MS [34], with an important improvement for FTOs of about three to four order of magnitude. The intraday precision on the determination of the target compounds was examined by analysing in triplicate two standard solutions at concentrations very close (low level) and around ten times higher (medium level) than the limits of quantification (Table S2), achieving relative standard deviations (RSD %) lower than 10%. Moreover, the trueness in the determination of the target compounds showed relative errors lower than 10%. These results demonstrated the performance and validity of the developed GC-APPI-HRMS for the determination of the neutral PFASs.

3.2. Optimisation of HS-SPME procedure

The feasibility of headspace solid-phase microextraction to the determination of neutral PFASs in water samples at low concentration levels (ng L^{-1}) was investigated. The first step in the optimisation of the SPME procedure was the selection of the appropriate fibre. To obtain the best sensitivity and selectivity, the following five SPME fibres were tested: DVB/CAR/PDMS, PDMS/CAR, PDMS/DVB, PDMS and PA (section 2.3.). For this purpose, the fibres were evaluated using 10 mL of water samples spiked at 500 ng L^{-1} and the analytes were extracted from the headspace by exposing the fibre during 15 min at 60 °C using constant stirring (750 rpm). The desorption temperature was 250 °C for all fibres, which is within the recommended operating temperature range. Among the studied fibres, the PDMS and PA showed the worst results with a very low extraction efficiency of FOSAs, FOSEs and FTOs. Fig. 3 shows the extraction efficiency of the DVB/CAR/PDMS, PDMS/CAR and PDMS/DVB fibres for the determination of all the compounds. As can be seen in Fig. 3a, FTOHs showed a similar behaviour on the three fibres, while FOSAs and FOSEs achieved the best extraction yields with the DVB/CAR/PDMS fibre. In contrast, for FTOs the highest responses were achieved using the PDMS/CAR fibre, although the DVB/CAR/PDMS fibre also provided a high
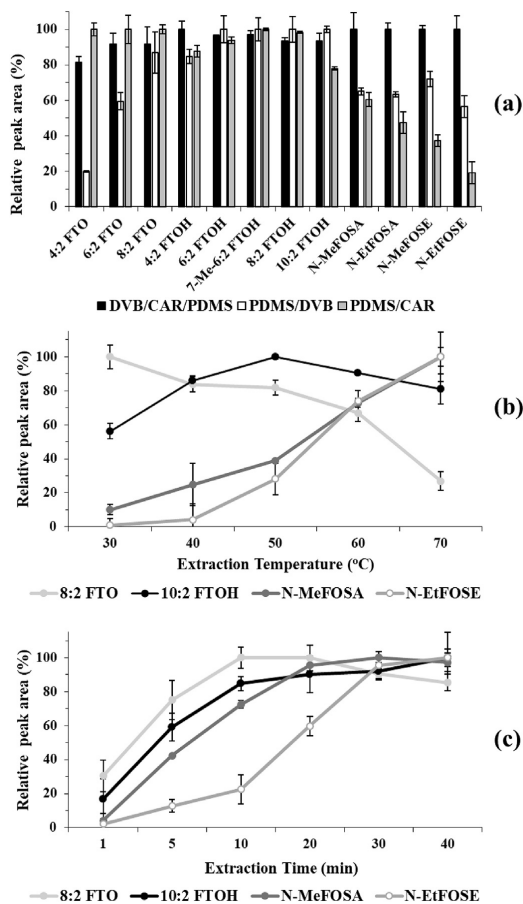
Fig. 3. (a) Extraction efficiency of the SPME fibres on the response of neutral PFASs. (b) Effect of extraction temperature and (c) extraction time on the absorption of 8:2 FTO, 10:2 FTOH, *N*-MeFOSA, and *N*-EtFOSE, using a DVB/CAR/PDMS fibre.

extraction efficiency. As a compromise, the DVB/CAR/PDMS was selected for all subsequent experiments.

Extraction temperature was then evaluated (from 30 °C to 70 °C) to improve the extraction of the analytes. As can be seen in Fig. 3b, the responses of FOSAs and FOSEs increased with the temperature, while a high extraction efficiency for FTOs and FTOHs was observed at temperatures ranging between 30 and 50 °C (Fig. 3b). This may be due to a decrease in the distribution constants between the headspace and the fibre coating of the FTOs and FTOHs when the temperature increases, since they have a higher vapour pressure than FOSAs and FOSEs (Table 1). Therefore, an extraction temperature of 60 °C was selected as optimum value for the extraction of all the compounds. In addition, the extraction time was evaluated from 1 to 40 min. As shown in Fig. 3c, an extraction time of 30 min was enough to reach the equilibrium and it was chosen as the optimal value for subsequent experiments. Finally, the effect of salt addition (0–30% NaCl) and pH adjustment (2–10) on extraction yield were investigated and, as expected, no significant differences in response were observed for any of the compounds.

## 3.3. Performance of the HS-SPME GC-APPI-HRMS method for river water analysis

In order to study the applicability of the proposed HS-SPME GC-APPI-HRMS method for the determination of neutral PFASs at low concentration levels, several river water samples were analysed in triplicate. As none of the analysed samples showed detectable concentrations of the target compounds for quantification, they were considered suitable for determining the figures of merit of the developed method and demonstrate its feasibility for achieving an accurate determination. For this purpose, quality parameters of the HS-SPME GC-APPI-HRMS method were established and the results are summarised in Table 3. Linearity was estimated by analysing seven calibration water solutions using HS-SPME over the range of 0.2–2000 ng L^{-1} and high correlation coefficients were obtained ($r > 0.998$) for all the compounds. Method limits of detection (MLODs) were stablished and ranged from 0.02 to 0.24 ng L^{-1} for most of the analytes, except for 4:2 FTO which was 15 ng L^{-1}, while method limits of quantification (MLOQs) were comprised between 0.08 and 50 ng L^{-1}. These values were about 40–200 times lower than those previously reported for some FTOHs and FOSAs (20–100 ng L^{-1}) using HS-SPME GC-MS with electron ionisation [40]. For LC-MS/MS with electrospray ionisation, the proposed method also provided lower MLOQs values of at least 500 times for FTOHs (60–90 ng L^{-1}) [41], 2–4 times for FOSAs (0.29–0.62 ng L^{-1}) [32,42] and around 30 times for FOSEs (2.2 ng L^{-1}) [43]. In addition, the reported MLOQs for the analysis of the target compounds using LC-MS/MS methods with APPI or APCI sources were 2–100 times higher for FTOHs, FOSAs and FOSEs (0.3–6 ng L^{-1}) [34] and at least 400 times higher for FTOs (0.07–6 μg L^{-1}) [20]. These results confirm the good detectability of the HS-SPME GC-APPI-HRMS method. The repeatability (intra-day precision) of the developed method was determined using a blank river water sample spiked at two concentration levels (low: 0.4–200 ng L^{-1}; medium: 5–2500 ng L^{-1}). Good repeatability was achieved with a relative standard deviation (RSD, %) values ranged from 2 to 11% ($n = 3$). Moreover, trueness, expressed as the relative error (RE, %), was also examined at the two same concentration levels, and the results were always lower than 12% ($n = 3$) (Table 3). Fig. 4 shows as an example of the GC-APPI-HRMS extracted high resolution full-scan chromatograms obtained by spiking 10 mL of a blank river water sample (from 0.4 ng L^{-1} to 4 ng L^{-1}, except for 4:2 FTO which was 200 ng L^{-1}). Under these conditions, it was possible to separate all the analytes in less than 22 min with a good sensitivity and selectivity. On base of this finding, the validity of the HS-SPME GC-APPI-HRMS method has been demonstrated and can be propose for the reliable determination of FTOs, FTOHs, FOSAs and FOSEs in water samples at low concentration levels.

4. Conclusions

The feasibility of a new analytical method based on HS-SPME combined with GC-APPI-HRMS for the determination of neutral PFASs in water samples has been demonstrated. The use of dopant-assisted APPI in the negative-ion mode with vapours of acetone as dopant allowed a high ionisation efficiency for all the compounds, providing characteristic in-source CID fragment ions to ensure the proper quantification and confirmation of the target compounds. In addition, the information provided by the high resolution mass spectra makes it possible to ensure unequivocal identification of the analytes and detect possible related compounds. The HS-SPME using a DVB/CAR/PDMS fibre has proven to be a fast and effective technique for the extraction of the target compounds from water samples, simplifying the sample treatment and avoiding possible losses of the analytes. The developed HS-SPME GC-APPI-HRMS

Table 3
Quality parameters of the developed HS-SPME GC-APPI-HRMS method.

Parameter		4:2 FTO	6:2 FTO	8:2 FTO	4:2 FTOH	6:2 FTOH	7-Me-6:2 FTOH
MLOD (ng L^{-1})		15	0.24	0.09	0.12	0.06	0.06
MLOQ (ng L^{-1})		50	0.80	0.30	0.40	0.20	0.20
Spiked conc. (ng L^{-1})	Low level	200	4.0	1.6	2.0	1.0	1.0
	Medium level	2500	50	20	25	12.5	12.5
Found conc. ± SD^a (ng L^{-1})	Low level	210 ± 14	3.5 ± 0.4	1.5 ± 0.1	2.1 ± 0.1	0.99 ± 0.09	1.02 ± 0.06
	Medium level	2342 ± 167	52 ± 4	19 ± 2	24 ± 1	12.1 ± 0.9	12 ± 1
Repeatability (RSD, %)^a	Low level	6	11	9	6	9	11
	Medium level	7	8	9	3	8	6
Trueness (Rel. Error, %)^a	Low level	5	−12	−3	5	−1	2
	Medium level	−3	4	−3	5	−3	−8

Parameter		8:2 FTOH	10:2 FTOH	N-MeFOSA	N-EtFOSA	N-MeFOSE	N-EtFOSE
MLOD (ng L^{-1})		0.06	0.02	0.15	0.15	0.02	0.02
MLOQ (ng L^{-1})		0.20	0.08	0.50	0.50	0.08	0.08
Spiked conc. (ng L^{-1})	Low level	1.0	0.4	3.0	3.0	0.4	0.4
	Medium level	12.5	5.0	37.5	37.5	5.0	5.0
Found conc. ± SD^a (ng L^{-1})	Low level	0.9 ± 0.1	0.39 ± 0.01	3.3 ± 0.2	3.2 ± 0.2	0.44 ± 0.03	0.39 ± 0.04
	Medium level	11.6 ± 0.8	5.0 ± 0.6	40.6 ± 0.4	39.5 ± 0.5	4.7 ± 0.1	4.9 ± 0.4
Repeatability (RSD, %)^a	Low level	11	11	6	6	8	11
	Medium level	7	6	2	2	2	8
Trueness (Rel. Error, %)^a	Low level	−5	−3	12	7	10	−3
	Medium level	−7	1	8	5	7	−2

^{a} $n = 3$.
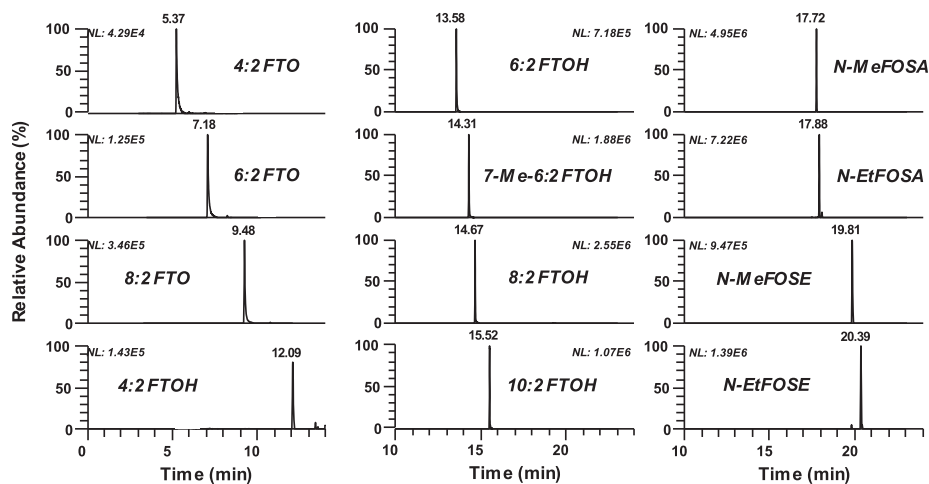
Fig. 4. GC-APPI-HRMS extracted ion chromatograms of a blank river water sample spiked at concentrations ranging from 0.4 ng L^{-1} to 4 ng L^{-1} for all the compounds, except for 4:2 FTO which was 200 ng L^{-1}.

method provided low limits of detection (0.02–15 ng L^{-1}) a good repeatability (RSD% < 11) and trueness (RE% < 12), demonstrating the good performance of the method for the analysis river water at low concentration levels (ng L^{-1}). As far as we know, this article reports for the first time the excellent performance of the GC-APPI interface coupled to HRMS (Q-Orbitrap) for the analysis of neutral PFAS, providing significant advantages over existing methods in terms of sensitivity and selectivity.

Author Contributions Section

J. F. Ayala-Cabrera: Conceptualization, Methodology, Investigation, Validation, Formal analysis, Writing-Original draft preparation. A. Contreras-Llin: Methodology, Investigation, Validation, Formal analysis. E. Moyano: Conceptualization, Methodology, Supervision, Project administration, Writing- Reviewing and Editing. F. J. Santos: Conceptualization, Methodology, Supervision, Project administration, Writing- Reviewing and Editing.

Declaration of competing interest

The authors declare that they have no known competing financial interests or personal relationships that could have appeared to influence the work reported in this paper.

Appendix A. Supplementary data

Supplementary data to this article can be found online at https://doi.org/10.1016/j.aca.2019.12.004.

References

[1] E. Kissa, Fluorinated Surfactants and Repellents, second ed., Marcel Dekker, New York, 2001.

[2] F.M. Hekster, R.W.P.M. Laane, P. de Voogt, Environmental and toxicity effects of perfluoroalkylated substances, in: G.W. Ware (Ed.), Reviews of Environmental Contamination and Toxicology, vol. 179, Springer, New York, 2003, pp. 99–121.

[3] H.J. Lehmler, Synthesis of environmentally relevant fluorinated surfactants - a review, Chemosphere 58 (2005) 1471–1496, https://doi.org/10.1016/j.chemosphere.2004.11.078.

[4] H. Fromme, S.A. Tittlemier, W. Völkel, M. Wilhelm, D. Twardella, Perfluorinated compounds - exposure assessment for the general population in western countries, Int. J. Hyg Environ. Health 212 (2009) 239–270, https://doi.org/10.1016/j.ijheh.2008.04.007.

[5] R.C. Buck, J. Franklin, U. Berger, J.M. Conder, I.T. Cousins, P. De Voogt, A.A. Jensen, K. Kannan, S.a. Mabury, S.P.J. van Leeuwen, Perfluoroalkyl and polyfluoroalkyl substances in the environment: terminology, classification, and origins, Integr, Environ. Assess. Manag. 7 (2011) 513–541, https://doi.org/10.1002/ieam.258.

[6] D.A. Ellis, J.W. Martin, A.O. De Silva, S.a. Mabury, M.D. Hurley, M.P. Sulbaek Andersen, T.J. Wallington, Degradation of fluorotelomer alcohols: a likely atmospheric source of perfluorinated carboxylic acids, Environ. Sci. Technol. 38 (2004) 3316–3321, https://doi.org/10.1021/es049860w.

[7] M.J.A. Dinglasan, Y. Ye, E.A. Edwards, S.A. Mabury, Fluorotelomer alcohol biodegradation yields poly- and perfluorinated acids, Environ. Sci. Technol. 38 (2007) 2857–2864, https://doi.org/10.1021/es0350177.

[8] Decision SC-4/17 of 4–8 May 2009 of Listing of perfluorooctane sulfonic acid, its salts and perfluorooctano sulfonyl fluoride, United Nation Environment Programme. Stockholm Convention on Persistent Organic Pollutants. UNEP/POPS/COP-4/38:66–9. Available at: https://www.pops.int/TheConvention/Overview/TextoftheConvention/tabid/2232/Default.aspx. accessed 16.08.19.

[9] Council Decision (EU) 2015/633 of 20 April 2015 on the submission, On behalf of the European union, of a proposal for the listing of additional chemicals in annex A to the stockholm convention on persistent organic pollutants, Off. J. Eur. Union. L 104 (2015) 14–15. http://data.europa.eu/eli/dec/2015/633/oj.

[10] S. Poothong, E. Lundanes, C. Thomsen, L.S. Haug, High throughput online solid phase extraction-ultra high performance liquid chromatography-tandem mass spectrometry method for polyfluoroalkyl phosphate esters, perfluoroalkyl phosphonates, and other perfluoroalkyl substances in human serum, plasma, and whole blood, Anal. Chim. Acta 957 (2017) 10–19, https://doi.org/10.1016/j.aca.2016.12.043.

[11] G. Munoz, P. Ray, S. Mejia-Avendaño, S.V. Duy, D.T. Do, J. Liu, S. Sauvé, Optimization of extraction methods for comprehensive profiling of perfluoroalkyl and polyfluoroalkyl substances in firefighting foam impacted soils, Anal. Chim. Acta 1034 (2018) 74–84, https://doi.org/10.1016/j.aca.2018.06.046.

[12] F. Xiao, S.A. Golovko, M.Y. Golovko, Identification of novel non-ionic, cationic, zwitterionic, and anionic polyfluoroalkyl substances using UPLC-TOF-MS^E high-resolution parent ion search, Anal. Chim. Acta 988 (2017) 41–49, https://doi.org/10.1016/j.aca.2017.08.016.

[13] J.W. Martin, D.C.G. Muir, C. a Moody, D. a Ellis, W.C. Kwan, K.R. Solomon, S. a Mabury, Collection of airborne fluorinated organics and analysis by gas chromatography/chemical ionization mass spectrometry, Anal. Chem. 74 (2002) 584–590, https://doi.org/10.1021/ac015630d.

[14] B. Szostek, K.B. Prickett, Determination of 8:2 fluorotelomer alcohol in animal plasma and tissues by gas chromatography-mass spectrometry, J. Chromatogr. B Anal. Technol. Biomed. Life Sci. 813 (2004) 313–321, https://doi.org/

[15] A.M. Piekarz, T. Primbs, J.A. Field, D.F. Barofsky, S. Simonich, Semivolatile fluorinated organic compounds in Asian and western U.S. air masses, Environ. Sci. Technol. 41 (2007) 8248–8255, https://doi.org/10.1021/es0713678.

[16] J.L. Barber, U. Berger, C. Chaemfa, S. Huber, A. Jahnke, C. Temme, K.C. Jones, Analysis of per- and polyfluorinated alkyl substances in air samples from Northwest Europe, J. Environ. Monit. 9 (2007) 530–541, https://doi.org/10.1039/b701417a.

[17] J. Li, S. Del Vento, J. Schuster, G. Zhang, P. Chakraborty, Y. Kobara, K.C. Jones, Perfluorinated compounds in the asian atmosphere, Environ. Sci. Technol. 45 (2011) 7241–7248, https://doi.org/10.1021/es201739t.

[18] Y. Wu, V.W.C. Chang, Development of analysis of volatile polyfluorinated alkyl substances in indoor air using thermal desorption-gas chromatography-mass spectrometry, J. Chromatogr., A 1238 (2012) 114–120, https://doi.org/10.1016/j.chroma.2012.03.053.

[19] W.M. Henderson, E.J. Weber, S.E. Duirk, J.W. Washington, M.A. Smith, Quantification of fluorotelomer-based chemicals in mammalian matrices by monitoring perfluoroalkyl chain fragments with GC/MS, J. Chromatogr. B 846 (2007) 155–161, https://doi.org/10.1016/j.jchromb.2006.08.042.

[20] J.F. Ayala-Cabrera, E. Moyano, F.J. Santos, Gas chromatography and liquid chromatography coupled to mass spectrometry for the determination of fluorotelomer olefins, fluorotelomer alcohols, perfluoroalkyl sulfonamides and sulfonamidoethanols in water, J. Chromatogr. A (2019), https://doi.org/10.1016/j.chroma.2019.460463 in press.

[21] I.A. Revelsky, Y.S. Yashin, T.G. Sobolevsky, A.I. Revelsky, B. Miller, V. Oriedo, Electron ionization and atmospheric pressure photochemical ionization in gas chromatography-mass spectrometry analysis of amino acids, Eur. J. Mass Spectrom. 9 (2003) 497–507, https://doi.org/10.1255/ejms.581.

[22] C.N. McEwen, R.G. McKay, A combination atmospheric pressure LC/MS:GC/MS ion source: advantages of dual AP-LC/MS:GC/MS instrumentation, J. Am. Soc. Mass Spectrom. 16 (2005) 1730–1738, https://doi.org/10.1016/j.jasms.2005.07.005.

[23] D.X. Li, L. Gan, A. Bronja, O.J. Schmitz, Gas chromatography coupled to atmospheric pressure ionization mass spectrometry (GC-API-MS): Review, Anal. Chim. Acta 891 (2015) 43–61, https://doi.org/10.1016/j.aca.2015.08.002.

[24] M. Haapala, L. Luosujärvi, V. Saarela, T. Kotiaho, R.A. Ketola, S. Franssila, R. Kostiainen, Microchip for combining gas chromatography or capillary liquid chromatography with atmospheric pressure photoionization-mass spectrometry, Anal. Chem. 79 (2007) 4994–4999, https://doi.org/10.1021/ac070157a.

[25] I.A. Revelsky, Y.S. Yashin, New approach to complex organic compounds mixtures analysis based on gas chromatography-atmospheric pressure photoionization-mass-spectrometry, Talanta 102 (2012) 110–113, https://doi.org/10.1016/j.talanta.2012.07.023.

[26] L. Luosujärvi, M.-M. Karikko, M. Haapala, V. Saarela, S. Huhtala, S. Franssila, R. Kostiainen, T. Kotiaho, T.J. Kauppila, Gas chromatography/mass spectrometry of polychlorinated biphenyls using atmospheric pressure chemical ionization and atmospheric pressure photoionization microchips, Rapid Commun. Mass Spectrom. 22 (2008) 425–431, https://doi.org/10.1002/rcm.3379.

[27] R.A. Di Lorenzo, V.V. Lobodin, J. Cochran, T. Kolic, S. Besevic, J.G. Sled, E.J. Reiner, K.J. Jobst, Fast gas chromatographu-atmospheric pressure (photo) ionization mass spectrometry of polybrominated diphenylether flame retardants, Anal. Chim. Acta 1056 (2019) 70–78, https://doi.org/10.1016/j.aca.2019.01.007.

[28] T.J. Kauppila, H. Kersten, T. Benter, Ionization of EPA contaminants in direct and dopant-assisted atmospheric pressure photoionization and atmospheric pressure laser ionization, J. Am. Soc. Mass Spectrom. 26 (2015) 1036–1045, https://doi.org/10.1007/s13361-015-1092-3.

[29] A. Kondyli, W. Schrader, High-resolution GC/MS studies of a light crude iol fraction, J. Mass Spectrom. 54 (2019) 47–54, https://doi.org/10.1002/jms.4306.

[30] H. Kersten, K. Kroll, K. Haberer, K.J. Brockmann, T. Benter, A. Peterson, A. Makarov, Design study of an atmospheric pressure photoionization interface for GC-MS, J. Am. Soc. Mass Spectrom. 27 (2016) 607–614, https://doi.org/10.1007/s13361-015-1320-x.

[31] S. Taniyasu, K. Kannan, K.S. Man, A. Gulkowska, E. Sinclair, T. Okazawa, N. Yamashita, Analysis of fluorotelomer alcohols, fluorotelomer acids, and short- and long-chain perfluorinated acids in water and biota, J. Chromatogr., A 1093 (2005) 89–97, https://doi.org/10.1016/j.chroma.2005.07.053.

[32] O.S. Arvaniti, A.G. Asimakopoulos, M.E. Dasenaki, E.I. Ventouri, A.S. Stasinakis, N.S. Thomaidis, Simultaneous determination of eighteen perfluorinated compounds in dissolved and particulate phases of wastewater, and in sewage sludge by liquid chromatography-tandem mass spectrometry, Anal. Methods. 6 (2014) 1341, https://doi.org/10.1039/c3ay42015a.

[33] T. Portolés, L.E. Rosales, J.V. Sancho, F.J. Santos, E. Moyano, Gas chromatography-tandem mass spectrometry with atmospheric pressure chemical ionization for fluorotelomer alcohols and perfluorinated sulfonamides determination, J. Chromatogr., A 1413 (2015) 107–116, https://doi.org/10.1016/j.chroma.2015.08.016.

[34] J.F. Ayala-Cabrera, F.J. Santos, E. Moyano, Negative-ion atmospheric pressure ionisation of semi-volatile fluorinated compounds for ultra-high-performance liquid chromatography tandem mass spectrometry analysis, Anal. Bioanal. Chem. 410 (2018) 4913–4924, https://doi.org/10.1007/s00216-018-1138-z.

[35] P. Herbert, A.L. Silva, M.J. João, L. Santos, A. Alves, Determination of semi-volatile priority pollutants in landfill leachates and sediments using

microwave-assisted headspace solid-phase microextraction, Anal. Bioanal. Chem. 386 (2006) 324—331, https://doi.org/10.1007/s00216-006-0632-x.

[36] Y. Huang, Y.-C. Yang, Y.Y. Shu, Analysis of semi-volatile organic compounds in aqueous samples by microwave-assisted headspace solid-phase micro-extraction coupled with gas chromatography-electron capture detection, J. Chromatogr., A 1140 (2007) 35—43, https://doi.org/10.1016/j.chroma.2006.11.074.

[37] A.N. Saber, H. Zhang, M. Yang, Optimization and validation of headspace solid-phase microextraction method coupled with gas chromatography-triple quadrupole tandem mass spectrometry for simultaneous determination of volatile and semi-vo.latile organic compounds in coking wastewater treat-ment plant, Environ. Monit. Assess. 191 (2019) 411, https://doi.org/10.1007/s10661-019-7554-5.

[38] A. Dreyer, C. Temme, R. Sturm, R. Ebinghaus, Optimized method avoiding solvent-induced response enhancement in the analysis of volatile and semi-volatile polyfluorinated alkylated compounds using gas chromatography—mass spectrometry, J. Chromatogr., A 1178 (2008) 199—205, https://doi.org/10.1016/j.chroma.2007.11.050.

[39] X. Liu, Z. Guo, E.E. Folk IV, N.F. Roache, Determination of fluorotelomer

alcohols in selected consumer products and preliminary investigation of their fate in the indoor environment, Chemosphere 129 (2015) 81—86, https://doi.org/10.1016/j.chemosphere.2014.06.012.

[40] C. Bach, V. Boiteux, J. Hemard, A. Colin, C. Rosin, J.F. Munoz, X. Dauchy, Simultaneous determination of perfluoroalkyl iodides, perfluoroalkane sul-fonamides, fluorotelomer alcohols, fluorotelomer iodides and fluorotelomer acrylates and methacrylates in water and sediments using solid-phase microextraction-gas chromatography/mas, J. Chromatogr., A 1448 (2016) 98—106, https://doi.org/10.1016/j.chroma.2016.04.025.

[41] B. Szostek, K.B. Prickett, R.C. Buck, Determination of fluorotelomer alcohols by liquid chromatography/tandem mass spectrometry in water, Rapid Commun. Mass Spectrom. 20 (2006) 2837—2844, https://doi.org/10.1002/rcm.2667.

[42] C. González-Barreiro, E. Martínez-Carballo, A. Sitka, S. Scharf, O. Gans, Method optimization for determination of selected perfluorinated alkylated sub-stances in water samples, Anal. Bioanal. Chem. 386 (2006) 2123—2132, https://doi.org/10.1007/s00216-006-0902-7.

[43] B. Boulanger, J. Vargo, J.L. Schnoor, K.C. Hornbuckle, Detection of per-fluorooctane surfactants in Great Lakes water, Environ. Sci. Technol. 38 (2004) 4064—4070, https://doi.org/10.1021/es0496975.

Supporting Information

A novel methodology for the determination of neutral perfluoroalkyl and polyfluoroalkyl substances in water by gas chromatography-atmospheric pressure photoionisation-high resolution mass spectrometry

J. F. Ayala-Cabrera [a], A. Contreras-Llin [a], E. Moyano [a,b], F. J. Santos [a,b,*]

[a] Department of Chemical Engineering and Analytical Chemistry, University of Barcelona. Av. Diagonal 645, E–08028 Barcelona, Spain

[b] Water Research Institute (IdRA), University of Barcelona, Montalegre 6, E–08001 Barcelona, Spain

*Corresponding author (F. J. Santos): e-mail: javier.santos@ub.edu

Table of Contents

Supporting Tables

Table S1.
Main ions generated in the GC-APPI interface depending on the dopant.

Analyte	Toluene		Acetone		Chlorobenzene		Tetrahydrofuran		Anisole	
	m/z	Assignation	m/z	Assignation	m/z	Assignation	m/z	Assignation	m/z	Assignation
4:2 FTO	192.9894 (100%)	$[C_5F_7]^-$	192.9894 (100%)	$[C_5F_7]^-$	192.9894 (100%)	$[C_5F_7]^-$	192.9894 (100%)	$[C_5F_7]^-$	192.9894 (100%)	$[C_5F_7]^-$
	208.9843 (37%)	$[C_5OF_7]^-$	208.9843 (19%)	$[C_5OF_7]^-$	208.9843 (57%)	$[C_5OF_7]^-$	208.9843 (50%)	$[C_5OF_7]^-$	208.9843 (53%)	$[C_5OF_7]^-$
	185.9910 (20%)	$[C_6F_6]^{-\bullet}$	185.9910 (16%)	$[C_6F_6]^{-\bullet}$	185.9910 (53%)	$[C_6F_6]^{-\bullet}$	185.9910 (40%)	$[C_6F_6]^{-\bullet}$	185.9910 (28%)	$[C_6F_6]^{-\bullet}$
6:2 FTO	292.9830 (100%)	$[C_7F_{11}]^-$	292.9830 (100%)	$[C_7F_{11}]^-$	292.9830 (100%)	$[C_7F_{11}]^-$	292.9830 (100%)	$[C_7F_{11}]^-$	292.9830 (100%)	$[C_7F_{11}]^-$
	308.9779 (95%)	$[C_7OF_{11}]^-$	308.9779 (45%)	$[C_7OF_{11}]^-$	308.9779 (80%)	$[C_7OF_{11}]^-$	308.9779 (80%)	$[C_7OF_{11}]^-$	308.9779 (80%)	$[C_7OF_{11}]^-$
	285.9846 (63%)	$[C_8F_{10}]^{-\bullet}$	340.9841 (16%)	$[M+O_2-HF_2O]^-$	285.9846 (21%)	$[C_8F_{10}]^{-\bullet}$	340.9841 (60%)	$[M+O_2-HF_2O]^-$	285.9846 (55%)	$[C_8F_{10}]^{-\bullet}$
8:2 FTO	385.9782 (100%)	$[C_{10}F_{14}]^{-\bullet}$	392.9766 (88%)	$[C_9F_{15}]^-$	392.9766 (100%)	$[C_9F_{15}]^-$	392.9766 (88%)	$[C_9F_{15}]^-$	392.9766 (100%)	$[C_9F_{15}]^-$
	392.9766 (88%)	$[C_9F_{15}]^-$	408.9715 (42%)	$[C_9OF_{15}]^-$	408.9715 (71%)	$[C_9OF_{15}]^-$	408.9715 (78%)	$[C_9OF_{15}]^-$	385.9782 (97%)	$[C_{10}F_{14}]^{-\bullet}$
	408.9715 (47%)	$[C_9OF_{15}]^-$	440.9770 (26%)	$[M+O_2-HF_2O]^-$	385.9782 (45%)	$[C_{10}F_{14}]^{-\bullet}$	440.9770 (49%)	$[M+O_2-HF_2O]^-$	408.9715 (49%)	$[C_9OF_{15}]^-$
4:2 FTOH	192.9894 (100%)	$[C_5F_7]^-$	192.9894 (100%)	$[C_5F_7]^-$	192.9894 (100%)	$[C_5F_7]^-$	192.9894 (100%)	$[C_5F_7]^-$	192.9894 (100%)	$[C_5F_7]^-$
	296.0101 (35%)	$[M+O_2]^{-\bullet}$	296.0101 (27%)	$[M+O_2]^{-\bullet}$	296.0101 (30%)	$[M+O_2]^{-\bullet}$	154.9926 (41%)	$[C_5F_3]^-$	296.0101 (29%)	$[M+O_2]^{-\bullet}$
	154.9926 (24%)	$[C_5F_5]^-$	154.9926 (26%)	$[C_5F_5]^-$	154.9926 (26%)	$[C_5F_5]^-$	296.0101 (26%)	$[M+O_2]^{-\bullet}$	154.9926 (25%)	$[C_5F_5]^-$
6:2 FTOH	292.9830 (100%)	$[C_7F_{11}]^-$	396.0037 (100%)	$[M+O_2]^{-\bullet}$	292.9830 (100%)	$[C_7F_{11}]^-$	292.9830 (100%)	$[C_7F_{11}]^-$	292.9830 (100%)	$[C_7F_{11}]^-$
	396.0037 (40%)	$[M+O_2]^{-\bullet}$	292.9830 (36%)	$[C_7F_{11}]^-$	396.0037 (66%)	$[M+O_2]^{-\bullet}$	396.0037 (89%)	$[M+O_2]^{-\bullet}$	396.0037 (48%)	$[M+O_2]^{-\bullet}$
	254.9862 (26%)	$[C_7F_9]^-$	254.9862 (21%)	$[C_7F_9]^-$	254.9862 (31%)	$[C_7F_9]^-$	254.9862 (56%)	$[C_7F_9]^-$	254.9862 (29%)	$[C_7F_9]^-$
7-Me-6:2 FTOH	305.9908 (100%)	$[C_8HF_{11}]^{-\bullet}$	305.9908 (100%)	$[C_8HF_{11}]^{-\bullet}$	305.9908 (100%)	$[C_8HF_{11}]^{-\bullet}$	305.9908 (100%)	$[C_8HF_{11}]^{-\bullet}$	305.9908 (100%)	$[C_8HF_{11}]^{-\bullet}$
	333.9856 (15%)	$[M-4HF]^{-\bullet}$	446.0005 (85%)	$[M+O_2]^{-\bullet}$	333.9856 (14%)	$[M-4HF]^{-\bullet}$	446.0005 (15%)	$[M+O_2]^{-\bullet}$	333.9856 (14%)	$[M-4HF]^{-\bullet}$
	446.0005 (5%)	$[M+O_2]^{-\bullet}$	342.9798 (80%)	$[C_8F_{13}]^-$	446.0005 (6%)	$[M+O_2]^{-\bullet}$	342.9798 (8%)	$[C_8F_{13}]^-$	446.0005 (4%)	$[M+O_2]^{-\bullet}$

Table S1 (Cont.).
Main ions generated in the GC-APPI interface depending on the dopant.

Analyte	Toluene		Acetone		Chlorobenzene		Tetrahydrofuran		Anisole	
	m/z	Assignation	*m/z*	Assignation	*m/z*	Assignation	*m/z*	Assignation	*m/z*	Assignation
8:2 FTOH	495.9973 (100%)	$[\mathrm{M+O_2}]^{-\bullet}$	495.9973 (100%)	$[\mathrm{M+O_2}]^{-\bullet}$	495.9973 (100%)	$[\mathrm{M+O_2}]^{-\bullet}$	495.9973 (100%)	$[\mathrm{M+O_2}]^{-\bullet}$	495.9973 (100%)	$[\mathrm{M+O_2}]^{-\bullet}$
	383.9825 (60%)	$[\mathrm{M-4HF}]^{-\bullet}$	392.9766 (89%)	$[\mathrm{C_9F_{15}}]^-$	383.9825 (48%)	$[\mathrm{M-4HF}]^{-\bullet}$	392.9766 (62%)	$[\mathrm{C_9F_{15}}]^-$	383.9825 (50%)	$[\mathrm{M-4HF}]^{-\bullet}$
	392.9766 (33%)	$[\mathrm{C_9F_{15}}]^-$	402.9809 (33%)	$[\mathrm{M-H-3HF}]^-$	392.9766 (28%)	$[\mathrm{C_9F_{15}}]^-$	402.9809 (33%)	$[\mathrm{M-H-3HF}]^-$	392.9766 (37%)	$[\mathrm{C_9F_{15}}]^-$
10:2 FTOH	483.9762 (100%)	$[\mathrm{M-4HF}]^{-\bullet}$	595.9909 (100%)	$[\mathrm{M+O_2}]^{-\bullet}$	483.9762 (100%)	$[\mathrm{M-4HF}]^{-\bullet}$	483.9762 (100%)	$[\mathrm{M-4HF}]^{-\bullet}$	483.9762 (100%)	$[\mathrm{M-4HF}]^{-\bullet}$
	595.9909 (66%)	$[\mathrm{M+O_2}]^{-\bullet}$	492.9702 (53%)	$[\mathrm{C_9F_{15}}]^-$	463.9699 (65%)	$[\mathrm{M-5HF}]^{-\bullet}$	595.9909 (79%)	$[\mathrm{M+O_2}]^{-\bullet}$	595.9909 (82%)	$[\mathrm{M+O_2}]^{-\bullet}$
	463.9699 (65%)	$[\mathrm{M-5HF}]^{-\bullet}$	502.9746 (30%)	$[\mathrm{M-H-3HF}]^-$	595.9909 (46%)	$[\mathrm{M+O_2}]^{-\bullet}$	463.9699 (52%)	$[\mathrm{M-5HF}]^{-\bullet}$	463.9699 (66%)	$[\mathrm{M-5HF}]^{-\bullet}$
N-MeFOSA	511.9619 (100%)	$[\mathrm{M-H}]^-$	511.9619 (100%)	$[\mathrm{M-H}]^-$	511.9619 (100%)	$[\mathrm{M-H}]^-$	511.9619 (100%)	$[\mathrm{M-H}]^-$	511.9619 (100%)	$[\mathrm{M-H}]^-$
	464.9447 (31%)	$[\mathrm{M-NFCH_3}]^-$	482.9353 (6%)	$[\mathrm{M-NHCH_3}]^-$	464.9447 (15%)	$[\mathrm{M-NFCH_3}]^-$	464.9447 (33%)	$[\mathrm{M-NFCH_3}]^-$	464.9447 (42%)	$[\mathrm{M-NFCH_3}]^-$
	482.9353 (11%)	$[\mathrm{M-NHCH_3}]^-$	464.9447 (3%)	$[\mathrm{M-NFCH_3}]^-$	418.9734 (14%)	$[\mathrm{C_8F_{17}}]^-$	418.9734 (29%)	$[\mathrm{C_8F_{17}}]^-$	418.9734 (33%)	$[\mathrm{C_8F_{17}}]^-$
N-EtFOSA	525.9775 (100%)	$[\mathrm{M-H}]^-$	525.9775 (100%)	$[\mathrm{M-H}]^-$	525.9775 (100%)	$[\mathrm{M-H}]^-$	525.9775 (100%)	$[\mathrm{M-H}]^-$	525.9775 (100%)	$[\mathrm{M-H}]^-$
	464.9447 (22%)	$[\mathrm{M-NFC_2H_5}]^-$	482.9353 (4%)	$[\mathrm{M-NHCH_3}]^-$	464.9447 (22%)	$[\mathrm{M-NFC_2H_5}]^-$	464.9447 (26%)	$[\mathrm{M-NFC_2H_5}]^-$	464.9447 (36%)	$[\mathrm{M-NFC_2H_5}]^-$
	482.9353 (8%)	$[\mathrm{M-NHC_2H_5}]^-$	464.9447 (2%)	$[\mathrm{M-NFCH_3}]^-$	418.9734 (21%)	$[\mathrm{C_8F_{17}}]^-$	418.9734 (25%)	$[\mathrm{C_8F_{17}}]^-$	418.9734 (31%)	$[\mathrm{C_8F_{17}}]^-$
N-MeFOSE	511.9619 (100%)	$[\mathrm{M-C_2H_5O}]^-$	511.9619 (100%)	$[\mathrm{M-C_2H_5O}]^-$	511.9619 (100%)	$[\mathrm{M-C_2H_5O}]^-$	418.9734 (100%)	$[\mathrm{M-C_2H_5O}]^-$	511.9619 (100%)	$[\mathrm{M-C_2H_5O}]^-$
	418.9734 (89%)	$[\mathrm{C_8F_{17}}]^-$	418.9734 (44%)	$[\mathrm{C_8F_{17}}]^-$	418.9734 (90%)	$[\mathrm{C_8F_{17}}]^-$	511.9619 (89%)	$[\mathrm{C_8F_{17}}]^-$	588.9857 (81%)	$[\mathrm{M+O_2}]^{-\bullet}$
	588.9857 (87%)	$[\mathrm{M+O_2}]^{-\bullet}$	588.9857 (38%)	$[\mathrm{M+O_2}]^{-\bullet}$	588.9857 (79%)	$[\mathrm{M+O_2}]^{-\bullet}$	588.9857 (83%)	$[\mathrm{M+O_2}]^{-\bullet}$	418.9734 (70%)	$[\mathrm{C_8F_{17}}]^-$
N-EtFOSE	525.9775 (100%)	$[\mathrm{M-C_2H_5O}]^-$	525.9775 (100%)	$[\mathrm{M-C_2H_5O}]^-$	525.9775 (100%)	$[\mathrm{M-C_2H_5O}]^-$	418.9734 (100%)	$[\mathrm{M-C_2H_5O}]^-$	525.9775 (100%)	$[\mathrm{M-C_2H_5O}]^-$
	418.9734 (99%)	$[\mathrm{C_8F_{17}}]^-$	418.9734 (44%)	$[\mathrm{C_8F_{17}}]^-$	603.0014 (93%)	$[\mathrm{M+O_2}]^{-\bullet}$	525.9775 (88%)	$[\mathrm{M-C_2H_5O}]^-$	418.9734 (74%)	$[\mathrm{C_8F_{17}}]^-$
	603.0014 (89%)	$[\mathrm{M+O_2}]^{-\bullet}$	603.0014 (41%)	$[\mathrm{M+O_2}]^{-\bullet}$	418.9734 (91%)	$[\mathrm{C_8F_{17}}]^-$	603.0014 (84%)	$[\mathrm{M+O_2}]^{-\bullet}$	603.0014 (63%)	$[\mathrm{M+O_2}]^{-\bullet}$

145

Table S2. Instrumental quality parameters of the GC-APPI-HRMS method.

Compound	Linear range (ng mL⁻¹)	Correlation coefficient (r)	ILOD (ng mL⁻¹)	ILOQ (ng mL⁻¹)	Spiked level (ng mL⁻¹)		Repeatability (RSD%)[a]		Trueness (Rel. error %)[a]	
					Low level	Medium level	Low level	Medium level	Low level	Medium level
4:2 FTO	25–500	0.9990	8	24	25	63	8	6	-0.5	1.3
6:2 FTO	2.5–500	0.9994	1	3	5.0	63	7	7	-10	0.6
8:2 FTO	1.0–500	0.9994	0.3	1.0	2.0	25	3	2	-1	1
4:2 FTOH	0.5–100	0.9993	0.2	0.7	1.0	13	5	4	-1	0.2
6:2 FTOH	0.25–100	0.9996	0.08	0.3	0.5	6.3	3	2	-8	-0.1
7-Me-6:2 FTOH	0.25–100	0.9990	0.08	0.3	0.5	6.3	2	2	5	-1
8:2 FTOH	0.25–100	0.9993	0.08	0.3	0.5	6.3	7	4	10	1
10:2 FTOH	0.10–100	0.9990	0.03	0.1	0.2	2.5	10	8	-6	-1
N-MeFOSA	0.75–100	0.9992	0.2	0.7	1.5	20	4	2	8	-7
N-EtFOSA	0.75–100	0.9994	0.2	0.7	1.5	20	4	2	9	-7
N-MeFOSE	0.10–100	0.9990	0.03	0.1	0.2	2.5	4	4	-3	2
N-EtFOSE	0.10–100	0.9996	0.03	0.1	0.2	2.5	9	5	-4	-0.2

[a] n=3

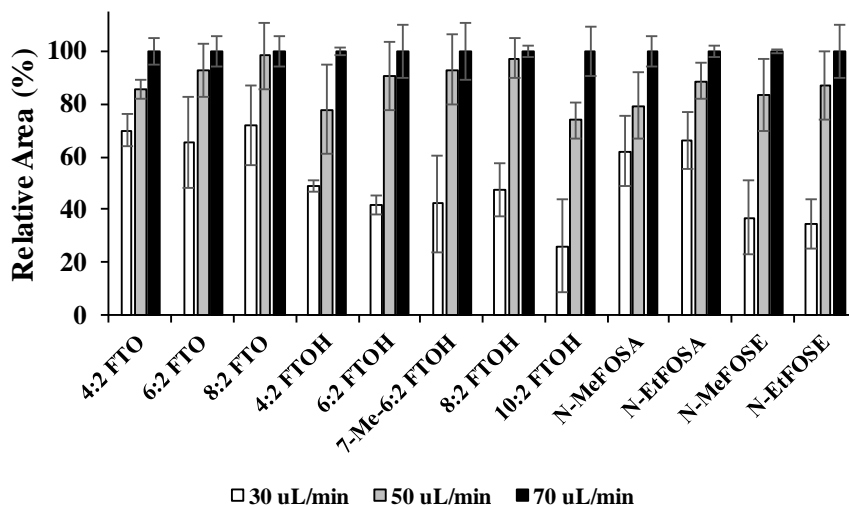## **Supporting Figures**

☐ **30 uL/min**   ☐ **50 uL/min**   ■ **70 uL/min**

Figure S1. Effect of acetone flow rate on the response of the target compounds using the dopant-assisted GC-APPI interface.

2.3. Discussion of the results

This section is devoted to the discussion of the results corresponding to the experimental work (*Articles I, II, III, and IV*) included in Section 2.4. The discussion is focused on two main topics: (i) new analytical methodologies for the determination of neutral PFAS, and (ii) novel API-based strategies for the non-targeted screening analysis of neutral PFAS.

2.3.1. New analytical methodologies for the determination of neutral PFAS

As mentioned before, the determination of neutral PFAS (FTOs, FTOHs, FOSAs, and FOSEs) requires selective and sensitive methods for their detection in environmental samples, where they are found at very low concentration levels. In this Thesis, different strategies based on liquid chromatography and gas chromatography coupled to mass spectrometry (LC-MS, GC-MS) methods have been proposed to overcome the problems observed in existing methods for their analysis in water samples.

The determination of neutral PFAS by gas chromatography coupled to mass spectrometry was evaluated in *Article II.* Regarding the chromatographic separation, the differences in the chemical structure of the neutral PFAS complicate both chromatographic separation and simultaneous determination. Moreover, short fluoroalkyl chain FTOs usually show low retention in both polar and non-polar stationary phases because of the high volatility of these compounds [137,284,285]. In this work, three different capillary columns (polar, non-polar, and semi-polar stationary phases) were tested (*Article II, Section 3.*1), achieving the best results using a poly(cyanopropylphenyldimethyl siloxane)-based column (DB-624) with a 60 m length. This semi-polar stationary phase not only allowed the separation of all neutral PFAS families but also produced enough retention of FTOs due to the high film thickness (1.4 µm). To avoid the chromatographic coelution of the most volatile fluorotelomer olefin (4:2 FTO) with the solvent peak, methanol was selected because it provided a narrow peak far enough to the FTOs. Nonetheless, even under these conditions, 4:2 FTO slightly overlapped with the tail of the methanol peak. Concerning the chromatographic separation of PFAS by ultra-high-performance liquid chromatography, in *Article II* (*Section 3.2*) four UHPLC columns packed with totally porous (Luna C_{18} and Luna Polar C_{18}) and superficially porous particles (Accucore C_{18} and Accucore PFP) were compared. The columns with totally porous particles provided better column efficiency, resolution, and peak symmetry, as well as good run-to-run precision in retention times than columns based on superficially porous particles. Among the columns with totally porous particles, Luna C_{18} column was able to completely separate almost all peaks (8 out of 12 peaks) and those analytes that partially coeluted did not show any ion suppression nor ion enhancement. Thus, the C_{18} stationary phase allowed enough retention for all the families of compounds, including FTOs, which is one of the main advantages over GC-MS methods.

The ionization of neutral PFAS using high-vacuum ionization techniques, such as EI, CI, and NICI, was also evaluated (*Article II, Section 3.1*). Regarding EI, most of the neutral PFAS showed highly fragmented mass spectra, especially FTOs, FTOHs, and FOSAs. Although EI is considered as an universal technique, it may lead to selectivity problems since the most abundant ions showed low *m/z* values (e.g. $[C_3H_3F_2]^+$ at *m/z* 77 for FTOs and $[C_3H_2F_3]^+$ at *m/z* 95 for FTOHs). In contrast, CI mass spectra only showed the protonated molecule for FTOHs, FOSAs, and FOSEs whereas the $[M–F]^+$ ion was the base peak of the mass spectra of FTOs. In the case of NICI, FTOs and FTOHs generated radical fragment ions due to losses of HF units (20 Da) from the molecular ion. For FOSAs and FOSEs, the base peak of the mass spectra corresponded to the *N*-alkyl sulfonamide $[NSO_2R]^-$ (R:-CH_3, -C_2H_5) and *N*-alkyl sulfonamido-ethanol $[NSO_2RC_2H_5O]^-$ (R:-CH_3, -C_2H_5) functional groups. Among these high-vacuum ionization techniques, NICI was discarded due to the low precision observed (RSD%, 10-55%, n=3), while CI generally provided lower iLODs than those obtained by EI. Besides, 4:2 FTO showed a high iLOD since it is the most volatile compound and its signal was slightly suppressed by the tail of the solvent peak.

Considering the difficulties that high-vacuum ionization techniques showed for the determination of neutral PFAS, API techniques were explored in this Thesis to evaluate their applicability for developing reliable UHPLC-MS/MS and GC-HRMS methods as alternatives to those previously reported in the literature. In this sense, the *Articles I and II* are devoted to the study of the ionization behavior of FTOs, FTOHs, FOSAs, and FOSEs using ESI, APCI, and APPI to develop new methods for their determination by UHPLC-MS/MS. Regarding ESI, the absence of polar functional groups on the structure of FTOs limited its application for the determination of these compounds. In contrast, FOSAs were easily ionized by ESI leading to deprotonated molecules (*Article I, Fig. 2*). On the other hand, FTOHs and FOSEs showed a high tendency to form adduct ions with mobile phase additives (e.g. $[M+HCOO]^-$ and $[M+CH_3COO]^-$) as well as with the anions like chloride, always present in the LC-MS system. However, these adduct ions showed the disadvantage of only generating the respective non-characteristic conjugate base ions (e.g., Cl^-, $HCOO^-$ or CH_3COO^-) in the tandem mass spectrometry, which was not suitable for their selective detection. The formation of these adduct ions can be prevented by labor-intense and time-consuming cleaning periods of the LC-MS system and, therefore, limiting the throughput of the laboratories. Unlike ESI source, negative ion APCI and APPI showed a better performance for the determination of neutral PFAS by UHPLC-MS/MS.

The mobile phase composition significantly affected the ionization efficiency of neutral PFAS. As an example, Fig. 2.4 shows the ionization mechanism of FTOHs using APCI in negative ion mode. When methanol/water mixtures were used as mobile phase, FTOHs were ionized by means of two series of ions: (i) even-electron ions coming from an abundant deprotonated molecule and (ii) odd-electron ions coming from an unstable molecular ion. In contrast, acetonitrile/water mixtures only favored the generation of odd-electron ions may be due to

some self-protonation processes in the acetonitrile/water cluster that hinders the deprotonation of FTOHs. This effect was not observed when working in negative ion APPI, where all the hydro-organic mobile phase mixtures tested allowed the formation of both series of ions. It must be pointed out that negative ion APPI is initiated by the photoionization of a dopant (toluene) that can trigger other reaction mechanisms (*see Chapter 1, Fig 1.15*) that finally led to the ionization of analytes by the generation of both the deprotonated molecule and odd-electron fragment ions. Regarding FOSAs, the deprotonated molecule was the only ion formed under all the conditions and sources tested, while FOSEs mainly formed the [M–CH$_2$CH$_2$OF]$^-$ ion and the [M+O$_2$]$^{-\bullet}$ ion in APCI and APPI, respectively. When FTOHs, FOSAs, and FOSEs were simultaneously determined using APCI, a methanol/water mixture was selected as mobile phase since it allowed the formation of an abundant [M–H]$^-$ ion for FTOHs. In contrast, an acetonitrile/water mixture was chosen when the APPI source was used since it permits not only a faster chromatographic separation but also the highest response of the analytes, especially for FTOHs. This fact may be attributed to the high capacity of methanol to compete with FTOHs in the proton abstraction mechanism, whereas the lack of acidic hydrogen might limit this competition when using acetonitrile as organic modifier. Among both systems, the UHPLC-APPI-MS/MS method provided the best performance leading to iLODs from 8 to 150 times lower than those achieved by UHPLC-APCI-MS/MS.
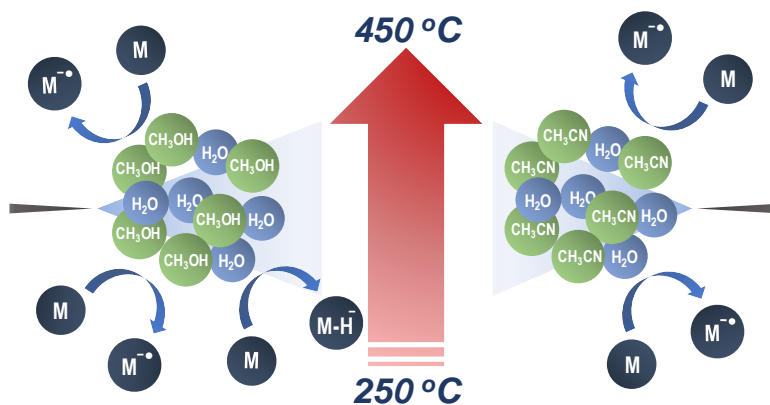

Fig. 2.4. Ionization mechanism of FTOHs in negative ion APCI using methanol/water (*left*) and acetonitrile/water (*right*) mixtures as mobile phase.

On the other hand, the development of a multi-class method to determine neutral PFAS, including FTOs, FTOHs, FOSAs, and FOSEs, by UHPLC-MS/MS required a re-optimization of the ion source conditions. *Article II* (*Section 3.2*) describes, for the first time, the ionization of FTOs using APCI and APPI. FTOs were ionized in both negative ion APCI and APPI through an unstable molecular ion that yielded odd-electron in-source collision-induced dissociation (CID) fragment ions. Among them, the ion [M–3HF]$^{-\bullet}$ was the main peak of the mass spectra. To improve the ionization of FTOs, high ion source temperatures (450 ºC) were required.

However, these conditions also increased the in-source CID fragmentation of the rest of the neutral PFAS. For instance, this increment on the ion source temperature almost hindered the formation of the deprotonated molecule for FTOHs while promoting the series of odd-electron fragment ions coming from the unstable molecular ion (Fig. 2.4). This effect was observed in both APCI and APPI ion source regardless of the mobile phase composition. Under these conditions, the UHPLC-APCI-MS/MS method provided the lowest iLODs (0.1-100 µg L^{-1}), especially for FTOs, which were 40 to 550 times lower than those obtained by UHPLC-APPI-MS/MS.

Table 2.1 summarizes the main chromatographic and mass spectrometric characteristics of the two UHPLC-MS/MS methods and the novel GC-APPI-HRMS method, as well as the sample treatment used in each of them for the determination of neutral PFAS in river water samples. This table allows an easy comparison of these developed methods. The ionization of target compounds using the GC-APPI source in negative ion mode slightly differed from the results obtained by negative ion APPI for LC-MS, especially for FTOs and FTOHs, which showed more significant differences. For instance, Fig. 2.5 shows the mass spectra of 8:2 FTOH using the conventional LC-APPI and the novel GC-APPI source.

Regarding FTOHs, the conventional LC-APPI promoted both the formation of the deprotonated molecule in addition to odd-electron ions coming from an unstable molecular ion, while the GC-APPI source mainly favored the generation of the superoxide ion, although some in-source CID fragment ions coming from the deprotonated molecule were also observed. Additionally, the presence of intense fluoroalkyl chain-related fragment ions (e.g. [C_9F_{15}]$^-$) was identified. These fluoroalkyl chain fragment ions were also observed for FTOs, being the base peak of the mass spectra, as well as some in-source CID fragment ion that incorporated the superoxide moiety. Thereby, it can be suggested this perfluoroalkyl chain ions may come from the fragmentation of the [M+O$_2$]$^{-\bullet}$ ion for both FTOHs and FTOs. The ionization of FOSAs did not show significant differences, while fragment ions generated by the loss of the ethanolic chain became the base peak of the mass spectra for FOSEs (*Article IV, Section 3.1*).

The nature of the optimal dopant to assist the APPI ionization was also different in both LC-MS/MS and GC-HRMS systems. While toluene was selected as the most suitable dopant in the LC-APPI-MS/MS method, acetone provided the best results using GC-APPI-HRMS. It must be pointed out that the absence of an active mobile phase (e.g., water, acetonitrile, methanol, etc.) in the GC-APPI source simplifies the ionization process since it may be just affected by the ionization energy of both analyte and dopant as well as other properties of the dopant such as vapor pressure or proton affinity. Therefore, we proposed the use of acetone as dopant since it provided the highest ionization efficiency, probably due to its higher vapor pressure. This may lead to a higher amount of dopant molecules in the gas-phase and, consequently, a high release of electrons after dopant photoionization that might enhance the ionization efficiency of the analytes.

Table 2.1. Main characteristics of the developed methods for the determination of neutral PFAS in water.

| Parameter	UHPLC-APPI-MS/MS	UHPLC-APCI-MS/MS	GC-APPI-HRMS
Analytes	FTOHs, FOSAs and FOSEs	FTOs, FTOHs, FOSAs and FOSEs	FTOs, FTOHs, FOSAs and FOSEs
Sample treatment			
Extraction technique	SPE	SPE	HS-SPME
Extraction phase	HLB® *(500 mg, 6 mL)*	HLB® *(500 mg, 6 mL)*	50/30 μm-DVB/CAR/PDMS
Sample volume	500 mL	500 mL	10 mL
Clean-up	Yes	Yes	No
Elution	Methanol *(4 mL)*	Methanol *(4 mL)*	Thermal desorption *(250 ºC)*
Evaporation	No	No	No
Dilution	Yes	Yes	No
Internal Standard	No	No	Yes
Chromatography			
Injection mode	Full loop *(10μL)*	Full loop *(10μL)*	Splitless *(3 min)*
Column	Accucore C_{18} *(100 x 2.1 mm; 2.6 μm)*	Luna C_{18} *(100 x 2.1 mm; 1.6 μm)*	DB-624 *(60 m x 0.25 mm; 1.4 μm)*
Mobile phase	CH_3CN/H_2O *(0.3 mL min^{-1})*	CH_3CN/H_2O *(0.3 mL min^{-1})*	He *(1.3 mL min^{-1})*
Mass spectrometry			
Ionization source			
API technique	APPI	APCI	APPI
Polarity	Negative	Negative	Negative
Energy	Kr lamp *(10.6 eV)*	Corona current *(12 μA)*	Kr lamp *(10.6 eV)*
Dopant	Toluene *(15 μL min^{-1})*	-	Acetone *(70 μL min^{-1})*
Make-up gas	N_2	N_2	N_2
Source temperature	250 ºC	450 ºC	225 ºC
Capillary temperature	275 ºC	275 ºC	175 ºC
Mass Analyzer			
Mass analyzer	Triple quadrupole	Triple quadrupole	Orbitrap *(Q-Exactive)*
Resolution	0.1-0.7 *m/z (peak width)*	0.7 *m/z (peak width)*	35,000 *(FWHM, at 200 m/z)*
Acquisition	MRM *(2 transitions/comp.)*	MRM *(2 transitions/comp.)*	Full scan *(100-800 m/z)*
Precursor ion / Monitored ion			
FTOs	-	[M–3HF]$^{-•}$	[M–CH_3F_2]$^-$
FTOHs	[M–H]$^-$	[M–4HF]$^{-•}$	[M+O_2]$^{-•}$/ [M–CH_5F_2O]$^-$
FOSAs	[M–H]$^-$	[M–H]$^-$	[M–H]$^-$
FOSEs	[M+O_2]$^{-•}$	[M–CH_2CH_2OF]$^-$	[M–CH_2CH_2O]$^-$
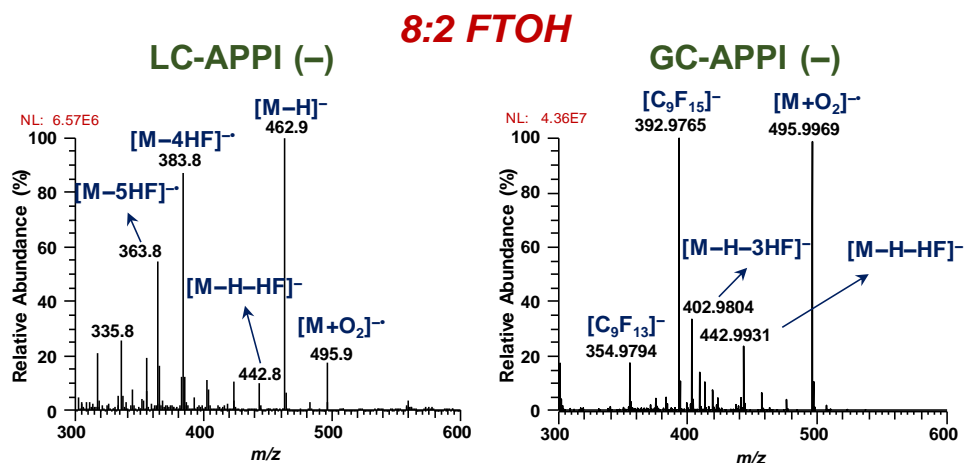
Fig. 2.5. Mass spectra of 8:2 FTOH in negative ion LC-APPI-MS using toluene as dopant (*left*) and GC-APPI-HRMS using acetone as dopant (*right*).

In contrast, the mobile phase in LC-MS could introduce more variables that may affect the APPI mechanisms, making toluene more suitable for the ionization of neutral PFAS. The ionization techniques were compared based on their detection capability. Fig. 2.6 shows the instrumental limits of detection determined for the different families of neutral PFAS using the different ionization techniques.

As it is pointed out in *Article IV* (*Section 3.1*), GC-APPI-HRMS provided the lowest iLODs, especially for FTOHs and FTOs, which were at least 30-fold and 4-fold lower than those obtained by the most sensitive UHPLC-MS/MS method, respectively. In contrast, FOSAs and FOSEs show a similar detection capability by negative ion APPI in both UHPLC-MS/MS and GC-HRMS systems. This may be due to the low volatility of these compounds in front of FTOs and FTOHs that might result in a less effective ionization at the GC-APPI source.

The sample treatment to extract neutral PFAS from river water samples have usually been performed by SPE. SPE constitutes an efficient extraction technique that offers a high pre-concentration capacity suitable for the analysis of water samples, where these analytes have been detected at ultra-trace concentration levels. Besides the enrichment capacity, SPE also works as a clean-up step, diminishing the number of interferences and, thereby, lowering the matrix effect in the instrumental analysis. For instance, Chen *et al.* [295] reported a SPE procedure using WAX cartridges as sorbent and acetonitrile for eluting FTOHs, achieving recoveries ranging from 93 to 96%. R. Ma and K. Shih [297] proposed the use of Oasis HLB® cartridge to extract FOSAs (81-85%) using methanol as elution solvent.
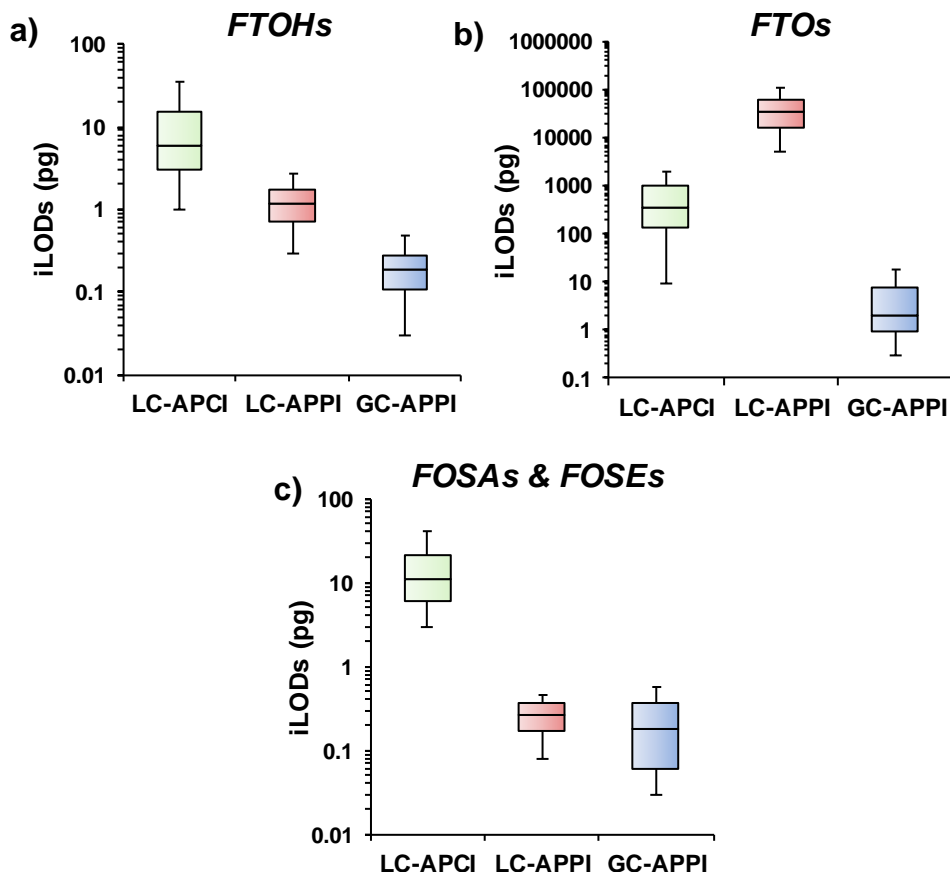
Fig. 2.6. iLODs determined for a) FTOHs, b) FTOs, and c) FOSAs and FOSEs using LC-APCI and LC-APPI in a triple quadrupole (MS/MS) and GC-APPI in an Orbitrap (HRMS) mass analyzer.

Nonetheless, the SPE extract often requires an evaporation step to concentrate the analytes at a concentration level high enough to be detected by the LC-MS or GC-MS systems. This evaporation process can result in important losses of the most volatile neutral PFAS, compromising their determination. As mentioned in the introduction (*Section 1.2.1, Sample Treatment*), Taniyasu *et al.* [100] reported a SPE method using Oasis WAX cartridges for the extraction of FTOHs and *N*-EtFOSA obtaining recoveries ranging from 35 to 55%. These low recoveries have been attributed to both the adsorption of target compounds on the polypropylene containers and the losses during the evaporation to concentrate the extracts under a nitrogen stream. In this thesis, all these problems were evaluated during the optimization of the sample treatment procedure, which is described in *Article I* and *Article II*. For this purpose, the different steps of the sample treatment were individually evaluated to maximize the extraction of analytes, to clean-up the extracts, and to concentrate the final extracts to the appropriate volume (Fig. 2.7). SPE procedure including both the extraction in

the Oasis HLB® cartridge and the clean-up (10 mL of methanol/water 5:95, *v/v*) yielded recoveries higher than 93% by eluting the analytes with 4 mL of methanol. Nevertheless, when the extracts were concentrated under a nitrogen stream, low recoveries were obtained, especially for FTOs (15-25%) and almost all the FTOHs (25-42%).
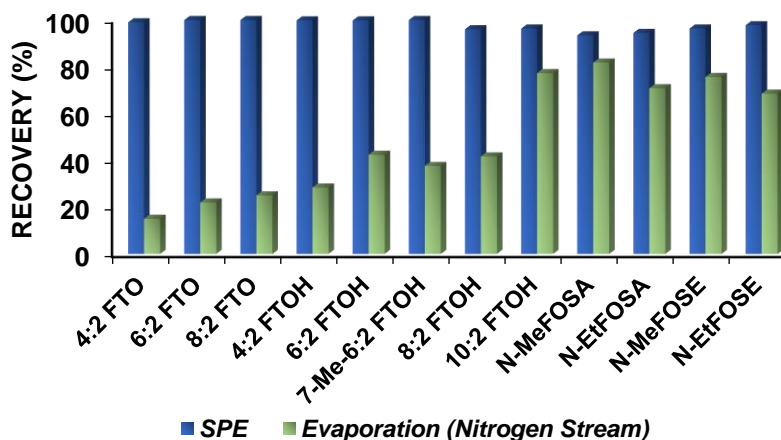

Fig. 2.7. Recoveries of the SPE and the evaporation steps for the analysis of neutral PFAS in water samples.

Thereby, considering the high preconcentration factor (from 500 mL of sample to 4 mL of extract), further evaporation steps of the SPE extract were avoided. Once the SPE method was established, a significant matrix effect was observed and ranged from 15 to 60%. Thus, an aliquot of the extract (1 mL) was diluted with Milli-Q water (3 mL), minimizing the matrix effect down to 20% and improving 4 to 5-fold the signal-to-noise ratio (*Article I, Section analysis of river water samples by UHPLC-APPI-MS/MS*). This strategy allowed us to propose very sensitive methodologies for the analysis of these compounds in water sample achieving mLODs ranging from 0.3 to 6 ng L^{-1} for the SPE UHPLC-APPI-MS/MS method and from 3 ng L^{-1} to 6 µg L^{-1} for the SPE UHPLC-APCI-MS/MS methodology.

Although SPE is an exhaustive extraction technique that involves both preconcentration and clean-up in one step, it also exhibits some disadvantages such as high solvent consumption, long analysis time (ca. 2h for 500 mL of water) as well as high sample volumes to achieve the optimal preconcentration. Thereby, *Article IV* proposes the use of HS-SPME in combination with a novel GC-APPI-HRMS (Orbitrap) methodology. The HS-SPME presents significant advantages in front of SPE: (i) rapid, inexpensive and solvent-free technique, (ii) low sample volume (10-15 mL), (iii) direct pre-concentration of the analytes in the exposed fiber coating, and (iv) highly selectivity of fibers towards the target compounds. Additionally, the absence of filament in the GC-APPI ion source and the low contribution to the background noise of the solvent (in this case methanol) make unnecessary to fix a delay time for the solvent elution. This avoids the suppression of the most volatile 4:2 FTO when eluted within the tail of the

solvent peak, which is an important advantage of the GC-APPI over the high-vacuum ionization techniques (EI, CI, and NICI) for the GC-HRMS determination of neutral PFAS. Although the UHPLC separations are faster (less than 10 min) than GC separation (ca. 20 min), the combination of GC-APPI-HRMS with HS-SPME allows the analysis of a sample in 65 min while the SPE UHPLC-MS/MS procedures require at least 2h. Moreover, GC separation fully resolved all the chromatographic peaks avoiding any possible ion suppression effect within coeluting peaks. The extraction procedure by HS-SPME using a DVB/CAR/PDMS fiber combined with the high potential of the GC-APPI-HRMS method provided a sensitive and selective method for detecting neutral PFAS in river water samples at very low concentration levels (mLODs: 20 pg L^{-1} – 240 pg L^{-1}, except for 4:2 FTO, which was 15 ng L^{-1}). Regarding detection capability of the whole method, mLODs were 2 to 100 times lower than those obtained using the UHPLC-APPI-MS/MS method (*Article I, Table 3*) and 50 to 400 times lower than those achieved by UHPLC-APCI-MS/MS (*Article II, Table 5*) for FTOHs, FOSAs, and FOSEs. It must be highlighted the significant decrease in the mLODs of FTOs, which were 400 to 8,500 times lower than those obtained using the UHPLC-APCI-MS/MS method. Bach *et al.* [105] reported a HS-SPME GC-EI-MS methodology to determine neutral PFAS in river water, achieving method limits of quantitation (mLOQs) 40 to 200 times higher than those obtained by HS-SPME GC-APPI-HRMS method developed in this Thesis. Furthermore, this method also improves the detection capability of the developed LC-MS/MS methods using the ESI source, as described in *Article IV* (*Section 3.2*). These results demonstrate the significant advantages that APCI and APPI techniques provide for the UHPLC-MS/MS and GC-HRMS determination of neutral PFAS in water samples.

It is also well-known that API sources may be subjected to matrix effect as well as ion suppression and/or ion enhancement. Since APCI and APPI mechanisms take place in the gas-phase, they generally show a lower matrix effect in LC-MS comparing to electrospray (*Article I, Section Analysis of river water samples by UHPLC-MS/MS, and Article II, Table 5)*. This effect has also been evaluated for the GC-APPI-HRMS method (Fig. 2.8). To achieve this goal, the SPE procedure proposed in *Article I* and *Article II*, avoiding the last dilution step, was applied to the GC-APPI-HRMS system. This matrix effect corresponds to the whole GC-APPI-HRMS system since it might affect both GC injection by discriminating between compounds and APPI ionization. Thus, the matrix effect was tested by analyzing different types of water samples (Milli Q-water, tap water, and river water from two areas with different levels of exposure to wastewater discharges). Briefly, 500 mL of a water sample was loaded onto an Oasis HLB® cartridge (500 mg, 6 mL) and, after washing the SPE cartridges with 10 mL of a Milli-Q water/methanol (95:5, *v/v*) mixture, analytes were eluted using 4 mL of methanol. The blank extract was then spiked at a concentration range from 2.5 to 65 pg µL^{-1} and the obtained results were compared with a standard solution at the same concentration level.
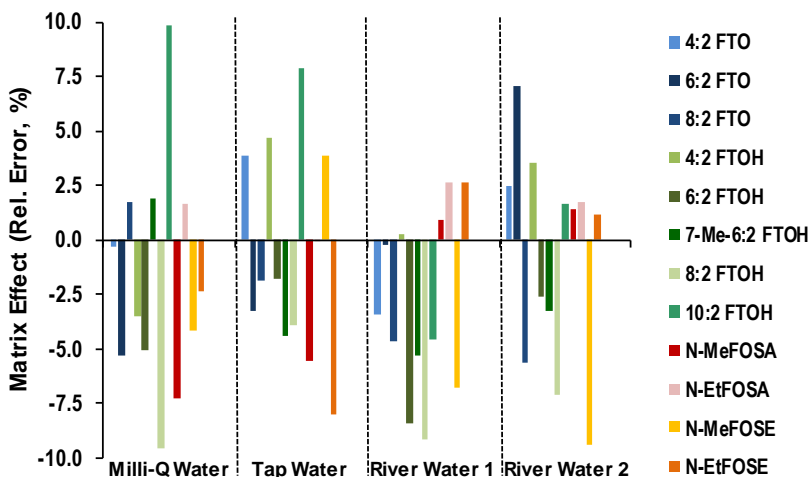
Fig. 2.8. Matrix effect on the GC-APPI-HRMS determination of neutral PFAS in water samples.

As can be observed in Fig. 2.8, the matrix effect was lower than 10% for all the target compounds in the analyzed water samples. When this approach was applied to the developed SPE UHPLC-APPI-MS/MS method in *Article I* the matrix effect ranged from 15 to 60%. Thus, the GC-APPI-HRMS method shows a significant decrease of the matrix effect in front of UHPLC-MS/MS methods. In fact, these results can even be associated to the instrumental variation of the GC-APPI-HRMS method (*Article IV, see supplementary information Table* S2). Thereby, it can be concluded that the matrix effect could be considered negligible in the GC-APPI-HRMS determination of neutral PFAS in water samples.

2.3.2. Novel API-based strategies for the non-targeted screening analysis of neutral PFAS

As mentioned in Chapter 1 (*Introduction, Section 1.1*), more than 6,300 PFAS have been reported during the last decades showing very different chemical structures and properties. This large number of substances is continuously increasing due to the widespread use of these compounds in industrial processes. Although targeted strategies such as those previously reported (*Section 2.3.2*) are very useful to monitor and quantify the levels of specific compounds in the environment, non-targeted strategies are required to simplify the unequivocal identification of new PFAS. In this sense, the establishment of fragmentation pathways for each family of compounds could help on the development of mass spectrometry strategies for the screening of neutral PFAS in real samples as well as for the identification and characterization of new and unknown related neutral PFAS and the differentiation of potential isobaric compounds.

The fragmentation pathways of neutral PFAS (FTOs, FTOHs, FOSAs, and FOSEs) using API techniques (ESI, APCI, and APPI) were tentatively proposed in *Article III*. To achieve this goal,

a linear ion trap-Orbitrap (LTQ-Orbitrap) mass analyzer was used since it allows multiple-stage mass spectrometry (MS^n) experiments by isolating precursor and products ions at low-resolution MS (ion-trap instruments) and the acquisition of both full-scan and product ion scan mass spectra at high-resolution MS (Orbitrap). Although in *Article III* is thoroughly detailed the fragmentation pathways proposed for PFAS in this Thesis, a summary of the most relevant trends in the fragmentation pathways of these compounds is included below.

Regarding FTOs, the odd-electron fragment ions observed in negative ion APCI and APPI were suggested to come from an unstable molecular ion. The main fragmentation pathway (*Article III, Fig. 2*) for FTOs initiates by consecutive losses of HF units *via* α,β-eliminations with charge retention between adjacent carbons from the fluoroalkyl chain. These losses can be identified in the mass spectra by the presence of ions shifting 20.0062 Da and their genealogical relationship can be confirmed by the one-unit increment of the ring double bond (RDB) equivalent due to the formation of a double bond on each HF elimination. This fragmentation pattern was also observed for the fragmentation of the deprotonated molecule of FTOHs as well as for the low-stable molecular ion under negative ion APCI and APPI (*Article III, Fig. 3*). These α,β-eliminations normally occur until exhausting all the hydrogens in the molecule. After that, losses of F atoms and CF_2 units (49.9668 Da) usually alternate. The loss of CF_2 units may involve the cleavage of the terminal C-C bond of the fluoroalkyl chain followed by the reattachment of one F atom to the fragmented molecule. In the case of FTOHs, initial losses of HF were followed by the fragmentation of the formed product ions through the loss of CO (27.9949 Da) or CF_2O (65.9917 Da) within the even-electron ion series (coming from the [M–H]$^-$ ion) or the loss of CO for the odd-electron ion series (coming from the molecular ion).

Concerning FOSEs, intense in-source CID fragment ions, dominated by the [M–C$_2$H$_4$OF]$^-$ ion, were observed when using both APCI and APPI techniques. This ion might be generated through the loss of the ethanolic chain where a hydrogen atom from the functional group and a fluorine atom from the fluoroalkyl chain may have suffered a rearrangement. The tentative fragmentation pathway (*Article III, Fig. 4*) initially involves the generation of a cyclic structure to yield the loss of one HF unit and further successive losses of HF units by α,β-eliminations until just two hydrogen atoms remain in the chemical structure. As happen with FTOs and FTOHs, this process involves a one-unit increment of the RDB equivalent and the formation of conjugated multiple bonds. In this stage, the loss of the SO_2 moiety (63.9619 Da) is promoted, opening the cycle structure although the RDB equivalent remains constant due to the formation of a double bond. After that, consecutive HF units are again lost by α,β-eliminations followed by losses of CF_2 units from the fluoroalkyl chain. In contrast, the acidity of the sulfonamide group strongly favored the formation of the [M–H]$^-$ ion for FOSAs using anyone of the API sources. The main fragmentation pathway of this ion (*Article III, Fig. 5*) yielded to an initial loss of the *N*-alkyl sulfonamide group (-NRSO$_2$, R: -CH$_3$, -C$_2$H$_5$) to obtain the [C$_8$F$_{17}$]$^-$ (*m/z* 418.9734) followed by different fragmentations of the fluoroalkyl chain

to form three intense shorter fluoroalkyl chain product ions: $[C_3F_7]^-$ (*m/z* 168.9894), $[C_4F_9]^-$ (*m/z* 218.9862), and $[C_5F_{11}]^-$ (*m/z* 268.9830). Other fragmentation pathways were observed for the deprotonated molecule.

As mentioned before, this information could be used to develop non-targeted strategies for the screening of PFAS in complex matrices. For instance, the product ions $[C_2F_5]^-$ (*m/z* 118.9926), $[C_3F_7]^-$ (*m/z* 168.9894), and $[C_4F_9]^-$ (*m/z* 218.9862) as well as the ion corresponding to the whole fluoroalkyl chain $[C_nF_{2n+1}]^-$ were identified in many of the new *N*-alkyl fluoroalkyl sulfonamides (FASAs) derivatives reported by Barzen-Hanson *et al.* [298] and Xiao *et al.* [299]. Thus, a fragmentation flagging approach with these common ions could be used to identify new unknown related PFAS as proposed by Liu *et al.* [300]. Although legacy PFAS such as PFCAs and PFSAs could also show these product ions, FASAs can be still differentiated from these compounds taking into account other common losses. For instance, PFSAs show $[SO_3]^{-\bullet}$ (*m/z* 79.9574) and $[FSO_3]^-$ (*m/z* 98.9558) as the main product ions, while PFCAs have an initial neutral loss of the functional group (-CO_2, 43.9898 Da) [301,302]. These fragmentation steps are not observed for FASAs for which the initial loss corresponded to the functional group (-$NRSO_2$, R: -CH_3, -C_2H_5) and, therefore, the presence or absence of these ions might also be used to differentiate within these families of PFAS. Moreover, Newton *et al.* [303] reported the loss of SO_2 (63.9619 Da) for perfluorobutane sulfonamido substances, which was also observed in *Article III* for structurally similar FOSAs and FOSEs.

Regarding FTOHs, Trier *et al.* [304] observed abundant in-source CID fragment ions corresponding to $[M-H-3HF]^-$, as well as another ion due to the loss of 108 Da from the deprotonated molecule. This last ion could be assigned to $[M-H-4HF-CO]^-$ according to the fragmentation pathway proposed in *Article III, Fig. 3a*. Successive losses of HF units were also reported by Martin *et al.* [305] and Fasano *et al.* [306] for different FTOH metabolites in rat hepatocytes as well as in rat urine, feces, bile, and plasma. These HF losses not only allowed the identification of FTOH related compounds but also new families of PFAS. Thus, Baygi *et al.* [307] discovered mono- ($C_nFH_{2n}CO_2^-$) and trifluoroalkyl carboxylic acids ($C_nF_3H_{2n-2}CO_2^-$) that showed successive HF losses until exhausting all the fluorine atoms in the molecule. Newton *et al.* [303] also observed that the difference of 20.0062 Da and 40.0124 Da indicates that some related PFAS compound alternates CH_2 and CF_2 units in the fluoroalkyl chain. These results demonstrate the usefulness of fragmentation pathways for the discovery of new families of PFAS.

It must be pointed out that both FTOHs and FOSEs have a high tendency to form adduct ions. For instance, they led to the generation of the $[M-H+CO_2]^-$ and the $[M+CH_3COO]^-$ adduct ions when operating in negative ion ESI under basic and acidic conditions, respectively. The acetate adduct ion has been widely reported when FTOHs and FOSEs were simultaneously determined with legacy PFAS such as PFCAs and PFSAs due to the addition of ammonium acetate to the mobile phase to improve the retention of these ionic PFAS. However, because these adduct ions only form the acetate as product ion, the selectivity of the LC-MS/MS

methods for determining FTOHs and FOSEs could be compromised. In contrast, the ionization of these compounds by negative ion APPI generates characteristic superoxide adduct ions. Contrarily to ESI adduct ions, the fragmentation of these $[M+O_2]^{-\bullet}$ ions required of high collision energies (25 to 40% in the case of FTOHs), which indicates a strong interaction with the molecule. In fact, for FOSEs, the fragmentation pathway of these ions yielded the cleavage of the O_2 moiety combined with the alkyl or the ethanolic chain, respectively (*Article III, supporting material Fig. S2*). In the case of FTOHs, the low intensity of these ions difficulted their isolation and, therefore, hindered the proposal of a reliable fragmentation pathway. Regardless of the low response of superoxide adduct ions in the traditional APPI source for LC-MS, the novel GC-APPI technique strongly promotes their formation as it was mentioned above (*Section 2.3.1, Fig. 2.5*). However, the narrow chromatographic peaks obtained in GC-APPI-HRMS (ca. 6 seconds) and the delay necessary to switch from full-scan to tandem mass spectrometry scan modes in the Q-Exactive Orbitrap did not allow a good quality of tandem mass spectra (few scans) which made difficult further interpretations.

During this Thesis, a collaborative research work, based on a paper spray-atmospheric pressure photoionization (PS-APPI)-HRMS methodology for the direct analysis of some of these families of neutral PFAS (FTOHs, FOSAs, and FOSEs) in waterproof impregnation sprays, was also performed [308]. Using the PS-APPI home-made device given in Fig. 2.9, few microliters of sample were deposit onto a triangle chromatographic paper and, after letting it dry, a fixed volume of a solvent containing a dopant was added at the same time a potential ranging from 0.5 to1.5 kV was also applied. Under these conditions, analytes were evaporated from the paper surface through field-assisted evaporation and ionized in the gas-phase by dopant-assisted photoionization.

Under the optimal conditions, FTOHs and FOSEs only led to the formation of a very intense superoxide ion that probably was due to the high percentage of oxygen in this ambient ionization source in front of traditional APPI and the novel GC-APPI sources. In contrast to GC-APPI, in the PS-APPI the signal was continuous and consisted of a broadband. This PS-APPI approach combined with the Q-Orbitrap system allowed the reliable acquisition of tandem mass spectra and, considering the same mass analyzer (Q-Exactive Orbitrap) was used with both GC-APPI and PS-APPI sources, it may help to the correct establishment of the fragmentation pathway for the superoxide adduct ions. Regarding FOSEs, the GC-APPI-HRMS mass spectra of *N*-MeFOSE (Fig. 2.10a) was mainly characterized by two series of ions coming from both the $[M-C_2H_4OF]^-$ ion (*green color*) and the superoxide adduct ion (*blue color*). This fact was assessed by MS/HRMS experiments using the PS-APPI source and observing that the superoxide adduct ion mainly yielded the loss of the fluoroalkyl or the ethanolic chain (Fig. 2.10b), which was in agreement with the fragmentation pathway proposed in *Article III* (*electronic material, Fig. S2*) (Fig. 2.10c).
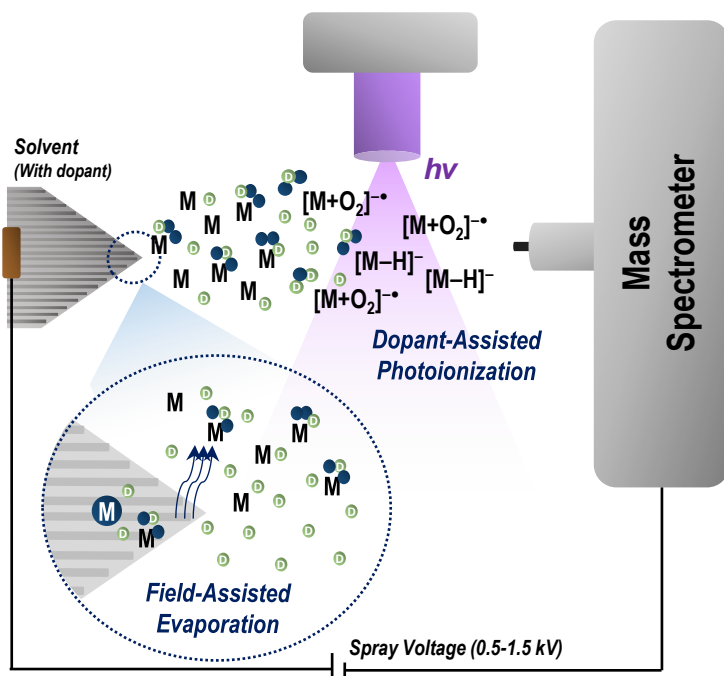
Fig. 2.9.   Scheme of the PS-APPI ionization process adapted from R. Seró [308] (*Figure is not drawn to scale*).

Moreover, the in-source CID fragmentation occurred in the GC-APPI source also provided the $[C_8F_{17}]^-$ ion, which was confirmed to come from the $[M+O_2-C_2H_5O_3]^-$ (*analog to the deprotonated molecule for FOSAs*) through the cleavage of the C-S bond and the stabilization of the charge on the fluoroalkyl chain. Additionally, a less intense product ion corresponding to the *N*-alkyl sulfonamido-ethanol functional group was also present in both mass spectra suggesting that it may be generated from the superoxide adduct ion by cleavage of the C-S bond with charge retention on the S atom. In contrast to FOSEs, the fragmentation of the adduct superoxide ion for FTOHs presented a higher complexity. Fig. 2.11a shows the GC-APPI-HRMS mass spectra of 10:2 FTOH were at least, two ion series could be initially identified coming from the deprotonated molecule (*green*) and the molecular ion (*red*). The other ions (*dark and light blue*) were suggested to come from the superoxide adduct ion based on the tandem mass spectrometry experiments carried out by PS-APPI (Fig. 2.11b). The fragmentation pathway of this ion was tentatively proposed (Fig. 2.11c) considering the product ions observed by PS-APPI-MS/HRMS, the in-source CID fragmentation achieved by GC-APPI-HRMS and the common losses reported for FTOHs (*Article III, fluorotelomer alcohols*). First, the addition of the superoxide moiety to the molecule might take place through the formation of a hydrogen bonding with one of the acidic hydrogens close to the fluoroalkyl chain. As reported in *Article III,* this may be a strong interaction as the ion can initially loss a HF unit through an α,β-elimination leading to a low abundant ion at *m/z* 575.9845. After that, the near position of the superoxide moiety to the hydrogen atom of the hydroxyl group may

162

induce the attack leading to the cleavage of the C-C bond that generates the ion at *m/z* 512.9758, which was assigned to $[C_{11}HF_{20}]^-$ (-1.2 ppm). Then, the ion at *m/z* 492.9699, corresponding to $[C_{11}F_{19}]^-$ (-0.6 ppm) could be formed due to the elimination of HF by means of the generation of a multiple bond. After that, the fragmentation pathway may follow through alternating losses of F atoms or CF_2 units as it was generally reported for neutral PFAS (*dark blue*). It must be pointed out that the tandem mass spectrum obtained by PS-APPI-MS/HRMS also showed a series of ions (*light blue*) with remaining O atoms in their chemical structures. Within this series of ions, *m/z* 540.9719 and *m/z* 536.9605 were assigned as the ion $[C_{12}HOF_{20}]^-$ (1.1 ppm) and $[C_{12}O_2F_{19}]^-$ (0.8 ppm), respectively. Both ions could come from the loss of a O atom or a HF unit from the ion $[C_{12}HO_2F_{20}]^-$ (*m/z* 556.9658, -0.8 ppm) also observed in the GC-APPI-HRMS spectrum (Fig. 2.11a). After that, different losses of HF units or F and O atoms may occur leading to an intense ion at *m/z* 501.9672 that was identified as $[C_{12}OF_{18}]^{-\bullet}$ (0.8 ppm). This fragmentation pathway is still challenging since it initially involves the loss of H_4FO moiety. In this case, MS^n experiments would be strongly needed to clarify the formation of this series of ions and to propose the fragmentation pathway. Nevertheless, it seems to be less favored under the optimal conditions used in the GC-APPI-HRMS method. Additionally, other series of ions (*green*) could also be identified in the tandem mass spectrum of 10:2 FTOH by PS-APPI-MS/HRMS. These ions are characteristic of the in-source CID fragmentation of the deprotonated molecule. In fact, the MS/HRMS profile of these ions strongly matched to that observed for the MS/MS fragmentation of the deprotonated molecule (*Article I, Fig.3b*). Taking into account these considerations and the formation of the [M–H]$^-$ ion (*m/z* 562.9936, 0.6 ppm) in the GC-APPI-HRMS, it could be suggested the formation of the deprotonated molecule from the [M+O$_2$]$^{-\bullet}$ ion probably due to the abstraction of a hydrogen atom by the superoxide moiety.

The Kendrick mass defect (KMD) plotting is also a useful tool that could provide additional information in the non-targeted screening of PFAS. These plots can easily identify homologous series of a family of compounds structurally related such as neutral PFAS. Most of these families of compounds (FTOs and FTOHs) differ on CF_2 units (49.9968 Da) and, therefore, the use of the CF_2 scale (monoisotopic mass x 50/49.99681) may achieve the same mass defect for homologous series shifting 50 Da. Perfluorinated compounds such as PFCAs and PFSAs usually have a negative mass defect because the F atom has a monoisotopic mass (18.9984 Da) lower than the nominal mass (19 Da). Meanwhile, polyfluorinated compounds such as neutral PFAS containing F and H atoms (1.0078 Da) may have positive and negative mass defects close to cero. When the KMD is based on the CF_2 scale, the general mass defects for known PFAS (ca. -0.1-0.15) [309] fall within two separate KMD ranges: -0.1-0 and 0-0.15, which required to focus on two separated regions of the KMD plot. For this reason, Liu *et al.* [300] proposed a transformation of the raw data that implies the addition of 1.0 to those KMD values below 0.1. This transformation allows to focus all the ions in only one region of the plot, and it has been extensively used for the non-targeted analysis of PFAS.
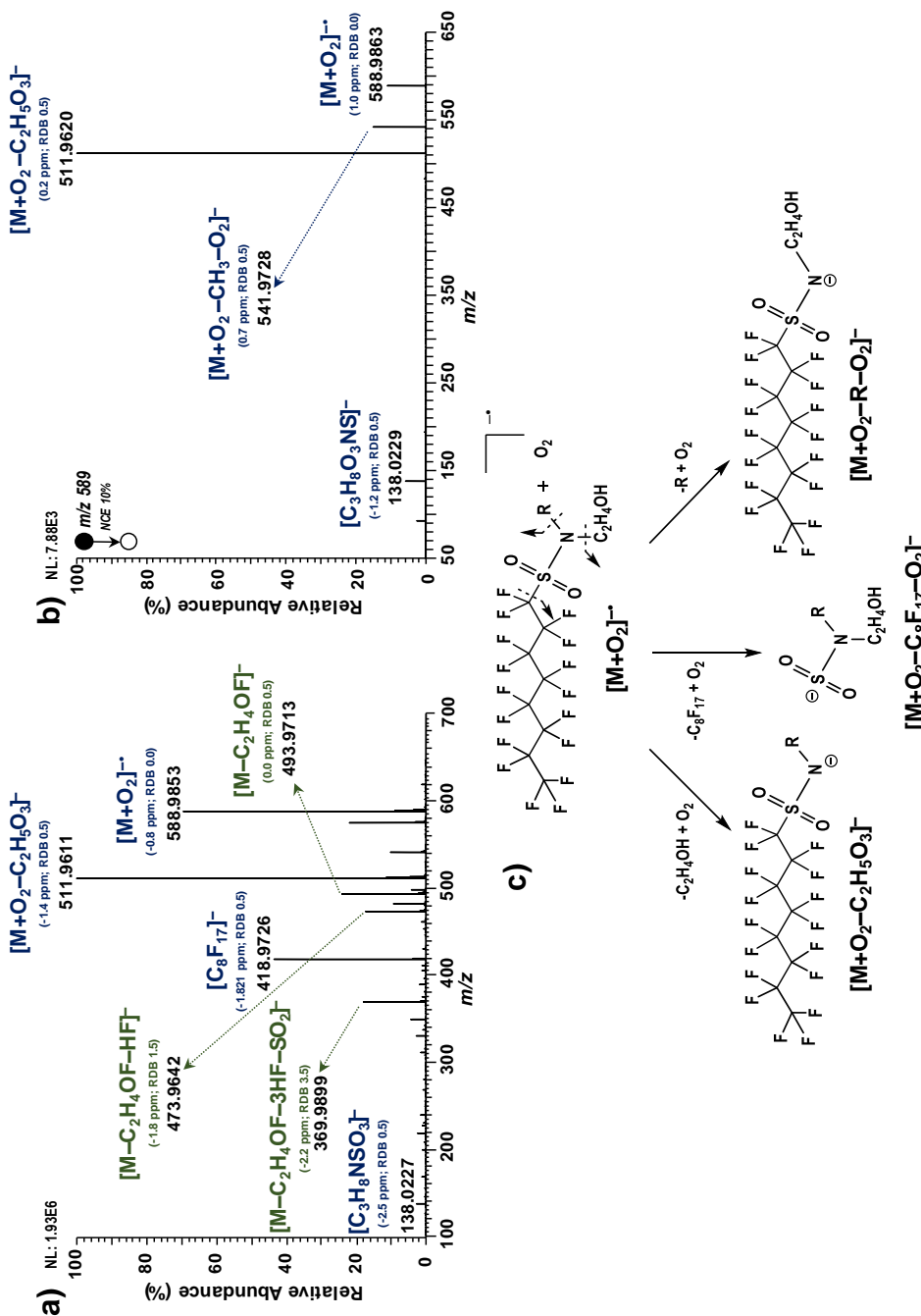
Fig. 2.10. Mass spectra of *N*-MeFOSE by a) GC-APPI-HRMS and b) PS-APPI-MS/HRMS, and the c) fragmentation pathway from the [M+O₂]⁻• ion.
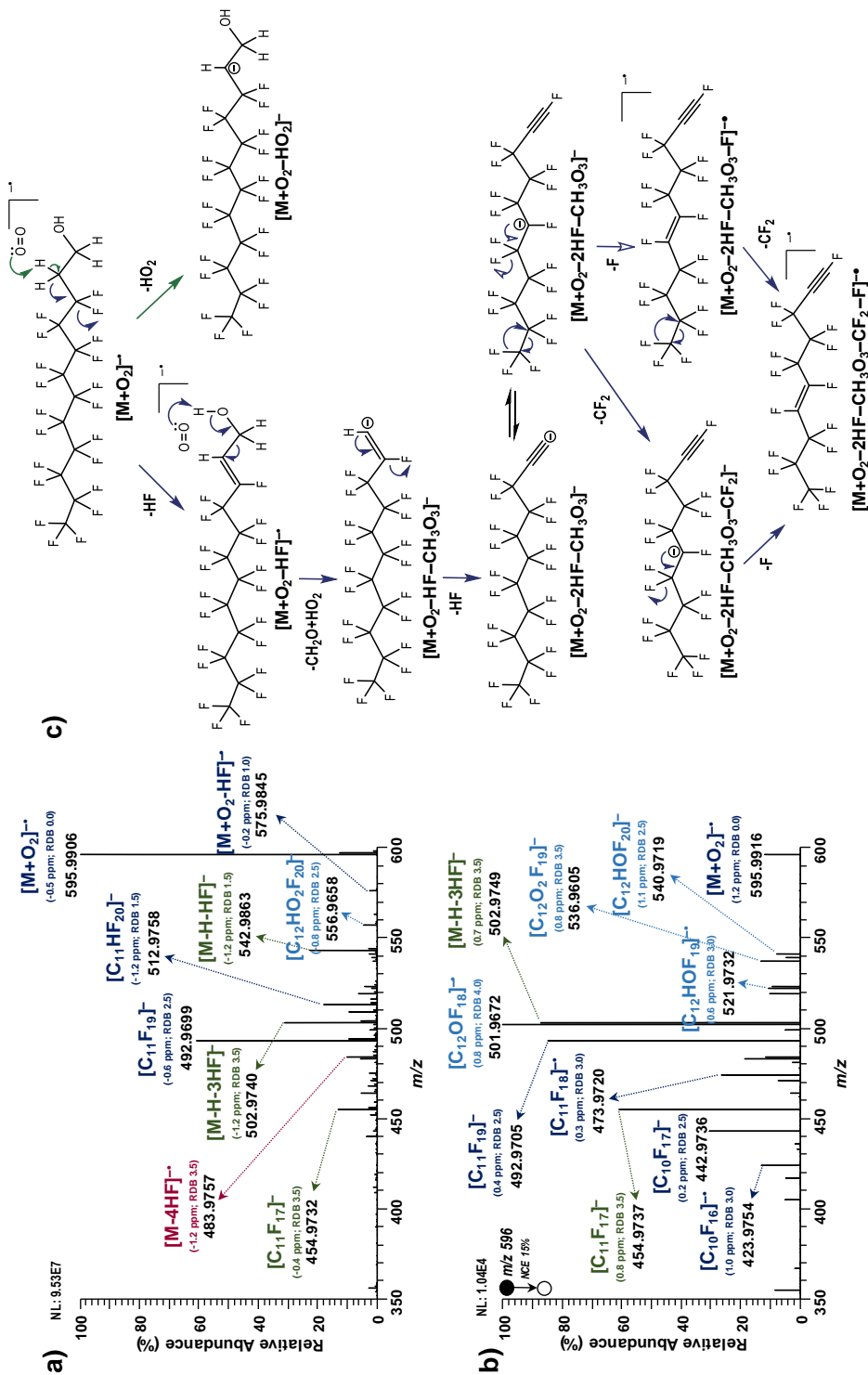
164

Fig. 2.11. Mass spectra of 10:2 FTOH by a) GC-APPI-HRMS and b) PS-APPI-MS/HRMS, and the c) fragmentation pathway from the [M+O₂]⁻• ion.

165

Thus, Fig. 2.12a and Fig. 2.12b show the adjusted Kendrick mass defect (AKMD, CF_2 scale) obtained by analyzing neutral PFAS standards using negative ion ESI and GC-APPI, respectively. As can be observed, ions from the same family of compounds with a different number of CF_2 units in the fluoroalkyl chain are distributed as horizontal lines in the AKMD plot. As the plot has been scaled using the CF_2 scale, compounds from the same family as *N*-MeFOSA *and N*-EtFOSA or *N*-MeFOSE and *N*-EtFOSE are not horizontally aligned since they differ on a CH_2 unit. The AKMD values varied using the different ionization techniques since analytes showed different precursor ions. Despite of that, these AKMD values are characteristic for each family of PFAS with each ionization technique allowing to distinguish not only between the targeted neutral PFAS but also within other families of PFAS such as legacy PFCAs and PFSAs (Fig. 2.12a). This provides additional identification criteria to the information provided using tandem mass spectrometry experiments to achieve the correct identification or discovery of new families of PFAS. In fact, both tandem mass spectrometry and mass defect information could be combined to identify some families of compounds. Fig. 2.12c shows the proposed HF-scaled KMD plot for the identification of neutral telomer-based PFAS using negative ion APPI. As mentioned above, these compounds show a characteristic in-source CID fragmentation leading to series of ions that shift 20.0062 Da (HF unit). Using this HF scale, ions with the same KMD value could be assigned to a molecular structure even if the molecular or deprotonated molecule is not observed in the mass spectrum. Moreover, series of ions that shift 0.019 in the KMD plot will correspond to compounds from the same family of telomer-based PFAS, just differing in one CF_2 unit of the fluoroalkyl chain. These types of plots that combined both mass defect and in-source CID fragment ions or even product ions (from tandem mass spectrometry experiments) can be very useful for the identification of families of compounds that present a repetitive neutral loss among the series of fragment ions observed in the mass spectra.
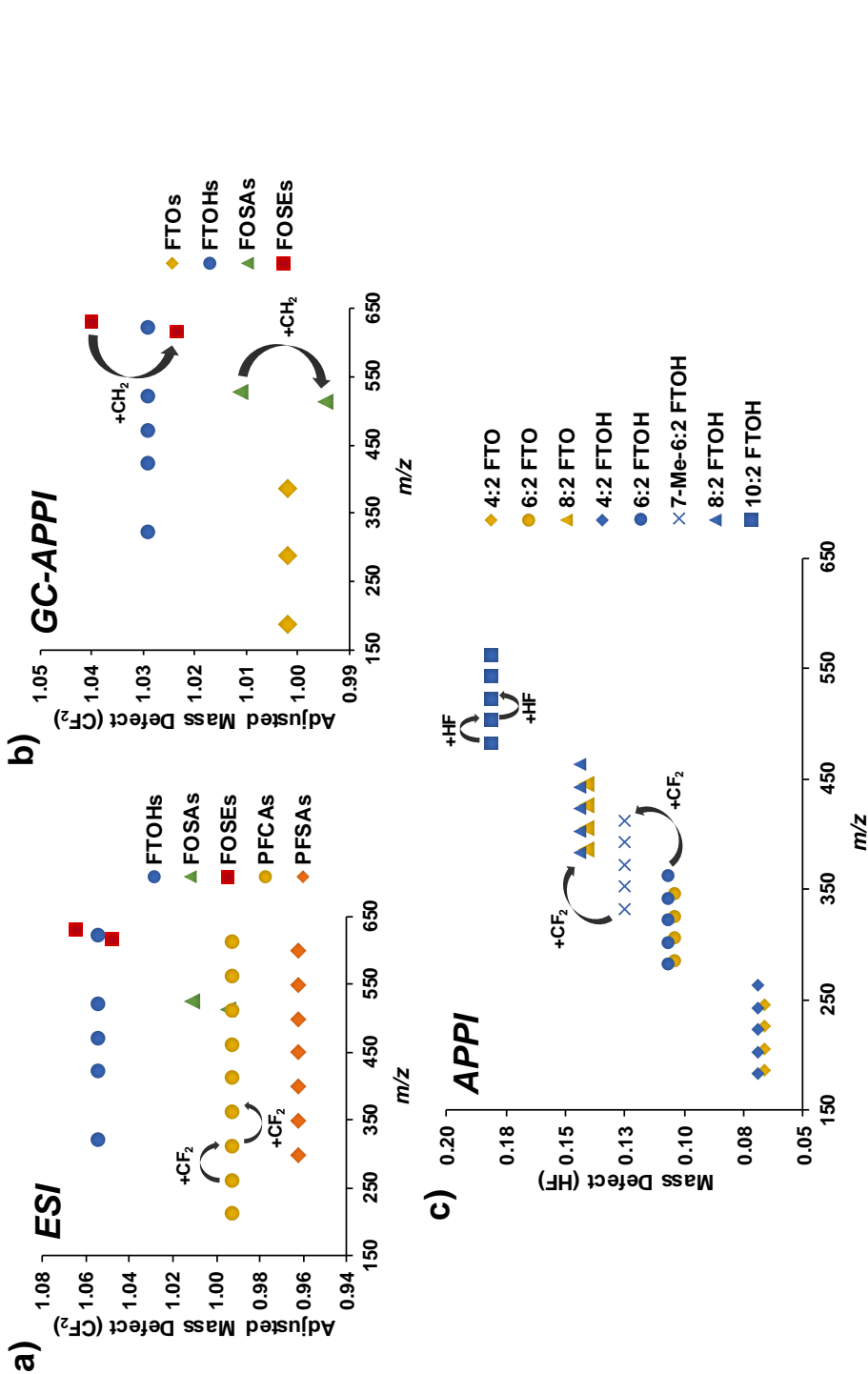
Fig. 2.12. Mass defect plots (CF$_2$ scale) of neutral PFAS using negative ion a) ESI, b) GC-APCI, and c) mass defect plot (HF scale) for FTOs (*yellow*) and FTOHs (*blue*) using APPI source.

CHAPTER 3.

DETERMINATION OF CHLORINATED ORGANIC COMPOUNDS

CHAPTER 3.DETERMINATION OF CHLORINATED ORGANIC COMPOUNDS

In this chapter, the performance of atmospheric pressure ionization sources is studied for the development of GC-HRMS methods to determine different families of chlorinated organic contaminants, including DP and analogs, PCNs, PCDD/Fs, dl-PCBs and SCCPs, in environmental samples. The proposed methodologies pursue the enhancement of the ionization efficiency by selecting the most appropriate gas-phase additives (dopants and modifier agents) as well as the optimal ionization source conditions. The feasibility of the developed methods is evaluated by applying them to the analysis of samples of environmental interest, such as gull eggs, marine sediments, fly ashes, or sludge, among others. Additionally, to achieve the separation of some of these complex families of compounds, novel multidimensional strategies are evaluated, such as comprehensive two-dimensional gas chromatography-mass spectrometry (GCxGC-MS) with ionic liquids as stationary phases and GCxGC combined with ion mobility-HRMS for improving separation capacity.

This chapter includes a brief introduction about these families of chlorinated contaminants, including their main applications, the relationship between their physicochemical properties and their occurrence in environmental compartments as well as the main features of the analytical methodologies currently used for their determination This introductory section is followed by the experimental and results section which includes five research publications. Four of these publications are focused in the development of new analytical methodologies using the novel GC-APPI source to determine DP and analogs (*Article V*), PCNs (*Article VII*), PCDD/Fs and dl-PCBs (*Article VIII*), and SCCPs (*Article IX*) by GC-HRMS (Orbitrap) in samples with environmental interest. The fifth research publication evaluates an ionic liquid stationary phase as a second dimension column to achieve the separation of all PCN congeners by GCxGC-MS (*Article VI*). Finally, all the results of these experimental works are discussed together focusing on two main topics: the new analytical methodologies to determine the chlorinated organic contaminants and the effect of dopants on the ionization of these compounds by GC-APPI..

.

3.1. Introduction

As mentioned in Chapter 1 (*Section 1.1*), SCCPs, PCNs, PCBs, and PCDD/Fs have been listed as POPs by the Stockholm Convention, while DP has been recently proposed as a candidate to be included in the POPs list after evaluating its the risk profile and occurrence in the environment. Some of them, like PCBs, PCNs, SCCPs, and DP, have been widely used during the last century in a vast number of applications due to their physicochemical properties. Concerning chlorinated paraffins, they are currently produced in many countries, being China the largest volume producer around the world. The major historical use of SCCPs is related to metalworking applications such as extreme-pressure additives in cutting fluids and lubricants. Moreover, they have also been used as flame retardants, in paints, adhesives and sealants, leather fat liquors, and as plasticizers in polymeric materials, especially polyvinyl chloride [310]. Since they were introduced in 1932, their production has grown to exceed 1 million ton/year in 2012 [311]. Right now, their use is mainly banned with specific exemptions such as additives in the production of transmission belts, lubricant additives, or plasticizers, among others [312]. With regards to Dechlorane Plus, it has been used as flame retardant since the 1960s. While it ranks among the high production volume chemical in the USA, it is considered a low production volume chemical in the EU. DP was firstly manufactured by OxyChem (Niagara Falls, USA) and it is currently marketed as a possible replacement for the banned decabromodiphenyl ether and Mirex [313]. Among its uses, DP is typically added in electrical wire and cable coatings, plastic roofing materials, automobiles, computer monitors, and connectors in TV as well as in non-plasticizing flame retardants in polymeric systems [314].

Regarding PCNs, their production started in the first decade of the 20th century for industrial applications as a wood preservative, additive to paints and engine oils, for cable insulation and in capacitors. They were also extensively used in paper inlays for gas masks in World War I [315]. After World War II, their production declined, and they were gradually substituted by plastics (for insulation cables) and PCBs in capacitors, although they remained as high volume chemicals until the 1970s [316]. While PCN applications have been ceased, they are still present in PCB formulations. They are also unintentionally produced by leaching from landfills or by thermal formation during waste incineration [317]. Concerning PCBs, they are used as heat exchange fluids in electric transformers and capacitors as well as additives in paint, carbonless copy paper, and plastics. The feasibility of PCBs for industrial applications relays on their chemical inertness, thermal stability, non-flammability, low vapor pressure, and high dielectric constant [318]. Nowadays, the Parties of the Stockholm Convention can no longer produce them, thus they have stopped the use of these chemicals and moved towards the elimination of PCBs. This process involves avoiding the use of PCBs in equipment by 2025 and achieving environmentally sound management as waste of liquids containing PCBs and instruments contaminated with them (content above 0.005% *w/w*) by 2028 [319]. PCBs can also be unintentionally produced due to inappropriate operation of the incinerator and the

combustion of waste at inadequate temperatures [320]. Additionally, they have also recently been identified as undesirable contaminants in dye pigments [321].

On the other hand, PCDDs and PCDFs are not used in any application. However, as also happen for PCBs and PCNs, they are unintentional byproducts generated during incomplete combustion in the presence of chlorine, as well as the manufacturing of pesticides and other chlorinated substances. PCDDs are emitted mostly from the burning of hospital waste, municipal waste, hazardous waste, and also from automobile emissions, peat, coal, and wood. On the other hand, PCDFs are mainly emitted from waste incinerators and automobiles. During recent history, different remarkable pollution episodes have been closely related to PCDD/Fs. The first effect related to these pollutants dates back to 1949 in a chemical facility from Virginia (USA) that mainly synthesized 2,4,5-trichlorphenol. Workers began to show skin alterations, tiredness, irritability, and nervousness. Eight years later, these symptoms were related to the exposure of the works to PCDD/Fs. However, the best-known event related to PCDD/Fs took place during the Vietnam War due to the indiscriminate use of the "Agent Orange," an herbicide and defoliant chemical that contained traces of 2,3,7,8-tetrachlorinated dibenzo-ρ-dioxin (TCDD). The use of this chemical produced the contamination of the population from that area, as well as the American soldiers who developed several symptoms and pathologies such as spontaneous abortion, fetal malformations, intoxications, chloracne, etc. [322,323]. Contamination episodes due to PCDD/Fs exposure have also taken place in Europe. For instance, in the summer of 1976, the explosion of a reactor in a 2,4,5-trichlorophenol factory in Seveso (Italy) caused the widespread dispersion of large amounts of TCDD. The accident supposed 73,000 deaths of domestic animals, vegetation destruction, as well as a vast number of symptoms on the local population [324,325]. Besides that, one of the latest episodes of PCDD/Fs contamination has occurred in Spain. In February 2020, the Zaldibar landfill (Basque Country) collapsed, releasing methane gas and causing the fire that produced low concentrations of PCDD/Fs. Although the effects of the event are still under evaluation, some official statements point to the lack of the implementation of the BAT and the BEP recommended by the Stockholm Convention in the landfill.

As a result of the extended use of PCNs, PCBs, SCCPs, and DP in many industrial applications as well as the unintentionally production of PCDD/Fs, PCNs and PCBs, these pollutants have been frequently detected in different environmental compartments. Table 3.1 summarizes the concentration levels of these pollutants determined in environmental samples. The environmental distribution of these contaminants is closely related to their physical properties. Regarding air samples, the low vapor pressure (VP) and high octanol-air partition coefficient (K_{OA}) of PCDD/Fs (VP: $6.61 \cdot 10^{-8}$ to $1.15 \cdot 10^{-5}$ Pa, log K_{OA}: 10.0-13.0) and DP (VP: $8.47 \cdot 10^{-8}$ to $1.59 \cdot 10^{-7}$ Pa, log K_{OA}: 12.2) make them prone to be associated with particles. For instance, Trinh *et al.* [326] reported that the gas/particle distribution of PCDD/Fs determined in different locations of East Asia clearly showed the predominance of these compounds in the particle phase (higher than 60%).

Table 3.1. Concentration levels of chlorinated organic contaminants determined in environment compartments (air, water, sediment, soil, and biota).

Environmental Compartment		DP Stereoisomers[a]	DP Analogs[b]	dl-PCBs[c]	PCDD/Fs[c]	PCNs	SCCPs
Air (pg m^{-3})	Urban Area Gas-phase	5.52-3,332	0.27-0.28	$1.9 \cdot 10^{-4}$-141.5	$6.4 \cdot 10^{-4}$-65.3	6.60-23.12	2,800-29,000
	Particle-phase	1.00-4,560	n.r.[d]			0.17-2.78	310-3,600
	Remote Area Gas-phase	0.17-0.22	0.0004-0.119	$4.36 \cdot 10^{-4}$	$7 \cdot 10^{-4}$-0.011	0.46-4.9	9.6-20.8
	Particle-phase	0.22-0.57	n.r.[d]	n.r.[d]		n.r.[d]	n.r.[d]
Water (ng L^{-1})	Urban Area	0.050-1.4	n.r.[d]	$2.61 \cdot 10^{-4}$-0.002	$7.7 \cdot 10^{-6}$-$4.4 \cdot 10^{-4}$	178-489	278-500
	Remote Area	0.069-0.303	n.d.[e]-0.106	$9.72 \cdot 10^{-5}$	$3 \cdot 10^{-6}$-$1.5 \cdot 10^{-5}$	n.r.[d]	3.7-117
Sediment (ng g^{-1} dw)	Urban Area	0.07-18.8	n.d.[e]-1.91	n.d.[e]-0.063	$1 \cdot 10^{-5}$-10	0.03-5.1	180-620
	Remote Area	0.116-0.885	n.d.[e]-0.020	n.r.[d]	0.134-0.230	0.23-1.9	9.2-138.1
Soil (ng g^{-1} dw)	Urban Area	0.17-1990	n.d.[e]-52.5	n.d.[e]-0.015	0.04-0.200	1-190	50-266
	Remote Area	0.109-1139	n.d.[e]-0.073	$5.39 \cdot 10^{-4}$	$7 \cdot 10^{-7}$-$6.5 \cdot 10^{-4}$	0.026-0.530	6.4-7.8
Biota (ng g^{-1} lw)		n.d.[e]-102	n.d.[e]-139	$1 \cdot 10^{-6}$-0.94[f]	$1 \cdot 10^{-6}$-0.087[f]	0.22-48.5	26-1,500

[a] *syn*- and *anti*-DP, [b] Dec-602, Dec-603, Dec-604, Cl$_{10}$-DP, and Cl$_{11}$-DP, [c] expressed as TEQ upper bound, [d] not reported, [e] non-detected, expressed as wet weight (ww).

175

Zhang *et al.* [327] and Salamova *et al.* [328] also indicated that the highest concentration of DP was found in the airborne particle-phase when analyzing air samples from areas near to the DP manufacturing plants in East China and areas close to the Great Lakes. The distribution levels reported in air-particles for dl-PCBs [329] was wider because of their higher vapor pressures ($4.77 \cdot 10^{-5}$-0.002 Pa) and lower log K_{OA} (9.62-11.3). In the case of PCNs, although they could also be found in airborne matter (log K_{OA}: 6.55-11.64), their high vapor pressures ($1.5 \cdot 10^{-6}$-0.352 Pa) make them more suitable to be transported by volatilization [317]. For example, Zhu *et al.* [330] reported that PCN concentrations determined in airborne matter contributed 11% (0.17-2.78 pg m^{-3}) to the total concentration of this family of pollutants in air samples from Beijing, China. These levels were even lower than those reported by Bidleman *et al*. [331] in the gas-phase of air samples from sub-arctic remote regions (0.46-4.9 pg m^{-3}). Concerning SCCPs, their relatively high vapor pressures ($2.8 \cdot 10^{-7}$-0.028 Pa) lead to higher proportions in the gas-phase. Nonetheless, this gas-/particle-phase partitioning depends on the group of SCCP congeners due to their high variation in the log K_{OA} values (4.07 to 12.55) [310]. For instance, Zhu *et al.* [332] reported the predominant presence of SCCPs with shorter carbon chains and lower chlorine content in the gas-phase from the urban air of Dalian (China), while long carbon chains and highly chlorinated SCCPs were more abundant in the particle-phase. Significant concentrations of SCCPs have been reported not only in urban air but also in air samples from remote areas. For instance, Ma *et al.* [333] found concentration levels ranging from 9.6 to 20.8 pg m^{-3} in the air samples from the Fildes Peninsula of Antarctica. Additionally, Henry's law constants ranged from 0.7-18 Pa·m^3 mol^{-1}, suggesting that SCCPs can move from water to air, contributing to the high concentrations observed in this environmental compartment [334].

Regarding the environmental partitioning of chlorinated pollutants between water and sediments, the behavior was quite similar to that observed in air samples. The high n-octanol/water partition coefficient (as log K_{OW}) of PCDD/Fs (6.13-8.48), dl-PCBs (6.47-7.15), PCNs (4.2-8.5), and DP (9.3) make these compounds more suitable to be adsorbed onto the sediments, especially for highly chlorinated congeners [326]. For instance, higher concentration levels of DP, PCDD/Fs, and dl-PCBs have been reported in sediment samples [108,335–337] compared to the very low concentration levels reported in water samples [95,335,336,338–340] as can be observed in Table 3.1. With regards to PCNs, they have been widely determined in sediments from both urban and remote regions finding concentration levels ranging from 0.03-5.1 ng g^{-1} dw and 0.23-1.9 ng g^{-1} dw, respectively [331,341]. Although PCN levels in water are not typically reported, Mahmood *et al.* [342] found unexpected high concentrations of them (178-489 ng L^{-1}) in the River Chenab (Pakistan), which may suggest local acute contamination. In contrast to DP, PCDD/Fs, dl-PCBs, and PCNs, the log K_{OW} values of SCCPs with chlorine content ranging from 49-71% variates from 4.39 to 5.37. This fact causes a higher distribution of this family of pollutants, finding significantly relevant concentrations in both water [343–345] and sediment samples [343,346] from urban and remote areas.

The occurrence of these pollutants has also been reported in soil samples. Zhao *et al.* [347] found SCCP concentrations of 50-266 ng g^{-1} dry weight (dw) in China while Li *et al.* [348] reported concentrations ranging from 6.4 to 7.8 ng g^{-1} dw in the Arctic. Significant levels of PCDD/Fs, dl-PCBs, and PCNs have also been detected in soil samples. For instance, PCDD/Fs concentrations of 0.04-0.2 ng TEQ g^{-1} dw and PCN levels ranging from 1-190 ng g^{-1} dw have been described in different countries from Europe and Asia [349,350], while lower concentration levels have been reported for dioxin-like PCBs in Vietnam e-waste processing sites [351]. These chlorinated aromatic compounds (PCDD/Fs, dl-PCBs, and PCNs) have also been detected in soils from remote areas (Arctic, Antarctic, Qinghai-Tibet Plateau, etc.) at lower concentrations, which may be the result of their air transportation [340,352,353]. Regarding DP, levels reported by Na *et al.* in soil from the Arctic Circle (0.109-1,139 ng g^{-1} dw) [336] were fairly similar to those found near to an e-waste recycling area in China (0.17-1,990 ng g^{-1} dw) [354]. These results differed from the other environmental compartments, where lower DP concentrations were found in remote areas. In the case of analogs and degradation products of DP, the concentration levels found in different environmental matrices were rather lower than those reported for DP stereoisomers [336,355–358].

Additionally, the occurrence of all these pollutants has also been reported in biota samples. Thus, Barón *et al.* [359] indicated the bioaccumulation of DP and analogs (Dec-602, Dec-603, and Dec-604) in bird eggs of 14 different species from a Natural Park of southwestern Spain. The authors highlighted the importance to monitor DP-related compounds since Dec-602 and Dec-603 were the predominant dechloranes. Moreover, these two analogs showed correlation evidence of biomagnification capacity, becoming a threat to human health. SCCPs were also detected in different marine and terrestrial animals (e.g., herring, sea eagle eggs, seal, moose, owl, wolf, lynx, etc.) from Scandinavia. Yuan *et al.* [360] reported concentration levels ranging from 26 to 1,500 ng g^{-1} lipidic weight (lw) depending on the animal. In general, fishes showed the lowest SCCP concentrations (34-97 ng g^{-1} lw) while higher levels were observed in seabirds and marine mammals (26-330 ng g^{-1} lw). These values were even higher for terrestrial mammal and birds (85-1,500 ng g^{-1} lw), suggesting the biomagnification of these pollutants through the intake of other smaller animals. These biomagnification processes could finally affect human health through the intake of food meat from this animal origin. In fact, food is considered the main source of exposure for humans to PCDD/Fs and dioxin-like compounds. For instance, great concentration levels of PCDD/Fs (1·10^{-6}-0.087 ng TEQ g^{-1} ww) and, especially, dioxin-like PCBs (1·10^{-6}-0.94 ng TEQ g^{-1} ww) have been reported in fish species from Africa, Europe and Asia [361]. Besides, the Arctic Monitoring and Assessment Programme (AMAP) has even reported significant levels of PCNs (0.22-48.5 ng g^{-1} lw) in seals, whales, and polar bears [362].

The worldwide occurrence of these pollutants demonstrated that they are prone to long-range transport, even to remote areas, and their bioaccumulation and biomagnification capacity

affect both humans and wildlife even at trace concentration levels. For these reasons, powerful analytical methodologies are needed to provide accurate and precise determination of these halogenated organic contaminants in environmental samples. Nonetheless, it is necessary to improve current analytical methodologies to overcome some of their drawbacks. Table 3.2. summarizes the main limitations of the methodologies typically used in the determination of these pollutants.

Table 3.2. Main limitations on the determination methods of chlorinated organic contaminants.

Family	Determination	Main Characteristics	Limitations
PCDD/Fs	GC-EI-HRMS	Moderate fragmentation	EI with low energies (<70 eV)
dl-PCBs	(sectors)	SIM acquisition	Loss of mass spectral information
PCNs	GC-EI-HRMS	Coeluting of some PCNs	No baseline separation[1]
	(sectors)	SIM acquisition	Loss of mass spectral information
	GCxGC-EI-MS	Baseline separation	Extended analysis time (>2.5h)
DP	GC-EI-MS	High fragmentation	Low selectivity
	GC-NICI-MS	Cl-losses fragmentation	High number of interferences
		Low ion source temperature	Frequent cleaning of the source
SCCPs	GC-NICI-MS	Coelution of SCCPs	No separation
		HCl/Cl-losses fragmentation	High number of interferences
		Chlorine content dependency	Tedious quantification approaches
	GC-NICI-HRMS	Coelution of SCCPs	No separation
		HCl/Cl-losses fragmentation	Possible internal interferences [a]
		Chlorine content dependency	Tedious quantification approaches

[a] Limitation for congener/homologue group-specific determination.

In the analysis of PCDD/Fs, there is a European normative (*Norma UNE-EN 1948*) that force to a minimum resolution of 10,000 FWHM as a quality control criterion to overcome interferences hindering the identification of PCDD/Fs congeners [363]. Thus, PCDD/Fs have been traditionally determined by GC-HRMS using a double-focusing magnetic sector mass analyzer and an EI source. This methodology fulfills all selectivity, specificity, and sensitivity criteria to ensure the correct quantification of these analytes at ultra-trace levels [364]. Additionally, it is generally applied to the determination of dl-PCBs and PCNs due to their structurally and physicochemical similarities. However, although this methodology has been accepted as the reference confirmatory method, some limitations can be pointed out. As mentioned in Section 1.2.1, the use of typical ionization energy of 70 eV produces a moderate fragmentation of PCDD/Fs, worsening the detection capability of these methods [148]. Thus, energies of ca. 35 eV are generally recommended to overcome these difficulties. Additionally, the double-focusing magnetic sector mass analyzers need to operate in SIM acquisition mode to achieve the required sensitivity for the detection of the analytes and, therefore, the mass spectral information is limited. In the case of PCNs, the use of GC-EI-HRMS system also hinders congener-specific determination because a single GC column cannot afford the separation of some of the most toxic PCN congeners [196]. In this sense, GCxGC achieves

the separation of all the most toxic congeners, although it requires long time analysis (more than 3h) [156].

Regarding DP and analogs, the determination is usually achieved by GC-MS using EI or NICI techniques. When GC-EI-MS is used, the $[C_5Cl_6]^+$ ion coming from the retro Diels-Alder fragmentation $[M]^{+\bullet}$ ion is usually monitored. This ion is also observed in the mass spectra of many organohalogen compounds, which reduces the selectivity when operating with low-resolution mass analyzers [313]. On the other hand, GC-NICI-MS methods showed a series of fragment ions corresponding to successive losses of 34 Da arising from the chlorine exchange by hydrogen atoms [365]. This fragmentation is generally reduced by applying low ion source temperatures (ca. 150-170 ºC), which increases both the selectivity and sensitivity of the method, although it requires more frequent cleaning, thus reducing laboratory throughput.

In the case of SCCPs, their analytical determination is one of the most challenging in the environmental field. From a chromatographic point of view, the use of one-dimension GC is not enough to achieve the full separation. GCxGC significantly improves the chromatographic separation of congener groups, although coelution still occurs due to the large number of compounds (more than 10,000) present in these complex mixtures [366]. Concerning the ionization, NICI is extensively used providing similar fragmentation patterns than those observed for DP through successive losses of Cl and HCl. As mentioned before (*Section 1.2.1*), the two most abundant peaks of the [M–Cl]⁻ ions are usually monitored. However, considering the vast number of SCCPs and the strong coelution observed in one-dimensional GC, GC-MS methods can be strongly affected by interferences coming from other halogenated compounds or other CP congeners including medium- and long-chain CPs [367]. Moreover, the large number of ions monitored may require several injections as a compromise between detection capacity and sensitivity to determine all the congener groups [206]. Some of these difficulties have been recently solved using novel HRMS systems such as Orbitrap that allows to overcome internal interferences and the analysis in a single run due to the high-speed of its full-scan acquisition mode [147]. Nevertheless, the NICI ionization of SCCPs is strongly affected by the chlorine content, being necessary to use a SCCP standard mixture with similar congener composition than that observed in the sample to avoid significant quantification errors [146,368]. This relationship between the response and the chlorine content requires the application of several quantification approaches to achieve a reliable quantification of SCCPs in the samples. One of the most accepted approaches is the Reth's method [206], which takes advantage of the linear relation between response factors and chlorine content to achieve the quantification of SCCPs regardless of the chlorine content. Although this method reduces potential quantification errors, both analysis and data processing are time-consuming.

Although current methodologies provide good enough results for the analysis of these contaminants, new analytical trends could overcome most of the difficulties observed on their

determination, improving chromatographic resolution, selectivity, sensitivity, as well as the throughput of the environmental laboratories. This chapter deals with the feasibility of the GC-HRMS (Orbitrap) interfaced with novel API sources, especially GC-APPI, to improve the determination of DP and analogs, PCNs, PCDD/Fs, dl-PCBs, and SCCPs in samples of environmental interest. Additionally, the use of multidimensional separations has also been tested to improve the separation of those compounds coeluting in one-dimensional GC separations during the analysis of highly complex mixtures of pollutants frequently studied in environmental applications.

3.2. Experimental work and results

This section includes five research publications related to the determination of the different families of chlorinated organic contaminants already mentioned in Section 3.1 in samples of environmental interest. To achieve this goal, the capabilities of the novel GC-APPI source was assessed for a selective and sensitive determination of target compounds. Thus, the *Article V* entitled "*Analysis of Dechlorane Plus and Analogues in Gull Eggs by GC-HRMS using a Novel Atmospheric Pressure Photoionization Source*" focuses on the study of the ionization of DP and analogs by GC-APPI and the feasibility of this method for the determination of these compounds in gull egg samples. On the other hand, *Articles VI and VII* are related to the determination of PCNs, which include the experimental work and the results achieved during the international stay (3.5 months) carried out in 2018 in the Applied Analytical Chemistry group (Universität Duisburg-Essen, Germany), headed by Prof. Oliver J. Schmitz. *Article VI* entitled "*Ionic Liquid Stationary Phase for Improving Comprehensive Multidimensional Gas Chromatographic Separation of Polychlorinated Naphthalenes*" reports the evaluation of an ionic liquid stationary phase as second dimension column to achieve the separation of closely coeluting PCN congeners while *Article VII* entitled "*Atmospheric Pressure Ionization for Gas Chromatography-High Resolution Mass Spectrometry Determination of Polychlorinated Naphthalenes in Marine Sediments*" compares the applicability of both atmospheric pressure ionization sources (GC-APCI and GC-APPI) to achieve a sensitive and selective determination of the content of PCNs in complex environmental samples such as marine sediments.

The GC-APPI ionization technique has also been evaluated to determine other families of POPs. *Article VIII* entitled "*Feasibility of gas chromatography-atmospheric pressure photoionization-high resolution mass spectrometry for the analysis of polychlorinated dibenzo-p-dioxins, dibenzofurans and dioxin-like polychlorinated biphenyls in environmental and feed samples*" reports the study of the ionization of PCDD/Fs and dl-PCBs using a GC-APPI source installed in a Q-Orbitrap mass spectrometer and the development of GC-APPI-HRMS methods for the accurate determination of these compounds in samples of environmental and feed interest. In this work, the atmospheric pressure ionization of the analytes allowed us to propose sensitive and selective methods that have been evaluated according to the current normative and that can be a good alternative to the traditional confirmatory GC-EI-HRMS (magnetic sectors) method. Finally, *Article IX* entitled "*Chloride-Enhanced Atmospheric Pressure Photoionisation as a Novel Determination of Short-Chain Chlorinated Paraffins in Environmental Samples*" focuses on the development of an alternative method to overcome the difficulties currently observed in the determination of SCCPs. In this sense, different ionization strategies, using the novel GC-APPI source, were evaluated to reduce the number of potential interferences over the response of these analytes. The chloride-attachment APPI ionization simplified the mass spectra and allowed the use of a quantification approach that reduced both analysis time and data treatment. This methodology is finally tested for the quantification of SCCPs in fish samples.

3.2.1. Article V

Analysis of Dechlorane Plus and Analogues in Gull Eggs by GC-HRMS using a Novel Atmospheric Pressure Photoionization Source

J. F. Ayala-Cabrera, S. Lacorte, E. Moyano, F. J. Santos

Analysis of Dechlorane Plus and Analogues in Gull Eggs by GC-HRMS using a Novel Atmospheric Pressure Photoionization Source

J. F. Ayala-Cabrera [a], S. Lacorte [b], E. Moyano [a], F. J. Santos [a,*]

[a] Department of Chemical Engineering and Analytical Chemistry, University of Barcelona. Av. Diagonal 645, E-08028 Barcelona, Spain

[b] Department of Environmental Chemistry, Institute of Environmental Assessment and Water Research (IDAEA-CSIC), C/Jordi Girona, 18-26, E-08034 Barcelona, Spain

* Corresponding author: Francisco Javier Santos Vicente
Phone: +34-93-403-4874
Fax: +34-93-402-1233
E-mail: javier.santos@ub.edu

Abstract

Here, a new gas chromatography-atmospheric pressure photoionization-high resolution mass spectrometry (GC-APPI-HRMS) method combined with selective pressurized liquid extraction (sPLE) has been developed and applied for the determination of Dechlorane Plus (DP) and analogues (Dechlorane 602, Dechlorane 603, and Dechlorane 604) in gull eggs from protected bird areas. The feasibility of the atmospheric pressure photoionization (GC-APPI) has been demonstrated for the first time to achieve selective and sensitive ionization of DP and analogues. The best results have been achieved using negative ion dopant-assisted (diethyl ether) ionization and a source temperature of 250 ºC. Under these conditions, mass spectra of the target compounds have shown intense in-source fragment ions as well as molecular ions and characteristic cluster ions containing oxygen atoms. The sPLE GC-APPI-HRMS method provided high recoveries (>91%) and low method limits of detection (0.05-2 pg g^{-1} wet weight). The developed methodology has been applied to the analysis of gull eggs (*L. michahellis* and *L. audouinii*) as bioindicators of environmental contamination from several Spanish natural and national parks, including the National Park of Atlantic Islands of Galicia, the Medes Islands, and the Ebro Delta Natural Park. The results obtained showed significant differences in the DP concentration profiles between the gull eggs from Atlantic and Medes islands and the Ebro Delta. Moreover, different concentration DP levels were obtained for each gull species within the same location. These results demonstrated the good performance of the GC-APPI-HRMS system to achieve a selective and sensitive determination of DP and analogues in complex biota samples.

1. Introduction

Over the last decades, the number of chemicals used as flame retardants (FRs) has grown very fast due to the needs to prevent ignition and combustion of flammable materials. Although flame retardants can protect from fires, environmental concerns have arisen for some of them, such as the polybrominated diphenyl ethers (PBDEs) or mirex, because of their widespread detection in the environment, bioaccumulation capacity in biota, high toxicity, and persistence. Consequently, strict regulations and banning have been addressed to reduce hazardous effects that they induce in human beings and wildlife [1] and alternative FRs has been proposed to replace them. Among the FRs, Dechlorane Plus (DP) is a highly chlorinated substance frequently used in wire coatings, furniture, and electrical plastic connectors in television and computer monitors. The technical DP mixture consists of two stereoisomers, *syn*-DP and *anti*-DP, in a ratio of about 1:3 [2]. Although DP was introduced in the market in the 1960s, it was first identified in the environment in 2006 when Hoh *et al.* [3] reported its presence in air and sediment samples from the Great Lakes. After that, a growing number of scientific studies has been published reporting the presence of DP in different environmental and biological matrices, such as house dust [4], gull eggs [5], human milk, maternal blood, placenta, and cord blood [6, 7], an even it has been detected in remote areas [8]. Additionally, the occurrence of DP-related analogues such Dechlorane-602 (Dec-602), Dechlorane-603 (Dec-603), Dechlorane-604 (Dec-604) as well as dechlorination products of DP isomers, such as mono- (Cl_{11}-DP) and didechlorinated DP (Cl_{10}-DP), has also been reported in air, sediments and wildlife [9–12]. The global distribution of DP and analogues and their bioaccumulation potential has recently led to propose DP as a candidate to be included in the persistent organic pollutant list of the Stockholm Convention [13].

The determination of DP and analogues is typically performed by gas chromatography coupled to mass spectrometry (GC-MS) using electron capture negative ionization (ECNI) [3, 14, 15]. Under ECNI conditions, low ion source temperatures (ca. 150 ºC) are needed to avoid high fragmentation of the molecular ion [2, 3]. Although this strategy provides a more selective and sensitive method, it may also result in the need for more frequent cleaning of the ion source, thus reducing laboratory throughput. GC-MS determination of DP using electron ionization (EI) has also been proposed [9, 16] although the high fragmentation observed results in the monitoring of low characteristic ions. In the last years, atmospheric pressure ionization (API) sources have been proposed as ionization techniques in GC-MS [17, 18], since they provide a soft ionization that reduces in-source fragmentation, leading to very selective and sensitive methodologies [19]. For instance, halogenated organic contaminants such as polychlorinated dibenzo-ρ-dioxins and dibenzofurans (PCDD/Fs) [20–22], polybrominated diethyl ethers (PBDEs) [23] or neutral per- and polyfluoroalkyl substances (nPFAS) [24, 25] have shown high ionization efficiency under atmospheric pressure chemical ionization (APCI) and atmospheric pressure photoionization (APPI). These API sources can be combined with high-resolution mass analysers, such as Orbitrap or time-of-flight (TOF), which can operate in a sensitive

full-scan acquisition mode allowing both targeted and non-targeted approaches. Moreover, they could also be coupled to both liquid and gas chromatography system, reducing costs and improving the throughput of environmental analysis laboratories. Regarding DP, Liu *et al.* [26] proposed the use of GC-APCI-HRMS (QTOF) for identifying two novel dechlorane analogues, structurally related with Dec-603, in peregrine falcon eggs and shark livers. Moreover, Megson *et al.* [27] determined the capability of the GC-APCI to ionize DP stereoisomers. However, to the best of our knowledge, the APPI source has never been used for the GC-MS determination of DP and analogues.

In the present work, we have investigated the ionization of DP and analogues using a GC-APPI source under different ion source conditions and dopants to develop a sensitive and sensitive GC-APPI-HRMS (Orbitrap) method for the analysis of these compounds. To evaluate the feasibility of the developed method, it has been applied for the determination of the target compounds in gull egg samples from natural protected areas of Spain.

2. Materials and Methods

2.1. Reagents and standards

The target compounds evaluated in this work are summarized in Fig. 1. Individual standard solutions of *syn*-DP, *anti*-DP, didechlorinated DP (Cl_{10}-DP) and monodechlorinated DP (Cl_{11}-DP) in toluene at 50 ng μL^{-1} were obtained from Wellington Laboratories Inc. (Guelph, ON, Canada), while individual standards (solids) of Dec-602, Dec-603 and Dec-604 at a purity higher than 99% were purchased from Toronto Research Chemicals Inc. (North York, ON, Canada). Individual stock solutions at 500 ng μL^{-1} of DP analogues (Dec-602, Dec-603 and Dec-604) were prepared in isooctane EMSURE® for analysis ($\geq$ 99.5%), supplied by Merck KGaA (Darmstadt, Germany). Working standard solutions were prepared by mixture and dilution of all analytes at a concentration of 500 pg μL^{-1}. A standard mixture solution (MXFR-PBDE) at 2 ng μL^{-1}, containing $^{13}C_{12}$-BDE-77 and $^{13}C_{12}$-BDE-138 in nonane (Wellington Laboratories Inc.) was used as surrogate standards to determine recovery rates, while a standard solution of CB-209 (5 μg mL^{-1}) in isooctane (Dr Ehrenstorfer GmbH, Ausburg, Germany) was used as injection internal standard. All the solutions were stored at 4 ºC before use.

Diethyl ether (EMSURE®, $\geq$ 99.7%) and acetone (LiChrosolv®, $\geq$ 99.8%), obtained from Merck KGaA, toluene and chlorobenzene (Chromasolv™ Plus, for HPLC analysis, purity $\geq$ 99%), supplied by Sigma-Aldrich (St Louis, MO, USA), and tetrahydrofuran (Photrex™ reagent, 99%), purchased from J. T. Baker (Deventer, Holland), were used as APPI dopant solvents. *n*-Hexane Unisolv® for organic trace analysis (99%, Merck) and dichloromethane for pesticide residue analysis (99%, Sigma-Aldrich) were used for extraction and clean-up procedures. Sulphuric acid (95-97%), anhydrous sodium sulphate (purity > 99%) of residue analysis grade, Florisil (0.15-0.25 mm) of residue analysis grade and silica gel (Gel 60) of chromatographic analysis quality were obtained from Merck. Before use, the Florisil and silica gel were baked
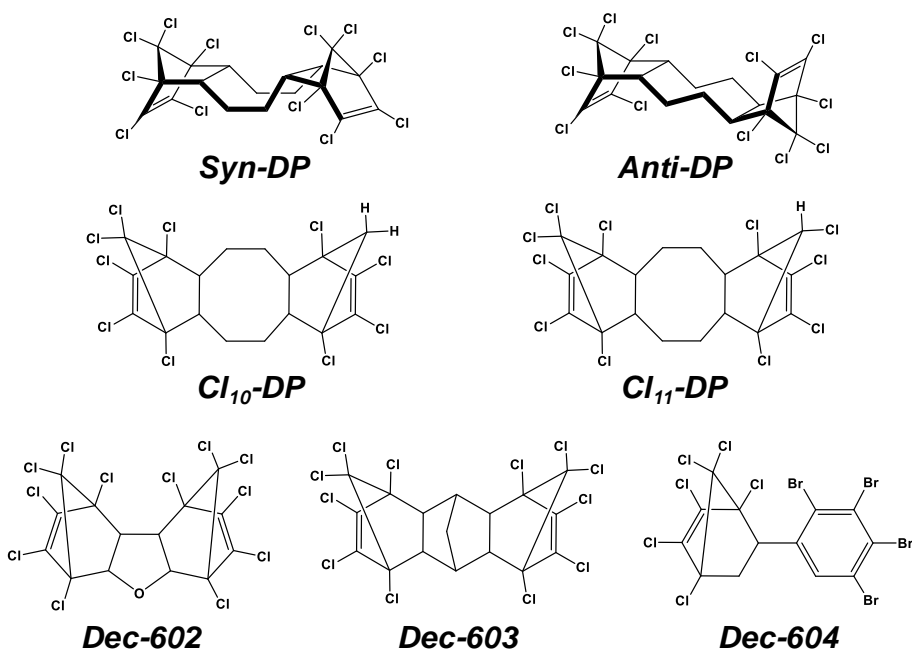
Fig. 1. Chemical structure of *syn-* and *anti*-DP, dechlorinated DPs (Cl$_{10}$-DP and Cl$_{11}$-DP), and analogues (Dec-602, Dec-603, and Dec-604).

overnight at 550 ºC and kept in an oven at 180 ºC. Silica gel modified with sulphuric acid (44%, *w/w*) was prepared by slowly adding an appropriate amount of sulphuric acid to the activated silica at room temperature. Helium Alphagaz™ 1 (≥ 99.999%), used as the carrier gas, was purchased from Air Liquide (Madrid, Spain) whereas nitrogen (≥ 99.995%), employed as make-up gas in the GC-APPI interface, was obtained from Linde (Barcelona, Spain).

2.2. Samples

Egg samples of yellow-legged gull (*Larus michahellis*) were collected in three protected areas from Spain: the National Park of Atlantic Islands of Galicia (thereafter Atlantic Islands) situated in the northwest coast of the Iberian Peninsula, the Medes Islands (thereafter Medes), which are a part of the Montgrí, les Illes Medes and the Baix Ter Natural Park, and the Ebro Delta Natural Park (thereafter Ebro Delta), both areas located in the north-eastern coast of Spain. Adouin's gull (*Larus audouinii*) eggs were sampled from the Ebro Delta Natural Park. The yellow-legged gull is one of the most common species in the Iberian Peninsula as well as a prevalent specie in Europe, the Middle East, and North Africa, and is an opportunistic species with an omnivorous diet that often scavenges on refuse tips. In contrast, Adouin's gull is a piscivorous species, considered a specialist in the capture of cuneiforms (pelagic fishes), but it can also feed on fishery discards and terrestrial preys. Adouin's gull is an endemic and protected species of the Mediterranean area and was classified globally as threatened species in 1988. However, due to an increasing number of breeding pairs (mainly in the Ebro Delta), it

is classified as least concern. A total of 36 samples were collected from each colony during the beginning of the breeding season of 2014 by specialized staff at three sub-colonies located within each park (12 egg per bird settlement). For comparing the results between colonies, only the first laid egg of each nest was collected since it contains the maximum contaminant burden transferred from the female gull at the egg-laying time. The eggs were transported to the laboratory in a cool box and the eggs of each sub-colony were then pooled, lyophilized and stored at -20ºC before analysis. To reproduce the sample matrix effect, chicken eggs with non-detectable amounts of the target compounds were obtained from a local supermarket in Barcelona. After pooling and lyophilizing the chicken eggs, the sample was used as blank for the optimization of the sample treatment and validation studies.

2.3. Sample treatment

DP and analogues were extracted from gull egg samples by selective pressurized liquid extraction (sPLE) using an ASE 100 Accelerated Solvent Extractor System (Dionex, Sunnyvale, CA, USA). Briefly, 1 g of the freeze-dried egg sample was spiked with adequate amounts of $^{13}C_{12}$-BDE-77 and $^{13}C_{12}$-BDE-138 surrogates standards and then kept overnight at room temperature to equilibrate. The sample mixed with anhydrous sodium sulphate at an egg/Na_2SO_4 ratio of 1:2 (*w/w*) was loaded on the extraction cells (34 mL) on the top of 20 g of silica modified with sulfuric acid (44% *w/w*), used as a fat retainer. The sample was extracted using a solvent mixture of *n*-hexane/dichloromethane (1:1 *v/v*) at 100 ºC for three static extraction cycles of 5 min working at a constant pressure of 1,500 psi, a flush volume of 60%, and a purge time of 90 s. After extraction, the extract was rotary evaporated up to 1 mL, after adding two times 3 mL of *n*-hexane for the complete removal of dichloromethane, it was then fractionated on 15 g of activated Florisil. Analytes were eluted from Florisil column using 30 mL of *n*-hexane followed by 80 mL of *n*-hexane/dichloromethane (95:5, *v/v*) to elute DP and analogues and others pollutants, such as PBDEs and polychlorinated biphenyls (PCBs). The extract was then rotary evaporated, and the final volume was adjusted to 50 µL using a gentle stream of nitrogen after adding an appropriate amount of CB-209 as injection internal standard.

The lipid content was gravimetrically determined on separate samples by evaporation of the extract obtained from the sPLE extraction process using a solvent mixture of *n*-hexane:dichloromethane (1:1, *v/v*). The percentage of lipids on wet weight basis for the samples were of 8.2 ± 0.9% for *L. michahellis* and 7 ± 1% for *L. audouinii*. The water content was analysed as the difference between the fresh weight and the freeze-dried weight, and the average water content for both species was 74 ± 1% for *L. michahellis* and 77 ± 1% for *L. audouinii*.

2.4. Instrumentation

Determination of DP and analogues was conducted on a Trace 1300 gas chromatograph, equipped with an AI-1310 autosampler, coupled to a Q-Exactive Orbitrap mass spectrometer (Thermo Fisher Scientific, San Jose, CA, USA). The GC-HRMS was interfaced with the

GC-APPI source (MasCom Technologies GmbH, Bremen, Germany) that disposes of a 10.6 eV krypton lamp (Syagen, Santa Ana, CA, USA). The injection of samples and standards (1 µL) was carried out in splitless mode (1 min) at a temperature of 280 ºC. The chromatographic separation of the target compounds was carried out into a TG-5ms fused-silica capillary column (15 m x 0.25 mm I.D.; 0.25 µm of film thickness), purchased from Thermo Fisher Scientific, using helium as carrier gas at a constant flow rate of 1.2 mL min^{-1}. The oven temperature program was set as follows: 90 ºC (held for 2 min) to 300 ºC (held for 9 min) at 15 ºC min^{-1}. Transfer line temperature was fixed at 280 ºC while the source and capillary temperature were set at 250 ºC and 180 ºC, respectively. Nitrogen was used as make-up gas in the GC-APPI ion source at a constant pressure of 5 a.u. (arbitrary units), whereas the S-lens radiofrequency was set at 50%. After optimization, the ionization of DP and analogues was achieved by dopant-assisted APPI using diethyl ether vapours as dopant at an optimum flow rate of 70 µL min^{-1} (see supplementary electronic material, Fig. S1). Orbitrap was operated in negative ion mode and data were acquired in full-scan acquisition mode (70-700 *m/z*) at a resolution of 35,000 full window at half maximum (FWHM, at *m/z* 200). Moreover, automatic gain control (AGC) target and the maximum injection time were fixed at $3\cdot10^6$ and 50 ms, respectively. The quantitation of the analytes was attained employing the internal calibration method and the extracted ion chromatograms (XICs) were filtered using a tolerance of 5 ppm in the mass extraction windows. The instrument control, data acquisition and processing were performed using the Xcalibur *v* 3.1 software.

2.5. Quality control

Quality control was performed through the analysis of procedural blanks and replicate analysis of egg samples. Procedural blanks covering instrumental and sample treatment procedures, as well as quality control standard solutions, were routinely analysed to guarantee the quality of the results and to check the chromatographic separation, the sensitivity of the ion source and the correct mass calibration. In addition, a quality control egg sample (a chicken egg samples with non-detectable amount of DP and analogues spiked at 2 ng g^{-1} wet weight) was analysed to ensure that the whole method was maintained under control and to rule out any possible carryover between samples. Recovery rates of the labelled $^{13}C_{12}$-BDE-77 and $^{13}C_{12}$-BDE-138 used as surrogate standards were higher than 90% and precisions of the whole method lower than 15% were established as acceptance criteria. Accurate mass calibration was carried out every 72h with a calibration solution consisting of caffeine, Ultramark 1621, butylamine and MRFA peptide in acetonitrile/methanol/water (2:1:1, *v/v/v*) using the electrospray source. To confirm the identification of the target compounds, the following restrictive criteria were applied: (a) the ion abundance ratios between the selected ions monitored should be within ±10 % of the theoretical value, and (b) the retention times should be within ±2 s of those observed for the standards.

3. Results and Discussion

3.1. Ionization of DP and analogues by atmospheric pressure photoionization

The ionization of DP and analogues was assessed using a standard mixture solution containing all the target compounds at 500 pg μL^{-1}. Experiments were carried out in negative ion GC-APPI mode since analytes were not ionized when operating in positive ion mode. To improve the ionization efficiency on the GC-APPI source different solvent vapours (chlorobenzene, toluene, acetone, tetrahydrofuran, and diethyl ether) were evaluated as potential dopants. In general, the ions observed in the mass spectra were not affected by the nature of the solvent used as dopant. As an example of the ionization observed, Fig. 2 shows the mass spectra obtained for *syn*-DP, Dec-602, Dec-603, Dec-604, and the dechlorinated-DPs, Cl_{10}-DP and Cl_{11}-DP, using diethyl ether as dopant (source temperature: 250 ºC).
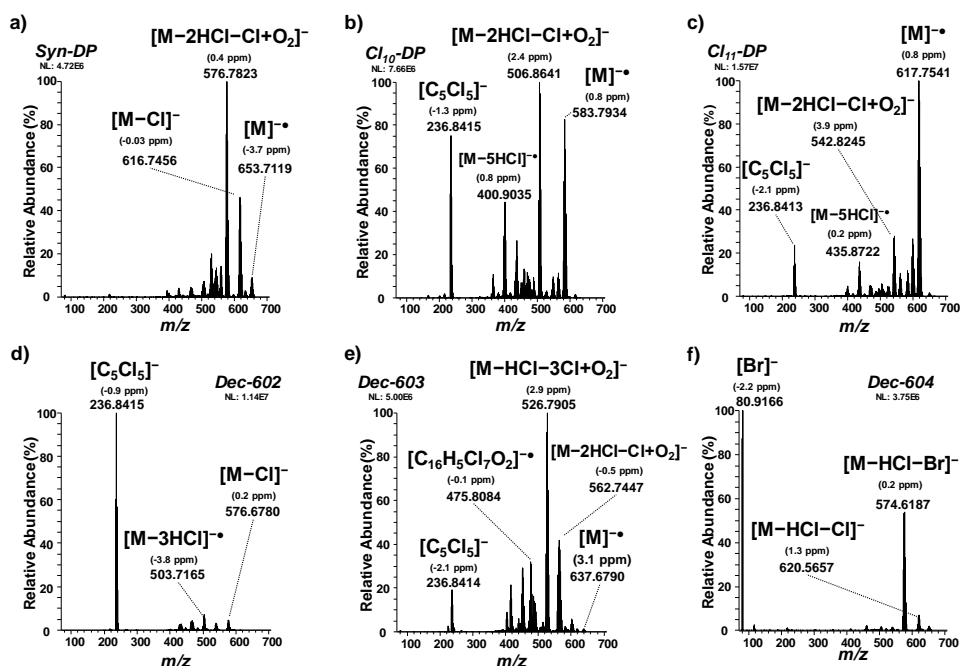

Fig. 2. GC-APPI-HRMS mass spectra of a) *syn*-DP, b) Cl_{10}-DP, c) Cl_{11}-DP, d) Dec-602, e) Dec-603, and f) Dec-604 in negative ion mode using diethyl ether as dopant *(250 ºC source temperature and 180 ºC capillary temperature).*

Both DP stereoisomers led to the formation of the $[M–2HCl–Cl+O_2]^-$ ion as the base peak of the mass spectra, as it could be observed for *syn*-DP in Fig. 2a. Ions including the attachment of a superoxide moiety have been previously reported for other halogenated compounds when operating in negative ion GC-APPI mode [22, 25]. These ions may be formed by clustering reactions in the gas-phase with the superoxide ion generated through the electrons released after dopant photoionization process [28]. DP also showed the formation of the molecular ion although at low relative intensity. In contrast, high abundant $[M]^{-•}$ ions were achieved for

dechlorinated-DPs being the base peak for Cl_{11}-DP and one of the most abundant ions for Cl_{10}-DP (Fig. 2b-c). Furthermore, a characteristic $[C_5Cl_5]^-$ ion, coming from a retro Diels-Alder fragmentation of DP molecular structure [3], was also observed in the Cl_{11}-DP and Cl_{10}-DP mass spectra and it could be used for their identification. This fragment ion was the base peak of the Dec-602 mass spectra (Fig. 2d), while Dec-603 mainly led to the formation of $[M–HCl–3Cl+O_2]^-$ cluster ion as the base peak of the mass spectra (Fig. 2e). In the case of Dec-604, the non-specific bromide ion was the base peak of the mass spectra (Fig. 2f), as it has also been reported in ECNI, which could be strongly interfered by other coeluting brominated compounds (e.g., PBDEs). Additionally, an intense $[M–HCl–Br]^-$ ion was formed, which may improve the selectivity of the method. To reduce in-source fragmentation, the effect of the ion source temperature (from 180 ºC to 250 ºC) over the ionization of DP and analogues was assessed. As it can be observed in Fig. 3, the in-source fragmentation of *anti*-DP decreased when the ion source temperature diminishes.
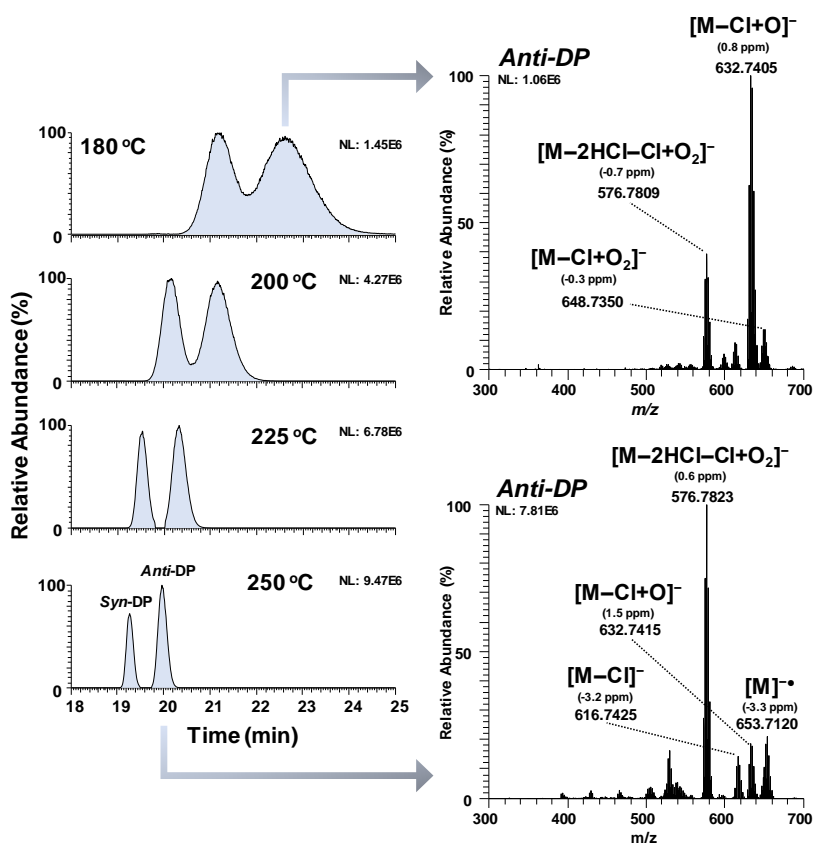

Fig. 3. Effect of the ion source temperature over the chromatographic separation and the mass spectra of *syn*-DP and *anti*-DP.

At a temperature of 180 ºC, the phenoxide ion became the base peak of the mass spectrum. Similar behaviour was observed for dechlorinated-DPs and analogues (Fig. S2). For instance,

the abundance of the molecular ion increased for both Dec-604 and Dec-602, being the base peak of the mass spectrum for the Dec-602 analogue. Moreover, Dec-603 showed an intense [M–Cl+O]$^-$ ion, whereas dechlorinated-DPs mainly formed the [M+O$_2$]$^{-\bullet}$ ion. Although the use of low ion source temperatures decreased the in-source fragmentation, a loss of the chromatographic efficiency was observed for all the compounds, especially worsening the resolution between *syn*-DP and *anti*-DP (Fig. 3). This effect has been already observed for low volatile compounds (e.g., PCDD/Fs) using the GC-APPI source [22]. The low volatility of DP and analogues (vapour pressure ranging from 1.59·10^{-7} to 8.47·10^{-8} Pa) and the GC-APPI source conical design may favour the condensation of the compounds on the source wall that caused an important chromatographic peak broadening and source contamination. Therefore, further cleaning of the ion source was required, reducing the throughput of the laboratory. Thereby, a high ion source temperature (250 ºC) was chosen since it ensured the chromatographic resolution and led to highly selective and abundant ions.

Under these ion source conditions, a specific base peak in the mass spectrum was obtained for each target compound regardless of the dopant tested. Table 1 lists all the monitored ions used for the study of the effect of the dopant (acetone, chlorobenzene, diethyl ether, tetrahydrofuran, and toluene) on the ionization efficiency of the analytes. Among the dopants evaluated, diethyl ether was the solvent that provided the highest responses for all the compounds (Fig. 4). This could be attributed to the high vapour pressure of the diethyl ether that may result in a higher gas-phase concentration of electrons released after the dopant photoionization, which consequently could cause the enhancement of subsequent gas-phase reactions of the target compounds.

Under these optimal GC-APPI conditions, the instrumental limits of detection (iLODs), defined as the lowest concentration of the analyte that provides a well-defined chromatographic peak, were established and ranged from 0.006 to 0.150 pg injected on the column. These values are in agreement with those previously reported using different GC-MS methods. For instance, Rjabova *et al.* [29] achieved iLODs ranging from 0.01 to 0.08 pg injected using GC-EI-HRMS (mass sectors analyzer), while Sales *et al.* [30] developed a GC-NICI-MS/MS (QqQ) providing iLODs ranging from 0.125 to 60 fg µL^{-1} by injecting a volume of 10 µL and using a solvent vent configuration (0.001-0.6 pg injected). Moreover, Megson *et al.* [27] reported iLODs for DP stereoisomers at least 5 times higher than those obtained in the present work using a novel GC-APCI-HRMS (TOF) method. These findings demonstrated the great detection capability of the developed GC-APPI-HRMS method for the determination of DP and analogues. Additional instrumental quality parameters, such as linearity, precision and trueness, were also determined and are summarized in Table S1. Good linearity (R^2 > 0.997) was observed along the working concentration range (0.5-200 pg µL^{-1}). Precision and trueness were estimated at three concentration levels: 0.5 pg µL^{-1} (low), 2.5 pg µL^{-1} (medium), and 50 pg µL^{-1} (high).

Table 1. Ions selected for the GC-APPI-HRMS analysis of DP and analogues.

Analyte	Ion	Formula	Q_1 ion (m/z)[a]	Formula	Q_2 ion (m/z)[a]	IR[b]	iLOD (pg)[c]
Dec-602	$[C_5Cl_5]^-$	$[C_5{}^{35}Cl_4{}^{37}Cl]^-$	**236.8419**	$[C_5{}^{35}Cl_3{}^{37}Cl_2]^-$	238.8389	1.56	0.006
Dec-603	$[M{-}HCl{-}3Cl{+}O_2]^-$	$[C_{17}H_7O_2{}^{35}Cl_7{}^{37}Cl]^-$	524.7930	$[C_{17}H_7O_2{}^{35}Cl_6{}^{37}Cl_2]^-$	**526.7901**	0.89	0.09
Dec-604	$[M{-}HCl{-}Br]^-$	$[C_{13}H_3{}^{79}Br_3{}^{35}Cl_3{}^{37}Cl_2]^-$	**574.6183**	$[C_{13}H_3{}^{79}Br_3{}^{35}Cl_2{}^{37}Cl_3]^-$	576.6163	1.03	0.15
Cl_{10}-DP	$[M{-}2HCl{-}Cl{+}O_2]^-$	$[C_{18}H_{12}O_2{}^{35}Cl_6{}^{37}Cl]^-$	**506.8633**	$[C_{18}H_{12}O_2{}^{35}Cl_5{}^{37}Cl_2]^-$	508.8603	1.04	0.03
Cl_{11}-DP	$[M]^{-\bullet}$	$[C_{18}H_{13}{}^{35}Cl_8{}^{37}Cl_3]^{-\bullet}$	**617.7538**	$[C_{18}H_{13}{}^{35}Cl_7{}^{37}Cl_4]^{-\bullet}$	619.7508	1.04	0.03
Syn-DP	$[M{-}2HCl{-}Cl{+}O_2]^-$	$[C_{18}H_{10}O_2{}^{35}Cl_8{}^{37}Cl]^-$	574.7854	$[C_{18}H_{10}O_2{}^{35}Cl_7{}^{37}Cl_2]^-$	**576.7824**	0.78	0.03
Anti-DP	$[M{-}2HCl{-}Cl{+}O_2]^-$	$[C_{18}H_{10}O_2{}^{35}Cl_8{}^{37}Cl]^-$	574.7854	$[C_{18}H_{10}O_2{}^{35}Cl_7{}^{37}Cl_2]^-$	**576.7824**	0.78	0.03
CB-209	$[M{-}Cl{+}O]^-$	$[C_{12}O{}^{35}Cl_8{}^{37}Cl]^-$	476.7122	$[C_{12}O{}^{35}Cl_7{}^{37}Cl_2]^-$	**478.7092**	0.78	-
$^{13}C_{12}$-BDE-77	$[M{-}Br{+}O]^-$	$[{}^{13}C_{12}H_6O_2{}^{79}Br_2{}^{81}Br]^-$	**432.8306**	$[{}^{13}C_{12}H_6O_2{}^{79}Br{}^{81}Br_2]^-$	434.8285	1.03	-
$^{13}C_{12}$-BDE-138	$[M{-}Br{+}O]^-$	$[{}^{13}C_{12}H_4O_2{}^{79}Br_3{}^{81}Br_2]^-$	**590.6495**	$[{}^{13}C_{12}H_4O_2{}^{79}Br_4{}^{81}Br]^-$	592.6475	1.03	-

a The most abundant ion is marked in bold, b IR: ion ratio, Q_1/Q_2, c Injection volume: 1 µL.
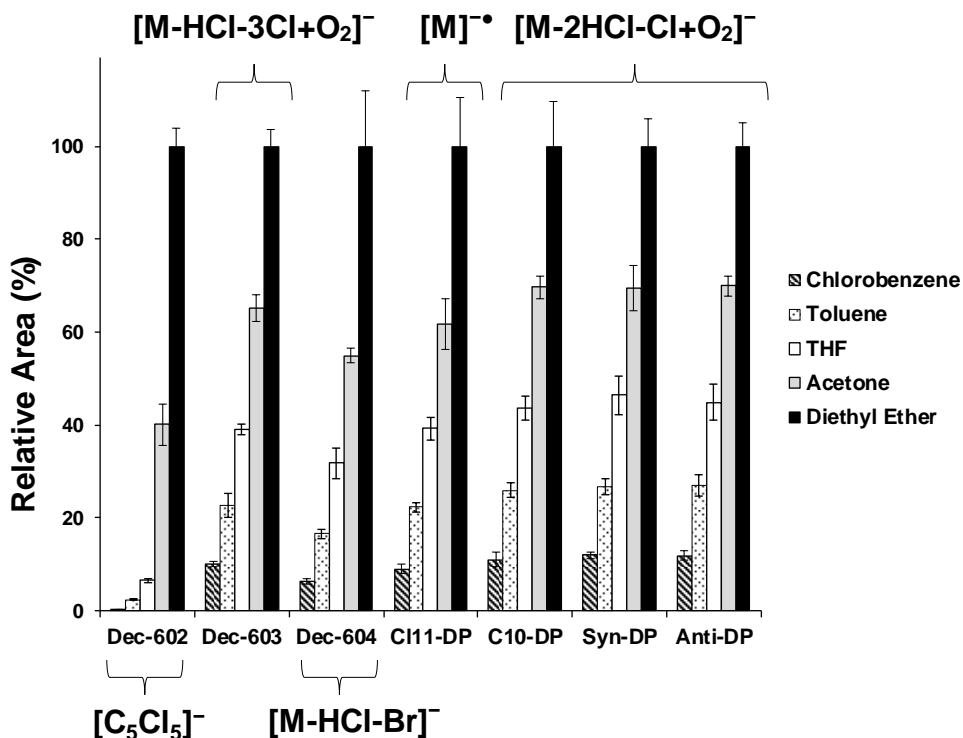
Fig. 4. Effect of the dopant vapours over the GC-APPI-HRMS response of DP and analogues.

Intra-day precision, expressed as the relative standard deviation (RSD, %, n=3), ranged from 2 to 8%, while inter-day precision, calculated in two non-consecutive days (n= 2 days x 3 replicate analyses), was lower than 9%. Moreover, the trueness expressed as relative error between the found and the theoretical concentration (RE, %, n=3), was always lower than 7%. These results, as well as the low variation observed for ion ratios (RSD: 1-2%, n=14), demonstrated the great reliability of the GC-APPI-HRMS method to achieve an accurate and precise determination of the target compounds.

3.2. Analysis of gull egg samples by GC-APPI-HRMS

To ensure a quantitative extraction of the analytes from the gull egg samples, recoveries of the sPLE extraction method were performed on a lyophilized blank chicken egg sample at two concentrations (n=9): 2 ng g^{-1} wet weight (low) and 42 ng g^{-1} ww (high), which are close to the levels often found in gull egg samples. The results showed recovery rates that ranged from 91 ± 7% to 95 ± 8% for the low concentration level, and between 91 ± 7% and 98 ± 6% for the high concentration level (Table 2). The detection capability of the sPLE GC-APPI-HRMS method was assessed through the estimation of the method limits of detection (mLODs) and quantitation (mLOQs), that were calculated using a blank chicken egg sample spiked at low concentration levels (0.5-5 pg g^{-1} wet weight, ww). The mLOD was defined as the lowest

concentration spiked in a blank chicken egg sample that provides a well-defined chromatographic peak (mass error threshold of 5 ppm for the extracted ion chromatogram)

Table 2. Method limits of detection and quantification (pg g^{-1} ww and pg g^{-1} lw) and recoveries (%) of the DP and analogues in egg samples by sPLE GC-APPI-HRMS method.

Analyte	mLOD		mLOQ		Recovery (%) ± SD[c]	
	(pg g^{-1} ww)	(pg g^{-1} lw)	(pg g^{-1} ww)	(pg g^{-1} lw)	Low[a]	High[b]
Dec-602	0.05	0.7	0.2	3	92 ± 7	93 ± 6
Dec-603	1	13	3	39	93 ± 8	92 ± 7
Dec-604	2	26	7	92	95 ± 8	98 ± 6
Cl_{10}-DP	0.3	4	1	13	93 ± 7	93 ± 7
Cl_{11}-DP	0.3	4	1	13	91 ± 7	91 ± 7
Syn-DP	0.3	4	1	13	93 ± 8	93 ± 6
Anti-DP	0.3	4	1	13	92 ± 8	94 ± 7

[a] Low level: 2 ng g^{-1} ww, [b] High level: 42 ng g^{-1} ww, [c] n=9.

while mLOQ was determined as 3.3 times the mLOD, since no background noise was detected on the extracted chromatograms. The values displayed in Table 2 (mLODs: 0.05-2 pg g^{-1} ww and mLOQs: 0.2-7 pg g^{-1} ww) were deemed low enough for the determination of DP and analogues at the concentration level generally found in gull egg samples. The detection capability of the sPLE GC-APPI-HRMS method was similar or even better than the methods reported in the literature using similar matrices. For instance, Su *et al.* [31] reported higher mLOQs ranging from 240-490 pg g^{-1} ww for the DP stereoisomers in herring gull eggs using PLE GC-ECNI-MS (Q) method. Similar values (mLOQs: 2.66-9.09 pg g^{-1} lipid weight, lw) were reported by Muñoz-Arnanz *et al.* [14] for DP stereoisomers and dechlorinated-DPs in gull egg samples using a matrix solid-phase dispersion procedure and an analyte determination by GC-ECNI-MS (Q). Neugebauer *et al.* [32] also proposed a PLE GC-APCI-MS/MS (QqQ) method achieving similar mLOQs for DP and analogues in herring gull eggs (2.7-54.6 pg g^{-1} dry weight (dw)). These findings demonstrated the feasibility of the developed method for the determination of the target compounds in complex biota samples.

The sPLE GC-APPI-HRMS method developed in this study was applied to the analysis of gull egg samples collected during the breeding season of 2014 from three Spanish natural and national parks, as detailed in section 2.2. Table 3 summarizes the concentration levels of DP and analogues found in the samples expressed as both wet weight and lipid weight basis. The levels of DP and analogues correlated to their respective locations, indicating common contamination sources for each protected area. Gull egg samples from island locations (Medes Islands and Atlantic Islands) showed *anti*-DP as the dominant compound, although relatively higher concentrations of these compounds were also observed in the Medes Island samples (0.73–0.80 ng g^{-1} ww). For samples from the Ebro Delta, similar concentration profiles were observed for both gull species. Dec-602 was the most abundant compound (0.74–0.84 ng g^{-1} ww) followed by Dec-603 (0.52–0.63 ng g^{-1} ww) and Dec-604 (0.28–0.63 ng g^{-1} ww).

Table 3. Mean and range concentrations of DP stereoisomers and analogues and fractional abundance values (f_{anti}) found in yellow-legged and Audouin's gull eggs from Ebro Delta, Atlantic Islands and Medes Islands.

Compound	Concentration in ng g^{-1} ww (ng g^{-1} lw)							
	Ebro Delta (*L. Audouinii*)		Ebro Delta (*L. Michahellis*)		Atlantic Is. Galicia (*L. Michahellis*)		Medes Islands (*L.Michahellis*)	
	Mean[a]	Range	Mean[a]	Range	Mean[a]	Range	Mean[a]	Range
Dec-602	0.79 (11.5)	0.77–0.82	0.79 (9.6)	0.74–0.84	0.30 (3.64)	0.30–0.31	0.19 (2.3)	0.16–0.207
Dec-603	0.56 (8.2)	0.52–0.59	0.59 (7.2)	0.55–0.63	0.13 (1.5)	0.10–0.14	0.36 (4.4)	0.29–0.410
Dec-604	0.29 (4.2)	0.28–0.30	0.56 (6.8)	0.51–0.63	0.23 (2.8)	0.21–0.24	n.d.[b]	–
Cl$_{10}$-DP	n.d.[b]	–	n.d.[b]	–	n.d.[b]	–	n.d.[b]	–
Cl$_{11}$-DP	n.d.[b]	–	0.011 (0.11)	0.010–0.014	0.013 (0.16)	0.012–0.014	0.015 (0.18)	0.011–0.019
Syn-DP	0.08 (1.2)	0.09–0.08	0.16 (2.0)	0.15–0.17	0.24 (3.0)	0.28–0.26	0.31 (3.8)	0.29–0.33
Anti-DP	0.19 (2.8)	0.19–0.21	0.38 (4.6)	0.35–0.41	0.63 (7.7)	0.61–0.65	0.76 (9.3)	0.73–0.80
Σ DPs	0.28 (4.0)	0.27–0.29	0.54 (6.6)	0.50–0.59	0.87 (10.6)	0.85–0.91	1.08 (13.1)	1.05–1.12
f_{anti} ± SD[c]	0.70 ± 0.01	0.68–0.71	0.70 ± 0.01	0.69–0.71	0.72 ± 0.01	0.71–0.73	0.71 ± 0.02	0.69–0.73

[a] n=3; [b] not detected; [c] f_{anti} = [anti-DP]/([anti-DP]+[syn-DP]).

Regarding dechlorinated DPs, Cl_{10}-DP was not found and Cl_{11}-DP was detected in all the yellow-legged gull eggs analysed at very low concentration levels (0.010-0.019 ng g^{-1} ww). The differences on the concentration profiles may suggest that Atlantic and Medes Islands colonies have been more exposed to DP stereoisomers probably due to the gull feeding habits in long-time contaminated areas which are close to industries or agricultural activities. In contrast, Ebro Delta concentration profile indicated nearby contamination since DP analogues are the dominant chemicals in the samples from this area. Concerning the total DP content (sum of both stereoisomer concentrations) accumulated by yellow-legged gull (*L. michahellis*) across the three areas, the highest concentration levels were observed in the Medes Islands (1.05–1.12 ng g^{-1} ww). In contrast, lower concentration levels of Dec-604 and total DP content were found for Adouin's gull protected species compared to common yellow-legged gull. Considering that both species share the same habitat and similar biology, the differences in DP levels may be mainly attributed to the feeding habits. While *L. audouinii* feeds exclusively on pelagic fish, *L. michahellis* has an opportunistic diet. In fact, Muñoz-Arnanz *et al*. [14] reported levels in eggs of yellow-legged gull (0.52–6.05 ng g^{-1} lw) and Audouin's gull (0.06–1.75 ng g^{-1} lw) collected in the Chafarinas Islands, (Mediterranean coast of Morocco), which were quite similar to those obtained in the present work. Regarding the *anti*-DP fraction, f_{anti}, the values remain in the range of 0.68–0.73 with an average value of 0.71 ± 0.01. This value was similar to the *anti*-DP fraction of the commercial technical DP mixture (f_{anti} = 0.65) [33], suggesting there was not stereoisomer enrichment in the samples analysed.

4. Conclusions

The suitability of the GC-APPI source coupled to HRMS (Orbitrap) has been demonstrated for the determination of DP and analogues in complex environmental samples such as gull eggs. The use of negative ion APPI ionization using dopants with high vapour pressures (e.g., diethyl ether) provided an efficient ionization of the target compounds leading to characteristic in-source fragment ions as well as the molecular ion and/or cluster ions with oxygen atoms, that ensure both quantitation and confirmation purposes. Moreover, high ion source temperatures are needed to avoid potential post-column peak broadening mainly due to the low vapour pressure of the analytes. Under these conditions, the GC-APPI-HRMS methods provided a high detection capability (iLODs: 0.006-0.15 pg injected) similar or slightly better than those obtained with high-vacuum ionization techniques (EI, NICI). Moreover, the acquisition of high-resolution full-scan mass spectra allows not only a selective and sensitive determination of the analytes but also the possibility to detect possible related compounds in the same sample. The developed method, combined with a selective pressurized liquid extraction, allowed an accurate determination of the target compounds in gull egg samples at very low concentration levels (mLODs: 0.05-2 pg g^{-1} ww) The results obtained showed that DP stereoisomers, *syn*-DP, *anti*-DP, were the most abundant compounds in Atlantic and Medes islands, while DP analogues (Dec-602, Dec-603, Dec-604) dominated in the Ebro Delta samples. In this last location, Adouin's gull protected species showed lower levels of DP

isomers compared to common yellow-legged gull, which might be correlated with their fish-based diet. Consequently, the developed GC-APPI-HRMS (Orbitrap) method can be proposed for the determination of DP and analogues in biota samples, providing significant advantages over existing methods in terms of sensitivity and selectivity.

Acknowledgements

Compliance with Ethical Standards

Conflict of Interest The authors declare that they have no conflict of interest.

References

1. Qiu X, Marvin CH, Hites RA. Dechlorane plus and other flame retardants in a sediment core from Lake Ontario. Environ Sci Technol. 2007;41:6014–9. https://doi.org/10.1021/es070810b.

2. Sverko E, Tomy GT, Reiner EJ, Li YF, McCarry BE, Arnot JA, Law RJ, Hites RA. Dechlorane Plus and related compounds in the environment: A review. Environ Sci Technol. 2011;45:5088–98. https://doi.org/10.1021/es2003028.

3. Hoh E, Zhu L, Hites RA. Dechlorane plus, a chlorinated flame retardant, in the Great Lakes. Environ Sci Technol. 2006;40:1184–9. https://doi.org/10.1021/es051911h.

4. Zhu J, Feng YL, Shoeib M. Detection of dechlorane plus in residential indoor dust in the City of Ottawa, Canada. Environ Sci Technol. 2007;41:7694–8. https://doi.org/10.1021/es071716y.

5. Gauthier LT, Hebert CE, Weseloh DVC, Letcher RJ. Current-use flame retardants in the eggs of herring gulls (*Larus argentatus*) from the Laurentian Great Lakes. Environ Sci Technol. 2007;41:4561–7. https://doi.org/10.1021/es0630487.

6. Siddique S, Xian Q, Abdelouahab N, Takser L, Phillips SP, Feng Y-L, Wang B, Zhu J. Levels of dechlorane plus and polybrominated diphenylethers in human milk in two Canadian cities. Environ Int. 2012;39:50–5. https://doi.org/10.1016/j.envint.2011.09.010.

7. Ben Y-J, Li X-H, Yang Y-L, Li L, Zheng M-Y, Wang W-Y, Xu X-B. Placental transfer of dechlorane plus in mother-infant pairs in an E-waste recycling area (Wenling, China). Environ Sci Technol. 2014;48:5187–93. https://doi.org/10.1021/es404106b.

8. Möller A, Xie Z, Sturm R, Ebinghaus R. Large-scale distribution of dechlorane plus in air and seawater from the Arctic to Antarctica. Environ Sci Technol. 2010;44:8977–82. https://doi.org/10.1021/es103047n.

9. Shen L, Reiner EJ, Macpherson KA, Kolic TM, Sverko E, Helm PA, Bhavsar SP, Brindle ID, Marvin CH. Identification and screening analysis of halogenated norbornene flame retardants in the Laurentian Great Lakes: Dechloranes 602, 603, and 604. Environ Sci Technol. 2010;44:760–6. https://doi.org/10.1021/es902482b.

10. Guerra P, Fernie K, Jiménez B, Pacepavicius G, Shen L, Reiner E, Eljarrat E, Barceló D, Alaee M. Dechlorane plus and related compounds in peregrine falcon (*Falco peregrinus*) Eggs from Canada and Spain. Environ Sci Technol. 2011;45:1284–90. https://doi.org/10.1021/es103333j.

11. Barón E, Giménez J, Verborgh P, Gauffier P, De Stephanis R, Eljarrat E, Barceló D. Bioaccumulation and biomagnification of classical flame retardants, related halogenated natural compounds and alternative flame retardants in three delphinids from Southern European waters. Environ Pollut. 2015;203:107–15. https://doi.org/10.1016/j.envpol.2015.03.041.

12. Widelka M, Lydy MJ, Wu Y, Chen D. Statewide surveillance of halogenated flame retardants in fish in Illinois, USA. Environ Pollut. 2016;214:627–34. https://doi.org/10.1016/j.envpol.2016.04.063.

13. UNEP. Proposal to list Dechlorane Plus (CAS No. 13560-89-9) and its syn-isomer (CAS No. 135821-03-3) and anti-isomer (CAS No. 135821-74-8) in Annexes A, B and/or C to the Stockholm Convention on Persistent Organic Pollutants. UNEP/POPS/POPRC.15/3. 2019.

14. Muñoz-Arnanz J, Roscales JL, Vicente A, Aguirre JI, Jiménez B. Dechlorane plus in eggs of two gull species (*Larus michahellis* and *Larus audouinii*) from the southwestern Mediterranean Sea. Anal Bioanal Chem. 2012;404:2765–73. https://doi.org/10.1007/s00216-012-6326-7.

15. Barón E, Eljarrat E, Barceló D. Analytical method for the determination of halogenated norbornene flame retardants in environmental and biota matrices by gas chromatography coupled to tandem mass spectrometry. J Chromatogr A. 2012;1248:154–60 . https://doi.org/10.1016/j.chroma.2012.05.079.

16. Malak IA, Cariou R, Guiffard I, Vénisseau A, Dervilly-Pinel G, Jaber F, Le Bizec B. Assessment of Dechlorane Plus and related compounds in foodstuffs and estimates of daily intake from Lebanese population. Chemosphere. 2019;235:492–7. https://doi.org/10.1016/j.chemosphere.2019.06.148.

17. Revelsky IA, Yashin YS, Sobolevsky TG, Revelsky AI, Miller B, Oriedo V. Electron ionization and atmospheric pressure photochemical ionization in gas chromatography-

mass spectrometry analysis of amino acids. Eur J Mass Spectrom. 2003;9:497–507. https://doi.org/10.1255/ejms.581.

18. McEwen CN, McKay RG. A combination atmospheric pressure LC/MS:GC/MS ion source: Advantages of dual AP-LC/MS:GC/MS instrumentation. J Am Soc Mass Spectrom. 2005;16:1730–8. https://doi.org/10.1016/j.jasms.2005.07.005.

19. Li DX, Gan L, Bronja A, Schmitz OJ. Gas chromatography coupled to atmospheric pressure ionization mass spectrometry (GC-API-MS): Review. Anal Chim Acta. 2015;891:43–61 . https://doi.org/10.1016/j.aca.2015.08.002.

20. Organtini KL, Haimovici L, Jobst KJ, Reiner EJ, Ladak A, Stevens D, Cochran JW, Dorman FL. Comparison of Atmospheric Pressure Ionization Gas Chromatography-Triple Quadrupole Mass Spectrometry to Traditional High-Resolution Mass Spectrometry for the Identification and Quantification of Halogenated Dioxins and Furans. Anal Chem. 2015;87:7902–8. https://doi.org/10.1021/acs.analchem.5b01705.

21. Van Bavel B, Geng D, Cherta L, Nácher-Mestre J, Portolés T, Ábalos M, Sauló J, Abad E, Dunstan J, Jones R, Kotz A, Winterhalter H, Malisch R, Traag W, Hagberg J, Ericson Jogsten I, Beltran J, Hernández F. Atmospheric-Pressure Chemical Ionization Tandem Mass Spectrometry (APGC/MS/MS) an Alternative to High-Resolution Mass Spectrometry (HRGC/HRMS) for the Determination of Dioxins. Anal Chem. 2015;87:9047–53. https://doi.org/10.1021/acs.analchem.5b02264.

22. Ayala-Cabrera JF, Ábalos M, Abad E, Moyano E, Santos FJ. Feasibility of gas chromatography-atmospheric pressure photoionization–high-resolution mass spectrometry for the analysis of polychlorinated dibenzo-p-dioxins, dibenzofurans, and dioxin-like polychlorinated biphenyls in environmental and feed samples. Anal Bioanal Chem. 2020;412:3703–16. https://doi.org/10.1007/s00216-020-02615-7.

23. Di Lorenzo RA, Lobodin V V., Cochran J, Kolic T, Besevic S, Sled JG, Reiner EJ, Jobst KJ. Fast gas chromatography-atmospheric pressure (photo)ionization mass spectrometry of polybrominated diphenylether flame retardants. Anal Chim Acta. 2019;1056:70–8. https://doi.org/10.1016/j.aca.2019.01.007.

24. Portolés T, Rosales LE, Sancho J V., Santos FJ, Moyano E. Gas chromatography-tandem mass spectrometry with atmospheric pressure chemical ionization for fluorotelomer alcohols and perfluorinated sulfonamides determination. J Chromatogr A. 2015;1413:107–16 . https://doi.org/10.1016/j.chroma.2015.08.016.

25. Ayala-Cabrera JF, Contreras-Llin A, Moyano E, Santos FJ. A novel methodology for the determination of neutral perfluoroalkyl and polyfluoroalkyl substances in water by gas chromatography-atmospheric pressure photoionisation-high resolution mass spectrometry. Anal Chim Acta. 2020;1100:97–106. https://doi.org/10.1016/j.aca.2019.12.004.

26. Liu X, Wu Y, Zhang X, Shen L, Brazeau AL, Adams DH, Marler H, Watts BD, Chen D. Novel Dechlorane Analogues and Possible Sources in Peregrine Falcon Eggs and Shark Livers from the Western North Atlantic Regions. Environ Sci Technol. 2019;53:3419–28. https://doi.org/10.1021/acs.est.8b06214.

27. Megson D, Robson M, Jobst KJ, Helm PA, Reiner EJ. Determination of halogenated flame retardants using gas chromatography with atmospheric pressure chemical ionization (APCI) and a high-resolution quadrupole time-of-flight mass spectrometer (HRqTOFMS). Anal Chem. 2016;88:11406–11. https://doi.org/10.1021/acs.analchem.6b01550.

28. Luosujärvi L, Karikko M-M, Haapala M, Saarela V, Huhtala S, Franssila S, Kostiainen R, Kotiaho T, Kauppila TJ. Gas chromatography/mass spectrometry of polychlorinated biphenyls using atmospheric pressure chemical ionization and atmospheric pressure photoionization microchips. Rapid Commun Mass Spectrom. 2008;22:425–31. https://doi.org/10.1002/rcm.3379.

29. Rjabova J, Viksna A, Zacs D. Development and optimization of gas chromatography coupled to high resolution mass spectrometry based method for the sensitive determination of Dechlorane plus and related norbornene-based flame retardants in food of animal origin. Chemosphere. 2018;191:597–606. https://doi.org/10.1016/j.chemosphere.2017.10.095.

30. Sales C, Poma G, Malarvannan G, Portolés T, Beltrán J, Covaci A. Simultaneous determination of dechloranes, polybrominated diphenyl ethers and novel brominated flame retardants in food and serum. Anal Bioanal Chem. 2017;409:4507–15. https://doi.org/10.1007/s00216-017-0411-x.

31. Su G, Letcher RJ, Moore JN, Williams LL, Martin PA, de Solla SR, Bowerman WW. Spatial and temporal comparisons of legacy and emerging flame retardants in herring gull eggs from colonies spanning the Laurentian Great Lakes of Canada and United States. Environ Res. 2015;142:720–30. https://doi.org/10.1016/j.envres.2015.08.018.

32. Neugebauer F, Dreyer A, Lohmann N, Koschorreck J. Determination of halogenated flame retardants by GC-API-MS/MS and GC-EI-MS: a multi-compound multi-matrix method. Anal Bioanal Chem. 2018;410:1375–87. https://doi.org/10.1007/s00216-017-0784-x.

33. Tomy GT, Pleskach K, Ismail N, Whittle DM, Helm PA, Sverko ED, Zaruk D, Marvin CH. Isomers of dechlorane plus in Lake Winnipeg and Lake Ontario food webs. Environ Sci Technol. 2007;41:2249–54. https://doi.org/10.1021/es062781v.

Supporting Information

Analysis of Dechlorane Plus and Analogues in Gull Eggs by GC-HRMS using a Novel Atmospheric Pressure Photoionization Source

J. F. Ayala-Cabrera [a], S. Lacorte [b], E. Moyano [a], F. J. Santos [a,*]

[a] Department of Chemical Engineering and Analytical Chemistry, University of Barcelona. Av. Diagonal 645, E-08028 Barcelona, Spain

[b] Department of Environmental Chemistry, Institute of Environmental Assessment and Water Research (IDAEA-CSIC), C/Jordi Girona, 18-26, E-08034 Barcelona, Spain

* Corresponding author: Francisco Javier Santos Vicente
Phone: +34-93-403-4874
Fax: +34-93-402-1233
E-mail: javier.santos@ub.edu

Table of Contents

Supporting Tables

Table S.1. Instrumental quality parameters of the GC-APPI-HRMS method.

Analyte	Linearity (R²)[a]	Intra-day precision (RSD, %)			Inter-day precision (RSD, %)			Trueness (RE, %)			IR (RSD, %)
		Low[b]	Medium[c]	High[d]	Low[b]	Medium[c]	High[d]	Low[b]	Medium[c]	High[d]	
Syn-DP	0.997	7	4	2	9	8	6	-6	6	1	0.79 (1%)
Anti-DP	0.998	8	3	3	7	9	5	-7	-1	-0.5	0.80 (1%)
Cl$_{10}$-DP	0.997	3	4	3	3	7	3	-2	-2	-1	1.07 (1%)
Cl$_{11}$-DP	0.998	4	6	3	7	7	6	-5	-2	2	1.03 (2%)
Dec-602	0.997	6	5	6	5	4	5	1	-7	-2	1.61 (2%)
Dec-603	0.997	2	3	1	5	5	4	1	-3	-7	0.87 (2%)
Dec-604	0.997	4	1	4	7	2	4	4	-7	-1	1.02 (2%)

[a] Concentration Range: 0.5-200 pg µL^{-1}, [b] Low level: 0.5 pg µL^{-1}, [c] Medium level: 2.5 pg µL^{-1}, [d] High level: 50 pg µL^{-1}
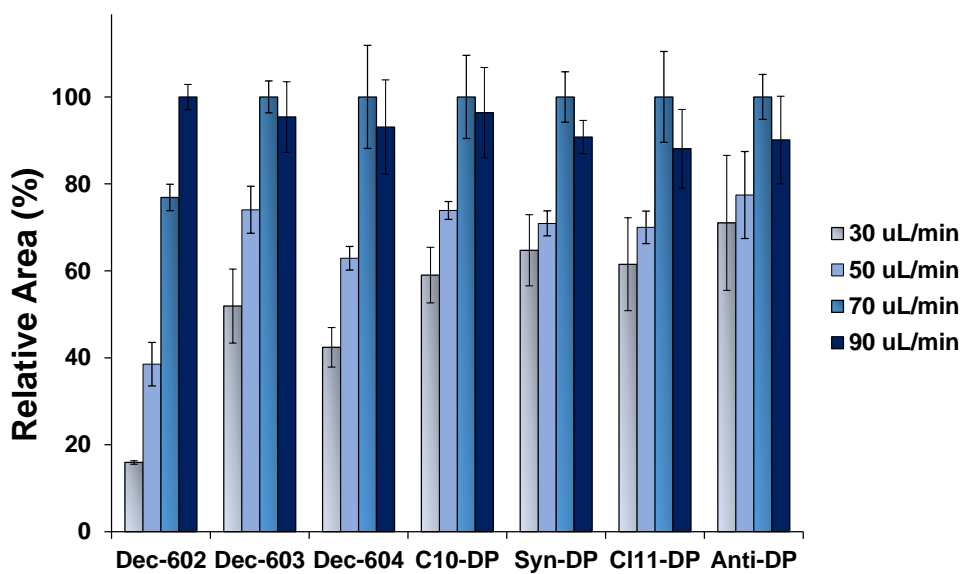
Supporting Figures

Figure S1. Effect of flow rate of diethyl ether as dopant over the GC-APPI response of DP and analogues.
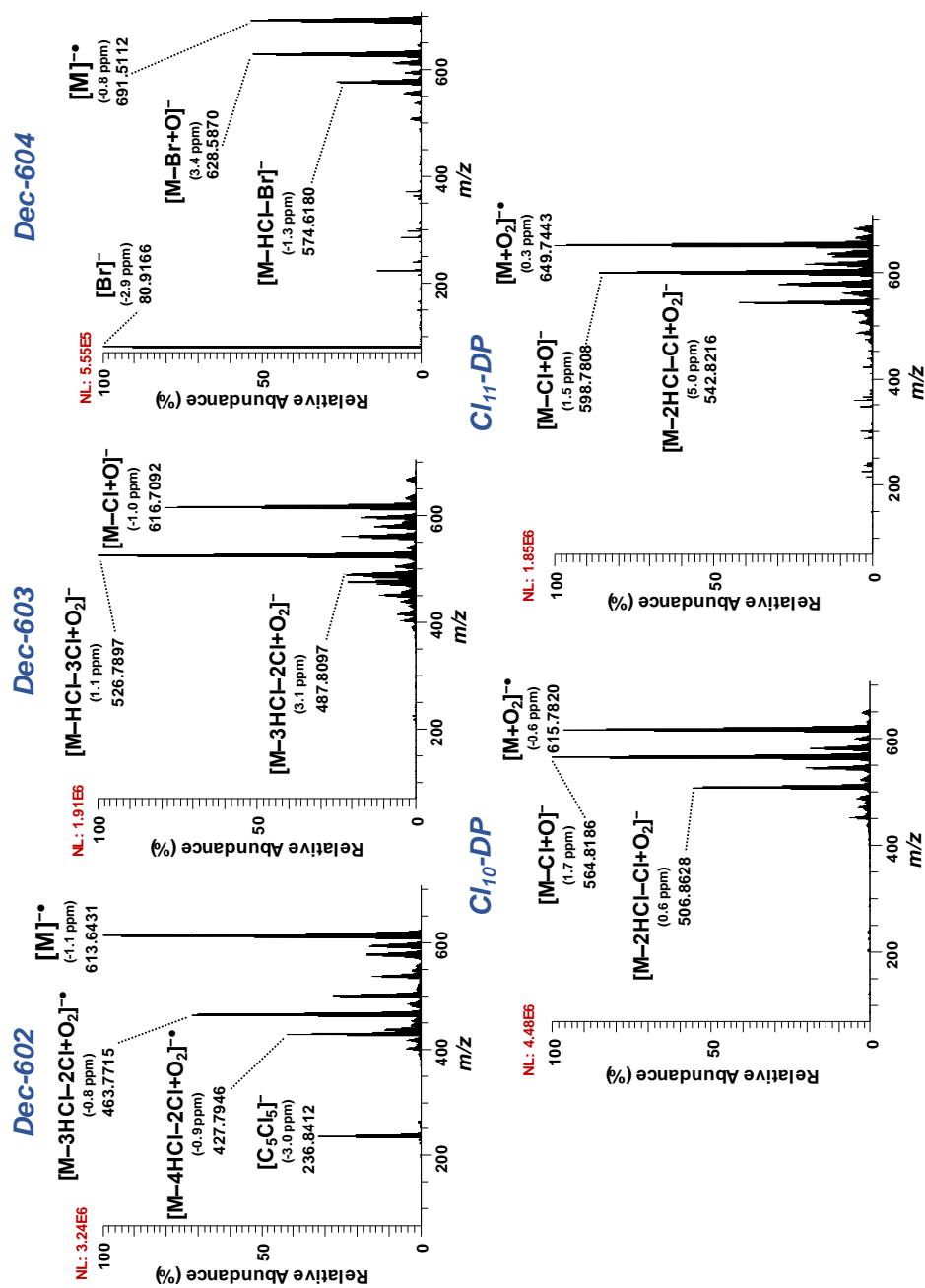
Figure S2. GC-APPI-HRMS mass spectra of dechlorinated DPs and DP analogues at an ion source temperature of 180 °C (*dopant: diethyl ether*).

3.2.2. Article VI

Ionic Liquid Stationary Phase for Improving Comprehensive Multidimensional Gas Chromatographic Separation of Polychlorinated Naphthalenes

J. F. Ayala-Cabrera, C. Lipok, J. Li, E. Moyano, O. J. Schmitz, F. J. Santos

Journal of Chromatography A, (**2020**) (*Under Review*)

Ionic Liquid Stationary Phase for Improving Comprehensive Multidimensional Gas Chromatographic Separation of Polychlorinated Naphthalenes

J. F. Ayala-Cabrera [a], C. Lipok [b,c], J. Li [b,c], E. Moyano [a], O. J. Schmitz [b,c], F. J. Santos [a,*]

[a] Department of Chemical Engineering and Analytical Chemistry, University of Barcelona. Av. Diagonal 645, E-08028 Barcelona, Spain

[b] Applied Analytical Chemistry, University of Duisburg-Essen, Universitatsstr. 5, D-45141 Essen, Germany.

[c] Teaching and Research Center for Separation, University of Duisburg-Essen, Universitatsstr. 5, D-45141 Essen, Germany.

* Corresponding author: Francisco Javier Santos Vicente
Phone: +34-93-403-4874
Fax: +34-93-402-1233
E-mail: javier.santos@ub.edu

Keywords: Polychlorinated naphthalenes, ionic liquid stationary phase, comprehensive two-dimensional gas chromatography, mass spectrometry.

Abstract

Here, we evaluate the use of an ionic liquid stationary phase to improve the comprehensive two-dimensional gas chromatographic separation (GCxGC) of polychlorinated naphthalenes (PCNs). The polarity and high thermal stability of ionic liquid stationary phases make them suitable as second dimension columns for GCxGC separations. For this purpose, the chromatographic resolution and the peak capacity of the system have been assessed using different temperature programs. The results obtained supply first data about the evaluation of these columns, allowing the congener-specific separation of PCNs in 140 min. These results represent an important decrease of time over the GCxGC-MS methodologies already published. The developed method has been applied to the characterization of different Halowax formulations, obtaining similar compositional profiles than those previously reported in the literature. These results make GCxGC-MS, using an ionic liquid stationary phase as second dimension, suitable for achieving a faster congener-specific determination of PCNs at the same time it may provide a useful tool to evaluate individual toxicity of closely eluting congeners.

1. Introduction

Polychlorinated naphthalenes (PCNs) are a group of chemicals based on a naphthalene ring in which one or more hydrogens have been replaced by chlorine atoms. They were used during the last century as multi-purpose synthetic resins and high-temperature boiling solvents in many industrial applications [1,2]. Recently, they have been classified as persistent organic pollutants by the Stockholm Convention, and nowadays, they are subject to large-scale monitoring programs to assess their occurrence and fate in the environment [3]. Some of the 75 potential congeners have even demonstrated dioxin-like toxicity [4]. Because of these dioxin-like properties, their global distribution, and accumulation in biota, the separation of all PCNs may help to understand better the toxicological contribution of each congener in the environment, humans, or food, among others [5,6]. While one-dimensional gas chromatography (1D-GC) coupled to mass spectrometry (GC-MS) allows the determination of the total content of PCNs, the congener specific analysis results more difficult due to the coelution of different congeners [7–9]. Thus, comprehensive two-dimensional gas chromatography coupled to mass spectrometry (GCxGC-MS) has been proposed to achieve their congener specific analysis [2]. Nonetheless, the theoretical 75 different congeners make challenge their determination from a chromatographic point of view, requiring prolonged temperature programs to enable the complete separation of closely eluting congeners [10].

In the last decades, the use of ionic liquid (ILs)-based stationary phases have exponentially increased [11]. ILs are organic molten salts that melt at temperatures below 100 ºC. They are constituted by a large organic cation that can be associated to a wide variety of anions and they are usually considered as 'designer solvents' due the unlimited structural variation through the combination of different organic cations and anions resulting in ILs with different physicochemical properties [12]. The most common IL organic cations contain N or P atoms (e.g., pyridinium, imidazolium, pyrrolidinium, tetra-alkyl phosphonium, etc.), combined with organic (e.g., bis(trifluoromethyl sulfonyl)imide, hexafluorophosphate, trifluoromethyl sulfate, dicyanamide, etc.) or inorganic anions (e.g., chloride, bromide, perchlorate, etc.). The interest in the use of ILs as stationary phases lies on their negligible vapor pressure, high thermal stability, and high selectivity towards different groups of chemicals. Additionally, the excellent wetting capacity on the inner wall of fused silica capillaries and the high viscosity of some ILs make them suitable as stationary phases for gas chromatography [13,14]. In fact, these characteristics as well as their high polarity provide important advantages for GCxGC separations in front of classical polyethylene glycol-based stationary phases to maximize peak capacity and reduce time analysis [11,14,15].

In this work, we explore the feasibility of an IL-stationary phase to improve the congener-specific determination of PCNs by GCxGC-MS.

2. Materials and methods

2.1. Reagents and standards

The PCN formulations (Halowax 1001, 1013, 1014 and 1099) at 10 µg mL^{-1} in cyclohexane were supplied by Dr. Ehrenstorfer GmbH (Ausburg, Germany). Equal amounts of the Halowax 1001, 1013, 1014 and 1099 (1:1:1:1 *v/v*) were mixed to obtain working standards. Moreover, a standard mixture solution (PCN-MXA) at 5 mg L^{-1} (in nonane) including 2-chloronaphthalene (CN-2), 1,5-dichloronaphthalene (CN-6), 1,2,3-trichloronaphthalene (CN-13), 1,2,3,5-tetrachloronaphthalene (CN-28), 1,2,3,5,7-pentachloronaphthalene (CN-52), 1,2,3,4,6,7-hexachloronaphthalene (CN-66), 1,2,3,4,5,6,7-heptachloronaphthalene (CN-73) and octachloronaphthalene (CN-75), was obtained from Wellington Laboratories Inc. (Guelph, ON, Canada). The isotopically labelled hexachlorobenzene ($^{13}C_6$-HCB) solution at 10 µg mL^{-1} in cyclohexane, purchased from Dr. Ehrenstorfer GmbH, was used as internal standard to correct injection variations. All the working solutions were prepared by dilution of the standards in n-hexane (Unisolv® for organic trace analysis, Merck, Darmstadt, Germany) and stored at 4 ºC before analyses.

2.2. Instrumentation

GCxGC-MS analysis was performed using a GC-2010 Plus gas chromatograph, equipped with an AOC-20 autosampler (Shimadzu, Kyoto, Japan) and coupled to a GCMS-QP2010 Ultra mass spectrometer including a quadrupole analyzer (Shimadzu). The instrument employs a two-jets cryogenic modulator using liquid nitrogen (cold-jet) and gaseous nitrogen (hot-jet) supplied by Air Liquide (Dusseldorf, Germany) as modulator gas. Modulation was performed using a modulation time of 12 s and a hot jet time of 200 ms. The 2D-separation was carried out using a non-polar DB-5MS (30 m x 0.25 mm ID; 0.25 µm) as first dimension and a polar IL-based SLB-IL60 (1.5 m x 0.1 mm ID; 0.08 µm) as second dimension. The temperature program was as follows: 80 °C (held for 5 min)-30 °C/min-160 °C (held for 5 min)-0.75°C/min-250°C (held for 0.5 min)- 5°C/min-280°C (held for 2 min) for a total run time of 140 min. Helium (Alphagaz 1, 99.9%, Air Liquid, Düsseldorf, Germany) was used as carrier gas at a constant flow rate of 1.9 mL min^{-1}. The injection (1 µL) was carried out in splitless mode (1 min) fixing the injector port temperature of 280 ºC while the transfer line temperature was set at 310 ºC. Electron ionization (EI) at 70 eV was used as ionization technique setting the ion source temperature at 200 ºC. The data acquisition was done in selected ion monitoring (SIM) mode by monitoring the two most intense peaks of the [M]$^{+•}$ cluster ion and using an event time of 0.04 s. GCMSsolution workstation software was used to control the GC-MS system while data processing was carried out with GC image *v.* 2.0 software. Moreover, peak identification was based on data previously reported in literature, comparison with chromatographic separation in one dimension (DB-5MS) as well as congeners standard solution mixture.

3. Results and discussion

3.1. GCxGC separation of PCNs

A mixture of four Halowax formulations (1001, 1013, 1014 and 1099) in the same proportion (1:1:1:1 *v/v*) was used in order to optimize the separation of the PCN congeners under the most difficult conditions. Firstly, four different modulation times were evaluated in order to take advantage of the second dimension. The IL stationary phase of SLB-IL60, consisting of a dicationic bis(trifluoromethylsulfonyl)imide [11], has a higher maximum temperature (up to 300 ºC) than traditional polyethylene glycol-based stationary phases, which may result on shorter analysis time. The first results concluded that a minimum modulation time of 8 s is needed to avoid wrap-around effects. Under these conditions, most of the analytes were separated following temperature program: 80 °C (5 min)-30 °C/min-160 °C (5 min)-1°C/min-260°C (5 min)-5°C/min-280°C (2 min) (run time: 124 min). Nonetheless, some tetra-, penta-, and hexaCN isomers were still coeluting. Therefore, a slower temperature program was proposed as an alternative to resolve these coelutions (temperature program: 80 °C (5 min)-30 °C/min-160 °C (5 min)-0.75°C/min-250°C (0.5 min)-5°C/min-280°C (2 min); run time: 140 min). Fig. 1 compares the chromatographic separation of closely eluting isomers.
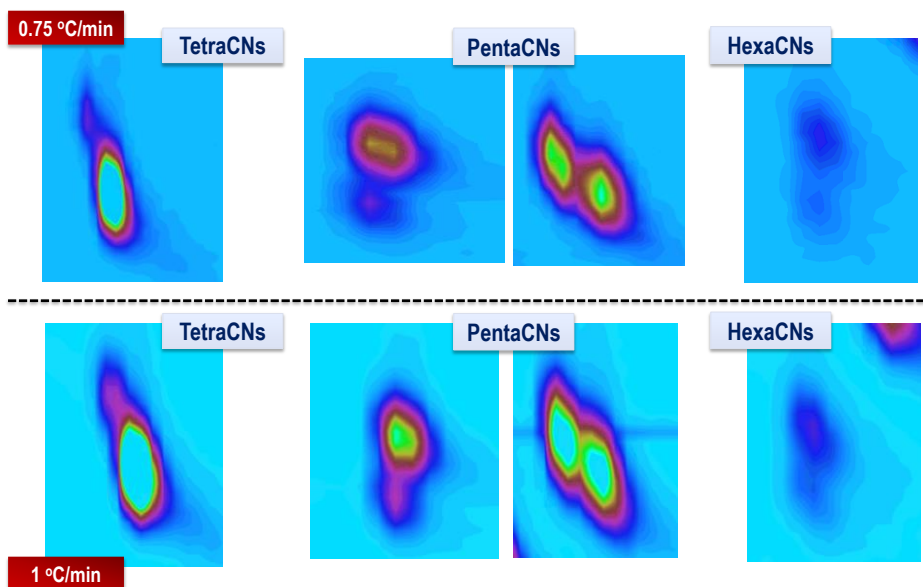
Fig. 1. Separation of closely eluting PCNs under different temperature programs.

The slower temperature program provided a better separation of the closely eluting isomers at the same time it only produced an increment of 16 minutes over the total run time. This fact was demonstrated by calculating the resolution in two-dimensional retention plane ($R_{S,2D}$) [16] of these isomers. Table 1 contains the quality parameters of the GCxGC separation of PCNs using both temperature programs. It can be observed that the resolution of the PCN pairs coeluting was higher when using the slow temperature program, achieving $R_{S,2D}$ higher than

1.0 for all of them. The use of this slow temperature program improved not only the chromatographic resolution of closely eluting PCNs but also the peak capacity of the system. The peak capacity (Eq. 1) was estimated using all the compounds detected in the 2D plot and applying the peak capacity equation corrected by the quantitative undersampling factor proposed by Davis et al. [17], although strictly speaking not all criteria for the GCxGC are fulfilled due to the long modulation time [18].

$$^{2D}n_{c,practical} = \frac{^{1}n_c \; x \; ^{2}n_c}{\sqrt{1 + 3.35 \; x \; \left(\frac{^{2}t_G \; ^{1}n_c}{^{1}t_G}\right)^2}}$$

Eq. 1. 2D peak capacity equation corrected by the quantitative undersampling factor (where n_c: peak capacity and t_G: final gradient time for each dimension).

Table 1. Peak capacity and resolution (for coeluting compounds) achieved using both temperature program methods.

Quality Parameter	Homologue group pair		1 °C/min method	0.75 °C/min method
Peak Capacity ($^{2D}n_c$)			3068.2	3707.6
Resolution ($R_{S,2D}$)	TetraCNs	(28/37)	0.81	1.27
	PentaCNs	(52/60)	0.80	1.16
		(53/62)	0.59	1.19
	HexaCNs	(68/69)	0.56	1.06
		(70/71)	0.77	1.27

As the slower temperature program provided better quality parameters, it was proposed for the GCxGC separation of PCNs (Fig. 2). The GCxGC separation using DB-5MS as first dimension and SLB-IL60 as second dimension allowed a selective determination of all the PCN congeners presented in the Halowax formulations studied, especially for tetraCNs, pentaCNs and hexaCNs. By applying an optimal modulation time of 12 s in order to take advantage of the second dimension, the method proposed achieved the baseline separation of all PCN congeners in a total run time of 140 min. This represents a decrease of 65 minutes over the analysis time of the reported method using a TG-WAX [10] stationary phase as second dimension, improving the congener specific analysis of PCNs and the throughput of the laboratories. These GCxGC separation clearly resolve overly complex coelutions previously reported in the literature, especially for tetra-, penta-, and hexaCNs. For instance, the separation of highly abundant CN-33, CN-34, and CN-37 (1,2,4,6-/1,2,4,7-/1,2,5,7-tetraCN) was easily achieved, thus representing a better separation capacity than GC-MS or fast GCxGC-MS determinations [2,7]. Regarding pentaCNs, the usually CN-52/CN-60 (1,2,3,5,7-/1,2,4,6,7-pentaCN) coeluting pair could also be completely separated by the proposed GCxGC separation using an ionic liquid column as the second dimension. Particular attention must be paid in hexaCNs, since some of them have shown the highest dioxin-like toxicity [4,19].
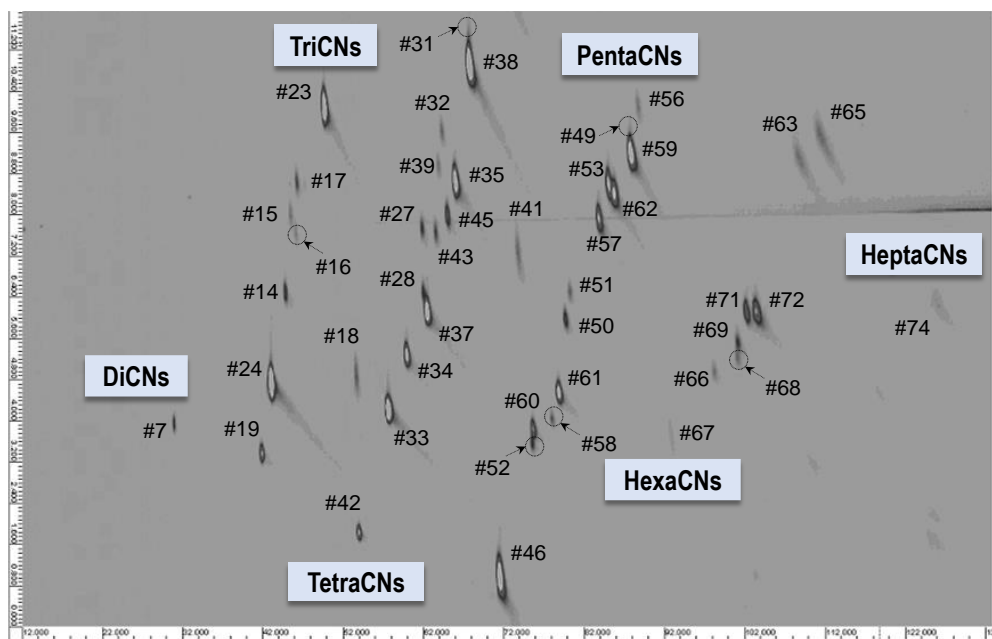
Fig. 2. GCxGC (DB-5MS, SLB-IL60) separation of PCNs (modulation time: 12 s).

Eight isomers were identified and separated, allowing the separation of CN-66/CN-67 (1,2,3,4,6,7-/1,2,3,5,6,7-hexaCN) and CN-71/CN-72 (1,2,4,5,6,8-/1,2,4,5,7,8-hexaCN), which are closely eluting by GC-MS. These results agree with those reported by Hanari *et al.* [10] demonstrating the potential of comprehensive two-dimensional gas chromatography to separate closely eluting compounds using slow temperature programs.

3.2. Characterization of Halowax formulations

The CN congener-specific characterization of four Halowax formulations (AccuStandard 1001, 1013, 1014 and 1099) is reported in Fig. 3. As can be observed, triCNs are the dominant homologue group in the Halowax 1001, being CN-23 (1,4,5-triCN) and CN-24 (1,4,6-triCN) the most abundant isomer among them. A similar profile was obtained for Halowax 1099, although the contribution of tetraCNs (from CN-27 to CN-48) was significantly higher, predominating both CN-38 (1,2,5,8-tetraCN) and CN-46 (1,4,5,8-tetraCN) isomers. In contrast, Halowax 1013 and 1014 showed a more distributed profile. Concerning Halowax 1013, the tetraCN homologue group clearly dominated the abundance profile, being CN-33 (1,2,4,6-tetraCN) and CN-38 (1,2,5,8-tetraCN) the most concentrated isomers. Besides tetraCN congeners, pentaCNs (from CN-49 to CN-62) and hexaCNs (from CN-63 to CN-72) predominated in the profile of the Halowax 1014 formulation, although triCNs also provided high abundances (4.7% for CN-23 and 8.2% for CN-24). Among them, CN-72 (1,2,4,5,7,8-hexaCN) was the most abundant PCN isomer. The results obtained were very similar to those previously reported for the characterization of Halowax formulations [10,20].
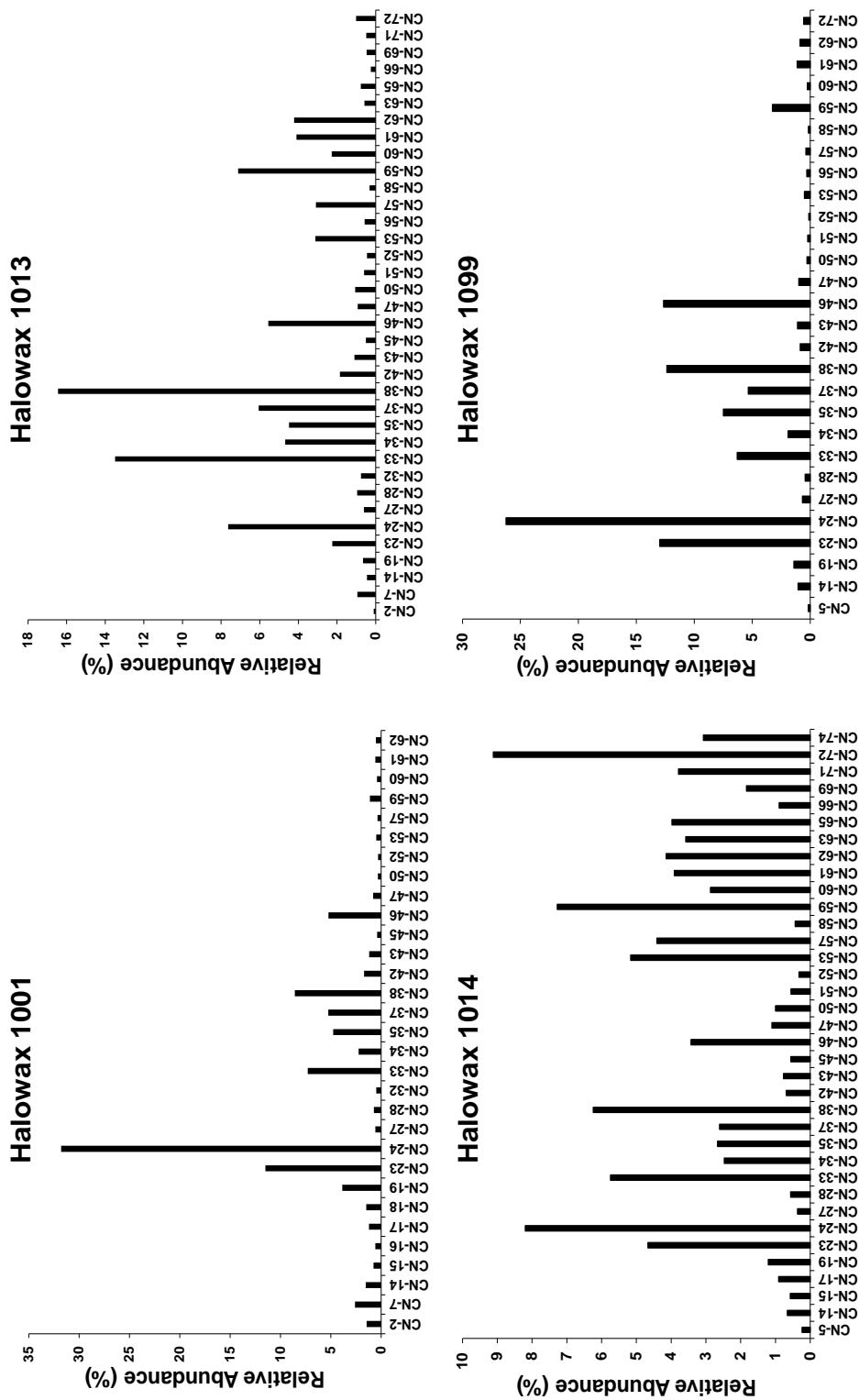
Fig. 3. Characterization of Halowax formulations (1001, 1013, 1014, and 1099) by GCxGC-MS (DB-5MS and SLB-IL60).

This fact demonstrated the feasibility of the GCxGC-MS method using an IL stationary phase as second dimension column for the specific-congener determination of PCNs.

4. Conclusions

A fast congener-specific separation of PCNs has been satisfactorily achieved by GCxGC-MS using a DB-5MS and an ionic liquid SLB-IL60 as first and second dimension columns, respectively. The application of a slow temperature program provided the complete separation of closely eluting congeners with a resolution higher than 1, at the same time an increment of 21% was observed for the peak capacity of the system. This GCxGC-MS system may allow determining the individual dioxin-like toxicity of all the PCN congeners. Moreover, the use of an IL column as second dimension allowed to achieve the separation of all PCN congeners in 140 min, which represents a decrease of 65 min over the methods already published. The feasibility of the method was finally demonstrated by means of the characterization of different Halowax formulations, obtaining very similar results than those previously reported in the literature.

Acknowledgements

Compliance with Ethical Standards

Conflict of Interest The authors declare that they have no conflict of interest.

References

[1] E. Jakobsson, L. Asplund, Polychlorinated Naphthalenes (PCNs), in: J. Paasivirta (Ed.), Handb. Environ. Chem. Vol. 3 Anthropog. Compd. Part K New Types Persistent Halogenated Compd., Springer-Verlag, Berlin, 2000: pp. 97–126. https://doi.org/10.1007/3-540-48915-0_5.

[2] E. Łukaszewicz, T. Ieda, Y. Horii, N. Yamashita, J. Falandysz, Comprehensive two-dimensional GC (GC x GC) qMS analysis of tetrachloronaphthalenes in Halowax formulations, J. Environ. Sci. Heal. - Part A Toxic/Hazardous Subst. Environ. Eng. 42 (2007) 1607–1614. https://doi.org/10.1080/10934520701517788.

[3] UNEP, Decision SC-7/14: Listing of polychlorinated naphthalenes, (2015).

[4] WHO, Concise International Chemical Assessment Document 34. Chlorinated naphthalenes, (2001).

[5] J. Falandysz, Chloronaphthalenes as food-chain contaminants: A review, Food Addit. Contam. 20 (2003) 995–1014. https://doi.org/10.1080/02652030310001615195.

[6] E.Ł. Gregoraszczuk, J. Jerzak, A. Rak-Mardyła, J. Falandysz, Halowax 1051 affects steroidogenesis, 17β-hydroxysteroid dehydrogenase (17β-HSD) and cytochrome P450arom (CYP19) activity, and protein expression in porcine ovarian follicles, Reprod. Toxicol. 32 (2011) 379–384. https://doi.org/10.1016/j.reprotox.2011.09.008.

[7] P. Castells, J. Parera, F.J. Santos, M.T. Galceran, Occurrence of polychlorinated naphthalenes, polychlorinated biphenyls and short-chain chlorinated paraffins in marine sediments from Barcelona (Spain), Chemosphere. 70 (2008) 1552–1562. https://doi.org/10.1016/j.chemosphere.2007.08.034.

[8] F. Li, J. Jin, X. Sun, X. Wang, Y. Li, S.M. Shah, J. Chen, Gas chromatography-triple quadrupole mass spectrometry for the determination of atmospheric polychlorinated naphthalenes, J. Hazard. Mater. 280 (2014) 111–117. https://doi.org/10.1016/j.jhazmat.2014.07.060.

[9] R. Lega, D. Megson, C. Hartley, P. Crozier, K. MacPherson, T. Kolic, P.A. Helm, A. Myers, S.P. Bhavsar, E.J. Reiner, Congener specific determination of polychlorinated naphthalenes in sediment and biota by gas chromatography high resolution mass spectrometry, J. Chromatogr. A. 1479 (2017) 169–176. https://doi.org/10.1016/j.chroma.2016.11.054.

[10] N. Hanari, J. Falandysz, T. Nakano, G. Petrick, N. Yamashita, Separation of closely eluting chloronaphthalene congeners by two-dimensional gas chromatography/quadrupole mass spectrometry: An advanced tool in the study and risk analysis of dioxin-like chloronaphthalenes, J. Chromatogr. A. 1301 (2013) 209–214. https://doi.org/10.1016/j.chroma.2013.05.070.

[11] A. Berthod, M.J. Ruiz-Ángel, S. Carda-Broch, Recent advances on ionic liquid uses in separation techniques, J. Chromatogr. A. 1559 (2018) 2–16. https://doi.org/10.1016/j.chroma.2017.09.044.

[12] C. Yao, J.L. Anderson, Retention characteristics of organic compounds on molten salt and ionic liquid-based gas chromatography stationary phases, J. Chromatogr. A. 1216 (2009) 1658–1712. https://doi.org/10.1016/j.chroma.2008.12.001.

[13] T.D. Ho, A.J. Canestraro, J.L. Anderson, Ionic liquids in solid-phase microextraction: A review, Anal. Chim. Acta. 695 (2011) 18–43. https://doi.org/10.1016/j.aca.2011.03.034.

[14] C. Ragonese, D. Sciarrone, P.Q. Tranchida, P. Dugo, L. Mondello, Use of ionic liquids as stationary phases in hyphenated gas chromatography techniques, J. Chromatogr. A. 1255 (2012) 130–144. https://doi.org/10.1016/j.chroma.2012.04.069.

[15] H. Nan, J.L. Anderson, Ionic liquid stationary phases for multidimensional gas chromatography, TrAC - Trends Anal. Chem. 105 (2018) 367–379. https://doi.org/10.1016/j.trac.2018.03.020.

[16] P. Jandera, Comprehensive Two-Dimensional Liquid Chromatography - Practical impacts of theoretical considerations. A review., Cent. Eur. J. Chem. 10 (2012) 844–875. https://doi.org/10.2478/s11532-012-0036-z.

[17] J.M. Davis, D.R. Stoll, P.W. Carr, Effect of first-dimension undersampling on effective peak capacity in comprehensive two-dimensional separations, Anal. Chem. 80 (2008) 461–473. https://doi.org/10.1021/ac071504j.

[18] P. Schoenmakers, P. Marriott, J. Beens, Nomenclature and conventions in comprehensive multidimensional chromatography, (2003).

[19] G. Suzuki, C. Michinaka, H. Matsukami, Y. Noma, N. Kajiwara, Validity of using a relative potency factor approach for the risk management of dioxin-like polychlorinated naphthalenes, Chemosphere. 244 (2020) 125448. https://doi.org/10.1016/j.chemosphere.2019.125448.

[20] J. Falandysz, K. Nose, Y. Ishikawa, E. Łukaszewicz, N. Yamashita, Y. Noma, HRGC/HRMS analysis of chloronaphthalenes in several batches of Halowax 1000, 1001, 1013, 1014 and 1099, J. Environ. Sci. Heal. - Part A. 41 (2006) 2237–2255. https://doi.org/10.1080/10934520600872748.

3.2.3. Article VII

Atmospheric Pressure Ionization for Gas Chromatography-High Resolution Mass Spectrometry Determination of Polychlorinated Naphthalenes in Marine Sediments

J. F. Ayala-Cabrera, C. Lipok, E. Moyano, O. J. Schmitz, F. J. Santos

Chemosphere, (**2020**) (*Under review*)

Atmospheric Pressure Ionization for Gas Chromatography-High Resolution Mass Spectrometry Determination of Polychlorinated Naphthalenes in Marine Sediments

J. F. Ayala-Cabrera [a], C. Lipok [b,c], E. Moyano [a], O. J. Schmitz [b,c], F. J. Santos [a,*]

[a] Department of Chemical Engineering and Analytical Chemistry, University of Barcelona. Av. Diagonal 645, E-08028 Barcelona, Spain

[b] Applied Analytical Chemistry, University of Duisburg-Essen, Universitatsstr. 5, D-45141 Essen, Germany.

[c] Teaching and Research Center for Separation, University of Duisburg-Essen, Universitatsstr. 5, D-45141 Essen, Germany.

* Corresponding author: Francisco Javier Santos Vicente
Phone: +34-93-403-4874
Fax: +34-93-402-1233
E-mail: javier.santos@ub.edu

Abstract

In this work, the performance of the atmospheric pressure chemical ionization (APCI) and photoionization (APPI) was assessed to develop a new selective and sensitive gas chromatography-high resolution mass spectrometry (GC-HRMS) method for the determination of polychlorinated naphthalenes (PCNs) in environmental samples. The capability of both APCI and APPI sources for the ionization of PCNs was investigated, showing the formation of the molecular ion and the [M–Cl+O]− ion in positive and negative ion modes, respectively. Positive ion APCI provided high responses using high corona ion current, while the use of high vapour pressure dopant-solvents, such as toluene in positive mode and diethyl ether in the negative mode, was required to achieve high ionization efficiencies in APPI. The performance of the two API sources in the PCN determination by GC-HRMS were instrumentally compared and the best results were achieved using the GC-APPI (+)-HRMS (Orbitrap), providing low limits of detection, good precision (RSD < 13%) and trueness (relative error <14%), although the GC-APPI (−)-HRMS (Orbitrap) also afforded a high detection capabilities from triCN to octaCNs. The GC-APPI (+)-HRMS (Orbitrap) method was applied to the characterisation of Halowax mixtures and the analysis of marine sediments collected near to the coastal area of Barcelona (NE, Spain), demonstrating a great detection capability and good enough quality parameters. Total PCN concentrations ranged from 0.35 to 5.04 ng g−1 dry weight and the presence of related compounds, such as polychlorinated biphenyls (PCBs), was also detected by combining positive and negative ion modes, providing complementary information to better

monitor the contamination of the samples. The results presented here show the feasibility of the GC-APPI-HRMS method for the suitable determination of PCNs.

1. Introduction

Polychlorinated naphthalenes (PCNs) are a family of naphthalene ring-based compounds with one or more hydrogens substituted by chlorine atoms that includes 75 potential congeners, ranging from mono- to octachlorinated napththalenes (WHO, 2001). PCNs are primarily industrial chemicals, whose production began in Germany around 1914, and their use became popular worldwide until the early 1970s (Falandysz et al., 2000; Jakobsson and Asplund, 2000). They have been employed in many industrial applications, such as high-temperature boiling solvents and multipurpose synthetic resins, as well as impregnation materials for waterproofness, flame resistance and protection again insects, among others (Jakobsson and Asplund, 2000; Łukaszewicz et al., 2007). However, PCNs are structurally similar to polychlorinated dibenzo-ρ-dioxins and dibenzofurans (PCDD/Fs) as well as polychlorinated biphenyls (PCBs), with some congeners showing dioxin-like toxicity (Kilanowicz et al., 2019a, 2019b). Currently, these compounds have been listed by the Stockholm Convention (UNEP, 2015) as persistent organic pollutants (POPs) under the annex A and C and their use and production has been banned with specific exemptions. Despite this, PCNs are still subjected to large-scale monitoring programs to evaluate their occurrence in the environment due to the great concern caused by their global distribution, high persistence, bioaccumulation capacity, and toxic effects for humans and wildlife (UNEP, 2019).

Gas chromatography coupled to mass spectrometry (GC-MS) using electron ionization (EI) is generally the method of choice for the determination of PCNs (Dat et al., 2019, Lega et al., 2017; Li et al., 2016, Noma et al., 2004, Schneider et al., 1998). EI allows an efficient ionization of PCNs, generating the molecular ion and leading to the formation of some fragment ions due to the successive losses of chlorine atoms (Castells et al., 2008). Negative ion chemical ionization (NICI) (Carrizo and Grimalt, 2006; Meijer et al., 2001; Pan et al., 2011) has also been proposed for the determination of PCNs showing high sensitivity from pentaCN to octaCN congeners, although the responses vary considerably between congeners of the same homologue group (Jakobsson and Asplund, 2000). Moreover, NICI causes a high fragmentation of PCNs (Carrizo and Grimalt, 2006) that could affect the quantification of these compounds.

In the last decades, GC-MS determinations have moved towards the use of atmospheric pressure ionization (API) sources in combination with high-resolution mass analysers, such as Orbitrap or time-of-flight (TOF) (McEwen and McKay, 2005; Revelsky et al., 2003). These high-resolution mass analysers offer important advantages with regard to the traditional magnetic sector instruments, since they can work in a very sensitive full-scan acquisition mode at the same time they are easy-handle instruments. Moreover, API sources have also additional advantages since they allow coupling gas and liquid chromatography systems to the same

high-resolution mass analyser, which could improve throughput and cost of the mass spectrometry instrument in the laboratory. The API sources, such as atmospheric pressure chemical ionization (APCI) and photoionization (APPI), provide a soft ionization and preserve the molecular ion, simplifying mass spectra interpretation obtained from complex samples. Besides, these ionization API techniques may ionize a wide range of analytes, from more polar to non-polar compounds (Li et al., 2015; Raro et al., 2014; Revelsky and Yashin, 2012). Among them, halogenated pollutants, such as PCDD/Fs, PCBs or polybrominated diphenyl ethers (PBDEs), have shown high ionization efficiency using APCI and APPI techniques (Di Lorenzo et al., 2019; Luosujärvi et al., 2008a; Portolés et al., 2016; Van Bavel et al., 2015). As far as we know, the ionization of PCNs using GC-API has not been evaluated yet and only the APPI source has been tested for PCN determination by liquid chromatography-tandem mass spectrometry (LC-MS/MS) (Moukas et al., 2016). Therefore, it is worth studying the applicability of GC-API-HRMS methods for the analysis of PCN congeners, since they would provide significant advantages not only for target analysis but also for the analysis of suspect and unknown compounds in complex samples.

In the present study, we investigate the feasibility of both APCI and APPI sources for the ionization of PCNs and their determination by GC-API-HRMS. The performance of the GC-APCI-HRMS (TOF) and GC-APPI-HRMS (Orbitrap) systems have been compared in positive and negative ion modes to select the most sensitive and selective method for the determination of PCNs in complex environmental matrices, such as marine sediments samples, and the characterization of Halowax formulations.

2. Materials and Methods

2.1. Reagents and standards

A standard mixture solution (PCN-MXA), which contains 2-chloronaphthalene (CN-2), 1,5-dichloronaphthalene (CN-6), 1,2,3-trichloronaphthalene (CN-13), 1,2,3,5-tetrachloronaphthalene (CN-28), 1,2,3,5,7-pentachloronaphthalene (CN-52), 1,2,3,4,6,7-hexachloronaphthalene (CN-66), 1,2,3,4,5,6,7-heptachloronaphthalene (CN-73) and octachloronaphthalene (CN-75) at 5 ng µL^{-1} in nonane, was purchased from Wellington Laboratories Inc. (Guelph, ON, Canada). Working solutions were prepared from the standard PCN-MXA solution by dilution with *n*-hexane (Unisolv® for organic trace analysis, Merck, Darmstadt, Germany) and stored at 4 °C prior to analysis. PCN formulations, Halowax 1001, 1013, 1014 and 1099, at 10 ng µL^{-1} in cyclohexane were obtained from Dr. Ehrenstorfer GmbH (Ausburg, Germany). The internal standard mixture ($^{13}C_{12}$-PCB), containing $^{13}C_{12}$ isotopic labelled PCBs from tri- to heptaCBs at 5 ng µL^{-1}, was also purchased from Wellington Laboratories Inc. Solvents used as APPI dopants were: toluene, chlorobenzene (Chromasolv™ Plus, for HPLC analysis, purity ≥ 99%), and anisole (anhydrous, purity > 99.7%) which were supplied by Sigma-Aldrich (St Louis, MO, USA), diethyl ether (EMSURE®, purity ≥ 99.7%) and acetone (LiChrosolv®, purity ≥ 99.8%) purchased from Merck,

and tetrahydrofuran (Photrex™ reagent, purity at 99%) obtained from J. T. Baker (Deventer, Holland). Dichloromethane for pesticide residue analysis (purity ≥ 99.9%) from Sigma-Aldrich, *n*-hexane and toluene were also used for the extraction and clean-up procedures. Helium Alphagaz™ 1 (purity ≥ 99.999%) was supplied by Air Liquide (Madrid, Spain), while nitrogen (purity > 99.995%) was purchased from Linde (Barcelona, Spain) and they were used as carrier gas and make-up gas in the GC-APPI-Orbitrap system, respectively. For the GC-APCI-TOF system, helium 5.0 as carrier gas and the nitrogen as make-up gas were obtained from Air Liquide.

2.2. Samples and sample treatment

Five coastal marine sediment samples were collected near of a submarine emissary located at 2 km from the mouth of Besòs River (Barcelona, NE Spain). This submarine emissary discharges the effluent coming from the wastewater treatment plant (WWTP) of the Besòs River. Samples were collected from sampling areas of 0.1 m^2 using a Van Veen grab sediment sampler. Afterwards, marine sediments were air-dried, grounded, sieved (125 µm mesh), homogenized and stored at 4 ^{o}C prior to their analysis. Marine sediments were submitted to a sample treatment previously described with slightly modifications (Castells et al., 2008). Briefly, 10 g of the dried marine sediment previously mixed with 10 g of anhydrous sodium sulphate and 2.5 g of activated copper powder (to remove sulphur) were Soxhlet extracted for 24 h using 300 mL *n*-hexane/dichloromethane (1:1 *v/v*). The extract was rotary evaporated to ca. 5 mL, concentrated to 1 mL under a gentle nitrogen stream and loaded onto a glass column packed with 15 g Florisil (activated at 650 ^{o}C for 12 h). Analytes were eluted in two fractions: (Fraction 1) 50 mL of n-hexane to remove PCBs interferences and (Fraction 2) 100 mL hexane/dichloromethane (1:1 *v/v*) to elute PCNs. Fraction 2 was concentrated to 100 µL and submitted to a clean-up in an ENVI-Carb Plus cartridge (400 mg, 1 mL) to remove potential non-planar chlorinated interferences. The ENVI-Carb Plus cartridge was pre-conditioned with 50 mL hexane before loading Fraction 2. The elution was carried out with 50 mL hexane to elute hydrocarbons (fraction discarded) and 50 mL toluene in backflush to elute PCNs. This extract was concentrated to 100 µL under a nitrogen stream and spiked with appropriate amounts of the $^{13}C_{12}$-PCBs internal standard mixture before its analysis by GC-API-HRMS. The recoveries of the method, which were estimated spiking a blank sediment at two different concentration levels (0.2 ng g^{-1} and 0.5 ng g^{-1}) ranged from 75 to 97%.

2.3. Instrumentation

2.3.1. GC-APPI-HRMS (Orbitrap)

A Trace 1300 gas chromatograph (Thermo Fisher Scientific, San Jose, CA, USA) equipped with a AI-1310 autosampler (Thermo Fisher Scientific) was coupled to a Q-Exactive Orbitrap mass spectrometer (Thermo Fisher Scientific) using the GC-APPI source (MasCom Technologies GmbH, Bremen, Germany), equipped with a 10.6 eV krypton lamp (Syagen,

Santa Ana, CA, USA). The chromatographic separation of PCNs was achieved using a DB-5MS fused-capillary column (30 m x 0.25 mm I.D., 0.25 µm of film thickness) supplied by Agilent Technologies (Santa Clara, CA, USA) and the oven temperature was programmed as follows: 90 ^{o}C (held for 1 min) to 160°C (held for 1 min) at 15°C min^{-1}, and then to 300 ^{o}C (held for 5 min) at 5°C min^{-1}.The carrier gas (helium) was set at constant flow rate at 1 mL min^{-1}. Transfer line was set at 280 ºC whereas the ion source and capillary temperatures were set at 210 ^{o}C after optimization (see Fig. S1a and S1b). Moreover, the pressure of the nitrogen make-up gas used in the GC-APPI interface was set at 5 a.u. and the S-lens radiofrequency was fixed at 50%. For the APPI dopant-assisted ionization of PCNs, toluene vapours flow rate was optimized from 10 to 90 µL min^{-1}, obtaining the highest responses at 70 µL min^{-1} (see Fig. S1c). Samples and standards were injected (1 µL) in splitless mode (1 min) at 280 ^{o}C. Data were acquired in both positive and negative ion full-scan mode (*m/z* 100-600) at a resolution of 35,000 full width at half maximum (FWHM) at *m/z* 200. Additionally, the maximum injection time and the AGC target were set at 50 ms and 3·10^6, respectively. Q-Exactive mass spectrometer was calibrated every 72 h using the electrospray source and a calibration solution that contained caffeine, MRFA peptide, Ultramark 1621 and butylamine in acetonitrile/methanol/water (2:1:1, v/v) with 1% (v/v) formic acid. The quantitation was performed using the internal calibration method and the ion chromatograms were extracted employing mass extraction windows with a tolerance of ±5 ppm. The instrument control, data acquisition, and data processing were carried out using the Xcalibur *v* 3.1 software.

2.3.2. GC-APCI-HRMS (TOF)

A 6890N Network GC system gas chromatograph equipped with 7683B series autosampler (Agilent Technologies) was coupled to a 6545 iFunnel Q-TOF LC/MS using the APCI source (Agilent Technologies). The chromatographic separation of PCNs was performed in a HP-5MS fused-capillary (30 m x 0.25 mm I.D., 0.25 µm film thickness) purchased from Agilent Technologies. The oven temperature program used was that previously described (*Section 2.3.1*) and the carrier gas was set at constant flow rate (He, 1 mL min^{-1}). A volume of 1 µL of samples and standards was injected in splitless mode (1 min). Moreover, the transfer line temperature was set at 280 ^{o}C, whereas the ion source temperature, optimized from 200 ºC to 275 ºC, was fixed at 275 ^{o}C (see Fig. S2). The corona current and the capillary voltage in the APCI source were fixed at 10 µA and 1,000 V, respectively. Additionally, nitrogen was used as make-up gas at a flow rate of 11 L min^{-1}, while de fragmentor voltage was set at 380 V. Data were acquired in positive and negative ion full-scan mode (*m/z* 100-600) working at a resolution of 40,000 (at *m/z* 2,722). Calibration of TOF mass analyser was performed each day before installing the APCI source by infusing a tuning mix (G1969-85000, Agilent Technologies) at low concentration. The gas chromatograph was controlled using the Leco chroma TOF GC *v*. 3.44 software, while the control of the mass spectrometer, data acquisition, and data processing were carried out using the Mass Hunter *v* B.09.00 software.

2.4. Quality assurance and quality control

The identification of each PCN congener was carried out by retention time compared to standards and elution orders previously stablished in the literature (Falandysz et al., 2006; Noma et al., 2004; Schneider et al., 1998), and quantified using and isotope ratio tolerance within ±15% of the theoretical values. The instrumental and method performance were checked by injecting quality control solutions and procedure blanks periodically. Moreover, the recoveries of the method, which were estimated spiking a blank sediment at two different concentration levels (0.2 ng g^{-1} and 0.5 ng g^{-1}), always ranged from 75 to 97%.

3. Results and Discussion

3.1. Atmospheric pressure ionization of PCNs

In this work, we have evaluated the use of atmospheric pressure chemical ionization (APCI) and atmospheric pressure photoionization (APPI) as alternative techniques to the traditionally used high-vacuum EI and NICI for the determination of PCNs by GC-HRMS. Initial experiments were conducted to investigate the behaviour of these ionization techniques and the optimal operational conditions for the sensitive measurements of all PCN congeners. Among the working conditions assessed, PCNs led only to the generation of the molecular ion [M]$^{+\bullet}$ in positive ion mode with both GC-APCI and GC-APPI, as can be seen as an example in the GC-APPI mass spectra showed in Fig. 1 for diCN (CN-6), pentaCN (CN-52) and octaCN (CN-75). However, the base peak of the mass spectra in negative ion mode under both API mechanisms was the ion [M–Cl+O]$^-$ (Fig. 1).

Regarding the APPI source, the addition of different dopants was evaluated to improve the ionization efficiency of the analytes (Fig. 2). In positive ion mode, the use of toluene and chlorobenzene significantly increased the abundance of the molecular ions of PCNs in front of the signals observed in the direct photoionization process (Fig. 2a). These solvents generated abundant dopant molecular ions (see Fig. S3) that interacted with neutral molecules of PCNs through charge-exchange reactions in the gas-phase to yield the molecular ion of PCNs (Kauppila et al., 2014). Although anisole generated the dopant molecular ion through the photoionization process, the low vapour pressure and the ionization potential (4.2 torr at 25 ºC, 8.20 eV) of this dopant, compared with toluene (27.7 torr at 25 ºC, 8.83 eV) and chlorobenzene (11.2 torr at 25 ºC, 9.07 eV), might limit its capacity to interact with the PCN molecules in gas-phase. On the other hand, PCNs also showed low responses using dopants with high proton affinity such as acetone, tetrahydrofuran and diethyl ether. These dopants mainly generated the [D+H]$^+$ ion (see Fig. S3) in the APPI source due to a self-protonation process after the dopant photoionization (Kauppila et al., 2015), which may hinder the ionization of PCNs that takes place by charge-exchange reactions. Among all dopants tested, toluene led to the highest ionization efficiency of this family of compounds and it was selected for further studies. Concerning the negative ion mode, phenoxide ion [M–Cl+O]$^-$ dominated
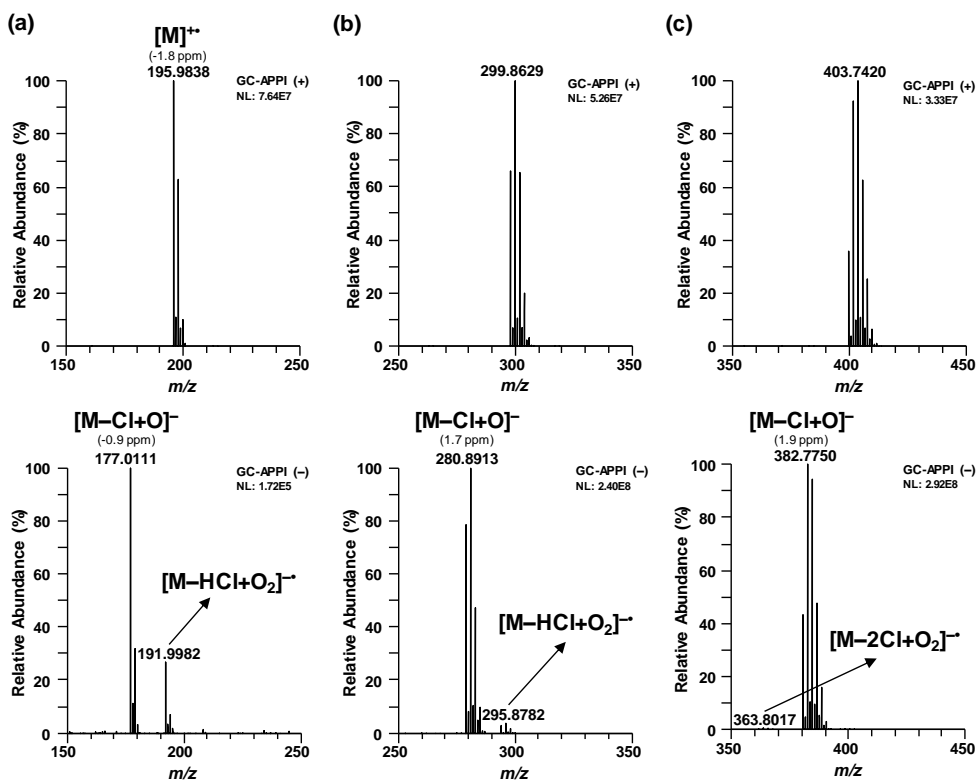
Fig. 1. GC-APPI mass spectra of (a) diCN (CN-6), (b) pentaCN (CN-52) and (c) octaCN (CN-75) in positive (dopant: toluene) and negative ion modes (dopant: diethyl ether) (source and capillary temperatures set at 210 °C).

the mass spectra of PCNs and it could have been generated through gas-phase reactions mediated by the oxygen or the ion $O_2^{-\bullet}$ as follows:

(1) $D + h\nu \rightarrow D^{+\bullet} + e^{-\bullet}$ (if ionization energy (D) < 10.6 eV)
(2) $O_2 + e^{-\bullet} \rightarrow O_2^{-\bullet}$
(3) $M + O_2^{-\bullet} \rightarrow [M–Cl+O]^{-\bullet} + OCl^{\bullet}$
(4) $M + e^{-\bullet} \rightarrow M^{-\bullet}$
(5) $M^{-\bullet} + O_2 \rightarrow [M–Cl+O]^{-\bullet} + OCl^{\bullet}$

In this mode, the best results were achieved using diethyl ether (Fig. 2b), which presents both the highest vapour pressure and the highest ionization potentials among the dopants tested (see. Table S1). The high vapour pressure ensured a high concentration of dopant in the gas-phase and, consequently, high number electrons released after the dopant photoionization process (Eq. 1), thus favouring the ionization of the oxygen (Eq. 2) and the subsequent gas-phase reactions of the superoxide ion with the analyte neutral molecules (Eq. 3). The high electronegativity of PCNs can also favour electron capture reactions to generate the molecular ion (Eq. 4), which can be further react with trace quantities of oxygen
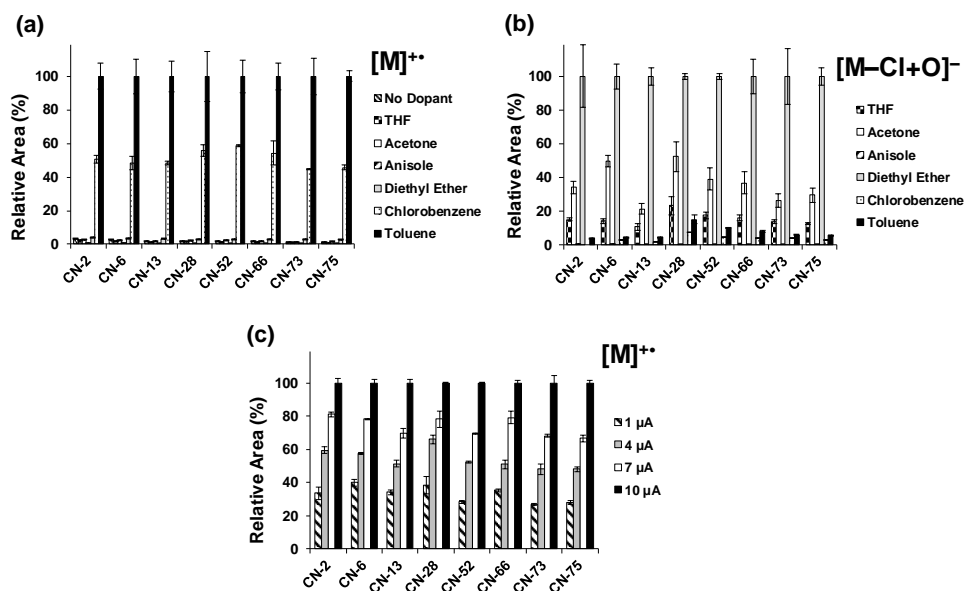
Fig. 2. Effect of dopants in (a) positive and (b) negative ion APPI and effect of (c) corona current in positive ion APCI over the response of PCNs.

to form the phenoxide ion (Eq. 5). At the same time, the high ionization potential of diethyl ether led to more energetic electrons that may also improve the ionization of PCN molecules.

Regarding APCI, PCN congeners were only efficiently ionized in positive ion mode. To improve the response, we tested the effect of corona discharge current (from 1 to 10 µA) over the ion signal and it was observed that the response of PCNs increased at high current values without any kind of in-source fragmentation (Fig. 2c). This result differed from those previously reported for similar compounds such as PCDD/Fs and PCBs (1-2 µA) (Geng et al., 2016; Portolés et al., 2016; ten Dam et al., 2016; Van Bavel et al., 2015), maybe due to the high stability of the molecular ion of PCNs. Consequently, a corona current of 10 µA working under dry conditions (no ion source humidity) was selected as the optimal conditions for the suitable ionization of PCNs using the APCI source.

The performance of the GC-APPI-Orbitrap and GC-APCI-TOF methods was evaluated to select the most suitable one for the determination of PCNs. The two most intense isotope ions of both molecular ion (in positive ion mode) and phenoxide ion (in negative ion mode) were monitored for quantitation and confirmation purposes. Moreover, the ion ratio (IR: abundance ratio between the ion with the lowest and the highest *m/z* values) was used as an additional confirmatory criterion (Table 1). In addition, run-to-run precision and trueness were estimated by triplicate analysis of standards solutions at three concentration levels (low: 0.25 pg µL^{-1}; medium: 5 pg µL^{-1} and high: 100 pg µL^{-1}). Run-to-run precision, expressed as the relative standard deviation (RSD, %), ranged from 2 to 13%, whereas the trueness (relative error between the calculated and the theoretical concentration) was always lower than 14%

Table 1. Selected ions for GC-APCI-HRMS and GC-APPI-HRMS analysis of PCNs in positive and negative ion modes.

Compound	Positive ion mode (APCI and APPI)					Negative ion mode (APPI)				
	Formula	Q-ion (m/z) [a]	Formula	q-ion (m/z) [b]	IR	Q-ion (m/z) [a]	Formula	q-ion (m/z) [b]	Formula	IR
MonoCNs	[M]+•	162.0231	[M+2]+•	164.0201	3.13	143.0502	[M−Cl+O]-	144.0536	[M+1−Cl+O]-	9.09
DiCNs	[M]+•	195.9841	[M+2]+•	197.9812	1.56	177.0113	[M−Cl+O]-	179.0083	[M+2−Cl+O]-	3.13
TriCNs	[M]+•	229.9451	[M+2]+•	231.9422	1.04	210.9723	[M−Cl+O]-	212.9693	[M+2−Cl+O]-	1.56
$^{13}C_{12}$-TriCBs	[M]+•	268.0010	[M+2]+•	269.9981	1.04	249.0282	[M−Cl+O]-	251.0253	[M+2−Cl+O]-	1.56
TetraCNs	[M+2]+•	265.9032	[M]+•	263.9062	0.79	244.9333	[M−Cl+O]-	246.9304	[M+2−Cl+O]-	1.04
$^{13}C_{12}$-TetraCBs	[M+2]+•	303.9591	[M]+•	301.9621	0.78	282.9881	[M−Cl+O]-	284.9852	[M+2−Cl+O]-	1.04
PentaCNs	[M+2]+•	299.8642	[M+4]+•	301.8613	1.56	280.8914	[M+2−Cl+O]-	278.8943	[M−Cl+O]-	0.78
$^{13}C_{12}$-PentaCBs	[M+2]+•	337.9201	[M+4]+•	339.9172	1.56	318.9462	[M+2−Cl+O]-	316.9492	[M−Cl+O]-	0.78
HexaCNs	[M+2]+•	333.8253	[M+4]+•	335.8223	1.25	316.8495	[M+2−Cl+O]-	314.8524	[M+4−Cl+O]-	1.56
$^{13}C_{12}$-HexaCBs	[M+2]+•	371.8812	[M+4]+•	373.8782	1.25	352.9072	[M+2−Cl+O]-	354.9043	[M+4−Cl+O]-	1.56
HeptaCNs	[M+2]+•	367.7863	[M+4]+•	369.7833	1.05	348.8135	[M+2−Cl+O]-	350.8105	[M+4−Cl+O]-	1.25
OctaCN	[M+4]+•	403.7444	[M+2]+•	401.7473	0.89	382.7745	[M+2−Cl+O]-	384.7715	[M+4−Cl+O]-	1.03
$^{13}C_{12}$-HeptaCBs	[M+2]+•	405.8422	[M+4]+•	407.8393	1.04	386.8683	[M+2−Cl+O]-	388.8653	[M+4−Cl+O]-	1.25

[a] Quantifier ion; [b] qualifier ion

(Table 2). Concerning the detection capability in positive ion mode (+), the instrumental limits of detection (ILODs), defined as the analyte concentration that led to a signal-to-noise ratio of 3 of the ion selected for confirmation purposes, achieved using GC-APPI (+)-Orbitrap were from 8 to 17 times lower than those obtained with GC-APCI (+)-TOF. Regarding the negative ion mode, GC-APPI (–)-Orbitrap provided the lowest ILODs for PCNs, from tetraCNs to OctaCN, with values ranging from 1.5 to 15 times lower than those obtained with GC-APPI (+)-Orbitrap and up to 160 times lower than the ILODs achieved using the GC-APCI (+)-TOF.

Table 2. Instrumental limits of detection for the analysis of PCN congers by positive and negative ion GC-APPI-Orbitrap and positive GC-APCI-TOF.

PCN congener	GC-APPI (+)-Orbitrap	GC-APPI (–)-Orbitrap	GC-APCI (+)-TOF
	ILOD (pg injected)[a]	ILOD (pg injected)[a]	ILOD (pg injected)[a]
CN-2 (MonoCN)	0.02	45	0.3
CN-6 (DiCN)	0.02	8	0.3
CN-13 (TriCN)	0.03	0.15	0.5
CN-28 (TetraCN)	0.03	0.02	0.5
CN-52 (PentaCN)	0.05	0.01	0.5
CN-66 (HexaCN)	0.05	0.01	0.7
CN-73 (HeptaCN)	0.10	0.01	0.8
CN-75 (OctaCN)	0.15	0.01	1.6

[a] Injection volumen: 1µL

Nonetheless, the GC-APPI (–)-Orbitrap also provided high ILODs for lowly chlorinated PCNs, especially mono- and diCNs. Considering the ionization of PCNs in negative ion APPI mode is subjected to electron capture or charge exchange reactions, a low number of highly electronegative Cl atoms may difficult these reactions thus reducing the ionization efficiency of these homologue groups and leading to high ILODs. Thereby, the GC-APPI (+)-Orbitrap method was chosen as the most suitable method for the analysis of PCNs, although the figures of merit of this method may be also determined in real samples. The ILODs achieved with the proposed method (0.02-0.15 pg injected on column) were similar to those reported using GC-HRMS (magnetic sector MS) operated in electron ionization (Lega et al., 2017). The main advantages of the GC-APPI (+)-Orbitrap were the absence of in-source fragmentation that increases the selectivity, the use of an easy-handle high-resolution mass spectrometer and the possibility to work in full scan mode with high an excellent sensitivity. Moreover, it also provided ILODs from 5 to 270 times lower than those obtained using UHPLC-APPI (–)-MS/MS (triple quadrupole) (Moukas et al., 2016), with a high selectivity that is necessary to avoid false positives and interferences when dealing with highly complex samples.

3.2. Characterization of PCN mixtures by GC-APPI-HRMS

In order to demonstrate the good instrumental performance of the developed method, the composition of different PCN mixtures (Halowax 1001, 1013, 1014 and 1099) was

characterized using by GC-APPI (+)-Orbitrap method. To achieve this goal, each Halowax standard mixture (total concentration of PCNs of 10 ng μL^{-1}) was spiked at 200 pg μL^{-1} with the $^{13}C_{12}$ isotopic labelled PCB standard mixture and quantified by internal standard method. This approach avoids possible sub- and overestimation of some PCNs due to strong differences in the response factor. Fig. 3 shows the results obtained for the different Halowax mixtures in terms of both homologue distribution and congener-specific compositional profile. Regarding the homologue distribution, for the Halowax 1001 and 1099 mixtures, tri- and tetraCNs were the predominant homologue groups covering 89.2% and 85.7% of the total concentration of PCNs, respectively. In contrast, the Halowax 1013 and 1014 composition of were more distributed between the different homologue groups. Thus, the tetraCNs (48.2%) and pentaCNs (38.3%) were the most abundant homologue groups in Halowax 1013 mixture, although triCNs and hexaCNs also accounted an important contribution (7.7% and 5.6%, respectively). Concerning the Halowax 1014 mixture, abundances higher than 5% were obtained from tri- to heptaCN homologue groups, showing the highest contribution for the hexaCNs (37.8%). In addition, the presence of monoCNs and octaCN was detected in all Halowax mixtures at low levels (lower than 1.2% and 0.15%, respectively). The homologue profiles are similar to those obtained by Noma *et al.* (Noma et al., 2004) using Halowax formulations from Foxboro. Nonetheless, pentaCNs and hexaCNs contribution was enriched in the Halowax formulations from Dr. Ehrenstorfer, especially for the Halowax 1013 and 1014. Yamashita *et al.* (Yamashita et al., 2003) reported that triCNs and tetraCNs were also the most abundant groups in the Halowax 1001 (85%) using a DB-1701 column, although the percentage relation (TriCNs/TetraCNs ratio of 0.98) different from the ratio of 1.4 in this study, which indicated a higher proportion of the tetraCN fraction. In contrast, the ratio was quite similar than that obtained for the same Halowax formulation when using an Ultra 2 column (ratio of 1.3) (Falandysz et al., 2008), which is analogue to the DB-5MS column used with the GC-APPI-HRMS system. The quantitative results obtained with the GC-APPI (+)-Orbitrap method were statistically compared with those previously reported by Falandysz *et al.* (Falandysz et al., 2006) for Halowax mixtures of the same brand. The results of the two-way analysis of variance (ANOVA) test showed no significant differences between the GC-APPI (+)-Orbitrap method and those previously reported with the GC-EI-HRMS (sectors) system, showing *p*-values ranging from 0.89 to 0.99, which were always higher than the significant level (0.05) for all the Halowax mixtures. These results indicated no significant variations on the homologue distribution of these Halowax formulations as well as the good performance of the proposed method for the analysis of PCNs in relatively simple samples.

Regarding the congener-specific profile, the compositional profiles obtained with the GC-APPI-HRMS are shown in Fig. 3. This methodology allowed a relatively fast separation of most of PCN congeners (ca. 31 minutes) while keeping a similar number of coeluting isomers than those reported in other mono-dimensional GC methods (Dat et al., 2019; Falandysz et al., 2008; Li et al., 2014; Noma et al., 2004). However, there are still some coeluting isomeric pairs which generally required comprehensive two-dimensional separation methods to achieve their
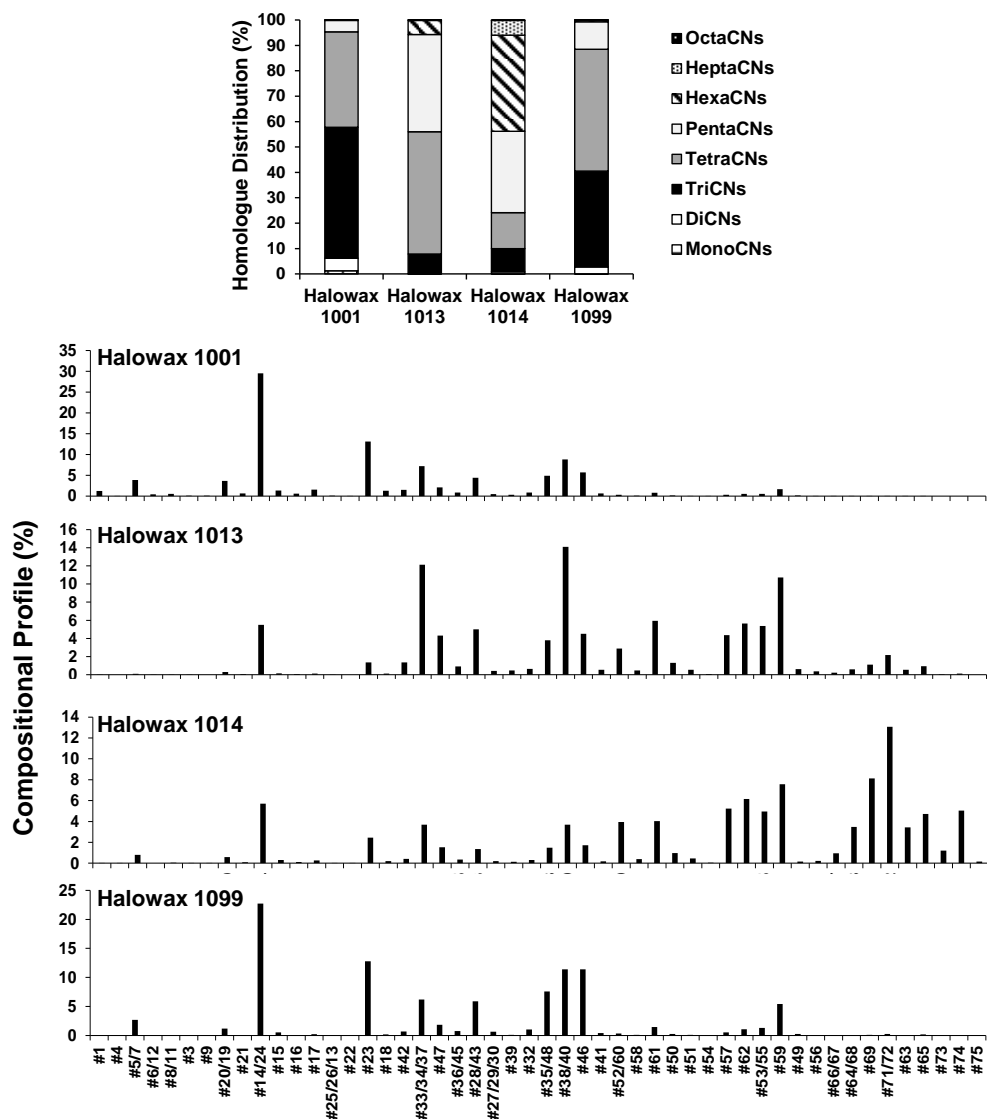
Fig. 3. Contribution of PCN homologue groups and specific-isomers (%) on the composition of Halowax formulations.

separation (Hanari et al., 2013). The compositional profiles also agree with those previously reported in the literature for AccuStandard Halowax mixtures (Falandysz et al., 2006), although some differences were also observed. For instance, the contribution of the 2-monoCN (CN-2, 2.5%) in the Halowax 1001 and 1,2,3,4,5,6,8-heptaCN (CN-74, 5.0%) in Halowax 1014 were higher than the values previously reported for the same formulations. Additionally, higher contributions were also obtained for the pair 1,4-diCN/1,6-diCN (CN-5/CN-7, 2.7%), 1,4,5,8-tetraCN (CN-46, 11.4%) and 1,2,4,5,8-pentaCN (CN-59, 5.4%) in Halowax 1099. On the other hand, regarding triCNs, the most abundant pair corresponding to 1,2,4-triCN/1,4,6-triCN

232

(CN-14/CN-24) differed from that generally reported in the literature 1,3,7-triCN/1,4,6-triCN (CN-21/CN-24) (Falandysz et al., 2006; Li et al., 2014). Thereby, it can be concluded that the CN-24 may be the triCN isomer contributing the most in these Halowax batches. These results demonstrate that GC-APPI-HRMS method could provide not only similar homologue distributions but also congener-specific compositional profiles than those previously reported in the literature.

3.3. Analysis of marine sediments by GC-APPI-HRMS

To examine the performance of the GC-APPI-HRMS method to the analysis of PCNs in environmental samples, several marine sediments, which are often considered a complex matrix due to the presence of a high concentration of hydrocarbons (Sanches Filho et al., 2017; Zaghden et al., 2007), were analysed using the method developed. Hence, an exhaustive extraction procedure and clean-up described above (see section 2.2) was carried out to remove all the potential matrix interferences. Nonetheless, it is well-known that the APPI (+) mode is highly sensitive for the detection of hydrocarbons (Gutiérrez Sama et al., 2018; Haapala et al., 2009; Huba and Gardinali, 2016; Kim et al., 2011; Kondyli and Schrader, 2019). This fact could lead to some matrix effect, even after removing most of the hydrocarbons present in the samples. As it can be observed in Fig. 4a, the total ion current (TIC) GC-APPI (+)-Orbitrap chromatogram of a marine sediment shows a broad hump from 15 min to 45 min due to the elution of the heavy fraction of hydrocarbons, which hinders the ionization of PCN homologue groups, especially from pentaCNs to the octaCN, (Fig. 4b). This effect was also observed when using the GC-APCI (+)-TOF system. To avoid this effect, those samples were re-injected in the GC-APPI-Orbitrap system working in negative ion mode and using diethyl ether as dopant (70 µL min^{-1}) in order to achieve the quantification of the interfered triCNs to octaCN homologue groups (Table 2) and prevent the ionization of hydrocarbons. Figure 4c shows the TIC chromatogram in negative ion mode of this sediment sample, where the absence of ionization for hydrocarbons allowed the adequate detection of PCN homologue groups (from triCNs to octaCN) as it can be observed in the extracted ion chromatogram (Fig. 4d).

To demonstrate the detection capability of the GC-APPI-Orbitrap, method limits of detection (MLODs), corresponding to a signal-to-noise ratio of 3 for the ion selected for confirmation purposes, were determined by analysing blank sediment samples spiked at low concentration levels. Regarding the positive ion mode, MLODs ranged between 0.2 and 1.6 pg g^{-1} dw while MLODs from 0.08 to 1.8 pg g^{-1} dw were obtained in the negative ion APPI mode for those homologue groups that were efficiently ionized (from triCNs to octaCN). These MLODs were comparable to those previously reported. For instance, Zhang *et al.* (Zhang et al., 2015) reported MLODs ranging from 0.48 to 12 pg g^{-1} using a GC-EI-MS/MS system while Pan *et al.* (Pan et al., 2011) achieved MLODs (20-70 pg g^{-1}) at least 10 times higher than those obtained by GC-APPI-HRMS. Moreover, they were also similar to those MLODs reported using GC-EI-HRMS (sectors) methods (0.06-10 pg g^{-1} dw) (Brack et al., 2003; Horii et al., 2004), which
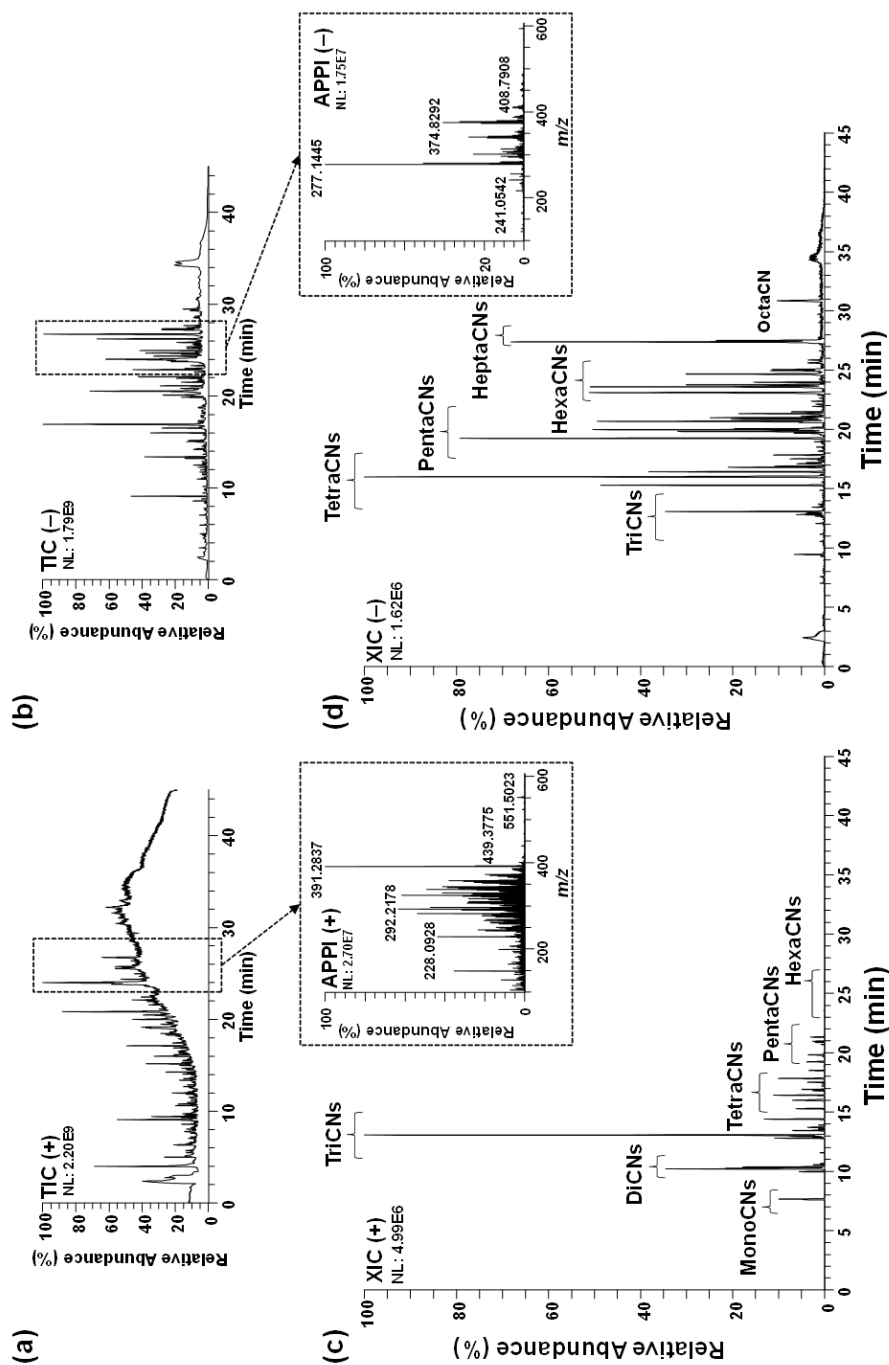
Fig. 4. GC-HRMS total ion current (TIC) and extracted ion chromatogram (XIC) of a marine sediment sample in (a, c) positive and (b, d) negative ion APPI.

234

Table 3. PCN homologue groups concentration in marine sediments from the Catalonian coast.

Homologue group	Concentration ± SD (ng g^{-1} dry weight)[a]				
	Sediment 1	Sediment 2	Sediment 3	Sediment 4	Sediment 5
∑ MonoCNs	0.104 ± 0.007	0.21 ± 0.01	0.086 ± 0.008	0.043 ± 0.003	0.0058 ± 0.0007
∑ DiCNs	0.86 ± 0.06	0.76 ± 0.05	0.27 ± 0.02	0.12 ± 0.007	0.03 ± 0.0003
∑ TriCNs	2.2 ± 0.1	1.6 ± 0.2	1.7 ± 0.3	0.35 ± 0.01	0.06 ± 0.004
∑ TetraCNs	0.84 ± 0.03	0.47 ± 0.05	0.32 ± 0.01	0.25 ± 0.02	0.07 ± 0.006
∑ PentaCNs	0.42 ± 0.05	0.24 ± 0.01	0.144 ± 0.003	0.13 ± 0.01	0.07 ± 0.004
∑ HexaCNs	0.38 ± 0.03	0.23 ± 0.02	0.13 ± 0.01	0.20 ± 0.02	0.058 ± 0.005
∑ HeptaCNs	0.147 ± 0.008	0.072 ± 0.003	0.071 ± 0.002	0.111± 0.009	0.027 ± 0.002
OctaCN	0.054 ± 0.004	0.027 ± 0.004	0.059 ± 0.005	0.054 ± 0.006	0.026 ± 0.003
∑ PCNs	5.0 ± 0.2	3.7 ± 0.3	2.8 ± 0.3	1.26 ± 0.06	0.35 ± 0.01

[a] n=3

demonstrate to good detection capability of the proposed methodology for the analysis of PCNs in sediment samples. Besides, the trueness of the method, defined as the relative error between the concentration found and the concentration spiked in a blank sediment, was determined at two concentration levels (0.2 ng g^{-1} and 0.5 ng g^{-1}), obtaining relative errors lower than 13%. The concentrations found for each homologue group of PCNs are summarized in Table 3. The analysis of these samples by triplicate showed the good intra-day precision of the method, achieving RSD values below 15%. Additionally, the concentrations found using GC-APPI-HRMS in both positive and negative ion mode showed very similar results (Table S2), which demonstrate the applicability of the GC-APPI (–)-HRMS method when highly chlorinated PCNs are interfered in the positive ion APPI mode.

In general, the highest concentrations were found for homologue groups from di- to hexaCNs with values up to 2.23 ng g^{-1} dry weight (dw). In addition, the total concentration of PCNs in marine sediments ranged from 0.35 to 5.04 ng g^{-1} dw. These results are very similar to those obtained in previous studies for sediments collected at the same coastal area in 2008 (0.17–6.6 ng g^{-1} dw) (Castells et al., 2008), confirming diffuse but uniform inputs of PCNs that could be attributed to permanent discharges of contaminated effluents coming from a wastewater treatment plant (WWTP) located near to the area. These results are also in agreement with data reported for marine sediments from the Salish Sea, Canada (0.007–1.487 ng g^{-1} dw) (Morales-Caselles et al., 2017), the Laizhou Bay area, China (0.12–5.1 ng g^{-1} dw) (Pan et al., 2011) and the Qingdao coastal sea, China (0.2–1.2 ng g^{-1} dw) (Pan et al., 2007), which are under the influence of industrial and urban inputs.

Regarding the homologue distribution of the samples analysed, different profiles were observed depending on the sampling site (see Fig. S4a). Those sediment samples that were located close to the submarine emissary outlet (sediment 1, 2, and 3) showed a higher proportion of di- to tetraCNs, which can be associated to the water discharges coming from

the Besòs River. These inputs are consequence of the long-range transportation and deposition from the river to the coast, favouring low molecular weight PCN congeners (Gevao et al., 2000). In contrast, those samples that were located between the seaside and the submarine emissary outlet (sediment 4 and 5) showed a higher contribution of highly chlorinated PCNs. These samples may indicate the historical distribution of PCNs in the water media after being affected by different environmental factors. Thus, highly chlorinated PCNs are more likely to be adsorbed onto the sediment due to their high octanol/water partitioning coefficient, and therefore, an enrichment on penta-, hexa-, hepta-, and octaCN contribution has been observed in these marine sediment samples.

Concerning the congener-specific compositional profile, the pair CN-14/CN-24 was the most abundant isomers in all the samples with concentrations ranging from 0.05 to 1.6 ng g^{-1} dw (see Fig. S4). These results are in agreement with those reported by Gevao *et al.* (0.108-1.486 ng g^{-1}) in sediments from Esthwaite Water (England) (Gevao et al., 2000). Besides that, the compositional profile also matched, observing predominant isomers within each homologue group. For instance, 1-monoCN (CN-1) and 1,4-/1,6-diCN (CN-5/CN-7), and 1,5-2,7-diCN (CN-6/CN-12) dominanted the monoCN and diCN series, respectively. On the other hand, 1,2,4,6-/1,2,4,7-/1,2,5,7-tetraCN (CN-33/CN-34/CN-37) were the most abundant tetraCN isomers while 1,2,3,5,7-/1,2,4,6,7-pentaCN (CN-52/CN-60) and 1,2,4,6,8-pentaCN (CN-61) dominated the pentaCN homologue group. Finally, hexaCNs composition was quite distributed being the isomeric pair 1,2,3,4,6,7-/1,2,3,5,6,7-hexaCN (CN-66/CN-67) the most intense while 1,2,3,4,5,6,7-heptaCN (CN-73) always showed a higher concentration than 1,2,3,4,5,6,8-heptaCN (CN-74). Considering potential sources of PCN contamination, the low abundance of congeners 2,3,6-triCN (CN-26), 1,2,3,6-/4,6,6,7-/2,3,6,7-tetraCNs (CN-29/CN-44/CN-48),and 1,2,3,6,7-pentaCN (CN-54) may indicate that the waste combustion (flue gas, fly ash) might not be the main source of PCN contamination (Horii et al., 2004). On the other hand, the ratios of CN-66/CN-67 to CN-71/CN-72 obtained in this work variated from 1.4 to 4.3 (mean: 2.6). These values were lower than those found from PCNs coming from the electric arc furnace gases emitted to the atmosphere (Liu et al., 2012), but they were similar than those reported for technical PCB formulations where PCNs are formed as by-products (Yamashita et al., 2000; Zhang et al., 2015). This suggests the formation of PCNs as by-products in the technical PCB formulations may be a potential main source of sediment contamination, as PCBs were extensively used in Europe during the last century. Other potential PCN source is coal burning process which led to the formation of CN-14/CN-24 isomers (Pan et al., 2012). The high concentration of di- to tetraCNs in sediments 1,2 and 3 can be also due to the atmospheric decomposition of hexaCNs and heptaCNs into the lower chlorinated congeners or the breakdown of hexa- to octaCN due to microbial activity in anaerobic conditions (Horii et al., 2004). On the other hand, highly chlorinated PCNs, especially CN-66/CN-67, CN-64/CN-68, CN-69, and CN-73, which have shown to be some of the most toxic PCNs (Falandysz and Fernandes, 2020; Li et al., 2020), have been found in all the samples at concentration levels ranging from 11 to 121 pg g^{-1} dw). In fact, the higher proportion of these isomers due to the

enrichment of coastal sediments with highly chlorinated PCNs may induce dioxin-like toxicity for human beings and wildlife. Additionally, the advantage of working at high sensitivity full-scan acquisition mode using the Orbitrap mass analyser allowed the detection in the sediment sample of other related compounds such as PCBs which could also present dioxin-like toxicity. Thus, some PCB congeners, such as HexaCBs (*m/z* 338.8719), HeptaCBs (*m/z* 372.8331) and OctaCBs (*m/z* 406.7939), which ionize by generating the ion [M–Cl+O]⁻ (Luosujärvi et al., 2008), were detected by GC-APPI (–)-Orbitrap in the time window of 22-29 min. This fact demonstrates the great capability of the GC-APPI-Orbitrap system not only the target analysis of PCNs but also for suspect or unknown analysis of other halogenated organic pollutants in complex matrices. In this sense, this methodology will provide more useful information to evaluate the concentration levels, potential sources of contamination as well as other relevant environmental information in complex samples such as marine sediments.

4. Conclusions

The APCI and APPI sources have demonstrated for the first time the high capability for the efficiently ionization of all PCN congeners, proving a high sensitivity in their determination by GC-HRMS. Regarding APCI, the ionization of the analytes was accomplished in positive ion mode at high corona currents under dry conditions. In contrast, the ionization in positive ion APPI was promoted using dopant vapours that favoured charge-exchange reactions (e.g., toluene), while dopants with high vapour pressure (e.g., diethyl ether) allowed the adequate ionization of all the compounds in negative ion mode. Comparing the performance of both GC-API-HRMS systems, it was observed that GC-APPI (+)-Orbitrap MS provided the lowest limits of detection for all PCNs with a good precision (RDS <13%) and trueness (RE%<14%), although negative ion APPI also showed a high detection capability and selectivity for homologues from triCNs to octaCN. Therefore, the GC-APPI (+)-Orbitrap method was proposed as a compromise for the simultaneous determination of all PCN congeners. The good performance of the proposed method allowed the adequate characterization of Halowax mixtures, obtaining similar results than those previously reported. The GC-APPI (+)-Orbitrap method also allowed the suitable PCN determination in marine sediment samples at low concentration levels, although the GC-APPI (–)-Orbitrap method can also provide a highly selective detection when the presence of high amounts of hydrocarbons may interfere the quantification of triCNs to octaCN congeners. Moreover, the use of an Orbitrap analyser for HRMS measurements, which operates at a very sensitive high-resolution full scan acquisition mode, allowed the retrospective analysis to detect related compounds such as PCBs. Hence, all these findings demonstrated the good performance of the GC-APPI-Orbitrap method and it can be proposed as an alternative to the traditional GC-MS methods generally used for the determination of PCNs in complex environmental matrices.

Acknowledgements

References

Brack, W., Kind, T., Schrader, S., Möder, M., Schüürmann, G., 2003. Polychlorinated naphthalenes in sediments from the industrial region of Bitterfeld. Environ. Pollut. 121, 81–85. https://doi.org/10.1016/S0269-7491(02)00200-2

Carrizo, D., Grimalt, J.O., 2006. Rapid and simplified method for the analysis of polychloronaphthalene congener distributions in environmental and human samples by gas chromatography coupled to negative ion chemical ionization mass spectrometry. J. Chromatogr. A 1118, 271–277. https://doi.org/10.1016/j.chroma.2006.03.108

Castells, P., Parera, J., Santos, F.J., Galceran, M.T., 2008. Occurrence of polychlorinated naphthalenes, polychlorinated biphenyls and short-chain chlorinated paraffins in marine sediments from Barcelona (Spain). Chemosphere 70, 1552–1562. https://doi.org/10.1016/j.chemosphere.2007.08.034

Dat, N.D., Chang, K.S., Wu, C.P., Chen, Y.J., Tsai, C.L., Chi, K.H., Chang, M.B., 2019. Measurement of PCNs in sediments collected from reservoir and river in northern Taiwan. Ecotoxicol. Environ. Saf. 174, 384–389. https://doi.org/10.1016/j.ecoenv.2019.02.087

Di Lorenzo, R.A., Lobodin, V. V., Cochran, J., Kolic, T., Besevic, S., Sled, J.G., Reiner, E.J., Jobst, K.J., 2019. Fast gas chromatography-atmospheric pressure (photo)ionization mass spectrometry of polybrominated diphenylether flame retardants. Anal. Chim. Acta 1056, 70–78. https://doi.org/10.1016/j.aca.2019.01.007

Falandysz, J., Kawano, M., Ueda, M., Matsuda, M., Kannan, K., Giesy, J.P., Wakimoto, T., 2000. Composition of chloronaphthalene congeners in technical chloronaphthalene formulations of the Halowax series. J. Environ. Sci. Heal. - Part A Toxic/Hazardous Subst. Environ. Eng. 35, 281–298. https://doi.org/10.1080/10934520009376971

Falandysz, J., Nose, K., Ishikawa, Y., Łukaszewicz, E., Yamashita, N., Noma, Y., 2006. HRGC/HRMS analysis of chloronaphthalenes in several batches of halowax 1000, 1001, 1013, 1014 and 1099. J. Environ. Sci. Heal. - Part A Toxic/Hazardous Subst. Environ. Eng. 41, 2237–2255. https://doi.org/10.1080/10934520600872748

Falandysz, J., Chudzyński, K., Takekuma, M., Yamamoto, T., Noma, Y., Hanari, N., Yamashita, N., 2008. Multivariate analysis of identity of imported PCN formulation. J. Environ. Sci. Heal. - Part A Toxic/Hazardous Subst. Environ. Eng. 43, 1381–1390. https://doi.org/10.1080/10934520802232022

Falandysz, J., Fernandes, A.R., 2020. Compositional profiles, persistency and toxicity of polychlorinated naphthalene (PCN) congeners in edible cod liver products from 1972 to 2017. Environ. Pollut. 260, 114035. https://doi.org/10.1016/j.envpol.2020.114035

Geng, D., Jogsten, I.E., Dunstan, J., Hagberg, J., Wang, T., Ruzzin, J., Rabasa-Lhoret, R., van Bavel, B., 2016. Gas chromatography/atmospheric pressure chemical ionization/mass spectrometry for the analysis of organochlorine pesticides and polychlorinated biphenyls in human serum. J. Chromatogr. A 1453, 88–98. https://doi.org/10.1016/j.chroma.2016.05.030

Gevao, B., Harner, T., Jones, K.C., 2000. Sedimentary record of polychlorinated naphthalene concentrations and deposition fluxes in a dated lake core. Environ. Sci. Technol. 34, 33–38. https://doi.org/10.1021/es990663k

Gutiérrez Sama, S., Barrère-Mangote, C., Bouyssière, B., Giusti, P., Lobinski, R., 2018. Recent trends in element speciation analysis of crude oils and heavy petroleum fractions. TrAC - Trends Anal. Chem. 104, 69–76. https://doi.org/10.1016/j.trac.2017.10.014

Haapala, M., Purcell, J.M., Saarela, V., Franssila, S., Rodgers, R.P., Hendrickson, C.L., Kotiaho, T., Marshall, A.G., Kostiainen, R., 2009. Microchip atmospheric pressure photoionization for analysis of petroleum by fourier transform ion cyclotron resonance mass spectrometry. Anal. Chem. 81, 2799–2803. https://doi.org/10.1021/ac802427m

Hanari, N., Falandysz, J., Nakano, T., Petrick, G., Yamashita, N., 2013. Separation of closely eluting chloronaphthalene congeners by two-dimensional gas chromatography/quadrupole mass spectrometry: an advanced tool in the study and risk analysis of dioxin-like chloronaphthalenes. J. Chromatogr. A 1301, 209–214. https://doi.org/10.1016/j.chroma.2013.05.070

Hori, Y., Falandysz, J., Hanari, N., Rostkowski, P., Puzyn, T., Okada, M., Amano, K., Naya, T., Taniyasu, S., Yamashita, N., 2004. Concentrations and fluxes of chloronaphthalenes in sediment from Lake Kitaura in Japan in past 15 centuries. J. Environ. Sci. Heal. - Part A Toxic/Hazardous Subst. Environ. Eng. 39, 587–609. https://doi.org/10.1081/ESE-120027727

Huba, A.K., Gardinali, P.R., 2016. Characterization of a crude oil weathering series by ultrahigh-resolution mass spectrometry using multiple ionization modes. Sci. Total Environ. 563–564, 600–610. https://doi.org/10.1016/j.scitotenv.2016.03.233

Jakobsson, E., Asplund, L., 2007. Polychlorinated Naphthalenes (PCNs), in J. Paasivirta (Ed.), New Types of Persistent Halogenated Compounds. The Handbook of Environmental Chemistry. Vol. 3 Anthropog. Compd. Part K 3, 97–126. https://doi.org/10.1007/3-540-48915-0_5

Kauppila, T.J., Kersten, H., Benter, T., 2015. Ionization of EPA contaminants in direct and dopant-assisted atmospheric pressure photoionization and atmospheric pressure laser ionization. J. Am. Soc. Mass Spectrom. 26, 1036–1045. https://doi.org/10.1007/s13361-015-1092-3

Kauppila, T.J., Kersten, H., Benter, T., 2014. The Ionization Mechanisms in Direct and Dopant-Assisted Atmospheric Pressure Photoionization and Atmospheric Pressure Laser Ionization. J. Am. Soc. Mass Spectrom. 25, 1870–1881. https://doi.org/10.1007/s13361-014-0988-7

Kilanowicz, A., Markowicz-Piasecka, M., Klimczak, M., Stragierowicz, J., Sikora, J., 2019a. Hexachloronaphthalene as a hemostasis disturbing factor in female Wistar rats – A pilot study. Chemosphere. 228, 557–585. https://doi.org/10.1016/j.chemosphere.2019.04.147

Kilanowicz, A., Sitarek, K., Stragierowicz, J., Klimczak, M., Bruchajzer, E., 2019b. Prenatal toxicity and maternal-fetal distribution of 1,3,5,8-tetrachloronaphthalene (1,3,5,8-TeCN) in Wistar rats. Chemosphere. 226, 75–84. https://doi.org/10.1016/j.chemosphere.2019.03.107

Kim, E., No, M.H., Koh, J., Kim, S., 2011. Compositional characterization of petroleum heavy oils generated from vacuum distillation and catalytic cracking by positive-mode APPI FT-ICR mass spectrometry. Mass Spectrom. Lett. 2, 41–44. https://doi.org/10.5478/MSL.2011.2.2.041

Kondyli, A., Schrader, W., 2019. High-resolution GC/MS studies of a light crude oil fraction. J. Mass Spectrom. 54, 47–54. https://doi.org/10.1002/jms.4306

Lega, R., Megson, D., Hartley, C., Crozier, P., MacPherson, K., Kolic, T., Helm, P.A., Myers, A., Bhavsar, S.P., Reiner, E.J., 2017. Congener specific determination of polychlorinated naphthalenes in sediment and biota by gas chromatography high resolution mass spectrometry. J. Chromatogr. A 1479, 169–176. https://doi.org/10.1016/j.chroma.2016.11.054

Li, D.X., Gan, L., Bronja, A., Schmitz, O.J., 2015. Gas chromatography coupled to atmospheric pressure ionization mass spectrometry (GC-API-MS): Review. Anal. Chim. Acta 891, 43–61. https://doi.org/10.1016/j.aca.2015.08.002

Li, F., Jin, J., Sun, X., Wang, X., Li, Y., Shah, S.M., Chen, J., 2014. Gas chromatography-triple quadrupole mass spectrometry for the determination of atmospheric polychlorinated naphthalenes. J. Hazard. Mater. 280, 111–117.

https://doi.org/10.1016/j.hazmat.2014.07.060

Li, F., Jin, J., Tan, D., Xu, J., Dhanjai, Ni, Y., Zhang, H., Chen, J., 2016. High performance solid-phase extraction cleanup method coupled with gas chromatography-triple quadrupole mass spectrometry for analysis of polychlorinated naphthalenes and dioxin-like polychlorinated biphenyls in complex samples. J. Chromatogr. A 1448, 1–8. https://doi.org/10.1016/j.chroma.2016.04.037

Li, C., Zhang, L., Li, J., Min, Y., Yang, L., Zheng, M., Wu, Y., Yang, Y., Qin, L., Liu, G., 2020. Polychlorianted naphthalenes in human milk: health risk assessment to nursing infants and source analysis. Environ. Int. 136, 105436. https://doi.org/10.1016/j.envint.2019.105436

Liu, G., Zheng, M., Du, B., Nie, Z., Zhang, B., Hu, J., Xiao, K., 2012. Identification and characterization of the most atmospheric emission of polychlorinated naphthalenes from electric arc furnaces. Environ. Sci. Pollut. Res. 19, 3645–3650. https://doi.org/10.1007/s11356-012-1038-2

Łukaszewicz, E., Ieda, T., Horii, Y., Yamashita, N., Falandysz, J., 2007. Comprehensive two-dimensional GC (GC x GC) qMS analysis of tetrachloronaphthalenes in Halowax formulations. J. Environ. Sci. Heal. - Part A Toxic/Hazardous Subst. Environ. Eng. 42, 1607–1614. https://doi.org/10.1080/10934520701517788

Luosujärvi, L., Karikko, M.-M., Haapala, M., Saarela, V., Huhtala, S., Franssila, S., Kostiainen, R., Kotiaho, T., Kauppila, T.J., 2008. Gas chromatography/mass spectrometry of polychlorinated biphenyls using atmospheric pressure chemical ionization and atmospheric pressure photoionization microchips. Rapid Commun. Mass Spectrom. 22, 425.431. https://doi.org/10.1002/rcm.3379

McEwen, C.N., McKay, R.G., 2005. A combination atmospheric pressure LC/MS:GC/MS ion source: Advantages of dual AP-LC/MS:GC/MS instrumentation. J. Am. Soc. Mass Spectrom. 16, 1730–1738. https://doi.org/10.1016/j.jasms.2005.07.005

Meijer, S.N., Harner, T., Helm, P.A., Halsall, C.J., Johnston, A.E., Jones, K.C., 2001. Polychlorinated naphthalenes in U.K. soils: Time trends, markers of source, and equilibrium status. Environ. Sci. Technol. 35, 4205–4213. https://doi.org/10.1021/es010071d

Morales-Caselles, C., Desforges, J.P.W., Dangerfield, N., Ross, P.S., 2017. A Risk-Based Characterization of Sediment Contamination by Legacy and Emergent Contaminants of Concern in Coastal British Columbia, Canada. Arch. Environ. Contam. Toxicol. 73, 1–15. https://doi.org/10.1007/s00244-017-0403-z

Moukas, A.I., Thomaidis, N.S., Calokerinos, A.C., 2016. Novel determination of polychlorinated naphthalenes in water by liquid chromatography-mass spectrometry with atmospheric pressure photoionization. Anal. Bioanal. Chem. 408, 191–201. https://doi.org/10.1007/s00216-015-9092-5

Noma, Y., Yamamoto, T., Sakai, S.I., 2004. Congener-specific composition of polychlorinated naphthalenes, coplanar PCBs, dibenzo-p-dioxins, and dibenzofurans in the Halowax Series. Environ. Sci. Technol. 38, 1675–1680. https://doi.org/10.1021/es035101m

Pan, J., Yang, Y.L., Xu, Q., Chen, D.Z., Xi, D.L., 2007. PCBs, PCNs and PBDEs in sediments and mussels from Qingdao coastal sea in the frame of current circulations and influence of sewage sludge. Chemosphere 66, 1971–1982. https://doi.org/10.1016/j.chemosphere.2006.07.070

Pan, X., Tang, J., Chen, Y., Li, J., Zhang, G., 2011. Polychlorinated naphthalenes (PCNs) in riverine and marine sediments of the Laizhou Bay area, North China. Environ. Pollut. 159, 3515–3521. https://doi.org/10.1016/j.envpol.2011.08.016

Pan, J., Yang, Y., Taniyasu, S., Yeung L.W.Y, Falandysz, J. Yamashita, N., 2012. Comparison of historical record of PCDD/Fs, dioxin-like PCBs and PCNs in sediment cores from Jiaozhou Bay and Coastal Yellow Sea : implication of different sources. Bull. Environ. Contam. Toxicol. 89, 1240–1246. https://doi.org/10.1007/s00128-012-0836-z

Portolés, T., Sales, C., Abalos, M., Sauló, J., Abad, E., 2016. Evaluation of the capabilities of atmospheric pressure chemical ionization source coupled to tandem mass spectrometry for the determination of dioxin-like polychlorobiphenyls in complex-matrix food samples. Anal. Chim. Acta 937, 96–105. https://doi.org/10.1016/j.aca.2016.06.038

Raro, M., Portolés, T., Sancho, J. V., Pitarch, E., Hernández, F., Marcos, J., Ventura, R., Gõmez, C., Segura, J., Pozo, O.J., 2014. Mass spectrometric behavior of anabolic androgenic steroids using gas chromatography coupled to atmospheric pressure chemical ionization source. Part I: Ionization. J. Mass Spectrom. 49, 509–521. https://doi.org/10.1002/jms.3367

Revelsky, I.A., Yashin, Y.S., 2012. New approach to complex organic compounds mixtures analysis based on gas chromatography-atmospheric pressure photoionization-mass-spectrometry. Talanta 102, 110–113. https://doi.org/10.1016/j.talanta.2012.07.023

Revelsky, I.A., Yashin, Y.S., Sobolevsky, T.G., Revelsky, A.I., Miller, B., Oriedo, V., 2003. Electron ionization and atmospheric pressure photochemical ionization in gas chromatography- mass spectrometry analysis of amino acids. Eur. J. Mass Spectrom. (Chichester, Eng). 507, 497–507. https://doi.org/10.1255/ejms.581

Schneider, M., Stieglitz, L., Will, R., Zwick, G., 1998. Formation of polychlorinated naphthalenes on fly ash. Chemosphere. 37, 2055–2070. https://doi.org/10.1016/S0045-6535(98)00269-0

Sanches Filho, P.J., Böhm, E.M., Böhm, G.M.B., Montenegro, G.O., Silveira, L.A., Betemps, G.R., 2017. Determination of hydrocarbons transported by urban runoff in sediments of São Gonçalo Channel (Pelotas – RS, Brazil). Mar. Pollut. Bull. 114, 1088–1095. https://doi.org/10.1016/j.marpolbul.2016.10.024

ten Dam, G., Pussente, I.C., Scholl, G., Eppe, G., Schaechtele, A., van Leeuwen, S., 2016. The performance of atmospheric pressure gas chromatography–tandem mass spectrometry compared to gas chromatography–high resolution mass spectrometry for the analysis of polychlorinated dioxins and polychlorinated biphenyls in food and feed samples. J. Chromatogr. A 1477, 76–90. https://doi.org/10.1016/j.chroma.2016.11.035

United Nation Environment Programme. Stockholm Convention on Persistent Organic Pollutants. UNEP-POPS-COP.7-SC-7-14, 2015. Decision SC-7/14 of 4-15 May 2015 of Listing of polychlorinated naphthalenes.

Van Bavel, B., Geng, D., Cherta, L., Nácher-Mestre, J., Portolés, T., Ábalos, M., Sauló, J., Abad, E., Dunstan, J., Jones, R., Kotz, A., Winterhalter, H., Malisch, R., Traag, W., Hagberg, J., Ericson Jogsten, I., Beltran, J., Hernández, F., 2015. Atmospheric-Pressure Chemical Ionization Tandem Mass Spectrometry (APGC/MS/MS) an Alternative to High-Resolution Mass Spectrometry (HRGC/HRMS) for the Determination of Dioxins. Anal. Chem. 87, 9047–9053. https://doi.org/10.1021/acs.analchem.5b02264

World Health Organization, 2001. Concise International Chemical Assessment Document 34: Chlorinated naphthalenes, Geneva.

Yamashita, N., Kannan, K., Imagawa, T., Miyazaki, A., Giesy, J.P., 2000. Concentration and profiles of polychlorinated naphthalene congeners in eighteen technical polychlorinated biphenyl preparations. Environ. Sci. Technol. 34, 4236–4241. https://doi.org/10.1021/es001122u

Yamashita, N., Taniyasu, S., Hanari, N., Hori, Y., Falandysz, J., 2003. Polychlorinated naphthalene contamination of some recently manufactured industrial products and commercial goods in Japan. J. Environ. Sci. Heal. - Part A Toxic/Hazardous Subst. Environ. Eng. 38, 1745–1759. https://doi.org/10.1081/ESE-120022876

Zaghden, H., Kallel, M., Elleuch, B., Oudot, J., Saliot, A., 2007. Sources and distribution of aliphatic and polyaromatic hydrocarbons in sediments of Sfax, Tunisia, Mediterranean Sea. Mar. Chem. 105, 70–89. https://doi.org/10.1016/j.marchem.2006.12.016

Zhang, L., Zhang, L., Dong, L., Huang, Y., Li, X., 2015. Concentrations and patterns of polychlorinated naphthalenes in surface sediments samples from Wuxi, Suzhou, and Nantong, in East China. Chemosphere. 138, 668–674. https://doi.org/10.1016/j.chemosphere.2015.07.045

Supplementary Material

Atmospheric Pressure Ionization for Gas Chromatography-High Resolution Mass Spectrometry Determination of Polychlorinated Naphthalenes in Marine Sediments

J. F. Ayala-Cabrera [a], C. Lipok [b,c], E. Moyano [a], O. J. Schmitz [b,c], F. J. Santos [a,*]

[a] Department of Chemical Engineering and Analytical Chemistry, University of Barcelona. Av. Diagonal 645, E-08028 Barcelona, Spain

[b] Applied Analytical Chemistry, University of Duisburg-Essen, Universitatsstr. 5, D-45141 Essen, Germany.

[c] Teaching and Research Center for Separation, University of Duisburg-Essen, Universitatsstr. 5, D-45141 Essen, Germany.

* Corresponding author: Francisco Javier Santos Vicente
Phone: +34-93-403-4874
Fax: +34-93-402-1233
E-mail: javier.santos@ub.edu

Table of Contents

Supporting Tables

Table S1. Vapour pressure and ionization potentials of the solvents used as dopants in APPI.

Dopant	Vapour Pressure (Torr, 25 °C)[a]	Ionization potential (eV)[b]
Acetone	348.4	9.703 ± 0.006
Anisole	4.2	8.20 ± 0.05
Chlorobenzene	11.2	9.07 ± 0.02
Diethyl Ether	566.8	9.51 ± 0.03
Tetrahydrofuran	152.4	9.40 ± 0.02
Toluene	27.7	8.828 ± 0.001

[a] *Predicted values using ACD/Labs Percepta Platform.*

[b] *NIST database.*

Table S2. PCN homologue group concentrations determined by GC-APPI-HRMS in both ionization modes.

| Homologue group | Concentration ± SD (ng g⁻¹ dry weight)[a] | | | | | | | | | |
| | Sediment 1 | | Sediment 2 | | Sediment 3 | | Sediment 4 | | Sediment 5 | |
	APPI (+)	APPI (−)	APPI (+)	APPI (−)	APPI (+)	APPI (−)	APPI (+)	APPI (−)	APPI (+)	APPI (−)
∑ MonoCNs	0.104 ± 0.007	n.d.	0.21 ± 0.01	n.d.	0.086 ± 0.008	n.d.	0.043 ± 0.003	n.d.	0.0058 ± 0.0007	n.d.
∑ DiCNs	0.86 ± 0.06	n.d.	0.76 ± 0.05	n.d.	0.27 ± 0.02	n.d.	0.12 ± 0.007	n.d.	0.03 ± 0.0003	n.d.
∑ TriCNs	2.2 ± 0.1	2.1 ± 0.2	1.6 ± 0.2	0.18 ± 0.1	1.7 ± 0.3	1.5 ± 0.2	0.35 ± 0.01	0.35 ± 0.02	0.06 ± 0.04	0.07 ± 0.03
∑ TetraCNs	0.84 ± 0.03	0.86 ± 0.05	0.47 ± 0.05	0.51 ± 0.06	0.32 ± 0.01	0.31 ± 0.02	0.25 ± 0.02	0.24 ± 0.01	0.07 ± 0.06	0.08 ± 0.04
∑ PentaCNs	0.42 ± 0.05	0.46 ± 0.04	0.24 ± 0.01	0.22 ± 0.02	0.144 ± 0.003	0.15 ± 0.1	0.13 ± 0.01	0.14 ± 0.03	0.07 ± 0.04	0.06 ± 0.03
∑ HexaCNs	n.d.	0.38 ± 0.03	n.d.	0.23 ± 0.02	0.13 ± 0.01	0.11 ± 0.02	0.20 ± 0.02	0.18 ± 0.03	0.058 ± 0.005	0.05 ± 0.04
∑ HeptaCNs	n.d.	0.147 ± 0.008	n.d.	0.072 ± 0.003	0.071 ± 0.002	0.08 ± 0.01	0.111 ± 0.009	0.13 ± 0.01	0.027 ± 0.002	0.033 ± 0.004
OctaCN	n.d.	0.054 ± 0.004	n.d.	0.027 ± 0.004	0.059 ± 0.005	0.051 ± 0.08	0.054 ± 0.006	0.05 ± 0.01	0.026 ± 0.008	0.030 ± 0.005

a n=3

246

<u>Supporting Figures</u>
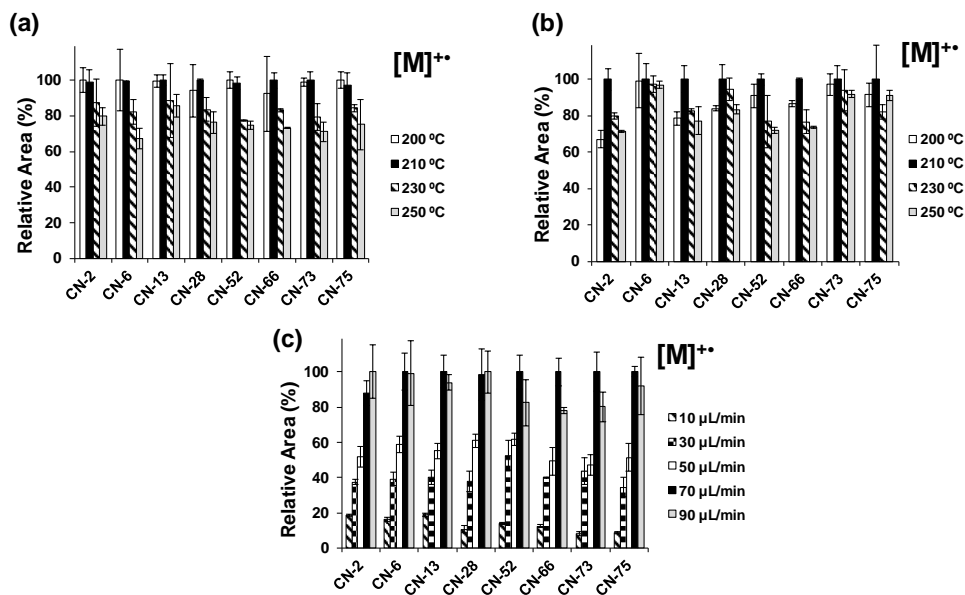
Figure S1. Effect of (a) source temperature, (b) capillary temperature, and (c) dopant flow rate over the response of PCNs using GC-APPI (*dopant: toluene*).
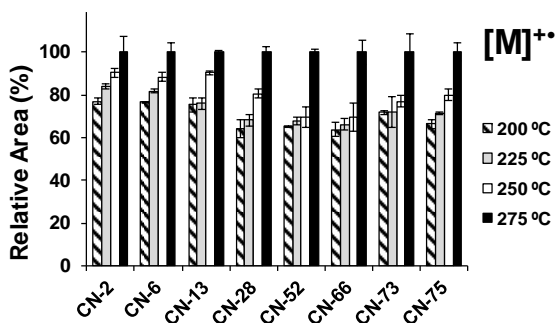
Figure S2. Effect of the source temperature over the response of PCNs using GC-APCI.
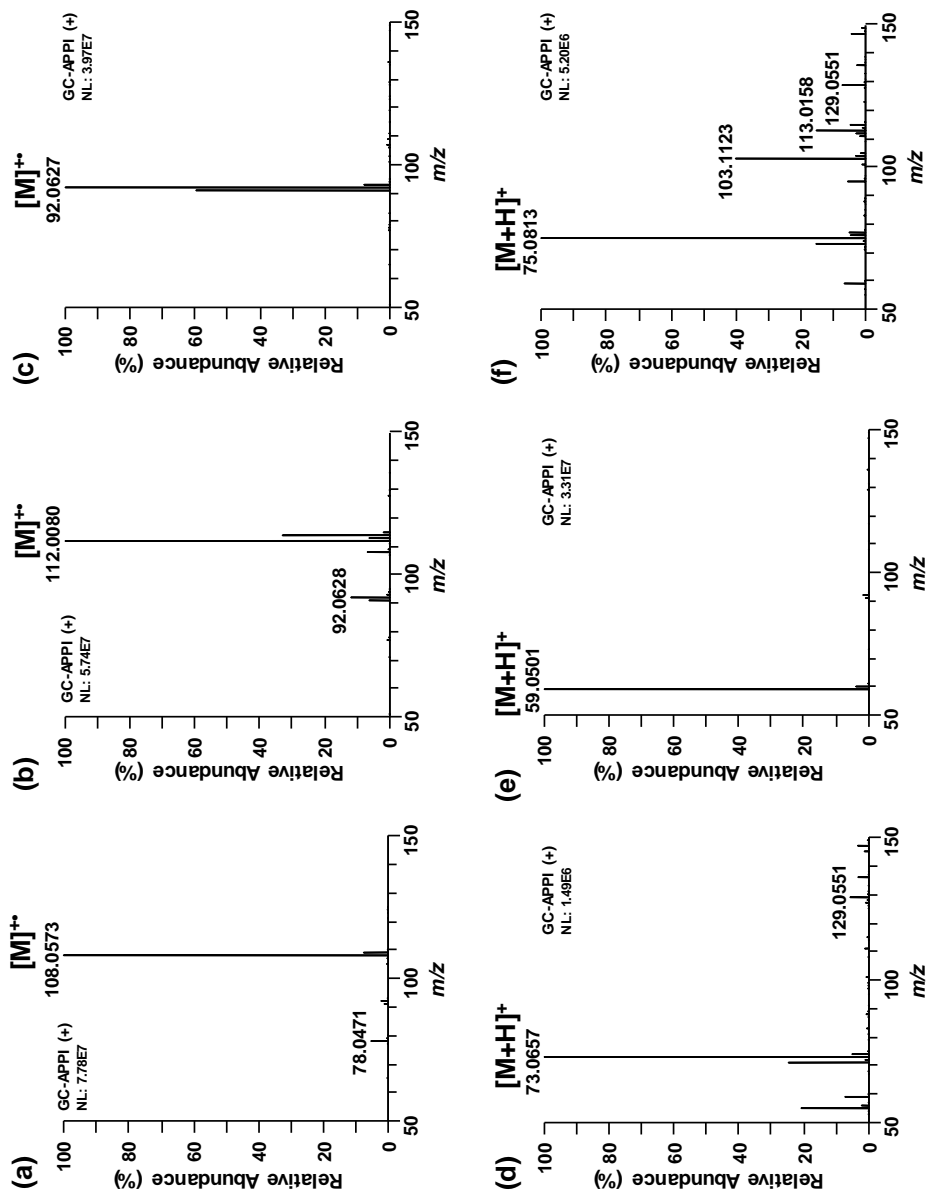
Figure S3. APPI mass spectra of a) anisole, b) chlorobenzene, c) toluene, d) tetrahydrofuran, e) acetone and f) diethyl ether dopants.
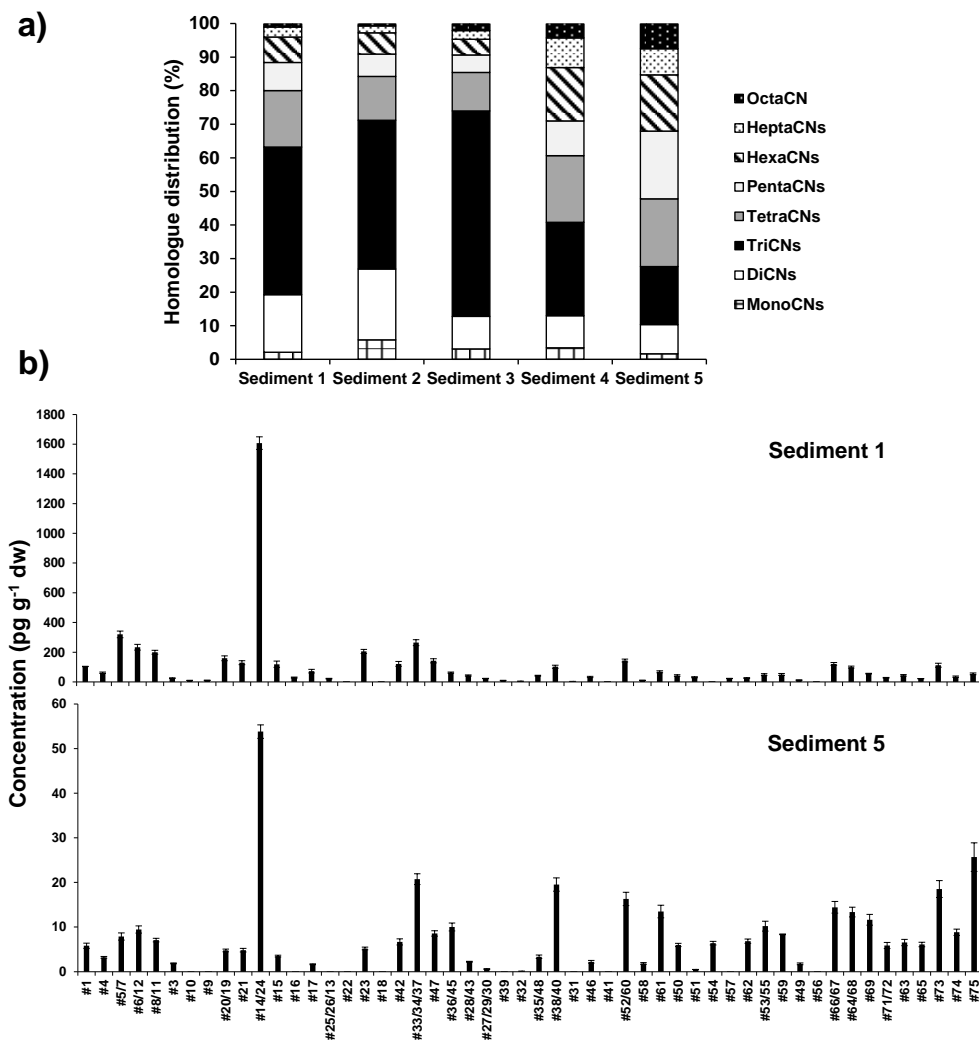
Figure S4. a) PCN homologue distribution in marine sediment samples, and b) PCN congener-specific compositional profile in marine sediments located at the submarine emissary outlet (*up*) and between the seaside and the submarine emissary outlet (*down*).

3.2.4. Article VIII

Feasibility of gas chromatography-atmospheric pressure photoionization-high resolution mass spectrometry for the analysis of polychlorinated dibenzo-p-dioxins, dibenzofurans and dioxin-like polychlorinated biphenyls in environmental and feed samples

J. F. Ayala-Cabrera, M. Ábalos, E. Abad, E. Moyano, F. J. Santos

RESEARCH PAPER

Feasibility of gas chromatography-atmospheric pressure photoionization–high-resolution mass spectrometry for the analysis of polychlorinated dibenzo-*p*-dioxins, dibenzofurans, and dioxin-like polychlorinated biphenyls in environmental and feed samples

J. F. Ayala-Cabrera [1] · M. Ábalos [2] · E. Abad [2] · E. Moyano [1] · F. J. Santos [1]

Abstract

In this work, the suitability of atmospheric pressure photoionization (APPI) has been assessed for the determination of polychlorinated dibenzo-*p*-dioxins and furans (PCDD/Fs) and dioxin-like polychlorinated biphenyls (dl-PCBs) by gas chromatography–high-resolution mass spectrometry (GC-HRMS). The APPI of target compounds has been tested in both positive and negative ion modes. Under positive ion mode, the analytes generated the molecular ion, which was favoured using dopants that promote charge exchange gas-phase reactions (i.e., benzene), while in negative ion mode, the ion $[M-Cl+O]^-$ for PCDFs and dl-PCBs were mainly formed, providing the best results using benzene and diethyl ether as dopants, respectively. Concerning PCDDs, highly chlorinated congeners were mainly ionized by means of the $[M-Cl]^-$ ion, whereas $[M-Cl+O_2]^-$ was the base peak for tetraCDD and $[M-Cl+O]^-$ for penta- and hexaCDDs. Method quality parameters, in accordance with the current EU Regulation guidelines for food and feed analysis, showed the good performance of the two GC-APPI-HRMS (Orbitrap) methods since they provided high detection capability (low fg levels), good linearity, and satisfactory precision (RSD% < 9%). In addition, the GC-APPI-HRMS (Orbitrap) methods were validated by analysing selected environmental and feed samples and the results were compared to those obtained using conventional GC-EI-HRMS, demonstrating the good performance in the analysis of the target compounds. Hence, the GC-APPI-HRMS technique can be proposed as alternative to the conventional methods for the determination of PCDD/Fs and dl-PCBs in environmental and feed matrices.

Keywords Atmospheric pressure photoionization · Gas chromatography–high-resolution mass spectrometry · Polychlorinated dibenzo-*p*-dioxins and furans · Dioxin-like polychlorinated biphenyls · Environmental samples · Feed samples

Introduction

To protect human health and the environment from hazardous substances, the Stockholm Convention establishes restriction and regulations for eliminating the production and

✉ F. J. Santos
  javier.santos@ub.edu

1   Department of Chemical Engineering and Analytical Chemistry, University of Barcelona, Av. Diagonal 645, 08028 Barcelona, Spain

2   Laboratory of Dioxins, Institute of Environmental Assessment and Water Research (IDAEA-CSIC), C/Jordi Girona, 18-26, 08034 Barcelona, Spain

introduction into the environment of several classes of persistent organic pollutants (POPs) [1, 2]. Among them, polychlorinated dibenzo-*p*-dioxins and dibenzofurans (PCDD/Fs) as well as dioxin-like polychlorinated biphenyls (dl-PCBs) constitute a class of environmental pollutants of great concern due to their high toxicity, bioaccumulation capacity, and persistence in the environment [1, 3, 4]. PCDD/Fs have never been deliberately produced, but they have been released into the environment as by-products from combustion processes and industrial synthesis of other chlorinated chemicals [5, 6]. In contrast, PCBs have been used in a wide range of industrial and commercial applications, including heat exchange fluids in transformers, capacitors, and other electrical instruments, as well as additives in paints and the production of carbonless copy paper and plastics, due to their high chemical stability and electrical insulating properties [7,

8]. Among the 209 possible chlorinated biphenyls (CBs), some congeners can take a planar conformation (dl-PCBs), which could confer similar harmful effect as PCDD/Fs for living organisms even at very low concentration levels [9]. Although PCDD/F and dl-PCB emissions in most countries have significantly decreased due to regulatory restrictions and control, they are still subjected to large-scale global monitoring programs in the environment and other important fields such as food and feed safety [10–13].

Traditionally, analyses of PCDD/Fs and dl-PCBs have been closely related and the developed methodologies are based on gas chromatography coupled to high-resolution mass spectrometry (GC-HRMS) using double-focusing magnetic sector as mass analyser and operating in electron ionization (EI) mode. This technique has been accepted as the reference standard method for confirmatory analysis of these compounds [14], since it guarantees the required sensitivity and selectivity for the determination of PCDD/Fs and dl-PCBs in food, feed, and environmental samples down to femtogram level, avoiding the contribution of potentially interfering chlorinated compounds [15]. Nevertheless, EI as an ionization technique produces significant fragmentation, even at low ionization energies (~ 35 eV), reducing the intensity of the molecular ion and, therefore, worsening the detection capabilities of the methods [2]. In addition, when operating double-focusing HRMS instruments in selected ion monitored mode, the sensitivity is inversely related to both the resolution and the number of masses monitored, which effectively limits the number of different compounds that can be monitored at any given time. In 2010, Peterson et al. [16] reported the use of a GC-EI-QLT-Orbitrap hybrid mass spectrometer to achieve high-mass accuracy and resolution in the determination of PCDD/Fs, achieving significant advantages over the traditional magnetic mass instruments, such as high detection capabilities and precision, even operating in full-scan acquisition mode, and an excellent versatility by performing measurements in tandem mass spectrometry. This instrumentation provides useful information on the molecular mass and chemical structure as well as the possibility to perform standard library search. In the last years, the advances achieved on triple quadrupole and ion trap technologies have allowed the development of new analytical methodologies based on gas chromatography coupled to tandem mass spectrometry (GC-MS/MS), which have been accepted as confirmatory methods for the determination of these families of compounds by the EU Regulations [17, 18]. These new methodologies provide enough sensitivity for the determination of PCDD/Fs and dl-PCBs [2, 19, 20] with the advantage of a lower instrumental cost. However, as GC-MS/MS operate at low mass resolution, it is subjected to more potential isobaric interferences, requiring more time-consuming sample fractionation procedures to be applied than those used with GC-HRMS methods to achieve and accurate and selective determination of the

analytes [21]. In the last decades, the use of atmospheric pressure ionization (API) sources for GC-MS analysis has significantly increased since they are soft ionization techniques that preserve molecular ion and/or protonated molecule [22, 23]. Moreover, API techniques are able to ionize a wider range of compounds than the high-vacuum ionization sources (e.g., electron and chemical ionization) and they have shown to be useful for the analysis of some families of persistent contaminants [24]. Among the API techniques, the atmospheric pressure chemical ionization (APCI) has been already applied to the GC-MS/MS analysis of both PCDD/Fs and dl-PCBs, obtaining intact molecular ions with low in-source collision-induced dissociation (CID) fragmentation and achieving high detection capability [2, 9, 21, 25–29]. Nevertheless, when APCI is combined with low-resolution tandem mass spectrometry working in multiple-reaction monitoring (MRM) mode, even though the selectivity achieved, the isotopic cluster information is lost, and also tedious sample clean-up procedures are necessary to avoid isobaric interferences. In the last years, a new atmospheric pressure photoionization (APPI) source has been commercialized and successfully applied to the analysis of different families of compounds [30–34]. In addition, this source is available for coupling to GC-MS instruments with Orbitrap mass analysers, which could overcome the limitations observed for MS/MS methods in the analysis of PCDD/Fs and dl-PCBs.

In this work, the performance and capability of the new coupling GC-APPI-HRMS (Orbitrap) for the reliable analysis of PCDD/Fs and dl-PCBs in selected feed and environmental samples have been evaluated as alternative to GC-EI-HRMS. For this purpose, several APPI parameters that affect the ionization of the target compounds were investigated. In addition, the GC-APPI-HRMS method was validated following the EU Regulations and the results were compared with those obtained using GC-EI-HRMS method. The real applicability of the proposed GC-APPI-HRMS method to the analysis of PCDD/Fs and dl-PCBs was assessed by analysing certified reference materials and reference samples used in several interlaboratory exercises.

Materials and methods

Standards and reagents

Calibration solutions of the seventeen regulated 2,3,7,8-chloro-substituted PCDD/Fs (CSL-CS4), EPA-1613, and twelve dl-PCBs (four non-ortho PCBs: CB 77, 81, 126, and 169, and eight mono-ortho PCBs: CB 105, 114, 118, 123, 156, 157, 167, and 189) (CS1-CS6), WP-CVS, containing the corresponding $^{13}C_{12}$-labelled compounds in nonane, were obtained from Wellington Laboratories Inc. (Guelph, Ontario, Canada) for quantification purposes. The calibration solutions

of PCDD/Fs and dl-PCBs covered a concentration range from 0.1 to 400 ng mL^{-1} and between 0.1 and 200 ng mL^{-1}, respectively. The $^{13}C_{12}$-labelled surrogate standard solutions, EPA-1613 LCS and WP-LCS, and injection standard solutions, EPA-1613 ISS and WP-ISS, for PCDD/Fs and dl-PCBs were also supplied by Wellington Laboratories Inc. Standards and calibration solutions were stored at 4 °C until their analyses.

Dichloromethane, toluene, cyclohexane, isooctane, and *n*-hexane for organic trace analysis were purchased from JT Baker (Deventer, The Netherlands). Ethyl acetate and nonane were supplied by Fluka (Fluka chemie GmbH., Switzerland). Silica gel was obtained from JT Baker (The Netherlands), basic Alumina ICN was purchased to MP Biomedicals (Germany), while Carbopack C 80/100 was achieved from Fluka (Switzerland). For the optimization of APPI of the target compounds, toluene and chlorobenzene (Chromasolv™ Plus, for HPLC analysis, purity ≥ 99%) from Sigma-Aldrich (St. Louis, MO, USA), acetone (LiChrosolv®, purity ≥ 99.8%), benzene (grade reagent for analysis, purity ≥ 99.7%), and diethyl ether (EMSURE® for analysis, purity ≥ 99.7%) from Merck, and tetrahydrofuran (Photrex™ reagent, purity at 99%) supplied by JT Baker (Deventer, The Netherland), were used as potential dopants. Helium Alphagaz™ 1 (purity ≥ 99.999%), supplied by Air Liquide (Madrid, Spain), was used as the GC carrier gas, whereas nitrogen (purity > 99.995%), from Linde (Barcelona, Spain), was employed as the make-up gas for the GC-APPI source. All glassware was cleaned using chromosulphuric acid and rinsed consecutively with Milli-Q water, methanol, and acetone, and dried at 180 °C overnight.

Samples and sample treatment

Certified reference materials BCR-677 (sewage sludge) and BCR-615 (fly ash) were obtained from the Institute for Reference Materials and Measurements (IRMM) of the European Commission-Joint Research (Geel, Belgium) and were used for validation of the GC-APPI-HRMS method. In addition, a chicken feed sample spiked with PCDD/Fs (0.12–2.27 pg g^{-1}) and dl-PCBs (12.8–30.7 pg g^{-1}), which is used as quality control material (QCM) for routine internal laboratory control, and some selected matrices (soybean meal, feed oil, and sediment) from several international interlaboratory studies were tested for evaluating the performance of the GC-APPI-HRMS method and comparing the results obtained with the two GC-HRMS systems.

Sample treatment was carried out following accredited analytical methods previously described elsewhere [35–37]. Owing to the variety of matrices, different extraction procedures were applied depending on the sample nature. All samples were spiked just before extraction step with known amounts of ^{13}C-labelled PCDD/Fs (EPA-1613 LCS) and

^{13}C-labelled dl-PCBs (WP-LCS). Appropriate amounts of soybean meal (40 g) and spiked chicken feed (9 g) samples were Soxhlet extracted for 24 h with 300 mL of toluene/cyclohexane (1:1, v/v), while for the fly ash (1 g), sludge (7 g), and sediment (1 g) samples, 300 mL of toluene was used. All the extracts were rotary evaporated to near dryness and the fatty residue was dissolved in 5 mL of *n*-hexane. For the feed oil sample, the matrix was directly diluted in *n*-hexane, after a previous homogenization by manual shaking for 5 min and spiked with known amounts of the ^{13}C-labelled PCDD/F and dl-PCB standard mixtures. Fat and other interfering substances were removed from all the extracts and the diluted feed oil by using an acidified silica gel column (H_2SO_4, 44%, w/w). Purification and fractionation of the extracts were carried out by sequential use of a multilayer silica, basic alumina, and carbon columns. The procedure provided two main fractions: fraction 1, containing the dl-PCB congeners, and fraction 2, where the PCDD/Fs were eluted. Both fractions were rotary concentrated and transferred into 1-mL conical vials. The remaining solvent was reduced to near dryness using a gentle stream of nitrogen and the final volume of the extract was adjusted to ca. 20 μL after addition in nonane of a known amount of the corresponding $^{13}C_{12}$-isotopically labelled injection standards (EPA-1613 ISS and WP-ISS). The extracts were then analysed by both GC-APPI-HRMS and GC-EI-HRMS.

Instrumentation

The determination of both PCDD/Fs and dl-PCBs by GC-APPI-HRMS was performed in a Trace 1300 gas chromatograph coupled to a Q-Exactive Orbitrap mass spectrometer (Thermo Fisher Scientific, San Jose, CA, USA), using an atmospheric pressure photoionization (GC-APPI) source supplied by MasCom Technologies GmbH (Bremen, Germany). The chromatographic separation of PCCD/Fs and dl-PCBs was carried out using the same GC column, a DB-5ms UI (60 m × 0.25 mm I.D., 0.25-μm film thickness) fused-silica capillary column (Agilent Technologies, Santa Clara, CA, USA). In both cases, the injector was operated at 280 °C in splitless mode (1 min), using helium as carrier gas at a constant flow mode (1.0 mL min^{-1}), and the injection volume was 1.5 μL for PCDD/Fs and 1 μL for dl-PCBs. The oven temperature program for PCDD/Fs was 140 °C (held for 1 min) to 200 °C at 20 °C min^{-1} (held for 1 min) and then to 300 °C at 2.5 °C min^{-1} (held for 20 min), and for dl-PCBs, 140 °C (held for 2 min) to 180 °C at 20 °C min^{-1} (held for 1 min) and to 300 °C at 2.5 °C min^{-1} (held for 5 min). The transfer line and capillary temperatures were set at 280 °C and 225 °C, whereas the source temperature was set at 250 °C and 225 °C for PCDD/F and dl-PCB analyses, respectively. The GC-APPI source was equipped with a 10.6-eV krypton lamp (Syagen, Santa Ana, CA, USA) and it was operated in negative ion

mode for PCDD/Fs and dl-PCBs. Nitrogen was employed as make-up gas (gas pressure of 5 a.u.) and vapours of benzene and diethyl ether at a flow rate of 90 μL min^{-1} were used as dopants for the APPI of PCDD/Fs and dl-PCBs, respectively. In addition, S-Lens radio frequency was set at 50% to enhance the ion transmission to the mass analyser. Data acquisition was performed in full-scan mode from 100 to 600 *m/z* at a mass resolution of 70,000 FWHM (full width at half maximum, at 200 *m/z*). To achieve the highest sensitivity with well-defined peaks (12 points per peak), the automatic gain control (AGC) and maximum injection time were set at 1×10^6 and 50 ms, respectively. The quantitation of the target compounds was performed using the isotope dilution method. The extracted ion chromatograms were obtained using mass extraction windows with a tolerance of ±5 ppm to guarantee a high selectivity and quality of the results. Xcalibur v 3.1 software was used to control the instrument setup and process the data acquisition.

The analysis of the target compounds by GC-EI-HRMS was performed using an Agilent 7890A gas chromatograph (Agilent Technologies, Santa Clara, CA, USA) coupled to a Micromass Premier (Waters, Manchester, UK) high-resolution mass spectrometer (EBE geometry) equipped with an electron ionization source. The separation of PCDD/Fs and dl-PCBs was carried out using the same GC column than that described above for GC-APPI-HRMS system. Injection (1 μL) was performed in splitless mode (1 min) at 280 °C using helium as carrier gas at a constant flow mode (1.0 mL min^{-1}). The oven temperature program was set as follows: 140 °C (held for 1 min) to 200 °C at 20 °C min^{-1} (held for 1 min) and then 310 °C at 5 °C min^{-1} (held for 6 min). The HRMS system was operated in EI+ mode at electron energy of 32 eV and at resolution of 10,000 (10% valley definition). The ion source and transfer line temperatures were set at 250 °C and 280 °C, respectively. The acquisition was carried out in selected ion monitoring (SIM) mode, where the two most abundant ions of the molecular cluster of each homologue group for PCDD/Fs and dl-PCBs were monitored at a 50-ms dwell time and a delay time of 20 ms. Trap current and acceleration voltage were set at 500 μA and 8000 V, respectively. Moreover, the quantitation was also performed using the isotope dilution method and a Masslynx data system (Waters) was used for data acquisition and instrument control.

Quality control criteria

Quality control procedures were applied for ensuring the quality of the results. Analyses including tests on isomer-specific GC separation, sensitivity, validity of the instrumental calibration and isotopic mass ratio, and recovery of the target compounds were carried out. In addition, procedural blanks, covering extraction, purification, and instrumental determination,

were periodically analysed to evaluate the potential contribution of interfering compounds or potential sample carryover. Recoveries of the target compounds were always in the range of 60 to 120% as indicated in the corresponding EU Regulation [18]. To ensure accurate mass measurements, the Orbitrap mass analyser was calibrated every 72 h using an electrospray source and a calibration solution containing caffeine, MRFA peptide, Ultramark 1621, and butylamine in acetonitrile/methanol/water (2:1:1, v/v/v) with 1% (v/v) formic acid. PCDD/F and dl-PCB results were expressed as individual congener concentration and in WHO-TEQ (World Health Organization Toxic Equivalent) using the toxic equivalent factors (TEFs) revised in 2005 [6]. TEQ values were calculated in upperbound assuming the method limits of detection for those congeners when they are below these limits.

Results and discussion

Ionization of PCDD/Fs and dl-PCBs by GC-APPI

To study the ionization of both native and ^{13}C-labelled compounds in the GC-APPI source, a calibration solution of PCDD/Fs (EN1613-CS4; 40–400 ng mL^{-1}) and dl-PCBs (WP-CS6; 200 ng mL^{-1}) were injected in the GC-APPI-HRMS system using vapours of different solvents (acetone, benzene, chlorobenzene, diethyl ether, tetrahydrofuran, and toluene) as dopants. As an example, Fig. 1 shows the mass spectra obtained for 1,2,3,7,8-PeCDD/Fs and CB-126 in both positive and negative ion modes, using as dopants benzene and diethyl ether, respectively. Generally, PCDD/Fs and dl-PCBs showed a similar ionization behaviour in positive ion mode using the tested dopants. Thus, all the target compounds led to the generation of the molecular ion [M]$^{+\bullet}$ without any in-source collision-induced dissociation (CID) fragment ions and the ionization efficiency of these analytes mainly depended on the nature of the dopant. For instance, Fig. 2 (a–c) shows the effect of different dopants on the response of the molecular ion [M]$^{+\bullet}$. As can be seen, all compounds showed higher responses with benzene, toluene, and chlorobenzene than those achieved with acetone and tetrahydrofuran. This could be attributed to the different ions generated by each dopant during the photoionization process (see Electronic Supplementary Material (ESM) Table S1). Dopants such as benzene, chlorobenzene, and toluene yielded their molecular ion [D]$^{+\bullet}$ (Table 1, reaction a), which was responsible of the ionization of the target compounds by charge exchange reactions (Table 1, reaction b). In contrast, acetone and tetrahydrofuran underwent a rapid self-protonation due to their high proton affinity that prevented the presence of radical dopant ions in the APPI source (Table 1, reaction c). Since benzene was the dopant that provided the highest responses for most of PCDD/Fs and dl-
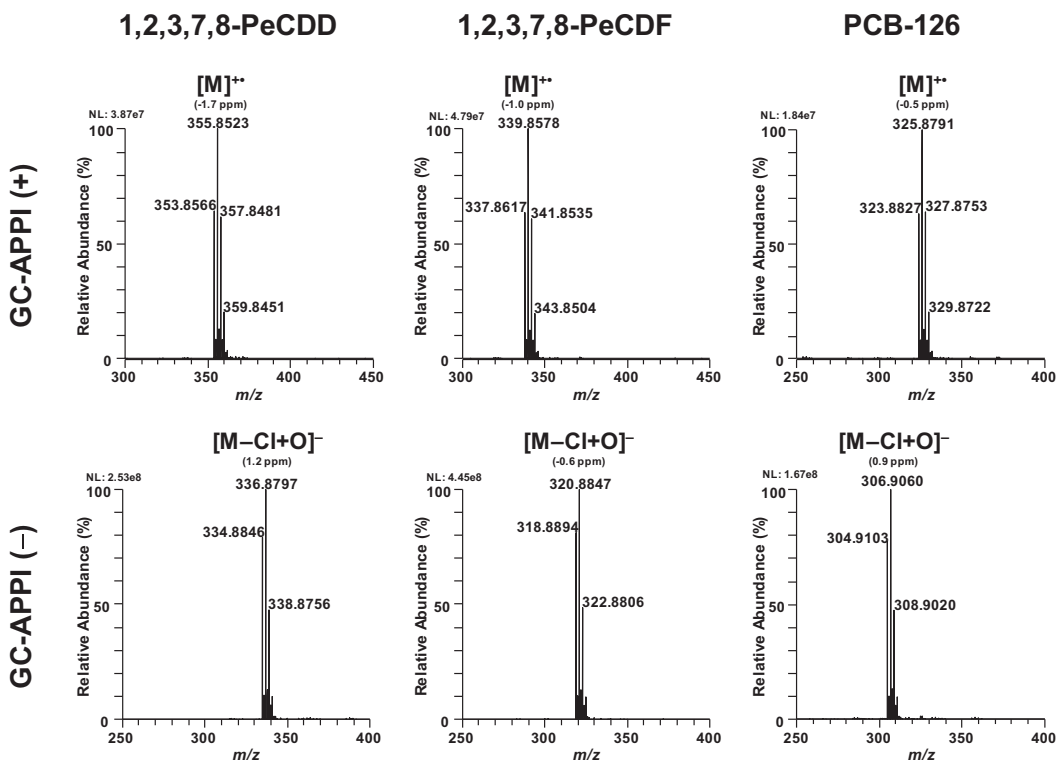
Fig. 1 GC-APPI-HRMS mass spectra of 1,2,3,7,8-PeCDD/F and PCB-126 in positive (dopant: benzene) and negative (dopant: diethyl ether) ion mode (250 °C source temperature and 225 °C capillary temperature)

PCBs in positive ion mode, it was selected as the most appropriate dopant to achieve a high ionization efficiency of the target compounds.

Concerning the negative ion mode, the APPI was generally mediated by the superoxide ion (Table 1, reaction d), which is formed when an oxygen molecule captures the electrons released during the photoionization process of the dopant. Thus, PCDD/Fs and dl-PCBs led to the generation of the phenoxide ion ([M−Cl+O]⁻) without any in-source CID fragmentation (Fig. 1). For the PCDDs, the nature of the most abundant ion (base peak) was closely related with the number of chlorine atoms in the molecule (Fig. 3). Thus, the tetrachlorinated dibenzo-p-dioxins (TCDD) yielded the [M−Cl+O₂]⁻ as base peak (Fig. 3a), whereas pentachlorinated (PeCDDs) and hexachlorinated dibenzo-p-dioxins (HxCDDs) mainly led to the phenoxide ion [M−Cl+O]⁻ (Fig. 3b). In contrast, the highly chlorinated dioxins, such as heptachlorinated (HpCDDs) and octachlorinated dibenzo-p-dioxins (OCDDs), yielded the ion [M−Cl]⁻ (Fig. 3c). This could be due to both a steric hindrance and repulsion effect of chlorine atoms in the

molecule that hinders the interaction of the superoxide ion with aromatic rings of the PCDDs. This phenomenon was not observed for PCDFs and dl-PCBs, which only yielded the phenoxide ion. This fact may be due to the less sterically hindered structures to generate the [M−Cl+O]⁻ ion, since they only have one or none oxygen atoms, respectively.

Additionally, a relationship was observed between vapour pressure of the dopant and the analyte ionization efficiency in negative ion mode (Fig. 2). Thus, the higher the vapour pressure of the dopant, the greater the ionization efficiency of the compounds. Dopants with high vapour pressure (e.g., diethyl ether and acetone) may provide a higher number of electrons during the photoionization process, which could promote the subsequent reactions with the analytes in gas-phase (Table 1, reactions e–g). Moreover, PCDD/Fs, especially the TCDD, showed a high ionization efficiency in the presence of benzene (Fig. 2), even though the lower vapour pressure of this dopant, which was probably compensated by its lower ionization potential. Therefore, as a compromise, diethyl ether and benzene were selected as dopants for further studies in negative ion mode.

🙋 Springer

257
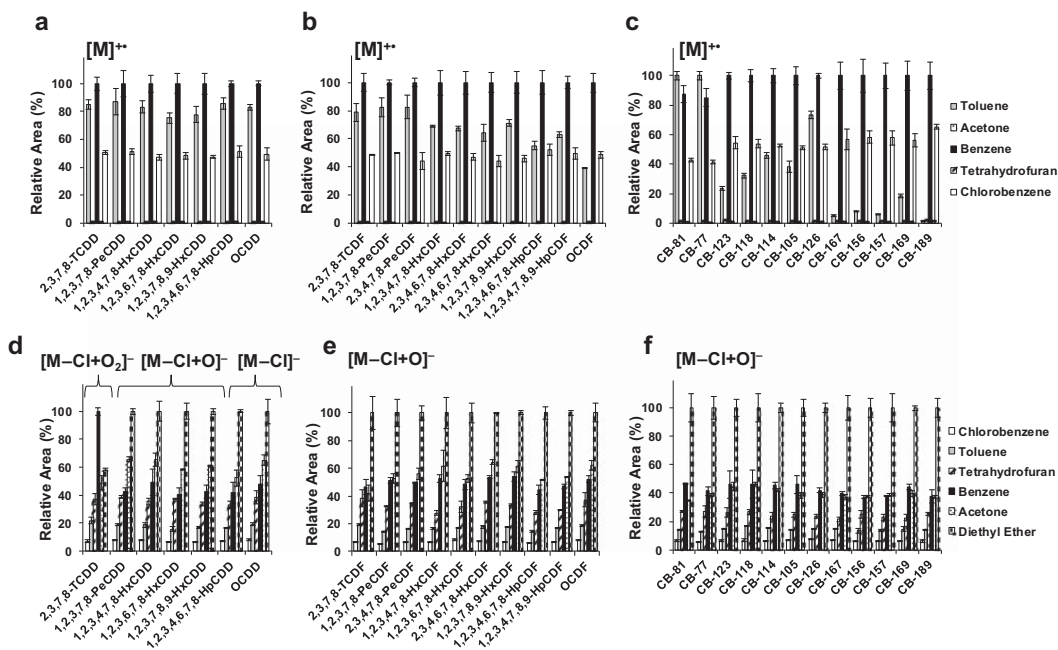
Fig. 2 Dopant vapour effect over PCDDs, PCDFs, and dl-PCBs responses in positive (**a**–**c**) and negative ion mode (**d**–**f**), respectively

To maximize the ionization efficiency of the target compounds, the effect of the APPI source (from 180 to 250 °C) and capillary temperatures (from 175 to 225 °C) on the response of the analytes were also investigated. As it can be observed in Fig. 4 for the chromatographic separation of HxCDDs, a decrease on the source temperature resulted in an important peak broadening that negatively affected the chromatographic separation of the compounds. This effect was also observed for PCDFs and dl-PCBs, and it could be related with both the relatively low vapour pressure of the analytes and the source design that could lead to some condensation problems. Thus, high source (250 °C) and capillary temperatures (225 °C) were required to preserve the adequate chromatographic separation for all the compounds.

Performance of the GC-APPI-HRMS methods

In order to select the most suitable dopant for the determination of PCDD/Fs and dl-PCBs by GC-APPI-HRMS, instrumental limits of detection (iLODs) were determined using the dopant that provided the best responses in positive ion (benzene) and negative ion (benzene and diethyl ether) modes and monitoring the ions selected for quantification and confirmation of PCDD/Fs and dl-PCBs (Table 2). Since the extracted ion chromatograms present almost no baseline noise due to the narrow mass error threshold (< 5 ppm), the iLODs were defined as the smallest analyte concentration that provides a well-defined chromatographic peak. Table 3 shows the iLODs achieved for those dopants previously selected in both

Table 1 The reactions in dopant-assisted positive and negative APPI

APPI	Gas-phase reaction	
Photoionization	(a) $D + h\nu \rightarrow D^{+\bullet} + e^{-\bullet}$	
Positive ion mode	(b) $D^{+\bullet} + M \rightarrow [M]^{+\bullet} + D$	(If $IE_M < IE_D$)
	(c) $D^{+\bullet} + D \rightarrow [D+H]^+ + [D-H]^\bullet$	(If D has a high proton affinity)
Negative ion mode	(d) $O_2 + e^{-\bullet} \rightarrow O_2^{-\bullet}$	
	(e) $M + e^{-\bullet} \rightarrow [M-Cl]^- + Cl^\bullet$	(If M has a high electron affinity)
	(f) $M + O_2^{-\bullet} \rightarrow [M-Cl+O_2]^- + Cl^\bullet$	
	(g) $M + O_2^{-\bullet} \rightarrow [M-Cl+O]^- + OCl^\bullet$	

D, dopant; *M*, PCDDs, PCDFs, and dl-PCBs; IE_M, ionization energy of M; IE_D, ionization energy of the dopant
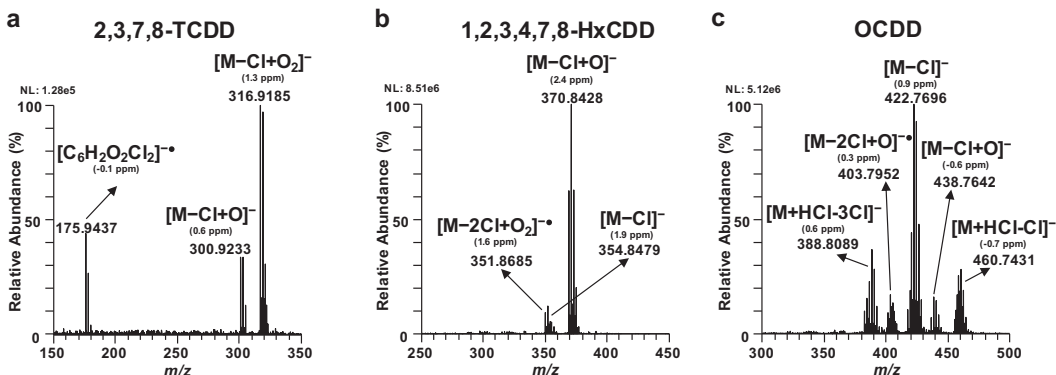
Fig. 3 Negative ion GC-APPI-HRMS mass spectra of **a** 2,3,7,8-TCDD, **b** 1,2,3,4,7,8-HxCDD, and **c** OCDD using benzene as dopant

positive and negative ion modes. For most of the PCDD/Fs, the lowest iLOD values were obtained in negative ion mode using diethyl ether as dopant (0.25–3 fg on-column), which were around twofold lower than those found with benzene (0.5–8 fg on-column) in negative mode and 100-fold lower (10–49 fg on-column) than those achieved in positive ion mode. Nevertheless, the iLOD for the 2,3,7,8-TCDD using diethyl ether (150 fg on-column) was 5 times higher than that achieved employing benzene as dopant (25 fg on-column) due to the high fragmentation observed in the APPI source (ESM Fig. S1 a). This could be attributed to the higher ionization potential of diethyl ether (9.53 eV) compared with benzene (9.24 eV) that may lead to more energetic electrons, which could induce a higher in-source CID fragmentation on this analyte, thus increasing the corresponding iLOD. As a compromise, benzene was selected as the most suitable dopant for the PCDD/F determination by negative ion GC-APPI-HRMS. Concerning the dl-PCBs, the use of diethyl ether as dopant in negative ion mode provided iLODs ranging from 2.5 to 100 times lower than those obtained in positive ion mode (Table 3). Therefore, negative ion GC-APPI-HRMS using

diethyl ether as dopant was chosen for the determination of dl-PCBs. In addition, the iLODs achieved with the GC-APPI-HRMS methods were compared with those obtained by GC-EI-HRMS. As can be seen in Table 3, iLODs obtained for most of dl-PCBs by negative ion GC-APPI-HRMS were at least 2 times lower than those achieved by GC-EI-HRMS and even up to a maximum of 60-fold lower than those estimated for the confirmatory method in the case of PCDD/Fs. These results demonstrate the high detection capability of the developed GC-APPI-HRMS methods.

The performance of the proposed GC-APPI-HRMS methods for the determination of PCDD/Fs and dl-PCBs was investigated in compliance with the requirements established in the current EU Regulation (EU Regulation 2017/664-771) [17, 18]. As mentioned before, the GC-APPI-HRMS methods allowed the adequate detection of the target compounds at low femtogram levels (Table 2), which successfully satisfies the analytical criteria established in the EU Regulations. In addition, the chromatographic separation achieved for 1,2,3,4,7,8-HxCDD and 1,2,3,6,7,8-HxCDD congeners was enough (co-elution lower than 7%) to fulfil

Fig. 4 Effect of the source temperature over the chromatographic separation of HxCDDs

Table 2 Selected ions for GC-APPI-HRMS analysis of PCDD/Fs and dl-PCBs in both positive and negative ion modes

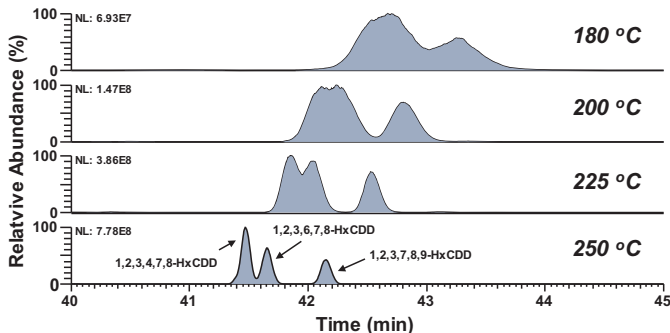| Compound	Positive ion mode[a]						Negative ion mode[a]					
	Ion	Formula	Q_1 ion (m/z)	Formula	Q_2 ion (m/z)	IR	Ion	Formula	Q_1 ion (m/z)	Formula	Q_2 ion (m/z)	IR
TCDD	$[C_{12}H_4Cl_4O_2]^{+•}$	$[M]^{+•}$	319.8960	$[M+2]^{+•}$	**321.8930**	0.78	$[C_{12}H_4Cl_4O_4]^-$	$[M-Cl+O_2]^-$	**316.9181**	$[M+2-Cl+O]^-$	318.9151	1.04
$^{13}C_{12}$-TCDD	$[^{13}C_{12}H_4Cl_4O_2]^{+•}$	$[M]^{+•}$	331.9362	$[M+2]^{+•}$	**333.9333**	0.78	$[^{13}C_{12}H_4Cl_4O_4]^-$	$[M-Cl+O_2]^-$	**328.9572**	$[M+2-Cl+O_2]^-$	330.9543	1.04
PeCDD	$[C_{12}H_3Cl_5O_2]^{+•}$	$[M+2]^{+•}$	**355.8541**	$[M+4]^{+•}$	357.8511	1.56	$[C_{12}H_3Cl_4O_3]^-$	$[M-Cl+O]^-$	334.8842	$[M+2-Cl+O]^-$	**336.8812**	0.78
$^{13}C_{12}$-PeCDD	$[^{13}C_{12}H_3Cl_5O_2]^{+•}$	$[M+2]^{+•}$	**367.8943**	$[M+4]^{+•}$	369.8914	1.56	$[^{13}C_{12}H_3Cl_4O_3]^-$	$[M-Cl+O]^-$	346.9233	$[M+2-Cl+O]^-$	**348.9204**	0.78
HxCDDs	$[C_{12}H_2Cl_6O_2]^{+•}$	$[M+2]^{+•}$	**389.8151**	$[M+4]^{+•}$	391.8121	1.25	$[C_{12}H_2Cl_6O_3]^-$	$[M+2-Cl+O]^-$	**370.8423**	$[M+4-Cl+O]^-$	372.8393	1.56
$^{13}C_{12}$-HxCDDs	$[^{13}C_{12}H_2Cl_6O_2]^{+•}$	$[M+2]^{+•}$	**401.8554**	$[M+4]^{+•}$	403.8524	1.25	$[^{13}C_{12}H_2Cl_6O_3]^-$	$[M+2-Cl+O]^-$	**382.8814**	$[M+4-Cl+O]^-$	384.8785	1.56
HpCDD	$[C_{12}HCl_7O_2]^{+•}$	$[M+2]^{+•}$	**423.7761**	$[M+4]^{+•}$	425.7732	1.04	$[C_{12}HCl_6O_2]^-$	$[M+2-Cl]^-$	**388.8084**	$[M+4-Cl]^-$	390.8054	1.25
$^{13}C_{12}$-HpCDD	$[^{13}C_{12}HCl_7O_2]^{+•}$	$[M+2]^{+•}$	**435.8164**	$[M+4]^{+•}$	437.8134	1.04	$[^{13}C_{12}HCl_6O_2]^-$	$[M+2-Cl]^-$	**400.8475**	$[M+4-Cl]^-$	402.8446	1.25
OCDD	$[C_{12}Cl_8O_2]^{+•}$	$[M+2]^{+•}$	457.7372	$[M+4]^{+•}$	**459.7342**	0.89	$[C_{12}Cl_8O_2]^-$	$[M+2-Cl]^-$	**422.7694**	$[M+4-Cl]^-$	424.7664	1.04
$^{13}C_{12}$-OCDD	$[^{13}C_{12}Cl_8O_2]^{+•}$	$[M+2]^{+•}$	469.7774	$[M+4]^{+•}$	**471.7745**	0.89	$[^{13}C_{12}Cl_8O_2]^-$	$[M+2-Cl]^-$	**434.8086**	$[M+4-Cl]^-$	436.8056	1.04
TCDF	$[C_{12}H_4Cl_4O]^{+•}$	$[M]^{+•}$	303.9011	$[M+2]^{+•}$	**305.8981**	0.78	$[C_{12}H_4Cl_4O_2]^-$	$[M-Cl+O]^-$	**284.9282**	$[M+2-Cl+O]^-$	286.9253	1.04
$^{13}C_{12}$-TCDF	$[^{13}C_{12}H_4Cl_4O]^{+•}$	$[M+2]^{+•}$	315.9413	$[M+2]^{+•}$	**317.9384**	0.78	$[^{13}C_{12}H_4Cl_4O_2]^-$	$[M-Cl+O]^-$	**296.9674**	$[M+2-Cl+O]^-$	298.9644	1.04
PeCDFs	$[C_{12}H_3Cl_5O]^{+•}$	$[M+2]^{+•}$	**339.8592**	$[M+4]^{+•}$	341.8562	1.56	$[C_{12}H_3Cl_4O_2]^-$	$[M-Cl+O]^-$	318.8893	$[M+2-Cl+O]^-$	**320.8863**	0.78
$^{13}C_{12}$-PeCDDs	$[^{13}C_{12}H_3Cl_5O]^{+•}$	$[M+2]^{+•}$	**351.8994**	$[M+4]^{+•}$	353.8965	1.56	$[^{13}C_{12}H_3Cl_4O_2]^-$	$[M-Cl+O]^-$	330.9284	$[M+2-Cl+O]^-$	**332.9255**	0.78
HxCDFs	$[C_{12}H_2Cl_6O]^{+•}$	$[M+2]^{+•}$	**373.8202**	$[M+4]^{+•}$	375.8172	1.25	$[C_{12}H_2Cl_6O_2]^-$	$[M+2-Cl+O]^-$	**354.8473**	$[M+4-Cl+O]^-$	356.8444	1.56
$^{13}C_{12}$-HxCDDs	$[^{13}C_{12}H_2Cl_6O]^{+•}$	$[M+2]^{+•}$	**385.8604**	$[M+4]^{+•}$	387.8575	1.25	$[^{13}C_{12}H_2Cl_6O_2]^-$	$[M+2-Cl+O]^-$	**366.8865**	$[M+4-Cl+O]^-$	368.8836	1.56
HpCDFs	$[C_{12}HCl_7O]^{+•}$	$[M+2]^{+•}$	**407.7812**	$[M+4]^{+•}$	409.7783	1.04	$[C_{12}HCl_6O_2]^-$	$[M+2-Cl+O]^-$	**388.8084**	$[M+4-Cl+O]^-$	390.8054	1.25
$^{13}C_{12}$-HpCDDs	$[^{13}C_{12}HCl_7O]^{+•}$	$[M+2]^{+•}$	**419.8240**	$[M+4]^{+•}$	421.8185	1.04	$[^{13}C_{12}HCl_6O_2]^-$	$[M+2-Cl+O]^-$	**400.8475**	$[M+4-Cl+O]^-$	402.8446	1.25
OCDF	$[C_{12}Cl_8O]^{+•}$	$[M+2]^{+•}$	441.7422	$[M+4]^{+•}$	**443.7393**	0.89	$[C_{12}Cl_8O_2]^-$	$[M+2-Cl+O]^-$	**422.7694**	$[M+4-Cl+O]^-$	424.7664	1.04
TCBs	$[C_{12}H_6Cl_4]^{+•}$	$[M]^{+•}$	289.9218	$[M+2]^{+•}$	**291.9189**	0.78	$[C_{12}H_6Cl_4O]^-$	$[M-Cl+O]^-$	**270.9479**	$[M+2-Cl+O]^-$	272.9449	1.04
$^{13}C_{12}$-TCBs	$[^{13}C_{12}H_6Cl_4]^{+•}$	$[M]^{+•}$	301.9621	$[M+2]^{+•}$	**303.9591**	0.78	$[^{13}C_{12}H_6Cl_4O]^-$	$[M-Cl+O]^-$	**282.9881**	$[M+2-Cl+O]^-$	284.9852	1.04
PeCBs	$[C_{12}H_5Cl_5]^{+•}$	$[M+2]^{+•}$	**325.8799**	$[M+4]^{+•}$	327.8769	1.56	$[C_{12}H_5Cl_4O]^-$	$[M-Cl+O]^-$	304.9089	$[M+2-Cl+O]^-$	**306.9060**	0.78
$^{13}C_{12}$-PeCBs	$[^{13}C_{12}H_5Cl_5]^{+•}$	$[M+2]^{+•}$	**337.9201**	$[M+4]^{+•}$	339.9172	1.56	$[^{13}C_{12}H_5Cl_4O]^-$	$[M-Cl+O]^-$	316.9492	$[M+2-Cl+O]^-$	**318.9462**	0.78
HxCBs	$[C_{12}H_4Cl_6]^{+•}$	$[M+2]^{+•}$	**359.8409**	$[M+4]^{+•}$	361.8380	1.25	$[C_{12}H_4Cl_6O]^-$	$[M+2-Cl+O]^-$	**340.8670**	$[M+4-Cl+O]^-$	342.8640	1.56
$^{13}C_{12}$-HxCBs	$[^{13}C_{12}H_4Cl_6]^{+•}$	$[M+2]^{+•}$	**371.8812**	$[M+4]^{+•}$	373.8782	1.25	$[^{13}C_{12}H_4Cl_6O]^-$	$[M+2-Cl+O]^-$	**352.9072**	$[M+4-Cl+O]^-$	354.9043	1.56
HpCBs	$[C_{12}H_3Cl_7]^{+•}$	$[M+2]^{+•}$	**393.8019**	$[M+4]^{+•}$	395.7990	1.04	$[C_{12}H_3Cl_6O]^-$	$[M+2-Cl+O]^-$	**374.8280**	$[M+4-Cl+O]^-$	376.8251	1.25
$^{13}C_{12}$-HpCBs	$[^{13}C_{12}H_3Cl_7]^{+•}$	$[M+2]^{+•}$	**405.8422**	$[M+4]^{+•}$	407.8393	1.04	$[^{13}C_{12}H_3Cl_6O]^-$	$[M+2-Cl+O]^-$	**386.8683**	$[M+4-Cl+O]^-$	388.8653	1.25

[a] The most abundant ion is marked in bold. *IR* theoretical ion ratio, Q_1/Q_2

Table 3 Instrumental limits of detection (fg on-column) for the GC-APPI-HRMS analysis of both PCDD/Fs and dl-PCBs using benzene and diethyl ether as dopants

Compound	GC-APPI-HRMS[a]			GC-EI-HRMS[b]
	Positive ion	Negative ion		
	Benzene	Benzene	Diethyl ether	
2,3,7,8-TCDD	100	25	150	10
1,2,3,7,8-PeCDD	25	2	1	22
1,2,3,4,7,8-HxCDD	40	0.5	0.25	30
1,2,3,6,7,8-HxCDD	40	0.5	0.25	30
1,2,3,7,8,9-HxCDD	40	5	3	33
1,2,3,4,6,7,8-HpCDD	50	5	2	29
OCDD	100	8	2	30
2,3,7,8-TCDF	100	2	1.5	11
1,2,3,7,8-PeCDF	25	0.5	0.25	19
2,3,4,7,8-PeCDF	25	1	0.5	17
1,2,3,4,7,8-HxCDF	50	0.5	0.25	25
1,2,3,6,7,8-HxCDF	50	0.5	0.25	26
1,2,3,7,8,9-HxCDF	50	1	0.5	26
2,3,4,6,7,8-HxCDF	50	1	0.5	36
1,2,3,4,6,7,8-HpCDF	75	0.5	0.5	22
1,2,3,4,7,8,9-HpCDF	75	2	1	30
OCDF	150	4	1	49
CB-81	25	-	8	8
CB-77	25	-	10	8
CB-123	50	-	8	14
CB-118	50	-	2	13
CB-114	50	-	4	13
CB-105	50	-	4	15
CB-126	50	-	4	16
CB-167	50	-	1	12
CB-156	50	-	0.5	12
CB-157	50	-	1.5	13
CB-169	50	-	2	14
CB-189	75	-	1	12

[a] Injection volume: 1.5 μL (PCDD/Fs) and 1.0 μL (dl-PCBs)

[b] Injection volume: 1.0 μL (PCDD/Fs and dl-PCBs)

with the EU Regulation (co-elution < 25%) [17], working at a source temperature of 250 °C (Fig. 4). The linearity was evaluated over the 0.1–400 pg μL^{-1} range for PCDD/Fs and from 0.1 to 40 pg μL^{-1} for dl-PCBs (Table 4). Calibration curves were established, and good linearity was obtained within the calibration range with determination coefficients (r^2) higher than 0.9997 for all the compounds. In addition, reproducible relative response factors (RRFs) were obtained from the analysis of calibration solutions with relative standard deviations lower than 12% for both PCDD/Fs and dl-PCBs (Table 4). Moreover, the differences between the RRF average obtained for all points and the corresponding values for only the lowest calibration point were less than 14% (Table 4). These

differences fulfilled with the criterion established by the EU Regulation (< 30%), demonstrating the high stability on the response of the target compounds using GC-APPI-HRMS methods, even working at very low concentration levels. The ion abundance ratio (IR) of the two ions selected for quantification (see Table 2) along the calibration range was quite stable and ranging from 0.3 to 7% RSD% (Table 4), which also met with the maximum permitted tolerance established in the EU Regulation (± 15%). Moreover, run-to-run and day-to-day precisions were assessed by analysing seven replicates ($n = 7$) of a standard calibration solution at low concentration levels (PCDD/Fs, 0.25–2.5 pg μL^{-1}; dl-PCBs, 0.5 pg μL^{-1}) on 1 day for run-to-run and on three

Table 4 Quality parameters of the GC-APPI-HRMS methods for the determination of PCDD/Fs and dl-PCBs

Compound	t_R (min)	Calibration range (pg μL^{-1})	Relative response factor (RRF)		Difference RRF$_1$–RRF$_{all}$ (%)	Ion ratio (IR)		Precision (RSD, %)		iLOQ (pg μL^{-1})
			Mean[a]	RSD (%)		Mean[a]	RSD (%)	Intra-day[b]	Inter-day[c]	
2,3,7,8-TCDD	28.54	0.1–40	0.94	5	−4	1.03	2	6	8	0.06
1,2,3,7,8-PeCDD	35.11	0.5–200	1.01	0.6	0.08	0.79	1	2	2	0.004
1,2,3,4,7,8-HxCDD	41.26	0.5–200	1.05	1	−0.06	1.58	0.8	6	8	0.002
1,2,3,6,7,8-HxCDD	41.45	0.5–200	1.02	0.7	1	1.57	1	8	8	0.002
1,2,3,7,8,9-HxCDD	41.95	0.5–200	0.38	10	15	1.56	1	6	5	0.01
1,2,3,4,6,7,8-HxCDD	47.80	0.5–200	1.13	2	2	1.27	0.7	3	3	0.01
OCDD	53.89	1.0–400	3.39	1	4	1.04	2	3	4	0.02
2,3,7,8-TCDF	27.67	0.1–40	1.07	1	2	1.05	0.8	3	4	0.004
1,2,3,7,8-PeCDF	33.13	0.5–200	1.01	4	7	0.79	1	4	6	0.002
2,3,4,7,8-PeCDF	34.60	0.5–200	1.09	2	2	0.78	1	3	4	0.002
1,2,3,4,7,8-HxCDF	39.63	0.5–200	1.09	4	6	1.57	1	9	9	0.002
1,2,3,6,7,8-HxCDF	39.85	0.5–200	1.05	4	6	1.58	0.3	8	9	0.002
1,2,3,7,8,9-HxCDF	40.93	0.5–200	1.06	5	9	1.58	1	4	8	0.002
2,3,4,6,7,8-HxCDF	42.54	0.5–200	1.10	3	5	1.58	0.9	4	8	0.002
1,2,3,4,6,7,8-HpCDF	45.53	0.5–200	1.07	3	6	1.27	1	4	6	0.007
1,2,3,4,7,8,9-HpCDF	48.79	0.5–200	1.06	3	3	1.27	0.6	3	6	0.004
OCDF	54.18	1.0–400	3.39	6	−4	1.06	0.8	6	7	0.01
CB-81	28.33	0.1–40	1.02	11	1	1.10	6	4	4	0.03
CB-77	29.01	0.1–40	0.97	5	−4	1.06	0.8	6	6	0.03
CB-123	30.38	0.1–40	1.01	5	−8	0.77	4	5	6	0.03
CB-118	30.62	0.1–40	1.08	8	−7	0.79	5	5	6	0.007
CB114	31.29	0.1–40	1.08	3	−3	0.79	1	3	3	0.01
CB-105	32.32	0.1–40	1.11	12	−11	0.78	2	4	5	0.01
CB-126	34.57	0.1–40	1.04	6	−1	0.77	7	4	4	0.01
CB-167	35.83	0.1–40	1.06	3	−4	1.57	1	3	4	0.003
CB-156	37.34	0.1–40	1.15	6	−6	1.54	6	3	4	0.002
CB-157	37.65	0.1–40	1.06	4	−0.8	1.54	4	3	3	0.005
CB-169	39.93	0.1–40	1.08	2	−3	1.56	2	4	5	0.007
CB-189	42.42	0.1–40	1.09	2	−0.4	1.28	2	2	2	0.003

[a] $n = 5$; [b] $n = 7$; [c] $n = 7$ replicates × 3 days

non-consecutive days for day-to-day. The precision achieved on the variation of quantitative results, expressed as RSD% values, was always lower than 9% (Table 4), showing the good performance of the GC-APPI-HRMS methods for the analysis of PCDD/Fs and dl-PCBs, respectively.

Analysis of reference samples

Once the instrumental methods were validated for the determination of PCDD/Fs and dl-PCBs, selected environmental and feed samples were analysed to evaluate the real applicability in the GC-APPI-HRMS technique. The analysed samples consisted on two certified reference materials, a fly ash (BCR-615) and a sewage sludge (BCR-677), three interlaboratory materials (soybean meal, feed oil, and sediment), and one quality control sample (a spiked chicken feed sample), which is used for the internal laboratory control. All these samples were analysed by triplicate using the sample treatment described in the experimental section ("Samples and sample treatment" section) and the extracts were injected in both GC-EI-HRMS and GC-APPI-HRMS systems. Tables 5 and 6 summarize the results obtained using the proposed GC-APPI-HRMS method, the reference GC-EI-HRMS method, and the certified or assigned value. In addition, quantitative results for the internal quality sample are also given in ESM

Table 5   PCDD/F concentrations in certified reference materials

Compound	Fly ash BCR-615 (pg g^{-1} ± SD)			Sludge BCR-677 (pg g^{-1} ± SD)		
	Reference value	GC-EI-HRMS	GC-APPI-HRMS	Reference value	GC-EI-HRMS	GC-APPI-HRMS
2,3,7,8-TCDD	27 ± 5	26 ± 5	22 ± 3	1.5 ± 0.2	1.4 ± 0.1	1.35 ± 0.08
1,2,3,7,8-PeCDD	92 ± 12	79 ± 15	78.98 ± 0.08	4.1 ± 0.9	4.0 ± 0.2	3.90 ± 0.08
1,2,3,4,7,8-HxCDD	74 ± 12	61 ± 9	60.9 ± 0.5	2.7 ± 0.9	2.9 ± 0.4	3.2 ± 0.2
1,2,3,6,7,8-HxCDD	103 ± 13	89 ± 8	84.9 ± 0.4	235 ± 17	253 ± 14	204 ± 16
1,2,3,7,8,9-HxCDD	108 ± 16	111 ± 14	113 ± 5	79 ± 7	93 ± 5	71 ± 4
1,2,3,4,6,7,8-HxCDD	870 ± 130	752 ± 84	741 ± 4	3500 ± 400	3373 ± 135	3177 ± 84
OCDD	1750 ± 200	1911 ± 278	1980 ± 14	12,700 ± 800	13,155 ± 521	11,574 ± 347
2,3,7,8-TCDF	86 ± 28	70 ± 10	59.9 ± 0.3	45 ± 4	46 ± 4	41 ± 1
1,2,3,7,8-PeCDF	176 ± 26	145 ± 21	128.5 ± 0.4	25 ± 2	23 ± 2	23.0 ± 0.9
2,3,4,7,8-PeCDF	125 ± 20	106 ± 19	91.9 ± 0.9	17 ± 2	15 ± 1	14.1 ± 0.4
1,2,3,4,7,8-HxCDF	203 ± 21	170 ± 17	160 ± 1	14 ± 2	14 ± 1	13 ± 1
1,2,3,6,7,8-HxCDF	204 ± 23	181 ± 20	172 ± 2	6.1 ± 0.8	5.7 ± 0.4	5.7 ± 0.5
1,2,3,7,8,9-HxCDF	13 ± 2	12 ± 10	12.6 ± 0.3	0.8 ± 0.3	0.89 ± 0.07	0.91 ± 0.04
2,3,4,6,7,8-HxCDF	130 ± 15	144 ± 13	130 ± 1	5.6 ± 0.6	7.1 ± 0.5	6.2 ± 0.3
1,2,3,4,6,7,8-HpCDF	750 ± 90	664 ± 55	641 ± 1	62 ± 3	54 ± 28	55 ± 2
1,2,3,4,7,8,9-HpCDF	61 ± 6	70 ± 6	53.99 ± 0.02	6.3 ± 0.8	5 ± 1	4.8 ± 0.1
OCDF	290 ± 40	349 ± 25	317 ± 2	177 ± 7	182 ± 203	166 ± 10

Table S2. As can be seen, a good agreement between both GC-MS methods was achieved for all individual congeners, with differences in the mean value lower than 23%. To compare these results and extract useful conclusions, statistical treatment of the data was performed using a two-way analysis of variances (ANOVA) test. The p-values obtained were always higher than the significance level of 0.05 (p values for PCDD/Fs, 0.15–0.52 and for dl-PCBs, 0.37–0.90), which indicated that there were no statistically significant differences between both GC-EI-HRMS and GC-APPI-HRMS methods. In addition, the statistical study also showed that the results were not significantly different from the reference concentration values. Moreover, the results were also compared in terms of toxic equivalents (TEQs) and the upperbound TEQs corresponding to the reference materials and those achieved using both GC-EI-HRMS and GC-APPI-HRMS methods are shown in Fig. 5. As it can be observed, the results were similar with no significant differences between them (p values from 0.26 to 0.77), which indicates that the GC-APPI-HRMS methods allow the estimation of the TEQ values as well as the reference GC-EI-HRMS methods. In fact, the differences between the lower and the upperbound TEQs did not exceed the 15% for all the samples analysed (15% for PCDD/Fs and 0.02% for dl-PCBs), which fulfils the requirements of the current EU Regulation (< 20%) [18]. These results demonstrate the suitability of the developed method for the analysis of

PCDD/Fs and dl-PCBs in environmental and feed samples.

Conclusions

The feasibility of the developed GC-APPI-HRMS (Orbitrap) (negative ion mode) methods for the analysis of both PCDD/Fs and dl-PCBs in environmental and feed samples has been demonstrated. The use of dopants with a high vapour pressure in the negative ion mode provided the highest ionization efficiency for the analytes, being benzene and diethyl ether the dopants that provided the best results for the determination of PCDD/Fs and dl-PCBs, respectively. Under the optimal GC-APPI-HRMS conditions, most of the analytes generated the phenoxide ion as the base peak of the mass spectrum. The two GC-APPI-HRMS methods allowed the detection of target compounds down to low femtogram level (PCDD/Fs, 0.5–25 fg injected; dl-PCBs, 0.5–10 fg injected) and showed a good performance in terms of linearity (RSD% of the RFF lower than 12%), run-to-run and day-to-day precision (RSD < 9%), and stability of the ion ratio values (RSD < 7%), which guarantee the analyte quantitation and confirmation even at very low concentration levels. Moreover, the results obtained for the analysis of selected environmental and feed samples showed that there were no statistically significant differences between the GC-APPI-HRMS methods and the GC-EI-HRMS reference method in terms of both analyte

Table 6 PCDD/F and dl-PCB concentrations in the interlaboratory materials

Compound	Sediment (pg g^{-1} ± SD)			Feed oil (pg g^{-1} ± SD)			Soybean meal (pg g^{-1} ± SD)		
	Assigned value	GC-EI-HRMS	GC-APPI-HRMS	Assigned value	GC-EI-HRMS	GC-APPI-HRMS	Assigned value[a]	GC-EI-HRMS	GC-APPI-HRMS
2,3,7,8-TCDD	0.08 ± 0.03	0.08 ± 0.03	n.d.	0.44 ± 0.09	0.37 ± 0.09	0.35 ± 0.01	0.01	n.d.	n.d.
1,2,3,7,8-PeCDD	0.25 ± 0.07	0.19 ± 0.07	n.d.	0.45 ± 0.08	0.31 ± 0.08	0.377 ± 0.008	0.03	0.03	0.033 ± 0.001
1,2,3,4,7,8-HxCDD	0.37 ± 0.07	0.36 ± 0.07	0.402 ± 0.05	0.41 ± 0.08	0.34 ± 0.08	0.43 ± 0.03	0.06	0.06	0.071 ± 0.004
1,2,3,6,7,8-HxCDD	0.51 ± 0.08	0.33 ± 0.08	0.55 ± 0.01	0.40 ± 0.06	0.31 ± 0.06	0.402 ± 0.004	2.29	2.02	1.98 ± 0.02
1,2,3,7,8,9-HxCDD	0.45 ± 0.09	0.45 ± 0.09	n.d.	0.42 ± 0.06	0.36 ± 0.06	0.394 ± 0.007	0.80	0.73	0.71 ± 0.03
1,2,3,4,6,7,8-HxCDD	6.4 ± 0.8	6.2 ± 0.8	6.3 ± 0.4	0.44 ± 0.09	0.32 ± 0.09	0.38 ± 0.02	122	101	103 ± 3
OCDD	30 ± 4	31 ± 4	30 ± 1	7.6 ± 0.6	5.0 ± 0.6	5.87 ± 0.08	747	462	601 ± 3
2,3,7,8-TCDF	2.2 ± 0.3	2.0 ± 0.3	1.82 ± 0.05	0.38 ± 0.05	0.29 ± 0.05	0.235 ± 0.002	0.02	0.008	0.020 ± 0.001
1,2,3,7,8-PeCDF	2.5 ± 0.3	2.5 ± 0.3	2.56 ± 0.03	0.35 ± 0.05	0.30 ± 0.05	0.328 ± 0.001	0.02	0.014	0.017 ± 0.001
2,3,4,7,8-PeCDF	1.9 ± 0.5	1.5 ± 0.5	1.69 ± 0.09	0.38 ± 0.06	0.24 ± 0.06	0.261 ± 0.006	0.03	n.d.	0.027 ± 0.001
1,2,3,4,7,8-HxCDF	8.5 ± 0.9	8.1 ± 0.9	8.3 ± 0.2	0.37 ± 0.06	0.27 ± 0.06	0.307 ± 0.001	0.096	0.082	0.094 ± 0.006
1,2,3,6,7,8-HxCDF	4.8 ± 0.5	4.9 ± 0.5	5.10 ± 0.06	0.36 ± 0.06	0.26 ± 0.06	0.35 ± 0.01	0.090	0.075	0.087 ± 0.007
1,2,3,7,8,9-HxCDF	3 ± 1	3 ± 1	3.82 ± 0.05	0.36 ± 0.10	0.27 ± 0.10	0.274 ± 0.006	0.19	0.19	0.227 ± 0.006
2,3,4,6,7,8-HxCDF	1.0 ± 0.7	0.7 ± 0.7	n.d.	0.34 ± 0.07	0.24 ± 0.07	0.30 ± 0.03	0.04	n.d.	0.042 ± 0001
1,2,3,4,6,7,8-HpCDF	45 ± 7	46 ± 7	49 ± 1	0.5 ± 0.1	0.5 ± 0.1	0.52 ± 0.03	1.9	1.7	1.77 ± 0.04
1,2,3,4,7,8,9-HpCDF	6.2 ± 0.7	6.6 ± 0.7	6.7 ± 0.2	0.36 ± 0.07	0.29 ± 0.07	0.429 ± 0.009	0.2	0.2	0.20 ± 0.01
OCDF	84 ± 10	110 ± 10	79 ± 8	10 ± 1	8 ± 1	8.2 ± 0.8	4	3	4.18 ± 0.08
CB-81	0.8 ± 0.2	n.d.	0.67 ± 0.03	2.2 ± 0.7	1.8 ± 0.7	2.32 ± 0.07	0.34	1.70	n.d.
CB-77	29 ± 3	26 ± 3	31 ± 2	3.0 ± 0.6	n.d.	3.2 ± 0.2	12 ± 2	15 ± 2	11.9 ± 0.7
CB-123	6 ± 3	12 ± 3	11.4 ± 0.6	143 ± 17	83 ± 17	119 ± 6	46 ± 8	42 ± 8	43 ± 2
CB-118	483 ± 44	493 ± 44	467 ± 23	151 ± 18	141 ± 18	129 ± 6	2840 ± 320	3319 ± 320	2499 ± 125
CB114	4.1 ± 0.9	3.3 ± 0.9	5.1 ± 0.2	146 ± 17	126 ± 17	119 ± 4	80 ± 10	101 ± 10	94 ± 3
CB-105	121 ± 13	123 ± 13	117 ± 5	119 ± 16	99 ± 16	89 ± 4	1270 ± 140	1388 ± 140	1198 ± 48
CB-126	2.8 ± 0.4	2.2 ± 0.4	2.33 ± 0.09	2.5 ± 0.4	2.3 ± 0.4	2.24 ± 0.09	2.0 ± 0.3	2.6 ± 0.3	2.14 ± 0.09
CB-167	26 ± 3	19 ± 3	27.6 ± 0.8	139 ± 14	129 ± 14	119 ± 4	300 ± 37	368 ± 37	353 ± 11
CB-156	43 ± 6	39 ± 6	41 ± 1	144 ± 15	122 ± 15	114 ± 3	835 ± 93	925 ± 93	842 ± 25
CB-157	11 ± 2	10 ± 2	11.1 ± 0.3	152 ± 16	136 ± 16	127 ± 4	86 ± 9	97 ± 9	97 ± 3
CB-169	0.8 ± 0.2	n.d.	0.61 ± 0.02	2.3 ± 0.5	1.9 ± 0.5	1.90 ± 0.08	0.6 ± 0.1	0.6 ± 0.1	0.8 ± 0.03
CB-189	7.4 ± 0.8	7.9 ± 0.8	7.1 ± 0.1	162 ± 19	138 ± 19	133 ± 3	115 ± 11	132 ± 11	123 ± 2

[a] Assigned according to the median value since standard deviation could not be assigned. *n.d.* not detected
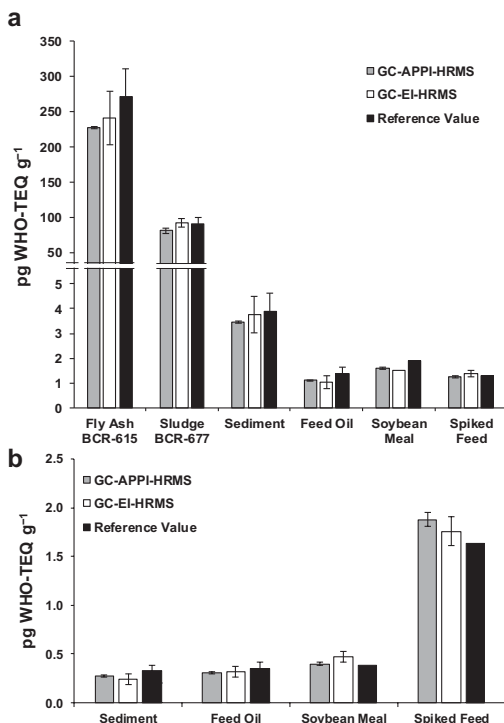
Fig. 5 Mean concentrations (pg WHO-TEQ g^{-1}) of **a** PCDD/Fs and **b** dl-PCBs, obtained in the analysis of selected environmental and food samples (p values from 0.26 to 0.79)

concentration and TEQs. As far as we know, this is the first time that the GC-APPI-HRMS (Orbitrap) (negative ion mode) has been proposed for the analysis of PCDD/Fs and dl-PCBs, showing important advantages over the traditional GC-EI-HRMS confirmatory method.

Compliance with ethical standards

Conflict of interest   The authors declare that they have no conflict of interest.

References

1. Xu W, Wang X, Cai Z. Analytical chemistry of the persistent organic pollutants identified in the Stockholm Convention: a review. Anal Chim Acta. 2013;790:1–13.

2. Van Bavel B, Geng D, Cherta L, Nácher-Mestre J, Portolés T, Ábalos M, et al. Atmospheric-pressure chemical ionization tandem mass spectrometry (APGC/MS/MS) an alternative to high-resolution mass spectrometry (HRGC/HRMS) for the determination of dioxins. Anal Chem. 2015;87:9047–53.

3. Safe S, Hutzinger O, Hill TA. Polychlorinated dibenzo-ρ-dioxins and -furans (PCDDs/PCDFs): sources and environmental impact, epidemiology, mechanisms of action, health risks. 1st ed. Berlin: Springer; 1990.

4. Kanan S, Samara F. Dioxins and furans: a review from chemical and environmental perspectives. Trends Environ Anal Chem. 2018;17:1–13.

5. Dioxins: a technical guide, 9th ed. Ministry of Health, Wellington; 2016.

6. Van den Berg M, Birnbaum LS, Denison M, De Vito M, Farland W, Feeley M, et al. The 2005 World Health Organization reevaluation of human and mammalian toxic equivalency factors for dioxins and dioxin-like compounds. Toxicol Sci. 2006;93:223–41.

7. Toxicological profile for polychlorinated biphenyls (PCBs). Agency for Toxic Substances and Disease Registry; 2000.

8. Batang ZB, Alikunhi N, Gochfeld M, Burger J, Al-Jahdali R, Al-Jahdali H, et al. Congener-specific levels and patterns of polychlorinated biphenyls in edible fish tissue from the Central Red Sea coast of Saudi Arabia. Sci Total Environ. 2016;572:915–25.

9. Portolés T, Sales C, Abalos M, Sauló J, Abad E. Evaluation of the capabilities of atmospheric pressure chemical ionization source coupled to tandem mass spectrometry for the determination of dioxin-like polychlorobiphenyls in complex-matrix food samples. Anal Chim Acta. 2016;937:96–105.

10. Kauppila TJ, Kersten H, Benter T. Ionization of EPA contaminants in direct and dopant- and atmospheric pressure laser ionization. J Am Soc Mass Spectrom. 2015;26:1036–45.

11. Abalos M, Abad E, Van Leeuwen SPJ, De Boer J, Lindström G, Van Bavel B, et al. Results for PCDD/PCDF and dl-PCBs in the first round of UNEPs biennial global interlaboratory assessment on persistent organic pollutants. TrAC - Trends Anal Chem. 2013;46: 98–109.

12. Van Leeuwen SPJ, Leslie HA, De Boer J, Van Leeuwen SPJ, Van Bavel B, Abad E, et al. POPs analysis reveals issues in bringing laboratories in developing countries to a higher quality level. TrAC - Trends Anal Chem. 2013;46:198–206.

13. Leslie HA, van Bavel B, Abad E, de Boer J. Towards comparable POPs data worldwide with global monitoring data and analytical capacity building in Africa, Central and Latin America, and the South Pacific. TrAC - Trends Anal Chem. 2013;46:85–97.

14. Reiner EJ, Clement RE, Okey AB, Marvin CH. Advances in analytical techniques for polychlorinated dibenzo-p-dioxins, polychlorinated dibenzofurans and dioxin-like PCBs. Anal Bioanal Chem. 2006;386:791–806.

15. Reiner EJ. The analysis of dioxins and related compounds. Eric Mass Spectrom Rev. 2009;29:526–59.

16. Peterson AC, Mcalister GC, Quarmby ST, Griep-raming J, Coon JJ. Development and characterization of a GC-enabled QLT-Orbitrap for high-resolution and high-mass accuracy GC / MS. 2010;82: 8618–28.

17. Commission Regulation (EU) 2017/771 of 3 of May amending Regulation (EC) No 152/2009 as regards the methods for the determination of the levels of dioxins and polychlorinated biphenyls. Off J Eur Union. 2017;115/22–115/42.

18. Commission Regulation (EU) 2017/644 of 5 of April 2017 Laying down methods of sampling and analysis for the control of levels of dioxins, dioxin-like PCBs and non-dioxin like PCBs in certain foodstuffs and repealing Regulation (EU) No 589/2014. Off J Eur Union. 2017;92/9–92/34.

19. Malavia J, Santos FJ, Galceran MT. Comparison of gas chromatography-ion-trap tandem mass spectrometry systems for the determination of polychlorinated dibenzo-p-dioxins, dibenzofurans and dioxin-like polychlorinated biphenyls. J Chromatogr A. 2008;1186:302–11.

20. L'Homme B, Scholl G, Eppe G, Focant JF. Validation of a gas chromatography-triple quadrupole mass spectrometry method for confirmatory analysis of dioxins and dioxin-like polychlorobiphenyls in feed following new EU Regulation 709/2014. J Chromatogr A. 2015;1376:149–58.

21. Organtini KL, Haimovici L, Jobst KJ, Reiner EJ, Ladak A, Stevens D, et al. Comparison of atmospheric pressure ionization gas chromatography-triple quadrupole mass spectrometry to traditional high-resolution mass spectrometry for the identification and quantification of halogenated dioxins and furans. Anal Chem. 2015;87:7902–8.

22. Revelsky IA, Yashin YS, Sobolevsky TG, Revelsky AI, Miller B, Oriedo V. Electron ionization and atmospheric pressure photochemical ionization in gas chromatography- mass spectrometry analysis of amino acids. Eur J Mass Spectrom. 2003;507:497–507.

23. McEwen CN, McKay RG. A combination atmospheric pressure LC/MS:GC/MS ion source: advantages of dual AP-LC/MS:GC/MS instrumentation. J Am Soc Mass Spectrom. 2005;16:1730–8.

24. Li DX, Gan L, Bronja A, Schmitz OJ. Gas chromatography coupled to atmospheric pressure ionization mass spectrometry (GC-API-MS): review. Anal Chim Acta. 2015;891:43–61.

25. ten Dam G, Pussente IC, Scholl G, Eppe G, Schaechtele A, van Leeuwen S. The performance of atmospheric pressure gas chromatography–tandem mass spectrometry compared to gas chromatography–high resolution mass spectrometry for the analysis of polychlorinated dioxins and polychlorinated biphenyls in food and feed samples. J Chromatogr A. 2016;1477:76–90.

26. Rivera-Austrui J, Martínez K, Ábalos M, Sales C, Portoles T, Beltran J, et al. Analysis of polychlorinated dibenzo-p-dioxins and dibenzofurans in stack gas emissions by gas chromatography-atmospheric pressure chemical ionization-triple-quadrupole mass spectrometry. J Chromatogr A. 2017;1513:245–9.

27. Luosujärvi L, Karikko M-M, Haapala M, Saarela V, Huhtala S, Franssila S, et al. Gas chromatography/mass spectrometry of polychlorinated biphenyls using atmospheric pressure chemical ionization and atmospheric pressure photoionization microchips. Rapid Commun Mass Spectrom. 2008;20:425–31.

28. Geng D, Jogsten IE, Dunstan J, Hagberg J, Wang T, Ruzzin J, et al. Gas chromatography/atmospheric pressure chemical ionization/mass spectrometry for the analysis of organochlorine pesticides and polychlorinated biphenyls in human serum. J Chromatogr A. 2016;1453:88–98.

29. Stubleski J, Kukucka P, Salihovic S, Lind PM, Lind L, Kärrman A. A method for analysis of marker persistent organic pollutants in low-volume plasma and serum samples using 96-well plate solid phase extraction. J Chromatogr A. 2018;1546:18–27.

30. Hintikka L, Haapala M, Franssila S, Kuuranne T, Leinonen A, Kostiainen R. Feasibility of gas chromatography-microchip atmospheric pressure photoionization-mass spectrometry in analysis of anabolic steroids. J Chromatogr A. 2010;1217:8290–7.

31. Haapala M, Luosujärvi L, Saarela V, Kotiaho T, Ketola RA, Franssila S, et al. Microchip for combining gas chromatography or capillary liquid chromatography with atmospheric pressure photoionization-mass spectrometry. Anal Chem. 2007;79:4994–9.

32. Revelsky IA, Yashin YS. Talanta new approach to complex organic compounds mixtures analysis based on gas chromatography – atmospheric pressure photoionization – mass-spectrometry. Talanta. 2012;102:110–3.

33. Kondyli A, Schrader W. High-resolution GC/MS studies of a light crude oil fraction. J Mass Spectrom. 2019;54:47–54.

34. Di Lorenzo RA, Lobodin VV, Cochran J, Kolic T, Besevic S, Sled JG, et al. Fast gas chromatography-atmospheric pressure (photo)ionization mass spectrometry of polybrominated diphenylether flame retardants. Anal Chim Acta. 2019;1056:70–8.

35. Ábalos M, Parera J, Rivera J, Abad E. PCDD/F and DL-PCB levels in meat from broilers and rabbits fed with fish-oil enriched feeds. Chemosphere. 2010;78:175–84.

36. Martínez K, Rivera-Austrui J, Adrados MA, Abalos M, Llerena JJ, van Bavel B, et al. Uncertainty assessment of polychlorinated dibenzo-p-dioxins and dibenzofuran and dioxin-like polychlorinated biphenyl analysis in stationary source sample emissions in accordance with the impending European standard EN-1948 using fly ashes. J Chromatogr A. 2010;1216:5888–94.

37. Ábalos M, Barceló D, Parera J, la Farré M, Llorca M, Eljarrat E, et al. Levels of regulated POPs in fish samples from the Sava River Basin. Comparison to legislated quality standard values. Sci Total Environ. 2019;647:20–8.

Publisher's note Springer Nature remains neutral with regard to jurisdictional claims in published maps and institutional affiliations.

Analytical and Bioanalytical Chemistry

Electronic Supplementary Material

Feasibility of gas chromatography-atmospheric pressure photoionization–high-resolution mass spectrometry for the analysis of polychlorinated dibenzo-*p*-dioxins, dibenzofurans, and dioxin-like polychlorinated biphenyls in environmental and feed samples

J. F. Ayala-Cabrera, M. Ábalos, E. Abad, E. Moyano, F. J. Santos

Table of Contents

Supporting Tables

Table S1 Mass spectra information of APPI dopants

Compound	*m/z* (Rel. ab., %)	Ion Assignment	Error (mDa)
Acetone	59.0501 (100%)	[D+H]$^+$	0.9
Benzene	78.0470 (100%)	[D]$^{+\bullet}$	0.6
Chlorobenzene	112.0080 (100%)	[D]$^{+\bullet}$	0.6
Diethyl Ether	73.0657 (15%)	[D−H]$^+$	0.9
	75.0813 (100%)	[D+H]$^+$	0.9
Tetrahydrofuran	71.0501 (23%)	[D−H]$^+$	0.9
	73.0657 (100%)	[D+H]$^+$	0.9
Toluene	91.0552 (43%)	[D−H]$^+$	1.0
	92.0626 (100%)	[D]$^{+\bullet}$	0.6

Table S2 PCDD/Fs and dl-PCBs concentrations in an internal reference material

Compound	Spiked Feed (pg g^{-1} ± SD)	
	GC-EI-HRMS	GC-APPI-HRMS
2,3,7,8-TCDD	0.12 ± 0.01	n.d.[a]
1,2,3,7,8-PeCDD	0.60 ± 0.05	0.60 ± 0.01
1,2,3,4,7,8-HxCDD	0.66 ± 0.05	0.72 ± 0.04
1,2,3,6,7,8-HxCDD	0.63 ± 0.03	0.71 ± 0.06
1,2,3,7,8,9-HxCDD	0.65 ± 0.05	0.59 ± 0.04
1,2,3,4,6,7,8-HxCDD	0.64 ± 0.09	0.67 ± 0.02
OCDD	2 ± 1	2.48 ± 0.07
2,3,7,8-TCDF	0.1 ± 0.1	0.130 ± 0.004
1,2,3,7,8-PeCDF	0.63 ± 0.08	0.61 ± 0.02
2,3,4,7,8-PeCDF	0.56 ± 0.06	0.54 ± 0.02
1,2,3,4,7,8-HxCDF	0.57 ± 0.06	0.60 ± 0.05
1,2,3,6,7,8-HxCDF	0.60 ± 0.04	0.62 ± 0.05
1,2,3,7,8,9-HxCDF	0.58 ± 0.06	0.57 ± 0.02
2,3,4,6,7,8-HxCDF	0.57 ± 0.04	0.57 ± 0.02
1,2,3,4,6,7,8-HpCDF	0.66 ± 0.06	0.75 ± 0.03
1,2,3,4,7,8,9-HpCDF	0.60 ± 0.06	0.60 ± 0.02
OCDF	1.3 ± 0.7	1.9 ± 0.1
CB-81	14 ± 1	15.0 ± 0.6
CB-77	18 ± 4	20 ± 1
CB-123	14.4 ± 0.9	15.2 ± 0.8
CB-118	31 ± 4	30 ± 1
CB114	15 ± 1	15.1 ± 0.4
CB-105	20 ± 2	19.0 ± 0.8
CB-126	13 ± 1	14.6 ± 0.6
CB-167	15.3 ± 0.8	16.1 ± 0.5
CB-156	14 ± 1	14.7 ± 0.4
CB-157	14 ± 1	14.7 ± 0.4
CB-169	13 ± 1	13.7 ± 0.6
CB-189	15 ± 1	13.5 ± 0.3

[a] non detected.

Supporting Figures

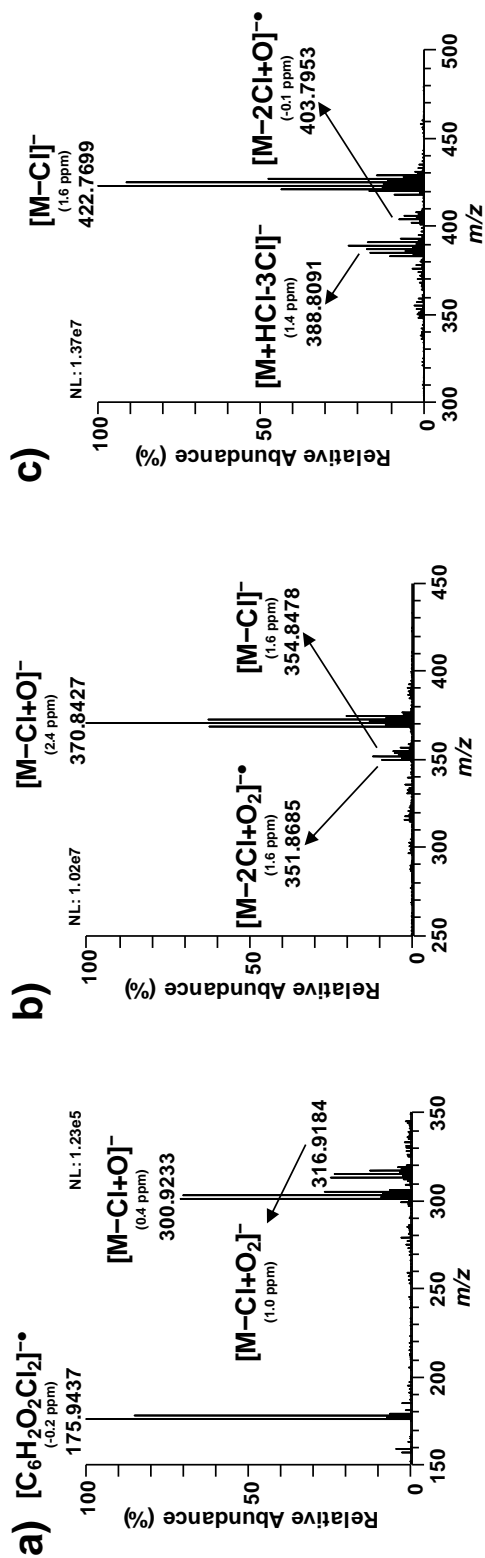**Fig. S1** Negative ion GC-APPI-HRMS mass spectra of a) 2,3,7,8-TCDD, b) 1,2,3,4,7,8-HxCDD and c) OCDD using diethyl ether as dopant

3.2.5. Article IX

Chloride-attachment Atmospheric Pressure Photoionisation for the Determination of Short-Chain Chlorinated Paraffins by Gas Chromatography-High-Resolution Mass Spectrometry

J. F. Ayala-Cabrera, M. T. Galceran, E. Moyano, F. J. Santos

Chloride-attachment Atmospheric Pressure Photoionisation for the Determination of Short-Chain Chlorinated Paraffins by Gas Chromatography-High-Resolution Mass Spectrometry

J. F. Ayala-Cabrera[(1)], M. T. Galceran[(1,2)], E. Moyano[(1,2)], F. J. Santos[(1,2)*]

[(1)] Department of Chemical Engineering and Analytical Chemistry, University of Barcelona. Av. Diagonal 645, E–08028 Barcelona, Spain

[(2)] Water Research Institute (IdRA), University of Barcelona, Montalegre 6, E–08001 Barcelona, Spain

* Corresponding author: Francisco Javier Santos Vicente
Phone: +34-93-403-4874
Fax: +34-93-402-1233
E-mail: javier.santos@ub.edu

Keywords: Gas Chromatography, Atmospheric Pressure Photoionisation, High-Resolution Mass Spectrometry, Chloride Attachment, Short-Chain Chlorinated Paraffins.

Abstract

In this work, a new gas chromatography-high-resolution mass spectrometry (GC-HRMS) method based on atmospheric pressure photoionization (APPI) has been developed for the accurate determination of short-chain chlorinated paraffins (SCCPs) in fish samples as a reliable alternative to the reported methods. The efficient ionization of SCCPs using the GC-APPI source was investigated, achieving the formation of an abundant $[M+Cl]^-$ adduct ion using dopant-assisted APPI in negative ion mode with acetone/CCl_4 (3:1 *v/v*) mixture. Operating at a resolution of 70,000 FWHM (full width at half maximum) and using the adduct ion, a selective determination of the different congener groups was achieved, avoiding isobaric interferences between them and with other halogenated compounds. Moreover, the effect of the number of chlorine atoms on the GC-APPI-HRMS response was also investigated and was shown to be negligible being mainly influenced by the concentration. Thus, the concentrations of the different homologue groups of congeners in the SCCP mixtures were determined by the internal normalization method, and the quantification was performed independently of the SCCP standard mixture employed. The developed GC-APPI-HRMS method provides significant advantages over the existing methods, providing an important time-saving in the quantification. Additionally, the GC-APPI-HRMS method allowed the determination of SCCPs at low concentration levels with high accuracy and precision and can be proposed as a reliable alternative for the determination of these pollutants in environmental samples.

1. Introduction

Chlorinated paraffins (CPs) are complex mixtures of chlorinated n-alkanes containing thousands of isomers with carbon chain lengths from C10 to C30 and variable chlorination degree between 30% and 70% by weight [1]. To deal with this diverse class of compounds, CPs are categorized according to their chain lengths as short-chain (SCCPs, from C10 to C13), medium-chain (MCCPs, from C14 to C17) and long-chain chlorinated paraffins (LCCPs, more than C17) [2]. These compounds are used in a wide scope of industrial applications, such as additives in metalworking fluids, plasticizers, and flame retardants, and their production volume was estimated at around 13 million tonnes (1935-2012) [3], although it is still increasing (~1 million tonnes per year). Even though CPs have been extensively produced at high volume, data about their environmental fate is limited, mainly due to their challenging chemical analysis. Among CP mixtures, SCCPs are especially of concern since several studies revealed their persistence, toxicity, long-range transport capacity, and bioaccumulation and biomagnification potential through the food chain [4–6]. As a result, SCCPs are listed as persistent organic pollutants (POPs) by the Stockholm Convention for the elimination of their production and use (Annex A) [7]. They are also included in several regulatory lists such as the European Water Framework Directive [8].

The analytical determination of SCCPs is challenging mainly due to the high complexity of the mixtures, the insufficient resolution between congeners, and the difficulties to perform an accurate quantification [9,10]. SCCPs are currently analysed by gas chromatography (GC), although their separation remains unachieved by a single-column GC, resulting in a broad hump in the chromatogram corresponding to a large number of co-eluting peaks that could be interfered with other CP mixtures (e.g., MCCPs) or halogenated compounds with similar retention times (e.g., PCBs and organochlorine pesticides). Comprehensive two-dimensional gas chromatography (GCxGC) has been used to improve the separation of SCCPs, but this technique only allowed a partial separation between congener groups with significant overlapping between homologues with different chlorination degrees [11]. Generally, the determination of SCCP mixtures has been mainly performed by gas chromatography coupled to electron-capture negative ion low-resolution mass spectrometry (GC-ECNI-LRMS) [12–15] by monitoring the [M–Cl]⁻ and [M–HCl]⁻ ions for congener group-specific analysis. However, multiple injections are needed to monitor all the ions corresponding to each homologue group [15] and interferences with longer chained CPs and between congeners with different chlorination degrees strongly affect the quantitative results [16]. Furthermore, the ionization efficiencies achieved with ECNI are highly dependent on the chlorination degree of CP congeners, and differences in the homologue composition between standards and samples often cause significant errors in the quantification (>300%) [17]. To decrease the strong dependency of ECNI with the chlorination degree some approaches have been employed based on a linear relationship between the response factors of the CP homologue groups and their chlorine content [15] and multiple linear regression [18]. Nevertheless, it is necessary the

use of SCCP standards with a homologue composition similar to the sample for achieving an accurate quantification [15,17,19]. GC-ECNI-HRMS has also been proposed to remove the isobaric CP interferences but a mass resolution higher than 20.000 [20] and multiple injections per sample are needed [19]. Recently, a fast method based on GC-ECNI-Orbitrap/HRMS has been reported, allowing the analysis of SCCPs and MCCPs in a single run, since it showed fewer interferences coming from other halogenated compounds [10]. As an alternative to GC-ECNI-MS methods, anion-attachment atmospheric pressure chemical ionisation (APCI) coupled to HRMS (APCI-qTOF/HRMS) has been proposed for the analysis of SCCPs by monitoring the chloride or bromide adduct ions generated by the addition of a halogenated reagent (e. dichloromethane, chloroform, or even bromoform) to the mobile phase [9,21–23]. These methods provide responses less affected by the chlorination degree, although in some cases they required a complex mathematical deconvolution method to achieve reliable quantification of CPs because the mass resolution obtained was not high enough to reach a complete removal of the isobaric interferences [24].

During the last decades, the use of atmospheric pressure chemical ionisation (GC-APCI) and atmospheric pressure photoionisation (GC-APPI) in the GC-MS determination has been extensively explored since they are soft ionisation techniques which allow preserving the integrity of the molecular ion and provide efficient ionisation of a wide range of compounds [25]. Thus, GC-APPI interface has been recently developed [26] and successfully applied to the GC-HRMS determination of several pollutants, such as PCBs [27], polycyclic aromatic hydrocarbons [28,29], phthalates [29], neutral fluorinated compounds [30], and several families of environmental contaminants [31].

The aim of the present work was to develop a new GC-APPI-HRMS method for a reliable determination of SCCPs in environmental samples based on chloride-attachment to propose a sensitive and selective method for the congener group quantification. To this end, the GC-APPI parameters, as well as the use of several chlorinated solvents and dopants that affect the ionization of the target compounds, were optimized to avoid isobaric interferences between CP congeners and to achieve a response less affected by the chlorination degree. Several mathematical approaches were also tested to ensure accurate quantification of SCCPs. The developed GC-APPI-HRMS method was validated and applied to the analysis of selected fish samples.

2. Materials and Methods

2.1. Chemical and standards

A standard solution of CP congeners (Mix 2), containing 1,2,5,6,9-pentachlorodecane (CP-3), 1,2,4,5,9,10-hexachlorodecane (CP-6), 1,2,4,5,6,9,10-heptachlorodecane (CP-7), 2,3,4,5,6,7,8,9-octachlorodecane (CP-9) and 1,2,3,4,5,6,7,8,9-nonachlorodecane (CP-10), at concentrations ranging from 0.5 to 19 µg mL^{-1} was purchased from Dr. Ehrenstofer GmbH (Ausburg, Germany). Standard mixtures of SCCPs (100 µg mL^{-1}) with a total chlorine content

of 51.5%, 55.5%, and 63%, and standard solutions of ^{13}C-hexachlorobenzene ($^{13}C_6$-HCB, 100 µg mL^{-1}) and δ-hexachlorocyclohexane (δ-HCH, 100 µg mL^{-1}), used respectively as injection and surrogate internal standard, were also supplied by Dr Ehrenstofer GmbH. Working standard solutions at concentrations lower than 10 µg mL^{-1} were prepared by appropriate dilution of the stock solutions in isooctane and stored at 4 °C until their analysis. To study the effect of potentially interfering compounds on the determination of SSCPs, two standard solutions, containing a mixture of seven polychlorinated biphenyls (PCB-Mix 1, CBs: 28, 52, 101, 118, 138, 153 and 180) at a concentration of 10 µg mL^{-1} in isooctane and twenty-two organochlorine pesticides (Pesticide-Mix 1037) at a concentration of 10 µg mL^{-1} in cyclohexane, were purchased from Dr Ehrenstorfer (LGC Standards, Teddington, UK).

Isooctane, dichloromethane, and *n*-hexane (for gas chromatography SupraSolv®, purity ≥ 99.8%) were obtained from Merck (Darmstadt, Germany). Besides, acetone (LiChrosolv®, purity ≥99.8%) supplied by Merck, tetrahydrofuran (Photrex™ reagent, purity at 99%) from J. T. Baker (Deventer, Holland), and anisole (analytical standard, purity ≥ 99,9 %), chlorobenzene and toluene (Chromasolv™ Plus, for HPLC analysis, purity ≥ 99%) supplied by Sigma-Aldrich (St Louis, MO, USA), were used as dopants for the optimization of APPI ionisation of the SCCPs. Helium Alphagaz™ 1 (purity ≥ 99.999%), used as GC carrier gas, was supplied by Air Liquide (Madrid, Spain), while nitrogen (purity > 99.995%), from Linde (Barcelona, Spain), was employed as make-up gas for GC-APPI source. Sulphuric acid (95-97%) and anhydrous sodium sulphate (purity > 99%) of residue analysis grade were obtained from Merck. Florisil (0.15-0.25 mm) of residue analysis grade and silica gel (Gel 60) of chromatographic analysis quality were also obtained from Merck. Before use, the Florisil and silica gel were baked overnight at 550 ºC and kept in an oven at 180 ºC. Silica gel modified with sulphuric acid (44%, *w/w*) was prepared by slowly adding an appropriate amount of sulphuric acid to the activated silica at room temperature. All glassware was cleaned using chromosulphuric acid and rinsed consecutively with Milli-Q water, methanol, and acetone, and dried overnight at 180 ºC before use.

2.2. Samples and sample treatment

Fish samples (salmon and tuna) were purchased from a local supermarket and were selected for the analysis of SCCPs since they are among the most frequently fish products found in the Spanish diet [32]. Salmon was of agriculture origin, while tuna was caught in the Mediterranean Sea. Once fish was washed, the non-edible parts were removed to obtain the muscle clean tissue and it was triturated, homogenized, and lyophilized for three days. Then, the dried tissue was ground in a glass mortar to a fine powder and stored in glass vials in the dark at 4 ºC before analysis.

The extraction of the lyophilized fish samples was performed on an ASE 100 Accelerated Solvent Extractor System (Dionex, Sunnyvale, CA). Before PLE extraction, an adequate amount of the δ-HCH was added to 1 g of the freeze-dried fish sample, which was left overnight

at room temperature to equilibrate. The sample was then mixed with sodium sulphate at a fish/Na_2SO_4 ratio of 1:2 (*w/w*) in a mortar until a homogenous mixture was obtained. The extraction cell was loaded by inserting a glass fibre filter into the cell outlets, followed by 20 g of acidified silica (44% sulphuric acid) as the fat retainer and the sample. Fish samples were extracted at 100 ºC with a solvent mixture of n-hexane:dichloromethane (1:1, *v/v*) using 3 cycles of 5 min each and working at a pressure of 1500 psi, a flush volume of 60% and a purge time of 90 s for a 34 mL PLE extraction cell. For fractionation, the extract was then concentrated to ca. 2 ml using a rotary evaporator at room temperature and carefully transferred to the top of a glass column (200 mm x 15 mm I.D.) filled with 15 g of activated Florisil, previously rinsed with 50 mL of n-hexane. Two fractions were collected: (F1) with 30 mL of n-hexane followed by 80 ml of a solvent mixture of n-hexane/DCM (95:5, *v/v*), that contained the PCBs and PBDEs, and (F2) with 30 mL of a mixture of n-hexane/DCM (1:1, *v/v*) where the SCCPs were eluted. The extracts were then rotary evaporated to approximately 2 mL adding 100 µL of isooctane as a keeper. Afterwards, the extract was carefully concentrated under a gentle nitrogen stream up to 50 µL and 1 µL was injected into the GC-APPI-HRMS system after adding an adequate amount of $^{13}C_6$-HCB as injection internal standard to obtain a final concentration of 5 ng mL^{-1} in the final extract.

2.3. GC-APPI-HRMS instrumentation

SCCP determination was achieved on a Trace 1300 gas chromatograph coupled to a Q-Exactive Orbitrap mass spectrometer (Thermo Fisher Scientific, San Jose, CA, USA), employing an atmospheric pressure photoionisation ion source (GC-APPI) (MasCom Technologies GmbH, Bremen, Germany). The chromatographic separation was carried out using a TG-5MS (15 m x 0.25 mm I.D., 0.25 µm film thickness) fused-silica capillary column (Thermo Fisher Scientific), using helium as carrier gas at a constant flow rate of 1.0 mL min^{-1}. The injector was operated at 270 ºC in splitless injection mode (1 min) and the injection volume for standards and samples was 1 µL. The oven temperature was set as follows: 90 ºC (held for 1 min) to 200 ºC at 20 ºC min^{-1} and then to 300 ºC at 15 ºC min^{-1} (held for 5 min). The transfer line, source and capillary temperatures were set at 280 ºC, 200 ºC and 180 ºC, respectively. The GC-APPI source was equipped with a 10.6 eV krypton lamp (Syagen, Santa Ana, CA, USA) and operated in the negative ion mode due to the high electronegativity of the target compounds. For the APPI ionization of SCCPs, vapours of acetone/carbon tetrachloride (3:1 *v/v*, 70 µL min^{-1}) were used as optimal dopant/chlorination agent mixture, and nitrogen was employed as make-up gas (gas pressure of 5 a.u.). Moreover, S-Lens RF was set at 20% to improve the ion transmission to the mass analyser. Data were acquired in full-scan mode from 60 *m/z* to 700 *m/z* at a mass resolution of 70,000 FWHM (full width at half maximum at 200 *m/z*). Besides, to achieve the highest sensitivity with well-defined peak shape (at least 12 points per peak), the automatic gain control (AGC) and maximum injection time were set at 1·10^6 and 50 ms, respectively. The extracted ion chromatograms (XICs) were obtained using mass extraction windows with a tolerance of ±5 ppm to guarantee a high selectivity and quality

of the results. Xcalibur *υ* 3.1 software was employed to control the instrument setup and process the data acquisition.

2.4. Quality control criteria

Specific tests to check the GC separation, the sensitivity of the GC-APPI-HRMS and the validity of the calibration were carried out daily. Procedural blanks (both instrumental and method) were routinely performed during the analysis, and a quality control material consisted of a salmon sample with non-detectable amounts of the SCCPs spiked at 0.5 ng g^{-1} wet weight, was periodically analysed to ensure that the whole analytical method was maintained under control. Recoveries of target compounds were routinely checked and ranged between 91-96%. Moreover, the Orbitrap mass analyser was calibrated every 72 h using an electrospray source with a calibration solution, containing caffeine, MRFA peptide, Ultramark 1621 and butylamine in acetonitrile/methanol/water (2:1:1, *v/v*) with 1% (*v/v*) formic acid, to ensure the accuracy on the mass-to-ratio values reported.

3. Results and Discussion

3.1. Ionisation of SCCPs by GC-APPI

The ionisation of SCCPs by GC-APPI was focused on the formation of characteristic ions of each homologue group that both avoids potential isobaric interferences between CP congeners with different carbon lengths and chlorination degrees and provides responses less affected by the number of chlorine atoms present in the molecule. The ionisation must be assisted by a dopant since they cannot be directly photoionised in the negative ion mode. Thus, vapours of several organic solvents, such as toluene, acetone, chlorobenzene, anisole, and tetrahydrofuran, were evaluated as possible dopant using a mixture of individual CP congeners (Mix 2). For all evaluated dopants, similar behaviour was observed in the mass spectra for all the compounds. For instance, the mass spectrum of a $C_{10}H_{15}Cl_7$ paraffin using toluene vapours as dopant showed two abundant clusters corresponding to the superoxide $[M+O_2]^{-\bullet}$ and chloride $[M+Cl]^-$ adduct ions (see Fig. S1). In addition, some intense in-source CID fragments corresponding to the losses of Cl and HCl from the adduct ions were generated, increasing the number of potential isobaric interferences with other CP congeners. Under these conditions, differences in the ion abundance of mass spectra were observed depending on the number of chlorine atoms of the molecule. Fig. 1 shows the GC-APPI-HRMS mass spectra of different C_{10}-paraffins, using acetone vapours as a dopant. As can be seen, when the number of chlorine atoms presents in the molecule was low than six chlorine atoms, the base peaks of mass spectra were the $[M+O_2]^{-\bullet}$ and $[M+Cl]^-$ adduct ions, while for heptachlor-substituted congeners ($C_{10}H_{15}Cl_7$) the $[M+O_2–Cl]^-$ and $[M+Cl–HCl]^-$ in-source CID fragments were the most abundant cluster ions of the mass spectrum. However, SCCPs with a high number of chlorine atoms (≥ 8 Cl), the superoxide adduct ion was not generated and different in-source CID fragments coming from losses of HCl or Cl units were only observed
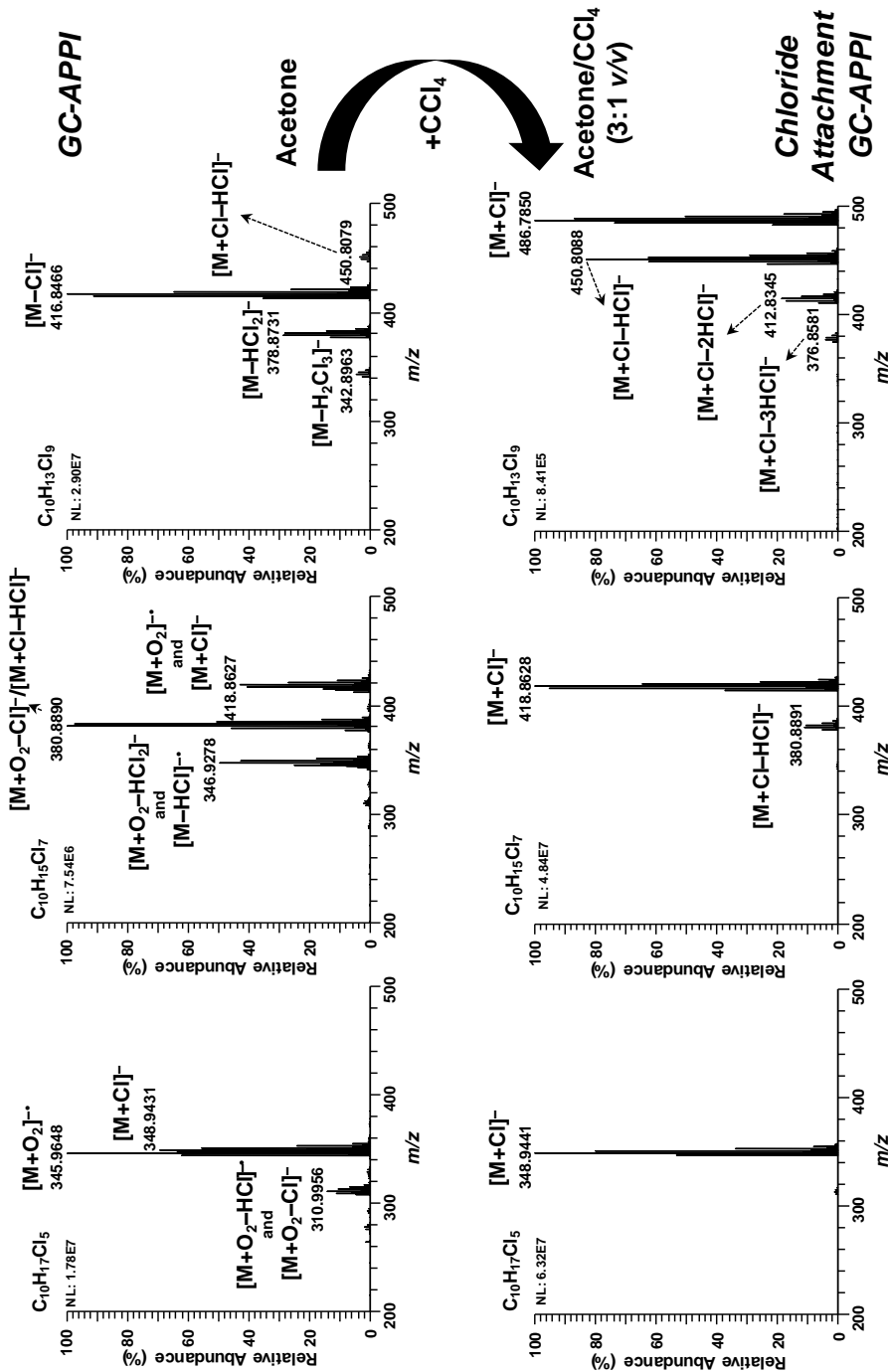
Figure 1. GC-APPI-HRMS (*above*) *versus* chloride-anion attachment GC-APPI-HRMS (*down*) mass spectra of a penta-, hepta-, and nonachlorodecane.

279

These different ionisation behaviours could lead to isobaric mass interferences due to the overlap of ions coming from the coelution of CP congeners. Considering the last advances on the anion-attachment APCI as an alternative technique for the ionisation of short-chain chlorinated paraffins [9,22–24,33], the generation of a chloride adduct ion could be investigated for the ionization of these compounds by GC-APPI. Thus, the addition of chlorinated solvent to the dopant for favouring the formation of chloride adduct ions was evaluated. For this, a mixture of acetone/CCl$_4$ vapours (3:1 *v/v*) was introduced into the GC-APPI source for optimizing the response of the [M+Cl]$^-$ as the base peak of the mass spectra (Fig. 1). The use of this dopant mixture hindered the formation of [M+O$_2$]$^{-\bullet}$ since the proportion of oxygen in the source decreased as a result of its displacement by the CCl$_4$. Moreover, the abundance of in-source CID fragments diminished and only ions coming from successive losses of HCl from the chloride adduct ion were observed in the mass spectra. To maximise the ionisation efficiency of the [M+Cl]$^-$ ion several organic solvents (toluene, acetone, tetrahydrofuran, chlorobenzene, and anisole) were mixed with CCl$_4$ (3:1 *v/v*). Fig. 2a shows the effect of these dopant mixtures on the response of individual CP congeners, being the acetone the solvent that provided the best results. This fact could be related to the highest vapour pressure of acetone, which allowed the release of a greater number of electrons after the photoionisation process, thus promoting better ionisation efficiency of the analytes. To select the most appropriate chlorination agent, mixtures of acetone with chlorobenzene, dichloromethane, chloroform, and carbon tetrachloride (3:1 *v/v*) were also tested (Fig. 2b). Under these conditions, it was observed the highest responses of [M+Cl]$^-$ adduct ions when the dopant contained CCl$_4$, which is the highest chlorinated solvent and can easily release more chlorine atoms. Moreover, for SCCPs with more than seven chlorine atoms, the base peak of the mass spectrum depended on the employed chlorination agent. For instance, the C$_{10}$H$_{14}$Cl$_8$ generated a chloride adduct ion as base peak when chloroform or carbon tetrachloride was used, whereas the most intense ion was [M+Cl–2HCl]$^-$ using dichloromethane or chlorobenzene as chlorinated agent (see Fig. S2). The dopant/chlorination agent ratio was also optimised from 10:1 (*v/v*) to 1:10 (*v/v*) at a fixed flow rate of 70 µL min^{-1}, obtained the maximum response of the chloride adduct with a mixture acetone/carbon tetrachloride 3:1 (*v/v*). Consequently, this solvent mixture was selected as the most suitable dopant mixture to achieve an efficient ionisation of SCCPs by chloride-enhanced APPI.

Other GC-APPI critical parameters, such as source and capillary temperatures, were also optimised. The source and capillary temperatures were evaluated between 200 ºC and 250 ºC and from 160 ºC to 200 ºC, respectively (see Fig. S3). Since the source temperature strongly affected the fragmentation of chloride adduct ions, a source temperature of 200 ºC was selected. Also, the best responses for all the compounds were obtained at a capillary temperature of 180 ºC and it was chosen as optimum value. Thus, it was possible to obtain a low fragmentation in mass spectra and, therefore, diminishing the risk of possible isobaric interferences between congeners. Under these conditions, a minimum resolution of 28,441 FWHM was required to avoid these internal interferences between congeners, avoiding the
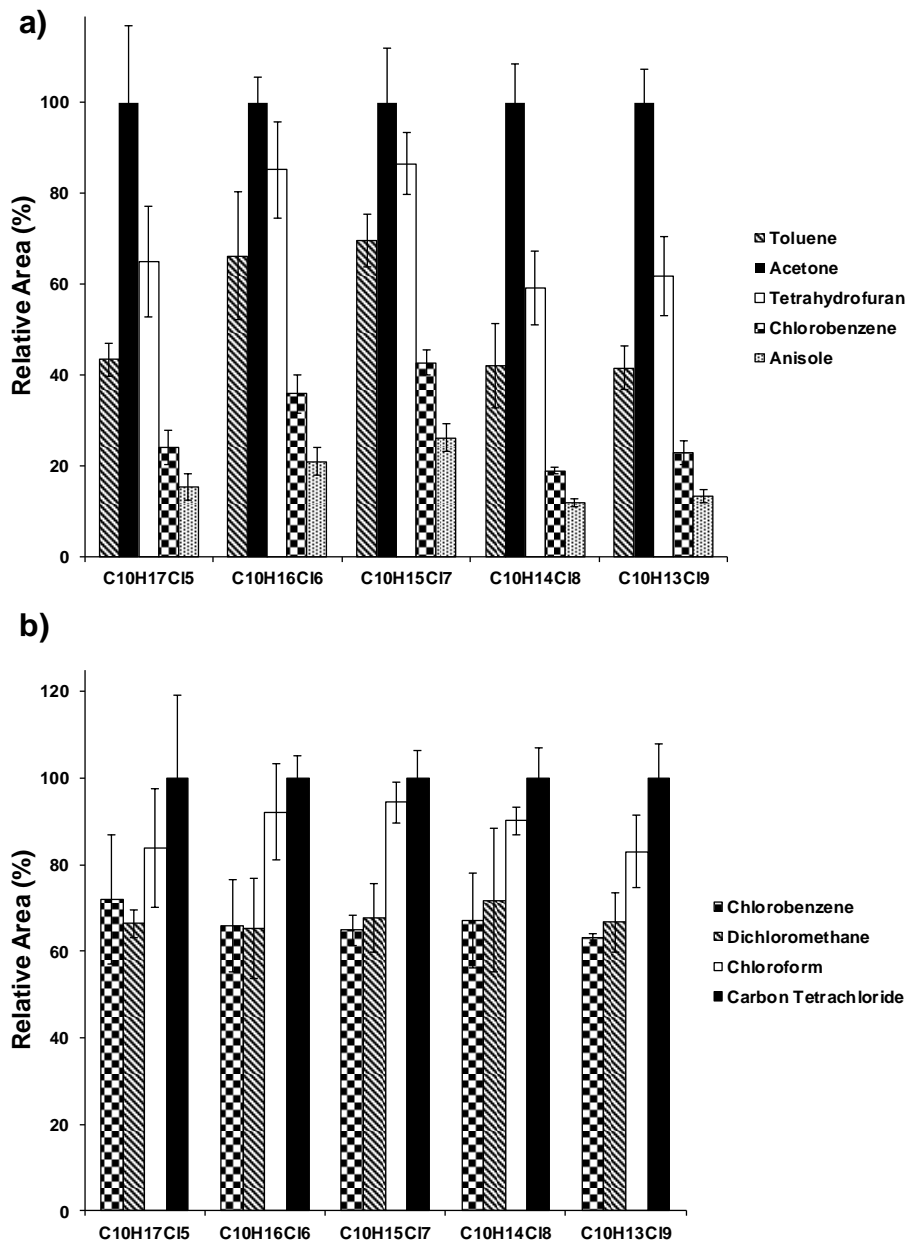
Figure 2. Effect of dopant mixtures a) solvent/CCl_4 (3:1 *v/v*) and b) acetone/chlorinated agent (3:1 *v/v*) on the abundance of chloride adduct ion for individual C_{10}-paraffins.

application of a deconvolution approach. Moreover, the monitorization of the chloride adduct ion allowed to separate the response of each homologue group in a SCCP mixture.

As mentioned before, an important disadvantage of GC-ECNI-MS methods is the strong dependence of the response with the number of total chlorine atoms present in the molecule.

Thus, the ECNI responses increase with the number of chlorine atoms. To evaluate the response of the GC-APPI source with the chlorination degree of SCCP congeners, several experiments were conducted to determine the response factor of each homologue group. Thus, a mixture of individual CP congeners (Mix 2) was analysed with the GC-APPI-HRM by monitoring the most abundant ions of the [M+Cl]$^-$ cluster (see Table S1). As it can be observed in Fig. 3, where the response factor of each CP congener relative to $C_{10}H_{17}Cl_5$ is represented, the effect of the number of chlorine atoms was strongly hindered, compared with the ECNI response, using chloride-attachment APPI for the ionisation of SCCPs.
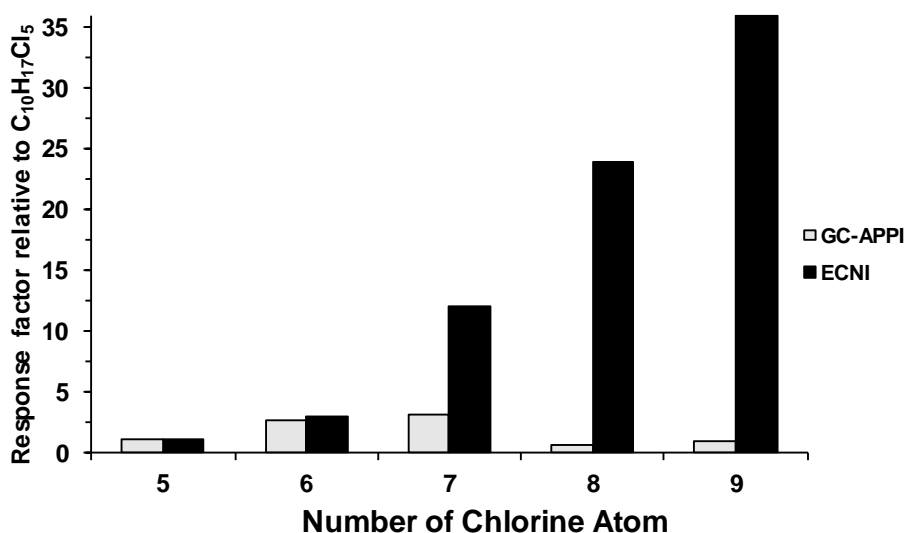
Figure 3. Effect of the number of chlorine atoms on the response of the [M+Cl]$^-$ and [M–Cl]$^-$ ions obtained by GC-APPI-HRMS and GC-ECNI-MS, respectively.

Moreover, the small differences observed on the response between congeners may be also attributed to the effect of the position of the chlorine substituents in the molecule over the ionisation. Therefore, it can be deduced that the response of the chloride adduct ions by GC-APPI mainly depended on the concentration, considering negligible the effect on the response of both the number and the position of chlorine atoms in the molecule.

3.2. Quantification of SCCPs by GC-APPI-HRMS

As the GC-APPI response mainly depends on the concentration, it is possible to determine the concentration of each homologue group of congeners by an internal normalization. Thus, the contribution of each homologue group to the total SCCP area can be related to their concentrations in the SCCP mixture. Using this approach, the concentration of each homologue group was determined in three commercial SCCP standard mixtures with a total chlorine content of 63%, 55.5%, and 51.5% (see Table S2-S4). These profile concentrations were similar to those previously described in the literature using APCI-HRMS (TOF) method

[22]. For quantitative purposes, calibration solutions of each SCCP standard mixtures were prepared at concentrations ranged from 0.5 to 5 mg L^{-1} (total concentration of SCCPs) and the calibration curves for each homologue group were determined using the internal standard method. As an example, Fig. 4 shows the calibration curves obtained for the $C_{13}H_{22}Cl_6$ homologue group in the three available SCCP mixtures.
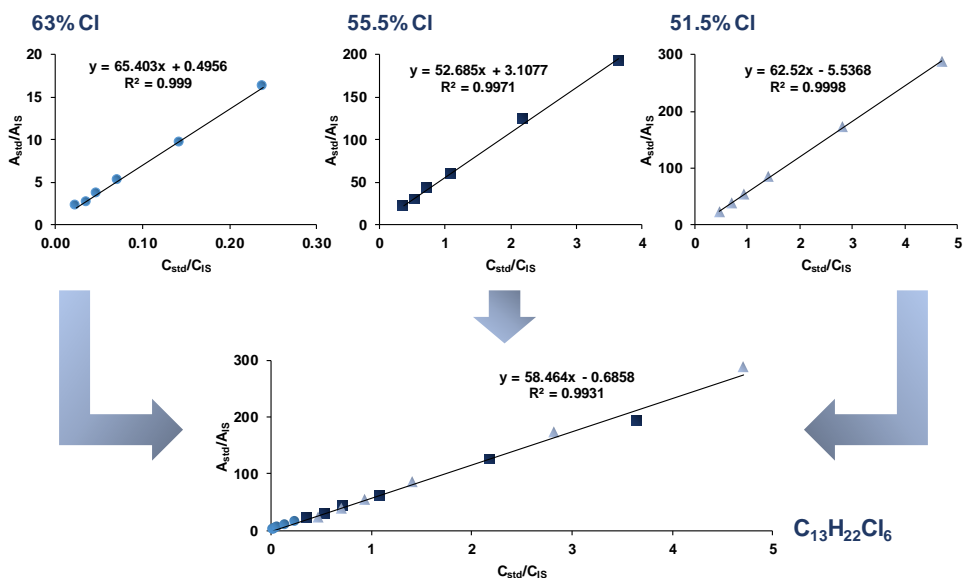
Figure 4. Calibration curves of the homologue group $C_{13}H_{22}Cl_6$, by monitoring the [M+Cl]$^-$ ion and using for calibration individual SCCP standards and a mixture of the SCCPs with a total chlorine content of 51.5%, 55.5% and 63% Cl.

Generally, good linearity was achieved for all the homologue groups with correlation coefficients ranging from 0.998 to 0.999. Moreover, by combining the calibration data of each homolog group corresponding to the three SCCP mixtures, there was still a good correlation between areas and concentrations, demonstrating that the calibration of each homologue group did not depend of the SCCP mixture used for quantification. Therefore, it is not necessary to know the chlorination content of the samples before analysing for selecting the adequate standard for the quantification. Using this approach, a considerable reduction in the analysis and data treatment time was achieved.

3.3. Quality parameters of the GC-APPI-HRMS method

To examine the feasibility of the developed GC-APPI-HRMS method for the determination of SCCPs several quality parameters were established. Instrumental limit of detection (ILOD), defined as the lowest amount injected that is possible to detect on a well-defined broad hump of at least one group of SCCPs isomers, was established for all the SCCP mixtures (51.5% Cl, 55.5% Cl and 63% Cl). ILODs ranged from 1 (SCCPs with 51.5% Cl) to 2 pg injected (SCCPs with 55.5% Cl and 63% Cl) of the total amount of SCCPs. Moreover, ILODs of each

homologue group of congeners were also determined (Table 1) and ranging from 0.07 to 0.19 pg injected. These values were lower than those achieved by direct injection-APCI-qTOF (0.2–100 pg µL^{-1} for 5 µL injected) [22], and slightly lower than the values obtained by GC-ECNI-HRMS (0.03–2.02 pg injected) using an Orbitrap mass analyser [10].

Table 1. Instrumental limits of detection (pg injected) of CP homologue groups by GC-APPI-HRMS method.

Homologue	ILOD (pg injected)			
	51.5% Cl	55.5% Cl	63%Cl	Mean ± SD
$C_{10}H_{18}Cl_4$	0.10	0.10	–	0.10[1]
$C_{10}H_{17}Cl_5$	0.15	0.10	0.10	0.12 ± 0.03
$C_{10}H_{16}Cl_6$	0.14	0.07	0.10	0.10 ± 0.04
$C_{10}H_{15}Cl_7$	0.12	0.16	0.10	0.13 ± 0.03
$C_{10}H_{14}Cl_8$	–	0.18	0.08	0.13[1]
$C_{10}H_{13}Cl_9$	–	–	0.10	0.10[1]
$C_{10}H_{12}Cl_{10}$	–	–	0.07	0.07[1]
$C_{11}H_{20}Cl_4$	0.14	0.14	–	0.14[1]
$C_{11}H_{19}Cl_5$	0.10	0.07	0.09	0.09 ± 0.01
$C_{11}H_{18}Cl_6$	0.10	0.07	0.05	0.07 ± 0.02
$C_{11}H_{17}Cl_7$	0.12	0.08	0.13	0.11 ± 0.02
$C_{11}H_{16}Cl_8$	0.20	0.15	0.11	0.15 ± 0.05
$C_{11}H_{15}Cl_9$	–	0.10	0.17	0.14 ± 0.05
$C_{11}H_{14}Cl_{10}$	–	–	0.10	0.10[1]
$C_{12}H_{22}Cl_4$	0.10	0.11	–	0.10[1]
$C_{12}H_{21}Cl_5$	0.08	0.08	0.05	0.07 ± 0.02
$C_{12}H_{20}Cl_6$	0.07	0.10	0.12	0.10 ± 0.03
$C_{12}H_{19}Cl_7$	0.08	0.10	0.10	0.09 ± 0.01
$C_{12}H_{18}Cl_8$	0.15	0.08	0.14	0.12 ± 0.04
$C_{12}H_{17}Cl_9$	0.20	0.10	0.19	0.16 ± 0.05
$C_{12}H_{16}Cl_{10}$	–	0.20	0.19	0.19[1]
$C_{13}H_{24}Cl_4$	0.20	0.12	–	0.16[1]
$C_{13}H_{23}Cl_5$	0.10	0.11	0.06	0.09 ± 0.03
$C_{13}H_{22}Cl_6$	0.15	0.10	0.15	0.13 ± 0.03
$C_{13}H_{21}Cl_7$	0.08	0.10	0.11	0.10 ± 0.01
$C_{13}H_{20}Cl_8$	0.15	0.06	0.19	0.15 ± 0.08
$C_{13}H_{19}Cl_9$	0.22	0.14	0.19	0.19 ± 0.04
$C_{13}H_{18}Cl_{10}$	–	0.14	0.21	0.18[1]
Total SCCPs	2	2	1	1.7 ± 0.6

[1] Not present in all the SCCP formulation.

Table 2 shows the quality parameters of the developed method calculated using the SCCP standard mixtures in a working range from 0.25 to 5 ng μL^{-1} (total amount of SCCPs) at two different concentration levels (depending on the homologue group). Good precisions were achieved for the homologue groups and the total SCCPs with relative standard deviation lower than 7%. The trueness of the developed method was also quite good with relative errors (RE, %) lower than 8%. Method limits of detection (MLODs) were determined by analysing a blank salmon samples spiked with the target compounds at low concentration levels. MLOD values ranged from 0.017 to 0.035 ng g^{-1} wet weight. All these figures of merit demonstrated the good performance of the GC-APPI-HRMS method for the reliable quantification of SCCPs.

To evaluate the selectivity of the GC-APPI-HRMS method the effect of some potential interfering compounds, such as PCBs and organochlorine pesticides, in the determination of SCCPs was investigated. Two standard mixtures containing seven CB congeners (PCB-Mix 1) and twenty-two organochlorine pesticides (Pesticide-Mix 1037) (see section 2.2.) at a concentration of 1 ng μL^{-1}, were injected under the established GC-APPI-HRMS conditions. The ionisation efficiency achieved for most of these compounds was very low even at these high concentration levels. PCBs yielded the [M–Cl+O]$^-$ ions while most of the studied pesticides generated the [M+Cl]$^-$ ion as the base peak of the mass spectra. The minimal resolution (R$_{min}$) required preventing these possible external interferences for the different SCCP homologue groups was 13,251 FWHM (Tables S5). This minimal resolution was even lower than that required for avoiding the potential isobaric interferences between CP congeners (28,441 FWHM). Therefore, the use of the proposed GC-APPI-HRMS method which operated at a resolution of 70,000 FWHM (resolution measured at *m/z* 200) provided a high selectivity on the determination of SCCPs with a negligible contribution of internal and external interferences.

3.4. Analysis of fish samples

To evaluate the real applicability of the developed HC-APPI-HRMS method for the determination of SCCPs in environmental samples, selected fish samples were analysed. Three salmon and two tune samples were analysed in triplicate and procedural blanks were also included to guarantee the absence of possible carryover between samples, assessing the quality of the results. Table 3 summarizes the results of the total SCCPs applying the two quantification approaches based on the use of a SCCP standard mixture (SCCPs 63%Cl) with a similar homologue composition to the analysed samples and a standard mixture of the three SCCP standards with a total chlorine content of 51.5%, 55.5% and 63%Cl. Total SCCP concentrations ranged between 25.8 and 28.3 ng g^{-1} wet weight, while the tune samples varied from 6.3 to 30 ng g^{-1} wet weight with good precision (RSD% <7%). In addition, a good agreement between the results obtained with the two calibration methods was achieved and no significant differences were observed between them (*p*-value > 0.82), demonstrating the feasibility of the quantification approaches.

Table 2. Quality parameters of the GC-APPI-HRMS method using SCCP standard mixtures.

Homologue Group	Conc.± SD (pg µL^{-1})	Precision (RSD %)	Conc.± SD (pg µL^{-1})	Precision (RSD %)	Trueness (RE %)	
	Low Level		Medium Level		Low Level	Medium Level
$C_{10}H_{18}Cl_4$	0.49 ± 0.03	6	1.35 ± 0.06	4	1	–8
$C_{10}H_{17}Cl_5$	6.2 ± 0.2	3	16.8 ± 0.4	2	5	–5
$C_{10}H_{16}Cl_6$	10.6 ± 0.5	4	29 ± 1	4	5	–3
$C_{10}H_{15}Cl_7$	9.3 ± 0.4	4	27 ± 1	4	3	1
$C_{10}H_{14}Cl_8$	3.58 ± 0.04	2	10.5 ± 0.2	2	5	2
$C_{10}H_{13}Cl_9$	0.19 ± 0.01	5	0.56 ± 0.01	2	–4	–4
$C_{10}H_{12}Cl_{10}$	n.d.[1]	n.d.[1]	n.d.[1]	n.d.[1]	n.d.[1]	n.d.[1]
$C_{11}H_{20}Cl_4$	4.0 ± 0.1	3	11.5 ± 0.6	5	8	3
$C_{11}H_{19}Cl_5$	34 ± 2	6	94 ± 5	5	4	–5
$C_{11}H_{18}Cl_6$	50 ± 2	4	135 ± 5	4	3	–7
$C_{11}H_{17}Cl_7$	49.9 ± 0.3	1	135 ± 3	2	4	–6
$C_{11}H_{16}Cl_8$	56 ± 2	4	154 ± 4	3	1	–8
$C_{11}H_{15}Cl_9$	6.7 ± 0.5	7	19.3 ± 0.8	4	–0.4	–5
$C_{11}H_{14}Cl_{10}$	0.35 ± 0.02	6	1.04 ± 0.02	2	–5	–6
$C_{12}H_{22}Cl_4$	3.7 ± 0.1	3	10.0 ± 0.4	4	7	–4
$C_{12}H_{21}Cl_5$	32 ± 1	3	87.9 ± 0.9	2	4	–5
$C_{12}H_{20}Cl_6$	47.5 ± 0.7	2	128 ± 4	3	5	–6
$C_{12}H_{19}Cl_7$	48 ± 3	6	141 ± 2	2	3	0.2
$C_{12}H_{18}Cl_8$	32 ± 1	3	91.8 ± 0.7	1	1	–5
$C_{12}H_{17}Cl_9$	13.3 ± 0.7	5	38 ± 1	3	1	–5
$C_{12}H_{16}Cl_{10}$	1.98 ± 0.09	5	5.4 ± 0.2	4	5	–4
$C_{13}H_{24}Cl_4$	1.62 ± 0.06	4	4.4 ± 0.1	2	4	–7
$C_{13}H_{23}Cl_5$	15.4 ± 0.4	3	42 ± 2	5	4	–5
$C_{13}H_{22}Cl_6$	26 ± 1	4	71 ± 1	2	2	–6
$C_{13}H_{21}Cl_7$	24 ± 1	4	69 ± 3	4	1	–4
$C_{13}H_{20}Cl_8$	20.3 ± 0.9	4	59 ± 2	3	–1	–5
$C_{13}H_{19}Cl_9$	12.1 ± 0.3	3	34.6 ± 0.7	2	1	–4
$C_{13}H_{18}Cl_{10}$	2.7 ± 0.1	4	8.0 ± 0.1	2	–2	–2
Total SCCPs	515 ± 16	3	1429 ± 80	6	3	–5

[1] non detected in the SCCP standard mixture.

Besides, the concentrations of each homologue groups were also determined for the analysed samples and the results showed that the C_{11}-SCCPs were found at high concentration levels, especially for the $C_{11}H_{19}Cl_5$ and $C_{11}H_{18}Cl_6$, which were determined at the highest values (Table 4).

Table 3. Concentrations of the total SCCPs (ng g^{-1} wet weight) found in selected fish samples using different quantification approaches.

Sample	Quantification approach	
	SCCP standard with similar % Cl [1]	Mixture of SCCP standards[1,2]
Salmon #1	25.8 ± 1.2	25.3 ± 1.2
Salmon #2	26.0 ± 0.3	25.3 ± 0.2
Salmon #3	28.3 ± 0.9	27.5 ± 0.9
Tuna #1	6.3 ± 0.4	5.7 ± 0.4
Tuna #2	30.0 ± 1.0	28.5 ± 1.3

[1] Calculated as mean (n=3) ± standard deviation.

[2] Mixture of SCCP standards with a total chlorine content of 51.5%, 55.5% and 63%.

As an example, Fig. 5 shows the concentration profile of the individual groups of isomers found in a salmon sample. The concentration profile of the homologue groups showed similarities with the homologue distribution of SCCPs with 55.5% and 51.5% chlorine content. So, a mixture of them should be used to avoid quantification errors when working with ECNI-based methods. Therefore, the use of the developed GC-APPI-HRMS method allowed the adequate quantification of both the total amount of SCCPs and the individual group of congeners using a mixture of commercially available SCCP standards, which involves an important time reduction and a better selectivity than the traditional methods.

4. Conclusions

This work demonstrates, for the first time, the capabilities of the new GC-APPI source for the accurate determination SCCP congeners in fish samples by GC-HRMS (Orbitrap). The efficient ionization of the CP congeners was accomplished by dopant-assisted GC-APPI using solvent vapours of acetone/CCl$_4$, (3:1 *v/v*) as a dopant and operating in the negative-ion mode. Under these conditions, the GC-APPI source allowed the formation of intense [M+Cl]$^-$ adduct ions for all the homologue groups with a very low fragmentation. Monitoring these adduct ions in full-scan mode at a high mass resolution (70,000 FWHM) provided suitable sensitivity and selectivity for the determination of SCCPs, minimizing the possible isobaric interferences between CP congeners and with other halogenated compounds. In addition, the GC-APPI-HRMS provided responses no dependent on the number of chlorine atoms of the molecule and were mainly proportional to the concentration, allowing a selective determination of the CP congener groups without interferences. Thus, the concentration of each of homologue group in the SCCP mixture was estimated by the internal normalization method, and the quantification was accomplished by the internal standard method using mixtures of SCCP standards with 51.5, 55.5, 63% Cl as calibration solution for quantification.
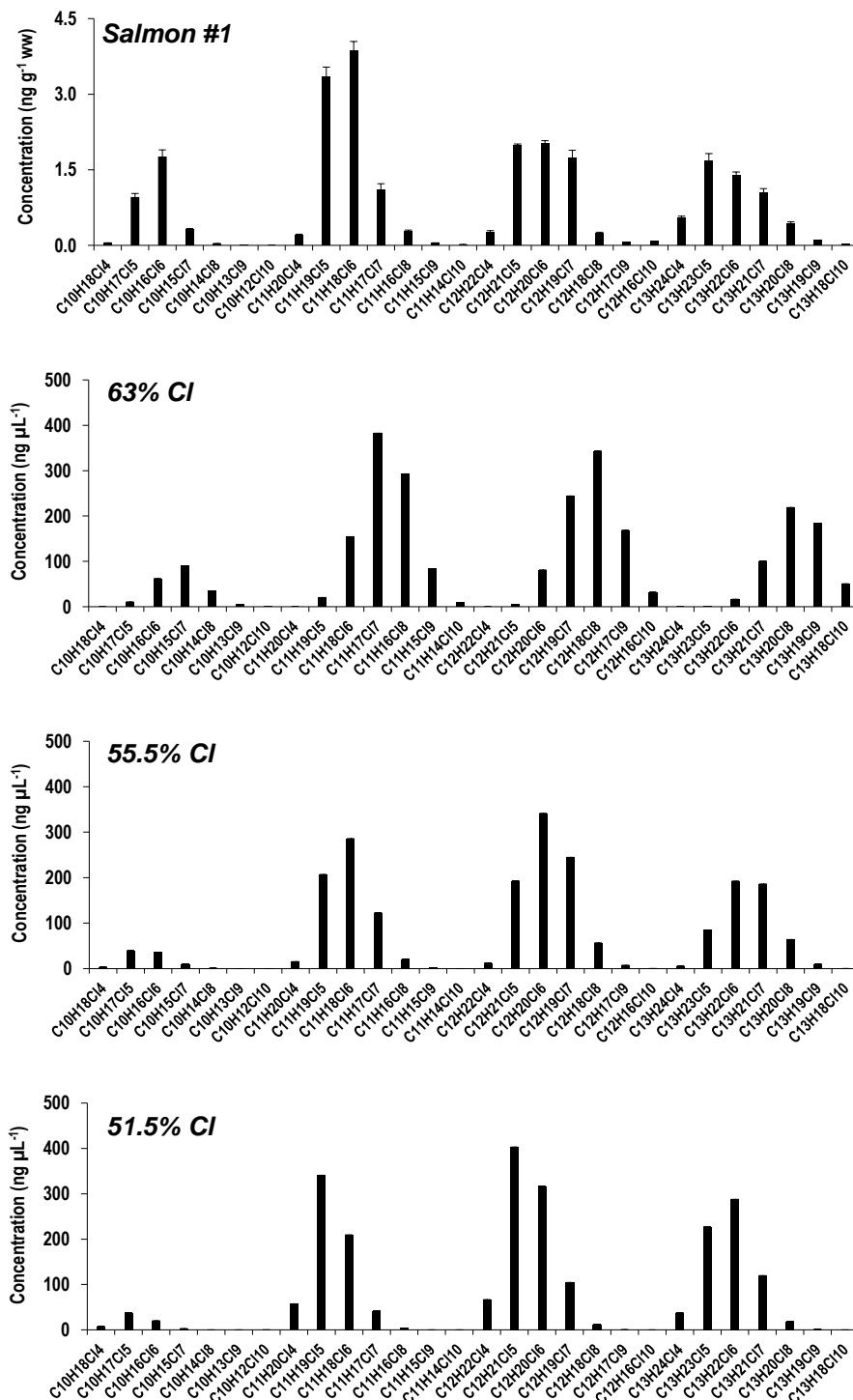
Figure 5. Concentration profile of each homologue group of SCCPs obtained for the salmon #1 sample and the standard formulations (63%, 55.5%, 51.5% Cl).

. **Table 4.** SCCP concentration of each homologue group (ng g^{-1} wet weight) in selected fish samples.

Homologue	Concentration (ng g^{-1} wet weight)[1]				
	Salmon #1	Salmon #2	Salmon #3	Tuna #1	Tuna #2
$C_{10}H_{18}Cl_4$	0.0531 ± 0.0005	0.071 ± 0.006	0.050 ± 0.006	0.005 ± 0.001	<MLOQ[3]
$C_{10}H_{17}Cl_5$	0.96 ± 0.07	1.35 ± 0.02	1.06 ± 0.03	0.040 ± 0.003	0.0117 ± 0.0003
$C_{10}H_{16}Cl_6$	1.8 ± 0.1	2.56 ± 0.04	1.69 ± 0.04	6.4 ±0.4	0.0032 ± 0.0004
$C_{10}H_{15}Cl_7$	0.31 ± 0.02	0.31 ± 0.01	0.231 ± 0.005	–	<MLOQ[3]
$C_{10}H_{14}Cl_8$	0.035 ± 0.002	0.025 ± 0.002	0.009 ± 0.001	–	–
$C_{10}H_{13}Cl_9$	<MLOQ[2]	–	–	–	–
$C_{10}H_{12}Cl_{10}$	–	–	–	–	–
$C_{11}H_{20}Cl_4$	0.21 ± 0.01	0.28 ± 0.01	0.23 ± 0.02	0.012 ± 0.001	1.00 ± 0.03
$C_{11}H_{19}Cl_5$	3.3 ± 0.2	4.46 ± 0.08	3.9 ± 0.2	0.035 ± 0.003	10.9 ± 0.1
$C_{11}H_{18}Cl_6$	3.9 ± 0.2	4.52 ± 0.03	4.1 ± 0.1	0.012 ± 0.001	10.2 ± 0.7
$C_{11}H_{17}Cl_7$	1.1 ± 0.1	1.01 ± 0.05	1.00 ± 0.04	0.0054 ± 0.0004	4.7 ± 0.4
$C_{11}H_{16}Cl_8$	0.28 ± 0.02	0.10 ± 0.01	0.125 ± 0.004	0.0032 ± 0.002	1.8 ± 0.1
$C_{11}H_{15}Cl_9$	0.046 ± 0.006	<MLOQ[2]	<MLOQ[2]	–	0.19 ± 0.01
$C_{11}H_{14}Cl_{10}$	0.017 ± 0.001	–	–	–	0.045 ± 0.004
$C_{12}H_{22}Cl_4$	0.27 ± 0.02	0.40 ± 0.01	0.36 ± 0.04	0.007 ± 0.001	<MLOQ[3]
$C_{12}H_{21}Cl_5$	1.98 ± 0.03	2.45 ± 0.04	2.5 ± 0.1	0.0032 ± 0.003	0.011 ± 0.001
$C_{12}H_{20}Cl_6$	2.03 ± 0.05	1.91 ± 0.05	2.21 ± 0.09	<MLOQ[3]	0.022 ± 0.002
$C_{12}H_{19}Cl_7$	1.7 ± 0.2	0.48 ± 0.03	1.94 ± 0.03	<MLOQ[3]	0.015 ± 0.002
$C_{12}H_{18}Cl_8$	0.24 ± 0.02	0.0162 ± 0.0003	0.180 ± 0.006	<MLOQ[3]	0.0047 ± 0.0009
$C_{12}H_{17}Cl_9$	0.059 ± 0.005	<MLOQ[2]	0.013 ± 0.001	–	<MLOQ[3]
$C_{12}H_{16}Cl_{10}$	0.079 ± 0.007	–	–	–	–
$C_{13}H_{24}Cl_4$	0.54 ± 0.04	0.69 ± 0.05	0.63 ± 0.06	0.0052 ± 0.0002	<MLOQ[3]
$C_{13}H_{23}Cl_5$	1.7 ± 0.1	1.66 ± 0.03	1.9 ± 0.1	0.0033 ± 0.0005	<MLOQ[3]
$C_{13}H_{22}Cl_6$	1.40 ± 0.06	1.10 ± 0.06	1.77 ± 0.06	<MLOQ[3]	<MLOQ[3]
$C_{13}H_{21}Cl_7$	1.04 ± 0.09	0.11 ± 0.01	1.22 ± 0.02	<MLOQ[3]	<MLOQ[3]
$C_{13}H_{20}Cl_8$	0.43 ± 0.04	0.13 ± 0.02	0.44 ± 0.02	<MLOQ[3]	<MLOQ[3]
$C_{13}H_{19}Cl_9$	0.098 ± 0.008	<MLOQ[2]	0.032 ± 0.002	–	<MLOQ[3]
$C_{13}H_{18}Cl_{10}$	0.024 ± 0.003	–	–	–	–

[1] Calculated as the mean (n=3) ± standard deviation.

[2] MLOQ (Salmon): 0.002-0.008 ng g^{-1} ww.

[3] MLOQ (Tuna): 0.001-0.003 ng g^{-1} ww.

The proposed GC-APPI-HRMS allowed the analysis of both the total amount of SCCPs and the homologue groups of congeners, providing valuable information on the homologue composition and achieving a reduction on the analysis time and data treatment compared with

the classical approaches. Besides, the developed GC-APPI-HRMS method showed a great detection capability (ILODs:1-2 pg injected and MLODs: 0.017-0.034 ng g^{-1} ww for total SCCPs) and also a good precision (RSD% <7%) and trueness (RE% <8%). The GC-APPI-HRMS method has been successfully applied to the analysis of SCCPs in fish samples demonstrating its excellent performance and it is proposed as a reliable alternative to the GC-ECNI-MS methods.

Declaration of Competing Interest

The authors declare that they have no conflict of interest.

Acknowledgements

References

[1] D.C.G. Muir, G. Stern, G. Tomy, Chlorinated Paraffins, in: O. Hutzinger, J. Paasivirta (Eds.), New Types Persistent Halogenated Compd., 1st ed., Springer, Berlin, Heidelberg, 2000: pp. 203–236. https://doi.org/https://doi.org/10.1007/3-540-48915-0.

[2] H. Fiedler, Short-Chain Chlorinated Paraffins: Production, Use and International Regulations, in: J. de Boer (Ed.), Chlorinated Paraffins, 1st ed., Springer Verlag, Berlin Heidelberg, 2010: pp. 1–40. https://doi.org/https://doi.org/10.1007/978-3-642-10761-0.

[3] J. Glüge, Z. Wang, C. Bogdal, M. Scheringer, K. Hungerbühler, Global production, use, and emission volumes of short-chain chlorinated paraffins – A minimum scenario, Sci. Total Environ. 573 (2016) 1132–1146. https://doi.org/10.1016/j.scitotenv.2016.08.105.

[4] M. Houde, D.C.G. Muir, G.T. Tomy, D.M. Whittle, C. Teixeira, S. Moore, Bioaccumulation and trophic magnification of short- and medium-chain chlorinated paraffins in food webs from Lake Ontario and Lake Michigan, Environ. Sci. Technol. 42 (2008) 3893–3899. https://doi.org/10.1021/es703184s.

[5] N. Geng, H. Zhang, L. Xing, Y. Gao, B. Zhang, F. Wang, X. Ren, J. Chen, Toxicokinetics of short-chain chlorinated paraffins in Sprague-Dawley rats following single oral administration, Chemosphere. 145 (2016) 106–111. https://doi.org/10.1016/j.chemosphere.2015.11.066.

[6]   D. Xia, L. Gao, M. Zheng, J. Li, L. Zhang, Y. Wu, Q. Tian, H. Huang, L. Qiao, Human Exposure to Short- and Medium-Chain Chlorinated Paraffins via Mothers' Milk in Chinese Urban Population, Environ. Sci. Technol. 51 (2017) 608–615. https://doi.org/10.1021/acs.est.6b04246.

[7]   United Nation Environment Programme - UNEP: Eighth meeting of the Conference of the Parties., Decision SC-8/11: Listing of short-chain chlorinated paraffins, Stockholm, (2017).

[8]   European Union, Directive 2013/39/EU of the European Parliament and of the Council of 12 August 2013 amending Directives 2000/60/EC and 2008/105/EC as regards priority substances in the field of water policy, Off. J. Eur. Communities. L226 (2013) 1–17.

[9]   C. Bogdal, T. Alsberg, P.S. Diefenbacher, M. Macleod, U. Berger, Fast quantification of chlorinated paraffins in environmental samples by direct injection high-resolution mass spectrometry with pattern deconvolution, Anal. Chem. 87 (2015) 2852–2860. https://doi.org/10.1021/ac504444d.

[10] K. Krätschmer, C. Cojocariu, A. Schächtele, R. Malisch, W. Vetter, Chlorinated paraffin analysis by gas chromatography Orbitrap high-resolution mass spectrometry: Method performance, investigation of possible interferences and analysis of fish samples, J. Chromatogr. A. 1539 (2018) 53–61. https://doi.org/10.1016/j.chroma.2018.01.034.

[11] P. Korytár, J. Parera, P.E.G. Leonards, F.J. Santos, J. De Boer, U.A.T. Brinkman, Characterization of polychlorinated n-alkanes using comprehensive two-dimensional gas chromatography-electron-capture negative ionisation time-of-flight mass spectrometry, J. Chromatogr. A. 1086 (2005) 71–82. https://doi.org/10.1016/j.chroma.2005.05.003.

[12] O. Froescheis, K. Ballschmiter, Electron capture negative ion (ECNI) mass spectrometry of complex mixtures of chlorinated decanes and dodecanes: An approach to ECNI mass spectra of chlorinated paraffins in technical mixtures, Fresenius. J. Anal. Chem. 361 (1998) 784–790. https://doi.org/10.1007/s002160051016.

[13] P. Castells, F.J. Santos, M.T. Galceran, Evaluation of three ionisation modes for the analysis of chlorinated paraffins by gas chromatography/ion-trap mass spectrometry., Rapid Commun. Mass Spectrom. 18 (2004) 529–536. https://doi.org/10.1002/rcm.1366.

[14] Z. Zencak, A. Borgen, M. Reth, M. Oehme, Evaluation of four mass spectrometric methods for the gas chromatographic analysis of polychlorinated n-alkanes, J. Chromatogr. A. 1067 (2005) 295–301. https://doi.org/10.1016/j.chroma.2004.09.098.

[15] M. Reth, Z. Zencak, M. Oehme, New quantification procedure for the analysis of chlorinated paraffins using electron capture negative ionization mass spectrometry, J. Chromatogr. A. 1081 (2005) 225–231. https://doi.org/10.1016/j.chroma.2005.05.061.

[16] M. Reth, M. Oehme, Limitations of low resolution mass spectrometry in the electron capture negative ionization mode for the analysis of short- and medium-chain chlorinated paraffins, Anal. Bioanal. Chem. 378 (2004) 1741–1747. https://doi.org/10.1007/s00216-004-2546-9.

[17] T.P. Rusina, P. Korytár, J. de Boer, Comparison of quantification methods for the analysis of polychlorinated alkanes using electron capture negative ionisation mass spectrometry, Int. J. Environ. Anal. Chem. 91 (2011) 319–332. https://doi.org/10.1080/03067311003602583.

[18] S. Geiss, M. Schneider, G. Donnevert, J.W. Einax, N. Lettmann, A. Rey, H. Lepper, B. Korner, T. Prey, B. Hilger, M. Engelke, M.P. Strub, H. Adrien, G. Sawal, D. Loffler, T. Schillings, I. Hussy, P. Steinbichl, S. Scharf, A. Ruderisch, J.E. Olmos, F.J. Santos, A. Bartolome, J. Caixach, Validation interlaboratory trial for ISO 12010: Water quality-Determination of short-chain polychlorinated alkanes (SCCP) in water, Accredit. Qual. Assur. 17 (2012) 15–25. https://doi.org/10.1007/s00769-011-0820-z.

[19] G.T. Tomy, G.A. Stern, D.C.G. Muir, A.T. Fisk, C.D. Cymbalisty, J.B. Westmore, Quantifying C10-C13 Polychloroalkanes in Environmental Samples by High-Resolution Gas Chromatography/Electron Capture Negative Ion High-Resolution Mass Spectrometry, Anal. Chem. 69 (1997) 2762–2771. https://doi.org/10.1021/ac961244y.

[20] L. Schinkel, S. Lehner, N. V. Heeb, P. Lienemann, K. McNeill, C. Bogdal, Deconvolution of Mass Spectral Interferences of Chlorinated Alkanes and Their Thermal Degradation Products: Chlorinated Alkenes, Anal. Chem. 89 (2017) 5923–5931. https://doi.org/10.1021/acs.analchem.7b00331.

[21] S.H. Brandsma, L. Van Mourik, J.W. O'Brien, G. Eaglesham, P.E.G. Leonards, J. De Boer, C. Gallen, J. Mueller, C. Gaus, C. Bogdal, Medium-Chain Chlorinated Paraffins (CPs) Dominate in Australian Sewage Sludge, Environ. Sci. Technol. 51 (2017) 3364–3372. https://doi.org/10.1021/acs.est.6b05318.

[22] B. Yuan, C. Bogdal, U. Berger, M. MacLeod, W.A. Gebbink, T. Alsberg, C.A. De Wit, Quantifying Short-Chain Chlorinated Paraffin Congener Groups, Environ. Sci. Technol. 51 (2017) 10633–10641. https://doi.org/10.1021/acs.est.7b02269.

[23] B. Yuan, J.P. Benskin, C.E.L. Chen, Å. Bergman, Determination of Chlorinated Paraffins by Bromide-Anion Attachment Atmospheric-Pressure Chemical Ionization Mass Spectrometry, Environ. Sci. Technol. Lett. 5 (2018) 348–353. https://doi.org/10.1021/acs.estlett.8b00216.

[24] B. Yuan, T. Alsberg, C. Bogdal, M. MacLeod, U. Berger, W. Gao, Y. Wang, C.A. De Wit, Deconvolution of Soft Ionization Mass Spectra of Chlorinated Paraffins to Resolve Congener Groups, Anal. Chem. 88 (2016) 8980–8988. https://doi.org/10.1021/acs.analchem.6b01172.

[25]   D.-X. Li, L. Gan, A. Bronja, O.J. Schmitz, Gas chromatography coupled to atmospheric pressure ionization mass spectrometry (GC-API-MS): Review, Anal. Chim. Acta. 891 (2015) 43–61. https://doi.org/10.1016/j.aca.2015.08.002.

[26]   I. Revelsky, Y. Yashin, T. Sobolevsky, A. Revelsky, B. Miller, V. Oriedo, Electron ionization and atmospheric pressure photochemical ionization in gas chromatography-mass spectrometry analysis of amino acids, Eur. J. Mass Spectrom. 9 (2003) 497. https://doi.org/10.1255/ejms.581.

[27]   L. Luosujärvi, M.-M. Karikko, M. Haapala, V. Saarela, S. Huhtala, S. Franssilla, R. Kostiainen, T. Kotiaho, T.J. Kauppila, Gas chromatography/mass spectrometry of polychlorinated biphenyls using atmospheric pressure chemical ionization and atmospheric pressure photoionization microchips, Rapid Commun. Mass Spectrom. 22 (2008) 425–431. https://doi.org/https://doi.org/10.1002/rcm.3379.

[28]   M. Haapala, L. Luosujǎrvi, V. Saarela, T. Kotiaho, R.A. Ketola, S. Franssila, R. Kostiainen, Microchip for combining gas chromatography or capillary liquid chromatography with atmospheric pressure photoionization-mass spectrometry, Anal. Chem. 79 (2007) 4994–4999. https://doi.org/10.1021/ac070157a.

[29]   I.A. Revelsky, Y.S. Yashin, New approach to complex organic compounds mixtures analysis based on gas chromatography-atmospheric pressure photoionization-mass-spectrometry, Talanta. 102 (2012) 110–113. https://doi.org/10.1016/j.talanta.2012.07.023.

[30]   J.F. Ayala-Cabrera, A. Contreras-Llin, E. Moyano, F.J. Santos, A novel methodology for the determination of neutral perfluoroalkyl and polyfluoroalkyl substances in water by gas chromatography-atmospheric pressure photoionisation-high resolution mass spectrometry, Anal. Chim. Acta. 1100 (2020) 97–106. https://doi.org/10.1016/j.aca.2019.12.004.

[31]   T.J. Kauppila, H. Kersten, T. Benter, Ionization of EPA contaminants in direct and dopant-assisted atmospheric pressure photoionization and atmospheric pressure laser ionization, J. Am. Soc. Mass Spectrom. 26 (2015) 1036–1045. https://doi.org/10.1007/s13361-015-1092-3.

[32]   Ministerio de Agricultura, Pesca y Alimentación, Survey of the Spanish population's food comsumption - 2018, (2019).

[33]   Z. Zencak, M. Oehme, Chloride-enhanced atmospheric pressure chemical ionization mass spectrometry of polychlorinated n-alkanes., Rapid Commun. Mass Spectrom. 18 (2004) 2235–40. https://doi.org/10.1002/rcm.1614.

Supporting Information

Chloride-attachment Atmospheric Pressure Photoionisation for the Determination of Short-Chain Chlorinated Paraffins by Gas Chromatography-High-Resolution Mass Spectrometry

J. F. Ayala-Cabrera[(1)], M. T. Galceran[(1,2)], E. Moyano[(1,2)], F. J. Santos[(1,2)*]

[(1)] Department of Chemical Engineering and Analytical Chemistry, University of Barcelona. Av. Diagonal 645, E–08028 Barcelona, Spain

[(2)] Water Research Institute (IdRA), University of Barcelona, Montalegre 6, E–08001 Barcelona, Spain

* Corresponding author: Francisco Javier Santos Vicente
Phone: +34-93-403-4874
Fax: +34-93-402-1233
E-mail: javier.santos@ub.edu

Table of Contents

Supporting Tables

Table S1. Mass-to-charge (*m/z*) ratio of [M+Cl]− cluster ions for the SCCP homologue groups.

Homologue Group	M [M+Cl]−	Rel.Ab (%)	M+2	Rel.Ab (%)	M+4	Rel.Ab (%)	M+6	Rel.Ab (%)	M+8	Rel.Ab (%)	M+10	Rel.Ab (%)
$C_{10}H_{18}Cl_4$	312.9857	62.6	314.9827[1]	100.0	316.9798[1]	63.9	318.9768	20.4	320.9739	3.3	322.9709	0.2
$C_{10}H_{17}Cl_5$	346.9467	52.2	348.9437	100.0	350.9408	79.9	352.9738	34.1	354.9349	8.2	356.9319	1.0
$C_{10}H_{16}Cl_6$	380.9077	44.7	382.9048	100.0	384.9018	95.9	386.8989	51.1	388.8959	16.3	390.8930	3.1
$C_{10}H_{15}Cl_7$	414.8688	35.0	416.8658	89.4	418.8629	100.0	420.8599	63.9	422.8570	25.5	424.8540	6.5
$C_{10}H_{14}Cl_8$	448.8298	27.2	450.8268	78.2	452.8239	100.0	454.8209	74.6	456.8180	35.8	458.8150	11.4
$C_{10}H_{13}Cl_9$	482.7908	21.8	484.7879	69.5	486.7849	100.0	488.7820	85.2	490.7790	47.7	492.7761	18.3
$C_{10}H_{12}Cl_{10}$	516.7518	17.8	518.7489	62.6	520.7459	100.0	522.7430	95.9	524.7400	61.3	526.7371	27.4
$C_{11}H_{20}Cl_4$	327.0013	62.6	328.9984	100.0	330.9954	63.9	332.9925	20.4	334.9895	3.3	336.9866	0.2
$C_{11}H_{19}Cl_5$	360.9623	52.2	362.9594	100.0	364.9564	79.9	366.9535	34.1	368.9505	8.2	370.9476	1.0
$C_{11}H_{18}Cl_6$	394.9234	44.7	396.9204	100.0	398.9175	95.9	400.9145	51.1	402.9116	16.3	404.9086	3.1
$C_{11}H_{17}Cl_7$	428.8844	35.0	430.8815	89.4	432.8785	100.0	434.8756	63.9	436.8726	25.5	438.8697	6.5
$C_{11}H_{16}Cl_8$	462.8454	27.2	464.8425	78.2	466.8395	100.0	468.8366	74.6	470.8336	35.8	472.8307	11.4
$C_{11}H_{15}Cl_9$	496.8065	21.8	498.8035	69.5	500.8006	100.0	502.7976	85.2	504.7947	47.7	506.7917	18.3
$C_{11}H_{14}Cl_{10}$	530.7675	17.8	532.7645	62.6	534.7616	100.0	536.7586	95.9	538.7557	61.3	540.7527	27.4

[1] Ions selected for quantification (green) and confirmation (blue) purposes.
[2] Internal standard.

Table S1 (cont.). Mass-to-charge (*m/z*) ratio of [M+Cl]⁻ cluster ions for the SCCP homologue groups.

Homologue Group	[M+Cl]⁻											
	M	Rel.Ab (%)	M+2	Rel.Ab (%)	M+4	Rel.Ab (%)	M+6	Rel.Ab (%)	M+8	Rel.Ab (%)	M+10	Rel.Ab (%)
$C_{12}H_{22}Cl_4$	341.0170	62.6	343.0140[1]	100.0	345.0111[1]	63.9	347.0081	20.4	349.0052	3.3	351.0022	0.2
$C_{12}H_{21}Cl_5$	374.9780	52.2	376.9750	100.0	378.9721	79.9	380.9691	34.1	382.9662	8.2	384.9632	1.0
$C_{12}H_{20}Cl_6$	408.9390	44.7	410.9361	100.0	412.9331	95.9	414.9302	51.1	416.9272	16.3	418.9243	3.1
$C_{12}H_{19}Cl_7$	442.9001	35.0	444.8971	89.4	446.8942	100.0	448.8912	63.9	450.8883	25.5	452.8853	6.5
$C_{12}H_{18}Cl_8$	476.8611	27.2	478.8581	78.2	480.8552	100.0	482.8522	74.6	484.8493	35.8	486.8463	11.4
$C_{12}H_{17}Cl_9$	510.8221	21.8	512.8192	69.5	514.8162	100.0	516.8133	85.2	518.8103	47.7	520.8074	18.3
$C_{12}H_{16}Cl_{10}$	544.7831	17.8	546.7802	62.6	548.7772	100.0	550.7743	95.9	552.7713	61.3	544.7684	27.4
$C_{13}H_{24}Cl_4$	355.0326	62.6	357.0297	100.0	359.0267	63.9	361.0238	20.4	363.0271	3.3	365.0179	0.2
$C_{13}H_{23}Cl_5$	388.9936	52.2	390.9907	100.0	392.9877	79.9	394.9848	34.1	396.9818	8.2	398.9789	1.0
$C_{13}H_{22}Cl_6$	422.9547	44.7	424.9517	100.0	426.9488	95.9	428.9458	51.1	430.9429	16.3	432.9399	3.1
$C_{13}H_{21}Cl_7$	456.9157	35.0	458.9128	89.4	460.9098	100.0	462.9069	63.9	464.9039	25.5	466.9010	6.5
$C_{13}H_{20}Cl_8$	490.8767	27.2	492.8738	78.2	494.8708	100.0	496.8679	74.6	498.8649	35.8	500.8620	11.4
$C_{13}H_{19}Cl_9$	524.8378	21.8	526.8348	69.5	528.8319	100.0	530.8289	85.2	532.8260	47.7	534.8230	18.3
$C_{13}H_{18}Cl_{10}$	558.7988	17.8	560.7958	62.6	562.7929	100.0	564.7899	100.0	566.7870	95.9	568.7840	27.4
^{13}C-HCB[2]	268.8599	63.8	270.8568	100.0	272.8536	100.0	274.8513	51.4	276.8484	18.4	278.8447	0.2

[1] Ions selected for quantification (green) and confirmation (blue) purposes.
[2] Internal standard.

Table S2. Concentration of each homologue group in the SCCP standard mixture with a total chlorine content of 51.5%.

Homologue Group	$A_{CxHyClz}/\Sigma A_{SCCP}$[1]	P1 ($\mu g\ L^{-1}$)	P2 ($\mu g\ L^{-1}$)	P3 ($\mu g\ L^{-1}$)	P4 ($\mu g\ L^{-1}$)	P5 ($\mu g\ L^{-1}$)	P6 ($\mu g\ L^{-1}$)
$C_{10}H_{18}Cl_4$	0.0022	1.1	1.7	2.2	3.4	6.7	11.2
$C_{10}H_{17}Cl_5$	0.013	6.5	9.8	13.1	19.6	39.2	65.3
$C_{10}H_{16}Cl_6$	0.0075	3.8	5.6	7.5	11.3	22.5	37.6
$C_{10}H_{15}Cl_7$	0.0012	0.59	0.88	1.17	1.76	3.52	5.87
$C_{10}H_{14}Cl_8$	-	-	-	-	-	-	-
$C_{10}H_{13}Cl_9$	-	-	-	-	-	-	-
$C_{10}H_{12}Cl_{10}$	-	-	-	-	-	-	-
$C_{11}H_{20}Cl_4$	0.016	8.2	12.3	16.4	24.7	49.3	82.2
$C_{11}H_{19}Cl_5$	0.12	58	87	116	175	349	582
$C_{11}H_{18}Cl_6$	0.093	46	70	93	139	279	464
$C_{11}H_{17}Cl_7$	0.023	11	17	23	34	68	113
$C_{11}H_{16}Cl_8$	0.0020	1.0	1.5	2.0	2.9	5.9	9.8
$C_{11}H_{15}Cl_9$	-	-	-	-	-	-	-
$C_{11}H_{14}Cl_{10}$	-	-	-	-	-	-	-
$C_{12}H_{22}Cl_4$	0.020	10	15	20	29	59	98
$C_{12}H_{21}Cl_5$	0.16	80	120	160	239	479	798
$C_{12}H_{20}Cl_6$	0.16	82	124	165	247	494	824
$C_{12}H_{19}Cl_7$	0.056	28	42	56	84	168	279
$C_{12}H_{18}Cl_8$	0.0065	3.2	4.9	6.5	9.7	19.5	32.4
$C_{12}H_{17}Cl_9$	0.00026	0.13	0.19	0.26	0.39	0.77	1.29
$C_{12}H_{16}Cl_{10}$	-	-	-	-	-	-	-
$C_{13}H_{24}Cl_4$	0.012	6.2	9.4	12.5	18.7	37.4	62.4
$C_{13}H_{23}Cl_5$	0.11	54	80	107	161	321	535
$C_{13}H_{22}Cl_6$	0.13	66	100	133	199	399	664
$C_{13}H_{21}Cl_7$	0.057	28	43	57	85	171	284
$C_{13}H_{20}Cl_8$	0.0092	4.6	6.9	9.2	13.8	27.6	46.0
$C_{13}H_{19}Cl_9$	0.00068	0.34	0.51	0.68	1.03	2.05	3.42
$C_{13}H_{18}Cl_{10}$	-	-	-	-	-	-	-
ΣSCCP	1.00	500	750	1000	1500	3000	5000

[1]Calculated from [SCCP] of 3 mg L^{-1} (51.5% Cl formulation, n=3).

Table S3. Concentration of each homologue group in the SCCP standard mixture with a total chlorine content of 55.5%.

Homologue Group	$A_{CxHyClz}/\Sigma A_{SCCP}$[1]	P1 ($\mu g\ L^{-1}$)	P2 ($\mu g\ L^{-1}$)	P3 ($\mu g\ L^{-1}$)	P4 ($\mu g\ L^{-1}$)	P5 ($\mu g\ L^{-1}$)	P6 ($\mu g\ L^{-1}$)
$C_{10}H_{18}Cl_4$	0.0012	0.58	0.87	1.15	1.73	3.46	5.77
$C_{10}H_{17}Cl_5$	0.015	7.7	11.6	15.4	23.2	46.3	77.2
$C_{10}H_{16}Cl_6$	0.016	8.2	12.4	16.5	24.7	49.5	82.5
$C_{10}H_{15}Cl_7$	0.0049	2.5	3.7	4.9	7.4	14.8	24.6
$C_{10}H_{14}Cl_8$	0.00051	0.25	0.38	0.51	0.76	1.52	2.54
$C_{10}H_{13}Cl_9$	-	-	-	-	-	-	-
$C_{10}H_{12}Cl_{10}$	-	-	-	-	-	-	-
$C_{11}H_{20}Cl_4$	0.0059	2.9	4.4	5.9	8.8	17.6	29.4
$C_{11}H_{19}Cl_5$	0.093	46	70	93	139	279	465
$C_{11}H_{18}Cl_6$	0.14	68	102	136	204	408	679
$C_{11}H_{17}Cl_7$	0.062	31	46	62	92	185	308
$C_{11}H_{16}Cl_8$	0.011	5.4	8.1	10.8	16.1	32.3	53.8
$C_{11}H_{15}Cl_9$	0.00091	0.46	0.68	0.91	1.37	2.74	4.56
$C_{11}H_{14}Cl_{10}$	-	-	-	-	-	-	-
$C_{12}H_{22}Cl_4$	0.0037	1.8	2.8	3.7	5.5	11.1	18.4
$C_{12}H_{21}Cl_5$	0.086	43	65	86	130	259	432
$C_{12}H_{20}Cl_6$	0.17	85	127	169	254	507	845
$C_{12}H_{19}Cl_7$	0.11	54	81	109	163	326	543
$C_{12}H_{18}Cl_8$	0.028	14	21	28	42	84	140
$C_{12}H_{17}Cl_9$	0.0035	1.7	2.6	3.5	5.2	10.5	17.5
$C_{12}H_{16}Cl_{10}$	0.000084	0.04	0.06	0.08	0.13	0.25	0.42
$C_{13}H_{24}Cl_4$	0.0023	1.1	1.7	2.3	3.4	6.8	11.3
$C_{13}H_{23}Cl_5$	0.040	20	30	40	60	121	201
$C_{13}H_{22}Cl_6$	0.10	49	73	98	147	293	489
$C_{13}H_{21}Cl_7$	0.087	43	65	87	130	260	433
$C_{13}H_{20}Cl_8$	0.022	11	17	22	34	67	112
$C_{13}H_{19}Cl_9$	0.0049	2.4	3.7	4.9	7.3	14.6	24.4
$C_{13}H_{18}Cl_{10}$	0.00019	0.10	0.15	0.19	0.29	0.58	0.97
ΣSCCP	1.00	500	750	1000	1500	3000	5000

[1]Calculated from [SCCP] of 3 mg L^{-1} (55.5% Cl formulation, n=3).

**Table S4.** Concentration of each homologue group in the SCCP standard mixture with a total chlorine content of 63%.

Homologue Group	$A_{C_xH_yCl_z}/\Sigma A_{SCCP}$[1]	P1 (µg L^{-1})	P2 (µg L^{-1})	P3 (µg L^{-1})	P4 (µg L^{-1})	P5 (µg L^{-1})	P6 (µg L^{-1})
$C_{10}H_{18}Cl_4$	0.0000066	0.003	0.005	0.007	0.010	0.020	0.033
$C_{10}H_{17}Cl_5$	0.0034	1.7	2.5	3.4	5.1	10.1	16.9
$C_{10}H_{16}Cl_6$	0.021	10	16	21	31	62	104
$C_{10}H_{15}Cl_7$	0.030	15	22	30	44	89	148
$C_{10}H_{14}Cl_8$	0.013	7	10	13	20	40	66
$C_{10}H_{13}Cl_9$	0.0019	1.0	1.4	1.9	2.9	5.7	9.6
$C_{10}H_{12}Cl_{10}$	0.000032	0.02	0.02	0.03	0.05	0.10	0.16
$C_{11}H_{20}Cl_4$	0.000011	0.005	0.008	0.011	0.016	0.033	0.055
$C_{11}H_{19}Cl_5$	0.0061	3.0	4.6	6.1	9.1	18.3	30.5
$C_{11}H_{18}Cl_6$	0.044	22	33	44	66	132	220
$C_{11}H_{17}Cl_7$	0.15	76	114	152	228	455	759
$C_{11}H_{16}Cl_8$	0.11	56	84	112	168	335	559
$C_{11}H_{15}Cl_9$	0.032	16	24	32	48	96	160
$C_{11}H_{14}Cl_{10}$	0.0037	1.8	2.8	3.7	5.5	11.0	18.4
$C_{12}H_{22}Cl_4$	–	–	–	–	–	–	–
$C_{12}H_{21}Cl_5$	0.0016	0.80	1.20	1.60	2.40	4.79	7.99
$C_{12}H_{20}Cl_6$	0.027	14	21	27	41	82	137
$C_{12}H_{19}Cl_7$	0.11	54	81	109	163	326	543
$C_{12}H_{18}Cl_8$	0.13	67	100	133	200	400	667
$C_{12}H_{17}Cl_9$	0.070	35	52	70	104	209	348
$C_{12}H_{16}Cl_{10}$	0.014	6.8	10.2	13.6	20.3	40.7	67.8
$C_{13}H_{24}Cl_4$	–	–	–	–	–	–	–
$C_{13}H_{23}Cl_5$	0.00021	0.10	0.15	0.21	0.31	0.62	1.03
$C_{13}H_{22}Cl_6$	0.0064	3.2	4.8	6.4	9.6	19.2	31.9
$C_{13}H_{21}Cl_7$	0.041	20	30	41	61	122	203
$C_{13}H_{20}Cl_8$	0.086	43	64	86	129	258	430
$C_{13}H_{19}Cl_9$	0.073	36	54	73	109	218	363
$C_{13}H_{18}Cl_{10}$	0.022	11	16	22	33	65	109
ΣSCCP	1.00	500	750	1000	1500	3000	5000

[1]Calculated from [SCCP] of 3 mg L^{-1} (63% Cl formulation, n=3).

Table S5. Resolution required to avoid potential interferences from PCBs and organochlorine pesticides on the [M+Cl]⁻ ion monitoring of SCCPs.

Short-Chain Chlorinated Paraffin			Interference on the [M+Cl]⁻ adduct ion				
Homologue	[M+Cl]⁻ (m/z)	Isotope	Compound	Interfering Ion	Mass (m/z)	Isotope (Abund., %)	R_{min}
$C_{10}H_{16}Cl_6$	382.9048	M+2	CB80	[M–Cl+O]⁻	382.8173	M+10 (1.2)	4,380
$C_{10}H_{15}Cl_7$	418.8629	M+4	Dieldrin/Endrin	[M+Cl]⁻	418.8312	M+6 (11.5)	13,251
$C_{11}H_{20}Cl_4$	328.9984	M+2	α-HCH/γ-HCH	[M+Cl]⁻	328.8207	M+6 (51.5)	1,852
$C_{11}H_{19}Cl_5$	362.9594	M+2	2,4'-DDD/4,4'-DDD	[M+Cl]⁻	362.9083	M+10 (0.2)	7,102
$C_{12}H_{22}Cl_4$	343.0140	M+2	CB138/CB153	[M–Cl+O]⁻	342.8651	M+4 (59.2)	2,304
$C_{12}H_{21}Cl_5$	376.9750	M+2	CB180	[M–Cl+O]⁻	376.826	M+4 (86.2)	2,530
			C-Chlordene	[M+Cl]⁻	376.8205	M+6 (47.7)	2,440
$C_{12}H_{19}Cl_7$	446.8942	M+4	C-Chlordane/T-Chlordane	[M+Cl]⁻	446.7681	M+6 (74.0)	3,545
$C_{12}H_{18}Cl_8$	480.8552	M+4	T-Nonachlor	[M+Cl]⁻	480.7192	M+6 (88.2)	3,538
$C_{13}H_{24}Cl_4$	357.0297	M+2	2,4'-DDD/4,4'-DDD	[M+Cl]⁻	356.9173	M+4 (67.3)	3,177

Supporting Figures
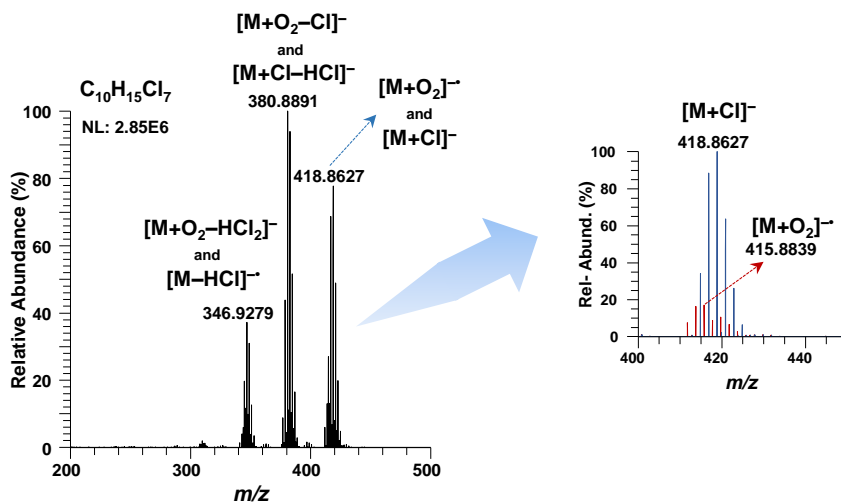
Figure S1. Mass spectrum of $C_{10}H_{15}Cl_7$ by GC-APPI-HRMS using toluene vapours as dopant.
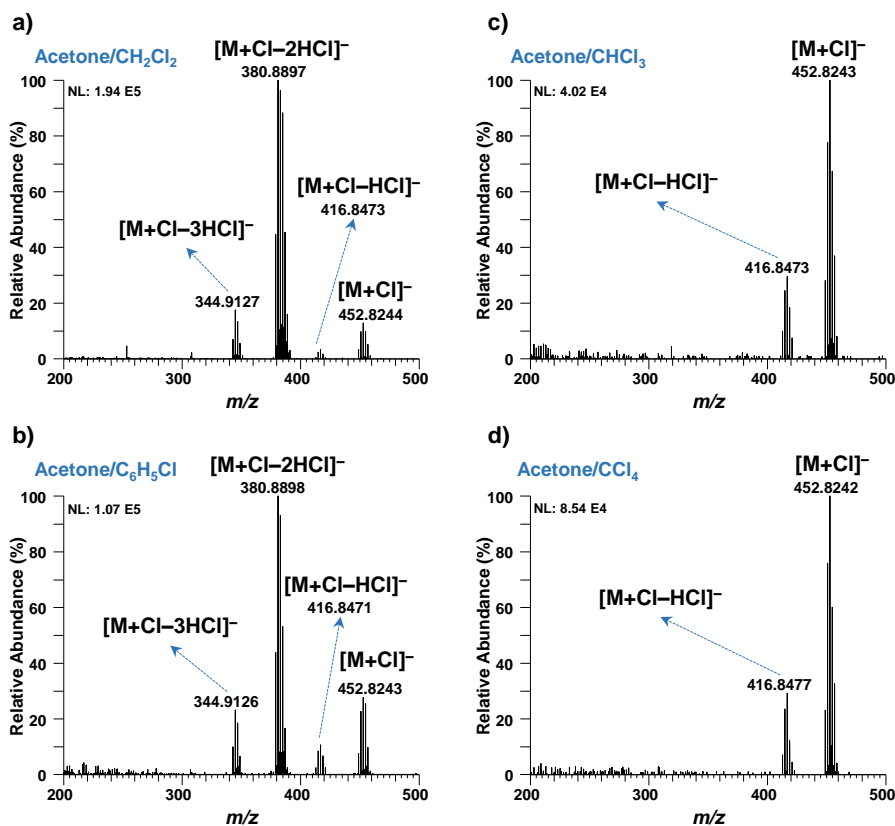
Figure S2. GC-APPI-HRMS mass spectra for a $C_{10}H_{14}Cl_8$ using acetone vapours mixed with a) dichloromethane, b) chlorobenzene, c) chloroform and d) carbon tetrachloride (3:1 *v/v*).
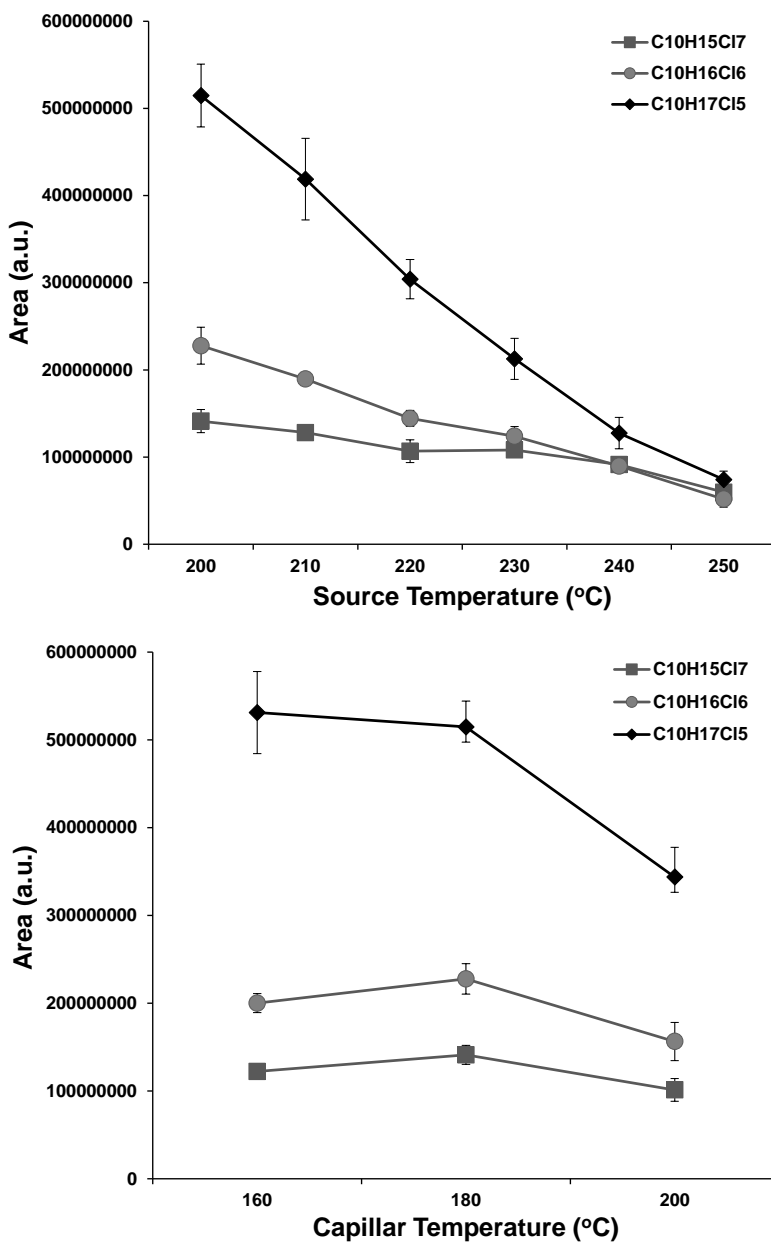
301

Figure S3. Effect of source (above) and capillary (down) temperatures on the chloride adduct ion abundance of peta-, hexa- and heptachlorodecanes.

3.3. Discussion of the results

This section includes the discussion of the results corresponding to the experimental works (*Article V, VI, VII, VIII, and IX*) described in this chapter. The discussion focuses on two main subjects: (i) new analytical methodologies for the determination of chlorinated organic contaminants, emphasizing the advantages for achieving a sensitive and selective determination of the different families of compounds in environmental samples, and (ii) effects of dopants on the ionization of halogenated organic contaminants by GC-APPI, studying the significant role of physicochemical properties in the ionization efficiency.

3.3.1. New analytical methodologies for the determination of chlorinated organic contaminants

As can be seen in Table 3.2, most of the common analytical determinations of chlorinated organic contaminants show some limitations in terms of chromatographic separation, ionization, or resolution/sensitivity of some mass analyzer, which might be faced by using new analytical trends, especially when dealing with very complex samples.

With regards to chromatographic separations, one-dimensional gas chromatography has limitations to separate very complex mixtures that contain a large number of compounds with similar chemical structures. For instance, in this Thesis the chromatographic separation of the complex mixture of PCNs using a single column has not been enough to achieve the complete congener-specific determination. Different authors have reported the use of comprehensive two-dimensional gas chromatography to improve the chromatographic separation of these compounds, although these methods required long analysis time. For instance, Hanari *et al.* [156] proposed a GCxGC-MS method (runtime: 3h 25min) using 14% cyanopropylphenyl/86% dimethyl polysiloxane (Rt-βDEXcst) as the first dimensional column and a a polyethylene glycol-based stationary phase (DB-WAX) as the second-dimensional column. Although the orthogonality of these stationary phases allows a good separation of PCNs (closely eluted) for tetra-, penta- and hexaCNs isomers, some difficulties may also arise due to the low maximum temperature allowed on the column, which requires a very slow temperature program to achieve the complete chromatographic separation of the analytes. *Article VI* deals with the evaluation of an ionic liquid (IL) stationary phase as a second dimension to improve the congener-specific determination of PCNs. The proposed IL-based column consists of a 1,12-di(tripropylphosphonium)dodecane bis(trifluoromethylsulfonyl)imide stationary phase ($[C_{12}(P_{333})_2]^+[NTf_2]^-$), which has exceptional physicochemical properties, such as negligible vapor pressure, high thermal stability, and high wetting capacity and viscosity, to be used as a chromatographic column for the separation of these compounds [369,370]. In addition, this IL-based column retains PCNs similarly to polyethylene glycol-based columns, like DB-WAX, but with better phase stability (lower column bleeding) and higher maximum temperature (ca. 50 ºC higher than DB-WAX). Thus, faster temperature programs can be carried out, achieving the separation of PCN congeners in only 2h 20min, as it can be observed in Fig. 2

of *Article VI*, which represents a decrease of 32% over the already reported GCxGC separation [156]. This GCxGC separation using the $([C_{12}(P_{333})_2]^+[NTf_2]^-$ stationary phase as second dimension column even allowed the separation of the most problematic tetra-, penta- and hexaCNs pairs. The characterization of Halowax formulations using this new column provided similar abundance profiles than those reported in the literature [156,371], which demonstrated the good performance of the GCxGC (DB-5MS/SLB-IL60)-MS method proposed in this Thesis. The separation of all PCN congeners may help on a better estimation of PCN relative potencies (RPs), especially those pairs of high toxicity that generally coelute like 1,2,3,4,6,7- and 1,2,3,5,6,7-hexaCNs (CN-66 and CN-67).

The determination of CPs is another analytical challenge from the chromatographic separation point of view. In this sense, the use of GCxGC can be a good alternative and it has already shown great potential in the separation of congeners of CPs [111,366,372]. However, this technique does not yet allow complete separation of all SCCP and MCCP congener groups. As mentioned in Section 1.2.1, the ion mobility-mass spectrometry (IM-MS) may be an interesting technique to improve the separation of small molecules, such as SCCPs and MCCPs. During the research stay at the Applied Analytical Chemistry group at the University of Duisburg-Essen, GCxGC (1st dimension: DB-5MS, 30 m x 0.25 mm; I.D. 0.25 μm; 2nd dimension: Rtx-17silMS, 2 m x 0.15 mm; I.D. 0.15 μm; modulator: double hot/cold jet modulator using liquid nitrogen) was coupled to a high-resolution mass spectrometer equipped with a drift tube as ion mobility cell, consisting of an Agilent 6560 Ion Mobility Q-TOF (Agilent Technologies) that used N_2 as drift gas. Additionally, this system used a GC-APPI source as an alternative ionization system to overcome some of the limitations observed when using μECD or NICI-MS [373]. The GCxGC-APPI-HRMS allowed a more selective detection of SCCP and MCCP congener groups from 4 to 12 chlorine atoms, although some of them still coelute being able to act as potential interferences. Thus, the addition of one more dimension through the use of ion mobility (GCxGC-APPI-IM-HRMS) was explored to increase the separation capacity to solve the remaining separation problems. Fig. 3.1a shows the separation of SCCPs and MCCPs (represented as the drift time *vs.* acquisition time) by monitoring [M+Cl]⁻ ions. Under these conditions, ion mobility did not provide an improvement over the separation of the analytes already achieved by GCxGC-APPI-HRMS. In fact, if we extract one frame of the IM separation (Fig. 3.1b), it can be observed that different congener groups have the same drift time, leading to a unique peak and, therefore, not improving peak capacity and separation from that achieved by GCxGC. Different strategies such as multiplexing were also tried, although any positive results were obtained due to the probable small differences in the CCS values between all congeners. Moreover, the labile [M+Cl]⁻ adduct ion was fragmented in some cases due to the collision of the molecules with the nitrogen drift gas, thus reducing the advantages of the GC-APPI source. Therefore, these results show that current IM-MS systems do not produce any improvement over GCxGC, and further advances in IM-MS technology are required to face the complete separation of SCCP
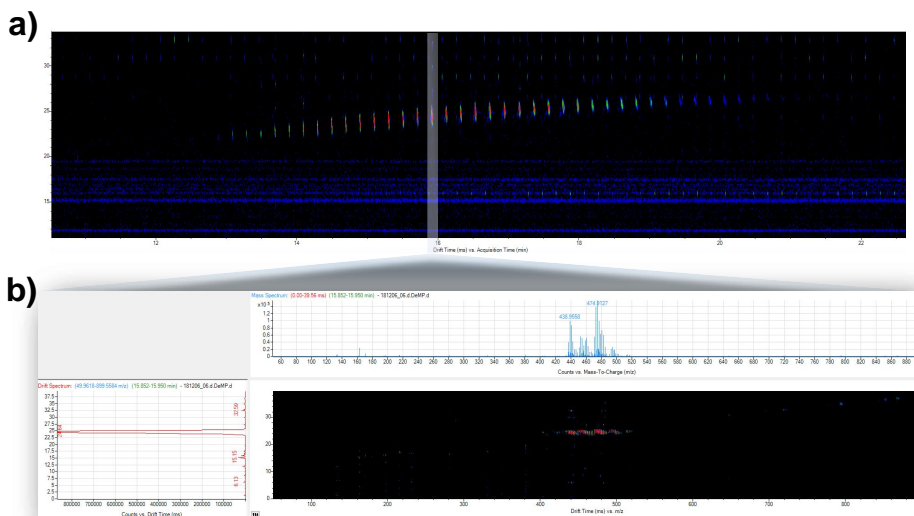
Fig. 3.1. GCxGC-APPI-IM-HRMS (QTOF) separation of SCCPs and MCCPs represented as a) drift time (IM) *vs.* acquisition time (GC) and b) drift time *vs. m/z* value in the frame 15.85-15.95 min.

and MCCP congener groups. However, the potential of GCxGC-APPI-HRMS could be assessed to avoid possible underestimation of the concentrations when using NICI [373].

Regarding the ionization, the feasibility of GC-API-HRMS, especially with the GC-APPI source, was assessed for several families of contaminants to provide a selective and sensitive determination. Table 3.3 summarizes the most relevant characteristics of the developed analytical determinations based on GC-APPI-HRMS for the analysis of PCDD/Fs, dl-PCBs, and PCNs. In general, negative ion GC-APPI provided the highest ionization efficiency through the phenoxide ion and other related ions. The formation of these ions was fully described in *Article VIII* (*Table 1*). Generally, the electrons released after the dopant photoionization process may interact with trace amounts of oxygen in the gas-phase to generate the superoxide ion. After that, this ion could interact with analyte molecules leading to the formation of the characteristic $[M–Cl+O]^-$ cluster ion as it has been shown in Fig 1.15b (*Chapter 1, Section 1.2.2*). These cluster ions could also be formed by electron capture of the neutral molecules and further interactions with the oxygen in the gas-phase [207]. Although phenoxide ions were the only peaks observed in the mass spectra for PCDFs, dl-PCBs, and PCNs, other ions were also detected for PCDDs depending on the number of chlorine atoms present in the molecule. Fig. 3.2 shows the tentative ion structures proposed for some ions generated for PCDDs using negative ion GC-APPI. As showed in *Article VIII* (*Fig.* 3), $[M–Cl+O_2]^-$ ion was the base peak of the 2,3,7,8-TCDD mass spectrum, whereas $[M–Cl+O]^-$ was the most abundant ion for PeCDDs and HxCDDs. In contrast, HpCDDs and OCDD mainly yielded the $[M–Cl]^-$ ion.

Table 3.3. Sample treatment and the main operational parameters of the GC-APPI-HRMS (Orbitrap) methods developed to determine PCDD/Fs, dl-PCBs and PCNs.

Parameter	PCDD/Fs	dl-PCBs	PCNs
Sample treatment			
Sample type	Fly ash, sludge, sediment, soybean meal, feed oil		Marine sediments
Sample amount	1-40 g		10 g
Extraction	Soxhlet *(24 h)*		Soxhlet *(24 h)*
Solvent	Toluene/cyclohexane *(1:1, v/v, 300 mL)*		Hexane/CH$_2$Cl$_2$ *(1:1, v/v, 300 mL)*
Clean-up Fractionation	Acidified silica gel column *(H$_2$SO$_4$, 44% w/w)* 1. Multilayer silica column 2. Basic alumina column *(F1: dl-PCBs)* *(F2: PCDD/Fs)* 3. Carbon column *(only for F2: PCDD/Fs)*		1. Activated Florisil column *(F1: 50 mL hexane, PCBs, rejected)* *(F2: 100 mL hexane/CH$_2$Cl$_2$, PCNs and SCCPs)* 2. SPE *(ENVI-Carb Plus)* *(F1: 50 mL hexane, SCCPs, rejected)* *(F2: 50 mL toluene, PCNs)[a]*
Surrogate IS	^{13}C$_{12}$-PCDD/Fs	^{13}C$_{12}$-dl-PCBs	–
Injection IS	^{13}C$_{12}$-PCDDs	^{13}C$_{12}$-PCBs	^{13}C$_{12}$-PCBs
Chromatography			
Injection volume	1.5 µL	1 µL	1 µL
Injection mode	Splitless *(1 min, 280 ºC)*	Splitless *(1 min, 280 ºC)*	Splitless *(1 min, 280 ºC)*
Column	DB-5MS UI *(60 m x 0.25 mm; 0.25 µm)*	DB-5MS UI *(60 m x 0.25 mm; 0.25 µm)*	DB-5MS UI *(30 m x 0.25 mm; 0.25 µm)*
Mobile phase	He *(1.0 mL min^{-1})*	He *(1.0 mL min^{-1})*	He *(1.0 mL min^{-1})*
Mass spectrometry			
Ionization source			
Polarity	Negative	Negative	Positive
Dopant	Benzene *(90 µL min^{-1})*	Diethyl ether *(90 µL min^{-1})*	Toluene *(70 µL min^{-1})*
Make-up gas	N$_2$ *(5 a.u.)*	N$_2$ *(5 a.u.)*	N$_2$ *(5 a.u.)*
S-Lens (%)	50	50	50
Source temp.	250 ºC	225 ºC	210 ºC
Capillary temp.	225 ºC	225 ºC	210 ºC
Mass Analyzer			
Resolution	70,000 FWHM	70,000 FWHM	35,000 FWHM
Acquisition	Full scan *(100-600 m/z)*	Full scan *(100-600 m/z)*	Full scan *(100-600 m/z)*
Monitored ions	[M–Cl+O$_2$]$^-$/ [M–Cl+O]$^-$/ [M–Cl]$^-$	[M–Cl+O]$^-$	[M]$^{+\bullet}$

[a] Backflushed.

Differences in the nature of the ions observed for this family of compounds could be related to both steric hindrance and the repulsion effect of chlorine atoms in the molecule. While TCCD is less affected by these effects, allowing the attachment of the superoxide moiety, PeCDDs and HxCDDs only may stabilize one oxygen atom in their chemical structure. In the case of HpCDDs and OCDD, the significant steric hindrance and repulsion can make the interaction with oxygen atoms difficult, and, therefore, the molecule is better stabilized by the loss of one chlorine atom. As mentioned above, this clear influence of the number of chlorine atoms in the
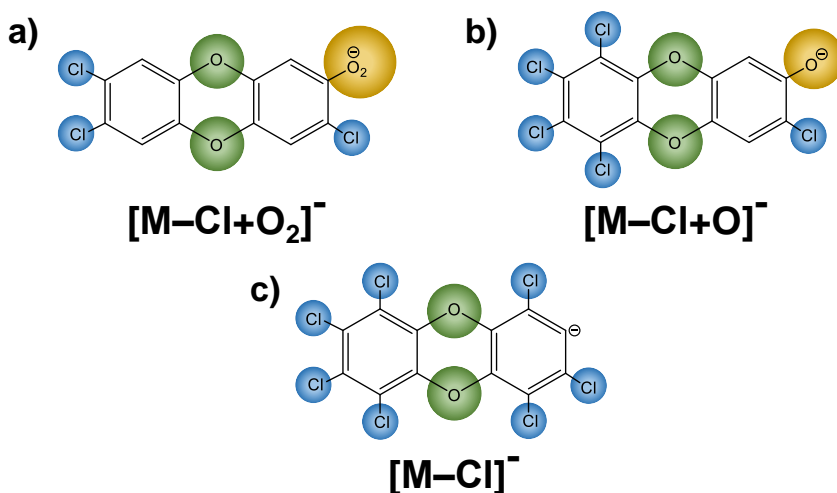
a) $[M-Cl+O_2]^-$

b) $[M-Cl+O]^-$

c) $[M-Cl]^-$

Fig. 3.2. Tentative structures of the ions generated for a) 2,3,7,8-TCDD, b) 1,2,3,4,7,8-HxCDD, and c) OCDD in negative ion GC-APPI.

ionization is completely different from that observed with other planar related compounds (PCDFs, dl-PCBs, and PCNs). The lower number of oxygen atoms in the structure (one for PCDFs, and none for dl-PCBs and PCNs) may reduce both the steric hindrance and the repulsion effect, thus promoting the formation of the phenoxide ion. Negative ion APPI provided a high ionization efficiency of compounds with more than 3 chlorine atoms. However, mono- and diCNs showed poor responses under the same conditions. The low number of chlorine atoms in the structure may reduce the electronegativity of the molecule, decreasing the tendency to eliminate a chlorine atom and, thereby, hampering the formation of the phenoxide ion. In contrast, PCNs also showed a high ionization efficiency for all the PCN congener groups working in positive ion GC-APPI and GC-APCI through the molecular ion formation (*Article VII, Fig. 1*).

APPI ionization is generally assisted by dopants such as toluene, chlorobenzene, anisole, tetrahydrofuran or acetone. However, low vapor pressure (VP) could lead to solvent condensation problems, thus reducing the concentration of these dopants in the gas-phase. For instance, the use of anisole, which has a low vapor pressure (VP: 4.2 Torr, 25 ºC), provided the lowest ionization efficiency of PCNs by negative ion GC-APPI (*Article VII, Fig. 2*). Additionally, this low vapor pressure leads to a longer residence time of the dopant in the GC-APPI ion source, which negatively affects the throughput of this technique since it requires a more exhaustive cleaning of the ion source. In contrast to anisole, other organic solvents with high vapor pressures and ionization energies (IE) lower than 10.6 eV have been evaluated as alternative dopants. In this Thesis, diethyl ether (IE: 9.53, VP: 440 Torr, 25 ºC) and benzene (IE: 9.24, VP: 75 Torr, 25 ºC) have been proposed for the first time as APPI dopants. Generally, the nature of the ions present in the mass spectra of the target compounds did not depend on the dopant vapor used in GC-APPI negative ion mode since the ionization is mediated by the

electrons released during the dopant photoionization process. Among the dopants tested, diethyl ether frequently provided the best ionization efficiency for most of PCDD/Fs, dl-PCBs, and PCNs. The high vapor pressure of this solvent may lead to higher dopant concentration in the gas-phase, increasing the number of electrons released after the dopant photoionization process and, thereby, promoting further gas-phase reactions to ionize the analytes. However, the dopant ionization energy also affects the ionization efficiency of the analytes. For instance, TCDD ionizes more efficiently using benzene as dopant, even though diethyl ether has a higher vapor pressure. Nevertheless, if we compared the TCDD mass spectra using both dopants (*Article VIII, Fig.3a (benzene) and Fig. S1a (diethyl ether)*), it could be deduced that diethyl ether favored the in-source fragmentation of this compound. This fact can be due to the higher ionization energy of diethyl ether, which might release more energetic electrons, thus inducing the in-source fragmentation and decreasing the response of the analyte. Concerning PCNs, these compounds could be ionized in positive ion GC-APPI by direct photoionization or charge-exchange reactions with dopants such as chlorobenzene or toluene. Among them, toluene provided the highest responses, probably due to its higher vapor pressure.

Another parameter that must be carefully considered is the ion source temperature. As reported in *Article VIII* (*Fig. 4*), the application of low ion sources temperatures (180-200 ºC) produced a significant peak broadening, worsening the chromatographic separation of these compounds, especially PCDD/Fs. This fact could be associated with the ion source design or even with the vapor pressure of the analytes. While the vapor pressure of dl-PCBs and PCNs ranged from $4.77 \cdot 10^{-5}$-0.002 Pa and $1.5 \cdot 10^{-6}$-0.352 Pa, respectively, PCDD/Fs show a lower vapor pressure ($6.61 \cdot 10^{-8}$ to $1.15 \cdot 10^{-5}$ Pa), which make them more vulnerable to this effect, requiring high ion source temperatures (250 ºC).

All cluster ions generated in negative ion APPI for dioxin-like compounds showed very high abundances and, therefore, they could be used to propose very sensitive and selective GC-APPI-HRMS methods. For instance, the method proposed for the determination of dl-PCBs using diethyl ether as dopant achieved very low iLODs ranging from 0.5 to 10 fg injected on column. These limits of detection are 2.5 to 50 times lower than those reported in the literature using a GC-APCI-MS/MS method [149]. Furthermore, these iLODs were quite similar and even lower for some specific dl-PCBs than those obtained using the traditional and confirmatory GC-EI-HRMS (magnetic sectors) method [139]. Contrarily to dl-PCBs, in the determination of PCDD/Fs, the best results were obtained when using benzene as dopant, which allowed us to achieve a lower iLOD for the most toxic TCDD (25 fg injected on column). The detection capability of the method proposed in this Thesis for PCDD/Fs (iLODs: 0.5-25 fg injected on column) was comparable to that of the GC-EI-HRMS method, being up to 60-fold and 75-fold lower than those obtained when using double-focusing magnetic sectors and Orbitrap [190] mass analyzers, respectively. Additionally, iLODs were in the same order than those obtained by GC-APCI-MS/MS except for TCDD (25-fold higher) [148,191,192], although the detection capability of this compound is good enough to achieve their determination in real

samples. In the case of PCNs, negative ion GC-APPI achieved exceptionally low iLODs for tri- to octaCN (10-150 fg injected on column). However, as mentioned above, mono- and diCNs showed a very low ionization efficiency, achieving iLODs ranging from 8 to 45 pg injected. In contrast, when GC-APPI operated in positive ion mode (dopant: toluene), the iLODs obtained for PCN congener groups ranged from 20-150 fg injected on column. The detection capability of the GC-APPI-HRMS method was again similar to those reported by GC-EI-HRMS (magnetic sectors) [196] and up to 150 times better than those obtained using the GC-APCI-HRMS (QTOF) (*Article VII,Table 2*).

The suitability of the GC-APPI source was also tested for DP and analogs, and SCCPs. Table 3.4 shows the most relevant characteristics of the developed analytical determinations based on GC-APPI-HRMS for the analysis of these compounds. In contrast to PCDD/Fs, dl-PCBs, and PCNs, the ionization of SCCPs and DP was only possible in negative ion APPI mode. Concerning DP and analogs, the monitored ions under the optimal conditions consisted of the molecular ions, cluster ions such as $[M–2HCl–Cl+O_2]^-$ and $[M–HCl–3Cl+O_2]^-$ and fragment ions like $[M−HCl−Br]^-$ or even the characteristic $[C_5Cl_5]^-$ ion coming from the retro-Diels Alder fragmentation of these compounds (*Article V, Fig. 2*). Furthermore, the use of diethyl ether as dopant achieved the highest ionization efficiency, as occurred for most of PCDD/Fs, dl-PCBs, and PCNs. These ions resulted from the thermal degradation of the molecular, cluster, or adduct ions like $[M–Cl+O]^-$ or $[M+O_2]^{-\bullet}$ since they were the most abundant ions of the mass spectra when decreasing the ion source temperature up to 180 °C. However, as it was observed for PCDD/Fs, the low vapor pressure of DP ($8.47·10^{-8}$ to $1.59·10^{-7}$ Pa) negatively affected the chromatographic resolution causing post-column peak broadening (*Article V, Fig. 3*). Thereby, as a compromise between chromatographic efficiency and ion intensity, but also taking into account the selectivity provided by the Orbitrap mass analyzer, the ion source temperature was finally fixed at 250 °C. This implies an important advantage over GC-NICI-MS methods, for which the required low temperature in the ion source (ca. 150-170 °C) makes necessary a more frequent cleaning of the system, reducing laboratory throughput.

Regarding SCCPs, the dopant-assisted photoionization led to a complex mass spectra consisting of ions coming from the in-source fragmentation of both $[M+Cl]^-$ and $[M+O_2]^{-\bullet}$ adduct ions. As happens for PCDD/Fs, highly chlorinated SCCPs ($>Cl_8$) also hindered the attachment of the superoxide moiety and only in-source fragment ions from the chloride adduct ion appeared in the mass spectra (*Article IX, Fig. 1*). Moreover, among the dopant tested, acetone provided the highest ionization efficiency of SCCPs, probably due to its high vapor pressure. Recently, Bogdal *et al.* [176] proposed the addition of dichloromethane to selectively form the chloride adduct ion by APCI-HRMS (QTOF). In this Thesis, this strategy was used for the ionization of SCCPs by GC-APPI by mixing the dopant with different chlorination agents (chlorobenzene, CH_2Cl_2, $CHCl_3$, and CCl_4). A mixture of acetone/CCl_4 (3:1, *v/v*) provided the best chloride-enhanced conditions, which hindered the formation of superoxide-related ions and promoted the formation of chloride adduct ion for all SCCP.

Table 3.4. Sample treatment and main operational parameters of the GC-APPI-HRMS (Orbitrap) methods developed to determine SCCPs, DP and analogs.

Parameter	SCCPs	DP and Analogs
Sample treatment		
Sample type	Fish	Gull eggs
Sample amount	1 g (lyophilized)	1 g (lyophilized)
Extraction	sPLE *(acidified silica, H_2SO_4, 44% w/w)* *(3 x 5 min, 100 ºC, 1500 psi, 60% flush vol.)*	sPLE *(acidified silica, H_2SO_4, 44% w/w)* *(3 x 5 min, 100 ºC, 1500 psi, 60% flush vol.)*
Solvent	Hexane/CH_2Cl_2 *(1:1, v/v)*	Hexane/CH_2Cl_2 *(1:1, v/v)*
Fractionation	Activated Florisil column *(F1: 30 mL hexane and 80 mL hexane/CH_2Cl_2 (95:5, v/v), PBDEs and PCBs)* *(F2: 30 mL hexane/CH_2Cl_2 (1:1, v/v), SCCPs)*	Activated Florisil column *(30 mL hexane and 80 mL hexane/CH_2Cl_2 (95:5, v/v), DP, PBDEs and PCBs)*
Surrogate IS	δ-HCH	$^{13}C_{12}$-BDE 77/ $^{13}C_{12}$-BDE 138
Injection IS	$^{13}C_6$-HCB	CB-209
Chromatography		
Injection volume	1 µL	1 µL
Injection mode	Splitless *(1 min, 280 ºC)*	Splitless *(1 min, 280 ºC)*
Column	TG-5MS *(15 m x 0.25 mm; 0.25 µm)*	TG-5MS *(15 m x 0.25 mm; 0.25 µm)*
Mobile phase	He *(1.0 mL min^{-1})*	He *(1.2 mL min^{-1})*
Mass spectrometry		
Ionization source		
Polarity	Negative	Negative
Dopant	Acetone/CCl_4 *(3:1, v/v)*[a] *(70 µL min^{-1})*	Diethyl ether *(70 µL min^{-1})*
Make-up gas	N_2 *(5 a.u.)*	N_2 *(5 a.u.)*
S-Lens (%)	20	50
Source temp.	200 ºC	250 ºC
Capillary temp.	225 ºC	180 ºC
Mass Analyzer		
Resolution	70,000 FWHM	35,000 FWHM
Acquisition	Full scan *(60-700 m/z)*	Full scan *(70-700 m/z)*
Monitored ions	$[M+Cl]^-$	$[M]^{-\bullet}$/ $[M-2HCl-Cl+O_2]^-$/ $[C_5Cl_5]^-$/ $[M-HCl-3Cl+O_2]^-$/ $[M-HCl-Br]^-$

[a] Dopant/chlorinated agent mixture.

As an example, Fig. 3.3 shows the GC-APPI mass spectrum for the $C_{10}H_{15}Cl_7$ isomer, where the chloride adduct is the base peak. It is important to highlight that the use of $CHCl_3$ and CCl_4 as chlorination agents enhanced the response of the $[M+Cl]^-$ ion (*Article IX, Fig. S2*), which may be due to the enrichment of chloride ions in the gas-phase. Yuan *et al.* [177] indicated that under chloride-enhanced conditions and using a APCI source and a mass analyzer with a resolution of 10,000 FWHM, the chloride adduct ion of each homologue group could be only interfered by $[M+Cl–HCl]^-$ fragment ion.
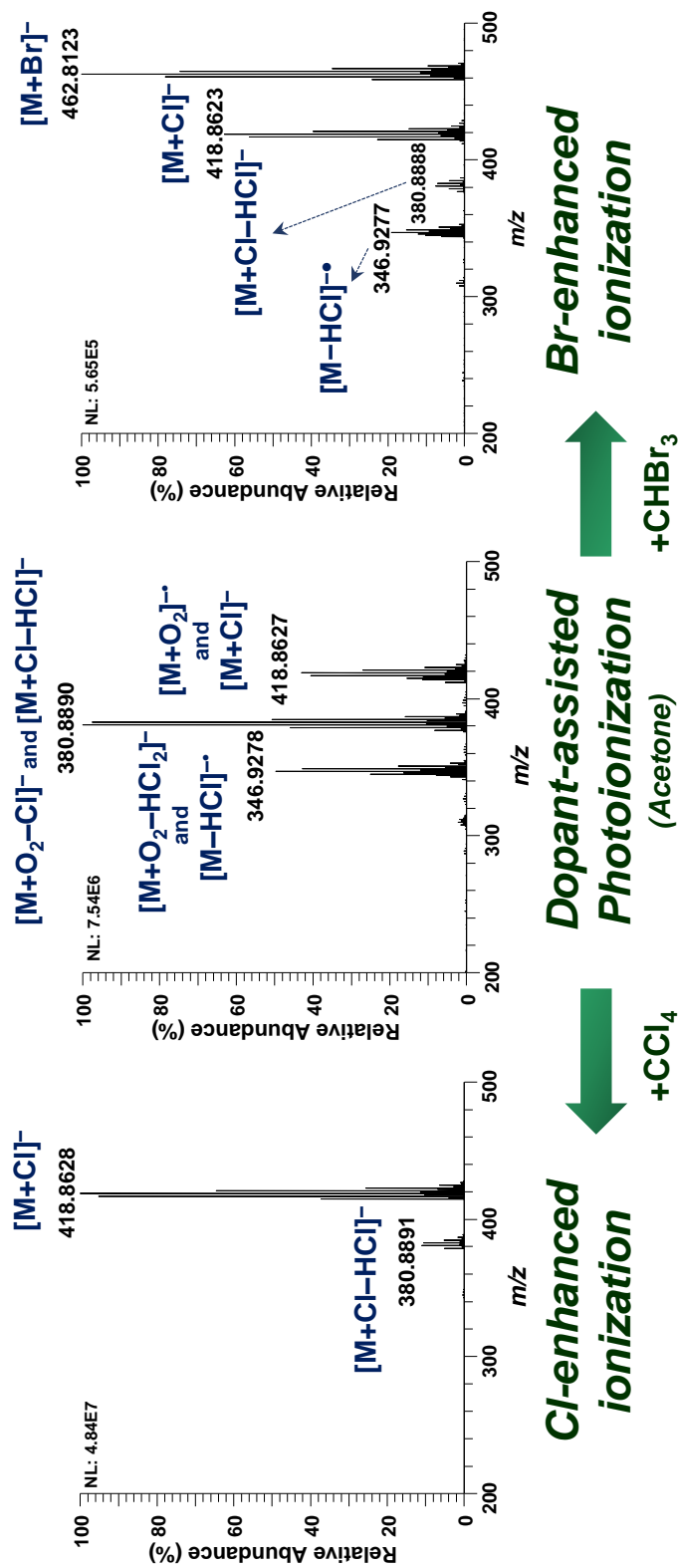
Fig. 3.3. GC-APPI-HRMS mass spectra of 1,2,4,5,6,9,10-heptachlorodecane obtained through chloride-enhanced ionization (acetone/CCl₄, 3:1 *v/v*, *left*), dopant-assisted photoionization (acetone, *center*), and bromide-enhanced ionization (acetone/CHBr₃, 3:1 *v/v*, *right*).

311

Hence, the accurate determination of individual C_nCl_m congener groups requires a time-consuming deconvolution approach to resolve these interferences. However, a resolution higher than 50,000 FWHM would allow the mass spectrometric separation of these ions, as reported by Li *et al.* (Li 2018). Therefore, in this Thesis, the Orbitrap was operated at a resolution of 70,000 FWHM (at *m/z* 200) to separate the interferent ions and to avoid the application of the deconvolution approach. Yuan *et al.* [179] also proposed the addition of bromoform instead of the chlorination agents to promote only the formation of the [M+Br]⁻ ion in the APCI source. This strategy was also considered in this Thesis for the ionization of SCCPs by GC-APPI. However, the mass spectra obtained when using a mixture of acetone/bromoform (3:1 *v/v*) consisted of a mixture of both chloride and bromide adduct ions (Fig. 3.3). Moreover, the response of the analytes significantly decreased, probably due to both the multiple ion species for one analyte and the low vapor pressure of bromoform (5 Torr, 25 ℃) that led to condensation problems similar to those observed when using anisole as dopant.

In contrast to the other families of chlorinated organic contaminants, the chloride adduct ion may be generated through a labile interaction between the molecule and the chlorine ion. Thereby, low ion source temperatures (ca. 180 ℃) are highly recommended to promote their efficient formation. The way the dopant/chlorination agent mixture is introduced also affects the ionization efficiency of SCCPs. For instance, Fig. 3.4 shows the effect over the response of C_{10}-SCCPs when adding this mixture *via* an uncapped vial (Fig. 3.4a) or a nitrogen make-up gas flow doped with the acetone/CCl_4 (3:1 *v/v*) mixture (Fig. 3.4b). These experiments were carried out using a 6890N Network GC system gas chromatograph coupled to a 6495 Triple Quad LC/MS mass spectrometer, equipped with an APPI source (Agilent Technologies, CA, USA). The use of a doped nitrogen make-up gas flow in the GC-APPI source supplies a constant flow of the dopant/chlorination agent mixture, ensuring the constant presence of chlorine atoms in the ion source. In contrast, the use of an uncapped vial may provide an uncontrolled flow of the dopant mixture, which is limited by the vial volume and the volatility of the dopant mixture, making the ionization less reproducible. Regarding the ionization efficiency, the results showed in Fig. 3.4c demonstrate that the use of a N_2 make-up gas flow doped with acetone/CCl_4 vapors improved the ionization of SCCPs. This system could be proposed as an alternative to the infusion syringe (10 mL) recommended by the manufacturer (MasCom) of the GC-APPI source. Although the infusion syringe device provides a constant flow of dopant vapors, it does not allow the continuous work, being necessary to refill the syringe every 3 hours.

The detection capability of the GC-APPI-HRMS methods was also evaluated for the determination of DP and analogs, and SCCPs. For instance, iLODs achieved for the determination of DP and analogs (6-150 fg injected on column) were similar or even slightly better than those achieved by GC-EI-HRMS and GC-NICI-MS/MS [145,374].
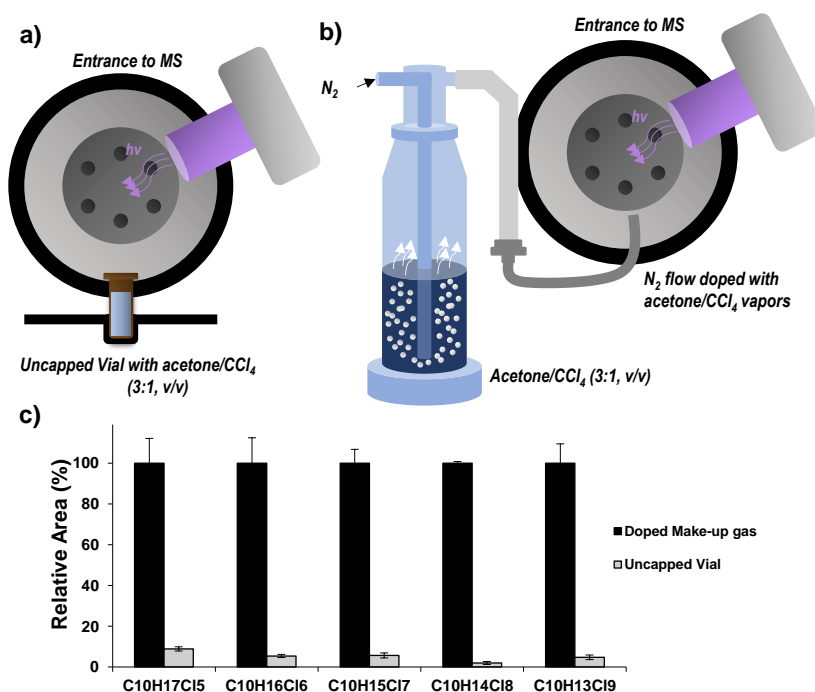
Fig. 3.4. Addition of dopant/chlorinated agent mixture (acetone/CCl₄, *v/v*) *via* a) an uncapped vial or b) a doped N₂ make-up gas flow and c) the effect of the dopant/chlorinated agent mixture addition over the response of C_{10}-SCCPs.

Additionally, the method also provided iLODs at least 5 times lower than those obtained by Megson *et al.* using the GC-APCI-HRMS (TOF) [186]. Regarding SCCPs, the chloride-enhanced GC-APPI-HRMS achieved the lowest iLODs for both the total SCCP content and the concentrations of the CP congener groups. Regarding the detection of the total SCCP, the iLOD was 1-2 pg injected on the column (injection volume: 1 µL) based on the measurement of the sum of congeners in each technical SCCP formulation. This value was from 50 to 600 times lower than those obtained by APCI-HRMS (100-1200 pg µL⁻¹) [176] and at least 7.5 times lower than those reported by LC-ESI-HRMS (15-20 pg µL⁻¹) [155] using the chloride-attachment ionization. In fact, they were even 12 times lower than the iLODs achieved by GC-NICI-HRMS (24-81 pg µL⁻¹) [174]. With regards to the iLODs for each homologue group of congeners, the iLODs (0.07-0.19 pg) were quite lower than those reported using bromide-attachment APCI-HRMS (0.1-160 pg µL⁻¹) [179] or both chloride-attachment APCI-HRMS (0.2-100 pg µL⁻¹) [178] and LC-ESI-HRMS (0.75-11.8 pg µL⁻¹) [155], or even lower than those achieved by GC-NICI-HRMS (Orbitrap) (0.03-2.02 pg µL⁻¹) [147]. These results, together with those achieved for PCDD/Fs, dl-PCBs, and PCNs, clearly demonstrated the high potential of the GC-APPI-HRMS system to determine chlorinated organic contaminants at very low concentration levels.

Another critical parameter on the determination of these families of pollutants is the quantification, which was carried out according to the general comments and recommendations included in Section 1.2.1 (*quantification methods*). Regarding PCDD/Fs and dl-PCBs, the quantification was carried out by isotope dilution, whereas PCNs, SCCPs, and DP with its analogs were quantified using the internal standard method. Nonetheless, quantification is, by far, one of the most significant challenges in the analytical determination of SCCPs. Since the NICI response of these analytes is strongly affected by the number of chlorine atoms in the molecule, quantitation requires approaches like Reth's method to overcome possible errors and over/underestimations [206]. This effect was taken into account in the determination of these compounds when using the chloride-attachment GC-APPI-HRMS method. It was observed that, in contrast to NICI, the response of C_{10}-SCCPs by GC-APPI-HRMS was less affected by the number of chlorine atoms, achieving response factors relative to $C_{10}H_{17}Cl_5$ close to 1 (*Article VIII, Fig. 3*). These relatively small variations on the congener response could be related to the position in the molecule of chlorine substituents and allowed us to conclude that the GC-APPI responses of each $C_nH_{2n+2-m}Cl_m$ congener group mainly depend on its concentration. Based on this hypothesis, *Article IX* describes a simple internal normalization approach to quantify SCCPs easily. Briefly, if we consider that the response is only affected by the concentration, the total contribution of each $C_nH_{2n+2-m}Cl_m$ homologue group to the whole area must be proportional to their contribution to the total concentration. Another advantage is that each homologue group, independently of the CP technical formulations used (51.5, 55.5 or 63% Cl), may have a common calibration curve. This implies that we do not need to know the homologue distribution and the total chlorine content of the sample before its analysis and we could achieve the quantification of all the samples using just one SCCP standard mixture that contains all the congener groups with different carbon chain lengths and chlorination degree. This quantification approach provides a significant reduction of time in both analysis and data processing.

The developed GC-APPI-HRMS methods and the most adequate sample treatment (Table 3.3 and 3.4) were applied to the analysis of halogenated organic contaminants in samples of environmental interest. Regarding PCDD/Fs and dl-PCBs, the figures of merits of both methods were investigated fulfilling all the requirements of the current EU regulations 2017/664 and 2017/771. These methods were compared with the traditional GC-EI-HRMS (magnetic sectors) method through the analysis of certified reference materials and reference samples used in several interlaboratory exercises of both environmental and feed interest. The results from both methodologies were similar in terms of analyte concentrations and WHO-TEQ values (accuracy and precision), demonstrating their excellent applicability to the analysis of PCDD/Fs and dl-PCBs, being reliable alternatives to the confirmatory method. Additionally, the use of an Orbitrap instead of traditional mass analyzers such as double-focusing magnetic sector or triple quadrupole, allowed the possibility of operating in a highly selective and sensitive full-scan acquisition mode. This fact could be useful not only for targeted analysis but also to overcome possible interferences from complex matrices. As an example, *Article VII*

describes the capabilities of the GC-APPI-HRMS to determine the total concentrations of PCNs in marine sediments. In this work, the analysis of some sediment samples showed the suppression of the ionization of penta- to octaCN when operating in positive GC-APPI ion mode. The rich information provided by the full-scan acquisition allowed us to detect a broad hump at the same retention times of the penta- to octaCN elution, which was identified as a heavy fraction of hydrocarbons (*Article VII, Fig. 4*). The presence of these interferences would require a more exhaustive clean-up of the extract to remove them if the samples are analyzed by GC-EI-MS. In contrast, the possibility of operating in both positive and negative ion mode with the GC-APPI-HRMS system, provided an easy solution to overcome these interferences. Since the highly chlorinated PCNs were the most affected analytes by the matrix, the sample extract was re-injected in GC-APPI negative ion mode. These groups of congeners showed a remarkably high ionization efficiency in this ion mode, while the hydrocarbons were not ionized under these conditions, so they did not affect the ionization efficiency of the coeluting compounds, allowing the correct quantification of these groups of congeners. As demonstrated, with this strategy, it is possible to continue using simple sample treatments while providing reliable quantitative results and improving the laboratory throughput.

Furthermore, the valuable information provided by the GC-APPI-HRMS system can be also used for the retrospective screening of suspect or unknow contaminants that could be present in these samples. Indeed, the characteristic isotopic cluster of halogenated compounds (chlorinated and brominated) and the sensitive high-resolution full-scan acquisition mode of the Orbitrap mass analyzer represent a huge advantage for non-targeted analysis. For instance, Fig. 3.5 shows the tentative identification of some suspect chlorinated pollutants in yellow-legged gull egg samples collected from the Delta Ebro natural park. Using a flagging approach that searched for the phenoxide ion, it was possible to tentatively identify the presence in the extract of tetra- to nona-CBs, as well as the hexachlorobenzene. This information is complementary to levels already reported for DP and analogs in these biota samples. Thereby, the high sensitivity of the GC-APPI to ionize halogenated compounds combined with the capabilities of Orbitrap to carry out non-targeted strategies could provide a particularly useful tool for the screening of known or unknown pollutants in environmental samples, while determining targeted compounds. Therefore, it is possible to have a more extensive estimation of the whole contamination of a given sample.

3.3.2. Effect of dopants on the ionization of chlorinated organic contaminants by GC-APPI

Nowadays, the main applications reporting GC-APPI-based methods are related to the evaluation of the ionization of selected families of compounds from a more quantitative point of view. However, few works have attempted to go into deep on the GC-APPI ionization mechanisms. Some of these studies are those of Kauppila *et al.* [238,241]*,* who proposed the
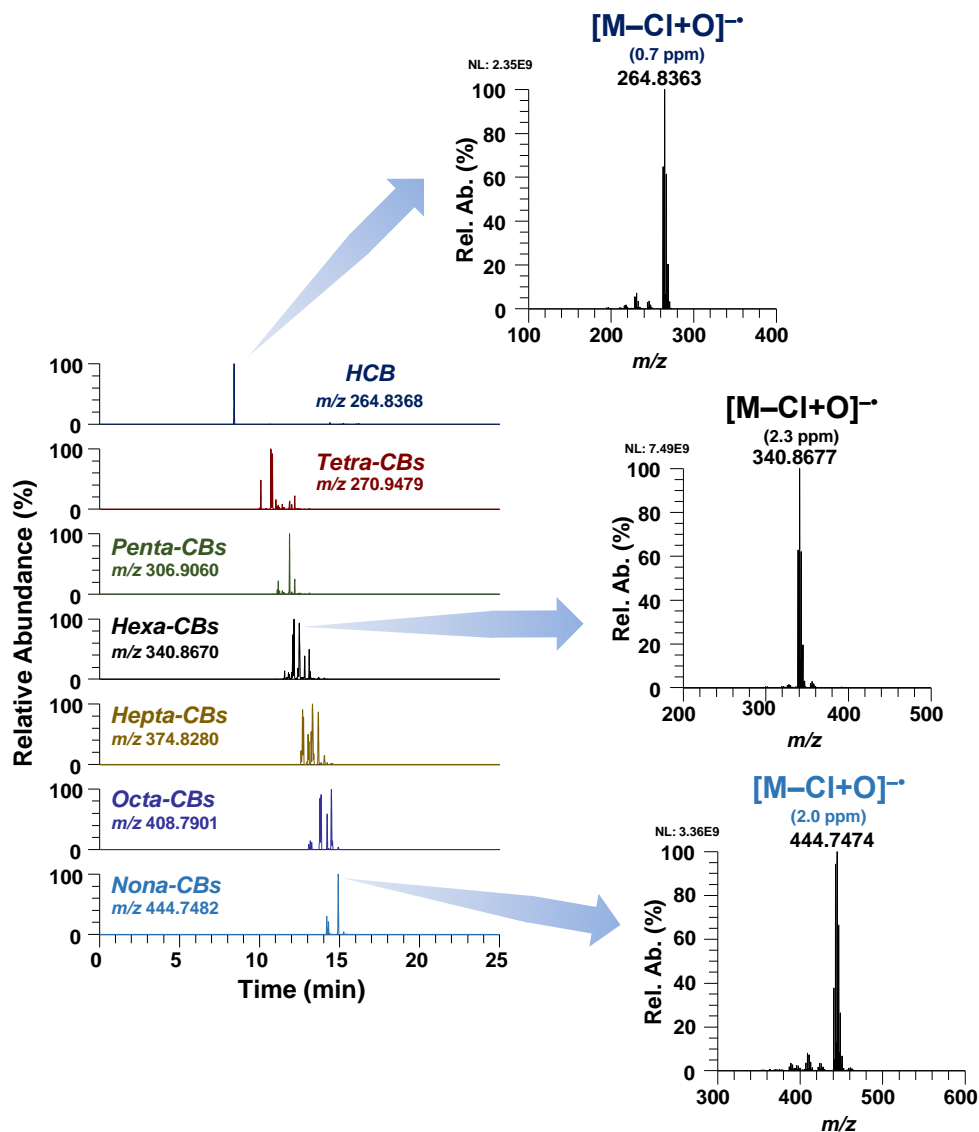
Fig. 3.5. Screening of suspect chlorinated organic contaminants in a yellow-legged gull egg sample (*L. Michahellis)* collected from the Ebro Delta natural park.

use of selected model compounds and traditional dopants (acetone, toluene, chlorobenzene, and anisole) to study the GC-APPI mechanism in positive ion mode. However, they only included a few halogenated compounds. In this Thesis we have demonstrated the potential of the GC-APPI technique to efficiently ionize chlorinated organic compounds and have shown that the ionization behavior was quite similar for the chlorinated organic compounds studied (*Sections 3.2 and 3.3.1*). Therefore, this section focuses on the most remarkable considerations and trends in the dopant-assisted GC-APPI ionization of chlorinated organic compounds.

Firstly, it must be considered that the design of the GC-APPI source consisted of an enclosed atmospheric pressure system where we can only introduce the column eluate (helium and analytes), the make-up gas (high purity nitrogen) and dopant vapors. Therefore, this implies the ionization will mainly depend on the analyte capabilities to be photoionized or to interact with the dopant and reactive air components (mainly oxygen). Moreover, the absence of reactive mobile phase in the system simplifies the main APPI ionization mechanisms. The main GC-APPI ionization mechanisms are summarized in Table 3.5.

Table 3.5. Main ionization mechanism by GC-APPI.

Reaction	Condition	Process
Positive ion GC-APPI		
(1) $M + hv \rightarrow M^{+\bullet} + e^{-\bullet}$	IE^a (M) < 10.6 eV	Direct photoionization reaction
(2) $M + M^{+\bullet} \rightarrow [M+H]^+ + [M–H]^\bullet$	PA^b (M) > PA ([M–H]$^\bullet$)	Analyte self-protonation reaction
(3) $D + hv \rightarrow D^{+\bullet} + e^{-\bullet}$	IE (D) < 10.6 eV	Dopant photoionization reaction
(4) $D + D^{+\bullet} \rightarrow [D+H]^+ + [D–H]^\bullet$	PA (D) > PA ([D–H]$^\bullet$)	Dopant self-protonation reaction
(5) $D^{+\bullet} + M \rightarrow M^{+\bullet} + D$	IE (M) < IE (D)	Charge exchange reaction
(6) $D^{+\bullet} + M \rightarrow [M+H]^+ + [D–H]^\bullet$	PA (M) > PA ([D–H]$^\bullet$)	Proton transfer reaction
Negative ion GC-APPI		
(7) $M + e^{-\bullet} \rightarrow M^{-\bullet}$	High EA^c (M)	Electron capture reaction
(8) $O_2 + e^{-\bullet} \rightarrow O_2^{-\bullet}$	High EA (O$_2$)	Superoxide formation
(9) $M + O_2^{-\bullet} \rightarrow M^{-\bullet} + O_2$	EA (M) > EA (O$_2$)	Charge exchange reaction
(10) $M + O_2^{-\bullet} \rightarrow [M–H]^- + [HO_2]^\bullet$	PA (M) > PA ([HO$_2$]$^\bullet$)	Proton transfer reaction
(11) $M + O_2^{-\bullet} \rightarrow [M+O_2]^{-\bullet}$	High EA and adduct tendency	Clustering reaction
(12) $M + O_2^{-\bullet} \rightarrow [M–X+O]^{-\bullet} + OX^\bullet$	High EA and aromaticity	Clustering reaction
(13) $M^{-\bullet} + O_2 \rightarrow [M–X+O]^{-\bullet} + OX^\bullet$	High EA and aromaticity	Clustering reaction

[a] IE: Ionization energy, [b] PA: Proton affinity, [c] EA: Electron affinity.

The dopants tested (Fig 3.6) can be classified in two different groups: (i) dopants that generate the molecular ion such as anisole, chlorobenzene, toluene, and benzene (Fig. 3.6a-d), and (ii) dopants that yield the [D+H]$^+$ as the base peak of their mass spectra such as tetrahydrofuran, acetone, and diethyl ether (Fig. 3.6e-g). The different photoionization behavior can be explained based on the dopant proton affinity (PA) (Table 3.6). Acetone, diethyl ether, and tetrahydrofuran have functional groups that are proton acceptor and they show the highest proton affinities. Consequently, the self-protonation of the dopant (Table 3.5, eq. 4) can take place after the dopant photoionization process (Table 3.5, eq. 3). In contrast, the absence of proton acceptors functional groups in the structure of the other dopants (lower PA) hinders this process. Regarding the ionization of these analytes in positive ion mode, only dioxin-like compounds (PCDD/Fs, dl-PCBs and PCNs) were ionized through the formation of the molecular ion as reported in *Article VII (Fig. 1) and Article VIII (Fig. 1)*. Although these compounds may show an IE low enough for their direct photoionization (Table 3.5, eq. 1), this ionization mechanism was not quite efficient. In contrast, the ionization efficiency for these compounds increased when using the dopant-assisted photoionization with dopant vapors that
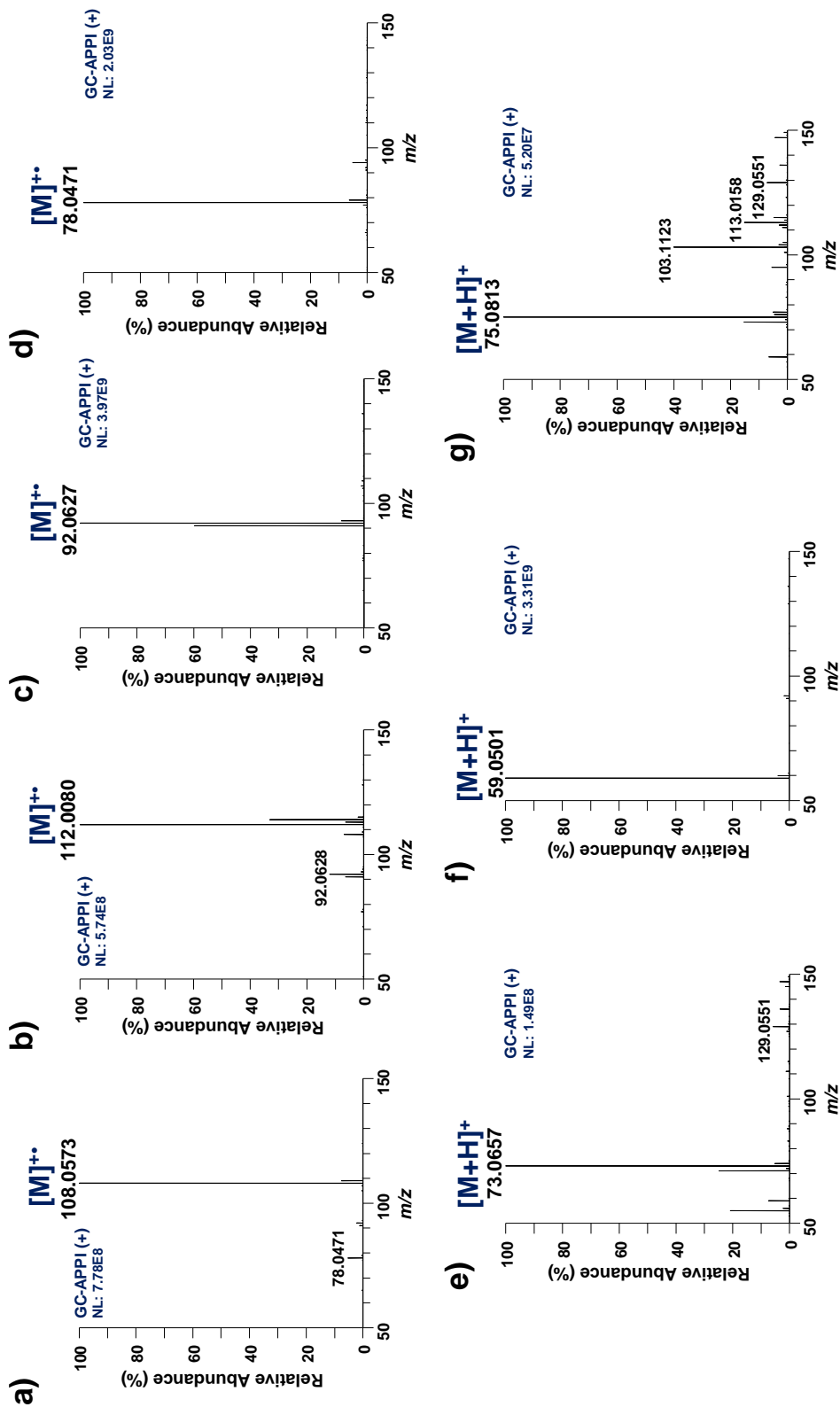
Fig. 3.6. Positive ion GC-APPI mass spectra of a) anisole, b) chlorobenzene, c) toluene, d) benzene, e) tetrahydrofuran, f) acetone, and g) diethyl ether.

Table 3.6. Main properties of the dopants affecting the GC-APPI ionization of chlorinated organic contaminants.

Dopant	Ionization Energy[a] (eV)	Vapor Pressure[b] (Torr, 25 °C)	Proton Affinity[a] (kJ mol^{-1}, 25 °C)
Acetone	9.703 ± 0.006	180	812
Anisole	8.20 ± 0.05	4.2	–
Benzene	9.2438 ± 0.0001	75	746.4
Chlorobenzene	9.07 ± 0.02	9	753.1
Diethyl Ether	9.51 ± 0.03	440	828.4
Tetrahydrofuran	9.40 ± 0.02	132	822.1
Toluene	8.828 ± 0.001	21	782.4

[a] NIST database, [b] Experimental values reported by NIOSH.

promote charge-exchange reactions (Table 3.5, equation 5). As mentioned in *Article VII (Section 3.1)* and *Article VIII (Ionization of PCDD/Fs and dl-PCBs by GC-APPI)*, chlorobenzene, toluene, and benzene may favor charge-exchange reactions since they easily generate the [D]$^{+\bullet}$ ion (Table 3.5, eq. 3). In contrast, the ionization efficiency of PCDD/Fs, dl-PCBs and PCNs significantly decreased using acetone or tetrahydrofuran, when the dopant self-protonation process may hinder these charge-exchange reactions. Kauppila *et al.* [238] reported that the addition of dopants could significantly suppress the direct photoionization of analytes due to a decrease of the VUV transparency (photon attenuation) and/or neutralizing reactions between the dopant and the analytes. This effect was observed in the ionization of PCNs. The signal from most of these compounds was slightly suppressed when dopants that promote proton-transfer reactions (e.g., tetrahydrofuran, acetone) were added instead of the expected improved ionization efficiency versus the direct photoionization (*Article VII, Fig. 2a*). This low ionization efficiency was observed when anisole was used as dopant, although, as mentioned above (*Section 3.3.1*), it formed the dopant molecular ion during the photoionization process, favoring charge-exchange reactions. Probably, its low vapor pressure (Table. 3.6) could produce some condensation in the ion source, which would have reduced the concentration of the [D]$^{+\bullet}$ ion in the gas-phase. Moreover, anisole also has the lowest IE (8.20 Torr, 25 °C) among all the dopants evaluated, which might hinder the charge exchange reactions with PCDD/Fs, dl-PCBs and PCNs (Table 3.5, eq. 5). Thus, the effect of the dopants over the way the analytes are ionized could help to establish ionization trends for families of compounds with similarities (same functional group, presence of aromatic rings, halogens, etc.) and, therefore, selecting the most suitable dopant that promotes those reactions of interest (charge exchange, proton transfer, etc.).

Concerning the ionization in negative ion mode, all the families of chlorinated organic contaminants were ionized through the formation of cluster ions with oxygen atoms (Table 3.5, eq. 11-13), except SCCPs for which the chloride-attachment ionization strategy provided the best results. Halogen atoms (F, Cl, and Br) have higher electron affinity than oxygen and, therefore, these cluster ions are quite common for chlorinated organic contaminants

[116,168,195]. In contrast to positive ion GC-APPI, the gas-phase reactions in negative ion mode are initiated by the electrons emitted after the dopant photoionization process, so any photoionized dopant could produce the ionization of high electronegative compounds. The gas-phase reactions to generate the analyte ions in negative ion mode can be produced by electron capture (Table 3.5, eq. 7) and the generation of the superoxide ion (Table 3.5, eq. 8) with further reactions with neutral molecules (Table 3.5, eq. 9, 11-12) or oxygen (Table 3.5, eq. 13), respectively. As all the dopants tested could ionize the analytes, different models were established for each family of compounds to determine the effect of the dopant vapor pressure over the GC-APPI ionization (Fig. 3.7).
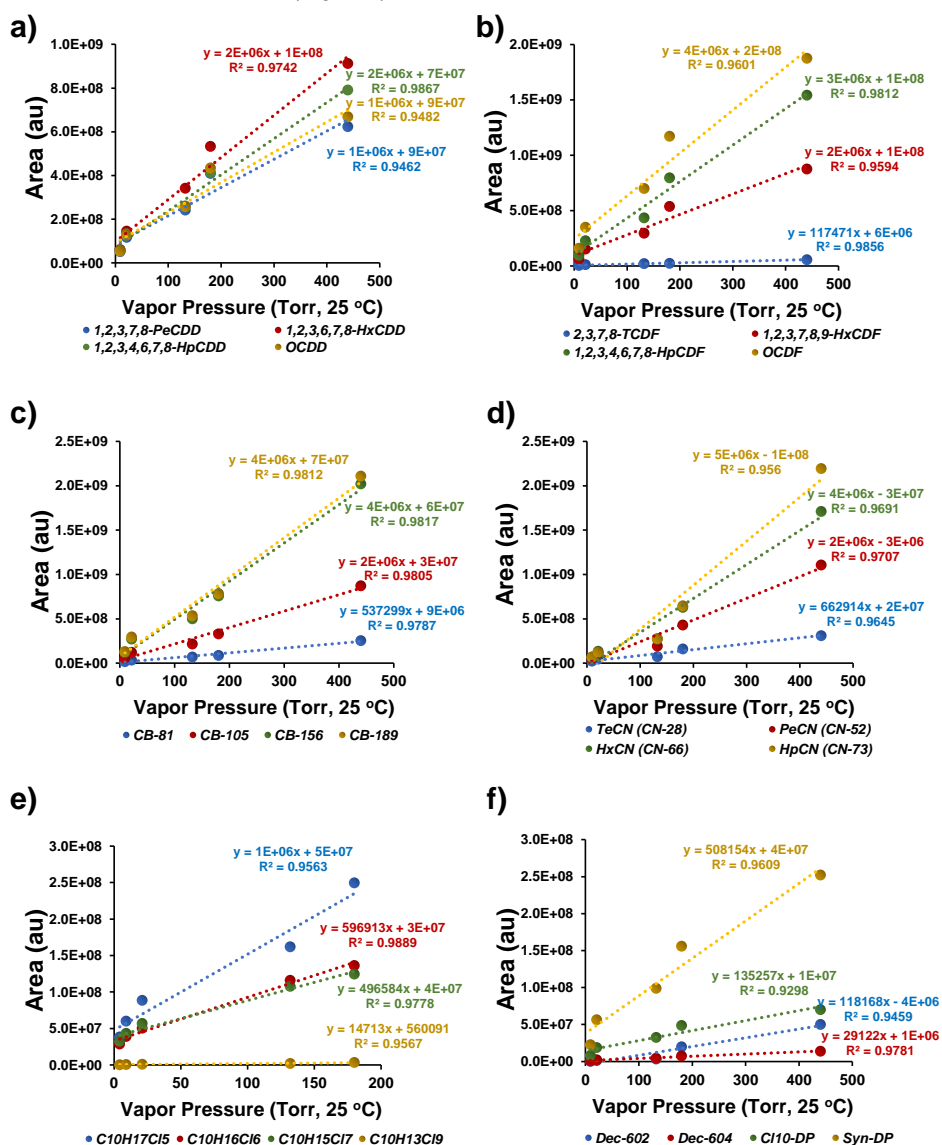

Fig. 3.7. Correlation between dopant vapor pressure and GC-APPI response of a) PCDDs, b) PCDFs, c) dl-PCBs, d) PCNs, e) SCCPs, and f) DP and analogs.

Fig. 3.7 represents the chromatographic peak area observed for each compound versus the experimental vapor pressure of the dopants (keeping constant the analyte concentration and ion source conditions). As can be observed, a good linear correlation was obtained for different compounds of each family of chlorinated organic contaminants. In fact, the determination coefficients (R^2) ranged from 0.926 to 0.988, which demonstrates the high influence of the dopant vapor pressure on the ionization efficiency of chlorinated organic contaminants. However, some aspects might be considered. With regards to benzene, the response-dopant vapor pressure correlation (R^2: 0.845-0.947) for PCDD/Fs and dl-PCBs was worse and did not follow the trends of the other dopants. This might be because the responses of analytes are also influenced by the ionization energy of the dopant. For instance, if we consider only those dopants with an IE lower than 9.3 eV (chlorobenzene, toluene, and benzene), the R^2 was higher than 0.980. The use of dopants with IE higher than 9.3 eV may can transfer a higher energy to analytes inducing a small in-source fragmentation on analytes such as PCDD/Fs and dl-PCBs, which slightly decrease the ion intensity. Nonetheless, the higher vapor pressure of these dopants may compensate this small fragmentation. In some cases, this fragmentation can even lead to lower responses than those obtained when using dopants with lower vapor pressures. In fact, this effect might explain the lower responses of 2,3,7,8-TCDD when using diethyl ether (compared to benzene). If we only consider the response of this compound using only those dopants with IE lower than 9.3 eV, the correlation significantly improves achieving a R^2 of 0.9995 (Fig. 3.8). Thereby, it can be concluded that diethyl ether, which presents the higher vapor pressure, provides the highest ionization efficiency for chlorinated organic contaminants. Nevertheless, when there is a strong in-source fragmentation, it is recommended the use of a dopant with a lower IE (e.g., benzene for 2,3,7,8-TCDD) to reduce the fragmentation and to check if the response could be enhanced even using dopants with lower vapor pressure.
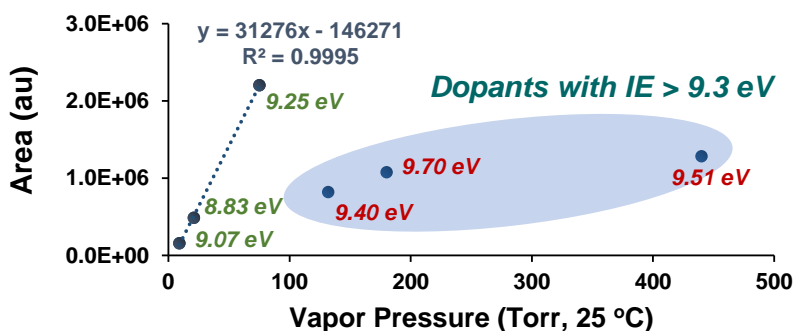

Fig. 3.8. Correlation of dopant vapor pressure-GC-APPI response for 2,3,7,8-TCDD.

CONCLUSIONS

CONCLUSIONS

In this Thesis, different strategies based on chromatography-atmospheric pressure ionization-mass spectrometry have been studied for the development of new methodologies that could overcome the main limitations on the analytical determination of several families of halogenated organic contaminants. These limitations have been faced out from different points of view, such as the sample treatment, the chromatographic separation, the ionization behavior and/or the ionization efficiency of the analytes, as well as the detection capability and selectivity of the developed methods. The suitability of the proposed methodologies has been demonstrated through the analysis of samples of environmental interest such as water, fly ashes, fish, gull eggs, marine sediments, or sludge, among others. Additionally, the in-source and MS/MS fragmentation of some of these families have also been studied to propose reliable non-targeted screening strategies.

The following conclusions can be drawn from the results obtained in this Thesis:

Concerning the sample treatment,

The extraction technique and the clean-up and fractionation steps (when required) were optimized according to the type of sample and the characteristics of analytes studied to obtain high recoveries and remove potential matrix interferences.

- To reduce losses of the most volatile neutral PFAS during sample treatment procedures, it has been recommended to avoid evaporation steps. For instance, to achieve recoveries higher than 93% for all target compounds using SPE (Oasis HLB sorbent), evaporation steps must be avoided and, in this Thesis, SPE has been recommended for the UHPLC-API-MS/MS analysis of neutral PFAS in river water samples. In contrast, the alternative use of HS-SPME (DVB/CAR/PDMS), faster than the SPE procedure, has been proposed in combination with GC-APPI-HRMS for both *in-situ* selective and efficient extraction of neutral PFAS from river water samples allowing the monitoring of their occurrence at low pg L^{-1} levels.

- For the extraction of PCDD/Fs, dl-PCBs and PCNs from solid samples (sediments, soybean meal, sludge, and fly ashes), it has been proposed the use of a Soxhlet extraction followed by clean-up and fractionation steps with acidified silica, Florisil, and carbon columns to allow high enough recoveries for all the target compounds with effective removal of interfering matrix components such as lipids or hydrocarbons. On the other hand, the use of a selective PLE method with acidified silica as fat retainer inside the extraction cell and employing a mixture of hexane/CH_2Cl_2 (1:1, *v/v*) as solvent extraction followed by a simultaneous clean-up and fractionation step in an activated Florisil column is proposed for the extraction of SCCPs and DP and analogs from biota samples (gull eggs and fish). These sample treatments have led to clean extracts and high recoveries for the target compounds (SCCPs: 91-96%, DP and analogs: 91-98%).

Concerning the chromatographic separation,

Different separation strategies consisted of UHPLC and GC with capillary columns, comprehensive two-dimensional gas chromatography or even ion mobility have been evaluated in this Thesis to improve the separation of those families of compounds showing retention difficulties (nPFAS) or coelution problems (SCCPs and PCNs).

- Regarding the GC-MS determination of neutral PFAS, the use of a long GC column (60 m) with a semi-polar stationary phase (poly(cyanopropylphenyldimethyl siloxane), DB-624) and a film thickness of 1.4 µm is proposed to achieve both the separation of FTOs, FTOHs, FOSAs, and FOSEs, and good enough retention of the most volatile FTOs. In contrast, when these compounds have to be determined by UHPLC-MS/MS, the use of a UHPLC column packed with totally porous particles and a C_{18} stationary phase (Luna C_{18}) has been proposed to allow the baseline separation of most of the analytes and to efficiently retain the most volatile FTOs.

- For the congener-specific separation of PCNs, GCxGC using a DB-5 (5% diphenyl 95% dimethylpolysiloxane) as first dimension column combined with a thermally stable ionic liquid stationary phase (IL-SLB60) column in the second dimension is proposed since it significantly improves the separation of these compounds in front of other polar stationary phases such as polyethylene glycol-based columns, and it also allows to reduce 32% the analysis time.

- For the separation of SCCPs, GCxGC-IM did not show any improvement over GCxGC separations. Nonetheless, the separation capacity of GCxGC combined with the selectivity of HRMS and the soft GC-APPI source could provide a very powerful technique not only for the analysis of SCCPs, but also for the screening of other pollutants in complex environmental matrices.

Concerning the ionization behavior and efficiency,

The use of atmospheric pressure ionization was evaluated to reduce in-source fragmentation and to achieve an efficient ionization of the target compounds included in this Thesis.

- For those families of compounds determined by UHPLC-MS/MS like neutral PFAS, the negative ion APCI and APPI sources have demonstrated to efficiently ionize them through the generation of deprotonated molecules (FTOHs, FOSEs) or odd-electron fragment ions coming from the loss of HF units (FTOs, FTOHs) or part of the functional group (FOSEs). The ionization studies indicated that the mobile phase composition strongly affected the ionization of the analytes, especially FTOHs, which makes it highly recommended to carefully select the mobile phase composition. The best results have been obtained using negative ion APCI and APPI with acetonitrile/water mixtures.

326

- The tandem mass spectrometry fragmentation studies of ions generated in API sources (ESI, APCI and APPI) for neutral PFAS allowed the establishment of fragmentation pathways for the different families of compounds and the identification of common product ions ($[C_2F_5]^-$, $[C_3F_7]^-$, and $[C_4F_9]^-$ for FOSAs), neutral losses (HF units for FTOs and FTOHs, SO_2 for FOSAs and FOSEs or general CF_2 losses) and common fragmentation patterns (successive HF losses for fluorotelomer-based neutral PFAS). Moreover, for the fragmentation pathway of superoxide adduct ions, in addition to the information obtained in the fragmentation studies, it has also been required the information achieved from both the in-source CID fragmentation observed in GC-APPI-HRMS and the tandem mass spectrometry using PS-APPI-MS/HRMS. Furthermore, these studies have allowed to identify the most characteristic and abundant ions in both full-scan and tandem mass spectrometry, which has allowed the development of selective and sensitive determination methods for these families of compounds.

- The fragmentation studies have also allowed the development of new non-targeted screening strategies, such as fragmentation flagging approaches for screening the occurrence of target, suspect, as well as new and unknown PFAS in complex environmental samples. This information could be even complemented with Kendrick mass defect plots to verify the unequivocal identification of PFAS from the same family (using the CF_2 scale) as well as fluorotelomer-based neutral PFAS that present successive neutral losses among the series of fragment ions observed in the mass spectra (using the HF scale).

On the other hand, the GC-APPI has demonstrated for the first time its feasibility for the efficient ionization of the halogenated organic contaminants studied in this Thesis.

- Under the optimal ionization conditions, the GC-APPI, especially in negative-ion mode, has provided an efficient ionization of all analytes yielding characteristic ions, which improve the selectivity of the methods. Neutral PFAS were ionized through the formation of characteristic superoxide adduct ions (FTOHs and FOSEs), the deprotonated molecule (FOSAs) or odd-electron in-source fragment ions (FTOs) while DP and analogs yielded the formation of cluster ions that contains oxygen atoms. Moreover, PCDD/Fs, dl-PCBs, and PCNs could be ionized in both positive and negative ion mode by means of the generation of molecular ions and phenoxide ions, respectively. In the case of SCCPs, the use of dopant/chlorination agent mixtures is highly recommended to promote the formation of $[M+Cl]^-$ ions (chloride-attachment APPI) which significantly reduce the number of potential interferences coming from other CP congener groups with higher carbon chain length and chlorination degree. Additionally, it has been observed that the response of these ions mainly depends on the concentration, which greatly simplifies the quantification of these complex mixture of compounds.

- The ionization of analytes in positive ion GC-APPI (PCDD/Fs, dl-PCBs, and PCNs through the formation of $[M]^{+\bullet}$ ion) was strongly dependent on the dopant nature, being significantly favored when using dopants that promote ionization *via* charge-exchange reactions (e.g., benzene, toluene, and chlorobenzene). In contrast, the ionization in negative ion GC-APPI mainly depended on the dopant vapor pressure, achieving the best results when using highly volatile dopants (e.g., diethyl ether, acetone). In fact, the dopant vapor pressure was positively correlated with the analyte response for all families of halogenated organic contaminants. However, in those cases that a high in-source fragmentation is observed, the dopant must be carefully selected taking into account its ionization energy.

- For the analysis of compounds with low vapor pressures (e.g., PCDD/Fs, or DP and analogs), in this Thesis it is suggested to apply high temperatures (ca. 250 ºC) in the ion source to avoid post-column peak broadening that could lead to the partial chromatographic coelution of some compounds. In contrast, when using the chloride-attachment strategy proposed for SCCPs, it is recommended the use of low temperatures (ca. 200 ºC) in the ion source to enhance the formation of labile chloride adduct ions.

Concerning the figures of merit of the developed methods,

The high ionization efficiency provided by APCI and APPI sources, especially in negative ion mode, has allowed to develop sensitive and selective UHPLC-MS/MS and GC-APPI-HRMS methods for the accurate and precise determination of halogenated organic contaminants in environmental samples.

- Among the developed methodologies for the determination of neutral PFAS, GC-APPI-HRMS has shown the best detection capability, especially for FTOs and FTOHs. The iLODs achieved with this method are at least between 4 and 30-fold lower than those previously obtained using the most sensitive UHPLC-API-MS/MS method, with the additional advantage of showing a negligible matrix effect, which ensure the quantitation procedure.

- The GC-APPI-HRMS (Orbitrap) system provided a very high detection capability for all the studied chlorinated organic contaminants. These methodologies provided iLODs ranging from 0.5 to 190 fg injected on the column. These values were comparable or even better than those obtained using traditional GC-HRMS methodologies based on high-vacuum ionization techniques (EI and NICI) or even GC-APCI-HRMS. The methods developed in this Thesis allow to fulfil the criteria indicated on the current EU regulation for PCCD/Fs, and dl-PCBs, while the proposed methodologies for PCNs and DP and analogs make possible their sensitive and selective determination in complex environmental samples such as marine sediments and gull eggs, respectively. In the case of SCCPs, the use of the chloride-attachment GC-APPI-HRMS method has

provided important advantages over ECNI-based methods. The low influence of the number of chlorine atoms over the response and the use of the Orbitrap mass analyzer at a resolution of 70,000 FWHM (at *m/z* 200) allowed the quantification of both the total SCCP content and the different homologue groups by internal normalization. This methodology not only leads to a very sensitive determination of SCCPs but also significantly reduces both the analysis time and the data processing.

- The capability of the GC-APPI-HRMS system to operate in both polarities (positive and negative ion mode) and to acquire data in a sensitive high-resolution full-scan mode allows the easy identification of potential interferences and the design of non-targeted strategies for the screening of suspect or new contaminants in environmental samples. Due to these advantages and the high capacity to achieve highly sensitive and selective targeted analyses, the GC-APPI-HRMS (Orbitrap) system can be proposed as a universal technique to monitor halogenated contaminants in environmental samples. Thereby, the swappability of GC-APPI with LC-API interfaces in the same HRMS instrument (Orbitrap) makes it possible to unify the instrumentation normally required (GC-EI-HRMS (sectors), GC-CI-MS, UHPLC-ESI-MS/MS, GC-NICI-MS, and GC-NICI-HRMS) in laboratories focused on the environmental occurrence of these contaminants.

REFERENCES

REFERENCES

[1] Stockholm Convention Web Page. (*accessed May 7,2020*).
http://www.pops.int/TheConvention/ThePOPs/tabid/673/Default.aspx.

[2] POPs listed in the Stockholm Convention Web Page. (*accessed May 7, 2020*).
http://www.pops.int/TheConvention/ThePOPs/AllPOPs/tabid/2509/Default.aspx.

[3] UNEP, Proposal to list Dechlorane Plus (CAS No. 13560-89-9) and its syn-isomer (CAS No. 135821-03-3) and anti-isomer (CAS No. 135821-74-8) in Annexes A, B and/or C to the Stockholm Convention on Persistent Organic Pollutants. UNEP/POPS/POPRC.15/3, (**2019**).

[4] UNEP, Proposal to list methoxychlor in Annex A to the Stockholm Convention on Persistent Organic Pollutants. UNEP/POPS/POPRC.15/4, (**2019**).

[5] UNEP, Proposal to list perfluorohexane sulfonic acid (CAS No: 355-46-4, PFHxS), its salts and PFHxS-related compounds in Annexes A, B and/or C to the Stockholm Convention on Persistent Organic Pollutants. UNEP/POPS/POPRC.13/4, (**2017**).

[6] Global Monitoring Plan Data Warehouse for Persistent Organic Pollutants under the Stockholm Convention (*accessed May 7, 2020*). http://visualization.pops-gmp.org/2014/.

[7] S.D. Richardson, T.A. Ternes, Water Analysis: Emerging Contaminants and Current Issues, *Anal. Chem.* 90 (**2018**) 398–428. https://doi.org/10.1021/acs.analchem.7b04577.

[8] S.D. Richardson, S.Y. Kimura, Emerging environmental contaminants: Challenges facing our next generation and potential engineering solutions, *Environ. Technol. Innov.* 8 (**2017**) 40–56. https://doi.org/10.1016/j.eti.2017.04.002.

[9] S.D. Richardson, S.Y. Kimura, Water Analysis: Emerging Contaminants and Current Issues, *Anal. Chem.* 92 (**2020**) 473–505. https://doi.org/10.1021/acs.analchem.9b05269.

[10] L.W.Y. Yeung, N. Yamashita, J. Falandysz, Legacy and emerging perfluorinated and polyfluorinated compounds: An update, *Chemosphere.* 237 (**2019**) 124506. https://doi.org/10.1016/j.chemosphere.2019.124506.

[11] A. Jahnke, U. Berger, Trace analysis of per- and polyfluorinated alkyl substances in various matrices-How do current methods perform?, *J. Chromatogr. A.* 1216 (**2009**) 410–421. https://doi.org/10.1016/j.chroma.2008.08.098.

[12] Z. Wang, I.T. Cousins, M. Scheringer, R.C. Buck, K. Hungerbühler, Global emission inventories for C4-C14 perfluoroalkyl carboxylic acid (PFCA) homologues from 1951 to 2030, Part I: Production and emissions from quantifiable sources, *Environ. Int.* 70 (**2014**) 62–75. https://doi.org/10.1016/j.envint.2014.04.013.

[13] Y. Pan, H. Zhang, Q. Cui, N. Sheng, L.W.Y. Yeung, Y. Sun, Y. Guo, J. Dai, Worldwide Distribution of Novel Perfluoroether Carboxylic and Sulfonic Acids in Surface Water, *Environ. Sci. Technol.* 52 (**2018**) 7621–7629. https://doi.org/10.1021/acs.est.8b00829.

[14] S. Wang, J. Huang, Y. Yang, Y. Hui, Y. Ge, T. Larssen, G. Yu, S. Deng, B. Wang, C. Harman, First report of a Chinese PFOS alternative overlooked for 30 years: Its toxicity, persistence, and presence in the environment, *Environ. Sci. Technol.* 47 (**2013**) 10163–10170. https://doi.org/10.1021/es401525n.

[15] T. Ruan, Y. Lin, T. Wang, R. Liu, G. Jiang, Identification of novel polyfluorinated ether sulfonates as PFOS alternatives in municipal sewage sludge in China, *Environ. Sci. Technol.* 49 (**2015**) 6519–6527. https://doi.org/10.1021/acs.est.5b01010.

[16] W.A. Gebbink, R. Bossi, F.F. Rigét, A. Rosing-Asvid, C. Sonne, R. Dietz, Observation of emerging per- and polyfluoroalkyl substances (PFASs) in Greenland marine mammals, *Chemosphere*. 144 (**2016**) 2384–2391. https://doi.org/10.1016/j.chemosphere.2015.10.116.

[17] Y. Liu, T. Ruan, Y. Lin, A. Liu, M. Yu, R. Liu, M. Meng, Y. Wang, J. Liu, G. Jiang, Chlorinated Polyfluoroalkyl Ether Sulfonic Acids in Marine Organisms from Bohai Sea, China: Occurrence, Temporal Variations, and Trophic Transfer Behavior, *Environ. Sci. Technol.* 51 (**2017**) 4407–4414. https://doi.org/10.1021/acs.est.6b06593.

[18] Y. Shi, R. Vestergren, L. Xu, Z. Zhou, C. Li, Y. Liang, Y. Cai, Human Exposure and Elimination Kinetics of Chlorinated Polyfluoroalkyl Ether Sulfonic Acids (Cl-PFESAs), *Environ. Sci. Technol.* 50 (**2016**) 2396–2404. https://doi.org/10.1021/acs.est.5b05849.

[19] F. Chen, S. Yin, B.C. Kelly, W. Liu, Chlorinated Polyfluoroalkyl Ether Sulfonic Acids in Matched Maternal, Cord, and Placenta Samples: A Study of Transplacental Transfer, *Environ. Sci. Technol.* 51 (**2017**) 6387–6394. https://doi.org/10.1021/acs.est.6b06049.

[20] UNEP, Technical paper on the identification and assessment of alternatives to the use of perfluorooctane sulfonic acid in open applications. UNEP/POPS/PORC.8/INF/17, (**2012**).

[21] C. Wei, Q. Wang, X. Song, X. Chen, R. Fan, D. Ding, Y. Liu, Distribution, source identification and health risk assessment of PFASs and two PFOS alternatives in groundwater from non-industrial areas, *Ecotoxicol. Environ. Saf.* 152 (**2018**) 141–150. https://doi.org/10.1016/j.ecoenv.2018.01.039.

[22] P.B. Poulsen, L.K. Gram, A.A. Jensen, A.A. Rasmussen, C. Ravn, P. Møller, C.R. Jørgensen, K. Løkkegaard, Substitution of PFOS for use in non-decorative hard chrome plating, *Danish Environ. Prot. Agency.* 1371 (**2011**) 1–78. http://www2.mst.dk/udgiv/publications/2011/06/978-87-92779-10-6.pdf.

[23]   A. Urtiaga, A. Soriano, J. Carrillo-Abad, BDD anodic treatment of 6:2 fluorotelomer sulfonate (6:2 FTSA). Evaluation of operating variables and by-product formation, *Chemosphere.* 201 (**2018**) 571–577. https://doi.org/10.1016/j.chemosphere.2018.03.027.

[24]   H. Fromme, M. Wöckner, E. Roscher, W. Völkel, ADONA and perfluoroalkylated substances in plasma samples of German blood donors living in South Germany, *Int. J. Hyg. Environ. Health.* 220 (**2017**) 455–460. https://doi.org/10.1016/j.ijheh.2016.12.014.

[25]   F. Heydebreck, J. Tang, Z. Xie, R. Ebinghaus, Alternative and Legacy Perfluoroalkyl Substances: Differences between European and Chinese River/Estuary Systems, *Environ. Sci. Technol.* 49 (**2015**) 8386–8395. https://doi.org/10.1021/acs.est.5b01648.

[26]   M. Sun, E. Arevalo, M. Strynar, A. Lindstrom, M. Richardson, B. Kearns, A. Pickett, C. Smith, D.R.U. Knappe, Legacy and Emerging Perfluoroalkyl Substances Are Important Drinking Water Contaminants in the Cape Fear River Watershed of North Carolina, *Environ. Sci. Technol. Lett.* 3 (**2016**) 415–419. https://doi.org/10.1021/acs.estlett.6b00398.

[27]   Z. Wang, I.T. Cousins, M. Scheringer, K. Hungerbuehler, Hazard assessment of fluorinated alternatives to long-chain perfluoroalkyl acids (PFAAs) and their precursors: Status quo, ongoing challenges and possible solutions, *Environ. Int.* 75 (**2015**) 172–179. https://doi.org/10.1016/j.envint.2014.11.013.

[28]   G. Shi, Q. Cui, Y. Pan, N. Sheng, Y. Guo, J. Dai, 6:2 fluorotelomer carboxylic acid (6:2 FTCA) exposure induces developmental toxicity and inhibits the formation of erythrocytes during zebrafish embryogenesis, *Aquat. Toxicol.* 190 (**2017**) 53–61. https://doi.org/10.1016/j.aquatox.2017.06.023.

[29]   S.S. White, L.S. Birnbaum, An Overview of the Effects of Dioxins and Dioxin-like Compounds on Vertebrates, as Documented in Human and Ecological Epidemiology, *J. Environ. Sci. Health. - Part C Environ. Carcinog. Ecotoxicol. Rev.* 27 (**2009**) 197–211. https://doi.org/10.1080/10590500903310047.

[30]   S. Safe, S. Bandiera, T. Sawyer, L. Robertson, L. Safe, A. Parkinson, P.E. Thomas, D.E. Ryan, L.M. Reik, W. Levin, M.A. Denomme, T. Fujita, PCBs : Structure-Function Relationships and Mechanism of Action, *Environ. Health Perspect.* 60 (**1985**) 47–56.

[31]   L.S. Birnbaum, The mechanism of dioxin toxicity: relationship to risk assessment., *Environ. Health Perspect.* 102 (**1994**) 157–167.https://doi.org/10.1289/ehp.94102s9157.

[32]   WHO, Consultation on assessment of the health risk of dioxins; re-evaluation of the tolerable daily intake (TDI): Executive Summary, *Food Addit. Contam.* 17 (**2000**) 223–240. https://doi.org/10.1080/713810655.

[33] M. Engwall, B. Brunström, E. Jakobsson, Ethoxyresorufin O-deethylase (EROD) and aryl hydrocarbon hydroxylase (AHH)-inducing potency and lethality of chlorinated naphthalenes in chicken (Gallus domesticus) and eider duck (Somateria mollissima) embryos, *Arch. Toxicol.* 68 (**1994**) 37–42.

[34] OME, Scientific Criteria Document for Standard Development No. 4-84. Polychlorinated dibenzo-p-dioxins (PCDDs) and Polychlorinated dibenzofurans (PCDFs), (**1984**).

[35] NATO, Pilot study on international information exchange on dioxins and related compounds. International toxicity equivalency factor (I-TEF) method of risk assessment for complex mixtures of dioxins and related compounds, (**1988**).

[36] M. Van Den Berg, L. Birnbaum, A.T.C. Bosveld, B. Brunström, P. Cook, M. Feeley, J.P. Giesy, A. Hanberg, R. Hasegawa, S.W. Kennedy, T. Kubiak, J.C. Larsen, F.X.R. Van Leeuwen, A.K.D. Liem, C. Nolt, R.E. Peterson, L. Poellinger, S. Safe, D. Schrenk, D. Tillitt, M. Tysklind, M. Younes, F. Wærn, T. Zacharewski, Toxic equivalency factors (TEFs) for PCBs, PCDDs, PCDFs for humans and wildlife, *Environ. Health Perspect.* 106 (**1998**) 775–792. https://doi.org/10.1289/ehp.98106775.

[37] M. Van den Berg, L.S. Birnbaum, M. Denison, M. De Vito, W. Farland, M. Feeley, H. Fiedler, H. Hakansson, A. Hanberg, L. Haws, M. Rose, S. Safe, D. Schrenk, C. Tohyama, A. Tritscher, J. Tuomisto, M. Tysklind, N. Walker, R.E. Peterson, The 2005 World Health Organization reevaluation of human and mammalian toxic equivalency factors for dioxins and dioxin-like compounds, *Toxicol. Sci.* 93 (**2006**) 223–241. https://doi.org/10.1093/toxsci/kfl055.

[38] A. Hanberg, F. Wærn, L. Asplund, E. Haglund, S. Safe, Swedish dioxin survey: Determination of 2,3,7,8-TCDD toxic equivalent factors for some polychlorinated biphenyls and naphthalenes using biological tests, *Chemosphere.* 20 (**1990**) 1161–1164. https://doi.org/10.1016/0045-6535(90)90238-O.

[39] A.L. Blankenship, K. Kannan, S.A. Villalobos, D.L. Villeneuve, J. Falandysz, T. Imagawa, E. Jakobsson, J.P. Giesy, Relative potencies of individual polychlorinated naphthalenes and halowax mixtures to induce Ah receptor-mediated responses, *Environ. Sci. Technol.* 34 (**2000**) 3153–3158. https://doi.org/10.1021/es9914339.

[40] D.L. Villeneuve, K. Kannan, J.S. Khim, J. Falandysz, V.A. Nikiforov, A.L. Blankenship, J.P. Giesy, Relative potencies of individual polychlorinated naphthalenes to induce dioxin-like responses in fish and mammalian *in vitro* bioassays, *Arch. Environ. Contam. Toxicol.* 39 (**2000**) 273–281. https://doi.org/10.1007/s002440010105.

[41] G. Suzuki, C. Michinaka, H. Matsukami, Y. Noma, N. Kajiwara, Validity of using a relative potency factor approach for the risk management of dioxin-like polychlorinated naphthalenes, *Chemosphere*. 244 (**2020**) 125448. https://doi.org/10.1016/j.chemosphere.2019.125448.

[42] NTP, Toxicology and carcinogenesis studies of chlorinated paraffins (C12, 60% Chlorine) (CAS No. 63449-39-8) in F344/N rats and B6C3F$_1$ mice, (**1986**).

[43] D.M. Serrone, R.D.N. Birtley, W. Weigand, R. Millischer, Toxicology of Chlorinated Paraffins, *Food Chem. Toxicol.* 25 (**1987**) 553–562. https://doi.org/10.1016/0278-6915(87)90209-2.

[44] EC, European Union Risk Assessment Report. Alkanes, C10-13, Chloro- risk assessment, (**2000**).

[45] ECHA, Support document for identification of alkanes, C10-13, chloro as substances of very high concern, (**2008**).

[46] European Commission Environment Web Page. Substances of concern. (*accessed May 7, 2020*). https://ec.europa.eu/environment/chemicals/endocrine/strategy/substances_en.htm#sub1.

[47] NTP, Chlorinated Paraffins (C12, 60% Chlorine), (**2014**).

[48] J.C. O'Connor, S.M. Munley, T.L. Serex, R.C. Buck, Evaluation of the reproductive and developmental toxicity of 6:2 fluorotelomer alcohol in rats, *Toxicology.* 317 (**2014**) 6–16. https://doi.org/10.1016/j.tox.2014.01.002.

[49] T. Serex, S. Anand, S. Munley, E.M. Donner, S.R. Frame, R.C. Buck, S.E. Loveless, Toxicological evaluation of 6:2 fluorotelomer alcohol, *Toxicology.* 319 (**2014**) 1–9. https://doi.org/10.1016/j.tox.2014.01.009.

[50] C. Lau, K. Anitole, C. Hodes, D. Lai, A. Pfahles-Hutchens, J. Seed, Perfluoroalkyl acids: A review of monitoring and toxicological findings, *Toxicol. Sci.* 99 (**2007**) 366–394. https://doi.org/10.1093/toxsci/kfm128.

[51] D.A. Ellis, J.W. Martin, A.O. De Silva, S.A. Mabury, M.D. Hurley, M.P. Sulbaek Andersen, T.J. Wallington, Degradation of fluorotelomer alcohols: A likely atmospheric source of perfluorinated carboxylic acids, *Environ. Sci. Technol.* 38 (**2004**) 3316–3321. https://doi.org/10.1021/es049860w.

[52] Commission Regulation (EU) No 944/2013 of 2 October 2013 amending, for the purposes of its adaptation to technical and scientific progress, Regulation (EC) No 1272/2008 of the European Parliament and of the Council on classification, labelling and packaging of substances and mixtures, *Off. J. Eur. Union.* (**2013**).

[53] UNEP, Risk profile on pentadecafluorooctanoic acid (CAS No: 335-67-1, PFOA, perfluorooctanooic acid), its is salts and PPFOA-related compounds. UNEP/POPS/POPRC.12/11/Add.2, (**2016**).

[54] UNEP, Risk Profile on perfluorooctane sulfonate. UNEP/POPS/POPRC.2/17/Add.5, (**2006**).

[55] E. Barón, A. Dissanayake, J. Vilà-Cano, C. Crowther, J.W. Readman, A.N. Jha, E. Eljarrat, D. Barceló, Evaluation of the Genotoxic and Physiological Effects of Decabromodiphenyl Ether (BDE-209) and Dechlorane Plus (DP) Flame Retardants in Marine Mussels (*Mytilus galloprovincialis*), *Environ. Sci. Technol.* 50 (**2016**) 2700–2708. https://doi.org/10.1021/acs.est.5b05814.

[56] X.M. Hang, Y. Jiang, Y. Liu, H.L. Jia, Y.Q. Sun, An Integrated Study on Toxicity of Dechlorane Plus in Zebrafish, *Organohalogen Compd.* 75 (**2013**) 1085–1089.

[57] H. Kang, H.B. Moon, K. Choi, Toxicological responses following short-term exposure through gavage feeding or water-borne exposure to Dechlorane Plus in zebrafish (*Danio rerio*), *Chemosphere.* 146 (**2016**) 226–232. https://doi.org/10.1016/j.chemosphere.2015.12.024.

[58] X. Chen, Q. Dong, Y. Chen, Z. Zhang, C. Huang, Y. Zhu, Y. Zhang, Effects of Dechlorane Plus exposure on axonal growth, musculature and motor behavior in embryo-larval zebrafish, *Environ. Pollut.* 224 (**2017**) 7–15. https://doi.org/10.1016/j.envpol.2017.03.011.

[59] L. Zhang, F. Ji, M. Li, Y. Cui, B. Wu, Short-term effects of Dechlorane Plus on the earthworm *Eisenia fetida* determined by a systems biology approach, *J. Hazard. Mater.* 273 (**2014**) 239–246. https://doi.org/10.1016/j.jhazmat.2014.03.018.

[60] Y. Li, L. Yu, Z. Zhu, J. Dai, B. Mai, J. Wu, J. Wang, Accumulation and effects of 90-day oral exposure to Dechlorane Plus in quail (*Coturnix coturnix*), *Environ. Toxicol. Chem.* 32 (**2013**) 1649–1654. https://doi.org/10.1002/etc.2202.

[61] B. Wu, S. Liu, X. Guo, Y. Zhang, X. Zhang, M. Li, S. Cheng, Responses of mouse liver to dechlorane plus exposure by integrative transcriptomic and metabonomic studies, *Environ. Sci. Technol.* 46 (**2012**) 10758–10764. https://doi.org/10.1021/es301804t.

[62] ECHA, Proposal for identification of substance of very high concern on the basis of the criteria set out in REACH. Article 57, (**2017**).

[63] CEPA, Certain Organic Flame Retardants Grouping Risk Management Approach For Dechlorane Plus (DP) Chemical Abstracts Service Registry Number (CAS RN): 13560-89-9, (**2019**).

[64] Y. Li, L. Yu, J. Wang, J. Wu, B. Mai, J. Dai, Accumulation pattern of Dechlorane Plus and associated biological effects on rats after 90 d of exposure, *Chemosphere*. 90 (**2013**) 2149–2156. https://doi.org/10.1016/j.chemosphere.2012.10.106.

[65] Y.-J. Ben, X.-H. Li, Y.-L. Yang, L. Li, M.-Y. Zheng, W.-Y. Wang, X.-B. Xu, Placental transfer of dechlorane plus in mother-infant pairs in an E-waste recycling area (Wenling, China), *Environ. Sci. Technol.* 48 (**2014**) 5187–5193. https://doi.org/10.1021/es404106b.

[66] Y. Zhang, J.-P. Wu, X.-J. Luo, J. Wang, S.-J. Chen, B.-X. Mai, Tissue distribution of Dechlorane Plus and its dechlorinated analogs in contaminated fish: High affinity to the brain for *anti*-DP, *Environ. Pollut.* 159 (**2011**) 3647–3652. https://doi.org/10.1016/j.envpol.2011.07.026.

[67] L. Li, W. Wang, Q. Lv, Y. Ben, X. Li, Bioavailability and tissue distribution of Dechloranes in wild frogs (*Rana limnocharis*) from an e-waste recycling area in southeast China, *J. Environ. Sci.* 26 (**2014**) 636–642. https://doi.org/10.1016/S1001-0742(13)60447-7.

[68] J.-P. Wu, X.-Y. Chen, W. Si-Kang, Y. Sun, W.-L. Feng, L. Tao, X.-J. Luo, B.-X. Mai, Dechlorane Plus flame retardant in a contaminated frog species: Biomagnification and isomer-specific transfer from females to their eggs, *Chemosphere*. 211 (**2018**) 218–225. https://doi.org/10.1016/j.chemosphere.2018.07.146.

[69] Y.-H. Zeng, X.-J. Luo, B. Tang, B.-X. Mai, Habitat- and species-dependent accumulation of organohalogen pollutants in home-produced eggs from an electronic waste recycling site in South China: Levels, profiles, and human dietary exposure, *Environ. Pollut*. 216 (**2016**) 64–70. https://doi.org/10.1016/j.envpol.2016.05.039.

[70] H. Marler, D.H. Adams, Y. Wu, C.K. Nielsen, L. Shen, E.J. Reiner, D. Chen, Maternal Transfer of Flame Retardants in Sharks from the Western North Atlantic Ocean, *Environ. Sci. Technol*. 52 (**2018**) 12978–12986. https://doi.org/10.1021/acs.est.8b01613.

[71] S. Siddique, Q. Xian, N. Abdelouahab, L. Takser, S.P. Phillips, Y.-L. Feng, B. Wang, J. Zhu, Levels of dechlorane plus and polybrominated diphenylethers in human milk in two Canadian cities, *Environ. Int*. 39 (**2012**) 50–55. https://doi.org/10.1016/j.envint.2011.09.010.

[72] UNECE, Protocol to the 1979 Convention on Long-range Transboundary Air Pollution on persistent organic pollutants, (**1998**).

[73] UNECE, The 1998 Protocol on Persistent Organic Pollutants, Including the Amendments Adopted by the Parties on 18 December 2009. ECE/EB.AIR/104, (**2010**).

[74] Regulation (EC) No 850/2004 of the European Parliament and of the Council of 29 April 2004 on persistent organic pollutants and amending Directive 79/117/EEC, *Off. J. Eur. Union*. (**2004**).

[75] Regulation (EU) 2019/1242 of the European Parliament and of the Council of 20 June 2019 on persistent organic pollutants, *Off. J. Eur. Union*. (**2019**).

[76] Council Directive 96/59/EC of 16 September 1996 on the disposal of polychlorinated biphenyls and polychlorinated terphenyls (PCB/PCT), *Off. J. Eur. Union*. (**2009**).

[77] Regulation No 166/2006 of the European Parliament and of the Council of 18 January 2006 concerning the establishment of a European Pollutant Release and Transfer Register and amending Council Directives 91/689/EEC and 96/61/EC, *Off. J. Eur. Union*. (**2006**).

[78] Real Decreto 508/2007, de 20 de abril, por el que se regula el suministro de información sobre emisiones del Reglamento E-PRTR y de las autorizaciones ambientales integradas, BOE. (**2007**).

[79] Directive 2010/75/EU of the European Parliament and of the Council of 24 November 2010 on industrial emissions (integrated pollution prevention and control), *Off. J. Eur. Union*. (**2010**).

[80] Directive 2013/39/EU of the European Parliament and of the Council of 12 August 2013 amending Directives 2000/60/EC and 2008/105/EC as regards priority substances in the field of water policy*, Off. J. Eur. Union*. (**2013**).

[81] Real Decreto 817/2015, de 11 de septiembre, por el que se establecen los criterios de seguimiento y evaluación del estado de las aguas superficiales y las normas de calidad ambiental, BOE. (**2015**).

[82] Council Directive 98/83/EC of 3 November 1998 on the quality of water intended for human consumption, *Off. J. Eur. Communities*. (**1998**).

[83] Commission Directive (EU) 2015/1787 of 6 October 2015 amending Annexes II and III to Council Directive 98/83/EC on the quality of water intended for human consumption, *Off. J. Eur. Union*. (**2015**).

[84] EC, Proposal for a Directive of the European Parliament and of the Council on the quality of water intended for human consumption. 6060/1/20 REV 1, (**2020**).

[85] U.S. EPA, The Third Unregulated Contaminant Monitoring Rule (UCMR 3) Fact Sheet for Assessment Monitoring (List 1 Contaminants), (**2013**).
https://www.epa.gov/sites/production/files/2016-05/documents/ucmr3-factsheet-list1.pdf

[86] U.S. EPA, Fact Sheet PFOA & PFOS Drinking Water Health Advisories, (**2016**). https://www.epa.gov/sites/production/files/2016-06/documents/drinkingwaterhealthadvisories_pfoa_pfos_updated_5.31.16.pdf .

[87] Real Decreto 140/2003, de 7 de febrero, por el que se establecen los criterios sanitarios de la calidad del agua de consumo humano, BOE. (**2018**).

[88] Real Decreto 9/2005, de 14 de enero, por el que se establece la relación de actividades potencialmente contaminantes del suelo y los criterios y estándares para la declaración de suelos contaminados, BOE. (**2017**).

[89] EFSA, Risk for animal and human health related to the presence of dioxins and dioxin-like PCBs in feed and food, *EFSA J.* 16 (**2018**) 5333. https://doi.org/10.2903/j.efsa.2018.5333.

[90] Commission Regulation (EC) No 118/2006 of 19 December 2006 setting maximum levels for certain contaminants in foodstuffs, *Off. J. Eur. Union*. (**2019**).

[91] EFSA, Scientific Opinion. Risk to human health related to the presence of perfluoroalkyl substances in food, *EFSA J*. (**2020**).

[92] EFSA, Risk assessment of chlorinated paraffins in feed and food, *EFSA J.* 18 (**2020**) 5991. https://doi.org/10.2903/j.efsa.2020.5991.

[93] Commission Regulation (EU) 2018/192 of 8 February 2018 amending Annex VII to Regulation (EC) No 882/2004 of the European Parliament and of the Council as regards the EU reference laboratories in the field of contaminants in feed and food, *Off. J. Eur. Union*. (**2018**).

[94] A.I. Moukas, N.S. Thomaidis, A.C. Calokerinos, Determination of polychlorinated biphenyls by liquid chromatography-atmospheric pressure photoionization-mass spectrometry, *J. Mass Spectrom*. 49 (**2014**) 1096–1107. https://doi.org/10.1002/jms.3427.

[95] N. Xiang, L. Chen, X.Z. Meng, Y.L. Li, Z. Liu, B. Wu, L. Dai, X. Dai, Polybrominated diphenyl ethers (PBDEs) and dechlorane plus (DP) in a conventional wastewater treatment plant (WWTP) in Shanghai: Seasonal variations and potential sources, *Sci. Total Environ*. 487 (**2014**) 342–349. https://doi.org/10.1016/j.scitotenv.2014.04.014.

[96] B. Szostek, K.B. Prickett, R.C. Buck, Determination of fluorotelomer alcohols by liquid chromatography/tandem mass spectrometry in water, *Rapid Commun. Mass Spectrom*. 20 (**2006**) 2837–2844. https://doi.org/10.1002/rcm.2667.

[97] A. Bacaloni, L. Callipo, E. Corradini, P. Giansanti, R. Gubbiotti, R. Samperi, A. Laganà, Liquid chromatography-negative ion atmospheric pressure photoionization tandem mass spectrometry for the determination of brominated flame retardants in environmental water and industrial effluents, *J. Chromatogr. A*. 1216 (**2009**) 6400–6409. https://doi.org/10.1016/j.chroma.2009.07.039.

[98] A.I. Moukas, N.S. Thomaidis, A.C. Calokerinos, Novel determination of polychlorinated naphthalenes in water by liquid chromatography-mass spectrometry with atmospheric pressure photoionization, *Anal. Bioanal. Chem*. 408 (**2016**) 191–201. https://doi.org/10.1007/s00216-015-9092-5.

[99] T. Portolés, L.E. Rosales, J. V. Sancho, F.J. Santos, E. Moyano, Gas chromatography-tandem mass spectrometry with atmospheric pressure chemical ionization for fluorotelomer alcohols and perfluorinated sulfonamides determination, J*. Chromatogr. A*. 1413 (**2015**) 107–116. https://doi.org/10.1016/j.chroma.2015.08.016.

[100] S. Taniyasu, K. Kannan, K.S. Man, A. Gulkowska, E. Sinclair, T. Okazawa, N. Yamashita, Analysis of fluorotelomer alcohols, fluorotelomer acids, and short- and long-chain perfluorinated acids in water and biota, *J. Chromatogr. A*. 1093 (**2005**) 89–97. https://doi.org/10.1016/j.chroma.2005.07.053.

[101] N. Barco-Bonilla, A.J. Nieto-García, R. Romero-González, J.L. Martínez Vidal, A.G. Frenich, Simultaneous and highly sensitive determination of PCBs and PBDEs in environmental water and sediments by gas chromatography coupled to high resolution magnetic sector mass spectrometry, *Anal. Methods*. 7 (**2015**) 3036–3047. https://doi.org/10.1039/c5ay00017c.

[102] M. Qiao, W. Cao, B. Liu, X. Zhao, J. Qu, Simultaneous detection of chlorinated polycyclic aromatic hydrocarbons with polycyclic aromatic hydrocarbons by gas chromatography–mass spectrometry, *Anal. Bioanal. Chem*. 409 (**2017**) 3465–3473. https://doi.org/10.1007/s00216-017-0290-1.

[103] F. Han, Y. Gao, F. Hu, X. Yu, H. Xie, H. Li, Y. Zhao, S.Y. Kimura, Y. Zhang, M.E. Zubizarreta, S. Xiao, M. Zhan, W. Zheng, Solid-phase extraction of seventeen alternative flame retardants in water as determined by ultra-high-performance liquid chromatography-tandem mass spectrometry, *J. Chromatogr. A*. 1602 (**2019**) 64–73. https://doi.org/10.1016/j.chroma.2019.05.048.

[104] F. Gandolfi, L. Malleret, M. Sergent, P. Doumenq, Parameters optimization using experimental design for headspace solid phase micro-extraction analysis of short-chain chlorinated paraffins in waters under the European water framework directive, *J. Chromatogr. A*. 1406 (**2015**) 59–67. https://doi.org/10.1016/j.chroma.2015.06.030.

[105] C. Bach, V. Boiteux, J. Hemard, A. Colin, C. Rosin, J.-F. Munoz, X. Dauchy, Simultaneous determination of perfluoroalkyl iodides, perfluoroalkane sulfonamides, fluorotelomer alcohols, fluorotelomer iodides and fluorotelomer acrylates and methacrylates in water and sediments using solid-phase microextraction-gas chromatography/mass spectrometry, *J. Chromatogr. A.* 1448 (**2016**) 98–106. https://doi.org/10.1016/j.chroma.2016.04.025.

[106] I. Domínguez, F.J. Arrebola, R. Romero-González, A. Nieto-García, J.L. Martínez Vidal, A. Garrido Frenich, Solid phase microextraction and gas chromatography coupled to magnetic sector high resolution mass spectrometry for the ultra-trace determination of contaminants in surface water, *J. Chromatogr. A.* 1518 (**2017**) 15–24. https://doi.org/10.1016/j.chroma.2017.08.061.

[107] P. Tölgyessy, S. Nagyová, M. Sládkovičová, Determination of short chain chlorinated paraffins in water by stir bar sorptive extraction–thermal desorption–gas chromatography–triple quadrupole tandem mass spectrometry, *J. Chromatogr. A.* 1494 (**2017**) 77–80. https://doi.org/10.1016/j.chroma.2017.03.012.

[108] E. Barón, E. Eljarrat, D. Barceló, Analytical method for the determination of halogenated norbornene flame retardants in environmental and biota matrices by gas chromatography coupled to tandem mass spectrometry, *J. Chromatogr. A.* 1248 (**2012**) 154–160. https://doi.org/10.1016/j.chroma.2012.05.079.

[109] L. Aguilar, E.S. Williams, B.W. Brooks, S. Usenko, Development and application of a novel method for high-throughput determination of PCDD/Fs and PCBs in sediments, *Environ. Toxicol. Chem.* 33 (**2014**) 1529–1536. https://doi.org/10.1002/etc.2579.

[110] F. Li, J. Jin, D. Tan, J. Xu, Dhanjai, Y. Ni, H. Zhang, J. Chen, High performance solid-phase extraction cleanup method coupled with gas chromatography-triple quadrupole mass spectrometry for analysis of polychlorinated naphthalenes and dioxin-like polychlorinated biphenyls in complex samples, *J. Chromatogr. A.* 1448 (**2016**) 1–8. https://doi.org/10.1016/j.chroma.2016.04.037.

[111] D. Xia, L. Gao, M. Zheng, Q. Tian, H. Huang, L. Qiao, A Novel Method for Profiling and Quantifying Short- and Medium-Chain Chlorinated Paraffins in Environmental Samples Using Comprehensive Two-Dimensional Gas Chromatography-Electron Capture Negative Ionization High-Resolution Time-of-Flight Mass Spectrometry, *Environ. Sci. Technol.* 50 (**2016**) 7601–7609. https://doi.org/10.1021/acs.est.6b01404.

[112] Y. Zhao, Q. Li, X. Miao, X. Huang, B. Li, G. Su, M. Zheng, Determination of hexabromocyclododecanes in sediments from the Haihe River in China by an optimized HPLC–MS–MS method, *J. Environ. Sci.* 55 (**2017**) 174–183. https://doi.org/10.1016/j.jes.2016.07.013.

[113] X. Liu, Y. Wu, X. Zhang, L. Shen, A.L. Brazeau, D.H. Adams, H. Marler, B.D. Watts, D. Chen, Novel Dechlorane Analogues and Possible Sources in Peregrine Falcon Eggs and Shark Livers from the Western North Atlantic Regions, *Environ. Sci. Technol*. 53 (**2019**) 3419–3428. https://doi.org/10.1021/acs.est.8b06214.

[114] Z. Zhao, G. Zhong, A. Möller, Z. Xie, R. Sturm, R. Ebinghaus, J. Tang, G. Zhang, Levels and distribution of Dechlorane Plus in coastal sediments of the Yellow Sea, North China, *Chemosphere*. 83 (**2011**) 984–990. https://doi.org/10.1016/j.chemosphere.2011.02.011.

[115] D. Zacs, V. Bartkevics, A. Viksna, Content of polychlorinated dibenzo-p-dioxins, dibenzofurans and dioxin-like polychlorinated biphenyls in fish from Latvian lakes, *Chemosphere*. 91 (**2013**) 179–186. https://doi.org/10.1016/j.chemosphere.2012.12.041.

[116] D. Zacs, V. Bartkevics, Analytical capabilities of high performance liquid chromatography-Atmospheric pressure photoionization-Orbitrap mass spectrometry (HPLC-APPI-Orbitrap-MS) for the trace determination of novel and emerging flame retardants in fish, *Anal. Chim. Acta*. 898 (**2015**) 60–72. https://doi.org/10.1016/j.aca.2015.10.008 .

[117] P. Castells, J. Parera, F.J. Santos, M.T. Galceran, Occurrence of polychlorinated naphthalenes, polychlorinated biphenyls and short-chain chlorinated paraffins in marine sediments from Barcelona (Spain), *Chemosphere*. 70 (**2008**) 1552–1562. https://doi.org/10.1016/j.chemosphere.2007.08.034.

[118] G. Mascolo, V. Locaputo, G. Mininni, New perspective on the determination of flame retardants in sewage sludge by using ultrahigh pressure liquid chromatography-tandem mass spectrometry with different ion sources, *J. Chromatogr. A*. 1217 (**2010**) 4601–4611. https://doi.org/10.1016/j.chroma.2010.05.003.

[119] S. Chu, R.J. Letcher, Analysis of fluorotelomer alcohols and perfluorinated sulfonamides in biotic samples by liquid chromatography-atmospheric pressure photoionization mass spectrometry, *J. Chromatogr. A*. 1215 (**2008**) 92–99. https://doi.org/10.1016/j.chroma.2008.10.103.

[120] H. Peng, K. Hu, F. Zhao, J. Hu, Derivatization method for sensitive determination of fluorotelomer alcohols in sediment by liquid chromatography-electrospray tandem mass spectrometry, *J. Chromatogr. A*. 1288 (**2013**) 48–53. https://doi.org/10.1016/j.chroma.2013.02.085.

[121] M. Roszko, K. Szymczyk, R. Jedrzejczak, Separation of polychlorinated dibenzo-p-dioxins/furans, non-ortho/mono/di/tri/tetra-ortho-polychlorinated biphenyls, and polybrominated diphenyl ethers groups of compounds prior to their determination with large volume injection gas chromatography-Quadrupole ion storage tandem mass spectrometry, *Anal. Chim. Acta*. 799 (**2013**) 88–98. https://doi.org/10.1016/j.aca.2013.08.053.

[122] H. Zhang, S. Bayen, B.C. Kelly, Co-extraction and simultaneous determination of multi-class hydrophobic organic contaminants in marine sediments and biota using GC-EI-MS/MS and LC-ESI-MS/MS, *Talanta*. 143 (**2015**) 7–18. https://doi.org/10.1016/j.talanta.2015.04.084.

[123] V. Yusà, O. Pardo, A. Pastor, M. De La Guardia, Optimization of a microwave-assisted extraction large-volume injection and gas chromatography–ion trap mass spectrometry procedure for the determination of polybrominated diphenyl ethers, polybrominated biphenyls and polychlorinated naphthalenes in sediments, *Anal. Chim. Acta*. 557 (**2006**) 304–313. https://doi.org/10.1016/j.aca.2005.10.041.

[124] D. Lankova, M. Kockovska, O. Lacina, K. Kalachova, J. Pulkrabova, J. Hajslova, Rapid and simple method for determination of hexabromocyclododecanes and other LC-MS-MS-amenable brominated flame retardants in fish, *Anal. Bioanal. Chem*. 405 (**2013**) 7829–7839. https://doi.org/10.1007/s00216-013-7076-x.

[125] S. Iozza, P. Schmid, M. Oehme, Development of a comprehensive analytical method for the determination of chlorinated paraffins in spruce needles applied in passive air sampling, *Environ. Pollut*. 157 (**2009**) 3218–3224. https://doi.org/10.1016/j.envpol.2009.06.033.

[126] M. Gorga, E. Martínez, A. Ginebreda, E. Eljarrat, D. Barceló, Determination of PBDEs, HBB, PBEB, DBDPE, HBCD, TBBPA and related compounds in sewage sludge from Catalonia (Spain), *Sci. Total Environ*. 444 (**2013**) 51–59. https://doi.org/10.1016/j.scitotenv.2012.11.066.

[127] S. Pizzini, E. Marchiori, R. Piazza, G. Cozzi, C. Barbante, Determination by HRGC/HRMS of PBDE levels in edible Mediterranean bivalves collected from north-western Adriatic coasts, *Microchem. J*. 121 (**2015**) 184–191. https://doi.org/10.1016/j.microc.2015.03.010.

[128] Y. Moussaoui, L. Tuduri, Y. Kerchich, B.Y. Meklati, G. Eppe, Atmospheric concentrations of PCDD/Fs, dl-PCBs and some pesticides in northern Algeria using passive air sampling, *Chemosphere*. 88 (**2012**) 270–277. https://doi.org/10.1016/j.chemosphere.2012.02.025.

[129] R. Piazza, A. Gambaro, E. Argiriadis, M. Vecchiato, S. Zambon, P. Cescon, C. Barbante, Development of a method for simultaneous analysis of PCDDs, PCDFs, PCBs, PBDEs, PCNs and PAHs in Antarctic air, *Anal. Bioanal. Chem*. 405 (**2013**) 917–932. https://doi.org/10.1007/s00216-012-6464-y.

[130] F. Li, J. Jin, X. Sun, X. Wang, Y. Li, S.M. Shah, J. Chen, Gas chromatography-triple quadrupole mass spectrometry for the determination of atmospheric polychlorinated naphthalenes, *J. Hazard. Mater*. 280 (**2014**) 111–117. https://doi.org/10.1016/j.jhazmat.2014.07.060.

[131] R. Man, P. Ping-an, Z. Su-kung, D. Yun-yun, M. Bi-xian, S. Guo-ying, Determination of 2,3,7,8-Substitituted Polychlorinated Dibenzo-p-dioxins-Dibenzofurans and Dioxin-like Polychlorinated Biphenyls in Environmental Samples by Gas Chromatography/High Resolution Mass Spectrometry, *Chinese J. Anal. Chem*. 35 (**2007**) 176–180.

[132] Y. Fan, H. Zhang, D. Wang, M. Ren, X. Zhang, L. Wang, J. Chen, Simultaneous determination of chlorinated aromatic hydrocarbons in fly ashes discharged from industrial thermal processes, *Anal. Methods*. 9 (**2017**) 5198–5203. https://doi.org/10.1039/c7ay01545c.

[133] D. Megson, E.J. Reiner, K.J. Jobst, F.L. Dorman, M. Robson, J.-F. Focant, A review of the determination of persistent organic pollutants for environmental forensics investigations, *Anal. Chim. Acta*. 941 (**2016**) 10–25. https://doi.org/10.1016/j.aca.2016.08.027.

[134] N. Riddell, B. Van Bavel, I.E. Jogsten, R. McCrindle, A. McAlees, D. Potter, C. Tashiro, B. Chittim, Comparative assessment of the chromatographic separation of 2,3,7,8-substituted polychlorinated dibenzo-p-dioxins and polychlorinated dibenzofurans using supercritical fluid chromatography and high resolution gas chromatography, *Anal. Methods*. 7 (**2015**) 9245–9253. https://doi.org/10.1039/c5ay01644d.

[135] N. Riddell, B. van Bavel, I. Ericson Jogsten, R. McCrindle, A. McAlees, B. Chittim, Coupling supercritical fluid chromatography to positive ion atmospheric pressure ionization mass spectrometry: Ionization optimization of halogenated environmental contaminants, *Int. J. Mass Spectrom*. 421 (**2017**) 156–163. https://doi.org/10.1016/j.ijms.2017.07.005.

[136] N. Riddell, B. van Bavel, I. Ericson Jogsten, R. McCrindle, A. McAlees, B. Chittim, Coupling of supercritical fluid chromatography to mass spectrometry for the analysis of Dechlorane Plus: Examination of relevant negative ion atmospheric pressure chemical ionization mechanisms, *Talanta*. 171 (**2017**) 68–73. https://doi.org/10.1016/j.talanta.2017.04.066.

[137] J.L. Barber, U. Berger, C. Chaemfa, S. Huber, A. Jahnke, C. Temme, K.C. Jones, Analysis of per- and polyfluorinated alkyl substances in air samples from Northwest Europe, *J. Environ. Monit*. 9 (**2007**) 530–541. https://doi.org/10.1039/b701417a.

[138] R. Köppen, R. Becker, C. Jung, I. Nehls, On the thermally induced isomerisation of hexabromocyclododecane stereoisomers, *Chemosphere*. 71 (**2008**) 656–662. https://doi.org/10.1016/j.chemosphere.2007.11.009.

[139] Á. García-Bermejo, M. Ábalos, J. Sauló, E. Abad, M.J. González, B. Gómara, Triple quadrupole tandem mass spectrometry: A real alternative to high resolution magnetic sector instrument for the analysis of polychlorinated dibenzo-p-dioxins, furans and dioxin-like polychlorinated biphenyls, *Anal. Chim. Acta*. 889 (**2015**) 156–165. https://doi.org/10.1016/j.aca.2015.07.039.

[140] P. Xu, B. Tao, Z. Ye, L. Qi, Y. Ren, Z. Zhou, N. Li, Y. Huang, J. Chen, Simultaneous determination of three alternative flame retardants (dechlorane plus, 1,2-bis(2,4,6-tribromophenoxy) ethane, and decabromodiphenyl ethane) in soils by gas chromatography-high resolution mass spectrometry, *Talanta*. 144 (**2015**) 1014–1020. https://doi.org/10.1016/j.talanta.2015.07.031.

[141] C. Sales, T. Portolés, J.V. Sancho, E. Abad, M. Ábalos, J. Sauló, H. Fiedler, B. Gómara, J. Beltrán, Potential of gas chromatography-atmospheric pressure chemical ionization-tandem mass spectrometry for screening and quantification of hexabromocyclododecane, *Anal. Bioanal. Chem*. 408 (**2016**) 449–459. https://doi.org/10.1007/s00216-015-9146-8.

[142] A. Piersanti, T. Tavoloni, E. Bastari, C. Lestingi, S. Romanelli, R. Rossi, G. Saluti, S. Moretti, R. Galarini, A GC-EI-MS/MS Method for the Determination of 15 Polybrominated Diphenyl Ethers (PBDEs) in Fish and Shellfish Tissues, *Food Anal. Methods*. 11 (**2018**) 355–366. https://doi.org/10.1007/s12161-017-1006-z.

[143] R.A. Di Lorenzo, V. V. Lobodin, J. Cochran, T. Kolic, S. Besevic, J.G. Sled, E.J. Reiner, K.J. Jobst, Fast gas chromatography-atmospheric pressure (photo)ionization mass spectrometry of polybrominated diphenylether flame retardants, *Anal. Chim. Acta*. 1056 (**2019**) 70–78. https://doi.org/10.1016/j.aca.2019.01.007.

[144] H.M. Stapleton, Instrumental methods and challenges in quantifying polybrominated diphenyl ethers in environmental extracts: A review, *Anal. Bioanal. Chem*. 386 (**2006**) 807–817. https://doi.org/10.1007/s00216-006-0400-y.

[145] J. Rjabova, A. Viksna, D. Zacs, Development and optimization of gas chromatography coupled to high resolution mass spectrometry based method for the sensitive determination of Dechlorane plus and related norbornene-based flame retardants in food of animal origin, Chemosphere. 191 (2018) 597–606. https://doi.org/10.1016/j.chemosphere.2017.10.095.

[146] T.P. Rusina, P. Korytár, J. de Boer, Comparison of quantification methods for the analysis of polychlorinated alkanes using electron capture negative ionisation mass spectrometry, *Int. J. Environ. Anal. Chem*. 91 (**2011**) 319–332. https://doi.org/10.1080/03067311003602583.

[147] K. Krätschmer, C. Cojocariu, A. Schächtele, R. Malisch, W. Vetter, Chlorinated paraffin analysis by gas chromatography Orbitrap high-resolution mass spectrometry: Method performance, investigation of possible interferences and analysis of fish samples, *J. Chromatogr. A*. 1539 (**2018**) 53–61. https://doi.org/10.1016/j.chroma.2018.01.034.

[148] B. Van Bavel, D. Geng, L. Cherta, J. Nácher-Mestre, T. Portolés, M. Ábalos, J. Sauló, E. Abad, J. Dunstan, R. Jones, A. Kotz, H. Winterhalter, R. Malisch, W. Traag, J. Hagberg, I. Ericson Jogsten, J. Beltran, F. Hernández, Atmospheric-Pressure Chemical Ionization Tandem Mass Spectrometry (APGC/MS/MS) an Alternative to High-Resolution Mass Spectrometry (HRGC/HRMS) for the Determination of Dioxins, *Anal. Chem.* 87 (**2015**) 9047–9053. https://doi.org/10.1021/acs.analchem.5b02264.

[149] T. Portolés, C. Sales, M. Abalos, J. Sauló, E. Abad, Evaluation of the capabilities of atmospheric pressure chemical ionization source coupled to tandem mass spectrometry for the determination of dioxin-like polychlorobiphenyls in complex-matrix food samples, *Anal. Chim. Acta*. 937 (**2016**) 96–105. https://doi.org/10.1016/j.aca.2016.06.038.

[150] D. Geng, I.E. Jogsten, J. Dunstan, J. Hagberg, T. Wang, J. Ruzzin, R. Rabasa-Lhoret, B. van Bavel, Gas chromatography/atmospheric pressure chemical ionization/mass spectrometry for the analysis of organochlorine pesticides and polychlorinated biphenyls in human serum, *J. Chromatogr. A*. 1453 (**2016**) 88–98. https://doi.org/10.1016/j.chroma.2016.05.030.

[151] J. Stubleski, P. Kukucka, S. Salihovic, P.M. Lind, L. Lind, A. Kärrman, A method for analysis of marker persistent organic pollutants in low-volume plasma and serum samples using 96-well plate solid phase extraction, *J. Chromatogr. A*. 1546 (**2018**) 18–27. https://doi.org/10.1016/j.chroma.2018.02.057.

[152] S.N. Zhou, E.J. Reiner, C.H. Marvin, P.A. Helm, L. Shen, I.D. Brindle, Liquid chromatography/atmospheric pressure photoionization tandem mass spectrometry for analysis of Dechloranes, *Rapid Commun. Mass Spectrom*. 25 (**2011**) 436–442. https://doi.org/10.1002/rcm.4874.

[153] O. Lacina, P. Hradkova, J. Pulkrabova, J. Hajslova, Simple, high throughput ultra-high performance liquid chromatography/tandem mass spectrometry trace analysis of perfluorinated alkylated substances in food of animal origin: Milk and fish, *J. Chromatogr. A*. 1218 (**2011**) 4312–4321. https://doi.org/10.1016/j.chroma.2011.04.061.

[154] S.Y. Baek, S. Lee, B. Kim, Separation of hexabromocyclododecane diastereomers: Application of C18 and phenyl-hexyl ultra-performance liquid chromatography columns, *J. Chromatogr. A*. 1488 (**2017**) 140–145. https://doi.org/10.1016/j.chroma.2017.01.047.

[155] L. Zheng, L. Lian, J. Nie, Y. Song, S. Yan, D. Yin, W. Song, Development of an ammonium chloride-enhanced thermal-assisted-ESI LC-HRMS method for the characterization of chlorinated paraffins, *Environ. Pollut*. 255 (**2019**) 113303. https://doi.org/10.1016/j.envpol.2019.113303.

[156] N. Hanari, J. Falandysz, T. Nakano, G. Petrick, N. Yamashita, Separation of closely eluting chloronaphthalene congeners by two-dimensional gas chromatography/quadrupole mass spectrometry: An advanced tool in the study and risk analysis of dioxin-like chloronaphthalenes, *J. Chromatogr. A*. 1301 (**2013**) 209–214. https://doi.org/10.1016/j.chroma.2013.05.070.

[157] S. Hashimoto, Y. Takazawa, A. Fushimi, K. Tanabe, Y. Shibata, T. Ieda, N. Ochiai, H. Kanda, T. Ohura, Q. Tao, S.E. Reichenbach, Global and selective detection of organohalogens in environmental samples by comprehensive two-dimensional gas chromatography-tandem mass spectrometry and high-resolution time-of-flight mass spectrometry, *J. Chromatogr. A*. 1218 (**2011**) 3799–3810. https://doi.org/10.1016/j.chroma.2011.04.042.

[158] D. Xia, L. Gao, M. Zheng, S. Wang, G. Liu, Simultaneous analysis of polychlorinated biphenyls and polychlorinated naphthalenes by isotope dilution comprehensive two-dimensional gas chromatography high-resolution time-of-flight mass spectrometry, *Anal. Chim. Acta*. 937 (**2016**) 160–167. https://doi.org/10.1016/j.aca.2016.07.018.

[159] K. Janák, A. Covaci, S. Voorspoels, G. Becher, Hexabromocyclododecane in marine species from the Western Scheldt Estuary: Diastereoisomer- and enantiomer-specific accumulation, *Environ. Sci. Technol*. 39 (**2005**) 1987–1994. https://doi.org/10.1021/es0484909.

[160] S.A. Mackintosh, A. Pérez-Fuentetaja, L.R. Zimmerman, G. Pacepavicius, M. Clapsadl, M. Alaee, D.S. Aga, Analytical performance of a triple quadrupole mass spectrometer compared to a high resolution mass spectrometer for the analysis of polybrominated diphenyl ethers in fish, *Anal. Chim. Acta*. 747 (**2012**) 67–75. https://doi.org/10.1016/j.aca.2012.08.021.

[161] N. Barco-Bonilla, P. Plaza-Bolaños, N.M.V. Tarifa, R. Romero-González, J.L.M. Vidal, A.G. Frenich, Highly sensitive determination of polybrominated diphenyl ethers in surface water by GC coupled to high-resolution MS according to the EU Water Directive 2008/105/EC, *J. Sep. Sci*. 37 (**2014**) 69–76. https://doi.org/10.1002/jssc.201300757.

[162] J.J. Ellington, J.W. Washington, J.J. Evans, T.M. Jenkins, S.C. Hafner, M.P. Neill, Analysis of fluorotelomer alcohols in soils: Optimization of extraction and chromatography, *J. Chromatogr. A*. 1216 (**2009**) 5347–5354. https://doi.org/10.1016/j.chroma.2009.05.035.

[163] U.E. Fridén, M.S. McLachlan, U. Berger, Chlorinated paraffins in indoor air and dust: Concentrations, congener patterns, and human exposure, *Environ. Int.* 37 (**2011**) 1169–1174. https://doi.org/10.1016/j.envint.2011.04.002.

[164] Z. Zencak, A. Borgen, M. Reth, M. Oehme, Evaluation of four mass spectrometric methods for the gas chromatographic analysis of polychlorinated n-alkanes, *J. Chromatogr. A*. 1067 (**2005**) 295–301. https://doi.org/10.1016/j.chroma.2004.09.098.

[165] E. Jakobsson, L. Asplund, Polychlorinated Naphthalenes (PCNs), in: J. Paasivirta (Ed.), *Handb. Environ. Chem. Vol. 3 Anthropog. Compd. Part K New Types Persistent Halogenated Compd*., Springer-Verlag, Berlin, (**2000**): pp. 97–126. https://doi.org/10.1007/3-540-48915-0_5.

[166] C. Perazzolli, I. Mancini, G. Guella, Benzene-assisted atmospheric-pressure chemical ionization: A new liquid chromatography/mass spectrometry approach to the analysis of selected hydrophobic compounds, *Rapid Commun. Mass Spectrom*. 19 (**2005**) 461–469. https://doi.org/10.1002/rcm.1807.

[167] L. Debrauwer, A. Riu, M. Jouahri, E. Rathahao, I. Jouanin, J.P. Antignac, R. Cariou, B. Le Bizec, D. Zalko, Probing new approaches using atmospheric pressure photo ionization for the analysis of brominated flame retardants and their related degradation products by liquid chromatography-mass spectrometry, *J. Chromatogr. A.* 1082 (**2005**) 98–109. https://doi.org/10.1016/j.chroma.2005.04.060.

[168] R. McCulloch, A. Alvaro, A.M. Astudillo, J.C. del Castillo, M. Gómez, J.M. Martín, M. Amo-González, A novel atmospheric pressure photoionization – Mass spectrometry (APPI-MS) method for the detection of polychlorinated dibenzo P- dioxins and dibenzofuran homologues in real environmental samples collected within the vicinity of industrial incinerators, *Int. J. Mass Spectrom*. 421 (**2017**) 135–143. https://doi.org/10.1016/j.ijms.2017.05.016.

[169] A. Riu, D. Zalko, L. Debrauwer, Study of polybrominated diphenyl ethers using both positive and negative atmospheric pressure photoionization and tandem mass spectrometry, *Rapid Commun. Mass Spectrom*. 20 (**2006**) 2133–2142. https://doi.org/10.1002/rcm.2557.

[170] M.A.E. Abdallah, S. Harrad, A. Covaci, Isotope dilution method for determination of polybrominated diphenyl ethers using liquid chromatography coupled to negative ionization atmospheric pressure photoionization tandem mass spectrometry: Validation and application to house dust, *Anal. Chem*. 81 (**2009**) 7460–7467. https://doi.org/10.1021/ac901305n.

[171] X. Wang, X. Zhang, Z. Wang, Y. Chen, X. Li, Z. Cui, Determination of hexabromocyclododecane in soil by supercritical fluid extraction and gas chromatography mass spectrometry, *Anal. Methods*. 10 (**2018**) 1181–1189. https://doi.org/10.1039/c8ay00018b.

[172] C. Gremmel, T. Frömel, T.P. Knepper, Systematic determination of perfluoroalkyl and polyfluoroalkyl substances (PFASs) in outdoor jackets, *Chemosphere*. 160 (**2016**) 173–180. https://doi.org/10.1016/j.chemosphere.2016.06.043.

[173] Y. Gao, H. Zhang, L. Zou, P. Wu, Z. Yu, X. Lu, J. Chen, Quantification of Short-Chain Chlorinated Paraffins by Deuterodechlorination Combined with Gas Chromatography-Mass Spectrometry, *Environ. Sci. Technol*. 50 (**2016**) 3746–3753. https://doi.org/10.1021/acs.est.5b05115.

[174] W. Gao, J. Wu, Y. Wang, G. Jiang, Quantification of short- and medium-chain chlorinated paraffins in environmental samples by gas chromatography quadrupole time-of-flight mass spectrometry, J*. Chromatogr. A.* 1452 (**2016**) 98–106. https://doi.org/10.1016/j.chroma.2016.04.081.

[175] T. Li, Y. Wan, S. Gao, B. Wang, J. Hu, High-Throughput Determination and Characterization of Short-, Medium-, and Long-Chain Chlorinated Paraffins in Human Blood, *Environ. Sci. Technol*. 51 (**2017**) 3346–3354. https://doi.org/10.1021/acs.est.6b05149.

[176] C. Bogdal, T. Alsberg, P.S. Diefenbacher, M. Macleod, U. Berger, Fast quantification of chlorinated paraffins in environmental samples by direct injection high-resolution mass spectrometry with pattern deconvolution, *Anal. Chem*. 87 (**2015**) 2852–2860. https://doi.org/10.1021/ac504444d.

[177] B. Yuan, T. Alsberg, C. Bogdal, M. MacLeod, U. Berger, W. Gao, Y. Wang, C.A. De Wit, Deconvolution of Soft Ionization Mass Spectra of Chlorinated Paraffins to Resolve Congener Groups, *Anal. Chem*. 88 (**2016**) 8980–8988. https://doi.org/10.1021/acs.analchem.6b01172.

[178] B. Yuan, C. Bogdal, U. Berger, M. MacLeod, W.A. Gebbink, T. Alsberg, C.A. De Wit, Quantifying Short-Chain Chlorinated Paraffin Congener Groups, *Environ. Sci. Technol*. 51 (**2017**) 10633–10641. https://doi.org/10.1021/acs.est.7b02269.

[179] B. Yuan, J.P. Benskin, C.E.L. Chen, Å. Bergman, Determination of Chlorinated Paraffins by Bromide-Anion Attachment Atmospheric-Pressure Chemical Ionization Mass Spectrometry, *Environ. Sci. Technol. Lett*. 5 (**2018**) 348–353. https://doi.org/10.1021/acs.estlett.8b00216.

[180] Y. Wang, Y. Sun, T. Chen, Z. Shi, X. Zhou, Z. Sun, L. Zhang, J. Li, Determination of polybrominated diphenyl ethers and novel brominated flame retardants in human serum by gas chromatography-atmospheric pressure chemical ionization-tandem mass spectrometry, *J. Chromatogr. B*. 1099 (**2018**) 64–72. https://doi.org/10.1016/j.jchromb.2018.09.015.

[181] F.L. Chiriac, L. Cruceru, M. Niculescu, L.F. Pascu, C.B. Lehr, T. Galaon, Simultaneous Determination of α-,β-and γ-hexabromocyclododecane Diastereoisomers in Sewage Sludge using Liquid Chromatography Tandem Mass Spectrometry, *Rev. Chim*. 68 (**2017**) 1685–1689.

[182] D. Zacs, J. Rjabova, V. Bartkevics, New perspectives on diastereoselective determination of hexabromocyclododecane traces in fish by ultra high performance liquid chromatography-high resolution orbitrap mass spectrometry, *J. Chromatogr. A*. 1330 (**2014**) 30–39. https://doi.org/10.1016/j.chroma.2014.01.023.

[183] J. Feng, Y. Wang, T. Ruan, G. Qu, G. Jiang, Simultaneous determination of hexabromocyclododecanes and tris (2,3-dibromopropyl) isocyanurate using LC-APCI-MS/MS, *Talanta*. 82 (**2010**) 1929–1934. https://doi.org/10.1016/j.talanta.2010.08.014.

[184] M.S. Ross, C.S. Wong, Comparison of electrospray ionization, atmospheric pressure photoionization, and anion attachment atmospheric pressure photoionization for the analysis of hexabromocyclododecane enantiomers in environmental samples, *J. Chromatogr. A*. 1217 (**2010**) 7855–7863. https://doi.org/10.1016/j.chroma.2010.09.083.

[185] M. Smoluch, J. Silberring, E. Reszke, J. Kuc, A. Grochowalski, Determination of hexabromocyclododecane by flowing atmospheric pressure afterglow mass spectrometry, *Talanta*. 128 (**2014**) 58–62. https://doi.org/10.1016/j.talanta.2014.04.042.

[186] D. Megson, M. Robson, K.J. Jobst, P.A. Helm, E.J. Reiner, Determination of halogenated flame retardants using gas chromatography with atmospheric pressure chemical ionization (APCI) and a high-resolution quadrupole time-of-flight mass spectrometer (HRqTOFMS), *Anal. Chem*. 88 (**2016**) 11406–11411. https://doi.org/10.1021/acs.analchem.6b01550.

[187] V. Hloušková, D. Lanková, K. Kalachová, P. Hrádková, J. Poustka, J. Hajšlová, J. Pulkrabová, Brominated flame retardants and perfluoroalkyl substances in sediments from the Czech aquatic ecosystem, *Sci. Total Environ*. 470–471 (**2014**) 407–416. https://doi.org/10.1016/j.scitotenv.2013.09.074

[188] T. Portolés, C. Sales, B. Gómara, J.V. Sancho, J. Beltrán, L. Herrero, M.J. González, F. Hernández, Novel Analytical Approach for Brominated Flame Retardants Based on the Use of Gas Chromatography-Atmospheric Pressure Chemical Ionization-Tandem Mass Spectrometry with Emphasis in Highly Brominated Congeners, *Anal. Chem*. 87 (**2015**) 9892–9899. https://doi.org/10.1021/acs.analchem.5b02378.

[189] X. Zheng, K.T. Dupuis, N.A. Aly, Y. Zhou, F.B. Smith, K. Tang, R.D. Smith, E.S. Baker, Utilizing ion mobility spectrometry and mass spectrometry for the analysis of polycyclic aromatic hydrocarbons, polychlorinated biphenyls, polybrominated diphenyl ethers and their metabolites, *Anal. Chim. Acta*. 1037 (**2018**) 265–273. https://doi.org/10.1016/j.aca.2018.02.054.

[190] D.G. Hayward, J.C. Archer, S. Andrews, R.D. Fairchild, J. Gentry, R. Jenkins, M. McLain, U. Nasini, S. Shojaee, Application of a High-Resolution Quadrupole/Orbital Trapping Mass Spectrometer Coupled to a Gas Chromatograph for the Determination of Persistent Organic Pollutants in Cow's and Human Milk, *J. Agric. Food Chem*. 66 (**2018**) 11823–11829. https://doi.org/10.1021/acs.jafc.8b03721.

[191] K.L. Organtini, L. Haimovici, K.J. Jobst, E.J. Reiner, A. Ladak, D. Stevens, J.W. Cochran, F.L. Dorman, Comparison of Atmospheric Pressure Ionization Gas Chromatography-Triple Quadrupole Mass Spectrometry to Traditional High-Resolution Mass Spectrometry for the Identification and Quantification of Halogenated Dioxins and Furans, *Anal. Chem*. 87 (**2015**) 7902–7908. https://doi.org/10.1021/acs.analchem.5b01705.

[192] J. Rivera-Austrui, K. Martínez, M. Ábalos, C. Sales, T. Portoles, J. Beltran, J. Sauló, B.H. Aristizábal, E. Abad, Analysis of polychlorinated dibenzo-p-dioxins and dibenzofurans in stack gas emissions by gas chromatography-atmospheric pressure chemical ionization-triple-quadrupole mass spectrometry, *J. Chromatogr. A*. 1513 (**2017**) 245–249. https://doi.org/10.1016/j.chroma.2017.07.039.

[193] G. ten Dam, I.C. Pussente, G. Scholl, G. Eppe, A. Schaechtele, S. van Leeuwen, The performance of atmospheric pressure gas chromatography–tandem mass spectrometry compared to gas chromatography–high resolution mass spectrometry for the analysis of polychlorinated dioxins and polychlorinated biphenyls in food and feed samples, *J. Chromatogr. A*. 1477 (**2016**) 76–90. https://doi.org/10.1016/j.chroma.2016.11.035.

[194] F. Hernández, M. Ibáñez, T. Portolés, M.I. Cervera, J. V. Sancho, F.J. López, Advancing towards universal screening for organic pollutants in waters, *J. Hazard. Mater*. 282 (**2015**) 86–95. https://doi.org/10.1016/j.jhazmat.2014.08.006.

[195] L. Luosujärvi, M.-M. Karikko, M. Haapala, V. Saarela, S. Huhtala, S. Franssila, R. Kostiainen, T. Kotiaho, T.J. Kauppila, Gas chromatography/mass spectrometry of polychlorinated biphenyls using atmospheric pressure chemical ionization and atmospheric pressure photoionization microchips, *Rapid Commun. Mass Spectrom*. 22 (**2008**) 425–431. https://doi.org/10.1002/rcm.3379.

[196] R. Lega, D. Megson, C. Hartley, P. Crozier, K. MacPherson, T. Kolic, P.A. Helm, A. Myers, S.P. Bhavsar, E.J. Reiner, Congener specific determination of polychlorinated naphthalenes in sediment and biota by gas chromatography high resolution mass spectrometry, *J. Chromatogr. A*. 1479 (**2017**) 169–176. https://doi.org/10.1016/j.chroma.2016.11.054.

[197] D. Carrizo, J.O. Grimalt, Rapid and simplified method for the analysis of polychloronaphthalene congener distributions in environmental and human samples by gas chromatography coupled to negative ion chemical ionization mass spectrometry, *J. Chromatogr. A*. 1118 (**2006**) 271–277. https://doi.org/10.1016/j.chroma.2006.03.108.

[198] I.A. Revelsky, Y.S. Yashin, T.G. Sobolevsky, A.I. Revelsky, B. Miller, V. Oriedo, Electron ionization and atmospheric pressure photochemical ionization in gas chromatography-mass spectrometry analysis of amino acids, *Eur. J. Mass Spectrom*. 9 (**2003**) 497–507. https://doi.org/10.1255/ejms.581.

[199] C.N. McEwen, R.G. McKay, A combination atmospheric pressure LC/MS:GC/MS ion source: Advantages of dual AP-LC/MS:GC/MS instrumentation, *J. Am. Soc. Mass Spectrom*. 16 (**2005**) 1730–1738. https://doi.org/10.1016/j.jasms.2005.07.005.

[200] B. Szostek, K.B. Prickett, Determination of 8:2 fluorotelomer alcohol in animal plasma and tissues by gas chromatography-mass spectrometry, *J. Chromatogr. B.* 813 (**2004**) 313–321. https://doi.org/10.1016/j.jchromb.2004.10.031.

[201] G. Lindström, H. Wingfors, M. Dam, B. van Bavel, Identification of 19 polybrominated diphenyl ethers (PBDEs) in long- finned pilot whale (Globicephala melas) from the Atlantic, *Arch. Environ. Contam. Toxicol*. 36 (**1999**) 355–363. https://doi.org/10.1007/s002449900482.

[202] T. Ieda, S. Hashimoto, T. Isobe, T. Kunisue, S. Tanabe, Evaluation of a data-processing method for target and non-target screening using comprehensive two-dimensional gas chromatography coupled with high-resolution time-of-flight mass spectrometry for environmental samples, *Talanta*. 194 (**2019**) 461–468. https://doi.org/10.1016/j.talanta.2018.10.050.

[203] K.J. Jobst, L. Shen, E.J. Reiner, V.Y. Taguchi, P.A. Helm, R. McCrindle, S. Backus, The use of mass defect plots for the identification of (novel) halogenated contaminants in the environment, *Anal. Bioanal. Chem*. 405 (**2013**) 3289–3297. https://doi.org/10.1007/s00216-013-6735-2.

[204] T. Portolés, J.G.J. Mol, J. V. Sancho, F. Hernández, Use of electron ionization and atmospheric pressure chemical ionization in gas chromatography coupled to time-of-flight mass spectrometry for screening and identification of organic pollutants in waters, *J. Chromatogr. A*. 1339 (**2014**) 145–153. https://doi.org/10.1016/j.chroma.2014.03.001.

[205] N.D. Dat, K.-S. Chang, C.P. Wu, Y.-J. Chen, C.-L. Tsai, K.H. Chi, M.-B. Chang, Measurement of PCNs in sediments collected from reservoir and river in northern Taiwan, *Ecotoxicol. Environ. Saf*. 174 (**2019**) 384–389. https://doi.org/10.1016/j.ecoenv.2019.02.087.

[206] M. Reth, Z. Zencak, M. Oehme, New quantification procedure for the analysis of chlorinated paraffins using electron capture negative ionization mass spectrometry, *J. Chromatogr. A*. 1081 (**2005**) 225–231. https://doi.org/10.1016/j.chroma.2005.05.061.

[207] E.C. Horning, D.I. Carroll, I. Dzidic, S.-N. Lin, R.N. Stillwell, J.P. Thenot, Atmospheric pressure ionization mass spectrometry studies of negative ion formation for detection and quantification purposes, J. Chromatogr. 142 (**1977**) 481–495.

[208] I. Dzidic, D.I. Carroll, R.N. Stillwell, E.C. Horning, Comparison of Positive Ions Formed in Nickel-63 and Corona Discharge Ion Sources Using Nitrogen, Argon, Isobutane, Ammonia and Nitric Oxide as Reagents in Atmospheric Pressure Ionization Mass Spectrometry, *Anal. Chem*. 48 (**1976**) 1763–1768. https://doi.org/10.1021/ac50006a035.

[209] R.K. Mitchum, W.A. Korfmacher, G.F. Moler, Capillary Gas Chromatography/Atmospheric Pressure Negative Chemical Ionization Mass Spectrometry of the 22 Isomeric Tetrachlorodibenzo-*p*-dioxins, *Anal. Chem*. 54 (**1982**) 719–722.

[210] R.K. Mitchum, G.F. Moler, W.A. Korfmacher, Combined Capillary Gas Chromatography/Atmospheric Pressure Negative Chemical Ionization/Mass Spectrometry For The Determination Of 2, 3, 7, 8-Tetrachlorodibenzo-*ρ*-Dioxin In Tissue, *Anal. Chem*. 52 (**1980**) 2278–2282. https://doi.org/10.1021/ac50064a011.

[211] W.A. Korfmacher, K.R. Rowland, R.K. Mitchum, J.J. Daly, R.C. McDaniel, M. V. Plummer, Analysis of snake tissue and snake eggs for 2,3,7,8-tetrachlorodibenzo-*p*-dioxin via fused silica GC combined with atmospheric pressure ionization MS, *Chemosphere*. 13 (**1984**) 1229–1233. https://doi.org/10.1016/0045-6535(84)90123-1.

[212] W.A. Kofmacher, G.F. Moler, R.R. Delongchamp, R.K. Mitchum, Validation study for the gas chromatographic-atmospheric pressure ionization-mass spectrometric method for the isomer-specific determination of 2,3,7,8-tetrachlorodibenzo-p-dioxin, Chemosphere. 13 (**1984**) 669–685.

[213] W.A. Korfmacher, R.K. Mitchum, F.D. Hileman, T. Mazer, Analysis of 2,3,7,8-tetrachlorodibenzofuran by fused silica GC combined with atmospheric pressure ionization MS, *Chemosphere*. 12 (**1983**) 1243–1249. https://doi.org/10.1016/0045-6535(83)90129-7.

[214] W.A. Korfmacher, P.P. Fu, M. Chou, R.K. Mitchum, Separation and Analysis of 3-Nitrobenzo[e]pyrene and 1-,3-, and 6-Nitrobenzo[a]pyrene via Fused Silica GC Combined with Negative Ionization Atmospheric Pressure Ionization Mass Spectrometry, *J. High Resolut. Chromatogr*. 7 (**1984**) 41–42.

[215] W.A. Korfmacher, D.W. Miller, Analysis of 1- and 4-nitropyrene and 1-nitropyrene-d9 via fused silica GC combined with negative ion atmospheric pressure ionization mass spectrometry, J. High Resolut. Chromatogr. 7 (1984) 581–583. https://doi.org/10.1002/jhrc.1240071009.

[216] W.A. Korfmacher, L.G. Rushing, J. Arey, B. Zielinska, J.N. Pitts, Identification of mononitropyrenes and mononitrofluoranthenes in air particulate matter via fused silica gas, chromatography combined with negative ion atmospheric pressure ionization mass spectrometry, *J. High Resolut. Chromatogr*. 10 (**1987**) 641–646. https://doi.org/10.1002/jhrc.1240101204.

[217] R.J. Engelbach, W.A. Korfmacher, L.G. Rushing, Analysis of nitropyrenamines and methylated nitropyrenamines via gas chromatography-negative ion atmospheric pressure ionization mass spectrometry, *J. High Resolut. Chromatogr*. 11 (**1988**) 661–663. https://doi.org/10.1002/jhrc.1240110909.

[218] T. Kinouchi, A.T.L. Miranda, L.G. Rushing, F.A. Beland, W.A. Korfmacher, Detection of 2-aminofluorene at femtogram levels via high resolution gas chromatography combined with negative ion atmospheric pressure ionization mass spectrometry, *J. High Resolut. Chromatogr*. 13 (**1990**) 281–284. https://doi.org/10.1002/jhrc.1240130415.

[219] C.-Y. Lee, J. Shiea, Gas Chromatography Connected to Multiple Channel Electrospray Ionization Mass Spectrometry for the Detection of Volatile Organic Compounds, *Anal. Chem*. 70 (**1998**) 2757–2761. https://doi.org/10.1021/ac971325.

[220] C. Wu, W.F. Siems, H.H. Hill, Secondary electrospray ionization ion mobility spectrometry/mass spectrometry of illicit drugs, *Anal. Chem*. 72 (**2000**) 396–403. https://doi.org/10.1021/ac9907235.

[221] R. Schiewek, M. Schellenträger, R. Mönnikes, M. Lorenz, R. Giese, K.J. Brockmann, S. Gäb, T. Benter, O.J. Schmitz, Ultrasensitive determination of polycyclic aromatic compounds with atmospheric-pressure laser ionization as an interface for GC/MS, *Anal. Chem.* 79 (**2007**) 4135–4140. https://doi.org/10.1021/ac0700631.

[222] R. Schiewek, M. Lorenz, R. Giese, K. Brockmann, T. Benter, S. Gäb, O.J. Schmitz, Development of a multipurpose ion source for LC-MS and GC-API MS, *Anal. Bioanal. Chem.* 392 (**2008**) 87–96. https://doi.org/10.1007/s00216-008-2255-x.

[223] R. Schiewek, R. Mönnikes, V. Wulf, S. Gäb, K.J. Brockmann, T. Benter, O.J. Schmitz, A universal ionization label for the APLI-(TOF)MS analysis of small molecules and polymers, *Angew. Chemie - Int. Ed.* 47 (**2008**) 9989–9992. https://doi.org/10.1002/anie.200804106.

[224] A.W. Nørgaard, V. Kofoed-Sørensen, B. Svensmark, P. Wolkoff, P.A. Clausen, Gas chromatography interfaced with atmospheric pressure ionization-quadrupole time-of-flight-mass spectrometry by low-temperature plasma ionization, *Anal. Chem.* 85 (**2013**) 28–32. https://doi.org/10.1021/ac301859r.

[225] C. Stader, F.T. Beer, C. Achten, Environmental PAH analysis by gas chromatography-atmospheric pressure laser ionization-time-of-flight-mass spectrometry (GC-APLI-MS), *Anal. Bioanal. Chem.* 405 (**2013**) 7041–7052. https://doi.org/10.1007/s00216-013-7183-8.

[226] C. Achten, F.T. Beer, C. Stader, S.G. Brinkhaus, Wood-Specific Polycyclic Aromatic Hydrocarbon (PAH) Patterns in Soot Using Gas Chromatography-Atmospheric Pressure Laser Ionization-Mass Spectrometry (GC-APLI-MS), *Environ. Forensics.* 16 (**2015**) 42–50. https://doi.org/10.1080/15275922.2014.991004.

[227] P. Benigni, J.D. Debord, C.J. Thompson, P. Gardinali, F. Fernandez-Lima, Increasing Polyaromatic Hydrocarbon (PAH) Molecular Coverage during Fossil Oil Analysis by Combining Gas Chromatography and Atmospheric-Pressure Laser Ionization Fourier Transform Ion Cyclotron Resonance Mass Spectrometry (FT-ICR MS), *Energy and Fuels.* 30 (**2016**) 196–203. https://doi.org/10.1021/acs.energyfuels.5b02292.

[228] S. Große Brinkhaus, J.B. Thiäner, C. Achten, Ultra-high sensitive PAH analysis of certified reference materials and environmental samples by GC-APLI-MS, *Anal. Bioanal. Chem.* 409 (**2017**) 2801–2812. https://doi.org/10.1007/s00216-017-0224-y.

[229] A. Leider, S. Richter-Brockmann, B.J. Nettersheim, C. Achten, C. Hallmann, Low-femtogram sensitivity analysis of polyaromatic hydrocarbons using GC-APLI-TOF mass spectrometry: Extending the target window for aromatic steroids in early Proterozoic rocks, *Org. Geochem.* 129 (**2019**) 77–87. https://doi.org/10.1016/j.orggeochem.2019.01.015.

[230] J.F. Dohmann, J.B. Thiäner, C. Achten, Ultrasensitive detection of polycyclic aromatic hydrocarbons in coastal and harbor water using GC-APLI-MS, *Mar. Pollut. Bull*. 149 (**2019**) 110547. https://doi.org/10.1016/j.marpolbul.2019.110547.

[231] M. Raro, T. Portolés, J. V. Sancho, E. Pitarch, F. Hernández, J. Marcos, R. Ventura, C. Gómez, J. Segura, O.J. Pozo, Mass spectrometric behavior of anabolic androgenic steroids using gas chromatography coupled to atmospheric pressure chemical ionization source. Part I: Ionization, *J. Mass Spectrom*. 49 (**2014**) 509–521. https://doi.org/10.1002/jms.3367.

[232] T. Portolés, J. V. Sancho, F. Hernández, A. Newton, P. Hancock, Potential of atmospheric pressure chemical ionization source in GC-QTOF MS for pesticide residue analysis, *J. Mass Spectrom*. 45 (**2010**) 926–936. https://doi.org/10.1002/jms.1784.

[233] C.J. Wachsmuth, K. Dettmer, S.A. Lang, M.E. Mycielska, P.J. Oefner, Continuous water infusion enhances atmospheric pressure chemical ionization of methyl chloroformate derivatives in gas chromatography coupled to time-of-flight mass spectrometry-based metabolomics, *Anal. Chem*. 86 (**2014**) 9186–9195. https://doi.org/10.1021/ac502133r.

[234] C. Stultz, K.J. Jobst, L. Haimovici, R. Jones, S. Besevic, J. Byer, K.L. Organtini, T. Kolic, E.J. Reiner, F.L. Dorman, Evaluation of multiple alternative instrument platforms for targeted and non-targeted dioxin and furan analysis, *J. Mass Spectrom*. 53 (**2018**) 504–510. https://doi.org/10.1002/jms.4086.

[235] D.X. Li, L. Gan, A. Bronja, O.J. Schmitz, Gas chromatography coupled to atmospheric pressure ionization mass spectrometry (GC-API-MS): Review, *Anal. Chim. Acta*. 891 (**2015**) 43–61. https://doi.org/10.1016/j.aca.2015.08.002.

[236] C.N. McEwen, GC/MS on an LC/MS instrument using atmospheric pressure photoionization, *Int. J. Mass Spectrom*. 259 (**2007**) 57–64. https://doi.org/10.1016/j.ijms.2006.07.004.

[237] T. Suominen, M. Haapala, A. Takala, R.A. Ketola, R. Kostiainen, Neurosteroid analysis by gas chromatography – atmospheric pressure photoionization – tandem mass spectrometry, *Anal. Chim. Acta*. 794 (**2013**) 76–81. https://doi.org/10.1016/j.aca.2013.07.055.

[238] T.J. Kauppila, H. Kersten, T. Benter, The Ionization Mechanisms in Direct and Dopant-Assisted Atmospheric Pressure Photoionization and Atmospheric Pressure Laser Ionization, *J. Am. Soc. Mass Spectrom*. 25 (**2014**) 1870–1881. https://doi.org/10.1007/s13361-014-0988-7.

[239] H. Kersten, K. Kroll, K. Haberer, K.J. Brockmann, T. Benter, A. Peterson, A. Makarov, Design Study of an Atmospheric Pressure Photoionization Interface for GC-MS, *J. Am. Soc. Mass Spectrom*. 27 (**2016**) 607–614. https://doi.org/10.1007/s13361-015-1320-x.

[240] A.C. Peterson, H. Kersten, D. Krumwiede, S. Quarmby, K. D'Silva, K. Kroll, K. Haberer, M. Bromirski, A. Makarov, T. Benter, Analytical performance of a novel, dopant-free GC-APPI source with femtogram-level sensitivity for quadrupole-Orbitrap GC/MS, (**2013**).

[241] T.J. Kauppila, H. Kersten, T. Benter, Ionization of EPA Contaminants in Direct and Dopant-Assisted Atmospheric Pressure Photoionization and Atmospheric Pressure Laser Ionization, *J. Am. Soc. Mass Spectrom*. 26 (**2015**) 1036–1045. https://doi.org/10.1007/s13361-015-1092-3.

[242] E. Hoffmann, V. Stroobant, Mass Spectrometry. Principles and Applications, 3er ed., John Wiley & Sons Ltd., New Jersey, (**2007**). https://doi.org/10.1007/978-1-4939-7877-9_17.

[243] I.A. Revelsky, Y.S. Yashin, New approach to complex organic compounds mixtures analysis based on gas chromatography-atmospheric pressure photoionization-mass-spectrometry, *Talanta*. 102 (**2012**) 110–113. https://doi.org/10.1016/j.talanta.2012.07.023.

[244] Y.J. Lee, E.A. Smith, J.H. Jun, Gas Chromatography-High Resolution Tandem Mass Spectrometry Using a GC-APPI-LIT Orbitrap for Complex Volatile Compounds Analysis, *Mass Spectrom. Lett*. 3 (**2012**) 29–38. https://doi.org/10.5478/MSL.2012.3.2.29.

[245] A. Kondyli, W. Schrader, High-resolution GC/MS studies of a light crude oil fraction, *J. Mass Spectrom*. 54 (**2019**) 47–54. https://doi.org/10.1002/jms.4306.

[246] H. Kersten, V. Derpmann, I. Barnes, K.J. Brockmann, R. O'Brien, T. Benter, A novel APPI-MS setup for in situ degradation product studies of atmospherically relevant compounds: Capillary atmospheric pressure photo ionization (cAPPI), *J. Am. Soc. Mass Spectrom*. 22 (**2011**) 2070–2081. https://doi.org/10.1007/s13361-011-0212-y.

[247] M. Haapala, T. Suominen, R. Kostiainen, Capillary photoionization: A high sensitivity ionization method for mass spectrometry, *Anal. Chem*. 85 (**2013**) 5715–5719. https://doi.org/10.1021/ac4002673.

[248] M. Haapala, L. Luosujǎrvi, V. Saarela, T. Kotiaho, R.A. Ketola, S. Franssila, R. Kostiainen, Microchip for combining gas chromatography or capillary liquid chromatography with atmospheric pressure photoionization-mass spectrometry, *Anal. Chem*. 79 (**2007**) 4994–4999. https://doi.org/10.1021/ac070157a.

[249] L. Luosujärvi, M. Haapala, M. Thevis, V. Saarela, S. Franssila, R.A. Ketola, R. Kostiainen, T. Kotiaho, Analysis of Selective Androgen Receptor Modulators by Gas Chromatography-Microchip Atmospheric Pressure Photoionization-Mass Spectrometry, *J. Am. Soc. Mass Spectrom*. 21 (**2010**) 310–316. https://doi.org/10.1016/j.jasms.2009.10.019.

[250] L. Hintikka, M. Haapala, S. Franssila, T. Kuuranne, A. Leinonen, R. Kostiainen, Feasibility of gas chromatography-microchip atmospheric pressure photoionization-mass spectrometry in analysis of anabolic steroids, *J. Chromatogr. A*. 1217 (**2010**) 8290–8297. https://doi.org/10.1016/j.chroma.2010.10.074.

[251] L. Hintikka, M. Haapala, T. Kuuranne, A. Leinonen, R. Kostiainen, Analysis of anabolic steroids in urine by gas chromatography-microchip atmospheric pressure photoionization-mass spectrometry with chlorobenzene as dopant, *J. Chromatogr. A*. 1312 (**2013**) 111–117. https://doi.org/10.1016/j.chroma.2013.08.098.

[252] T.J. Kauppila, P. Östman, S. Marttila, R.A. Ketola, T. Kotiaho, S. Franssila, R. Kostiainen, Atmospheric pressure photoionization-mass spectrometry with a microchip heated nebulizer, *Anal. Chem*. 76 (**2004**) 6797–6801. https://doi.org/10.1021/ac049058c.

[253] P. Östman, S.J. Marttila, T. Kotiaho, S. Franssila, R. Kostiainen, Microchip atmospheric pressure chemical ionization source for mass spectrometry, *Anal. Chem*. 76 (**2004**) 6659–6664. https://doi.org/10.1021/ac049345g.

[254] R.C. Buck, J. Franklin, U. Berger, J.M. Conder, I.T. Cousins, P. De Voogt, A.A. Jensen, K. Kannan, S.A. Mabury, S.P.J. van Leeuwen, Perfluoroalkyl and polyfluoroalkyl substances in the environment: terminology, classification, and origins, *Integr. Environ. Assess. Manag*. 7 (**2011**) 513–541. https://doi.org/10.1002/ieam.258.

[255] R.E. Banks, B.E. Smart, J.C. Tatlow, Organofluorlne Chemistry. Principles and Commercial Applications, in: A.R. Katritzky, G.J. Sabongi (Eds.), 1st ed., Springer Science, New York, (**1994**).

[256] E. Kissa, Fluorinated Surfactants and Repellents, 2nd ed., Marcel Dekker, New York, (**2001**).

[257] J.H. Simons, Electrochemical process of making fluorine-containing carbon-compounds, (**1948**).

[258] R.N. Haszeldine, The reactions of fluorocarbon radicals. Part I. The reaction of iodotrifluoromethane with ethylene and tetrafluoroethylene, *J. Chem. Soc*. (**1949**) 2856–2861. https://doi.org/10.1039/JR9490002856.

[259] R.E. Parsons, Improvement in the preparation of perfluoroalkyl iodides from tetrafluoroethylene, (**1964**). https://doi.org/10.1145/178951.178972 .

[260] J.P. Giesy, K. Kannan, Global distribution of perfluorooctane sulfonate in wildlife, *Environ. Sci. Technol*. 35 (**2001**) 1339–1342. https://doi.org/10.1021/es001834k.

[261] K.J. Hansen, L.A. Clemen, M.E. Ellefson, H.O. Johnson, Compound-specific, quantitative characterization of organic fluorochemicals in biological matrices, *Environ. Sci. Technol*. 35 (**2001**) 766–770. https://doi.org/10.1021/es001489z.

[262] R. Renner, Growing concern over perfluorinated chemicals, *Environ. Sci. Technol*. 35 (**2001**) 155–160. https://doi.org/10.1021/es012317k.

[263] U.S. EPA, Letter Inviting Participation in the PFOA Stewardship Program, (**2006**). https://www.epa.gov/sites/production/files/2015-10/documents/dupont.pdf.

[264] CEPA, Perfluorocarboxylic acids and their precursors: environmental performance agreement overview (*accessed May 7, 2020*). https://www.canada.ca/en/environment-climate-change/services/environmental-performance- agreements/list/perfluorocarboxylic-acids-overview.html.

[265] OECD, Strategic Approach to International Chemicals Management, (**2011**). https://doi.org/10.1201/b11064-22.

[266] UNEP, Decision SC-4/17: Listing of perfluorooctane sulfonic acid, its salts and perfluorooctane sulfonyl fluoride, (**2009**).

[267] UNEP, Decision SC-9/12: Listing of perfluorooctanoic acid (PFOA), its salts and PFOA-related compounds, (**2019**).

[268] T. Ruan, G. Jiang, Analytical methodology for identification of novel per- and polyfluoroalkyl substances in the environment, *TrAC - Trends Anal. Chem*. 95 (**2017**) 122–131. https://doi.org/10.1016/j.trac.2017.07.024.

[269] A. Ritscher, Z. Wang, M. Scheringer, J.M. Boucher, L. Ahrens, U. Berger, S. Bintein, S.K. Bopp, D. Borg, A.M. Buser, I. Cousins, J. Dewitt, T. Fletcher, C. Green, D. Herzke, C. Higgins, J. Huang, H. Hung, T. Knepper, C.S. Lau, E. Leinala, A.B. Lindstrom, J. Liu, M. Miller, K. Ohno, N. Perkola, Y. Shi, L.S. Haug, X. Trier, S. Valsecchi, K. van der Jagt, L. Vierke, Zürich Statement on Future Actions on Per- and Polyfluoroalkyl Substances (PFASs), *Environ. Health Perspect*. 126 (**2018**) 1–5. https://doi.org/10.1289/EHP4158.

[270] OECD/UNEP Global PFC Group, Synthesis paper on per- and polyfluorinated chemicals (PFCs), *Environ. Heal. Safety, Environ. Dir*. (**2013**) 1–58.

[271] 3M, Fluorochemical use, distribution and release overview, (**1999**).

[272] H.J. Lehmler, Synthesis of environmentally relevant fluorinated surfactants - A review, *Chemosphere*. 58 (**2005**) 1471–1496. https://doi.org/10.1016/j.chemosphere.2004.11.078.

[273] C.T. Olson, M.E. Andersen, The Acute Toxicity of Perfluorooctanoic and Perfluorodecanoic in Male Rats and Effects on Tissue Fatty Acids Acids, *Toxicol. Appl. Pharmacol*. 70 (**1983**) 362–372.

[274] OECD, Hazard Assesment of Perfluorooctane Sulfonate (PFOS) and its salts, (**2002**).

[275] S.C. Gordon, Toxicological evaluation of ammonium 4,8-dioxa-3H-perfluorononanoate, a new emulsifier to replace ammonium perfluorooctanoate in fluoropolymer manufacturing, *Regul. Toxicol. Pharmacol*. 59 (**2011**) 64–80. https://doi.org/10.1016/j.yrtph.2010.09.008.

[276] REACH, Criteria for the identification of persistent, bioaccumulative and toxic substances, and very persistent and very bioaccumulative substances, (*accessed May 10, 2020*) https://reachonline.eu/reach/en/annex-xiii.html.

[277] Y. Shi, R. Vestergren, Z. Zhou, X. Song, L. Xu, Y. Liang, Y. Cai, Tissue Distribution and Whole Body Burden of the Chlorinated Polyfluoroalkyl Ether Sulfonic Acid F-53B in Crucian Carp (*Carassius carassius*): Evidence for a Highly Bioaccumulative Contaminant of Emerging Concern, *Environ. Sci. Technol*. 49 (**2015**) 14156–14165. https://doi.org/10.1021/acs.est.5b04299.

[278] W. Liu, J. Li, L. Gao, Z. Zhang, J. Zhao, X. He, X. Zhang, Bioaccumulation and effects of novel chlorinated polyfluorinated ether sulfonate in freshwater alga Scenedesmus obliquus, *Environ. Pollut*. 233 (**2018**) 8–15. https://doi.org/10.1016/j.envpol.2017.10.039.

[279] S.F. Nakayama, M. Yoshikane, Y. Onoda, Y. Nishihama, M. Iwai-Shimada, M. Takagi, Y. Kobayashi, T. Isobe, Worldwide trends in tracing poly- and perfluoroalkyl substances (PFAS) in the environment, *TrAC - Trends Anal. Chem*. 121 (**2019**) 115410. https://doi.org/10.1016/j.trac.2019.02.011.

[280] M. Lorenzo, J. Campo, Y. Picó, Analytical challenges to determine emerging persistent organic pollutants in aquatic ecosystems, *TrAC - Trends Anal. Chem*. 103 (**2018**) 137–155. https://doi.org/10.1016/j.trac.2018.04.003.

[281] U.S. EPA, Method 537.1 Determination of selected Per- and Polyfluorinated Alkyl Substances in Drinking Water by Solid Phase Extraction and Liquid Chromatography/Tandem Mass Spectrometry (LC/MS/MS), (**2018**).

[282] U. Berger, I. Langlois, M. Oehme, R. Kallenborn, Comparison of Three Types of Mass Spectrometer for High-Performance Liquid Chromatography/Mass Spectrometry Analysis of Perfluoroalkylated Substances and Fluorotelomer Alcohols, *Eur. J. Mass Spectrom*. 10 (**2004**) 579–588. https://doi.org/10.1255/ejms.679.

[283] W.M. Henderson, E.J. Weber, S.E. Duirk, J.W. Washington, M.A. Smith, Quantification of fluorotelomer-based chemicals in mammalian matrices by monitoring perfluoroalkyl chain fragments with GC/MS, *J. Chromatogr. B*. 846 (**2007**) 155–161. https://doi.org/10.1016/j.jchromb.2006.08.042.

[284] A.M. Piekarz, T. Primbs, J.A. Field, D.F. Barofsky, S. Simonich, Semivolatile fluorinated organic compounds in Asian and western U.S. air masses, *Environ. Sci. Technol*. 41 (**2007**) 8248–8255. https://doi.org/10.1021/es0713678.

[285] J. Li, S. Del Vento, J. Schuster, G. Zhang, P. Chakraborty, Y. Kobara, K.C. Jones, Perfluorinated compounds in the Asian atmosphere, *Environ. Sci. Technol*. 45 (**2011**) 7241–7248. https://doi.org/10.1021/es201739t.

[286] M. Kotthoff, J. Müller, H. Jürling, M. Schlummer, D. Fiedler, Perfluoroalkyl and polyfluoroalkyl substances in consumer products, *Environ. Sci. Pollut. Res*. 22 (**2015**) 14546–14559. https://doi.org/10.1007/s11356-015-4202-7.

[287] P. Favreau, C. Poncioni-Rothlisberger, B.J. Place, H. Bouchex-Bellomie, A. Weber, J. Tremp, J.A. Field, M. Kohler, Multianalyte profiling of per- and polyfluoroalkyl substances (PFASs) in liquid commercial products, *Chemosphere*. 171 (**2017**) 491–501. https://doi.org/10.1016/j.chemosphere.2016.11.127.

[288] X. Liu, Z. Guo, E.E. Folk, N.F. Roache, Determination of fluorotelomer alcohols in selected consumer products and preliminary investigation of their fate in the indoor environment, *Chemosphere*. 129 (**2015**) 81–86. https://doi.org/10.1016/j.chemosphere.2014.06.012.

[289] G. Yuan, H. Peng, C. Huang, J. Hu, Ubiquitous Occurrence of Fluorotelomer Alcohols in Eco-Friendly Paper-Made Food-Contact Materials and Their Implication for Human Exposure, *Environ. Sci. Technol*. 50 (**2016**) 942–950. https://doi.org/10.1021/acs.est.5b03806.

[290] Z. Xie, Z. Zhao, A. Möller, H. Wolschke, L. Ahrens, R. Sturm, R. Ebinghaus, Neutral poly- and perfluoroalkyl substances in air and seawater of the North Sea, *Environ. Sci. Pollut. Res*. 20 (**2013**) 7988–8000. https://doi.org/10.1007/s11356-013-1757-z.

[291] Y. Wu, V.W.C. Chang, Development of analysis of volatile polyfluorinated alkyl substances in indoor air using thermal desorption-gas chromatography-mass spectrometry, *J. Chromatogr. A*. 1238 (**2012**) 114–120. https://doi.org/10.1016/j.chroma.2012.03.053.

[292] M.A.M. Mahmoud, A. Kärrman, S. Oono, K.H. Harada, A. Koizumi, Polyfluorinated telomers in precipitation and surface water in an urban area of Japan, *Chemosphere*. 74 (**2009**) 467–472. https://doi.org/10.1016/j.chemosphere.2008.08.029.

[293] A.I. García-Valcárcel, E. Miguel, J.L. Tadeo, Determination of ten perfluorinated compounds in sludge amended soil by ultrasonic extraction and liquid chromatography-tandem mass spectrometry, *Anal. Methods*. 4 (**2012**) 2462–2468. https://doi.org/10.1039/c2ay25387a.

[294] H. Zhang, B. Wen, X. Hu, Y. Wu, L. Luo, Z. Chen, S. Zhang, Determination of fluorotelomer alcohols and their degradation products in biosolids-amended soils and plants using ultra-high performance liquid chromatography tandem mass spectrometry, *J. Chromatogr. A*. 1404 (**2015**) 72–80. https://doi.org/10.1016/j.chroma.2015.05.063.

[295] H. Chen, H. Peng, M. Yang, J. Hu, Y. Zhang, Detection, Occurrence, and Fate of Fluorotelomer Alcohols in Municipal Wastewater Treatment Plants, *Environ. Sci. Technol*. 51 (**2017**) 8953–8961. https://doi.org/10.1021/acs.est.7b00315.

[296] I. Zabaleta, E. Bizkarguenaga, D.B.O. Nunoo, L. Schultes, J. Leonel, A. Prieto, O. Zuloaga, J.P. Benskin, Biodegradation and Uptake of the Pesticide Sulfluramid in a Soil-Carrot Mesocosm, *Environ. Sci. Technol*. 52 (**2018**) 2603–2611. https://doi.org/10.1021/acs.est.7b03876.

[297] R. Ma, K. Shih, Perfluorochemicals in wastewater treatment plants and sediments in Hong Kong, *Environ. Pollut*. 158 (**2010**) 1354–1362. https://doi.org/10.1016/j.envpol.2010.01.013.

[298] K.A. Barzen-Hanson, S.C. Roberts, S. Choyke, K. Oetjen, A. McAlees, N. Riddell, R. McCrindle, P.L. Ferguson, C.P. Higgins, J.A. Field, Discovery of 40 Classes of Per- and Polyfluoroalkyl Substances in Historical Aqueous Film-Forming Foams (AFFFs) and AFFF-Impacted Groundwater, *Environ. Sci. Technol*. 51 (**2017**) 2047–2057. https://doi.org/10.1021/acs.est.6b05843.

[299] F. Xiao, S.A. Golovko, M.Y. Golovko, Identification of novel non-ionic, cationic, zwitterionic, and anionic polyfluoroalkyl substances using UPLC–TOF–MS E high-resolution parent ion search, *Anal. Chim. Acta*. 988 (**2017**) 41–49. https://doi.org/10.1016/j.aca.2017.08.016.

[300] Y. Liu, A.D.S. Pereira, J.W. Martin, Discovery of C5-C17 Poly- and perfluoroalkyl substances in water by in-line Spe-HPLC-Orbitrap with in-source fragmentation flagging, *Anal. Chem*. 87 (**2015**) 4260–4268. https://doi.org/10.1021/acs.analchem.5b00039.

[301] A. Rotander, A. Kärrman, L.-M.L. Toms, M. Kay, J.F. Mueller, M.J. Gómez Ramos, Novel fluorinated surfactants tentatively identified in firefighters using liquid chromatography quadrupole time-of-flight tandem mass spectrometry and a case-control approach, *Environ. Sci. Technol*. 49 (**2015**) 2434–2442. https://doi.org/10.1021/es503653n.

[302] N. Yu, H. Guo, J. Yang, L. Jin, X. Wang, W. Shi, X. Zhang, H. Yu, S. Wei, Non-Target and Suspect Screening of Per- and Polyfluoroalkyl Substances in Airborne Particulate Matter in China, *Environ. Sci. Technol*. 52 (**2018**) 8205–8214. https://doi.org/10.1021/acs.est.8b02492.

[303] S. Newton, R. McMahen, J.A. Stoeckel, M. Chislock, A. Lindstrom, M. Strynar, Novel Polyfluorinated Compounds Identified Using High Resolution Mass Spectrometry Downstream of Manufacturing Facilities near Decatur, Alabama, *Environ. Sci. Technol*. 51 (**2017**) 1544–1552. https://doi.org/10.1021/acs.est.6b05330.

[304] X. Trier, K. Granby, J.H. Christensen, Polyfluorinated surfactants (PFS) in paper and board coatings for food packaging, *Environ. Sci. Pollut. Res*. 18 (**2011**) 1108–1120. https://doi.org/10.1007/s11356-010-0439-3.

[305] J.W. Martin, S.A. Mabury, P.J. O'Brien, Metabolic products and pathways of fluorotelomer alcohols in isolated rat hepatocytes, *Chem. Biol. Interact*. 155 (**2005**) 165–180. https://doi.org/10.1016/j.cbi.2005.06.007.

[306] W.J. Fasano, S.C. Carpenter, S.A. Gannon, T.A. Snow, J.C. Stadler, G.L. Kennedy, R.C. Buck, S.H. Korzeniowski, P.M. Hinderliter, R.A. Kemper, Absorption, distribution, metabolism, and elimination of 8-2 fluorotelomer alcohol in the rat, *Toxicol. Sci*. 91 (**2006**) 341–355. https://doi.org/10.1093/toxsci/kfj160.

[307] S.F. Baygi, B.S. Crimmins, P.K. Hopke, T.M. Holsen, Comprehensive emerging chemical discovery: Novel polyfluorinated compounds in lake Michigan trout, *Environ. Sci. Technol*. 50 (**2016**) 9460–9468. https://doi.org/10.1021/acs.est.6b01349.

[308] R. Seró Llor, Noves estratègies per a l'anàlisi directa de compostos orgànics per espectrometria de masses, University of Barcelona, (**2019**). http://diposit.ub.edu/dspace/handle/2445/145082.

[309] B.J. Place, J.A. Field, Identification of novel fluorochemicals in aqueous film-forming foams used by the US military, *Environ. Sci. Technol*. 46 (**2012**) 7120–7127. https://doi.org/10.1021/es301465n.

[310] UNEP, Risk profile on short-chained chlorinated paraffins. UNEP/POPS/POPRC.11/10/Add.2, 2015.

[311] J. Glüge, Z. Wang, C. Bogdal, M. Scheringer, K. Hungerbühler, Global production, use, and emission volumes of short-chain chlorinated paraffins – A minimum scenario, *Sci. Total Environ*. 573 (**2016**) 1132–1146. https://doi.org/10.1016/j.scitotenv.2016.08.105.

[312] UNEP, Decision SC-8 / 11: Listing of short-chain chlorinated paraffins, (**2017**).

[313] E. Hoh, L. Zhu, R.A. Hites, Dechlorane plus, a chlorinated flame retardant, in the Great Lakes, *Environ. Sci. Technol*. 40 (**2006**) 1184–1189. https://doi.org/10.1021/es051911h.

[314] P. Wang, Q. Zhang, H. Zhang, T. Wang, H. Sun, S. Zheng, Y. Li, Y. Liang, G. Jiang, Sources and environmental behaviors of Dechlorane Plus and related compounds - A review, *Environ. Int*. 88 (**2016**) 206–220. https://doi.org/10.1016/j.envint.2015.12.026.

[315] D. Hayward, Identification of Bioaccumulating Polychlorinated Naphthalenes and Their Toxicological Significance, *Environ. Res*. 76 (**1998**) 1–18. https://doi.org/10.1006/enrs.1997.3777.

[316] AMAP, AMAP Assessment 2002: Persistent organic pollutants in the Arctic, (**2004**).

[317] UNEP, Risk profile on chlorinated naphthalenes. UNEP/POPS/POPRC.8/16/Add.1, (**2012**).

[318] L. Ritter, K.. Solomon, J. Forget, Persistent Organic Pollutants - An Assessment Report on: DDT- Aldrin- Dieldrin- Endrin- Chlordane- Heptachlor- Heptachlorobenzene- Mirex- Tozapene- Polychlorinated Biphenyls- Dioxins and Furans, (**1995**).

[319] UNEP, Report on progress towards the elimination of polychlorinated biphenyls. UNEP/POPS/COP.9/INF/10, (**2019**).

[320] UNEP, Technical guidelines on the environmentally sound management of wastes containing or contaminated with unintentionally produced polychlorinated dibenzo-p-dioxins, polychlorinated dibenzofurans, hexachlorobenzene, polychlorinated biphenyls or pentachlorobenzene. UNEP/CHW.12/5/Add.4/Rev.1, (**2015**).

[321] E. Grossman, Non Legacy PCBs. Pigment Manufacturing By-Products. Get a Second Look, *Environ. Health Perspect*. 121 (**2013**) 87–93. https://doi.org/10.1289/ehp.121-a86.

[322] M.C. Catlin, Health effects of agent orange: the more recent national academy of science efforts, *Organohalogen Compd*. 226 (**2003**) 223–226.

[323] S.D. Stellman, J.M. Stellman, Exposure opportunity models for Agent Orange, dioxin, and other military herbicides used in Vietnam, 1961-1971, *J. Expo. Anal. Environ. Epidemiol*. 14 (**2004**) 354–362. https://doi.org/10.1038/sj.jea.7500331.

[324] G.U. Fortunati, The Seveso accident, *Chemosphere*. 14 (**1985**) 729–737.

[325] P. Mocarelli, Seveso: A teaching story, *Chemosphere*. 43 (**2001**) 391–402. https://doi.org/10.1016/S0045-6535(00)00386-6.

[326] M.M. Trinh, M.B. Chang, Review on occurrence and behavior of PCDD/Fs and dl-PCBs in atmosphere of East Asia, *Atmos. Environ*. 180 (**2018**) 23–36. https://doi.org/10.1016/j.atmosenv.2018.02.037.

[327] Q. Zhang, C. Zhu, H. Zhang, P. Wang, Y. Li, D. Ren, G. Jiang, Concentrations and distributions of Dechlorane Plus in environmental samples around a Dechlorane Plus manufacturing plant in East China, *Sci. Bull*. 60 (**2015**) 792–797. https://doi.org/10.1007/s11434-015-0768-1.

[328] A. Salamova, R.A. Hites, Dechlorane plus in the atmosphere and precipitation near the Great Lakes, *Environ. Sci. Technol*. 45 (**2011**) 9924–9930. https://doi.org/10.1021/es202762n.

[329] C. Degrendele, H. Fiedler, A. Kočan, P. Kukučka, P. Přibylová, R. Prokeš, J. Klánová, G. Lammel, Multiyear levels of PCDD/Fs, dl-PCBs and PAHs in background air in central Europe and implications for deposition, *Chemosphere*. 240 (**2020**) 124852. https://doi.org/10.1016/j.chemosphere.2019.124852.

[330] Q. Zhu, X. Zhang, S. Dong, L. Gao, G. Liu, M. Zheng, Gas and particle size distributions of polychlorinated naphthalenes in the atmosphere of Beijing, China, *Environ. Pollut*. 212 (**2016**) 128–134. https://doi.org/10.1016/j.envpol.2016.01.065.

[331] T.F. Bidleman, P.A. Helm, B.M. Braune, G.W. Gabrielsen, Polychlorinated naphthalenes in polar environments - A review, *Sci. Total Environ*. 408 (**2010**) 2919–2935. https://doi.org/10.1016/j.scitotenv.2009.09.013.

[332] X. Zhu, H. Bai, Y. Gao, J. Chen, H. Yuan, L. Wang, W. Wang, X. Dong, X. Li, Concentrations and inhalation risk assessment of short-chain polychlorinated paraffins in the urban air of Dalian, China, *Environ. Sci. Pollut. Res*. 24 (**2017**) 21203–21212. https://doi.org/10.1007/s11356-017-9775-x.

[333] X. Ma, H. Zhang, H. Zhou, G. Na, Z. Wang, C. Chen, J. Chen, J. Chen, Occurrence and gas/particle partitioning of short- and medium-chain chlorinated paraffins in the atmosphere of Fildes Peninsula of Antarctica, *Atmos. Environ*. 90 (**2014**) 10–15. https://doi.org/10.1016/j.atmosenv.2014.03.021.

[334] X. Ma, Y. Wang, W. Gao, Y. Wang, Z. Wang, Z. Yao, G. Jiang, Air-Seawater Gas Exchange and Dry Deposition of Chlorinated Paraffins in a Typical Inner Sea (Liaodong Bay), North China, *Environ. Sci. Technol*. 52 (**2018**) 7729–7735. https://doi.org/10.1021/acs.est.8b01803.

[335] G. Cornelissen, K. Amstaetter, A. Hauge, M. Schaanning, B. Beylich, J.S. Gunnarsson, G.D. Breedveld, A.M.P. Oen, E. Eek, Large-scale field study on thin-layer capping of marine PCDD/F-contaminated sediments in Grenlandfjords, Norway: Physicochemical effects, *Environ. Sci. Technol*. 46 (**2012**) 12030–12037. https://doi.org/10.1021/es302431u.

[336] G. Na, W. Wei, S. Zhou, H. Gao, X. Ma, L. Qiu, L. Ge, C. Bao, Z. Yao, Distribution characteristics and indicator significance of Dechloranes in multi-matrices at Ny-Ålesund in the Arctic, *J. Environ. Sci.* 28 (**2015**) 8–13. https://doi.org/10.1016/j.jes.2014.07.019.

[337] M. Cai, Q. Hong, J. Sun, K. Sundqvist, K. Wiberg, K. Chen, Y. Wang, C. Qiu, S. Huang, Concentrations, distribution and sources of polychlorinated dibenzo-p-dioxins and dibenzofurans and dioxin-like polychlorinated biphenyls in coastal sediments from Xiamen, China, *Mar. Chem.* 185 (**2016**) 74–81. https://doi.org/10.1016/j.marchem.2016.05.008.

[338] R. Jing, S. Fusi, A. Chan, S. Capozzi, B. V. Kjellerup, Distribution of polychlorinated biphenyls in effluent from a large municipal wastewater treatment plant: Potential for bioremediation?, *J. Environ. Sci.* 78 (**2019**) 42–52. https://doi.org/10.1016/j.jes.2018.06.007.

[339] R. Lei, W. Liu, X. Wu, T. Ni, T. Jia, A review of levels and profiles of polychlorinated dibenzo-p-dioxins and dibenzofurans in different environmental media from China, *Chemosphere.* 239 (**2020**) 124685. https://doi.org/10.1016/j.chemosphere.2019.124685.

[340] R. Ullah, R. Asghar, M. Baqar, A. Mahmood, A. Alamdar, A. Qadir, M. Sohail, R.B. Schäfer, S.A.M.A.S. Eqani, Assessment of polychlorinated biphenyls (PCBs) in the Himalayan Riverine Network of Azad Jammu and Kashmir, *Chemosphere.* 240 (**2020**) 124762. https://doi.org/10.1016/j.chemosphere.2019.124762.

[341] X. Li, Y. Gao, Y. Wang, Y. Pan, Emerging persistent organic pollutants in Chinese Bohai sea and its coastal regions, *Sci. World J.* 2014 (**2014**). https://doi.org/10.1155/2014/608231.

[342] A. Mahmood, R.N. Malik, J. Li, G. Zhang, Congener specific analysis, spatial distribution and screening-level risk assessment of polychlorinated naphthalenes in water and sediments from two tributaries of the River Chenab, Pakistan, *Sci. Total Environ.* 485–486 (**2014**) 693–700. https://doi.org/10.1016/j.scitotenv.2014.03.118.

[343] T.A. Dick, C.P. Gallagher, G.T. Tomy, Short- and medium-chain chlorinated paraffins in fish, water and soils from the Iqaluit, Nunavut (Canada), area, *World Rev. Sci. Technol. Sustain. Dev.* 7 (**2010**) 387–401. https://doi.org/10.1504/WRSTSD.2010.032747.

[344] A. Rubirola, F.J. Santos, M.R. Boleda, M.T. Galceran, Routine Method for the Analysis of Short-Chain Chlorinated Paraffins in Surface Water and Wastewater, *Clean - Soil, Air, Water.* 46 (**2018**) 1600151. https://doi.org/10.1002/clen.201600151.

[345] R. Wang, L. Gao, M. Zheng, Y. Tian, J. Li, L. Zhang, Y. Wu, H. Huang, L. Qiao, W. Liu, G. Su, G. Liu, Y. Liu, Short- and medium-chain chlorinated paraffins in aquatic foods

from 18 Chinese provinces: Occurrence, spatial distributions, and risk assessment, *Sci. Total Environ*. 615 (**2018**) 1199–1206. https://doi.org/10.1016/j.scitotenv.2017.09.327.

[346] Y. Huang, L. Chen, G. Jiang, Q. He, L. Ren, B. Gao, L. Cai, Bioaccumulation and biomagnification of short-chain chlorinated paraffins in marine organisms from the Pearl River Estuary, South China, *Sci. Total Environ*. 671 (**2019**) 262–269. https://doi.org/10.1016/j.scitotenv.2019.03.346.

[347] N. Zhao, Y. Cui, P. Wang, S. Li, W. Jiang, N. Luo, Z. Wang, X. Chen, L. Ding, Short-chain chlorinated paraffins in soil, sediment, and seawater in the intertidal zone of Shandong Peninsula, China: Distribution and composition, *Chemosphere*. 220 (**2019**) 452–458. https://doi.org/10.1016/j.chemosphere.2018.12.063.

[348] H. Li, J. Fu, W. Pan, P. Wang, Y. Li, Q. Zhang, Y. Wang, A. Zhang, Y. Liang, G. Jiang, Environmental behaviour of short-chain chlorinated paraffins in aquatic and terrestrial ecosystems of Ny-Ålesund and London Island, Svalbard, in the Arctic, *Sci. Total Environ*. 590–591 (**2017**) 163–170. https://doi.org/10.1016/j.scitotenv.2017.02.192.

[349] B.O. Clarke, S.R. Smith, Review of "emerging" organic contaminants in biosolids and assessment of international research priorities for the agricultural use of biosolids, *Environ. Int*. 37 (**2011**) 226–247. https://doi.org/10.1016/j.envint.2010.06.004.

[350] K. Guemiza, L. Coudert, S. Metahni, G. Mercier, S. Besner, J.-F. Blais, Treatment technologies used for the removal of As, Cr, Cu, PCP and/or PCDD/F from contaminated soil: A review, *J. Hazard. Mater*. 333 (**2017**) 194–214. https://doi.org/10.1016/j.jhazmat.2017.03.021.

[351] G. Suzuki, M. Someya, H. Matsukami, N.M. Tue, N. Uchida, L.H. Tuyen, P.H. Viet, S. Takahashi, S. Tanabe, A. Brouwer, H. Takigami, Comprehensive evaluation of dioxins and dioxin-like compounds in surface soils and river sediments from e-waste-processing sites in a village in northern Vietnam: Heading towards the environmentally sound management of e-waste, *Emerg. Contam*. 2 (**2016**) 98–108. https://doi.org/10.1016/j.emcon.2016.03.001.

[352] S. Jia, Q. Wang, L. Li, X. Fang, Y. Shi, W. Xu, J. Hu, Comparative study on PCDD/F pollution in soil from the Antarctic, Arctic and Tibetan Plateau, *Sci. Total Environ*. 497–498 (**2014**) 353–359. https://doi.org/10.1016/j.scitotenv.2014.07.109.

[353] R. Jin, J. Fu, M. Zheng, L. Yang, A. Habib, C. Li, G. Liu, Polychlorinated Naphthalene Congener Profiles in Common Vegetation on the Tibetan Plateau as Biomonitors of Their Sources and Transportation, *Environ. Sci. Technol*. 54 (**2020**) 2314–2322. https://doi.org/10.1021/acs.est.9b06668.

[354] K. Xiao, P. Wang, H. Zhang, H. Shang, Y. Li, X. Li, D. Ren, W. Chen, Q. Zhang, Levels and profiles of Dechlorane Plus in a major E-waste dismantling area in China, *Environ. Geochem. Health*. 35 (**2013**) 625–631. https://doi.org/10.1007/s10653-013-9545-8.

[355] A. De La Torre, G. Pacepavicius, L. Shen, E. Reiner, B. Jiménez, M. Alaee, M.A. Martínez, Dechlorane Plus and Related Compounds in Spanish Air, *Organohalogen Compd*. 72 (**2010**) 929–932.

[356] D.G. Wang, M. Yang, H. Qi, E. Sverko, W.-L. Ma, Y.-F. Li, M. Alaee, E.J. Reiner, L. Shen, An Asia-specific source of Dechlorane Plus: Concentration, isomer profiles, and other related compounds, *Environ. Sci. Technol*. 44 (**2010**) 6608–6613. https://doi.org/10.1021/es101224y.

[357] E. Barón, G. Santín, E. Eljarrat, D. Barceló, Occurrence of classic and emerging halogenated flame retardants in sediment and sludge from Ebro and Llobregat river basins (Spain), *J. Hazard. Mater*. 265 (**2014**) 288–295. https://doi.org/10.1016/j.jhazmat.2013.10.069.

[358] Y. Yu, H. Hung, N. Alexandrou, P. Roach, K. Nordin, Multiyear Measurements of Flame Retardants and Organochlorine Pesticides in Air in Canada's Western Sub-Arctic, *Environ. Sci. Technol*. 49 (**2015**) 8623–8630. https://doi.org/10.1021/acs.est.5b01996.

[359] E. Barón, M. Máñez, A.C. Andreu, F. Sergio, F. Hiraldo, E. Eljarrat, D. Barceló, Bioaccumulation and biomagnification of emerging and classical flame retardants in bird eggs of 14 species from Doñana Natural Space and surrounding areas (South-western Spain), *Environ. Int*. 68 (**2014**) 118–126. https://doi.org/10.1016/j.envint.2014.03.013.

[360] B. Yuan, K. Vorkamp, A.M. Roos, S. Faxneld, C. Sonne, S.E. Garbus, Y. Lind, I. Eulaers, P. Hellström, R. Dietz, S. Persson, R. Bossi, C.A. De Wit, Accumulation of Short-, Medium-, and Long-Chain Chlorinated Paraffins in Marine and Terrestrial Animals from Scandinavia, *Environ. Sci. Technol*. 53 (**2019**) 3526–3537. https://doi.org/10.1021/acs.est.8b06518.

[361] P. Ssebugere, M. Sillanpää, H. Matovu, E. Mubiru, Human and environmental exposure to PCDD/Fs and dioxin-like PCBs in Africa: A review, *Chemosphere*. 223 (**2019**) 483–493. https://doi.org/10.1016/j.chemosphere.2019.02.065.

[362] AMAP, AMAP Assessment 2016: Chemicals of Emerging Arctic Concern, (**2017**).

[363] CEN, Noma Española UNE-EN 1948-3. Emisiones de fuentes estacionarias. Parte 3: identificación y cuantificación de PCDD/PCDF, (**2007**).

[364] E.J. Reiner, R.E. Clement, A.B. Okey, C.H. Marvin, Advances in analytical techniques for polychlorinated dibenzo-p-dioxins, polychlorinated dibenzofurans and dioxin-like PCBs, *Anal. Bioanal. Chem.* 386 (**2006**) 791–806. https://doi.org/10.1007/s00216-006-0479-1.

[365] E. Sverko, G.T. Tomy, E.J. Reiner, Y.F. Li, B.E. McCarry, J.A. Arnot, R.J. Law, R.A. Hites, Dechlorane Plus and related compounds in the environment: A review, *Environ. Sci. Technol.* 45 (**2011**) 5088–5098. https://doi.org/10.1021/es2003028.

[366] P. Korytár, J. Parera, P.E.G. Leonards, F.J. Santos, J. De Boer, U.A.T. Brinkman, Characterization of polychlorinated n-alkanes using comprehensive two-dimensional gas chromatography-electron-capture negative ionisation time-of-flight mass spectrometry, *J. Chromatogr. A.* 1086 (**2005**) 71–82. https://doi.org/10.1016/j.chroma.2005.05.003.

[367] M. Reth, M. Oehme, Limitations of low resolution mass spectrometry in the electron capture negative ionization mode for the analysis of short- and medium-chain chlorinated paraffins, *Anal. Bioanal. Chem.* 378 (**2004**) 1741–1747. https://doi.org/10.1007/s00216-004-2546-9.

[368] G.T. Tomy, G.A. Stern, D.C.G. Muir, A.T. Fisk, C.D. Cymbalisty, J.B. Westmore, Quantifying C10-C13 Polychloroalkanes in Environmental Samples by High-Resolution Gas Chromatography/Electron Capture Negative Ion High-Resolution Mass Spectrometry, *Anal. Chem.* 69 (**1997**) 2762–2771. https://doi.org/10.1021/ac961244y.

[369] T.D. Ho, A.J. Canestraro, J.L. Anderson, Ionic liquids in solid-phase microextraction: A review, *Anal. Chim. Acta.* 695 (**2011**) 18–43. https://doi.org/10.1016/j.aca.2011.03.034.

[370] C. Ragonese, D. Sciarrone, P.Q. Tranchida, P. Dugo, L. Mondello, Use of ionic liquids as stationary phases in hyphenated gas chromatography techniques, *J. Chromatogr. A.* 1255 (**2012**) 130–144. https://doi.org/10.1016/j.chroma.2012.04.069.

[371] J. Falandysz, K. Nose, Y. Ishikawa, E. Łukaszewicz, N. Yamashita, Y. Noma, HRGC/HRMS analysis of chloronaphthalenes in several batches of Halowax 1000, 1001, 1013, 1014 and 1099, *J. Environ. Sci. Heal. - Part A.* 41 (**2006**) 2237–2255. https://doi.org/10.1080/10934520600872748.

[372] A.M. Muscalu, D. Morse, E.J. Reiner, T. Górecki, The quantification of short-chain chlorinated paraffins in sediment samples using comprehensive two-dimensional gas chromatography with µECD detection, *Anal. Bioanal. Chem.* 409 (**2017**) 2065–2074. https://doi.org/10.1007/s00216-016-0153-1.

[373] L.M. van Mourik, R. Lava, J. O'Brien, P.E.G. Leonards, J. de Boer, M. Ricci, The underlying challenges that arise when analysing short-chain chlorinated paraffins in environmental matrices, *J. Chromatogr. A*. 1610 (**2020**) 460550. https://doi.org/10.1016/j.chroma.2019.460550.

[374] C. Sales, G. Poma, G. Malarvannan, T. Portolés, J. Beltrán, A. Covaci, Simultaneous determination of dechloranes, polybrominated diphenyl ethers and novel brominated flame retardants in food and serum, *Anal. Bioanal. Chem*. 409 (**2017**) 4507–4515. https://doi.org/10.1007/s00216-017-0411-x.